



University of  
Novi Sad  
Faculty of  
Technical Sciences  
Department of  
Production Engineering

14<sup>th</sup> International  
Scientific  
Conference

# MMA 2021

## FLEXIBLE TECHNOLOGIES

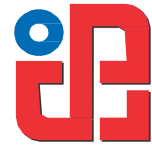


Novi Sad  
Serbia  
September 23-25, 2021



UNIVERSITY OF NOVI SAD  
FACULTY OF TECHNICAL SCIENCES  
DEPARTMENT OF PRODUCTION ENGINEERING  
NOVI SAD, SERBIA

---



14<sup>th</sup> INTERNATIONAL SCIENTIFIC CONFERENCE  
MMA 2021 - FLEXIBLE TECHNOLOGIES

**MMA 2021**  

---

**FLEXIBLE TECHNOLOGIES**

**PROCEEDINGS**

---

Novi Sad, September 23-25, 2021

PROCEEDINGS OF THE 14<sup>th</sup> INTERNATIONAL SCIENTIFIC CONFERENCE  
**MMA 2021 - FLEXIBLE TECHNOLOGIES**  
Novi Sad, 2021

---

*Publisher:* **FACULTY OF TECHNICAL SCIENCES**  
**DEPARTMENT OF PRODUCTION ENGINEERING**  
**21000 NOVI SAD, Trg Dositeja Obradovića 6**  
**SERBIA**

---

*Organization of this Conference was approved by Educational-scientific Council of Faculty of Technical Sciences in Novi Sad*

---

*Editor:* Dr Rade Doroslovački, Full Professor, Dean

*Technical treatment and design:* Dr Milenko Sekulić, Full Professor  
Dr Borislav Savković, Associate Professor  
Dr Dragan Rodić, Assistant Professor  
Dr Miroslav Dramićanin, Assistant Professor  
M. Sc. Anđelko Aleksić, Teaching assistant  
M. Sc. Nenad Kulundžić, Research associate

*Manuscript submitted for publication:* September 15, 2021

*Printing:* 1<sup>st</sup>

*Circulation:* 200 copies

*CIP classification:*

CIP - Каталогизacija y publikaciji  
Biblioteka Maticе српске, Нови Сад

621.7/.9(082)

621.9(082)

**INTERNATIONAL Scientific Conference MMA 2021 - Flexible Technologies (14 ; 2021 ; Novi Sad)**

Proceedings / 14th International Scientific Conference MMA 2021 - Flexible Technologies, Novi Sad, September 23-25, 2021 ; [editor Rade Doroslovački]. - 1st ed. - Novi Sad : Faculty of Technical Sciences, 2021 (Novi Sad : FTN, Graphic Centre Grid). - V, 254 str. : ilustr. ; 30 cm

Tiraž 200. - Tekst štampan dvostubačno. - Bibliografija uz svaki rad. - Registar.

ISBN 978-86-6022-364-9

a) Производно машинство - Зборници. b) Метали - Обрада - Зборници  
COBISS.SR-ID 45959689

*Printing by:* FTN, Graphic Centre  
GRID, Novi Sad

---

*Financing of the Proceedings was sponsored by the Ministry of Education, Science and Technological Development of the Republic of Serbia and supported by the Provincial Secretariat for Higher Education and Scientific Research of AP Vojvodina.*

---

CONFERENCE ORGANIZER

---

University of Novi Sad  
Faculty of Technical Sciences  
Department of Production Engineering  
Novi Sad, Serbia

INTERNATIONAL SCIENTIFIC COMMITTEE

---

Milenko Sekulić, Chairman, University of Novi Sad, SRB  
Bojan Ačko, University of Maribor, SVN  
Boris Agarski, University of Novi Sad, SRB  
Sergei Alexandrov, Russian Academy of Sciences, RUS  
Aco Antić, University of Novi Sad, SRB  
Jan C. Aurich, Technical University Kaiserslautern, GER  
Bojan Babić, University of Belgrade, SRB  
Sebastian Baloš, University of Novi Sad, SRB  
Dana Livia Beju, Lucian Blaga University of Sibiu, ROU  
Konstantinos D. Bouzakis, Aristotle University of Thessaloniki, GRE  
Miran Brezočnik, University of Maribor, SVN  
Erhan Budak, Sabanci University, TUR  
Igor Budak, University of Novi Sad, SRB  
Emanuele Carpanzano, Un. of App. Sci. and Arts of S. Switz., CHE  
Robert Čep, Technical University of Ostrava, CZE  
Ilija Ćosić, University of Novi Sad, SRB  
Predrag Ćosić, University of Zagreb, CRO  
Joao Paulo Davim, University of Aveiro, PRT  
Goran Devedžić, University of Kragujevac, SRB  
Lubomir Dimitrov, Technical University of Sofia, BGR  
Cristian Doicin, Polytechnica University of Bucharest, ROU  
Rade Doroslovački, University of Novi Sad, SRB  
Miroslav Dovica, University of Kosice, SVK  
Viorel Mircea Drăgoi, Transilvania University of Braşov, ROU  
Igor Drstvenšek, University of Maribor, SLO  
Numan M. Durakbasa, Vienna University of Technology, AUT  
Kornel Ehmann, Northwestern University, USA  
Sabahudin Ekinović, University of Zenica, BIH  
Luigi Maria Galantucci, Politecnico di Bari, ITA  
Adam Gaska, Cracow University of Technology, POL  
Valentina Gečevska, Ss. Cyril and Methodius University, MKD  
Gordana Globočki Lakić, University of Banja Luka, BIH  
Šefket Goletić, University of Zenica, BIH  
Dušan Golubović, University of East Sarajevo, BIH  
Marin Gostimirović, University of Novi Sad, SRB  
Miodrag Hadžistević, University of Novi Sad, SRB  
František Holešovský, Tomas Bata University, CZE  
Predrag Janković, University of Niš, SRB  
Jerzy Jędrzejewski, Wrocław Univ. of Science and Technology, POL  
Zoran Jurković, University of Rijeka, CRO  
Snežana Ćirić Kostić, University of Kragujevac, SRB  
Peter Krajnik, Chalmers University of Technology, SWE  
Davorin Kramar, University of Ljubljana, SVN

Janos Kundra, University of Miskolc, HUN  
Ivan Kuric, University of Zilina, SVK  
Mikolaj Kuzinovski, Ss. Cyril and Methodius U., MKD  
Dejan Lukić, University of Novi Sad, SRB  
Ognjan Lužanin, University of Novi Sad, SRB  
Miodrag Manić, University of Niš, SRB  
Ildikó Maňková, Technical University of Kosice, SVK  
Dorian Marjanović, University of Zagreb, CRO  
Mijodrag Milošević, University of Novi Sad, SRB  
Mladomir Milutinović, University of Novi Sad, SRB  
Zoran Miljković, University of Belgrade, SRB  
Radivoje Mitrović, University of Belgrade, SRB  
Slobodan Morača, University of Novi Sad, SRB  
Dimitris Mourtzis, University of Patras, GRE  
Bogdan Nedić, University of Kragujevac, SRB  
Duško Pavletić, University of Rijeka, CRO  
Darko Petković, University of Zenica, BIH  
Petar B. Petrović, University of Belgrade, SRB  
Franci Pušavec, University of Ljubljana, SVN  
Radovan Puzović, University of Belgrade, SRB  
Dragan Rajnović, University of Novi Sad, SRB  
Biserka Runje, University of Zagreb, CRO  
Borislav Savković, University of Novi Sad, SRB  
Antun Stoić, University of Osijek, CRO  
Tibor Szalay, Budapest U. of Technology and Eco., HUN  
Tomislav Šarić, University of Slavonski Brod, CRO  
Mladen Šerčer, University of Zagreb, CRO  
Leposava Šiđanin, University of Novi Sad, SRB  
Goran Šimunović, University of Osijek, CRO  
Branko Škorić, University of Novi Sad, SRB  
Lubomír Šooš, Slovak University of Technology, SVK  
Dušan Šormaz, Ohio University, USA  
Slobodan Tabaković, University of Novi Sad, SRB  
Branko Tadić, University of Kragujevac, SRB  
Ljubodrag Tanović, University of Belgrade, SRB  
Radoslav Tomović, University of Montenegro, MNE  
Nicolae Ungureanu, N. University of Baia Mare, ROU  
Đorđe Vukelić, University of Novi Sad, SRB  
Lihui Wang, KTH Royal Institute of Technology, SWE  
Wojciech Zebala, Cracow University of Technology, POL  
Milan Zeljković, University of Novi Sad, SRB  
Aleksandar Živković, University of Novi Sad, SRB

---

**HONORARY COMMITTEE**

*Slavko Arsovski, University of Kragujevac, SRB*  
*Pavao Bojanić, University of Belgrade, SRB*  
*Franc Čuš, University of Maribor, SLO*  
*Dragan Domazet, Metropolitan University, SRB*  
*Milenko Jovičić, University of Belgrade, SRB*  
*Vid Jovišević, University of Banja Luka, BIH*  
*Milislav Kalajdžić, University of Belgrade, SRB*  
*Janez Kopač, University of Ljubljana, SLO*  
*Pavel Kovač, University of Novi Sad, SRB*  
*Miodrag Lazić, University of Kragujevac, SRB*  
*Ljubomir Lukić, University of Kragujevac, SRB*

*Vidosav Majstorović, University of Belgrade, SRB*  
*Vučko Mečanin, University of Kragujevac, SRB*  
*Dragoje Milikić, University of Novi Sad, SRB*  
*Dragan Milutinović, University of Belgrade, SRB*  
*Ratko Mitrović, University of Kragujevac, SRB*  
*Miroslav Radovanović, University of Niš, SRB*  
*Sava Sekulić, University of Novi Sad, SRB*  
*Mirko Soković, University of Ljubljana, SLO*  
*Bogdan Sovilj, University of Novi Sad, SRB*  
*Velimir Todić, University of Novi Sad, SRB*  
*Dragiša Vilotić, University of Novi Sad, SRB*

---

**ORGANIZING COMMITTEE**

*Borislav Savković, University of Novi Sad, SRB, chairman*  
*Anđelko Aleksić, University of Novi Sad, SRB*  
*Dragan Rodić, University of Novi Sad, SRB*  
*Miroslav Dramićanin, University of Novi Sad, SRB*  
*Miloš Knežev, University of Novi Sad, SRB*  
*Zorana Lanc, University of Novi Sad, SRB*  
*Ivan Matin, University of Novi Sad, SRB*  
*Cvijetin Mladenović, University of Novi Sad, SRB*

*Nenad Kulundžić, University of Novi Sad, SRB, secretary*  
*Miloš Ranisavljev, University of Novi Sad, SRB*  
*Željko Santoši, University of Novi Sad, SRB*  
*Milana Ilić Mićunović, University of Novi Sad, SRB*  
*Mario Šokac, University of Novi Sad, SRB*  
*Branko Štrbac, University of Novi Sad, SRB*  
*Marko Zagoričnik, University of Novi Sad, SRB*

## ACKNOWLEDGEMENTS

Organisation of 14<sup>th</sup> International Scientific Conference MMA 2021 – FLEXIBLE TECHNOLOGIES was made possible with understanding and financial help of following sponsors and donators:

- **MINISTRY OF EDUCATION, SCIENCE AND TECHNOLOGICAL DEVELOPMENT OF THE REPUBLIC OF SERBIA** – Belgrade
- **PROVINCIAL SECRETARIAT FOR HIGHER EDUCATION AND SCIENTIFIC RESEARCH OF AP VOJVODINA** – Novi Sad
- **UNIVERSITY OF NOVI SAD** – Novi Sad
- **FACULTY OF TECHNICAL SCIENCES** – Novi Sad
- **DEPARTMENT OF PRODUCTION ENGINEERING AT THE FACULTY OF TECHNICAL SCIENCES** – Novi Sad
- **UNIMET d.o.o.** – Kać
- **TERMOVENT SC d.o.o.** – Temerin
- **TELSONIC d.o.o.** – Kać
- **SECO TOOLS SRB d.o.o.** – Novi Sad
- **ATB SEVER d.o.o.** – Subotica
- **PRECISE CASTING PLANT - LPO d.o.o.** – Ada
- **CHAMBER OF COMMERCE AND INDUSTRY OF VOJVODINA** – Novi Sad
- **FACTORY OF ROLLING BEARINGS AND CARDAN SHAFTS - FKL a.d.** – Temerin
- **IMPERIAL BUILDINGS d.o.o.** – Novi Sad
- **STREIT NOVA d.o.o.** – Stara Pazova
- **INTRAPROFIL d.o.o.** - Smederevo
- **TEHNOEXPORT d.o.o.** – Inđija
- **PEŠTAN d.o.o.** – Aranđelovac
- **VUVES COMMERCE d.o.o.** – Kać
- **GRUJIĆ & ГРУЈИЋ d.o.o.** – Novi Sad

**C**ontinuing a long tradition of more than **45 years**, the **Department of Production Engineering of the Faculty of Technical Sciences** organizes **14<sup>th</sup> International Scientific Conference MMA 2021 – Flexible Technologies**.

The conference will cover current issues in the field of production engineering as well as multidisciplinary fields of mechanical engineering, information technologies, environmental engineering, bio-medical engineering and other related engineering fields, that play a significant role in successful functioning of manufacturing industry, agriculture, transport, electric power industry, oil industry, military industry, health care and other branches of economy and society.

The scientific-expert conference MMA, with its long tradition and regular organization since 1976, aims to gather and exchange experience of researchers and experts from faculties, institutes and industry, and thus wants to contribute to more intensive scientific and economic development.

The fourteenth International Scientific Conference MMA 2021 - FLEXIBLE TECHNOLOGIES is being held for the eleventh time as an international conference. By the number of papers, their quality and participation of domestic and foreign authors achieved so far, the Conference has gained an enviable reputation among scientific and professional employees from both faculty and industry. The content of the MMA 2021 – FLEXIBLE TECHNOLOGIES involves the following areas:

- MATERIAL REMOVAL TECHNOLOGIES
- MACHINE TOOLS AND AUTOMATIC FLEXIBLE SYSTEMS, CAx AND CIM PROCEDURES AND SYSTEMS
- METROLOGY, QUALITY, FIXTURES, CUTTING TOOLS AND TRIBOLOGY
- PROCESS PLANNING, OPTIMIZATION, LOGISTICS AND INTERNET TECHNOLOGIES IN PRODUCTION ENGINEERING
- MATERIALS, METAL FORMING, CASTING AND WELDING
- MECHANICAL ENGINEERING AND ENVIRONMENTAL PROTECTION
- BIO-MEDICAL ENGINEERING
- ADDITIVE MANUFACTURING TECHNOLOGIES

With 58 scientific papers the **14<sup>th</sup> International Scientific Conference MMA 2021 - FLEXIBLE TECHNOLOGIES** keeps the pace of previous conferences. The participation of numerous national and foreign authors from 15 countries, as well as the topics covered in the papers, confirm the efforts put into the organization of the conference, thus contributing to the exchange of knowledge, research results and expert experiences from industry, research institutions and universities working in the field of production engineering.

On behalf of the International Scientific and Organizing Committee of the Conference we would like to thank all keynote speakers, domestic and foreign authors, reviewers, as well as institutions and individuals who contributed to the realization of the high-quality program of the Conference. Without their great help, the conference would have been difficult to organize under the conditions of the Covid 19 pandemic.

Novi Sad, September 2021

Chairman of the International Scientific Committee  
Dr Milenko Sekulić, Full Professor

Chairman of the Organizing Committee  
Dr Borislav Savković, Associate Professor

## Contents

### KEYNOTE PAPERS

<b>Budak, E.:</b> INCREASED PERFORMANCE AND FLEXIBILITY IN MACHINING THROUGH PROCESS MODELING .....	1
<b>Carpanzano, E.:</b> HARMONIZING DIGITAL TRANSFORMATION AND HUMAN ASPECTS IN NEXT GENERATION PRODUCTION SYSTEMS .....	3
<b>Galantucci, L. M., Pellegrini, A., Guerra, M. G., Lavecchia, F.:</b> 3D PRINTING OF PARTS USING METAL EXTRUSION: AN OVERVIEW OF SHAPING DEBINDING AND SINTERING TECHNOLOGY .....	5
<b>Gaška, A., Harmatys, W., Gaška, P., Śladek, J.:</b> RECENT ADVANCES IN SIMULATION METHODS FOR DETERMINATION OF MEASUREMENT UNCERTAINTY .....	13
<b>Pušavec, F.:</b> GREEN AND SUSTAINABLE MACHINING PROCESSES AS A BASIS FOR INNOVATIONS .....	17

### Section A: MATERIAL REMOVAL TECHNOLOGIES

<b>Madić, M., Janković, P., Petković, D., Gostimirović, M., Rodić, D.:</b> OPTIMIZATION OF MATERIAL REMOVAL RATE IN CO <sub>2</sub> LASER CUTTING OF AN ALUMINUM ALLOY .....	19
<b>Rodić, D., Gostimirović, M., Sekulić, M., Madić, M., Kulundžić, N.:</b> INFLUENCE OF PULSE DURATION ON SURFACE ROUGHNESS IN ASSISTING ELECTRODE ELECTRIC DISCHARGE MACHINING .....	23
<b>Trifunović, M., Madić, M., Vitković, N.:</b> CUTTING PARAMETERS OPTIMIZATION FOR MINIMIZING ENERGY CONSUMPTION IN MULTI-PASS TURNING OF GREY CAST IRON .....	27
<b>Sredanović, B., Čiča, Đ., Borojević, S., Tešić, S., Kramar, D.:</b> EXPERIMENTAL ANALYSIS AND OPTIMIZATION OF THIN-WALLED TUBULAR PARTS MILLING .....	31
<b>Pămîntaş, E., Banciu, F.V.:</b> METAL CUTTING IS IT STILL OF INTEREST TO ANYONE? .....	37
<b>Kurbegović, R., Janjić, M.:</b> JET LAGGING IN ABRASIVE WATER JET CUTTING OF TOOL STEEL .....	41



<b>Antić, A., Ungureanu, N., Čep, R., Lukić D., Milošević, M.:</b> TOOL WEAR CONDITION MONITORING BASED ON FUZZY SYSTEM .....	45
<b>Sekulić, M., Rodić, D., Gostimirović, M., Savković, B., Aleksić, A., Kulundžić, N.:</b> MODELING OF TORQUE AND THRUST FORCE IN DRILLING USING GENETIC ALGORITHM.....	49
<b>Nedić, B., Baralić, J.:</b> EXPERIMENTAL INVESTIGATION OF THE INFLUENCE OF MACHINING PARAMETERS ON CUT QUALITY IN MDF LASER CUTTING .....	53
<b>Aleksić, A., Sekulić, M., Gostimirović, M., Rodić, D., Savković, B., Antić, A.:</b> EFFECT OF CUTTING PARAMETERS ON CUTTING FORCES IN TURNING OF CPM 10V STEEL .....	59

## Section B: MACHINE TOOLS AND AUTOMATIC FLEXIBLE TECHNOLOGICAL SYSTEMS, CAx AND CIM PROCEDURES AND SYSTEMS

<b>Slavković, N., Vorkapić, N., Živanović, S., Dimić, Z., Kokotović, B.:</b> VIRTUAL BISCARA ROBOT INTEGRATED WITH OPEN-ARCHITECTURE CONTROL SYSTEM.....	63
<b>Nikolić, V., Tabakovic, S.:</b> DEVELOPMENT OF POST-PROCESSOR FOR CNC MACHINE TOOLS WITH HYBRID DEFINITION OF GEOMETRIC PARAMETERS OF TOOL PATH .....	67
<b>Tabaković, S., Živanović, S., Dimić, Z., Zeljković, M.:</b> PROGRAMMING AND PROGRAM VERIFICATION OF 3-AXIS HYBRID KINEMATICS CNC MACHINE FOR RAPID PROTOTYPING.....	71
<b>Ižol, P., Varga, J., Vrabelj, M., Demko, M., Greš, M.:</b> EVALUATION OF 3-AXIS AND 5-AXIS MILLING STRATEGIES WHEN MACHINING FREEFORM SURFACE FEATURES .....	75
<b>Grešová, Z., Ižol, P., Maňková, I. Vrabelj, M.:</b> THE EFFECT OF CUTTER PATH STRATEGIES ON SURFACE ROUGHNESS WHEN MACHINING TITANIUM ALLOY.....	79
<b>Bojanić Šejat, M., Rackov, M., Knežević, I., Živković, A.:</b> MODAL ANALYSIS OF BALL BEARINGS USING FINITE ELEMENT METHOD .....	83
<b>Šantoši, Ž., Šokac, M., Budak, I., Vukelić, Đ.:</b> INVESTIGATION OF DIFFERENT CIRCULAR IMAGE ACQUISITION METHODS IN CLOSE- RANGE PHOTOGRAMMETRY - VIRTUAL APPROACH .....	87
<b>Đekić, P., Milutinović, B., Ristić, M., Pavlović, M., Kostić, N., Nikolić, M., Jovković, S.:</b> REENGINEERING OF BRAKE TRIANGLE BY USING CAD/CAM APPLICATIONS .....	91

## Section C: METROLOGY, QUALITY, FIXTURES, CUTTING TOOLS AND TRIBOLOGY

<b>Ranisavljev, M., Štrbac, B., Janković, P., Lanc, Z., Matin, I., Hadžistević, M.:</b> THE IMPORTANCE OF MEASURING SYSTEM ANALYSIS IN PROCESS CAPABILITY ASSESSMENT .....	95
--	----

<b>Janković P., Madić M., Štrbac B., Hadžistević M., Mladenović P.:</b> APPLICATION OF GAGE R&R FOR EVALUATION MEASUREMENT SYSTEM PRECISION: CASE STUDY .....	99
<b>Terek, V., Miletić, A., Kovačević, L., Škorić, B., Kukuruzović, D., Drnovšek, A., Panjan, P., Terek, P.:</b> COMPARISON OF TWO METHODS USED FOR EVALUATION OF HIGH TEMPERATURE TRIBOLOGICAL PERFORMANCE OF PROTECTIVE COATINGS.....	103
<b>Anania F. D., Bisu C. F., But A., Canarache M. R.:</b> STUDY CONCERNING THE STIFFNESS EVALUATION FOR A MODULAR CLAMPING DEVICES.....	107
<b>Section D: PROCESS PLANNING, OPTIMIZATION, LOGISTICS AND INTERNET TECHNOLOGIES IN PRODUCTION ENGINEERING</b>	
<b>Majstorović, V., Stojadinović, S.:</b> RELATIONS BETWEEN ERP AND INDUSTRY 4.0 MODEL .....	111
<b>Tomov, M., Velkoska, C.:</b> ANALYSIS AND TRENDS OF THE CHANGES IN THE GRAPHIC INTERPRETATION OF THE QUALITY COSTS MODELS.....	115
<b>Nedeljković, D., Jakovljević, Ž.:</b> IMPLEMENTATION OF CNN BASED ALGORITHM FOR CYBER-ATTACKS DETECTION ON A REAL-WORLD CONTROL SYSTEM.....	119
<b>Banciu F.V., Pamintas E., Feier A. I.:</b> THE APPLICATION OF NEW INDUSTRIAL MAINTENANCE CONCEPTS - AN EASY WAY TO SAVING MONEY.....	123
<b>Turudija, R., Arandžević, J., Stojković, M., Korunović, N.:</b> ASSAY ON CLOUD BASED PRODUCT LIFECYCLE MANAGEMENT – OPEN PRODUCT AND TECHNOLOGY DEVELOPMENT WITHIN EDUCATION.....	127
<b>Trstenjak, M., Opetuk, T., Cajner, H., Đukić, G.:</b> PROCESS PLANNING AND INDUSTRY 4.0 – THE IMPORTANCE OF STRATEGICALLY DEFINED TRANSITION TOWARDS DIGITAL WORK ENVIRONMENT.....	131
<b>Randžević S., Milutinović M., Movrin D., Blagojević V., Kostić N.:</b> NEW GENERATION OF PRODUCTION SYSTEM ACCORDING TO THE CONCEPT OF I4.0 ...	135
<b>Milosavljević, M., Morača, S., Fajsi, A.:</b> INDUSTRY 4.0: A REVIEW OF TECHNOLOGY INFLUENCE ON BUSINESS MODELS.....	139
<b>But, A., Canarache, R., Gal, L.:</b> IMPROVE PRODUCTIVITY THROUGH DIGITAL MANUFACTURING .....	143
<b>Tešić, Z., Kuzmanović, B., Tasić, N., Škorić, B.:</b> KEY DIMENSIONS FOR SUCCESSFUL APPLICATION OF BUSINESS PROCESS MANAGEMENT MODEL .....	147
<b>Milošević, M., Lukić, D., Ostojić, G., Lazarević, M., Antić, A.:</b> APPLICATION OF CLOUD-BASED MACHINE LEARNING IN CUTTING TOOL CONDITION MONITORING.....	151

## Section E: MATERIALS, METAL FORMING, CASTING AND WELDING

<b>Bobić, Z., Petrović, B., Kojić, S., Terek, V., Škorić, B., Kovačević, L., Stojanović, G., Terek, P.:</b> A PRELIMINARY STUDY OF VARIOUS MOUTHWASH INFLUENCE ON NiTi ALLOY CORROSION .....	155
<b>Kukuruzović, D., Kovačević, L., Terek, P., Terek, V., Škorić, B., Miletić, A., Panjan, P., Čekada, M.:</b> THE INFLUENCE OF CRALN COATING DEFECTS AND CHEMICAL COMPOSITION ON DELAMINATION CAUSED BY AL CAST ALLOY SOLDENING .....	159
<b>Milutinović, M., Konjović, Z., Randelović, S., Movrin, D., Vilotić, M., Stefanović, Lj., Krašnik, M.:</b> RECENT ACHIEVEMENTS IN THE PRODUCTION OF BI AND MULTI-METAL COMPONENTS BY METAL FORMING TECHNOLOGIES .....	163
<b>Janjatović, P., Rajnović, D., Erić Čekić, O., Baloš, S., Dramićanin, M., Šidanin, L.:</b> THE PROPERTIES AND APPLICATION OF DUAL PHASE AUSTEMPERED DUCTILE IRONS.....	167
<b>Čabrilo, A.:</b> INFLUENCE OF HEAT INPUT ON THE BALLISTIC PERFORMANCE OF ARMOR STEEL WELDMENTS .....	171
<b>Dramićanin, M., Janjatović, P., Adamović, S., Kulundžić, N., Zabunov, I., Rajnović, D., Baloš, S.:</b> INFLUENCE OF MICRO AND NANO PARTICLES ON THE PERFORMANCE OF ACTIVATED TUNGSTEN INERT GAS WELDING.....	177
<b>Lanc, Z., Zeljković, M., Hadžistević, M., Štrbac, B., Labus Zlatanović, D., Baloš, S.:</b> EMISSIVITY OF METAL SURFACE COATINGS .....	181

## Section F: MECHANICAL ENGINEERING AND ENVIRONMENTAL PROTECTION

<b>Plavac, F., Pavković, D., Trstenjak, M., Cipek, M., Benić, J., Lisjak, D.:</b> SPEED CONTROL OF A SERIES DC DRIVE FOR DRILLING APPLICATIONS WITH VIBRATION DAMPING TORQUE FEEDBACK LOOP .....	185
<b>Miljković, Z., Jevtić, Đ., Svorcan, J.:</b> REINFORCEMENT LEARNING APPROACH FOR AUTONOMOUS UAV NAVIGATION IN 3D SPACE .....	189
<b>Ilić Mićunović, M., Novaković, T., Agarski, B., Čepić, Z., Vukelić, Đ., Budak, I.:</b> ECO-LABELS AS A TOOL FOR CIRCULAR ECONOMY AND CIRCULAR PACKAGING .....	193
<b>Kosec, B., Cigić, L., Ilić Mićunović, M., Klobčar, D., Nagode, A.:</b> DUST PARTICLES EMISSIONS AT STEEL CUTTING PROCESSES .....	197
<b>Mijanović, K., Kopač, J.:</b> SUSTAINABLE PRODUCTION TO LONG-TERM ECONOMIC DEVELOPMENT .....	201
<b>Stanivuk, T., Dujmović, M., Dumanić, N., Barač, M.:</b> AUTOMATION OF CONTROL OF ELECTRO-PNEUMATIC (PNEUMATIC) SYSTEM WITH AND WITHOUT PROGRAMMABLE LOGICAL CONTROLLER PLC .....	205
<b>Dudić, B., Kovač, P., Savković, B.:</b> INDUSTRIAL ROBOTS APPLICATION .....	211

## Section G: ADDITIVE MANUFACTURING TECHNOLOGIES

<b>Vasileska, E., Demir A. G., Colosimo B. M., Gečevska, V., Previtali, B.:</b> ENERGY INPUT ADAPTATION ACCORDING TO PART GEOMETRY IN SELECTIVE LASER MELTING THROUGH EMPIRICAL MODELLING OF THERMAL EMISSION.....	217
<b>Ignjatović Stupar, D., Chabrol, G.R., Baraze, A.R.I., Lecler S., Tessier, A., Cutard, T., Brendle, J.:</b> FEASIBILITY OF ADDITIVE MANUFACTURING PROCESSES FOR LUNAR SOIL SIMULANTS.....	223
<b>Dekić, P., Milutinović, B., Tomić, M., Nikolić, S.:</b> INFLUENCE OF PRINTING PARAMETARS AT MECHANICAL PROPERTIES OF FDM PRINTINGS PARTS MADE FROM ABS .....	229
<b>Movrin, D., Pintać, D., Knežević, P., Milutinović, M., Kojić, S., Premčevski, V.:</b> COMPARISON OF MECHANICAL PROPERTIES OF REGULAR AND ANTIBACTERIAL 3D PRINTED PLA SPECIMENS.....	233
<b>Ćirić Kostić, S., Bogojević, N., Croccolo, D., Olmi, G., Sindelić, V., Šoškić, Z.:</b> EFFECTS OF MACHINING ON THE FATIGUE STRENGTH OF STEEL COMPONENTS PRODUCED BY DMLS .....	237
<b>Sabotin, I., Jerman, M., Lebar, A., Valentinčič, J., Böttger, T., Kühnel, L., Zeidler, H.:</b> EFFECTS OF PLASMA ELECTROLYTIC POLISHING ON SLM PRINTED MICROFLUIDIC PLATFORM .....	241
<b>AUTHOR INDEX .....</b>	<b>245</b>
<b>INFORMATION ABOUT SPONSORS AND DONATORS .....</b>	<b>251</b>

Budak, E.

## INCREASED PERFORMANCE AND FLEXIBILITY IN MACHINING THROUGH PROCESS MODELING

***Abstract:** Machining is a commonly used manufacturing process in many industries such as automotive, aerospace, energy, die and mold, medical etc. due to its flexibility and ability to produce high quality parts. Although there have been significant advances in machine tool, control and CNC, CAD/CAM and cutting tool technologies over the last couple of decades, the productivity in these processes is still limited due to the process related problems such as excessive cutting temperatures and forces, process instability and chatter vibrations, part/tool/machine deflections etc. Current CAM systems or CNCs do not provide solutions to these problems. Process models (or digital twins), on the other hand, can be used to predict, avoid or reduce these problems through determination of the appropriate process conditions. In this talk, a brief overview of machining process modeling fundamentals such as chip formation mechanics, shearing, friction etc. will be given, and their use in calculation of process forces will be presented with examples. As one of the main and common problems in machining, cutting dynamics and stability will be explained through process-structure interactions where effects of structural dynamics and process conditions will be presented. Commonly used chatter suppression methods will be demonstrated with examples. Implementation of the models for production process simulations will be discussed, and process optimization will be demonstrated through industrial application examples. Modeling and simulation of special machining operations such as simultaneous turning/milling and turn-milling will also so be presented. The presentation will be concluded with future aspects machining process modeling and simulation.*

**Author:** Prof. dr Erhan Budak, Sabancı University, Orta Mahalle, Üniversite Caddesi No: 27 Tuzla, 34956 İstanbul, Turkey

E-mail: [ebudak@sabanciuniv.edu](mailto:ebudak@sabanciuniv.edu)



**Carpanzano, E.**

**HARMONIZING DIGITAL TRANSFORMATION AND HUMAN ASPECTS IN NEXT  
GENERATION PRODUCTION SYSTEMS**

***Abstract:** The impact of digitization on production systems is changing the relationship between humans, the technological system and the organization as a whole. Due to growing complexity of industrial processes and their digital automation systems, it is of major relevance to consider industrial workers' safety as well as their psychophysiological health. An innovative framework to model and design cognitive-digital closed loop control solutions is discussed, so as to achieve production performance as well as workers safety and well-being in a balanced way. Industrial application cases, experienced benefits and future perspectives are addressed throughout the talk.*

**Author:** Prof. dr Emanuele Carpanzano, University of Applied Sciences and Arts of Southern Switzerland, Le Gerre, Via Pobietto 11 CH-6928 Manno, Switzerland, Phone: +41 (0)58 666 60 00  
E-mail: [emanuele.carpanzano@supsi.ch](mailto:emanuele.carpanzano@supsi.ch)





Galantucci, L. M., Pellegrini, A., Guerra, M. G., Lavecchia, F.

**3D PRINTING OF PARTS USING METAL EXTRUSION: AN OVERVIEW OF SHAPING DEBINDING AND SINTERING TECHNOLOGY**

**Abstract:** Additive Manufacturing (AM) is the fabrication of real three-dimensional objects from plastics and metals by adding material, layer by layer. One of the most common AM processes is the Material Extrusion (ME) based on different approaches: plunger, filament and screw. Material Extrusion technologies of metal-polymer composites is expanding and it mainly uses the filament or plunger-based approaches. The feedstock used is a mixture of metal powder (from 55 vol% to about 80 vol%) dispersed in a thermoplastic matrix, as the Metal Injection Molding (MIM) materials. The process consists of three steps: shaping, debinding and sintering. The first step provides the extrusion of filament to realize a primary piece called “green part”; subsequent steps, debinding and sintering, allow to obtain a full metal part by dissolving the polymeric binder. The latter can be carried out using solvents, heat and the combination of them. The interest toward this technology is driven by the possibility to replace other Metal AM technologies, such as Selective Laser Melting or Direct Energy Deposition, in sectors like rapid-tooling or mass production, with several benefits: simplicity, safety to use and saving material and energy. The aim of this keynote is to provide a general overview of the main metal ME technologies considering the more technical aspects such as process methodologies, 3D printing strategy, process parameters, materials and possible applications for the manufacturing of samples on a 3D consumer printer.

**Key words:** Fused Filament Fabrication, Metal Extrusion, SDS process

**1. INTRODUCTION**

Several Additive Manufacturing processes are currently existing; they only differ in the way layers are deposited to create an object, in the operation modes and in the way the material is fed into the system. Some methods melt or soften materials (thermoplastics, composites, photopolymers and metals) to produce the layers, e.g., Material Extrusion (ME) or Fused Filament Fabrication (FFF), Selective Laser Sintering (SLS), Selective Laser Melting (SLM) and Electron Beam Melting (EBM), Direct Metal Laser Sintering (DMLS), while others cure liquid materials, e.g., Stereolithography (SLA) [1]. However, it is necessary for SLS, SLM and DMLS techniques to adopt high-energy beams including laser or electron beam as heating sources to fuse the metal powders during the whole manufacturing processing to obtain metal parts, which is very energy-consuming. In addition, these techniques usually require large investments for metal powders, machinery, and maintenance, limiting their applications mainly to the high value-added industries which are cost-insensitive. Therefore, it is of practical significance to explore other economical metal 3D printing techniques with less energy consumption.

Material Extrusion, conversely, is a cheaper 3D printing technique mainly developed for the additive manufacturing of polymer materials. During the manufacturing process, a polymeric filament is first melted in the printing nozzle at a temperature slightly higher than the melting point of the printing polymer, then deposited onto the printer hot bed layer by layer under the control of a computer, and finally fused with the bottom adjacent layers [2]. Whenever necessary, support structures are included in the process to enable the fabrication of complex geometrical features. This

basic principle enables the production of complex parts without a shaping tool other than a die with a simple geometry. Depending on the type of extruder used, one can classify material extrusion into different types: filament and plunger-based [3]. The first example of using FFF for the production of metal parts was presented in 1996 with a 17-4 PH stainless steel and tungsten carbide-cobalt [4,5] and this process was later on referred as FDMet (Fused Deposition of Metal) or Metal Fused Filament Fabrication (Metal FFF) [6]. This new AM method is based on the combination of FFF and Metal Injection Molding (MIM), a more conventional process which allows to obtain a close full density metal part with high complexity. The feedstock used is a mixture of metal powders with a different amount in percentage by volume (vol%) from 55 since to 88, as reported in open library, and a polymeric binder. This is constituted by three different component: a main binder (i.e., Polyoxymethylene (POM), Wax paraffin, Thermoplastic elastomer (TPE) or Polyethylene glycol (PEG)), a backbone binder like Polypropylene (PP), Low-Density Polyethylene (LDPE) or Grafted Polyolefin and in some cases also additives like stearic acid, the most common [3,7–9]. The printed part is defined as “Green Part”, the debinded part as “Brown Part”, and the sintered metal part as “White Part”, respectively, while the entire process chain is called “Shaping, Debinding and Sintering-SDS-Process”. In the first step, the green parts are printed from metal/polymer composite filament, during which polymer is melted as the binder but the metal particles remain solid subsequently, brown parts were obtained by subjecting the green parts to a debinding process to remove most of the polymer binder. The remaining polymer binder in the brown parts avoid the spreading of the metal particles and thus preserve the shape of the

parts. Finally, they are sintered to melt the metal particles together to form a dense material.

## 2. TYPES OF METAL EXTRUSION

### 2.1. Filament based process

The first way to extrude the filament and realize the green parts is the “filament-based” type (Fig. 1).

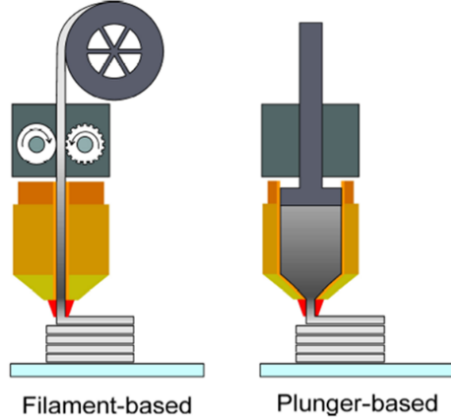


Fig. 1. Type of Material Extrusion [3]

The American company Markforged Inc. has realised a hybrid-process inspired by Metal FFF named Atomic Diffusion Additive Manufacturing™ (ADAM). The entire SDS process of Markforged system is controlled by a proprietary software called “Eiger”. The printing of green part takes place in the “Metal X” printer equipped with a heated nozzle of 0.4 mm, which softens and deposits material layer by layer with a height equal to 125 μm. As reported in Eiger slicer, this is the unique layer height available. Only for copper, the layer height is 129 μm. The feedstock used is a spool of different materials like: stainless steel 17-4 PH or H13, A2 and D2 tool steel, but also nickel superalloy (Inconel 625) and copper [10]. The used binder is completely thermally debound in the washing system with proprietary solvent (Opteon SF79, Opteon SF80, or Tergo Metal Cleaning Fluid). The last step useful for the realization of a dense metal part is the sintering, which varies in terms of temperatures and the time according of the selected material. Some examples of parts printed via ADAM are reported in Fig. 2.



Fig. 2. Examples of parts made via ADAM in 17-4 PH [11]

On the other hand, the German society BASF 3D Printing Solutions GmbH, offer two metal-composite filaments called Ultrafuse® 316L and Ultrafuse® 17-4 PH, opening the possibility to produce green parts with existing and, in some cases, very cost-effective, FFF printers, as shown in Fig. 3.

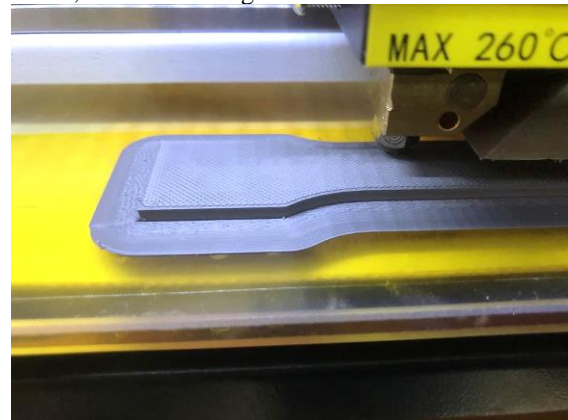


Fig. 3. Example of printing of sample in Ultrafuse 316L with a consumer 3D printer

Then, also in this case, the green parts are processed into pure metal parts using a debinding and sintering process [12].

The metal/polymer composites filament consists of a polymer matrix and an 88 vol% dispersed stainless steel particles with a different particle size. In Ultrafuse 316L filament, variable particle size of metal powder are dispersed in the matrix; they are indicated with white arrows in Fig. 4. Typical dimensions of metal powder grains are comprised in the range 1-10 μm, according to Tosto et al. [13], while Liu et al. [2] observed higher values, comprised between 30-50 μm. The polymer matrix (red arrows in Fig. 4), is composed of POM and Polyethylene (PE) with other additives such as polypropylene, dioctyl phthalate (DOP), dibutyl phthalate (DBP), and zinc oxide (ZnO) to increase the fluidity, plasticity, and thermo-stability of the composite [2].

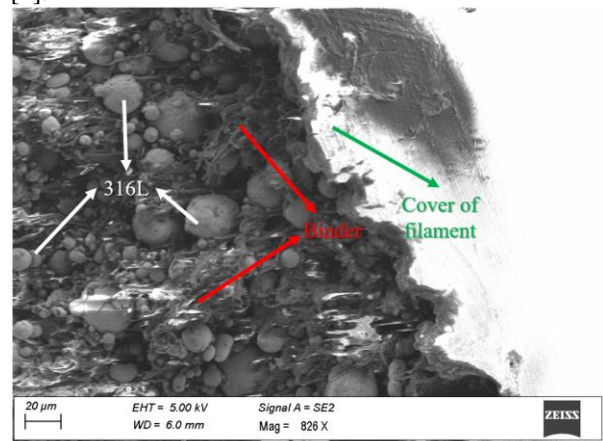


Fig. 4. SEM image of cross section of Ultrafuse 316L filament

In research laboratories, in other cases, it is possible to manufacture filaments with different percentage of metal and polymer [6,14–22]. In particular, it is possible to use stainless-steels, (316L and 17-4 PH the most common ones), titanium alloys (Ti-6Al-4V) [14,20],

hard-metals like carbide tungsten (WC) and tungsten carbide-cobalt (WC-Co) [18] and low-melting alloys (low-melting eutectic alloy of bismuth, non-eutectic alloy of bismuth, and a non-eutectic alloy of antimony) [21]. For the manufacturing of filament, it is necessary that it keeps a constant and uniform diameter during the entire process in order to maintain a constant delivery rate for a good printing result. The filament is usually manufactured using a single or twin-screw extruder. In addition, the material to be processed should have an even distribution of the binder, which should be easy to remove from the metal powder (by debinding or burning/evaporation). It is required a good fineness of metal powder to manufacture metal filaments. A uniform, as small as possible, size of the metal particles is important in order to obtain a uniform filament, to produce uniform prints and reproducible sintering results. It is a good practice to use grain sizes in the range between 2 and 44  $\mu\text{m}$ . According to Thompson et al. [6] the average size of metal powder for a 316L is 17.7  $\mu\text{m}$ .

The metal is preliminarily treated with an agent able to reduce the interaction forces between the particles and to lubricate the powder. Cyclohexane or stearic acid are the most used for this treatment. The metal powder is then gradually mixed with the polymer binder. The amount of metal powder is relevant for achieving a lower residual porosity after debinding and a better densification due to higher number of particle contacts.

Consequently, a high content of metal powder can generate voids and inhomogeneity in the extruded profiles due to higher feedstock viscosity and increasing particle friction [23]. The uniformity of distribution of the material components can be estimated through the viscosity of the mixed material and, therefore, through the torque value of the mixing device driving motor. Usually, due to the high metal content of these materials, it is recommended a nozzle in hard metal or ruby, with a diameter  $\geq 0.4$  mm [24].

## 2.2. Plunger based process

The second extrusion type is the “plunger-based” (Fig. 1). Another American company, Desktop Metal Inc. has patented a technology similar to FFF and MIM process called Bound Metal Deposition™ (BMD) enabling the printing of bound metal rods and the subsequent sintering to form a dense metal part. In the BMD process, the desired metal or alloy powder is compounded with an appropriate multi-component organic binder system to form the feedstock. The feedstock is shaped into a rod that has a well-defined and controlled diameter. Multiple rods of a fixed diameter and length are housed in a specially designed and padded dispensing cartridge. The cartridge feeds rod to an extruder which actuates and heats the rods to produce a quasi-molten composite. This composite is easily pushed by a plunger through a 0.4 mm nozzle, while the extruder moves on the build plate following a predetermined path to produce the green parts (Fig. 5).

This extrusion system enables precise printing and a minimum layer height of 50  $\mu\text{m}$ . In cases where the three-dimensional complexity of a part requires support structures to be printed, an interface layer is included in the design to allow for later separation [18,25].



Fig. 5. Example of green parts printed via BMD in 17-4 PH stainless steel

Desktop Metal’s materials available are similar to the ones provided by Markforged: 17-4 PH stainless steel, H13 tool steel and copper, but also 316L stainless steel and 4140 low alloy steel [26]. The binder used by Desktop Metal system is first debound by a solvent and then treated thermally. Later, there a sintering process is necessary to obtain a metal part. As Markforged, Desktop Metal provides a proprietary system composed by the 3D printer, debinder and furnace for sintering governed by a proprietary software called “Fabricate”.

## 3. SDS PROCESS

### 3.1 Shaping

The first phase of process is the shaping. In this phase the filament is extruded layer by layer until the entire green part is obtained. A right combination of printing parameters, such as infill density, flow rate, layer height and printing speed influence the success of print. In fact, when this does not happen, some troubles could be detected, such as a not perfect adhesion of the roads, which causes an incorrect filling of the green part, and subsequent voids in the metal part. In Fig. 6 three objects printed are shown; varying the flow rate, evident voids are created on the surface of these objects.

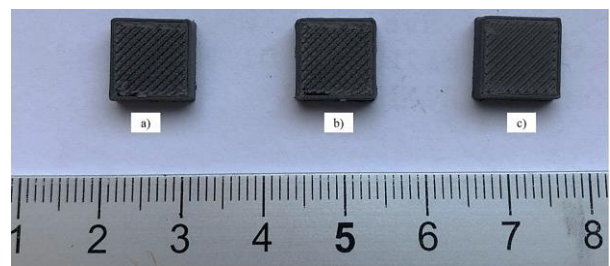


Fig. 6. Example of green parts with non-perfect adhesion between the rods.

Keeping constant the infill at 100% and the printing speed at 35 mm/s, instead increasing the flow rate from 110% (a) to 115% (b) and 125% (c), it has been possible to avoid the voids present in the first two parts. This behavior is confirmed from microscope images (Fig. 7) of these objects: in the a) and b) part holes in the vicinity of the wall layers also appear.

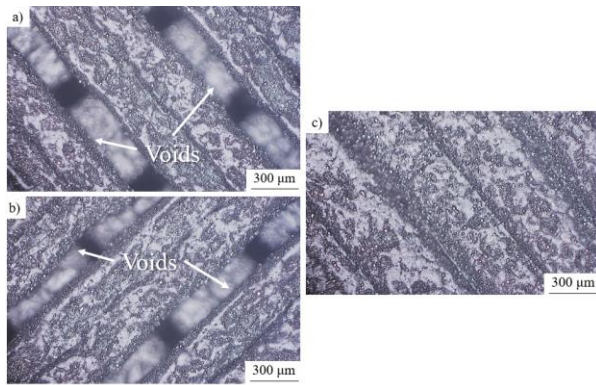


Fig. 7. Image at optical microscope of the green parts (140x)

### 3.2. Debinding

Once the green part is printed, the polymeric binder must be removed. This process is commonly referred to as “debinding” and it is very well known for parts produced by MIM. Polymers have to be removed completely from the green part since carbon residues can influence the sintering process and negatively affect the quality of the final product. Moreover, binder removal is one of the most critical steps in the SDS process, since defects can be produced by inadequate debinding. Some examples are blistering, surface cracking, and large internal voids. There are three main debinding techniques: thermal, solvent, and catalytic methods [3]. For a solvent debinding, the treatment time varies depending on the shape and size of the printed parts.

Gonzalez-Gutierrez et al. [27] suggest that printed parts should be kept in the solvent for at least 12 h. The same procedure is suggested by Thompson et al. [6] for parts having a wall thickness of 2 mm, while for a wall thickness of 6 mm the removing processing time of TPE should be 57 h. Removal of TPE of the printed green bodies generates interconnected pore channels. During solvent debinding, elimination of at least 99% of the contained TPE mass is necessary in order to enable successful realization of the following process steps. As rule, the mass loss of printed parts should be monitored during the debinding to determine the end of the treatment. Thermal debinding is performed by heating the parts in a vacuum furnace with a variation of pressures between  $10^{-3}$  to  $10^{-5}$  mbar, depending on variable levels of volatilized binder within the furnace during the burnout process. Debinding temperatures has to be evaluated in accordance with thermogravimetric analysis (TGA) of the backbone polymer. Heating rates have to be as high as possible, but slow enough to avoid blistering or crack formation within the samples [6]. Some studies proposed different temperatures depending on the geometry of the part and the material;

Thompson et al. [6] observed the complete degradation of backbone binder at 500 °C on a 316L stainless steel filament. Supriadi et al. [28] found the optimum debinding temperature for a 17-4 PH stainless at 510 °C, with a binder removal percentage of 6.2% and fewer oxides content. Choi et al. [29] studied the sintering of 316L stainless steel, and found that the weight loss of the molded part started at about 180 °C, and the weight became constant around 400 °C, with a

percentage of 5.70%. Thermal debinding can take place even after a solvent debinding, in the same furnace of sintering; in fact it is considered a preliminary sintering [30]. The last type of debinding is the catalytic debinding. This process is patented by BASF SE [31] for their metal-composite filament, but also for MIM feedstock, such as Catamold®. In fact, Catamold is totally unique in its ability for the catalytic gas phase decomposition of the binder and this ability is innate to the chemical structure of POM (Fig. 8).

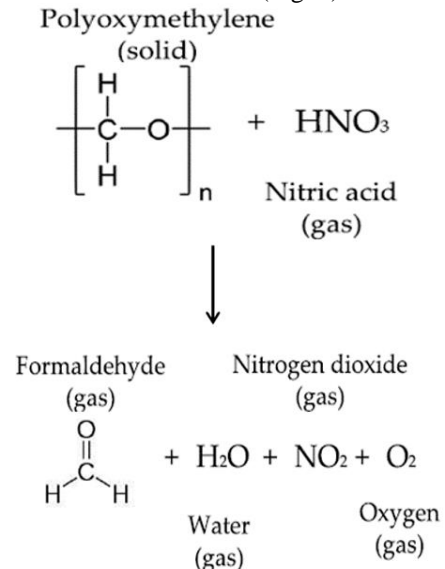


Fig. 8. Mechanism of decomposition of POM [8]

The oxygen atoms in the polymer chain are susceptible to acidic attack, causing the macro-molecule to split off successively  $\text{CH}_2\text{O}$  (formaldehyde) units when it is exposed to a suitable acidic catalyst and nitrogen dioxide ( $\text{NO}_2$ ). The catalyst used for the debinding process is gaseous nitric acid ( $\text{HNO}_3$ ), with a concentration higher than 98,5% [32]. First the exhaust is burned in a reducing atmosphere (no oxygen and rich in nitrogen) at a temperature of 600 °C, transforming nitric dioxide into nitrogen gas ( $\text{N}_2$ ). The second step consists is the burning in an oxidizing atmosphere at 800 °C to transform formaldehyde into water and carbon dioxide. It is important to mention that binders based on POM usually have a backbone polymer which is not susceptible to catalytic debinding. Such backbone polymer helps retain strength and shape stability in the “brown part”. However, sintering cannot begin until this backbone polymer is still present, and thus a thermal treatment between 200 and 600 °C is applied to the part prior to the start of the sintering process [8]. The guidelines of BASF for the catalytic debinding of green parts realized by FFF and MIM recommend a temperature between 110-120 °C, with a debinding rate of 1-2 mm/h and a holding time variable depending on the material weight in the furnace. The debinding process terminate when a minimal debinding loss of 10.5% is reached.

### 3.3. Sintering

The sintering is the last step necessary to obtain a full dense metal part realised via FFF or MIM. In general, this process is performed at temperatures below the

melting temperature of the major constituent in the metal, typically ranging from 1200 to 1600 °C. Also, the holding time is related to material and size of part. For small parts such as bushings, the average time varies from 1 to 1.5 h; for average-size ferrous parts, the sintering time can be 3 h. However, tungsten parts can have a sintering time of up to 8 h [8]. An important aspect to consider during sintering is the atmosphere inside the furnace. For low carbon iron/nickel steels and stainless steels, pure hydrogen is used. To obtain low-alloy steels containing carbon, this latter is introduced via the metal powder. During sintering under nitrogen, the carbon diffuses in the metal. It is not feasible to introduce or partially remove carbon via the sintering atmosphere, since this encounters considerable difficulties in practice. Stainless steels can also be sintered under reduced pressure. With appropriate process control, even the extremely low carbon content of stainless steels can be attained. BASF AG reports different examples of sintering atmosphere used for MIM process. For example, hydrogen is recommended for a 316L for a 430 stainless steels, but it is also possible use vacuum atmosphere. On the other hand, for a 17-4 PH stainless only hydrogen in atmosphere is recommended.

Sintering is essentially to remove pores; this is accompanied by growth and strong adhesion among the adjacent particles (Fig. 9), causing the shrinkage of the product whose dimensions usually reduce between 14 and 20%.

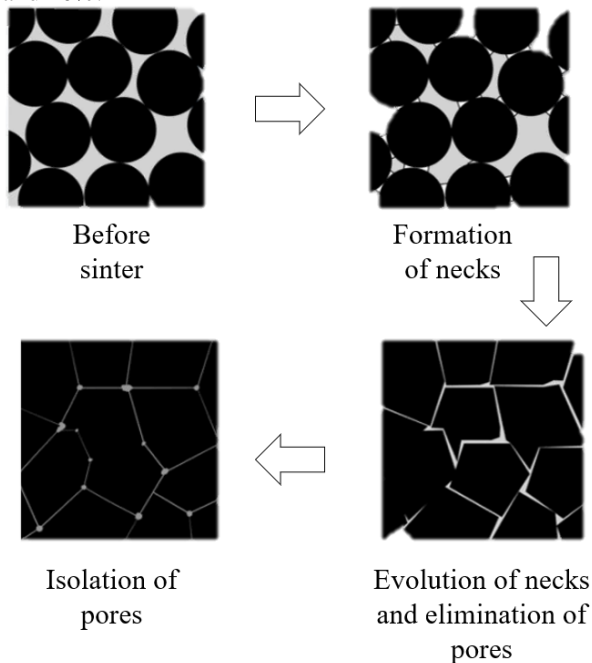


Fig. 9. Creation of pores after sintering process

The different choice of sintering parameters (holding time, temperature and atmosphere) caused different responses in mechanical aspects, as reported in Fig. 10. The graph reported shows the values recorded of mechanical properties like the Ultimate Tensile Strength (UTS), Yield Strength (YS) and the Elongation at break ( $\epsilon_b\%$ ) for a same material (17-4 PH stainless steel) provided by different companies.

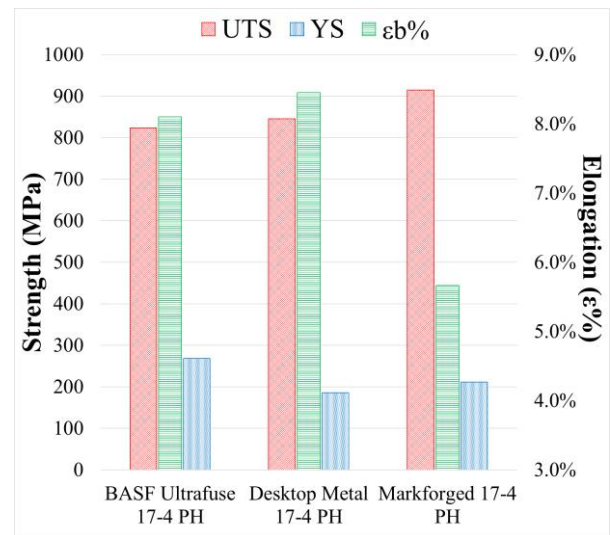


Fig. 10. Comparison of main mechanical properties for three different 17-4 PH stainless steel

### 3.3.1. Shrinkage Phenomenon

The green parts before printing, are oversized to compensate for the sintering shrinkage. [8] It is important to remark that the shrinkage does not occur in the same amount in all dimensions, as observed by Thompson et al. [6] and Kurose et al. [22] in samples printed with filament filled with respectively 55 vol% and 60 vol% of 316L stainless steel. Gong et al. [33,34] and Quarto et al. [35] have reported a similar shrinkage on X-Y axes, while a different one on Z axis, on a BASF Ultrafuse 316L, as found in parts printed by BMD in 17-4 PH and W-Cr [18,36]. On the contrary, Liu et al. [2] observed an equal shrinkage of 17% on all axes in 316L parts. With regard to the above, BASF 3D Printing Solutions GmbH in its guidelines, gave a nominal shrinkage for parts made in Ultrafuse® 316L and 17-4 PH: 16% on X-Y directions and 20% on Z direction [31].

The anisotropic shrinkage it was also found in parts manufactured by MIM [37]. Causes of this different shrinkage for a MIM process are to be pointed at polymer orientation which can be influenced by injection molding parameters. Besides polymer orientation, in filament highly filled, shrinkage and density can be influenced by the presence of gaps among deposited strands. The more gaps, the larger the shrinkage and the lower the density of the sintered parts, since larger gaps cannot be closed during sintering. The shrinkage can also be affected by the orientation of the filler particles [3].

Once sintering process is finished, the samples are subjected to cooling in the same furnace. Cooling is done in a protective atmosphere, in order to prevent oxidation of sintered parts.

### 3.4. Mechanical properties

The mechanical aspect is one of the most important, when a metal part is realized in AM. Parts printed in Metal FFF typically report worst mechanical properties if compared to the other Metal AM technology. The main cause is the not complete fullness of the parts, caused by some problems during the SDS process and the limitation of the ME technology. In Table 1 is

Material	Technology	Tensile strength (MPa)	Yield strength (MPa)	Tensile modulus (GPa)	Elongation at break (%)	References
17-4 PH	BMD	776	604	176	6.7	[36]
	BMD	1042	660	195	8.5	[37]
	ADAM	1050	800	140	5	[38]
	FFF	880	680	-	5.8	[39]
	FFF	497.40±9.90	443±6.90	108±6.90	0.79±0.05	[12]
	SLM	944	570	-	50	[40]
316L	FFF	465	167	152	31	[32]
	SLM	648	541	320	30	[32]
	FFF	436	167	152	-	[33]
	FFF	443.90±5.87	148.01±4.50	157.24±4.50	43.33±2.53	[12]

Table 1. Summary table of mechanical properties

reported a summary of some previous activities using stainless steel with compare to the data sheet and SLM technology.

### 3.5. Possible applications

The production of components in Metal ME is currently concentrated on few sectors: the most popular application for these technologies are Rapid tooling and prototyping. Thanks to the post-treatment capacity of sintered parts through machine tools, it could be possible to extent in the future the applications to other sectors, such as consumer goods or repair. Actually, limitations still exist for this technology related to the mechanical properties of these parts. Expansion of this technology also in others sectors required an increment of the precision and speed of printing, and an additional reduction of manufacturing cost.

## 4. CONCLUSIONS

Metal Extrusion is a new area of the most common AM process, Fused Filament Fabrication. For a full dense metal part, accurate dosing of metal powder and polymeric binder is necessary to avoid problems like porosity, low density or voids. In order to obtain a full metal part, the SDS process must be performed. Shaping requires an adequate choice of printing parameters.

Debinding can be execute with different methods to eliminate part of polymeric matrix, then during sintering the rest of polymer is burned and the grains of metal powder binded together. From a dimensional point of view, it is fundamental to take into account the phenomenon of shrinkage occurring during D&S, so the design of the part needs an oversizing factor for each of the three axes. Mechanical characteristics are lower if compared to parts made by SLM, however could satisfy the required strength requirements. Possibility to print metal on a traditional FFF printer or purchase an entire ME system, has allowed to expanding the material

portfolio of this technology and it has changed manufacturing scenarios in different sectors. Metal Extrusion could be an economical alternative to Powder Bed technologies for the type of material used, the safety in handling it. In fact, there are not specific recommendations when printing metal filaments, lower energy cost are needed compared to laser-beam or electron-beam technologies, and the ease of use of the machine can expand the application scenario of ME.

## 5. REFERENCES

- [1] Ojogba, Spencer, O.,: *Additive Manufacturing Technology Development*, A Trajectory Towards Industrial Revolution, Am. J. Mech. Ind. Eng. 3 (2018) 80. doi:10.11648/j.ajmie.20180305.12.
- [2] Liu B., Wang Y., Lin Z., Zhang T.: *Creating metal parts by Fused Deposition Modeling and Sintering*, Mater. Lett. 263 (2020) 127252. doi:10.1016/j.matlet.2019.127252.
- [3] Gonzalez-Gutierrez J., Cano S., Schuschnigg S., Kukla C., Sapkota J., Holzer C.: *Additive manufacturing of metallic and ceramic components by the material extrusion of highly-filled polymers*, A review and future perspectives, Materials (Basel). 11 (2018). doi:10.3390/ma11050840.
- [4] Agarwala M.K., Van Weeren R., Bandyopadhyay A., Safari A., Danforth S.C., Priedeman W.R.: *Filament Feed Materials for Fused Deposition Processing of Ceramics and Metals*, Proc. Of the Solid Free. Fabr. Symp. (1996) 451–458. <http://hdl.handle.net/2152/70277>.
- [5] Wu G., Langrana N.A., Rangarajan S., Mccuiston R., Sadanji R., Danforth S., Safari A.: *Fabrication of Metal Components using FDM*, Fused Deposition of Metals, Proc. Solid Free. Fabr. Symp. (1999) 775–782.
- [6] Thompson Y., Gonzalez-Gutierrez J., Kukla C., Felfer P.: *Fused filament fabrication, debinding and*

- sintering as a low cost additive manufacturing method of 316L stainless steel: *Addit. Manuf.* 30 (2019) 100861. doi:10.1016/j.addma.2019.100861.
- [7] Luquan Ren J.X. and X.L., Zhou X., Song Z., Zhao C., Liu Q.: *Process Parameter Optimization of Extrusion-Based*, (2017). doi:10.3390/ma10030305
- [8] González-Gutiérrez J., Stringari G.B., Emri I.: *Powder Injection Molding of Metal and Ceramic Parts*, Some Critical Issues for Injection Molding, *Some Crit. Issues Inject. Molding.* (2012) 65–88. <http://www.intechopen.com/books/some-critical-issues-for-injection-molding/powder-injection-molding-of-metal-and-ceramic-parts->.
- [9] Nurhuda A.I., Supriadi S., Whulanza Y., Saragih A.S.: *Additive manufacturing of metallic based on extrusion process*, A review, *J. Manuf. Process.* 66 (2021) 228–237. doi:10.1016/j.jmapro.2021.04.018.
- [10] Markforged Inc., *3D Printing Materials-Markforged*: (2021). <https://markforged.com/materials>.
- [11] Enrique P.D., DiGiovanni C., Mao N., Liang R., Peterkin S., Zhou N.Y.: *Resistance is not futile: The use of projections for resistance joining of metal additively and conventionally manufactured parts*, *J. Manuf. Process.* 66 (2021) 424–434. doi:10.1016/j.jmapro.2021.04.035.
- [12] Schumacher C., Moritzer E.: *Stainless Steel Parts Produced by Fused Deposition Modeling and a Sintering Process Compared to Components Manufactured in Selective Laser Melting*, 2000275 (2021) 4–7. doi:10.1002/masy.202000275.
- [13] Tosto C., Tirillò J., Sarasini F., Cicala G.: *Hybrid Metal/Polymer Filaments for Fused Filament Fabrication (FFF) to Print Metal Parts*, *Appl. Sci.* 11 (2021) 1444. doi:10.3390/app11041444.
- [14] Zhang Y., Bai S., Riede M., Garratt E., Roch A.: *A comprehensive study on fused filament fabrication of Ti-6Al-4V structures*, *Addit. Manuf.* 34 (2020) 101256. doi:10.1016/j.addma.2020.101256.
- [15] Wu G., Langrana N.A., Sadanji R., Danforth S.: *Solid freeform fabrication of metal components using fused deposition of metals*, *Mater. Des.* 23 (2002) 97–105. doi:10.1016/s0261-3069(01)00079-6.
- [16] Wang Y., Zhang L., Li X., Yan Z.: *On hot isostatic pressing sintering of fused filament fabricated 316L stainless steel – Evaluation of microstructure, porosity, and tensile properties*, *Mater. Lett.* 296 (2021) 129854. doi:10.1016/j.matlet.2021.129854.
- [17] Gonzalez-Gutierrez J., Kukla C., Schuschnigg S., Duretek I., Holzer C.: *Fused Filament Fabrication for Metallic Parts*, (2016).
- [18] Bose A., Schuh C.A., Tobia J.C., Tuncer N., Mykulowycz N.M., Preston A., Barbati A.C., Kernan B., Gibson M.A., Krause D., Brzezinski T., Schroers J., Fulop R., Myerberg J.S., Sowerbutts M., Chiang Y.M., John Hart A., Sachs E.M., Lomeli E.E., Lund A.C.: *Traditional and additive manufacturing of a new Tungsten heavy alloy alternative*, *Int. J. Refract. Met. Hard Mater.* 73 (2018) 22–28. doi:10.1016/j.ijrmhm.2018.01.019.
- [19] Lengauer W., Duretek I., Fürst M., Schwarz V., Gonzalez-Gutierrez J., Schuschnigg S., Kukla C., Kitzmantel M., Neubauer E., Lieberwirth C., Morrison V.: *Fabrication and properties of extrusion-based 3D-printed hardmetal and cermet components*, *Int. J. Refract. Met. Hard Mater.* 82 (2019) 141–149. doi:10.1016/j.ijrmhm.2019.04.011.
- [20] Singh P., Balla V.K., Tofangchi A., Atre S. V., Kate K.H.: *Printability studies of Ti-6Al-4V by metal fused filament fabrication (MF3)*, *Int. J. Refract. Met. Hard Mater.* 91 (2020) 105249. doi:10.1016/j.ijrmhm.2020.105249.
- [21] Warrior N., Kate K.H.: *Fused filament fabrication 3D printing with low-melt alloys*, *Prog. Addit. Manuf.* 3 (2018) 51–63. doi:10.1007/s40964-018-0050-6.
- [22] Kurose T., Abe Y., Santos M.V.A., Kanaya Y., Ishigami A., Tanaka S., Ito H.: *Influence of the layer directions on the properties of 316l stainless steel parts fabricated through fused deposition of metals*, *Materials (Basel)*. 13 (2020). doi:10.3390/ma13112493.
- [23] Gonzalez-Gutierrez J., Thompson Y., Handl D., Cano S., Schuschnigg S., Felfer P., Kukla C., Holzer C., Burkhardt C.: *Powder content in powder extrusion moulding of tool steel: Dimensional stability, shrinkage and hardness*, *Mater. Lett.* 283 (2021) 128909. doi:10.1016/j.matlet.2020.128909.
- [24] Poszvek G., Wiedermann C., Markl E., Bauer J.M., Seemann R., Durakbasa N.M., Lackner M.: *Fused Filament Fabrication of Ceramic Components for Home Use*, *Lect. Notes Mech. Eng.* (2021) 121–139. doi:10.1007/978-3-030-62784-3\_11.
- [25] Desktop Metal, *BMD Design Guide*, (2019) 1–15. <https://www.desktopmetal.com/> (accessed July 30, 2021).
- [26] Desktop Metal Inc., *Desktop Metal materials - engineered to perform* | Desktop Metal, (2020). <https://www.desktopmetal.com/materials>.
- [27] Gonzalez-Gutierrez J., Godec D., Kukla C., Schlauf T., Burkhardt C., Holzer C.: *Shaping, Debinding and Sintering of Steel Components Via Fused Filament Fabrication*, 16th Int. Sci. Conf. Prod. Eng. - CIM2017. (2017) 99–104.
- [28] Supriadi S., Suharno B., Hidayatullah R., Maulana G., Baek E.: *Thermal Debinding Process of SS 17-4 PH in Metal Injection Molding Process with Variation of Heating Rates, Temperatures, and Holding Times*, 266 (2017) 238–244. doi:10.4028/www.scientific.net/SSP.266.238.
- [29] Choi J., Lee G., Song J., Lee W., Lee J.: *Sintering behavior of 316L stainless steel micro – nanopowder compact fabricated by powder injection molding*, *Powder Technol.* 279 (2015) 196–202. doi:10.1016/j.powtec.2015.04.014.
- [30] Afian M., Subuki I.: *Sintering Characteristics of Injection Moulded 316L Component Using Palm-Based Biopolymer Binder*, *Sinter. - Methods Prod.* (2012). doi:10.5772/32737.
- [31] BASF 3D Printing Solutions, *Ultrafuse 316L: User guidelines for 3D printing metal parts*, BASF 3D Print. Solut. process in (2019) 1. <https://www.basf.com/global/en/who-we->

are/organization/locations/europe/german-companies/basf-3d-printing-solutions-gmbh/metal-solutions/Ultrafuse\_316L.html.

- [32] BASF Aktiengesellschaft, *Catamold Feedstock for Metal Injection Molding* : Processing - Properties - Applications, (2003).
- [33] Gong H., Snelling D., Kardel K., Carrano A.: *Comparison of Stainless Steel 316L Parts Made by FDM- and SLM-Based Additive Manufacturing Processes*, Miner. Met. Mater. Soc. 71 (2019) 880–885. doi:10.1007/s11837-018-3207-3.
- [34] Gong H., Crater C., Ordonez A., Ward C., Waller M., Ginn C.: *Material Properties and Shrinkage of 3D Printing Parts using Ultrafuse Stainless Steel 316LX Filament*, MATEC Web Conf. 249 (2018) 1–5. doi:10.1051/mateconf/201824901001.
- [35] Quarto M., Carminati M., D’Urso G.: *Density and shrinkage evaluation of AISI 316L parts printed via FDM process*, Mater. Manuf. Process. 00 (2021) 1–9. doi:10.1080/10426914.2021.1905830.
- [36] Watson A., Belding J., Ellis B. D.: *Characterization of 17-4 PH Processed via Bound Metal Deposition (BMD)*, Miner. Met. Mater. Ser. (2020) 205–216. doi:10.1007/978-3-030-36296-6\_19.
- [37] Huang M.S., Hsu H.C.: *Influence of injection moulding and sintering parameters on properties of 316L MIM compact*, Powder Metall. 54 (2011) 299–307. doi:10.1179/003258909X12502679013819.

**Authors: Full Prof. Luigi Maria Galantucci, M.Sc. Alessandro Pellegrini, PhD. Maria Grazia Guerra, Prof. Fulvio Lavecchia**, Politecnico di Bari, Dipartimento di Meccanica Matematica e Management Via Edoardo Orabona, 4 - 70125 Bari – Italy  
E-mail: [luigimaria.galantucci@poliba.it](mailto:luigimaria.galantucci@poliba.it)

#### **FUNDING**

This research received funding from the project PON “R&I” 2014– 2020 ARS01\_00806 “Soluzioni Innovative per la qualità e la sostenibilità dei processi di ADDitive manufacturing”.

This work was supported by the Italian Ministry of Education, University and Research under the Programme “Department of Excellence” Legge 232/2016 (Grant No. CUP - D94I18000260001).

#### **ACKNOWLEDGMENTS:**

Authors want to thank CMF Marelli s.r.l., Crea 3D s.r.l and Energy Group s.r.l. for their contribution to the production of samples.



Gąska, A., Harmatys, W., Gąska, P., Sladek, J.

**RECENT ADVANCES IN SIMULATION METHODS FOR DETERMINATION OF MEASUREMENT UNCERTAINTY**

**Abstract:** Simulation methods for measurement uncertainty estimation gain more interest and importance as they are the fastest and cheapest available solution. And the measurement speed along with low costs are ones of the most important requirement put for modern measurement and quality control systems. Recent advances in simulation methods applied to different types of measuring systems and various measuring tasks are presented in this paper. They include the recent works performed in Laboratory of Coordinate Metrology at Cracow University of Technology. The virtual models of tactile and optical CMMs are presented. Considerations are also given on adaptation of virtual CMM model for industrial conditions, development of five-axis CMM model and the concept of virtual laser tracker system.

**Key words:** uncertainty, CMM, optical measurements, industrial conditions, virtual model

**1. INTRODUCTION**

Result of the measurement stated without giving its uncertainty is barely useless from practical point of view. According to ISO 14253 series of international standards [1,2] measurement uncertainty plays crucial role in assessment of parts conformity with specifications and should always be taken into account during conformity verification. The uncertainty values determined in wrong way may be the cause for wrong decisions during assessing of the compliance with the GPS (Geometrical Product Specifications) requirements. Overestimated uncertainty may be the cause for rejecting properly manufactured parts, while the underestimated one, may be the reason of acceptance of faulty products [3].

Latterly, the simulation methods for uncertainty estimation are one of the most often used as they allow quick and straightforward measurement uncertainty determination of a single measurement and may easily be applied for determination of a task-specific uncertainty [4]. For many years its usage was narrowed to leading calibration laboratories in which stable ambient conditions were quite easily assured. Lately, thanks to advances in the field of development of virtual models of measuring systems, they are also used on Coordinate Measuring Machines (CMMs) working in industrial conditions. In following sections of this paper the idea of adapting the virtual CMMs to industrial conditions is presented and usage of virtual models of specific CMM types is discussed.

**2. CONCEPT – VIRTUAL CMM FOR CONTACT 3-AXIS COORDINATE MEASURING MACHINE WORKING IN INDUSTRIAL CONDITIONS**

In the past, there were two main reasons that limited implementation of virtual CMM models in industrial conditions. They were: temperature changes influences kinematic errors of CMM thus large changes of temperature values cause that models of kinematic

errors on which the virtual CMM is based also change and the second major reason was that long implementation experiments are necessary for determination of errors distributions and it would be hard to perform them on the machines that are used almost 100 % of plant working time and that are crucial point of production quality assurance system.

Model described in [5] were chosen as the one whose adaptation for use in industrial conditions should be possible. Solution to the first of mentioned problems was the determination of residual kinematic errors distributions for different temperature ranges. Temperature interval of 18 °C to 22 °C were divided into five smaller intervals and for them the residual errors were determined. Further optimisation of kinematic errors module showed that for mentioned temperature range three intervals are enough [6]. Second problem was solved through the optimization of reference points number in modules responsible for kinematic errors simulation and probe head errors simulation. Experimental data that is gathered during implementation is collected in reference points, so decrease of their number cause reduction of implementation experiments time. Thanks to the mentioned optimization, the total implementation time of VCMM was decreased from about 20 hours to about 5 hours for CMM with standard measuring volume. This virtual CMM model was successfully implemented in industrial conditions on the machine, which is used in a quality assurance system in a worldwide company that operates in automotive industry and is located near Krakow.

**3. VIRTUAL CMM FOR 5-AXIS COORDINATE MEASURING SYSTEM**

Reduction of the measurement duration can be obtained in case of classic tactile coordinate machines by introducing some changes into measuring system. One of good examples of such approach is a five axis coordinate system that utilizes articulating probing

system with ability of continuous indexation. This solution allows to measure points coordinates using rotating motion of probe head without, or with reduced, movements of other CMM's parts. For some measuring tasks, especially measurements of rotational elements (holes, shafts) it may results in significant reduction of measurement duration, improvement of machine repeatability and even increase of its accuracy. It is not surprising then that the number of installations of systems of such type in industry still growing. Of course, in the case of a system whose main advantage is acceleration of the quality control process, it is also

necessary to develop a method for estimating uncertainty which would allow to fully utilize its potential.

The virtual model of five axis system that utilizes special articulating probing system has been developed lately at LCM. It consist of two modules: one responsible for modelling the errors of CMM kinematics, and second one for simulation of probing system errors (Fig. 1).

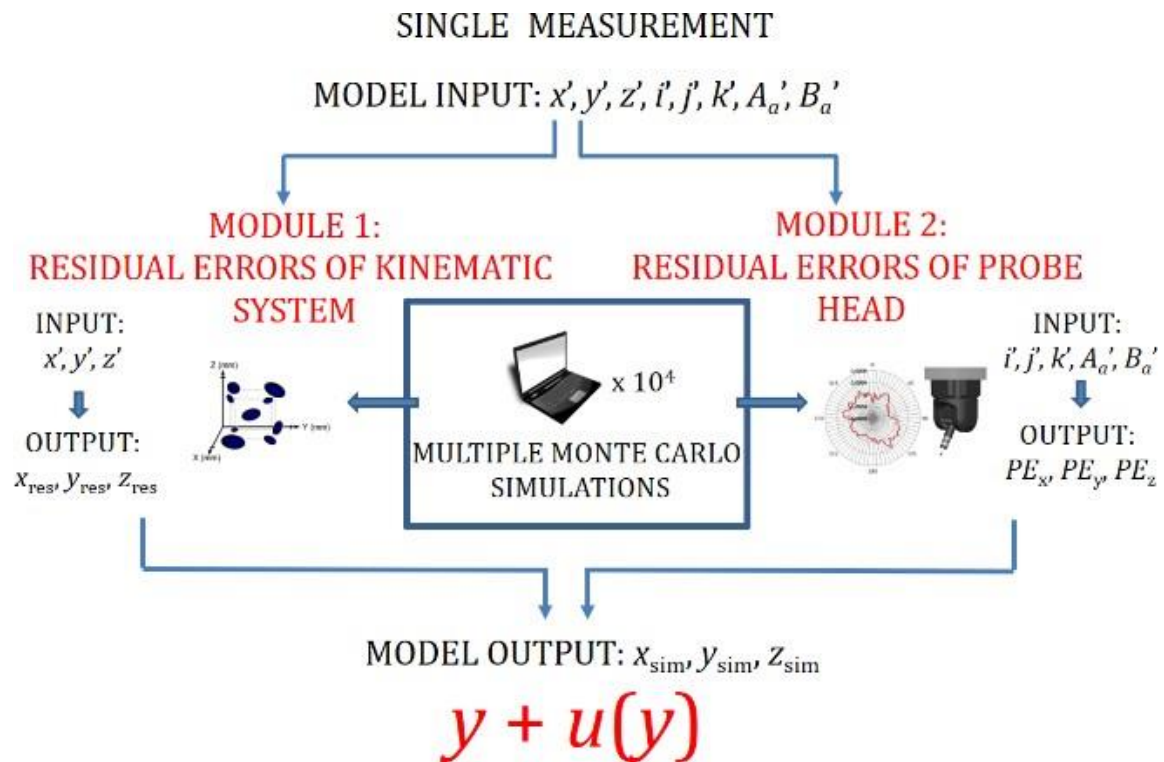


Fig. 1. Virtual CMM model for five-axis coordinate measuring system – schematic diagram [7]

First module utilizes concept of residual errors. As almost all of modern CMMs comes with software correction systems, the problem of kinematics errors analysis and modelling focuses on the errors that remained uncorrected and random errors, which together can be defined as a residual errors. Because of their random character residual errors can be described using probability density functions which are fit on the basis of results obtained during appropriate experiments. The experimental procedure is performed in the chosen points in the measuring volume of the machine which constitutes so called reference grid. The retroreflector is mounted in place of probing system and machine approaches on points included in the grid from different directions. Using laser tracking device of very high accuracy it is possible to measure the difference between the programmed position and the real position obtained by the reflector as well as dispersion of results. After these steps the simulation of errors can be performed using Monte Carlo method and nearest neighbour interpolation method for obtaining results in points which weren't included in experimental procedure.

Second module is based on the concept of Probing

Error Function which gives information about the errors associated with operation of probing system. Because probing process is influenced by many different factors which, among others depends on working principle of probe head, the error of probe is treated as sum of many components which are not examined separately, but can be determined in resultant form by measuring reference object (such as gauge ring or reference sphere) which is characterized by small dimensions (to minimize influence of machine's kinematics on measurement results) and negligible shape deviations. With such assumptions errors observed during measurements can be attributed mainly to the probing system and can be used for modelling its accuracy.

Articulating probing system with ability of continuous indexation can rotate around two perpendicular axes (vertical and horizontal ones). The probing errors strongly depend on the orientation of probing system used during measurements so it is necessary to measure reference object set in different positions in measuring volume of probing system. The positions are distributed in such a manner to evenly cover the measuring volume of probing system. The

variables needed for model operation are:  $x', y', z'$  – coordinates of measured point; the angles used by probing system  $A_a, B_b$  and direction cosines  $i', j', k'$  showed in Fig. 2. Next on the basis of obtained results the simulation can be done using Monte Carlo method and trilinear interpolation (needed to determine probing errors for orientations of probing system which weren't examined experimentally).

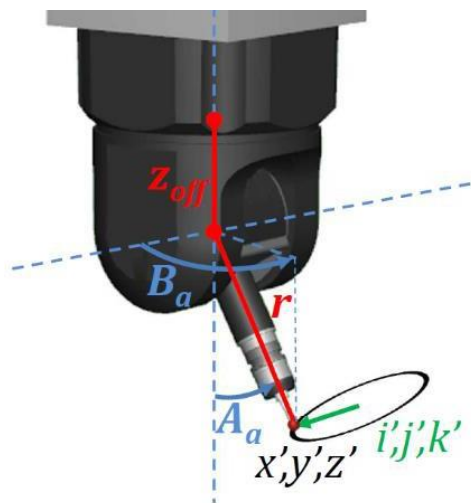


Fig. 2. Variables needed for virtual model functioning - variables described in test [7]

To integrate the two modules together two additional variables are used (Fig. 2):  $r$  which gives information about the distance between tip center and the position of probing system axes intersection point (which depends on the utilized stylus length);  $z_{off}$  which is distance between intersection point and center of reflector mounted in place of probing system during experiments needed for first module application (it depends on construction of specified CMM model).

Experiments performed at LCM shows that uncertainty given by Virtual CMM are consistent with those estimated using calibrated workpiece method, but Virtual CMM is capable of giving the task specific uncertainty right after the measurement. Additionally, experiments needed for application of virtual CMM on specific machine as well as verification measurements can be done in one day so the installation process doesn't cause the long-lasting downtime of the machine.

#### 4. VIRTUAL CMM FOR 5-AXIS COORDINATE MEASURING SYSTEM

CMMs equipped with an optical head are more and more appreciated in production plants. One of their advantages is that they can measure components that are sensitive to the application of force, e.g. small plastic parts. The use of an optical head for measurements is associated with the fact that the measurement is performed in a contactless manner, therefore the concept

of a virtual optical machine is based on different error components than in the case of models for classic machines. The research allowed to identify and determine several sources of errors that significantly affect the measurement result. One of the sources with the greatest impact is the illumination of the object, which in most cases of machines offered on the market, is manually adjusted, according to the subjective feeling of the operator. The main element of the optical head is a photosensitive electronic element in the form of a CMOS or CCD matrix, the operation of the elements is based on the measurement of the brightness of each pixel, therefore even small changes in the light intensity may affect the detection of the object's edge. The research showed a significant influence of this parameter on the measurement result. The conducted analysis allowed for the determination of the minimum and maximum range of illumination for which the results remained at a stable level. Another factor included in the model is the repeatability and reproducibility of the machine. The research showed a strong dependence of the direction of the point acquisition on the characteristics of the repeatability and reproducibility of the point. This has to do with the kinematics of the machine and the essence of recognizing edges in an image. The ambient temperature is another factor with a great influence. In most cases, measuring machines with optical heads are equipped with a temperature compensation system. Such machines are used in measuring laboratories and in production lines where fluctuations in ambient temperature can be very large. A significant influence on the characteristics of the repeatability and reproducibility of the points depending on the temperature was observed. Another influence included in the model is the use of the autofocus system. The variation of two parameters that can be set by the operator was checked - the size of the field and the backlight. For each of the above-mentioned impacts, a mathematical model and characteristic matrices were developed, which are used to simulate the points. The operation of the described simulation method begins after the measurement of the object (Fig. 3).

Measurement points of each feature along with additional data such as backlight value, direction cosine or AF area size are transferred to the developed software. Based on the provided data, the program selects appropriate simulation parameters for each of modules. Then the point simulation is started. After completing one simulation cycle, the points are substituted for the measured points so that all the features are calculated in the same way. Then the entire procedure is repeated many times. Each time the obtained results are collected in a data table, on the basis of which, after the simulation is finished, the measurement uncertainty of each feature is calculated.

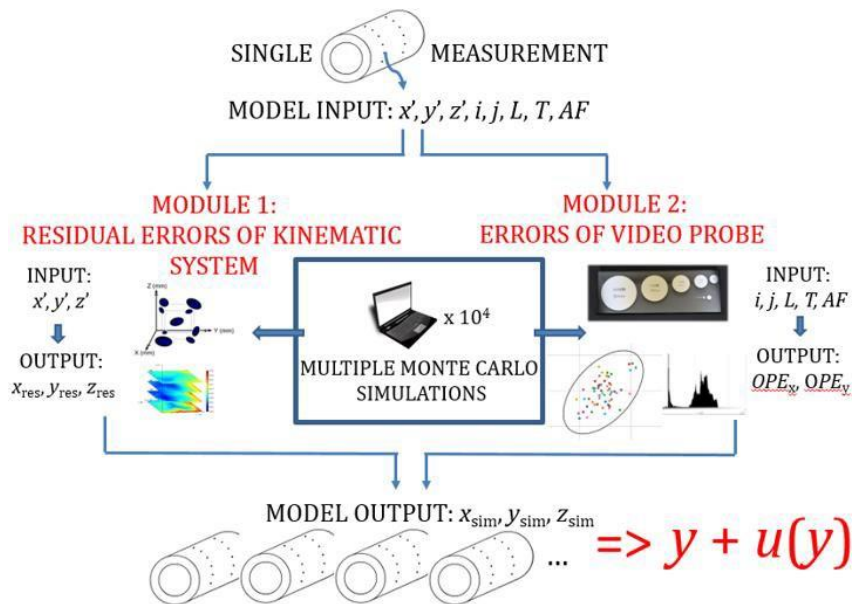


Fig. 3. Virtual optical CMM that may be used in shop floor conditions - schematic diagram

## 5. SUMMARY

Recently developed simulation models for simulation of measurement uncertainty applied to different types of measuring systems and various measuring tasks were presented. Proper functioning of all of them were validated before practical implementation and then again after models were implemented in real-life conditions. Validation was based on comparison of results given by developed models with results produced with use of methods that are known from the state-of-the-art and may be treated as already validated. Different validation models may be used for this purpose. For the virtual models presented in this paper, validation was based on the idea of statistical consistency and the A procedure for confirmation of the consistency of results, which is used during round robin interlaboratory comparisons. What is very important in that matter, is that no newly developed method should be used in practical applications before it is properly validated.

## 6. REFERENCES

- [1] ISO 14253-1:2017 *Geometrical product specifications (GPS) — Inspection by measurement of workpieces and measuring equipment — Part 1: Decision rules for verifying conformity or nonconformity with specifications.*
- [2] ISO 14253-2:2011 *Geometrical product specifications (GPS) — Inspection by measurement of workpieces and measuring equipment — Part 2: Guidance for the estimation of uncertainty in GPS measurement, in calibration of measuring equipment and in product verification.*
- [3] JCGM 106:2012 *Evaluation of measurement data – The role of measurement uncertainty in conformity assessment.*
- [4] Ramu, P., Yagüe, J.A., Hocken, R.J., Miller, J. *Development of a parametric model and virtual*

*machine to estimate task specific measurement uncertainty for a five-axis multi-sensor coordinate measuring machine* (2011) *Precision Engineering*, 35 (3), pp. 431-439.

- [5] Sładek, J., Gąska, A. *Evaluation of coordinate measurement uncertainty with use of virtual machine model based on Monte Carlo method* (2012) *Measurement: Journal of the International Measurement Confederation*, 45 (6), pp. 1564-1575.
- [6] Gąska, A., Harmatys, W., Gąska, P., Gruza, M., Gromczak, K., Ostrowska, K. *Virtual CMM-based model for uncertainty estimation of coordinate measurements performed in industrial conditions* (2017) *Measurement: Journal of the International Measurement Confederation*, 98, pp. 361-371.
- [7] Gąska, P., Gąska, A., Sładek, J., Jędrzejewski, J. *Simulation model for uncertainty estimation of measurements performed on five-axis measuring systems* (2019) *International Journal of Advanced Manufacturing Technology*, 104 (9-12), pp. 4685-4696.

**Authors: Assoc. Prof. Dr. Adam Gąska, M.Sc. Wiktor Harmatys, M.Sc. Piotr Gąska, Prof. Dr. Jerzy Sładek,** Cracow University of Technology, Faculty of Mechanical Engineering, Laboratory of Coordinate Metrology, al. Jana Pawła II 37, 31-864 Cracow, Poland, Phone.: +48 12 628-32-30, Fax: +48 374 32-38.  
E-mail: [adam.gaska@pk.edu.pl](mailto:adam.gaska@pk.edu.pl); [wharmatys@pk.edu.pl](mailto:wharmatys@pk.edu.pl); [piotr.gaska@pk.edu.pl](mailto:piotr.gaska@pk.edu.pl); [jerzy.sladek@pk.edu.pl](mailto:jerzy.sladek@pk.edu.pl)

Pušavec, F.

## GREEN AND SUSTAINABLE MACHINING PROCESSES AS A BASIS FOR INNOVATIONS

***Abstract:** The manufacturing industry is a global base for prosperity and key to Europe's economic, social and environmental sustainability. While the main driver for development are innovations, this does not mean to be focused just on the fundamental research innovations, but also to the innovations and their evolution to the level that make contribution to the society, are on lunched to the market, etc. For this purpose the EIT (European Institute of Innovation & Technology) has been established, also in the manufacturing field – EIT Manufacturing, with the objective to unite EU production in innovation ecosystem that would give to the EU products, processes and services unique value for making more global competitive and sustainable production. This is therefore emphasizing the need for usage of fundamental research results to be progressed in development and raised to high TRL levels and lunched into the industry, market, etc. In this presentation will be thus presented the EIT innovation community, with the challenges in manufacturing and machining industry, as well as EIT activities. Additionally, the speech will be focused on the case study on supported innovation project - Transitioning to a waste-free production – international cryogenic+MQL machining activity, with the road map of clean and dry cryogenic machining, where the fundamental research is lately been pushed to the industry and market with the help of EIT platform.*

**Author:** Prof. dr Franci Pušavec, University of Ljubljana, Faculty of Mechanical Engineering (FME), Aškerčeva 6, 1000 Ljubljana, Slovenia, Phone: +386 1 4771 200  
E-mail: [Franci.Pusavec@fs.uni-lj.si](mailto:Franci.Pusavec@fs.uni-lj.si)



# **MMA 2021**

---

**FLEXIBLE TECHNOLOGIES**

Section A:

## **MATERIAL REMOVAL TECHNOLOGIES**





Madić, M., Janković, P., Petković, D., Gostimirović, M., Rodić, D.

**OPTIMIZATION OF MATERIAL REMOVAL RATE IN CO<sub>2</sub> LASER CUTTING OF AN ALUMINUM ALLOY**

**Abstract:** *Technology of laser cutting is still of the widest used methods in industrial practice for contour cutting. The actual cutting process is very complex and diffuse affected by a number of process parameters. On the other hand, there are a number of performance characteristics used to characterize the process in terms of productivity, cut quality, costs, environmental aspects etc. The determination of the (near) optimal laser cutting regimes while considering several process performance characteristics is vital in laser cutting process planning. This study presents the optimization study related to the maximization of the material removal rate (MRR) in the CO<sub>2</sub> laser cutting of an aluminum alloy. In the formulation of the single-objective optimization problem with constraints, surface roughness and kerf width were taken as functional constraints so as to consider quality aspects of the cutting process. The developed laser cutting optimization model was solved using particle swarm optimization (PSO) metaheuristic.*

**Key words:** *CO<sub>2</sub> laser cutting, material removal rate, optimization, PSO*

**1. INTRODUCTION**

Technology of laser cutting is one of the leading non-conventional machining processes used in today's industry for high productive contour cutting of different engineering materials. The actual cutting process, in which the material from the kerf is removed by focusing the laser beam on the workpiece top surface and by using coaxial stream of assist gas, is very complex and diffuse, governed by a number of parameters related to the workpiece material, assist gas, optics and the applied cutting method. Thus, researchers and engineers, in order to get the best from this technology and/or ensure the achievement of the required quality, cost or productivity criteria, are aimed at quantification of the relationships between the process parameters and performance characteristics. Such approach enables detailed analysis of the process parameters effects, fulfillment of several requirements simultaneously, optimization of the process parameters and control of the actual cutting process [1].

Different analytical and empirical mathematical modeling techniques are being applied for analysis and modeling of the laser cutting process including analytical approaches [2-4], analysis of variance (ANOVA) [5], regression analysis [6, 7], design of experiment (DOE) [8], artificial neural network (ANN) [9], fuzzy logic [10] and genetic programming [11]. Also, a number of optimization studies using Taguchi method [12], MCDM [13], grey relational analysis (GRA) [14], response surface methodology (RSM) [15], desirability analysis [16] and classical formulation and solving of single and multi-objective optimization problems were performed [17].

The goal of the present study is the optimization of laser cutting parameter values in order to maximize material removal rate in CO<sub>2</sub> laser cutting of an aluminum alloy while considering several process constraints so as to take into account quality

characteristics. The single-objective laser cutting optimization problem was formulated considering mathematical models that were developed upon realization of experimental investigation in which three cutting parameters (cutting speed, nitrogen pressure and laser power) were varied at three levels. The developed laser cutting optimization model was solved using particle swarm optimization (PSO) metaheuristic.

**2. EXPERIMENTAL DETAILS**

The workpiece material selected for the present study is AA5754 aluminum alloy (AlMg3 by ISO designation). It is extensively used in construction, processing, aerospace and automotive industry due to its favorable weldability, corrosion resistance and weight to strength ratio. However, because of high thermal conductivity and reflectivity to CO<sub>2</sub> laser beam, laser cutting of aluminum alloys is considered difficult [18]. Thus, the experimental data used in the present study considers the high-power CO<sub>2</sub> laser cutting using non-conservative cutting speeds and assist gas pressure values [9]. Development of the required mathematical models for the definition of the laser cutting optimization problem uses the experimental data from the realization of full factorial design. The results obtained considered the variation of the laser power ( $P$ ), cutting speed ( $v$ ) and nitrogen pressure ( $p$ ) at three levels, thus enabling the development of second order mathematical models. The parameters were varied in the following range: laser power,  $P=3\div 4$  kW, cutting speed,  $v=3\div 3.5$  m/min, nitrogen pressure,  $p=6\div 10$  bar. More experimental details are given in [9]. For each experimental trial cut quality was assessed in terms of the kerf width and mean roughness depth. 3D coordinate measuring machine (Mitutoyo, QSL-200Z) and a digital measuring instrument MahrSurf-XR1 were used for measuring kerf width and surface roughness, respectively.

### 3. DEVELOPED MATHEMATICAL MODELS

On the basis of the experimentally measured cut quality characteristics mathematical models for the prediction of the average kerf width ( $K_w$ ) and mean roughness depth ( $R_z$ ) were developed in the following form:

$$K_w = 0.46 - 0.07P + 0.031p - 0.013v - 0.11P^2 + 0.021p^2 + 0.053v^2 + 0.003Pp - 0.022Pv - 0.023p \quad (1) \quad \text{¶}$$

$$R_z = 24.3 - 0.87P + 3.717p + 2.777v - 1.002P^2 + 0.403p^2 + 2.176v^2 + 3.558Pp - 2.311Pv - 1.227pv \quad (2) \quad \text{¶}$$

The coefficients of determination ( $R^2$ ) of 0.978 and 0.986 confirmed the statistical validity of the developed models, indicating that the derived equations can explain significant variability of the considered cut quality characteristics. It has to be noted that the developed models were obtained using coded values of the independent variables.

By multiplying the resulting average kerf width with the cutting speed and workpiece thickness one obtains the estimation of the volumetric material removal rate (MRR) as:

$$MRR = K_w \cdot s \cdot v \quad (3) \quad \text{¶}$$

This productivity criterion of the laser cutting technology refers to the volume of material removed per time unit when performing the actual cutting operation with a particular combination of the laser cutting parameter values. MRR belongs to the class of maximization criteria, where higher values are always preferred.

The aim of the present study was to develop laser cutting optimization model so as to determine optimal values of laser power, nitrogen pressure and cutting speed to maximize MRR and at the same time satisfy two imposed constraints related to the maximal allowable mean roughness depth ( $R_{zmax}$ ) and maximal allowable kerf width ( $K_{wmax}$ ).  $R_{zmax}$  is the maximal allowable surface roughness with respect to sheet thickness and desired cut class as defined by the ISO 9013 standard which is relevant for thermal cutting or specified by laser cutting machine manufacturers (such as Trumpf). Kerf width constraint was considered in order to enhance CNC path programming and also to prevent achieving high MRR at the expense of the wider cuts.

Given in mind the afore-mentioned, the following single-objective laser cutting optimization problem with constraints was formulated:

Determine  $P, v, p$  to maximize  $MRR$

subject to :  $K_w \leq K_{wmax} = 0.4\text{mm}$  (4) ¶

$$R_z \leq R_{zmax} = 22\mu\text{m}$$

### 4. PARTICLE SWARM OPTIMIZATION (PSO)

Particle swarm optimization (PSO) is a stochastic, population based, metaheuristic algorithm which is widely being used for solving different engineering optimization problems. This meta-heuristic optimization algorithm was proposed by Kennedy and Eberhart in 1995 [19]. The development of the algorithm is the result of inspiration from the nature, i.e. social behavior, dynamic movement and cooperation of insects, herds, birds and fishes. Although it a relatively recent optimization algorithm, from its origin until now it has undergone several changes and amendments in order to improve optimization speed, quality, robustness and entire control of the optimization process. In essence, the basic PSO algorithm can be summarized as follows [20-23]. At the very beginning of the optimization process, a swarm of particles (entities), as a set of potential solutions of the problem being solved, is initialized using random method. Each particle has its own position and velocity, and is able to memorize its best position in search history as well as optimal position of the entire swarm. Since the position of the particle represents the possible optimization solution of the problem each particle evaluates the fitness function at its current location. The search of the optimization hyper-space is achieved by swarm of flying particles, wherein each particle determines its movement on the basis of its own experience (current and best-fitness locations) and neighborhood experience (one or more members of the swarm), with some random perturbations. Consequently, in each iteration, new position of each particle is adjusted considering previous position, cognitive (individual) learning factor and social learning factor. If the cognitive learning factor is dominant, PSO intensifies exploration of the optimization hyper-space. Otherwise, the search mechanism is directed by the process of intensification (exploitation).

In the present work the canonical PSO algorithm was used which has significantly improved algorithm performance over the original PSO [20]. For solving the developed optimization problem, the following set of PSO parameter values was used: swarm size of  $m=100$ , linearly decreasing inertia weight with iteration number (with  $\omega_{min}=0.4$  and  $\omega_{max}=0.9$ ), cognitive learning factor  $c_1=2$ , social learning factor  $c_2=2$  and maximal number of iterations  $N=1000$ .

### 5. RESULTS AND DISCUSSION

In the present study in order to solve the defined laser cutting optimization problem, as given in equation 4, PSO algorithm was applied. As a result of the optimization process, the maximal feasible MRR of 4184 mm<sup>3</sup>/min was obtained with the following laser

cutting parameter values:  $P=3.93$  kW,  $p=6$  bar and  $v=3.46$  m/min. The determined optimal values of the laser cutting parameters along with functional constraints is given in Table 1.

Optimal laser cutting parameters			Objective function
$P$ (kW)	$p$ (bar)	$v$ (m/min)	MRR (mm <sup>3</sup> /min)
3.93	6	3.46	4184
Optimization constraints			
$R_z = 21.92 \mu\text{m}$		$K_w = 0.39 \text{ mm}$	

Table 1. Optimization problem solution

It is worth noting that the optimization process by the PSO algorithm was repeated several times to check the convergence of the PSO algorithm. What could be noted is the fact that PSO algorithm appeared to be robust by consistently producing the same set of independent variable values as the optimization result. In order to further check the optimality of the determined optimization solution, the developed software prototype was used [1]. This software solution enables the formulation of optimization problems with constraints and enables the application of the exhaustive iterative search algorithm which guarantees the optimality of the determined solution for the given discrete optimization hyper-space. As being confirmed with the use of the developed software solution, the optimization set of laser cutting parameter values was further experimentally verified and provided acceptable cut quality without dross formation. Although unconventional level of assist gas pressure is used, nozzle diameter of 2 mm provided sufficient gas flow inside the cutting kerf so as to ensure acceptable overall cut quality.

## 6. CONCLUSIONS

With an ultimate aim to enhance laser cutting process planning, the present study dealt with the determination of the optimal laser cutting parameter values so as to maximize MRR in CO<sub>2</sub> laser cutting of an aluminum alloy. In order to consider also cut quality aspects, surface roughness and kerf width mathematical models were considered as functional constraints in the proposed optimization problem which was solved using the PSO metaheuristic algorithm. The main derived conclusions are as follows:

- PSO metaheuristic proved capable of finding the feasible set of laser cutting parameter values within short optimization time.
- With the used set of main algorithm parameters PSO metaheuristic proved to be robust and capable to escape local minima consistently.
- In high-power CO<sub>2</sub> laser cutting of aluminum alloy using low assist gas pressure, there exists an optimal combination of the laser power and cutting speed ratio which ensures higher productivity without quality deterioration. The determination of the most suitable laser cutting regime by taking into account several process performance characteristics necessitates the development of a particular single or multi-objective optimization problem and its solving with an appropriate optimization algorithm.

Such approach, with respect to particular cutting method and workpiece material and thickness, may significantly outperform the traditional determination of laser cutting regimes based on trial and error approach or consideration of the different recommendations from laser cutting machine manufacturers.

## 7. REFERENCES

- [1] Madić, M., Kovačević, M., Radovanović, M., Blagojević, V.: *Software tool for laser cutting process control—solving real industrial case studies*, Facta Universitatis, Series: Mechanical Engineering, 14(2), pp. 135-145, 2016.
- [2] Fuchs, A.N., Woldrich, T., Heimhilger, K.M., Zaeh, M.F.: *Analytical model for laser cutting of carbon fiber fabrics: maximum cutting speed and the heat affected zone*, Lasers in Manufacturing Conference, pp. 1-9, Munich, German Scientific Laser Society (WLT), Munich, June 22-25, 2015.
- [3] Tani, G., Tomesani, L., Campana, G.: *Prediction of melt geometry in laser cutting*, Applied Surface Science, 208, pp. 142-147, 2003.
- [4] Yilbas, B.S.: *Effect of process parameters on the kerf width during the laser cutting process*, Proceedings of the Institution of Mechanical Engineers, Part B: Journal of Engineering Manufacture, 215(10), pp. 1357-1365, 2001.
- [5] Genna, S., Menna, E., Rubino, G., Tagliaferri, V.: *Experimental investigation of industrial laser cutting: The effect of the material selection and the process parameters on the kerf quality*, Applied Sciences, 10(14), pp. 4956, 2020.
- [6] Kadhim, K.J.: *Effect of laser process an inclined surface cutting of mild steel then analysis data statistically by RSM*, Journal of Engineering, 25(10), pp. 120-133, 2019.
- [7] Rajesh, K., Raju, V.M.K., Rajesh, S., Varma, N.S.K.: *Effect of process parameters on machinability characteristics of CO<sub>2</sub> laser process used for cutting SS-304 Stainless steels*, Materials Today: Proceedings, 18, pp. 2065-2072, 2019.
- [8] Girdu, C.C., Gheorghe, C., Radulescu, C., Cirtina, D.: *Influence of process parameters on cutting width in CO<sub>2</sub> laser processing of Hardox 400 steel*, Applied Sciences, 11(13), pp. 5998, 2021.
- [9] Janković, P., Madić, M., Radovanović, M., Petković, D., Mladenović, S.: *Optimization of surface roughness from different aspects in high-power CO<sub>2</sub> laser cutting of AA5754 aluminum alloy*, Arabian Journal for Science and Engineering, 44(12), pp. 10245-10256, 2019.
- [10] Kumar, A., Kumar, V., Sharma, G.: *Experimental investigation of multiple quality characteristics of laser beam machined surface using integrated Taguchi and fuzzy logic method*, Journal for Manufacturing Science and Production, 16(3), pp. 189-199, 2016.
- [11] Kondayya, D., Krishna, A.G.: *An integrated evolutionary approach for modelling and optimization of laser beam cutting process*, The International Journal of Advanced Manufacturing

- Technology, 65(1-4), pp. 259-274, 2013.
- [12] Mbithi, B.K., Byiringiro, J.B., Niyibizi, A.: *Experimental investigation and optimization of laser cutting parameters for solar cells based on Taguchi method*, IOSR Journal of Mechanical and Civil Engineering, 14(5), pp. 41-51, 2017.
- [13] Madić, M., Antucheviciene, J., Radovanović, M., Petković, D.: *Determination of laser cutting process conditions using the preference selection index method*. Optics and Laser Technology, 89, pp. 214-220, 2017.
- [14] Begic-Hajdarevic, D., Ficko, M., Cekic, A., Klancnik, S., Cohodar, M.: *Multi-response optimization of laser cutting parameters using grey relational analysis*. 30th DAAAM International Symposium on Intelligent Manufacturing and Automation, pp. 176-183, Zadar, DAAAM International, Vienna, October 23-26, 2019.
- [15] Shaikh, A.H.A., Varsi, A.M.: *Comparative statistical analysis for prediction of depth of cut in CO<sub>2</sub> laser machining*, International Journal of Management and Applied Science, 4(5), pp. 56-62, 2018.
- [16] Anghel, C., Gupta, K., Jen, T.C.: *Optimization of laser machining parameters and surface integrity analysis of the fabricated miniature gears*, Procedia Manufacturing, 51, pp. 878-884, 2020.
- [17] Madić, M., Mladenović, S., Gostimirović, M., Radovanović, M., Janković, P.: *Laser cutting optimization model with constraints: maximization of material removal rate in CO<sub>2</sub> laser cutting of mild steel*, Proceedings of the Institution of Mechanical Engineers, Part B: Journal of Engineering Manufacture, 234(10), pp. 1323-1332, 2020.
- [18] Leone, C., Genna, S., Caggiano, A., Tagliaferri, V., Molierno, R.: *Influence of process parameters on kerf geometry and surface roughness in Nd:YAG laser cutting of Al 6061T6 alloy sheet*, International Journal of Advanced Manufacturing Technology, 87, pp. 2745-2762, 2016.
- [19] Kennedy, J., Eberhart, R.C.: *Particle swarm optimization*, Proc. IEEE Int. Conf. On Neural Networks (Perth, Australia) IEEE Service Center, Piscataway, NJ, pp. 1942-1948, 1995.
- [20] Wang, D., Tan, D., Liu, L.: *Particle swarm optimization algorithm: an overview*, Soft Computing, 22(2), pp. 387-408, 2018.
- [21] Poli, R., Kennedy, J., Blackwell, T.: *Particle swarm optimization*, Swarm intelligence, 1(1), pp. 33-57, 2007.
- [22] Čupić, M.: *Prirodom inspirirani optimizacijski algoritmi: Metaheuristike*, 2013.
- [23] Aleksić, A., Sekulić M., Savković, B., Gostimirović, M., Kamenko, I., Kovač, P.: *Optimization of cutting parameters by nature-inspired algorithms*, Acta Technica Corviniensis-Bulletin of Engineering, 13(4), pp. 41-44, 2020.

**Authors:** Assist. Prof. Miloš Madić, Full Prof. Predrag Janković, Assist. Prof. Petković Dušan, Full Prof. Marin Gostimirović, Assist. Prof. Dragan Rodić, Faculty of Mechanical Engineering in Niš, University of Niš, Aleksandra Medvedeva 14, 18106 Niš, Serbia

Faculty of Technical Sciences, University of Novi Sad, Trg Dositeja Obradovića 6, 21102 Novi Sad, Serbia.

E-mail: [madic@masfak.ni.ac.rs](mailto:madic@masfak.ni.ac.rs);

[jape@masfak.ni.ac.rs](mailto:jape@masfak.ni.ac.rs);

[dulep@masfak.ni.ac.rs](mailto:dulep@masfak.ni.ac.rs);

[maring@uns.ac.rs](mailto:maring@uns.ac.rs);

[rodicdr@uns.ac.rs](mailto:rodicdr@uns.ac.rs)

**ACKNOWLEDGMENTS:** This research was financially supported by the Ministry of Education, Science and Technological Development of the Republic of Serbia (Contract No. 451-03-9/2021-14/200109).

Rodić, D., Gostimirović, M., Sekulić, M., Madić, M., Kulundžić, N.

## INFLUENCE OF PULSE DURATION ON SURFACE ROUGHNESS IN ASSISTING ELECTRODE ELECTRICAL DISCHARGE MACHINING

**Abstract:** *Electrical discharge machining (EDM) is an unconventional machining process that can machine all electrically conductive materials, regardless of their physical and metallurgical properties. Due to the efficiency of machining modern engineering materials, existing EDM methods are constantly being researched and improved or developed. This paper deals with an innovative method that enables EDM machining of non-conductive ceramic material, named Assisting Electrode Electrical Discharge Machining (AEEDM). It combines electrical discharge machining with a hybrid assisting electrode. The aim of the study is to find the influence of pulse duration on surface roughness. For the set machining conditions, it was found that the surface roughness was increased by increasing the pulse duration. It should be emphasized that the supporting electrode method is used only in the electroerosion of electrically non-conductive materials.*

**Key words:** EDM, hybrid assisting electrode, pulse duration, surface roughness

### 1. INTRODUCTION

Electrical discharge machining is a widely used and economically justified process that has wide applications and is most commonly used in the manufacture of tools for shaping materials, special and micro-particles, prototypes, etc. This machining can process all electrically conductive materials, but the main justification lies in the processing of high-alloy steels, difficult-to-cut steels and metal-ceramics. Recently, there are various innovative directions in the development of electrical discharge machining to process other modern but difficult-to-machine advanced materials [1].

EDM is used in the machining of electrically conductive materials, but its fundamental application is justified mainly in the machining of parts of specific structures made of materials that are difficult to cut [2]. In order to increase the efficiency of electrical discharge machining of modern engineering materials, existing or innovative EDM processes are constantly being researched and improved. Recently, a possible technological improvement of EDM process is achieved by an innovative method, such as Assisted Electrode Electrical Discharge Machining (AEEDM).

Compared to classical electrical discharge machining, only a few dozen papers have been published in the field of AEEDM. From the literature sources dealing with this field, some prominent works have been selected, on the basis of which an overview of the state of the art in the mentioned field has been presented. It should be emphasized that the assisting electrode method is used only in EDM of electronically non-conductive materials.

The foundations of Assisted Electrode Electrical Discharge Machining were laid in the early 1990s. The first appearance of EDM technology with an assisting electrode in academic circles was recorded in 1995 by Japanese scientists Fukuzawa et al [3]. In this paper, they described a new method that enables EDM of non-

conductive ceramic materials using a metal plate (assisting electrode) bonded to the workpiece and tools made of soft metal material. They concluded that discharge machining is achieved thanks to the modification of the ceramic surface, i.e. the continuous creation of an electrically conductive layer.

In this context, non-conductive ceramic materials can be machined by the EDM process using a supporting electrode layer [4]. The EDM process with assisting electrode is shown in Figure 1. The surface of the workpiece is covered with an electrically conductive material, allowing an initial electrical discharge, i.e., a discharge between the tool and the supporting electrode. This is followed by continuous erosion through the conductive layer to the workpiece material, on which the carbon layer (pyrolytic layer) is formed. During electrical discharge machining, a hydrocarbon layer is continuously formed on the workpiece, which is responsible for the stability of the process.

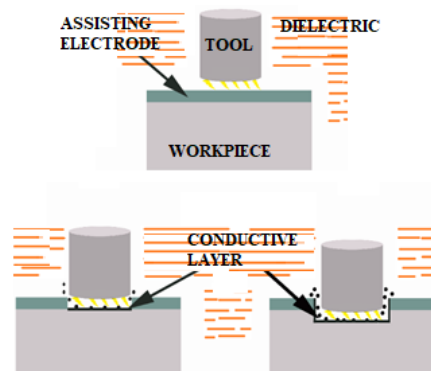


Fig. 1. Assisted Electrode Electrical Discharge Machining (AEEDM)

In order for AEEDM to process electrically nonconductive ceramic materials, hydrocarbon-based seed dielectrics could be used. By converting electrical energy to thermal energy, the resulting high temperature visibly affects the dielectric in the region of the

discharge channel. In the absence of oxygen in the region, the high temperature honestly leads to thermochemical decomposition of the dielectric [5]. The decomposition of materials under the influence of high temperature, without the influence of other forces, is called pyrolysis [6]. As a result of pyrolysis of the hydrocarbon-based dielectric, a carbon layer (pyrolytic layer) is formed. The resulting carbon layer is represented by the molten layer formed during EDM metal processing and is similar in structure to graphite, which makes it electrically conductive [6]. The electrically conductive layer is formed from electrically conductive particles, mainly carbon, formed by the dissolution of dielectric components and tool wear products during discharge [7]. This electrically conductive layer is essential for stable discharge during the AEEDM process.

Various metal foils can be used as assisting electrodes. The most common are metal foils made of aluminum and copper, which are mechanically applied to ceramics. The main advantage of this method is simplicity [8]. The main disadvantage of tightening the metal foil on ceramics is the lack of solid contact between the metal and the ceramic. Due to the lack of direct contact between the foil and the ceramic, the formation of the carbon layer is difficult, which leads to the instability of the AEEDM process, i.e., the interruption of the processing. The combination of metal foil and graphite coating is called hybrid assisting electrode. The metal foil provides robustness, i.e. it ensures the strength of the auxiliary electrode, while the graphite coating acts as an adhesive between the metal foil and the ceramic.

The influence of the assisting electrode material on the technological properties of the AEEDM was analyzed by the authors Tani et al. In their work [9], they machined zirconia ( $ZrO_2$ ) with copper and graphite tools. They found that the carbon layer was not completely generated by copper tools, resulting in a rough surface roughness. When a graphite tool was used, a significant reduction in the roughness of the treated surface was observed. In the previous two studies, they concluded that after the removal of the assisting electrode material, an electrically conductive carbon layer is continuously formed on the ceramic surface, without which machining would not be possible. The same authors concluded in the case of silicon nitride machining [10] that reducing the pulse length below 24 s improves the roughness of the treated surface, since in this way the excessive pulse length is prevented, which directly increases the discharge energy.

This research relates to the electrical discharge machining of electronically nonconductive ceramics. In order for electronically non-conductive materials, especially ceramics, to be processed by EDM, it is necessary to establish an electrical contact. By applying an electrically conductive layer (referred to as an assisting electrode - AE) to the ceramic surface, EDM machining of electrically non-conductive ceramic materials is made possible. One of the representatives of electronically non-conductive ceramics that has been used in this research is zirconia -  $ZrO_2$ .

Very few works have investigated the influence of

the main parameters of AEEDM, such as pulse duration, on surface roughness.

## 2. EXPERIMENTAL SETUP

The experiments were carried out on a die-sinking EDM machine Agie Charmilles of the SP1-U type, Figure 2. The isotropic graphite with a cross-section of  $10 \times 10 \text{ mm}^2$  was used as an electrode for machining insulating zirconium oxide  $ZrO_2$ . Before conducting the experiments, all tools were surface ground to ensure normality with the workpiece.



Fig. 2. EDM machine Agie Charmilles of the SP1-U type

For AEEDM of non-conducting materials to be possible, a hydrocarbon-based dielectric must be used. The commercial mineral oil (Castrol Ilocut 180) with a flash point of  $100^\circ\text{C}$  was used as the dielectric fluid in this study. As assisting electrode, the combination of metal foil and graphite coating used in this research. This type is called hybrid assisting electrode. A basic technique was developed in which a graphite layer (Graphite 33 lacquer) and an adhesive layer of copper foil (3M grade 1181) were applied to the workpiece surface.

The surface roughness measurements for the eroded surface were carried out using Perthometer, Mahr Surf PS1. The average surface roughness  $R_a$  [ $\mu\text{m}$ ] was used to quantitatively assess the quality of the machine surface.

In conducting the experiment, a lateral leaching was used with a dielectric with a flow rate of 20 l/min, through a nozzle with a diameter of 4 mm and the other with a nozzle with a cross section of  $2 \times 8 \text{ mm}$ . The tool lift-off time was 2 seconds at a distance of 1.5 mm. The erosion time of each experimental point was 60 min. For machining metallic materials, a duty factor of up to 95% is recommended. However, when machining ceramics, the increase has its limit to allow the formation of a carbon layer under the given machining conditions. According to sources from the literature, when machining ceramics, the duty factor ranges from  $20 \div 50\%$  [11, 12]. When machining with higher discharge currents and pulse duration, it is desirable that this coefficient moves to lower values.

Since the upper limit of discharge current of 2 A was chosen in this study, which is a relatively small discharge current, the chosen duty factor for machining with zirconia is 50%. Mostly, the open-circuit voltage can be set to 100 V or 300 V. When starting the machine

tool with a voltage of 100 V, it was difficult to start the AEEDM ZrO<sub>2</sub> due to the extremely low energy. To increase the energy, the machine has the option to turn on the auxiliary discharge current (high voltage current). When this option is enabled, the open circuit voltage is 300 V.

Under these processing conditions, it cannot affect the discharge voltage. During processing, a voltage value of about 240 V is automatically determined, which is measured by a DC voltmeter.

In this study, the negative polarity of the tool was used in AEEDM of zirconia. According to literature [4, 13, 14], when AEEDM insulating materials with negative tool polarity, the process is much more stable. Also, the transition time from the assisting electrode layer to the carbon layer is shorter than with the positive polarity of the tool.

### 3. RESULTS AND ANALYSYS

By applying an electrically conductive layer (Assisting Electrode) to the surface of the workpiece, it is possible to machine electronically non-conductive ceramic materials, which is called Assisting Electrode Electrical Discharge Machining. The assisting electrode allows the initial electrical discharge between the tool and the workpiece. After removing the assisting electrode layer, the dielectric decomposes due to the high temperature in the discharge zone, whereupon carbon particles are deposited on the surface of the workpiece and form an electrically conductive layer.

Before planning experimental trials, it is necessary to determine the range of variation of appropriate input parameters of machining, as well as other factors whose values are constant during the experiment. Based on the available literature sources and preliminary experimental studies, suitable conditions for the electrical discharge machining of ZrO<sub>2</sub> were assumed. The magnitude of the discharge current is limited by the dimensions of the frontal surface of the electrode, i.e. the current density. Here, the projection in the plane perpendicular to the direction of movement of the tool is taken as the governing surface of the tool. According to the previously published studies in the field of AEEDM, discharge currents up to 6 A have been used for electrode areas up to 1 cm<sup>2</sup> [15].

It is clear that as the discharge current increases, the discharge energy increases, resulting in better machining efficiency, but at higher values of discharge energy, the machining may become unstable, leading to the appearance of large craters on the workpiece surface, Figure 3.

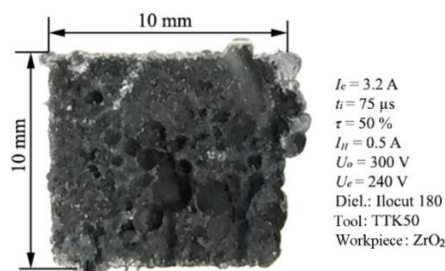


Fig. 3. Preliminary experimental trial, electrical discharge machining of ZrO<sub>2</sub>

Under the preliminary machining conditions: Discharge current 3.2 A, pulse duration 75 μs, duty factor 50%, auxiliary discharge current 0.5 A, open circuit voltage 300 V, the treated surface was obtained with high roughness, which could not be measured.

It is clear that as the discharge current increases, the discharge energy increases, resulting in better machining efficiency, but at higher values of discharge energy, the machining may become unstable, leading to the appearance of large craters on the workpiece surface. Accordingly, in this study on the electrical discharge machining of zirconia, the selected discharge current has been varied in the range of 1.5 A.

The purpose of the auxiliary discharge current in these experimental studies is to increase the energy to allow the transition of the assisting electrode layer into the carbon layer, without which the machining of insulating materials would not be possible. When the auxiliary current is activated, the machine control automatically switches the open circuit voltage to 300 V. The pulse duration is the time of the pulse in microseconds for which current flows in each cycle. During this time, the voltage is built up between the tool and the workpiece. According to the research published in the papers, the upper limit of the pulse duration for machining zirconia was 200 μs.

Accordingly, a discharge current of 1.5 A was used to investigate the effect of pulse duration on the surface roughness of AEEDM zirconia. The pulse duration was varied in three levels: 42, 75 and 110 μs. The test results are shown in Table 1.

Exp no.	I [A]	ti [μs]	Ra [μs]
1	1.5	42	9
2	1.5	75	10
3	1.5	110	13

Table 1. Table experimental trials

As the pulse length increases, the surface roughness increases at a constant discharge current. A test experiment was conducted at a constant discharge current of 1.5 A for the machining conditions set to determine the pulse duration up to which the erosion process is stable. It was found that for pulse lengths above 100 μs, Figure 4. For pulse durations below 42 μs, no carbon layer formed on the ceramic surface, which resulted in the AEEDM ZrO<sub>2</sub> process not being used.

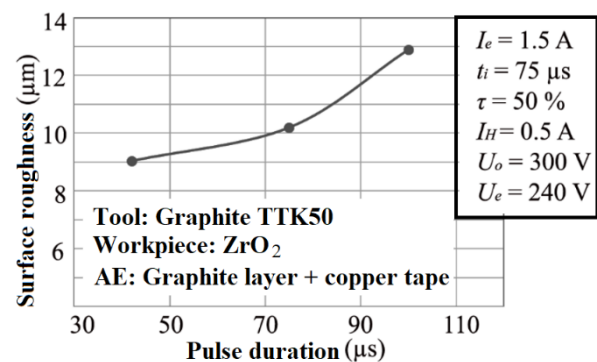


Fig. 4. Influence of pulse duration on surface roughness in AEEDM of ZrO<sub>2</sub>

## 5. CONCLUSION

The innovative development direction of Assisted Electrode Electrical Discharge Machining presented in this paper has elevated EDM to a higher level, especially from the aspect of machinability of electrically non-conductive materials. However, the research conducted in this paper covers only a small part of the field of electrical discharge machining of advanced engineering materials.

Based on previous research, the most influential parameter is the discharge current. However, very few works have investigated the extent to which pulse duration increases. According to the presented research, at constant discharge current, there is a pulse cutoff length of 100  $\mu$ s after which the AEEDM zirconium process becomes unstable.

The investigations in this work open some questions of new scientific knowledge, which impose themselves as guidelines for further development and future application of innovative methods of electroerosive treatment.

## 6. REFERENCES

- [1] Okada, A.: Ceramic technologies for automotive industry: Current status and perspectives. *Materials Science and Engineering: B*.Vol. 161(1-3): pp. 182-187, 2009.
- [2] Banu, A., M.Y. Ali, and M.A. Rahman: Micro-electro discharge machining of non-conductive zirconia ceramic: investigation of MRR and recast layer hardness. *The International Journal of Advanced Manufacturing Technology*.Vol. 75(1-4): pp. 257-267, 2014.
- [3] Fukuzawa, Y., et al.: Some Machining Methods of Insulating Materials by an Electrical Discharge Machine. *Journal of The Japan Society of Electrical Machining Engineers*.Vol. 29(60): pp. 11-21, 1995.
- [4] Fukuzawa, Y., et al.: Three-dimensional machining of insulating ceramics materials with electrical discharge machining. *Transactions of Nonferrous Metals Society of China* Vol. 19: pp. 150-156, 2009.
- [5] Gotoh, H., T. Tani, and N. Mohri: EDM of Insulating Ceramics by Electrical Conductive Surface Layer Control. *Procedia CIRP*.Vol. 42: pp. 201-205, 2016.
- [6] Kaneko, K., Y. Fukuzawa, and R. Yamada: Wire Electrical Discharge Machining Properties on Insulating SiC Ceramics. *Journal of The Japan Society of Electrical Machining Engineers*.Vol. 46(113): pp. 126-132, 2012.
- [7] Kucukturk, G. and C. Cogun: A New Method for Machining of Electrically Nonconductive Workpieces Using Electric Discharge Machining Technique. *Machining Science and Technology*.Vol. 14(2): pp. 189-207, 2010.
- [8] Lin, Y.J., et al.: Machining Characteristics of EDM for Non-Conductive Ceramics Using Adherent Copper Foils. *Advanced Materials Research*.Vol. 154-155: pp. 794-805, 2010.
- [9] Muttamara, A., et al.: Effect of electrode material on electrical discharge machining of alumina. *Journal of Materials Processing Technology*.Vol. 209(5): pp. 2545-2552, 2009.
- [10] Ojha, N., et al.: Analyzing the electrical pulses occurring during EDM of non-conductive Si<sub>3</sub>N<sub>4</sub> ceramics. *Key Engineering Materials*.Vol. 651-653: pp. 659-664, 2015.
- [11] Sabur, A., et al.: Investigation of material removal characteristics in EDM of nonconductive ZrO<sub>2</sub> ceramic. *Procedia Engineering*.Vol. 56: pp. 696-701, 2013.
- [12] Sabur, A., et al.: Investigation of surface roughness in micro-electro discharge machining of nonconductive ZrO<sub>2</sub> for MEMS application. *Materials Science and Engineering*.Vol. 53: pp. 1-6, 2013.
- [13] Tani, T., et al.: Effects of assisting electrode material on the EDM-ed characteristics for insulating sialon ceramics. *Journal of The Japan Society of Electrical Machining Engineers*.Vol. 30(65): pp. 17-24, 1996.
- [14] Tani, T., et al.: Machining Phenomena in EDM of Insulating Ceramics with Powder Mixed Oil. *Machining Phenomena in EDM of Insulating Ceramics with Powder Mixed Oil*.Vol. 36(81): pp. 39-46, 2002.
- [15] Gostimirovic, M., et al.: Inverse electro-thermal analysis of the material removal mechanism in electrical discharge machining. *The International Journal of Advanced Manufacturing Technology*: pp. 1-11, 2018.
- [16] Shabgard, M.R., A. Gholipour, and H. Baseri: A review on recent developments in machining methods based on electrical discharge phenomena. *The International Journal of Advanced Manufacturing Technology*.Vol. 87(5): pp. 2081-2097, 2016.

**Authors: Assist. Prof. Dragan Rodić, Full Prof. Marin Gostimirović, Full Prof. Milenko Sekulić, Research Assoc. Nenad Kulundžić**

<sup>1</sup>University of Novi Sad, Faculty of Technical Sciences, Department of Production Engineering, Trg Dositeja Obradovića 6, 21000 Novi Sad, Serbia, Phone.: +381 21 485-23-24, Fax: +381 21 454-495.

E-mail: [rodicdr@uns.ac.rs](mailto:rodicdr@uns.ac.rs); [maring@uns.ac.rs](mailto:maring@uns.ac.rs); [milenkos@uns.ac.rs](mailto:milenkos@uns.ac.rs); [kulundzic@uns.ac.rs](mailto:kulundzic@uns.ac.rs)

**Assist. Prof. Miloš Madić**, University of Nis, Faculty of Mechanical Engineering, Laboratory for Machine Tools and Machining, A. Medvedeva 14, 18000 Nis, Serbia, Phone.: +381 18 588 244, Fax: +381 18 500 635.

E-mail: [rodicdr@uns.ac.rs](mailto:rodicdr@uns.ac.rs); [maring@uns.ac.rs](mailto:maring@uns.ac.rs); [milenkos@uns.ac.rs](mailto:milenkos@uns.ac.rs); [madic@masfak.ni.ac.rs](mailto:madic@masfak.ni.ac.rs); [kulundzic@uns.ac.rs](mailto:kulundzic@uns.ac.rs)

**ACKNOWLEDGMENTS:** This paper has been supported by the Ministry of Education, Science and Technological Development through the project no. 451-03-68/2020-14/200156: "Innovative scientific and artistic research from the FTS (activity) domain".



Trifunović, M., Madić, M., Vitković, N.

## CUTTING PARAMETERS OPTIMIZATION FOR MINIMIZING ENERGY CONSUMPTION IN MULTI-PASS TURNING OF GREY CAST IRON

**Abstract:** Machine tools are dominant end users of electrical energy in the manufacturing industries, which account for one third of global energy consumption and 36 % of global carbon emissions. Optimization of cutting parameters is one of the key strategies for the reduction of energy consumption. The optimization problem for multi-pass turning of grey cast iron considering consumed energy as objective function was developed in the present study, and solved using a brute force optimization algorithm, which guarantees the optimality of the optimization solutions in the given discrete space of input variables values. The results show that consumed energy can be noticeably reduced by the optimization of cutting parameters, compared to the consumed energy for the cutting parameter values recommended by the insert manufacturer. For the production of one part, consumed energy can be reduced by 10.68 %. For the batch of 100 parts, total consumed energy can be reduced by 14.29 %.

**Key words:** multi-pass turning, optimization model, consumed energy, practical constraints, grey cast iron

### 1. INTRODUCTION

The manufacturing industries account for one third of global energy consumption and 36 % of global carbon emissions [1]. Machine tools are dominant end users of electrical energy in manufacturing, and responsible for high carbon emissions [2].

Turning is a machining method in which the material is removed from the surface of a rotating workpiece by using a single-point tool. Resulting geometry is determined by the feed trajectory of the cutting tool. Considering large number of lathes used in manufacturing, as well as low energy efficiency of machine tools in general [3], there is significant potential for energy saving in turning. Optimization of cutting parameters has been recognized as one of the key strategies for the reduction of energy consumption by several researchers recently [2,4].

There are only two recent multi-pass turning optimization studies based on analytical modelling, that consider consumed energy as objective function, either directly [5], or indirectly through carbon emissions [6]. There are also only two recent single-pass turning optimization studies based on analytical modelling, that consider consumed energy as objective function, either directly [7], or indirectly through carbon emissions [8]. Optimization problems in these studies were solved using meta-heuristic algorithms: backtracking search algorithm [5], non-dominated sorting genetic algorithm [6], particle swarm optimization [7], and genetic algorithm [8].

The present study considers newly developed optimization model for multi-pass rough turning [9]. Since meta-heuristic optimization algorithms cannot guarantee the global optimality of the solution [10], single-objective optimization problem developed in this study was solved using a deterministic approach, i.e., a brute force optimization algorithm, which guarantees the optimality of the optimization solutions in the given discrete space of input variables values.

### 2. CASE STUDY

The longitudinal multi-pass rough turning of grey cast iron using a carbide tool is considered to verify the proposed model and method (Fig. 1).

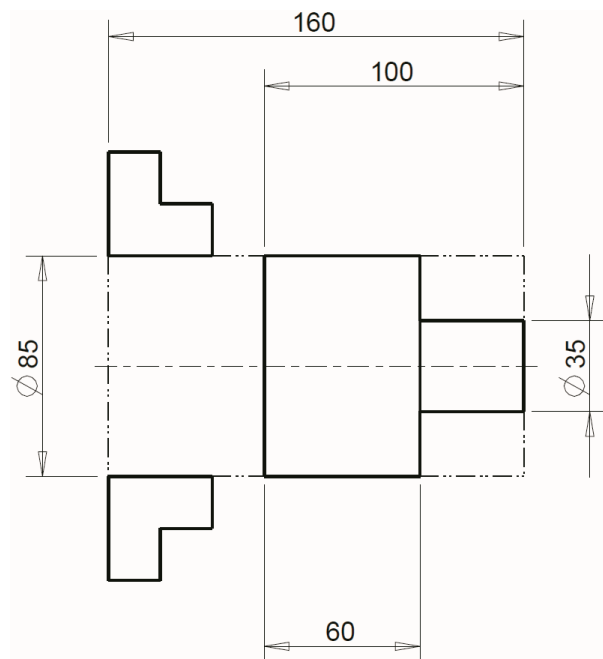


Fig. 1. Workpiece and stock dimensions

Stock is a bar with the diameter of 85 mm and the length of 160 mm made of EN-GJL-250 grey cast iron with a specific cutting force for the unit cutting cross-section  $k_{c1.1} = 1225 \text{ N/mm}^2$  and  $m_c = 0.25$ .

The multi-pass rough turning starts at the diameter of 85 mm, and finishes at the diameter of 35 mm. The mean cutting diameter for multi-pass rough turning is  $D_m = 60 \text{ mm}$ . The cutting length is  $L = 40 \text{ mm}$ .

To define the consumed energy, one needs to

analytically express the machining time. The machining time for multi-pass rough turning is defined as [11]:

$$t_m = \frac{L}{f \cdot n} \cdot i = \frac{L \cdot \pi \cdot D_m}{1000 \cdot f \cdot v_c} \cdot i \quad (1)$$

where  $t_m$  (min) is the machining time,  $L$  (mm) is the cutting length,  $f$  (mm/rev) is the feed rate,  $n$  (rpm) is the spindle speed,  $i$  is the number of passes,  $D_m$  (mm) is the mean cutting diameter, and  $v_c$  (m/min) is the cutting speed.

The machine tool is the CNC lathe Gildemeister NEF 520 with the motor power of  $P_m = 12$  kW and the efficiency of  $\eta = 0.8$ . The spindle speed range is  $n = 10 - 3000$  rpm.

The cutting tool is a toolholder PCLNR 2020K-12 (cutting edge angle of  $\kappa = 95^\circ$  and rake angle of  $\gamma_{oh} = -6^\circ$ ) with a CNMA 120408 insert for roughing, rake angle of  $\gamma_{oi} = 0^\circ$ , nose radius  $r_c = 0.8$  mm, and grade of IC8150 (coated carbide). Recommended cutting conditions are: depth of cut,  $a_p = [1.0 - 4.0]$  mm, feed rate,  $f = [0.05 - 0.43]$  mm/rev, and the cutting speed,  $v_c = [115 - 229]$  m/min. Recommended cutting conditions are valid for the tool life of  $T_c = 15$  min without a coolant [12].

### 3. FORMULATION OF OPTIMIZATION PROBLEM

The model for consumed energy in single-pass turning [13] can be extended for multi-pass turning. Thus, the extended model for consumed energy can be expressed as:

$$E = E_1 + E_2 + E_3 + E_4 \quad (2)$$

where  $E$  (J) is the total energy consumed,  $E_1$  (J) is the energy consumed during machine tool setup,  $E_2$  (J) is the energy consumed during machining,  $E_3$  (J) is the energy consumed during tool change, and  $E_4$  (J) is the energy footprint of the cutting tool.

The energy consumed during machine tool setup ( $E_1$ ) can be evaluated based on the machine tool idle power and total time needed for machine tool preparation and clamping the stock. The energy consumed during machining ( $E_2$ ) can be evaluated based on the machine tool idle power and the energy for material removal [14]. The energy consumed during tool change ( $E_3$ ) can be evaluated based on the machine tool idle power, tool change time, the machining time, and the tool life. Finally, the energy footprint of the cutting tool ( $E_4$ ) can be approximated based on the total energy per insert, number of insert cutting edges, the machining time, and the tool life [15].

The final form of the consumed energy model for multi-pass rough turning can be expressed as:

$$E = P_0 \cdot (t_{mp} + t_c) \cdot 60 + (P_0 + k \cdot MRR) \cdot t_m \cdot 60 + P_0 \cdot t_{tc1} \cdot \frac{t_m}{T} \cdot 60 + \frac{\gamma_E}{n_{ie}} \cdot \frac{t_m}{T} \quad (3)$$

where  $E$  (J) is the total energy consumed,  $P_0$  (W) is the machine tool idle power ( $P_0 = 2400$  W),  $t_{mp}$  (min) is the total machine tool preparation time ( $t_{mp} = 3$  min),  $t_c$  (min) is the time needed for clamping the stock ( $t_c = 0.25$  min),  $k$  (W·s/mm<sup>3</sup>) is the specific cutting energy for a given workpiece material, whose values are given in the referential literature [16] ( $k = 3.25$  W·s/mm<sup>3</sup>),  $MRR$  (mm<sup>3</sup>/s) is the material removal rate,  $t_m$  (min) is the machining time,  $t_{tc1}$  (min) is the tool changing time ( $t_{tc1} = 1$  min),  $T$  (min) is the tool life,  $\gamma_E$  (J) is the total energy

per cutting insert, whose values are given in the referential literature [15] ( $\gamma_E = 5.3 \cdot 10^6$  J), and  $n_{ie}$  is the number of insert cutting edges ( $n_{ie} = 4$ ).

The material removal rate in turning can be expressed as:

$$MRR = \frac{1000 \cdot a_p \cdot f \cdot v_c}{60} \quad (4)$$

where  $MRR$  (mm<sup>3</sup>/s) is the material removal rate for the cutting regime,  $a_p$  (mm) is the depth of cut,  $f$  (mm/rev) is the feed rate, and  $v_c$  (m/min) is the cutting speed.

From the Taylor's tool life equation, the tool life can be expressed as:

$$T = C_0 \cdot a_p^x \cdot f^y \cdot v_c^z \quad (5)$$

where  $T$  (min) is the tool life,  $C_0$ ,  $x$ ,  $y$ , and  $z$  are empirical constants (based on the data in [17],  $C_0 = 8.89 \cdot 10^6$ ,  $x = -0.399$ ,  $y = -0.759$ , and  $z = -2.75$  for turning EN-GJL-250 grey cast iron with a K10 grade carbide tool),  $a_p$  (mm) is the depth of cut,  $f$  (mm/rev) is the feed rate, and  $v_c$  (m/min) is the cutting speed.

The objective function, i.e., consumed energy, defined by equation (2), is subjected to several constraints during the multi-pass rough turning operation. These constraints are related to the part quality, machine tool and cutting tool limitations.

The goal in roughing is to achieve the highest possible productivity, while considering that cutting power does not exceed the allowable maximum power of the spindle motor of the machine tool:

$$\frac{P_c}{\eta} = \frac{F_c \cdot v_c}{60000 \cdot \eta} = \frac{k_{c1.1} \cdot a_p \cdot f \cdot v_c \cdot \left(\frac{1}{f \cdot \sin \kappa}\right)^{m_c} \cdot \left(1 - \frac{\gamma_0}{100}\right)}{60000 \cdot \eta} \leq P_m \quad (6)$$

where  $P_c$  (kW) is the cutting power,  $\eta$  is the machine tool efficiency,  $F_c$  (N) is the cutting force,  $v_c$  (m/min) is the cutting speed,  $k_{c1.1}$  (N/mm<sup>2</sup>) is the specific cutting force for the unit cutting cross-section of 1 mm<sup>2</sup>,  $a_p$  (mm) is the depth of cut,  $f$  (mm/rev) is the feed rate,  $\kappa$  (°) is the cutting edge angle,  $m_c$  is the material dependent constant,  $\gamma_0$  (°) is the rake angle, and  $P_m$  (kW) is the machine tool motor power.

The chip form is of great importance for undisturbed machining, part quality and the protection of the machine tool operator [18]. The chip morphology in turning depends on the ratio of the depth of cut and feed rate, known as cross sectional ratio [17]. To avoid unfavourable chip forms (ribbon, snarled, flat helical), this ratio must be kept at a certain range. With respect to favourable chip form the following constraint may be added:

$$4 \leq \frac{a_p}{f} \leq \xi_{max} \quad (7)$$

where  $a_p$  (mm) is the depth of cut,  $f$  (mm/rev) is the feed rate, and  $\xi_{max}$  is the maximal cross sectional ratio which depends on the workpiece material [19] ( $\xi_{max} = 6$  for grey cast iron).

The following set of constraints can be formulated based on the recommended cutting conditions provided by the cutting insert manufacturer (Iscar):

$$\begin{aligned} 115 &\leq v_c \leq 229 \\ 1.0 &\leq a_p \leq 4.0 \\ 0.05 &\leq f \leq 0.43 \end{aligned} \quad (8)$$

Additionally, considering the available spindle speed range on the machine tool used, as well as the change in the workpiece diameter during machining, the following cutting speed constraint is valid:

$$\frac{\pi \cdot D \cdot n_{min}}{1000} \leq v_c \leq \frac{\pi \cdot D \cdot n_{max}}{1000} \quad (9)$$

In order to avoid unmachined areas on the workpiece [18], the following inequality constraint was also considered:

$$f \leq r_e \quad (10)$$

where  $f$  (mm/rev) is the feed rate and  $r_e$  (mm) is the tool nose radius.

The proposed mathematical model of the multi-pass rough turning optimization problem aims at determining the set of cutting parameter values in order to minimize consumed energy, while considering several constraints. It considers one objective function, four parameters (feed rate, depth of cut, cutting speed and number of passes), four machining constraints and three machining parameter bounds, and can be defined as follows:

Minimize:

$$E = P_0 \cdot (t_{mp} + t_c) \cdot 60 + (P_0 + k \cdot MRR) \cdot t_m \cdot 60 + P_0 \cdot t_{tc1} \cdot \frac{t_m}{T} \cdot 60 + \frac{y_E}{n_{ie}} \cdot \frac{t_m}{T}$$

Subject to:

$$\frac{k_{c1.1} \cdot a_p \cdot f \cdot v_c \cdot \left(\frac{1}{f \cdot \sin \kappa}\right)^{m_c} \cdot \left(1 - \frac{v_0}{100}\right)}{60000 \cdot \eta} \leq P_m$$

$$4 \leq \frac{a_p}{f} \leq \xi_{max}$$

$$115 \leq v_c \leq 229$$

$$1.0 \leq a_p \leq 4.0$$

$$0.05 \leq f \leq 0.43$$

$$\frac{\pi \cdot D \cdot n_{min}}{1000} \leq v_c \leq \frac{\pi \cdot D \cdot n_{max}}{1000}$$

$$f \leq r_e$$

#### 4. RESULTS AND DISCUSSION

The optimization problem for multi-pass rough turning was coded and solved in the Brutomizer software tool [20], using the brute force algorithm. Values of all cutting parameters are discretized by defining appropriate step sizes, in order to obtain solutions that could be easily set on the machine tool. In this way all possible candidates for the solution are enumerated. By checking whether each candidate satisfies the problem's statement, brute-force algorithm guarantees the optimality of the solution for the given discrete space of input variables values.

The optimization problem was solved in 10 s, which is a reasonable optimization time.

The cutting regime which was realized with the depth of cut of  $a_p = 2.5$  mm (ten passes), feed rate of  $f = 0.43$  mm/rev, and cutting speed of  $v_c = 130$  m/min, ensured minimal consumed energy and represented the optimization solution. The values of constraints for this cutting regime are required machine tool power ( $P/\eta$ ) of 4.67 kW and cross sectional ratio of  $\xi = 5.81$ . The resulting tool life is  $T = 17.98$  min.

Recommended cutting regime (starting values at the middle of the range) for the insert used for roughing are: depth of cut of  $a_p = 2.5$  mm (ten passes), feed rate of  $f = 0.24$  mm/rev, and cutting speed of  $v_c = 172$  m/min. Resulting cross sectional ratio for the recommended cutting regime is  $\xi = 10.42$ , which is higher than the

maximal cross sectional ratio for grey cast iron. Consumed energy for the cutting regime representing the determined optimization solution is  $E = 1384574.31$  J, and is lower compared to the consumed energy of  $E = 1550089.63$  J for the recommended cutting regime. Machining time for the cutting regime representing the determined optimization solution is  $t_m = 1.35$  min, and is lower compared to the machining time of  $t_m = 1.83$  min for the recommended cutting regime.

#### 5. CONCLUSIONS

The following conclusions can be drawn from the analysis of the obtained results:

- Consumed energy can be noticeably reduced by optimizing the main cutting parameters starting from the cutting parameter ranges recommended by the cutting insert manufacturer. Consumed energy can be reduced by 10.68 % (165515.31 J).
- Machining time is reduced by 26.15 % (0.48 min) by implementing the cutting regime which represents the optimization solution of the developed single objective turning optimization problem with constraints.
- For the batch of 100 parts, total consumed energy can be reduced by 14.29 %, leading to total savings of 16551531.39 J.
- The cutting regime recommended by the cutting insert manufacturer do not necessarily satisfy certain constraints, such as the cross sectional ratio. On the other hand, the cutting regime determined with the help of the optimization model presented in this study satisfy all the constraints.

#### 6. REFERENCES

- [1] The International Energy Agency: *Tracking Industrial Energy Efficiency and CO<sub>2</sub> Emissions*, 2007. <https://doi.org/10.1787/9789264030404-en>
- [2] Sihag, N., Sangwan, K.S.: *A systematic literature review on machine tool energy consumption*, Journal of Cleaner Production, 275, Article ID: 123125, 2020.
- [3] He, Y., Liu, B., Zhang, X., Gao, H., Liu, X.: *A modeling method of task-oriented energy consumption for machining manufacturing system*, Journal of Cleaner Production, 23, pp. 167-174, 2012.
- [4] Su, Y., Zhao, G., Zhao, Y., Meng, J., Li, C.: *Multi-Objective Optimization of Cutting Parameters in Turning AISI 304 Austenitic Stainless Steel*, Metals, 10, Article ID: 217, 2020.
- [5] Lu, C., Gao, L., Li, X., Chen, P.: *Energy-efficient multi-pass turning operation using multi-objective backtracking search algorithm*, Journal of Cleaner Production, 137, pp. 1516-1531, 2016.
- [6] Liu, Z., Sun, D., Lin, C., Zhao, X., Yang, Y.: *Multi-objective optimization of the operating conditions in a cutting process based on low carbon emission costs*, Journal of Cleaner Production, 124, pp. 266-275, 2016.
- [7] Hassine, H., Barkallah, M., Bellacicco, A., Louati, J., Riviere, A., Haddar, M.: *Multi Objective*

- Optimization for Sustainable Manufacturing, Application in Turning*, International Journal of Simulation Modelling, 14, pp. 98-109, 2015.
- [8] Yi, Q., Li, C., Tang, Y., Chen, X.: *Multi-objective parameter optimization of CNC machining for low carbon manufacturing*, Journal of Cleaner Production, 95, pp. 256-264, 2015.
- [9] Trifunović, M., Madić, M., Radovanović, M.: *Pareto optimization of multi-pass turning of grey cast iron with practical constraints using a deterministic approach*, The International Journal of Advanced Manufacturing Technology, 110, pp. 1893-1909, 2020.
- [10] Diyaley, S., Chakraborty, S.: *Optimization of multi-pass face milling parameters using metaheuristic algorithms*, Facta Universitatis, Series: Mechanical Engineering, 17, pp. 365-383, 2019.
- [11] Panneerselvam, R., Sivasankaran, P.: *Process Planning and Cost Estimation*, PHI Learning, Delhi, India, 2016.
- [12] Iscar Ltd.: *Non-Rotating Tool Lines (Metric Version Catalog)*, 2017.
- [13] Rajemi, M.F., Mativenga, P.T., Aramcharoen, A.: *Sustainable machining: selection of optimum turning conditions based on minimum energy considerations*, Journal of Cleaner Production, 18, pp. 1059-1065, 2010.
- [14] Gutowski, T., Dahmus, J., Thiriez, A.: *Electrical Energy Requirements for Manufacturing Processes*, Proceedings of the 13th CIRP International Conference on Life Cycle Engineering, pp. 623-628, Leuven, Belgium, Katholieke Universiteit Leuven, 2006.
- [15] Dahmus, J.B., Gutowski, T.G.: *An environmental analysis of machining*, Proceedings of the 2004 ASME International Mechanical Engineering Congress and RD&D Expo, pp. 643-652, Anaheim, CA, USA, The American Society of Mechanical Engineers, 2004.
- [16] Kalpakjian, S., Schmid, S.: *Manufacturing Engineering and Technology, Fifth Edition*, Pearson Education, Upper Saddle River, NJ, USA, 2006.
- [17] Tschatsch, H.: *Applied Machining Technology*, Springer-Verlag, Berlin Heidelberg, Germany, 2009.
- [18] Klocke, F.: *Manufacturing Processes 1: Cutting*, Springer-Verlag, Berlin Heidelberg, Germany, 2011.
- [19] Kopač, J.: *Odrezavanje*, Fakulteta za strojništvo, Ljubljana, Slovenija, 1991.
- [20] Brutomizer, <http://www.virtuode.com/index.php/products/brutomizer/> 2021.

**Authors:** Assist. Prof. Milan Trifunović, Assist. Prof. Miloš Madić, Assist. Prof. Nikola Vitković, University of Niš, Faculty of Mechanical Engineering in Niš, Department of Production Information Technologies, Aleksandra Medvedeva 14, 18106, Niš, Serbia, Phone: +381 18 500-657, Fax: +381 18 588-244. E-mail: [milan.trifunovic@masfak.ni.ac.rs](mailto:milan.trifunovic@masfak.ni.ac.rs); [madic@masfak.ni.ac.rs](mailto:madic@masfak.ni.ac.rs); [nikola.vitkovic@masfak.ni.ac.rs](mailto:nikola.vitkovic@masfak.ni.ac.rs)

**ACKNOWLEDGMENTS:** This research was financially supported by the Ministry of Education, Science and Technological Development of the Republic of Serbia (Contract No. 451-03-9/2021-14/200109)

Sredanović, B., Čiča, Đ., Borojević, S., Tešić, S., Kramar, D.

## EXPERIMENTAL ANALYSIS AND OPTIMIZATION OF THIN-WALLED TUBULAR PARTS MILLING

**Abstract:** A certain percentage of mechanical parts in the engineering (parts in automotive industry, medical and measuring devices, parts in energetic sector, and etc.), refers to thin-walled structures with optimized shapes and dimensions. In addition to the requirements for a special shape of the structure, there are also requirements related to the dimensional accuracy and surface quality. In this paper, the milling of thin-walled tubular parts is analyzed. Workpiece of mentioned parts was C45E (AISI 1045) steel. Experimental analysis and optimization is based on Taguchi's experimental plan. The influence of cutting process parameters, depth of cut, feed per tooth and radial depth of cut, was analyzed. As the output cutting parameters, the dimensional accuracy and machined surface quality parameters, were measured and analyzed. Based on experimental data, modeling and optimization were performed. The obtained results defined the optimal input cutting process parameters, which give the best results in milling.

**Key words:** thin-walled structure, milling, experiment, optimization

### 1. INTRODUCTION

Thin-walled structures are most often used as structural parts in engineering due to their homogeneity and excellent load-to-weight ratio. Examples of such components are ribs, partitions, supports. These structures are technologically very complex because they are made of a wide materials range, have a complex geometry, and often relatively large dimensions. Many thin-walled structures forms have been developed, which can generally be divided into the next following types: line shapes, triangular shapes, rectangular shapes, hexagonal shapes, circular shapes and complex shapes. Complex forms of thin-walled structures are widely present in almost all branches of the metalworking industry (automotive, aerospace, energy, medicine devices, measuring devices, and etc.). They are most often used for the production of other assembly parts housings, as a base or supporting part for other parts in the assembly. These structures became technologically extremely complex, if stronger and harder materials are used for their production. The most common production technologies thin-walled structures are: casting and welding, in case simpler, bigger or non-functional surfaces on parts, and cutting technologies, in case of complex, smaller, or functional surfaces on parts.

Thin-walled structures, despite their simple design, bring problems to the machining in terms of technology and workability [1, 2, 3]. Although they have high rigidity in the vertical direction (wall extension direction), the most common cause of problems in their processing is their low rigidity in the perpendicular direction to the wall [4, 5]. Aluminum and its alloys are the dominant material of thin-walled structures, but other materials are often used. Other types of materials, such as steels or special alloys, are especially used in cases where the thin-walled structure construction requires higher strength, hardness, heat loads resistance, wear resistance, and etc. In addition to the problems in terms of manufacturability, this also complicates the

problems in terms of materials machinability. In the case of the application of cutting technology in the production of thin-walled structures from stronger materials, high machining accuracy and the machined surface quality are often required. If harder materials are used, the aforementioned machining problems became very complicated. Cylindrical shapes of thin-walled structures, made of relatively stronger and harder materials, are most often used as parts in the process industry, as parts of measuring devices, nozzles, burners, heaters, tools for plastics casting, tools in the textile and wood industry and the like. The milling is dominant method for machining of tubular thin-walled structures, due to the possibility of performing complex cutting tool movements, adequate precision and productivity. During machining, relatively higher cutting forces occur, which more intensively deform the thin walls (Figure 1).

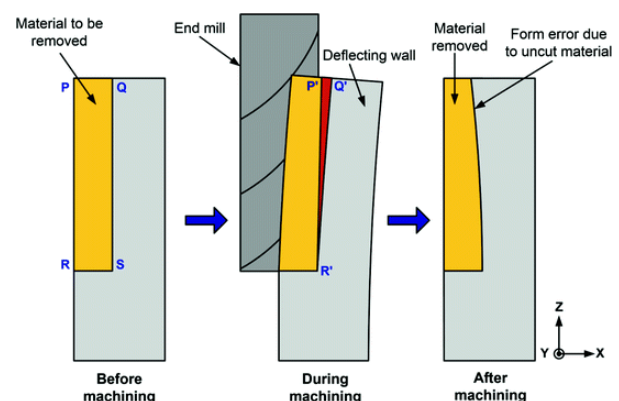


Fig. 1. Thin-walled structure deformation [3]

The action of a relatively higher cutting force on the thin and high structure wall, leads to a large deviation of dimensions and shapes due to elastic and plastic deformations of the thin walls of the structure [6]. The deviation of the dimensions of the cylindrical thin-walled structure is specific, and is reflected in the

changes in wall thickness in vertical direction, and deviations in terms of circularity and cylindricality. Higher cutting forces and a large height/base ratio of the structure causes the higher vibrations, and leads to poorer machined surface roughness.

In this paper, experimental investigates on influence of technological parameters on the machining accuracy and quality in milling of cylindrical thin-walled structures are shown. The surface roughness, wall thickness deviation and circularity of the wall were analyzed. Based on experimental obtained data, modeling and optimization are performed.

## 2. EXPERIMENTAL SETUP

The experiment were performed on three-axis milling machining center Emco Concept MILL 450 equipped with a Sinumerik 810D/840D control unit with Windows platform (Figure 2). Power of machine is 11 kW, and maximum main spindle revolutions per minute is 11000. The programming of the machining center was performed using the SolidCAM software. Movement on linear axis have acceleration of 2 m/s<sup>2</sup>. A milling cutter, marked as Dormer S814HA, was used to machining the experimental samples. The cutter has four teeth. The diameter of the cutter is  $d_c = 16$  mm. The length of the cutter body is of  $l_1 = 92$  mm, while the cutting length of the tool is  $l_2 = 32$  mm. The overhang of the tool was set to  $l_3 = 40$  mm. The tool mounting was performed with an ER32 elastic sleeve with an axial nut system, which is mounted in the ISO 40 holder.



Fig. 2. Experimental setup

Carbon steel C45E (Č.1530, DIN 17200, EN 10083) was used as the workpiece material for experimental research. This structural steel is used for the production of responsible parts, where increased wear resistance and strength are required. It has the possibility of heat treatment, such hardening and annealing. Workpiece was tubular, with outer diameter 40 mm, height 40 mm, and wall thickness 1.5 mm (Figure 3.).

The machined surface roughness was measured after workpiece samples machining, using a mobile measuring device Mitutoyo Surftest SJ 301. Measurement of wall thickness and circularity deviations was performed on Carl Zeiss Duramax 5/5/5 CNC coordinate measuring machine. Measurement accuracy of this device is  $\pm 2.3$   $\mu\text{m}$ , while repeatability

is 1.7  $\mu\text{m}$ . The measurement on machined workpiece was performed at five different points in height direction of the thin-walled structure, starting from 5 mm, with a step of 5 mm, to a height of 35 mm.

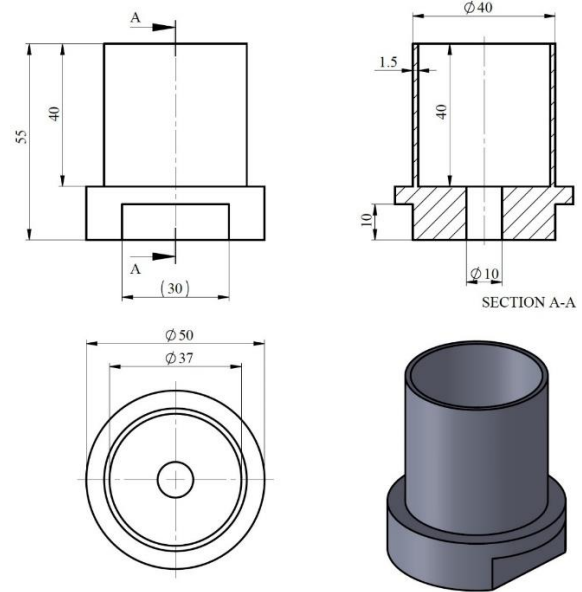


Fig. 3. Workpiece

Taguchi's orthogonal L9 ( $3^2$ ) experimental plan was used as the design of experiment. There was nine combinations of the three cutting process parameters at three levels, varied on three level (Table 1). All machining parameters, variable and constant, were adopted according to the recommendations of the cutting tool manufacturer. The depth of cutting ( $a_p$ ), as the first parameter (P1) was varied at three levels: 2, 4 and 6 mm; feed per tooth ( $f_z$ ), as the second parameter (P2) at three levels: 0.06, 0.12 and 0.18 mm/tooth, and as the third parameter (P3) milling width ( $a_e$ ), at three levels: 0.5, 1.0, and 1.5 mm.

No.	P1	P2	P3	$a_p$ (mm)	$f_z$ (mm/tooth)	$a_e$ (mm)
1	-1	-1	-1	2.0	0.06	0.5
2	-1	0	0	2.0	0.12	1.0
3	-1	+1	+1	2.0	0.18	1.5
4	0	-1	0	4.0	0.06	1.0
5	0	0	+1	4.0	0.12	1.5
6	0	+1	+1	4.0	0.18	0.5
7	+1	-1	+1	6.0	0.06	1.5
8	+1	0	-1	6.0	0.12	0.5
9	+1	+1	0	6.0	0.18	1.0

Table 1. Experiment runs

The cutting speed was kept at constant level for all combinations, on value of  $v_c = 120$  m/min. As a cooling and lubrication technique, flooding on the outside of the tool through two nozzles was used. A synthetic emulsion diluted in water, with a content of 5%, was used. The fluid pressure was 5 bar, and the flow was 40 l/min with recirculation of the fluid.

### 3. RESULTS AND DISCUSSIONS

The analysis of machining accuracy includes the analysis of the wall thickness deviation  $\delta$  (mm) from the nominal value of 1.5 mm, and the measurement of the mean circularity  $K$  (mm). Both parameters were measured at several points at five heights in the vertical direction of the thin-walled structure. Intervals between heights, starting from the bottom of the structure, was 5 mm. The analysis of the machined surface roughness included measurements in the vertical direction, along the height of the thin-walled structure  $R_{av}$  ( $\mu\text{m}$ ); and in the horizontal direction, in the direction of planar movement of the cutter  $R_{ah}$  ( $\mu\text{m}$ ). Machining time  $t$  (min), as economical parameter, was measured also.

No.	$a_p$	$f_z$	$a_e$	$\delta$ (mm)	$K$ (mm)	$R_{av}$ ( $\mu\text{m}$ )	$R_{ah}$ ( $\mu\text{m}$ )	$t$ (min)
1	2.0	0.06	0.5	0.136	0.027	0.90	0.72	26.53
2	2.0	0.12	1.0	0.266	0.034	1.40	0.83	7.47
3	2.0	0.18	1.5	0.216	0.039	1.88	1.06	3.78
4	4.0	0.06	1.0	0.216	0.029	1.37	0.70	7.47
5	4.0	0.12	1.5	0.230	0.046	1.74	0.89	2.95
6	4.0	0.18	0.5	0.214	0.041	0.78	1.14	4.82
7	6.0	0.06	1.5	0.144	0.039	1.71	0.79	3.95
8	6.0	0.12	0.5	0.135	0.033	0.84	0.92	5.03
9	6.0	0.18	1.0	0.165	0.061	1.02	1.16	2.10

Table 2. Experiment results

Figure 4 shows that measured wall thickness depends on the combination of the cutting parameters of the milling process and the measuring point height, along the vertical of the cylindrical thin-walled structure. Based on the diagram, it can be concluded that the thickness was the highest at a height of 5 mm, and then decreased. After the mentioned decreasing, it slightly increased at the measuring point at a height of 25 mm.

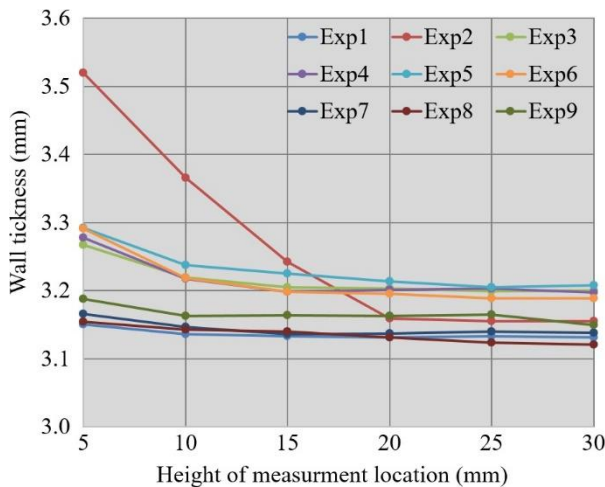


Fig. 4. Wall thickness for different experiment runs

The highest value of the mean deviation of the wall thickness of 0.266 mm was obtained using the cutting parameters  $a_p = 2.0$  mm,  $f_z = 0.12$  mm/tooth and

$a_e = 1.0$  mm, while the lowest value of 0.135 mm for the processing parameters  $a_p = 6.0$  mm,  $f_z = 0.12$  mm/tooth and  $a_e = 0.5$  mm. Higher deviation values were obtained for smaller depths of cutting. Based on the measuring, recalculating of circularity data was performed. Figure 5 shows diagrams of measured mean circularity.

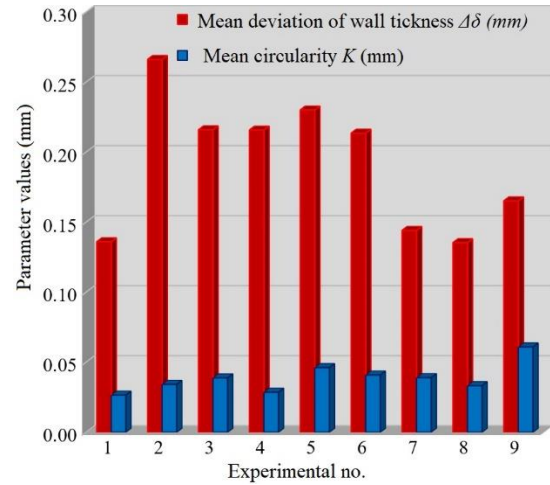


Fig. 5. Mean circularity for different experimental runs

The highest value of the mean circularity 0.061 mm, was obtained using the cutting parameters  $a_p = 6.0$  mm,  $f_z = 0.18$  mm/tooth and  $a_e = 1.0$  mm, while the lowest value of 0.029 mm with the cutting parameters  $a_p = 4.0$  mm,  $f_z = 0.06$  mm/tooth and  $a_e = 1.0$  mm (Figure 6). Higher mean circularity values were obtained for greater depths of cutting and cutting widths.

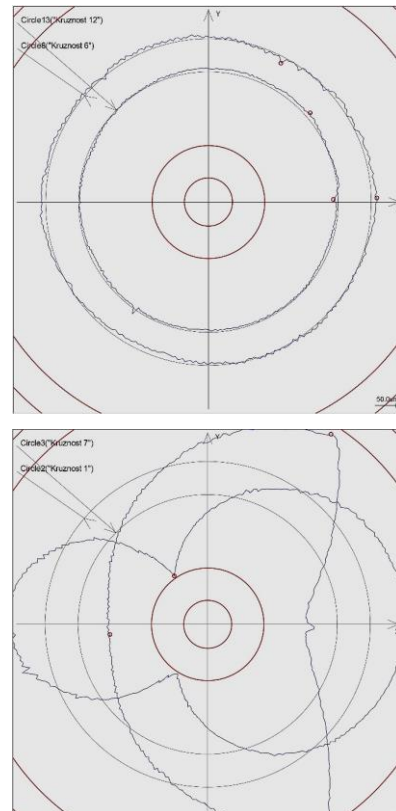


Fig. 6. The lowest (above) and highest (below) mean circularity measuring plot

The measured values of horizontal and vertical surface roughness depending on the combination of cutting parameters are shown in Figure 7.

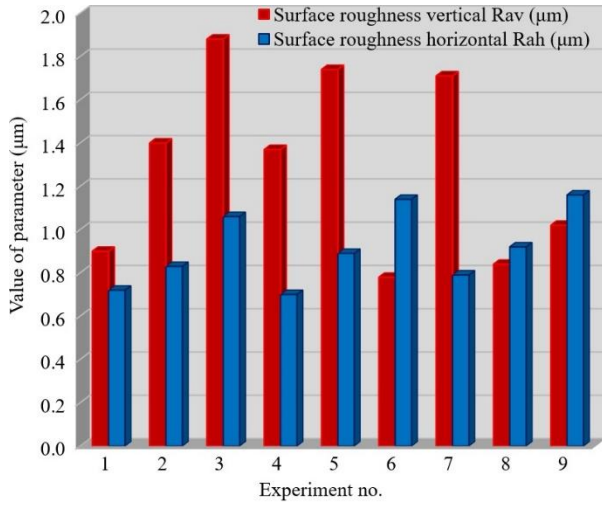


Fig. 7. Surface roughness for different experimental runs

The appearance of the machined surface, taken under a tool microscope Mitutoyo TM505, is shown in Figure 8. In the picture of the machined surface with the worst roughness, dark parts can be seen, which represent the waves created by the movement of the cutter. In the picture of machined surface with finest roughness, in some places, can be seen places of plunged and poorly separated material of the workpiece.

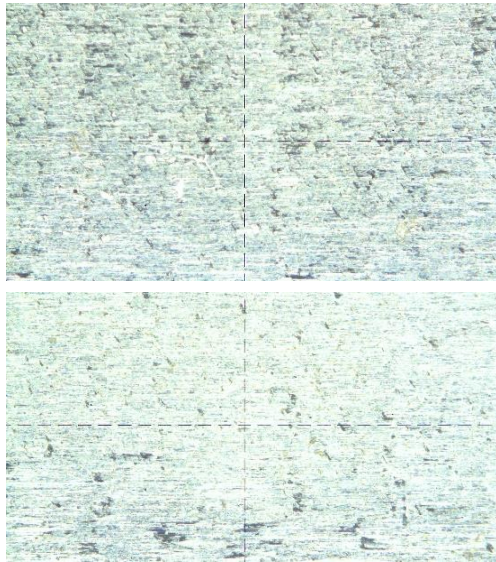


Fig. 8. The worst (above) and finest (below) machined surface under microscope

The highest value of the measured vertical roughness is 1.88 µm, which was obtained using the processing parameters  $a_p = 2.0$  mm,  $f_z = 0.18$  mm/tooth and  $a_e = 1.5$  mm, while the lowest value is 0.78 µm, obtained with the parameters  $a_p = 4.0$ ,  $f_z = 0.18$  mm/tooth and  $a_e = 0.5$  mm. Higher values of vertical roughness were obtained for larger machining widths. The highest value of horizontal roughness is 1.16 µm, which was obtained

with machining parameters  $a_p = 6.0$  mm,  $f_z = 0.18$  mm/tooth and  $a_e = 1.0$  mm, The lowest value is 0.70 µm, is obtained with  $a_p = 4.0$  mm,  $f_z = 0.06$  mm/tooth and  $a_e = 1.0$  mm. Higher values of horizontal roughness were obtained for larger steps per tooth.

### 3.1 Modeling of output parameters

For statistical analysis of experimentally measured data, and model generating, the software DesignExpert 7.1 was used. Statistical analysis is based on analysis of variance (ANOVA). Based on the measured, entered and untransformed experimental obtained values, the software proposed an appropriate models using the least sum of squares method. Determination of input parameters significance was based on F values (target is greater than 15) and P values (target is less than 0.05). The adequacy of the models was determined based on the coefficient of regression, signal-to-noise ratio, mean value and standard deviation. According to the previously presented results, statistical analysis and modeling of the following quantities were performed:

- mean deviation of wall thickness
- mean circularity
- surface roughness in vertical direction
- surface roughness in horizontal direction

Based on the mean values of the wall thickness deviation  $\Delta\delta$ , the software for statistical analysis proposed a model with the interaction of two parameters versus linear (2FI vs Linear). The P-value of the model is 0.028, while the most influential parameter is depth of cutting, whose P-value is 0.006. According to the analysis of variance, a mean value of  $\bar{x} = 0.19$ , and standard deviation of  $SD = 0.009$  were obtained. The signal-to-noise ratio is  $S/N = 15.61$ , and the regression coefficient is  $R^2 = 0.99$ . Based on these values, it is concluded that the model is adequate. By the surface response method (RSM), a mathematically formalized dependence of the mean deviation of the wall thickness depending on cutting parameters was obtained in form:

$$\Delta\delta = -0.107 - 0.028 \cdot a_p + 0.648 \cdot f_z + 0.719 \cdot a_e + 0.499 \cdot a_p \cdot f_z - 0.068 \cdot a_p \cdot a_e - 2.936 \cdot f_z \cdot a_e \quad (1)$$

The software proposed a model with the interaction of two parameters versus linear for model of mean circularity  $K$ . Calculated model P-value is 0.028, while the most influential parameter is feed, with P-value 0.003. Mean value is  $\bar{x} = 0.039$ , and standard deviation is  $SD = 0.00082$ . The signal-to-noise ratio is  $S/N = 47.39$ , and the regression coefficient is  $R^2 = 0.99$ . Based on these values, it is concluded that the model is adequate. Mathematically model was obtained in form of:

$$K = 0.035 - 0.008 \cdot a_p + 0.066 \cdot f_z + 0.004 \cdot a_e + 0.062 \cdot a_p \cdot f_z + 0.003 \cdot a_p \cdot a_e - 0.024 \cdot f_z \cdot a_e \quad (2)$$

Model response diagrams for mean values of the wall thickness deviation and mean circularity are shown on Figures 8 and 9, respectively.



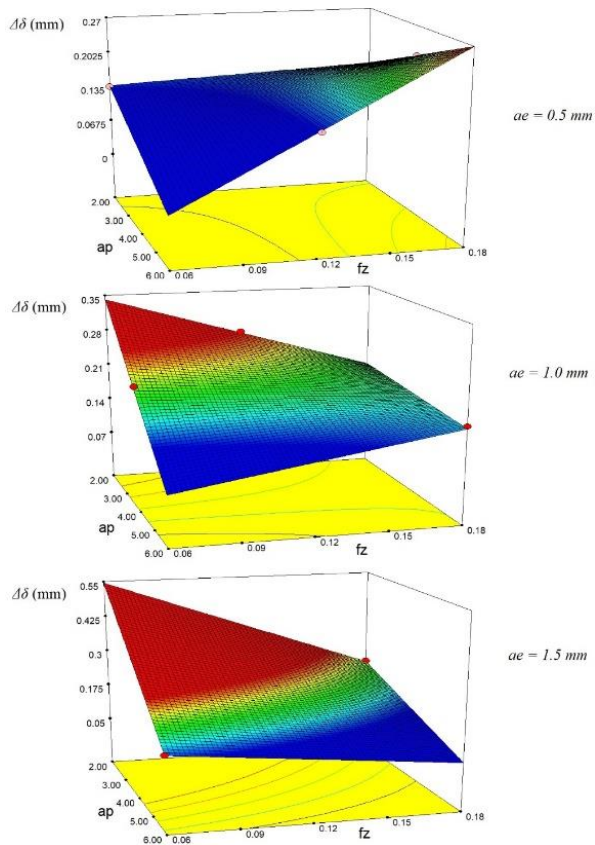


Fig. 8. Model response for  $\Delta\delta$

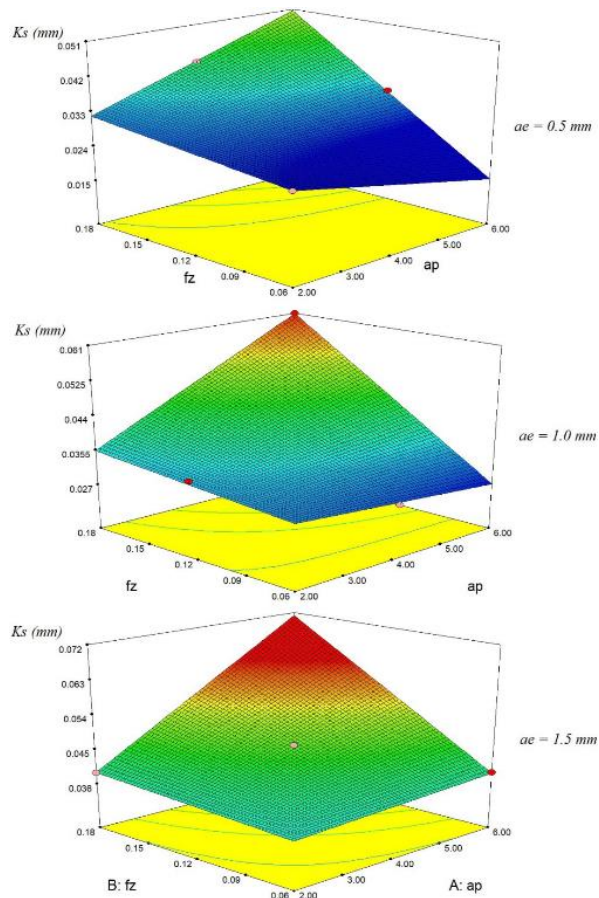


Fig. 8. Model response for  $\Delta K$

For both surface roughness parameters  $R_{av}$  and  $R_{ah}$ , the software proposed a model with the interaction of two parameters versus linear. P-values for model of  $R_{av}$  is 0.0002, and for  $R_{ah}$  is 0.0001. Most influential parameters for vertical surface roughness is milling width (P-value is 0.0001), and for horizontal surface roughness is feed per tooth (P-value is 0.0001 also). Mean values is  $\bar{x} = 1.29$  and standard deviation is  $SD = 0.057$ , for vertical surface roughness. Mean values is  $\bar{x} = 0.91$  and  $SD = 0.036$ , for horizontal surface roughness. Signal to noise ratio is 26.96 for vertical and 22.78 for horizontal surface roughness. Coefficients of regression is 0.991 and 0.97, respectively. The software gave a mathematical form of dependence between input and output parameters:

$$R_{av} = 0.348 + 0.053 \cdot a_p - 1.699 \cdot f_z + 1.353 \cdot a_e + -0.104 \cdot a_p \cdot a_e \quad (3)$$

$$R_{ah} = 0.442 + 0.022 \cdot a_p + 3.194 \cdot f_z \quad (4)$$

Using the previous mathematical formulas, a diagram or response surface is formed for horizontal surface roughness (Figure 9).

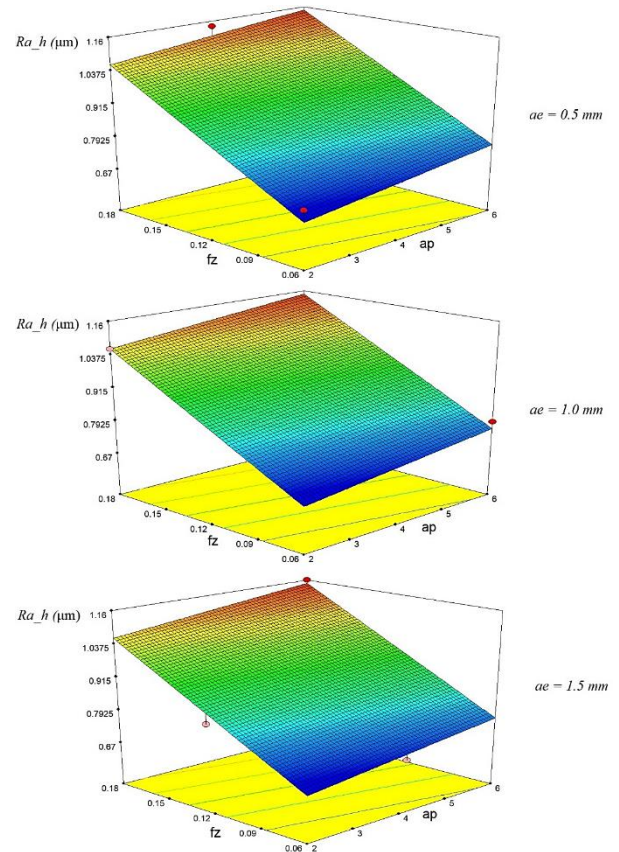


Fig. 9. Model response for  $R_{ah}$

### 3.2 Optimisation of process parameters

For the case of perform finish milling a cylindrical thin-walled structure, the minimum roughness of the machined surface, the minimum mean deviation of the wall, and the minimum mean circularity are chosen as the optimization target functions. The mathematical

framework of optimization, according to the mentioned requirements, is given in Table 3.

Parameter	Target	Lower	Upper	Lower	Upper	Para.
		Limit	Limit	Weight	Weight	W
$a_p$	In range	2.0	6.0	1	1	3
$f_z$	In range	0.06	0.18	1	1	3
$a_e$	In range	0.5	1.5	1	1	3
$R_{av}$	Minimized	0.026	0.061	1	1	3
$R_{ah}$	Minimized	0.78	1.88	1	1	3
$\Delta\delta$	Minimized	0.7	1.16	1	1	3
K	Minimized	0.135	0.266	1	1	3

Table 3. Optimisation framework

The optimization procedure, based on the previous mathematical framework, gave 27 possible solutions. As the optimal solution for finish milling, the cutting parameters  $a_p = 2.13$  mm,  $f_z = 0.066$  mm/tooth and  $a_e = 0.5$  mm were obtained. For these parameters, the desirability of optimization targets is 96.8%. Optimization solution desirability depending on the depth of cutting and feed at most (Figure 10). From the diagram, can be concluded that smaller values of cutting parameters should be used in finish milling. Higher values of depth of cutting can be used, which must be accompanied by a significant reduction in feed per tooth.

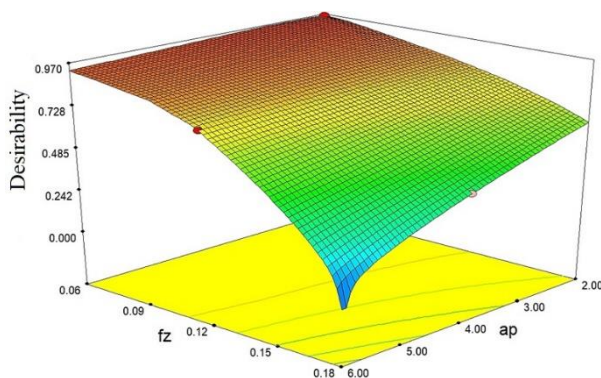


Fig. 10. Desirability for different parameters

#### 4. CONCLUSIONS

There was conducted experimental investigations of the influence of milling parameters: processing depth, feed per tooth and milling width, on the output parameters in milling of tubular thin-walled structure. The outputs are: deviation of wall thickness, circularity, and surface roughness.

Based on the analysis of variance, the significance of cutting parameters on the output parameters was determined. Linear models with a parameters combination, which describes the influence of the values of cutting parameters, have been developed. There is noted that the increase of cutting parameters, through the increase of cutting force, leads to a decrease in machining accuracy, according increase of the wall thickness and structure circularity. As a result of

optimization, optimal technological parameters were obtained. However, further research should focus on the analysis of the machining of thin-walled parts made of special materials.

#### 5. REFERENCES

- [1] Pompa, M.: *Computer Aided Process Planning for High-Speed Milling of Thin-Walled Parts-Strategy-Based Support*, PhD thesis, Department for Engineering Technology of the University of Twente, Enschede, 2010.
- [2] Weifang, C. et al.: *Deformation prediction and error compensation in multilayer milling processes for thin-walled parts*, International Journal of Machine Tools and Manufacture, vol. 49, no. 11, pp. 859 - 864, 2009.
- [3] Bolar, G. et al.: *Numerical modeling and experimental validation of machining of low-rigidity thin-wall parts*, pp. 99 - 122, in Precision Product - Process Design and Optimization, (ed.) S. Pande, S. Dixit, Springer, London, 2018.
- [4] Li, Z. L., Zhu, L. M.: *Compensation of deformation errors in five-axis flank milling of thin-walled parts via tool path optimization*, Precision Engineering, vol. 55, pp. 77-87, 2019.
- [5] Borojević, S., Lukić, D., Milošević, M., Vukman, J., Kramar, D.: *Optimization of process parameters for machining of Al 7075 thin-walled structures*, Advances in Production Engineering & Management, vol. 13, no. 2, pp. 125-135, 2018.
- [6] Cica, Dj., Borojevic, S., Jotic, G., Tesic, S., Sredanovic, B.: *Multiple performance characteristics optimization in end milling of thin-walled parts using desirability function*, Transactions of the Canadian Society for Mechanical Engineering, vol. 44, no. 1, pp. 84-94, 2020.

**Authors:** Assist. Prof. Branislav Sredanović, Full Prof. Đorđe Čiča, Assoc. Prof. Stevo Borojević, MSc. Saša Tešić, University of Banja Luka, Faculty of Mechanical Engineering, Department of Production and CAx Technologies, Bulevar Vojvode Stepe Stepanovića 75, 78000 Banja Luka, Republic of Srpska, Bosnia and Herzegovina, Phone: +387 51 433 001, Fax: +387 51 465 085,

E-mails: [branislav.sredanovic@mf.unibl.org](mailto:branislav.sredanovic@mf.unibl.org),

[djordje.cica@mf.unibl.org](mailto:djordje.cica@mf.unibl.org),

[stevo.borojevic@mf.unibl.org](mailto:stevo.borojevic@mf.unibl.org),

[sasa.tesic@mf.unibl.org](mailto:sasa.tesic@mf.unibl.org),

**Assoc. Prof. Davorin Kramar**, University of Ljubljana, Faculty of Mechanical Engineering, Department of Machining Technology Management, Aškerčeva 6, 1000 Ljubljana, Slovenia, Phone: +386 1 477 14 38, Fax: +386 1 477 17 68,

E-mail: [davorin.kramar@fs.uni-lj.si](mailto:davorin.kramar@fs.uni-lj.si)

**ACKNOWLEDGMENTS:** This paper is results of collaboration between Laboratory for cutting at FME Ljubljana and Laboratory for cutting technologies and machining systems at FME Banja Luka. Collaboration is supported by the ministries of the host countries.

Pămîntaş, E., Banciu, F.V.

## METAL CUTTING IS IT STILL OF INTEREST TO ANYONE?

**Abstract:** For almost 100 years, the phenomena in the metal cutting process have offered researchers in the field a wide range of research topics, and at the same time, as much satisfaction, both in terms of deepening theoretical knowledge, especially in terms of the practical results obtained. Interest in this field has declined dramatically, however, since the beginning of the third millennium. Has the cutting process reached the limits of knowledge by their exhaustion or has it become inefficient for industry compared to other new processes for manufacturing metallic, non-metallic materials and composites? Why is the field no longer as attractive to researchers? Here is what this paper tries to clarify and propose to researchers in the field to reinvent the approach of the cutting process, as an incomplete explored and still excellent perspective, not only for the manufacturing industry, but also for the theoretical foundations of the cutting phenomenon.

**Key words:** cutting process, the phenomenon of metal cutting, cutting geometry, fundamental research, applied research

### 1. INTRODUCTION

Chipping/metal cutting, as the initiates know, is the method by which, under the action of relative movements between the semi-finished part and the cutting tool, the surplus material is divided into layers, and then it is removed in the form of chips, until the shapes, dimensions and surface quality indicated in the execution drawing of a piece are obtained.

Some processes of the method are known since prehistory and can be documented by the existence of artifacts, most often non-metallic, that have undergone such a transformation (carving, trepanation, drills, scratches, grinding, etc.), and then of the inscriptions and pictograms made on different supports describing various working processes (i.e. in ancient Egypt, a rotating tool - wimble was used to drill stones and found in the museums of antiquities of the world.

During the Middle Ages (or rather, between Antiquity and the Renaissance) the cutting processes develop, less as a method but more as a number of objects subject to processing and as diversification of the fields of use, without mentioning, however, concerns to explain any process on the cause-effect relationship or to theorize the accompanying physical phenomena.

By the end of the 19th century, the demand for objects processed by processes specific to the cutting method leads to the development of rudimentary installations – usually with action based on human force and less often of the water fall – and of tools, devices and other aids.

After 1850, the first concerns began to appear regarding the explanation of how to form chips and the phenomena underlying this process, for the most common procedures such as drilling and turning.

Thus, around 1870, the first attempts to explain the phenomenon of chip formation are mentioned, and between 1881 and 1883 Arnulph Henry Reginald Mallock reveals the importance of chip shearing and friction at the tool-part interface [1] as well as the

influence of coolants-lubrication [2].

With the passage into the twentieth century, the concerns in the field intensify, in proportion to the scale of the industrial revolution and the transition to mass production, both from the point of view of materials subject to chipping and cutting tools, cutting processes and related machine tools, as well as in terms of researching the phenomenology of metal cutting and physical explanation of the cause-and-effect relationships involved.

The experimental equation of F.W. Taylor from 1907 that links the durability of the cutting tool blade to the cutting rate can be considered as the beginning of the experimental modeling of the phenomena in the cutting, for the purpose of their management, control and prediction.

The last century of the 2nd millennium is characterized by a large and rapid development of industrial production in which cutting processes occupy an increasingly significant percentage, so that the first years of the current millennium record a percentage of about 30% of the total manufactured parts that include cutting operations: turning, broaching, drilling, milling, threading, toothing, grinding, honing, lapping, etc.

At the same time, the interest of producers has gone from quantity to quality, optimization, efficiency, maximization of profit, minimization of resources used, etc. [2]. Normally, the attention paid to the phenomenology of metal cutting has increased proportionally. There were approached research topics belonging to all the cutting processes, looking for answers regarding the influence of:

- parameters of metal cutting process,
- the cutting tool geometry,
- the quality of the semi-finished materials and the tool materials,
- coolant-lubricating fluids,
- structural/ kinematic composition of machine tools,
- tool fastening/fixing/entrainment systems,

- the systems and fastening for semi finished (parts),
- on the following aspects (without their string being meant to be exhaustive):
- cutting forces,
  - the power / mechanical work consumed by the operation,
  - the durability of the cutting tool edge,
  - machinability of the material,
  - the shape of chips,
  - the time of phase/ cutting operation,
  - dynamic stability of the process,
  - the temperature released during the process,
  - the quality of the worked surface,
  - precision of processing.

The results of the researches in the field have been published - all over the world, especially in the countries that have been on the front line of industrialization - in the form of Research/Work Reports, Scientific Papers, Dissertations, PhD Theses. If all these results were gathered in one place – the current technique would allow the allocation of a "cloud" for this – it would result in a vast database, which analyzing it in terms of how it was or is or is or maybe will be used, we would find the following:

- A very small part of this huge database has been capitalized by adding and supplementing theoretical knowledge that leads to the description and understanding of the phenomena of splinting.
- Another small part of these researches were capitalized by the large companies producing cutting tools and machine tools respectively by compiling interactive libraries used to choose the type of tool, its geometry and the working parameters most appropriate to the desired machining by cutting.
- Another part, it was used to improve the performance of various cutting processes, usually for particular cases that generated the need for research and therefore lost their validity over time or became obsolete.
- Most of the results of the published applied researches have neither found their expected echo nor have been capitalized sustainably.

The above approximations, of the proportions of use of the results of research in the field of metal cutting and the way in which it was made, can give an overall picture of the decrease in interest in research work in the cutting of metals, non-metals and composites. Let's try to see why, because "only knowing the cause, the effect can be eliminated" ( sublata causa, tolitur effectus).

## 2. BASIC CONCEPTS

First of all, let us try to delimit our area of interest in the present argumentation. The directions of research taken into consideration refer to the classical processing processes belonging to the cutting method.

The research papers were carried out as a result of two distinct needs:

1. The first is in connection with the need to research the phenomenological bases of the method. These researches were approached first in universities with

scientific and technical profile and then also in departmental research institutions, governmental or private. In these cases, the research funds are not allocated mainly to research in the field of metal cutting but to the accompanying physical phenomena (temperatures, vibrations, mechanical work of elastic / plastic deformation, erosions, frictions, chemical dissociations, etc.) and the topics are chosen according to the curiosity / interest or skills of the research team participating in the national or international research grants competitions.

2. The second "engine" is the emergence of new materials, with mechanical characteristics so different from those of the existing ones that for their processing by cutting, the manufacturing companies cannot afford to extrapolate the working parameters of the usual processing processes, nor do they assume the risks of not knowing the output quantities from the cutting process in the form of forces, moments, consumed powers, temperatures released in the process, emissions, the quality of the surfaces obtained, the micro-structural integrity of the processed parts, etc. Research funds in these cases are allocated on the basis of topics specified by the private beneficiary through a research contract.

The goal is usually related to the behavior in chipping of new materials, recommended working regimes to improve the quality of the processed surface, reduce cutting efforts, introduce new types of cutting tools, coolants-lubrication or new load-bearing or kinematic structures or driving to advanced machine tools.

Regardless of how the research was initiated or the one in which the financing of the research contracts was made, the type of research approached is experimental research and their results are almost without exception, experimental computational (empirical) relationships, nomograms for choosing cutting regimes - the depth of cutting, the feed and the cutting speed (ap, f, v) - or pairs of their recommended values for various combinations of: cutting process, tool material, semi-finished material, quality of the processed surface, type of coolant-lubrication, specific working conditions, etc. For example, Figure 1 shows a generic form of experimental relationship very often used in the last 50... 70 years to describe the output size of the process - Cutting force - I (the cutting forces can be measured in terms of three components: cutting force Fc, feed force Ff and passive force Fp. - only the index in the formula changes: c, f, p).

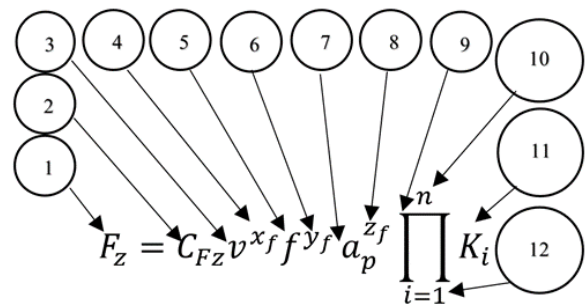


Fig. 1. Generic form of the empirical relationship for modeling the cutting force at turning

Analyzing the relationship, it is found that it takes into account the following components of the process: - input variables – the three parameters of the working regime  $v$  (3),  $f$  (5) and  $a_p$  (7), affected by the specific exponents  $x_f$ , (4)  $y_f$  (6) and  $z_f$  (8), - product  $\Pi$  (9) of a series from  $i = 1$  (12) to  $n$  (10) coefficients  $K_i$  (11) which take account of the influences:

- coolant-lubrication,
- tool material –steel, metal carbides, diamond, etc.,
- the material of the blank - steel, cast iron, non-ferrous, non-metallic - by its hardness HB,
- type of cutting – orthogonal, cutting, profiling,
- type of feed – longitudinal, tangential, mixed,
- the shape of the tool clearance face – with or without a splinter crusher, with or without a facet, etc.
- a CFz coefficient (2) resulting from the processing of the experimental data and which, in principle, identifies all other working conditions during the experiments and which cannot be individualised by  $K_i$ -type coefficients.

### 3. ARGUMENTATIVE EXAMPLES OF INTEREST IN CUTTING RESEARCH

Experiments, as a rule, are carried out in a number relevant to a previously adopted experimental program, in correlation with the type of mathematical regression that will be used for the processing of experimental data. The collection of experimental data was done, initially manually using analog mechanical measuring equipment, then dynamometers with tensometric stamps and electronic axes and in the last quarter of a century piezoelectric dynamometers with digital transformation of the measured signals. The equipment for processing the experimental results has evolved from manually drawn and rationally interpreted graphs to systems for automatic data collection and processing using dedicated software and high-performance electronic computing systems. Figure 2 exemplifies the way of graphical processing of the experimental results, with the specification that each of the points on the graph are actually the "poles" of some "clouds" of experimental data.

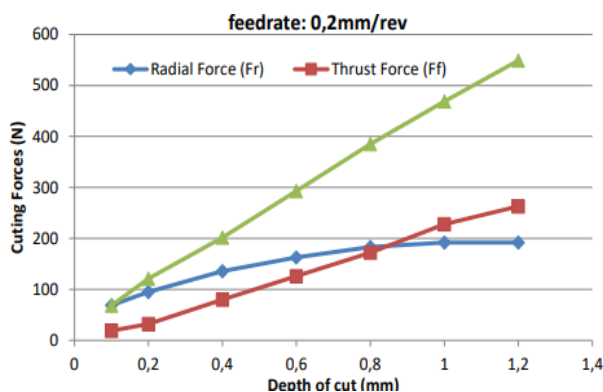


Fig. 2. Graphical representation of depth of cut  $a_p$  influences upon cutting forces at orthogonal turning

Not much different are other numerous cases of

studies of the influences of the different parameters of the splinter or cutting tool on wear, tool durability, machining quality and accuracy, splinter dynamics [4], high-speed turning [5], etc. For example:

- figure 3 shows the result of a study from 25 years ago on the wear on the laying face (VB) of the lathe knife reinforced with metal carbide plates depending on the depth of cutting ( $a_p$ ) when turning, for three types of semi-finished material;

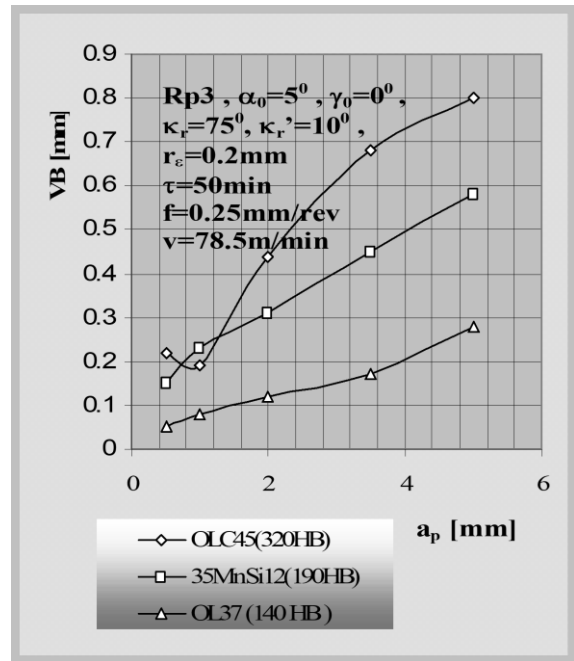


Fig. 3. The influence of depth of cut  $a_p$  on wear index VB

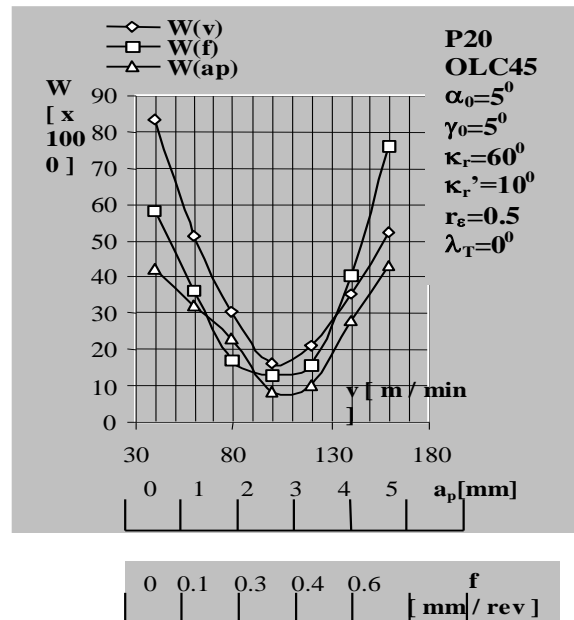


Fig. 4. The influences of  $a_p$ ,  $f$ ,  $v$ ) on the breakage degree of the chip  $W$  for OLC 45

- figure 4 is shown the result of a study from 20 years ago on the degree of crumbling of chips at adaptive turning that has as an automatic adjustment parameter the longitudinal advance.

The mentioned study also confirmed the aspects revealed by other researchers regarding the variation of the chip thickness which leads to the appearance of some phenomena such as: vibrations, variations in the size of components of the total turning force, acoustic phenomena, premature wear of the tool, a reduction of the dynamic stability field of the turning process [6].

- in Figure 5, the result of a study on the influence of the presence of coolant-lubrication in the processed area on the durability of the tool edge reinforced with metal carbide inserts is presented

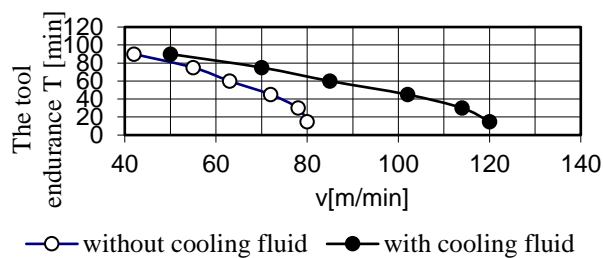


Fig. 5. The influence of the cutting speed  $v$  on  $T$  (tool life)

- the impact of the cutting parameters on the surface roughness and dimensional accuracy of hardened steel with CBN cutting tools was also experimentally studied, highlighting the variation of vibration, cutting forces, and tool wear under various cutting conditions.[7].

- other experimental study topics concerned the milling of composite materials for example to optimize and compare tilted helical milling processes in the case of carbon and glass fiber reinforced polymer composites. An uncoated carbide end mill were used and finally the microstructure were analyzed using optical-digital and scanning electron microscopy, respectively. [8].

- many other theoretical and/or experimental scientific papers aimed at streamlining the processing process, especially the optimization of the costs of processing by cutting through the control of working parameters. There are hundreds of such researches, but here we recall only the remarkable theoretical results obtained by the pioneers König & Depireaux [9], Spur Z. [10], Duca [11], Solomentsev [12] and practical ones of E. Dodon [13] and many others.

#### 4. FINAL REMARKS

The authors hope that this paper will remind researchers in the field, especially PhD students and young researchers, that chipping/metal cutting was, is and will be for a few more decades one of the predominant methods used in the manufacture of material goods.

Moreover, from the work emerges the idea that the physical phenomena that govern the phenomena during the cutting process are incompletely known, described mainly on the basis of experimental observations and is therefore far from being able to be conducted efficiently. In other words, the work is a plea, an encouragement for the sustained resumption of research in the field, introducing in the working instruments the latest conquests of the audio-video monitoring technique, of non-destructive investigation, of post-electron-

microscopic examination, metallographic, spectrographic, x-ray diffractometric, etc., of experiment planning, of data acquisition and processing using computational computing and simulation techniques, etc.

Consider the exposed ones as an encouragement, it being as necessary for the brilliant researcher as the beginner one, as is the sack for the bow of the most virtuous violinist.

#### 5. REFERENCES

- [1] Mallock, A. H. R.: *Action of Cutting Tools*, Proc. Roy. Soc. No 217, 1881.
- [2] Mallock, A. H. R.: *Shape of Drilled Holes*, Proc. Roy. Soc. No 226, 1883.
- [3] Wright, P.K., a.a.: *Manufacturing Intelligence*, Addison-Wesley Publisher, Massachusetts, 1988.
- [4] Hoshi, T.: *Measurement of cutting dynamics in orthogonal cutting condition*, Research report submitted to Ma T. C. of CIRP, Mars, 1975.
- [5] Gill, P.C.,a.a.: *Practical Optimisation*, Academic Press, New York, 1981.
- [6] Bagard, P., Palleau, M.: *Pour fabriquer les outillages, on gagne a les usiner a grande vitesse*, CETIM, - Information, nr.142, febr.1995.
- [7] Yousefi, S.; Zohoor, M.: *Effect of cutting parameters on the dimensional accuracy and surface finish in the hard turning of MDN250 steel with cubic boron nitride tool, for developing a knowledge base expert system*, International Journal of Mechanical and Materials Engineering 14:1, <https://doi.org/10.1186/s40712-018-0097-7>, 2019.
- [8] Pereszlai, C., Geier, N., Poór, D.I., Balázs, B.Z., Póka, G.: *Drilling fibre reinforced polymer composites (CFRP and GFRP): An analysis of the cutting force of the tilted helical milling process*, Composite structure, [Volume 262](#), 113646, ISSN:0263-822315, April 2021.
- [9] König, E., Depireux, W.: *How to optimize feedrate and cutting speed*. In: *Industrie Anzeiger*, nr.6/1969, Achen.
- [10] Spur, G.: *Adaptives System für Drehmaschinen zeitstrift für Wirtschaftliche*, Fertigung, 1971.
- [11] Duca, Z.: *Contributions to the method of calculating optimal cutting parameters*. In: *Buletin Științific*, I.P. București, Tom XIX, Fasc. 1-2, 1957 (in Romanian).
- [12] Solomentev, I. M., et. al: *Methodology for optimizing technological turning processes*. In: *Vesnic Mașinostroenie*, nr.6, pp. 62-66, 1974(in Romanian).
- [13] Dodon, E.: *On the adaptive control of the cutting parameters in turning*, Ph.D Thesis, I.P.București, 1960 (in Romanian).

**Authors: Lecturer Felicia Veronica Banciu, Assoc. Prof. Eugen Pamintas**, Politehnica University of Timișoara, Mechanical Faculty, Department of Materials and Manufacturing Engineering, No 1 M. Viteazul Av., Timișoara, Roamnia, Phone.: +40 2564009, Fax: +40 2563521.  
E-mail: [felicia.banciu@upt.ro](mailto:felicia.banciu@upt.ro); [eugen.pamintas@upt.ro](mailto:eugen.pamintas@upt.ro)

Kurbegović, R., Janjić, M.

## JET LAGGING IN ABRASIVE WATER JET CUTTING OF TOOL STEEL

**Abstract:** Abrasive water jet machining is an unconventional method for contour cutting of different types of materials. During machining with this method, as a consequence of jet lagging, curved lines appear on the material surface and cause machining errors. The aim of this work is to investigate the influence of machining parameters on jet lagging. The samples of tool steel DIN X165CrMoV12 (JUS c.4750) were machined with an abrasive water jet under varying pressure, traverse speed, abrasive flow rate, and stand-off distance. The jet lagging was measured at twenty places along with the depth of cut and the relationship between the jet lagging and machining parameters has been formed. In order to correctly select the process parameters, an empirical model for the prediction of jet lagging was developed using regression analysis. This developed model has been verified with the experimental results and reveals the high applicability of the model.

**Key words:** Jet lagging, Abrasive water jet, Empirical model, Tool steel, Regression analysis

### 1. INTRODUCTION

Abrasive Water jet Cutting [AWJC] has various distinct advantages over the other non-conventional cutting technologies, such as no thermal distortion, high machining versatility, minimum stresses on the workpiece, high flexibility and small cutting forces and has been proven to be an effective technology for processing various engineering materials [1]. It is superior to many other cutting techniques in processing a variety of materials and has found extensive applications in the industry [2]. However, AWJC has some drawbacks and limitations. It creates tapered edges on the kerf, especially when cutting at high traverse rates [3,4], generate loud noise and a messy working environment.

Several papers are dealing with the formation of cut front geometry and the factors that influence its final appearance. Mostly, the cutting front geometry of the workpiece machined by the abrasive water jet is influenced by machining parameters such as operating pressure, stand-off distance, traverse speed, abrasive flow rate [2,5].

Defining the geometry of the cutting front, is in fact, the determination of the deviation - lagging,  $Y_{lag}$ , of the abrasive water jet from the vertical line. Momber and Kovačević [2] explained the deviation of the cut front geometry from ideal as a consequence of energy loss during the cutting process.

The line that defines the lagging of abrasive water jet is described by Zeng, Heines and Kim [6] as a parabola.

M. Chithirai, P. Selvan, Mohana N. and S. Raju [7] observed the maximum cutting depth,  $h_{max}$ , as the main parameter for evaluating the applicability of the abrasive water jet machining process for a particular material. Using regression analysis, they developed a model for predicting the depth of cut of stainless steel. Their model is represented by a formula:

$$h_{max} = 678 \cdot \frac{p^{0,339} \cdot Ma^{0,107} \cdot d_a^{1,795} \cdot \rho_a^{0,878}}{E^{0,324} \cdot U^{0,137} \cdot Sd^{0,009} \cdot \rho_w \cdot d_j} \quad (1)$$

where  $p$  is the working pressure,  $Ma$  is the abrasive mass

flow rate,  $d_a$  is the mean value of the abrasive particle diameter,  $\rho_a$  is the density of the abrasive particles,  $E$  is the material modulus of elasticity,  $U$  is the traverse speed,  $Sd$  is the stand-off distance of the cutting head from the workpiece,  $\rho_w$  is the density of the water and  $d_j$  is the diameter of the water jet.

This model showed a good correlation with the experimentally obtained results and will be used as a basis for experimental analysis of the influence of the machining process parameters on the jet lagging.

As our previous research papers specimens [8,9] used annealed High-Speed Tool Steel EN HS6-5-2 (AISI M2, JUS č.7680) to see the influence of machining parameters on jet lagging, this work aims to investigate the influence of same machining parameters, such as operating pressure, standoff distance, traverse speed and abrasive mass flow rate on jet lagging and to make an empirical model for the prediction of jet lagging in abrasive water jet cutting of 60±1 HRC oil hardened tool steel DIN X165CrMoV12 (JUS č.4750). Some machining parameters, like low operating pressure (199,99 ÷ 299,9 MPa) and high traverse speeds (60 mm/min), showed large jet lagging and were omitted.

### 2. EXPERIMENTAL WORK

Water Jet System, model NCX 4020, was used for machining the samples. The diameter of the water orifice was 0,254 mm and the focusing tube diameter was 0,768 mm. The abrasive material was Garnet mesh 80.

The material used for the experiment is 60±1 HRC oil hardened tool steel JUS č.4750. Material is produced with the Electro Slag Remelting (ESR) method in a round-shaped ingot, normalized, cut with a bandsaw to 42 mm thick discs and lathe machined to 40±0,05 mm. Then, the material is oil hardened to 60±1 HRC.

Samples were water jet machined to 30x110 mm. The machining parameters used are shown in table 1.

Sample	p, MPa	U, mm/min	Ma, g/min	Sd, mm
1.	351,6	20	395	2
2.	413,7	20	395	2
3.	413,7	20	395	3
4.	413,7	20	395	4
5.	413,7	20	395	6
6.	413,7	5	395	2
7.	413,7	10	395	2
8.	413,7	30	395	2
9.	413,7	40	395	2
10.	413,7	20	166,5	2
11.	413,7	20	229	2
12.	413,7	20	274,5	2
13.	413,7	20	331,5	2

Table 1. Samples and its machining parameters

The cutting tool was perpendicular. The length of the cut is 25 mm and it was started 3 mm before the material. After that, the specimens were cut till the end with Wire Electric Discharge Machining (WEDM). Cutting with WEDM was done to avoid damaging the cut front line.

Measurements for determining water jet lagging were performed in twenty places (at the same distance) along the sample thickness using an optical microscope. Measured values of jet lagging are shown in Table 2.

	Sample 1	Sample 2	Sample 3	Sample 4	Sample 5
<b>h, mm</b>	<b>Y<sub>lag</sub>, mm</b>				
0	0	0	0	0	0
2	0	0	0,0550	0,0550	0,0185
4	0,1067	0	0,1085	0,1270	0,0834
6	0,1620	0,0412	0,1530	0,2232	0,1679
8	0,2631	0,1143	0,2261	0,2882	0,2261
10	0,3851	0,2491	0,2882	0,3543	0,2988
12	0,5304	0,3448	0,3973	0,4618	0,4146
14	0,7421	0,4508	0,5219	0,6282	0,5325
16	1,0248	0,5973	0,7105	0,7961	0,7004
18	1,3166	0,7608	0,9065	1,0035	0,8616
20	1,6307	0,9885	1,1278	1,2247	1,1110
22	2,0113	1,1988	1,4317	1,5057	1,3695
24	2,4142	1,5216	1,7266	1,8134	1,6675
26	2,8675	1,8591	2,0343	2,1625	1,9711
28	3,2453	2,1609	2,3420	2,5276	2,3631
30	3,7489	2,4827	2,6656	2,9812	2,7434
32	4,2080	2,8711	2,9823	3,4044	3,0848
34	4,7938	3,2502	3,4044	3,8227	3,4873
36	5,4050	3,6846	3,8926	4,2308	3,9682
38	6,1436	4,0361	4,4546	4,6459	4,4926
40	6,8057	4,4709	5,0667	5,4031	5,0999
<b>h, mm</b>	<b>Sample 6</b>	<b>Sample 7</b>	<b>Sample 8</b>	<b>Sample 9</b>	<b>Sample 10</b>
<b>h, mm</b>	<b>Y<sub>lag</sub>, mm</b>				
0	0	0	0	0	0
2	0	0	0,0723	0,0919	0
4	0	0	0,1290	0,1486	0,0755
6	0	0	0,2313	0,2296	0,1566
8	0	0,1582	0,3598	0,4006	0,2448
10	0	0,3062	0,6103	0,5588	0,3390
12	0	0,3758	0,8737	0,8221	0,5577
14	0	0,4655	1,0970	1,1568	0,7454
16	0,0000	0,5553	1,3526	1,6807	1,0050
18	0,0000	0,6152	1,5960	1,9374	1,3041
20	0,0590	0,6632	1,8992	2,5626	1,5905

22	0,0790	0,8795	2,1644	3,0884	1,9837
24	0,0945	1,0102	2,5478	3,5755	2,3054
26	0,1888	1,2053	2,9860	4,0353	2,7061
28	0,2568	1,3407	3,3653	4,4146	3,1593
30	0,3421	1,4589	3,8488	4,8531	3,6660
32	0,4165	1,5213	4,3483	5,3742	4,1394
34	0,5385	1,6894	4,8516	5,9856	4,6083
36	0,6552	1,7036	5,4102	6,7821	5,1674
38	0,8004	1,8258	6,0306	8,0956	5,7210
40	0,9308	2,0416	6,8237	9,1488	6,3526
	Sample 11	Sample 12	Sample 13		
<b>h, mm</b>	<b>Y<sub>lag</sub>, mm</b>				
0	0	0	0		
2	0,0858	0,0000	0,0960		
4	0,1395	0,0777	0,1668		
6	0,2240	0,1128	0,1668		
8	0,2890	0,1802	0,1965		
10	0,3774	0,2777	0,2487		
12	0,4819	0,4195	0,3169		
14	0,6892	0,5640	0,4732		
16	0,8907	0,7339	0,6385		
18	1,1191	1,0014	0,8687		
20	1,3573	1,2592	1,0379		
22	1,7053	1,5098	1,2301		
24	2,0929	1,8191	1,5819		
26	2,5196	2,1872	1,8953		
28	2,9004	2,6071	2,1948		
30	3,3133	3,0846	2,5462		
32	3,7792	3,5250	2,9752		
34	4,1996	4,0040	3,4527		
36	4,6453	4,4106	3,9046		
38	5,1515	4,8887	4,3667		
40	5,8289	5,3682	4,8709		

Table 2. Measured values of jet lagging

### 3. PREDICTIVE MODEL FOR JET LAGGING

AWJC process involves a large number of variables that affect the cutting performance. Using the MATLAB software package, multiple regression analysis was performed on the measured values of jet lagging. The constants in the models are statistically determined at a minimum 95 % confidence level. This model relates the jet lagging to four process variables, namely water pressure, nozzle traverse speed, abrasive mass flow rate and nozzle stand-off distance.

The mathematical model adopted for this research work will be as follows:

$$Y_{lag} = a \cdot h^b \cdot p^c \cdot U^d \cdot Ma^e \cdot Sd^f \quad (2)$$

where **a**, **b**, **c**, **d**, **e**, **f** are regression analysis coefficients.

The above model is valid for the operating parameters in the following range for practical purposes and machine limitations:

- Water pressure: 351,6 MPa < p < 413,7 MPa,
- Traverse speed: 5 mm/min < U < 40 mm/min,
- Abrasive mass flow rate: 166,5 g/min < ma < 395 g/min and
- Stand-off distance: 2 mm < Sd < 6 mm.

The mathematical model that describes the impact of the corresponding machining parameters on the jet lagging was given for each diagram.

$$Y_{lag} = 9076 \cdot h^{2,083} \cdot p^{-2,538} \quad (3)$$



Standard deviation of (3) is  $R = 0,999699$ .

$$Y_{lag} = 0.0001904 \cdot h^{1.886} \cdot U^{1.026} \quad (4)$$

Standard deviation of (4) is  $R = 0,996644$ .

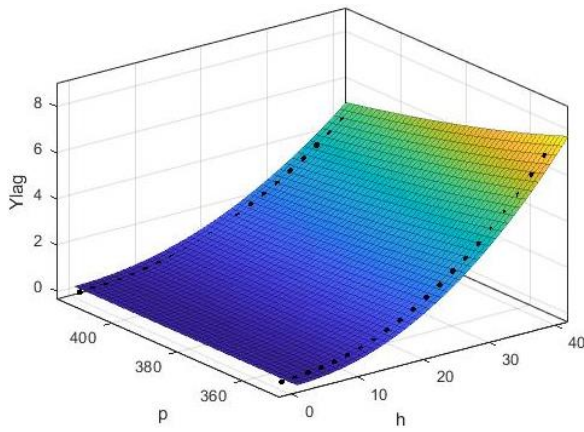
$$Y_{lag} = 0.0001904 \cdot h^{1.886} \cdot Ma^{1.026} \quad (5)$$

Standard deviation of (5) is  $R = 0,996594$ .

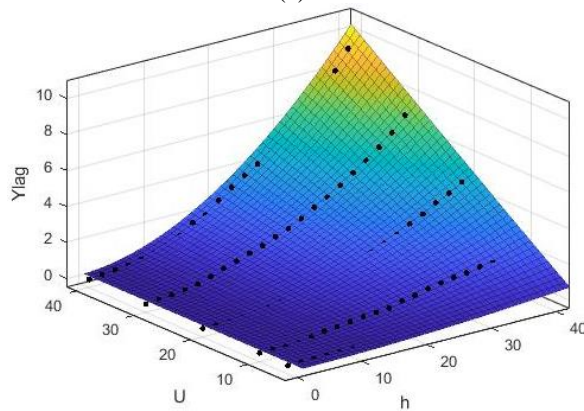
$$Y_{lag} = 0.00177 \cdot h^{2.119} \cdot Sd^{0.09561} \quad (6)$$

Standard deviation of (6) is  $R = 0,997346$ .

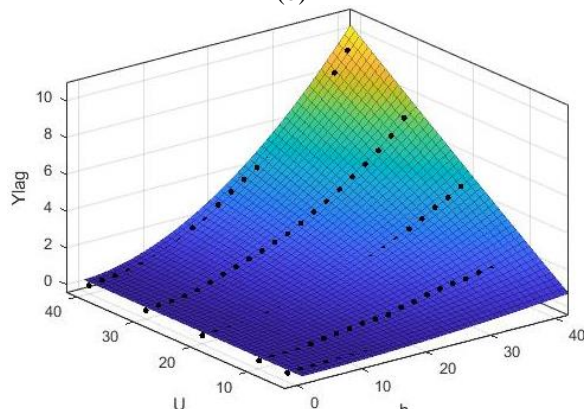
It is shown that the model predictions are in good agreement with the experimental data with deviations less than 3%. Also, using MATLAB, 3D representations of measured values of jet lagging and shown in Fig. 1, within the experimental range.



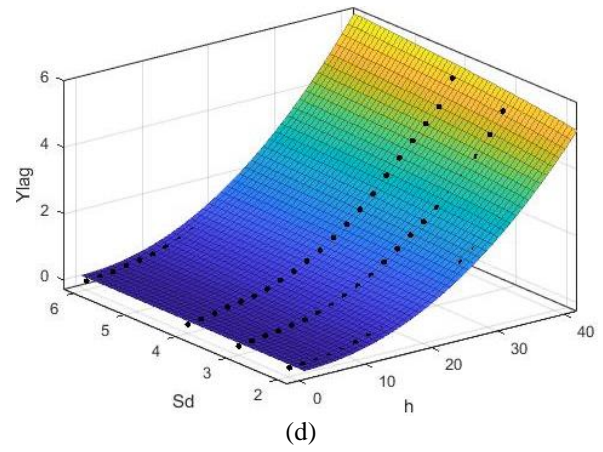
(a)



(b)



(c)



(d)

Fig. 1. Influence of (a) operating pressure, (b) traverse speed, (c) abrasive mass flow rate and (d) stand-off distance on jet lagging

Based on the measured values in Table 2, the relationship between the jet lagging and operating pressure, stand-off distance, traverse speed, abrasive mass flow rate and depth of cut, is formed. This relationship is represented by a mathematical model described in (2).

$$Y_{lag} = 656.3873 \cdot \frac{h^{1.71302} \cdot Sd^{0.12521} \cdot U^{1.224623}}{p^{2.14154} \cdot Ma^{0.40091}} \quad (7)$$

Standard deviation of (7) is  $R = 0.986712$ .

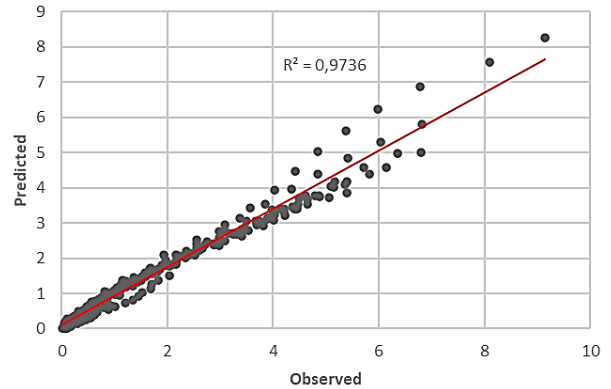


Fig. 2. Observed versus predicted values of the jet lagging

Fig. 2 shows the observed values of the jet lagging versus the values of the jet lagging predicted by the model presented in (7).

#### 4. CONCLUSIONS

Experimental investigations have been carried for the jet lagging in abrasive water jet cutting of  $60 \pm 1$  HRC oil hardened tool steel JUS č.4750. The effects of different operational parameters such as: pressure, abrasive mass flow rate, traverse speed and nozzle stand-off distance on jet lagging have been investigated.

The change of the jet lagging as the function of operating pressure, stand-off distance, traverse speed, and abrasive mass flow rate can be noted. With the increase of the traverse speed, there is an increase in the jet lagging. Furthermore, it can be observed that the increase of operating pressure and abrasive flow rate

causes the decrease of the water jet lagging. This clearly suggests a firm correlation between the water jet lagging and the referred machining parameters. The influence of the depth of cut on the jet lagging is also significant. With the increasing depth of cut, the jet lagging also increases.

It is interesting that the exponent associated with the depth of cut, in all Equations (3, 4, 5 and 6), has a value of about 2.

As a result of this study, it is observed that these operational parameters have a direct effect on jet lagging. It has been found that traverse speed has the most effect on jet lagging. An increase in traverse speed is associated with an increase in jet lagging. These findings indicate that the use of low traverse speed is preferred to obtain overall good cutting performance but at the cost of productivity. Jet lagging constantly decreases as the mass flow rate increases. It is recommended to use a more mass flow rate to decrease jet lagging. Among the process parameters considered in this study traverse speed and abrasive mass flow rate have a similar effect on jet lagging, but one opposite from another. Stand-off distance has no apparent effect on jet lagging, but to achieve an overall cutting performance, a low stand-off distance should be selected.

From the experimental results, an empirical model for the prediction of jet lagging in the AWJC process of tool steel JUS č.4750 has been developed using regression analysis. Also, verification of the developed model for using it as a practical guideline for selecting the parameters has been found to agree with the experiments. Therefore, the need for extensive experimental work to select the magnitudes of the most influential abrasive water jet cutting parameters on jet lagging of this tool steel can be eliminated.

Based on the model from (7), it can be concluded that with the proper selection of the machining parameters, the desired values of the jet lagging can be achieved. The entire length of the cut does not need to be machined with such selected machining parameters, but only the parts of the path that make the curve, because major mistakes occur there.

The obtained models are only valid for this material. It is necessary to carry out the experiments on the same material with different heat treatments to determine the effects of the mechanical properties of materials on the jet lagging.

It would also be interesting to carry out the experiments on the same material with different thicknesses and other mechanical properties and to investigate this phenomenon and its dependencies.

## 5. REFERENCES

- [1] Hascalik, A., Caydas, U., Gurun, H.: *Effect of Traverse Speed on Abrasive Water jet Machining of Ti-6Al-4V Alloy*, Materials and Design, Vol. 28(6), pp. 1953-1957, 2007.
- [2] Mombar, A.W., Kovačević, R.: *Principles of abrasive water jet machining*, Springer, London, 1998.
- [3] Azmir, M.A., Ahsan, A.K.: *Investigation on*

*glass/epoxy composite surfaces machined by abrasive water jet machining*, Journal of Materials Processing Technology, Vol.198, pp. 122-128, 2008.

- [4] Ma, C., Deam, R.T.: *A correlation for predicting the kerf profile from abrasive water jet cutting*, Experimental Thermal and Fluid Science, Vol.30, pp. 337-343, 2006.
- [5] Hasish, M.: *A modeling study of metal cutting with abrasive water jets*, Journal of Engineering Materials and Technology, Vol. 106, pp. 88-100, 1984.
- [6] Zeng, J., Heines, R., Kim, T.J.: *Characterization of energy dissipation phenomena in abrasive water jet cutting*, Proceedings of the 6th American Water Jet Conference, pp. 163-177, Houston, Water Jet Technology Association, 1991.
- [7] Chithirai, M., Selvan, P., Mohana, N., Raju, S.: *A Machinability Study of Stainless Steel Using Abrasive Water jet Cutting Technology*, International Conference on Mechanical, Automobile and Robotics Engineering, pp. 208-212, Penang, 2012.
- [8] Kurbegović, R., Janjić, M.: *Effect of abrasive water jet machining process parameters on jet lagging*, 42. Jupiter conference, Belgrade, pp. 3.81-3.87, Faculty of Mechanical Engineering, 2020.
- [9] Kurbegović, R., Janjić, M.: *Jet Lagging in Abrasive Water Jet Cutting of High-Speed Tool Steel*, Heavy Machinery - HM 2021, Vrnjačka Banja, pp. 3.81-3.87, Faculty of Mechanical and Civil Engineering in Kraljevo, 2021.

**Authors: Mr Ramiz Kurbegović, Full Prof. Mileta Janjić**, University of Montenegro, Faculty of Mechanical Engineering, Department of Production Engineering, Džordža Vašingtona bb, 81000 Podgorica, Montenegro, Phone.: +382.20.245.003.  
E-mail: [rkurbeg@gmail.com](mailto:rkurbeg@gmail.com); [mileta@ucg.ac.me](mailto:mileta@ucg.ac.me)

## ACKNOWLEDGEMENTS

This paper presents the results of research conducted on the doctoral research project "Investigation of Abrasive Water Jet Machining Parameters" which is financially supported by the Ministry of Science of Montenegro.

Antić, A., Ungureanu, N., Čep, R., Lukić D., Milošević, M.

## TOOL WEAR CONDITION MONITORING BASED ON FUZZY SYSTEM

**Abstract:** One of the biggest problems in production is the timely detection of tool failures in cutting operations such as turning. Performing the procedure with a worn tool can damage the final surface of the workpiece. On the other hand, it is unnecessary to change the cutting tool if it is still able to continue cutting. Therefore, an efficient diagnostic mechanism is necessary to automate the processing process in order to avoid losses and production delays. For that, signals obtained from the vibration sensor were used to make a decision about the status of the tool. In the first phase, features that are correlated with tool states such as statistical moments and were used as inputs to the fuzzy process were singled out. In conclusion, the outputs of this phase are taken into the functions of the thresholds whose output is used to classify the state of the tool.

**Key words:** tool wear, vibrations, fuzzy system, turning

### 1. INTRODUCTION

Continuous, online tool wear monitoring is very important in order to improve the quality of production systems in the cutting process. Premature replacement of usable tools or late replacement of worn tools can cause a waste of time and increase production costs. The complex mechanism of tool wear can cause unforeseen breakage at any time that could also lead to catastrophic consequences affecting other components in the system. By using efficient techniques for monitoring the condition of tool wear, not only such failures can be avoided, but also the maximum utilization of the cutting tool.

Monitoring the condition of tool wear uses methods that can be classified into two main groups: direct methods and indirect methods. Direct methods require direct tool measurements, while indirect methods use parameters that correlate with the cutting process such as: force, vibration, acoustic emission and power measured during the cutting process. Direct measurement of tool wear requires direct access to the cutting edge over a period of time or removal of the tool from the machine workspace to determine the degree of wear. However, both alternatives are not suitable for use in automated machining processes and cause downtime and loss of production time. Therefore, although direct methods are more accurate than indirect methods, indirect methods are more suitable for application than direct methods and most research in this area is concentrated on them.

Common physical quantities used in indirect methods are cutting force, vibration, acoustic emission, current, power and temperature. A large number of studies have focused on the analysis of time series and the frequency domain of these parameters [1]. In addition to these techniques, pattern recognition, statistical analysis [2], [3] Fourier transform, and artificial neural networks have been successfully applied [4]. These methods have the possibility of wider practical application to varying degrees compared to others. In addition to the methods used,

feature extraction is also very important for the design of an efficient condition monitoring system. A parameter that works well for one method may not be a good enough choice for another method. Therefore, diagnosing the mechanisms of wear and tear of tool wear depends on the applied sensor and the methods and techniques of distinguishing features and classification. Therefore, it is proposed to use multiple sensors in the same process [8].

### 2. CLASSIFICATION OF TOOL WEAR BY APPLICATION FUZZY C-mean ALGORITHM

The measured real-time vibration signal is defined as the actual values of the characteristics [So, Fo]. So and Fo are compared with the estimated characteristics for differently defined wear states (i.e., 0.25, 0.5, and 0.8 mm) to assess the degree of similarity between the actual wear condition with any of the estimated wear states.

For the purposes of classifying the condition of tool inserts in turning processing, the unclear algorithm of C-means (FCM) is applied [5], [6]. The Matlab software package was applied, i.e. the FCM and *genfis3* functions, which are an integral part of the Fuzzy Logic Toolbox.

The problem of FCM classification is reduced to minimizing the functions of the goal:

$$J_m = \sum_{i=1}^N \sum_{j=1}^C u_{ij}^m \|x_i - c_j\|^2, 1 \leq m < \infty$$

Also, in the sequel, we give the pseudo-code for the FCM algorithm:

1. Initialize the membership matrix  $U = [u_{ij}]$ ,
2. in the k-th step calculate the centers  $C^{(k)} = [c_j]$  for  $U^{(k)}$ ,

$$c_j = \frac{\sum_{i=1}^N u_{ij}^m x_i}{\sum_{i=1}^N u_{ij}^m}$$

3. updates  $U^{(k)}$  and  $U^{(k+1)}$

$$u_{ij} = \frac{1}{\sum_{k=1}^c \left( \frac{\|x_i - c_j\|}{\|x_i - c_k\|} \right)^{\frac{2}{m-1}}}$$

4. if the condition is met:

$$\|U^{(k+1)} - U^{(k)}\| < \varepsilon$$

For the purpose of clarification, we will observe the one-dimensional problem of classification of 20 elements. The parameters  $m = 2$  and  $\varepsilon = 0.3$  are set. Figure 1 shows the generated fuzzy sets after step 1, ie the initialization of the membership function matrix.

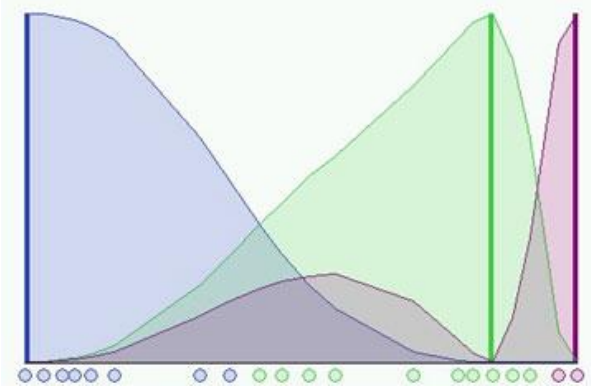


Fig. 1. Initial fuzzy sets

After eight iterations, the execution of the algorithms is stopped and the final matrix of membership functions is generated, on the basis of which the fuzzy sets shown in Figure 2 are defined.

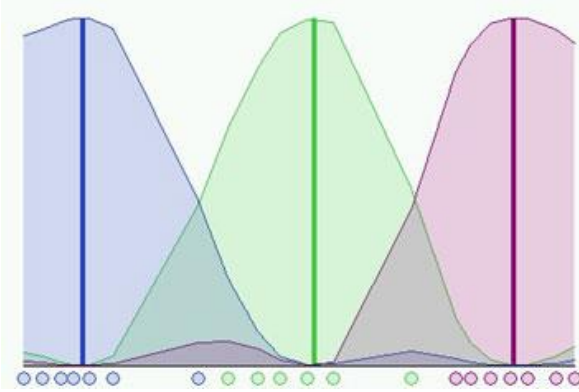


Fig. 2. Final look of fuzzy sets

Based on the obtained membership matrix, the fuzzy rule is generated in the following form:

$$\text{if } \alpha_i = FCM_i(x, C_x) \text{ then } y_i(x) = C_i^y$$

### 3. APPLIED FCM ALGORITHM

The Fuzzy C-mean algorithm was applied to the tool wear classification procedure. The implemented function is implemented within the Matlab software environment, Fuzzy Logic Tool Box.

The problem of finding clusters of a finite set  $X$  comes down to finding the centers of several clusters that adequately characterize clusters in  $X$ . Determining  $K$  regions, which correspond to individual subsystems

in a defined equivalent space so that system behavior in these regions can be described by simple dependency functions one feature assigned to each subsystem. However, the global model generated in this way cannot guarantee a qualitative approximation of the real system in certain situations. It is possible that there is a region in the state space that the generated model does not cover the best. In this case, the partitions of the set  $X$  become fuzzy partitions of  $X$ . Such fuzzy pseudo partitions of  $X$  are also called c-partitions, where  $c$  determines the number of classes in the partition. Improved pseudo code in the applied classification algorithm for fuzzy c-mean:

Input data: Unmarked object data  $X \subset R^p$   
 Settings: - set cluster number:  $1 \leq c \leq n$   
 - set max. number of iterations  $T$   
 - set the weight exponent:  
 $1 \leq m \leq \infty$   
 - average norm:  
 $J_m : \|x\|_A^2 = x^T A x$   
 - termination measure:  
 $E_i = \|V_i - V_{i-1}\| = \text{big value}$   
 - thrash hold terminations:  
 $0 < \varepsilon = \text{small value}$   
 - setting weights  $w_i = 0$

Guessing:  $V_0 = \{v_{1,0} \dots v_{c,0}\} \in R^{cp}$

Iterations:  $i \leftarrow 0$   
 repeat  
 $i \leftarrow i + 1$   

$$u_{ik} = \left[ \sum_{j=1}^c \left( \frac{D_{ik}}{D_{jk}} \right)^{\frac{2}{m-1}} \right]^{-1}$$
  

$$v_i = \frac{\sum_{k=1}^n u_{ik}^m x_k}{\sum_{k=1}^n u_{ik}^m}$$
  
 while valid ( $i < T$ )  $E_i \leq \varepsilon$   
 $(U, V) \leftarrow (U_i, V_i)$

The values of statistical moments c.m. were applied as discriminant features. kurtosis and c.m Skewness. That is, the problem of classification is reduced to a two-dimensional problem. Discriminant features are derived from a larger set of discriminant features, the smaller part of which is shown in Table 1. These features were chosen because their values change more clearly with the change in tile wear compared to other features.

Continuous classification of the degree of tool wear is a very complex part of monitoring, which involves the use of a large number of features isolated from the monitored process signal. The procedure of checking the selected classification model for the input data of the training feature set in the conducted experiments

was performed by determining six cluster centers, for each group of attrition, two in three different scales. By the selected method of linear classification by FCM algorithm, the selected features are grouped into clusters based on the affiliation matrix.

feature1	feature1
0.4257	0.8547
0.4257	0.9023
0.2686	0.9023
....	....
0.0919	0.9921

Table 1. Normalized set of input data carrying information feature 1 and feature 2

Cluster 1				
0.2686	0.8796	0.9862	0.9905	0.9828
0.7314	0.1204	0.0138	0.0095	0.0172
0.9712	0.9219	0.9916	0.9755	0.2579
0.0288	0.0781	0.0084	0.0245	0.7421
0.3843	0.9683	0.0415	0.1160	0.9236
0.6157	0.0317	0.9585	0.8840	0.0764
Cluster 2				
0.0966	0.0796	0.9380	0.6297	0.9580
0.9034	0.9204	0.0620	0.3703	0.0420
0.9887	0.9865	0.9815	0.9738	0.9533
0.0113	0.0135	0.0185	0.0262	0.0467
0.9867	0.9770	0.1211	0.7511	0.9640
0.0133	0.0230	0.8789	0.2489	0.0360
Cluster 3				
0.9919	0.9827	0.9744	0.1702	0.1674
0.0081	0.0173	0.0256	0.8298	0.8326
0.6320	0.6320			

Table 2. Affiliation matrix

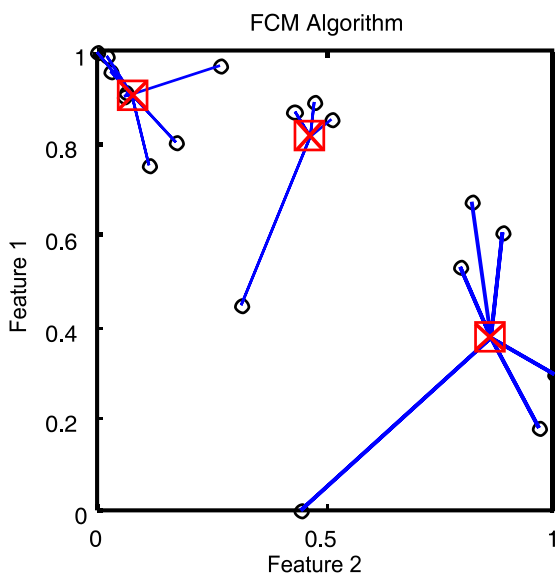


Fig. 3. Formed a priori clusters and grouping FCM by calcification of features

The first step is to define the input data, after highlighting the features, in the a priori group as shown in the figures 3 and 4.

In the classification procedure, the position of the

feature is defined at the same time by three vectors, ie. three central moments: variance, asymmetry coefficient (skewness), and (kurtosis) flattening coefficient. Previous analyzes have established that their simultaneous mutual combination gives the best characteristics for the chosen method of feature extraction.

Figures 3 show combinations of plane projections of feature space classified a priori and FCM algorithm for the first scale. The images can visually assess the agreement of the selected FCM clustering algorithm and a priori classified features.

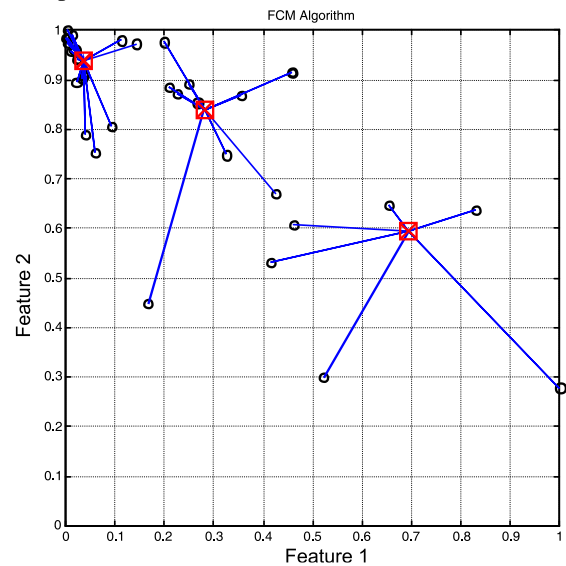


Fig. 4. Formed clusters for significant features skewness and kurtosis for training sets

#### 4. FUZZY TOOL WEAR CLASSIFIER TESTING

To determine the applicability of the proposed system model, method of feature extraction and fuzzy classifier, the complete procedure was tested on the example of processing for three degrees of tool wear. New and wear belt inserts VB 0.25 mm and VB 0.6 mm were also observed.

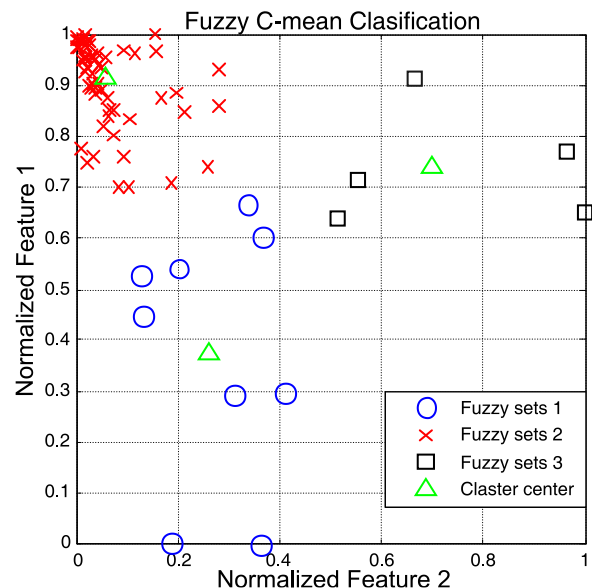


Fig. 5. Formed clusters for features Sskewness and kurtosis with Improved FCM algorithm

The statistical moments on the basis of which the fuzzy classifier was developed were taken into consideration. Also, the classification of plane projections of features classified a priori and the FCM algorithm for the first scale was presented. The images can visually assess the agreement of the selected FCM clustering algorithm and a priori classified features.

Verification of the developed tool wear classification system, using a linear FCM classification algorithm on a separate training set of features for the appropriate degree of plate wear, was performed on a test set of 12 samples for each degree of plate wear 4 test samples. Figures 5 and 6 show the results of longitudinal and transverse processing.

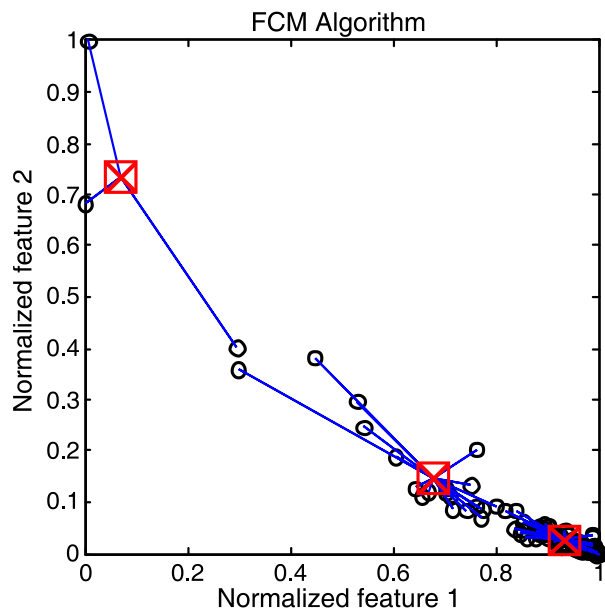


Fig. 6. Display clusters for selected cross turning operation features

Figure 7 presents a three-dimensional view of the cluster center layout for individual tool wear groups.

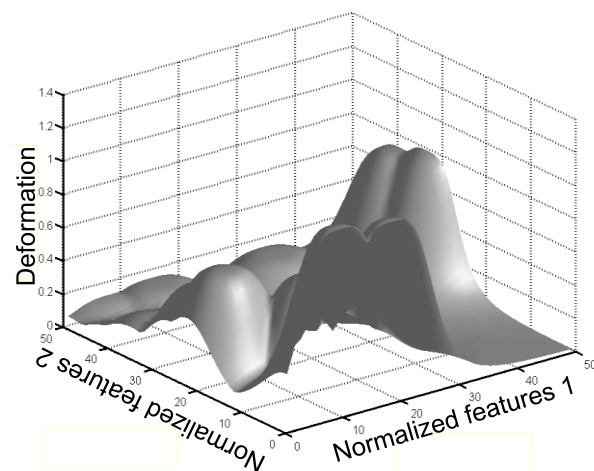


Fig. 7. Formed clusters for features skewness and kurtosis

## 5. CONCLUSION

The obtained results show that the highest percentage of successfully classified wear conditions is for the tool with the highest degree of wear, i.e. wear state VB 0.6 mm. Observing the results of the final classification of all test samples based on the developed fuzzy system for classification of tool wear condition, it can be concluded that they give good classification results, especially the classification of tools with the highest degree of wear.

## 6. REFERENCES

- [1] Guo, H.X. Zhu, K.J.: *Based on fuzzy c-means algorithm and the new genetic algorithm clustering method*, South China University of Technology Journal Natural Science, Vol. 32, (10): 93-96, 2004.
- [2] Tangjitsitcharoen, S., Moriwaki, T.: *Intelligent identification of turning process based on pattern recognition of cutting states*, Journal of Materials Processing Technology Vol. 192–193, 491–496, 2007.
- [3] Dong, Y., Zhang, Y.J., Chang, C.L.: *Improved genetic fuzzy clustering algorithm*, Fuzzy Systems and Mathematics, Vol. 19, (2):123-133, 2005.
- [4] Aliustaoglu, C., Metin Ertunc, H., Ocaik, H.: *Tool wear condition monitoring using a sensor fusion model based on fuzzy inference system*, Mechanical Systems and Signal Processing, Vol. 23, 539–546, 2009.
- [5] Bezdek, J.C., Keller, J., Krisnapuram, R., Pal, N.R.: *Fuzzy Models and Algorithms For Pattern Recognition And Image Processing*, Springer, 1999.
- [6] Miyamoto, S., Ichihashi, H. Honda, K.: *Algorithms for Fuzzy Clustering*, Springer, Vol. 229, 2008,

**Authors:** Full Prof. Aco Antić, Assoc. Prof. Dejan Lukić, Assoc. Prof. Mijodarg Milošević, University of Novi Sad, Faculty of Technical Sciences, Department of Production Engineering, Trg Dositeja Obradovića 6, 21000 Novi Sad, Serbia, Phone.: +381 21 485-23-24, Fax: +381 21 454-495, E-mail: [antica@uns.ac.rs](mailto:antica@uns.ac.rs); [lukić@uns.ac.rs](mailto:lukić@uns.ac.rs); [mido@uns.ac.rs](mailto:mido@uns.ac.rs)

**Full Prof. Nicolae Ungureanu**, Technical University of Cluj-Napoca, Dr. V. Babes 62/A, 430083 Baia Mare, Romania; Department of Machining, Assembly and Engineering Metrology,

E-mail: [nicolae.ungureanu@cunbm.utcluj.ro](mailto:nicolae.ungureanu@cunbm.utcluj.ro)

**Full Prof. Robert Čep**, Faculty of Mechanical Engineering, Technical University of Ostrava, 70800 Ostrava, Czech Republic

E-mail: [robert.cep@vsb.cz](mailto:robert.cep@vsb.cz)

**ACKNOWLEDGMENTS:** This paper is part of a research on the projects: "Application of smart manufacturing methods in Industry 4.0", No.142-451-3173/2020, and "Application of Edge Computing and Artificial Intelligence methods in smart products", No.142-451-2312/2021-01 supported by Provincial Secretariat for Higher Education and Scientific Research of the Autonomous Province of Vojvodina

Sekulić, M., Rodić, D., Gostimirović, M., Savković, B., Aleksić, A., Kulundžić, N.

## MODELING OF TORQUE AND THRUST FORCE IN DRILLING USING GENETIC ALGORITHM

**Abstract:** Modeling of the drilling process is very important as a tool for understanding the process and solving practical problems. This is especially important under the conditions of high cutting speeds and feeds associated with mass production. Mathematical drilling models are particularly important for determining thrust force and torque. A realistic estimation of these quantities is important both for the design of the drill geometry and for solving the main problems in production (surface defects, vibrations, tool wear, burr formation, etc.). Over the years, various mechanical-mathematical models have been developed to determine the cutting forces. In this paper, the application of a genetic algorithm for modeling torque and thrust force in drilling operation is presented. The predicted thrust force and torque, based on the models of GA, show good agreement with the experimental values.

**Key words:** modeling, torque, thrust force, genetic algorithm

### 1. INTRODUCTION

Drilling holes is a process that dates back to the Stone Age. It is one of the oldest and most commonly used machining processes. The twist drill is the most important drilling tool and its modern development began with the invention of high-speed steel around 1900. Twist drills account for about 20÷25 % of all metal cutting processes [1].

Very often drilling is performed as one of the last steps in the manufacture of a part, which places high demands on this operation and especially on the twist drill as a tool. In the 80s of the last century, 90 % of all drills were made of high-speed steel (HSS), today more than 50 % of drills are made of cemented carbide, which significantly increased the performance of the tools [1]. In order to increase the efficiency of drilling, research is moving towards the development of tools with internal cooling and the application of new tool materials and coatings, as well as towards modified processes, such as high-speed drilling and machining without coolant. This requires a combination of theoretical and experimental research to obtain realistic models on the basis of which the characteristics of the machining process can be determined with reasonable accuracy.

Mathematical drilling models are particularly important for estimating thrust force and torque. Cutting forces are the main cause of problems that occur in production, such as surface defects, vibration, tool wear, burr formation, etc. In other words, cutting forces contain information about the causes of the problem. A realistic estimation of the drilling torque and axial force is also important for the development of optimization techniques as well as for the intelligent control of machining systems.

This paper presents the application of evolutionary algorithms, more specifically the genetic algorithm, to model thrust and torque in the drilling process. The genetic algorithm (GA) is based on Darwin's theory of evolution. Two models have been developed using this method. One to predict torque and the other to predict

thrust. Drill diameter and feed rate were used as variable parameters. Existing well known Oxford and Shaw models were used for model development.

### 2. PLAN OF CUTTING FORCES IN DRILLING

By analyzing the plan of cutting forces in drilling (Fig. 1), it can be seen that the following loads act on the twist drill: torque  $M$ , which is the result of the two main cutting forces  $F_v$ , and thrust force  $F_f$ , which is the sum of the two feed forces  $F_{f1}$ . The sum of the penetration forces  $F_p$  is only zero if the two main cutting lips are identical and symmetrical to the drill axis.

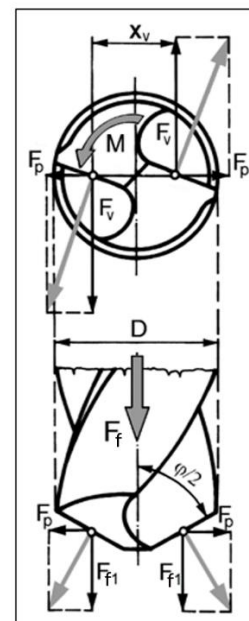


Fig. 1. Cutting forces applied to twist drill

Many empirical, analytical, numerical, and artificial intelligence (AI) based models have been developed by many researchers in the past 70 years for predicting torque and thrust force in drilling. The first models of

cutting forces were entirely empirical (Boston and Gilbert, 1936) and relied on empirical data to determine torque and axial force. The disadvantage of this approach is that specific experiments must be performed for many different materials, drills and types of machining.

One of the earliest cutting force models was the Merchant's model [2], applicable to both turning and drilling. By using the law of energy conservation, Merchant showed that the cutting force was proportional to the uncut chip area or the chip load.

Early drilling models have been developed by Shaw [3], Oxford [4], Shaw and Oxford [5], Williams [6], Armarego [7].

### 3. EXPERIMENTAL SETUP AND RESULTS

The experimental work explained in this paper was carried out at the Department of Production Engineering, Faculty of Technical Sciences, at the University of Novi Sad. The experiments were carried out on Index GU 600 machine tool and on C15 steel. The cutting tools used were HSS twist drills of different diameters under different cutting conditions (six different feed rates were used; the cutting speed was kept constant at 21÷22 m/min). The experimental conditions are summarized in Table 1.

Tool	HSS twist drill Diameter: 10 mm, 12 mm, 15 mm
Workpiece material	C15 steel
Machine tool	Index GU 600
Cutting conditions	Speed spindle: 450÷710 rpm; Feed: 0,056÷0,179 mm/rev; Coolant: Without

Table 1. Experimental conditions

During the experiments, torque and thrust force were measured using a Kistler dynamometer and sampled using a data acquisition system based on PC with LabVIEW software. Since a typical torque and thrust force signal can be divided into three phases (entry, steady state, exit), the average torque and thrust force are determined based on the second phase (steady state) by taking the signal value in the range of 1/4 to 3/4 of the full drilling phase (Fig. 2).

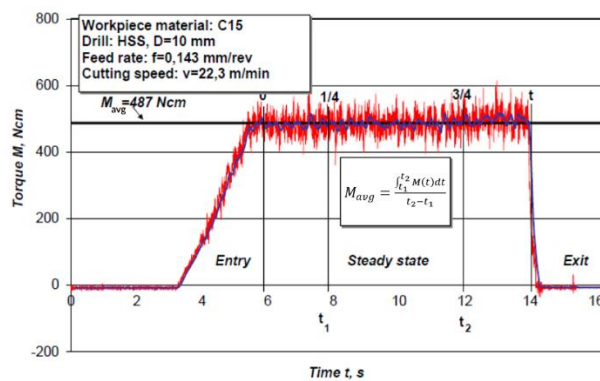


Fig. 2. Example of determining the mean value of the torque

This technique avoids the portions of the signal corresponding to drill bit input into the material and drill

bit output from the material. The following equations 1 and 2 were used to determine the mean values of the measured variables:

$$M_{avg} = \frac{\int_{t_1}^{t_2} M(t) dt}{t_2 - t_1} \quad (1) \quad F_{avg} = \frac{\int_{t_1}^{t_2} F_f(t) dt}{t_2 - t_1} \quad (2)$$

Measured results of torque and thrust force are presented in Table 2.

No	Parameters		Measured values	
	D, mm	f, mm/rev	M, Ncm	F <sub>f</sub> , N
1	10	0,056	247	969
2	10	0,071	300	1162
3	10	0,089	344	1312
4	10	0,1125	406	1488
5	10	0,143	487	1776
6	10	0,179	618	2362
7	12	0,056	385	1287
8	12	0,071	454	1501
9	12	0,089	523	1646
10	12	0,1125	619	1900
11	12	0,143	738	2164
12	12	0,179	883	2477
13	15	0,056	546	1457
14	15	0,071	660	1720
15	15	0,089	790	2014
16	15	0,1125	953	2374
17	15	0,143	1155	2808
18	15	0,179	1382	3285

Table 2. Experimental results for torque and thrust force

### 4. MODELING USING GENETIC ALGORITHM

Genetic algorithms (GA) are search tools based on the mechanisms of natural selection, genetics and evolution [8]. The aim of this work is to apply the GA principle, which is used to obtain the necessary equations to determine the torque and the thrust force.

To date, a large number of more or less complex equations have been developed to determine the thrust forces in drilling. One of the most valuable studies is the work of Oxford and Shaw. They developed simple equations based on analogy with turning tools. The required functions for torque and thrust force, already known in the literature, have the following equations 3 and 4:

$$M = C_M \cdot D^{x_M} \cdot f^{y_M} \quad (3)$$

$$F_f = C_F \cdot D^{x_F} \cdot f^{y_F} \quad (4)$$

where is  $D$  – drill diameter and  $f$  – feed rate

The goal of optimization GA is to obtain such solutions for values of coefficients  $C_M$ ,  $x_M$  and  $y_M$  for torque, and  $C_F$ ,  $x_F$  and  $y_F$  for thrust force. Under the condition that the difference between the experimental values and the values predicted by the model is as small as possible. In other words, this can be considered as a fitness function [9]. This function is essentially a measure of the success of each individual. The number  $n$  denotes the number of learning individuals in each



generation [10]. Each individual (chromosome) has five characteristic features (genes), the previously mentioned coefficients  $C_M$ ,  $x_M$  and  $y_M$  for torque, and  $C_F$ ,  $x_F$  and  $y_F$  for thrust force. All these coefficients are determined by minimizing  $\Delta$ , which is a sum of percentage errors for each parameter, expressed by equation 5:

$$\Delta = \sum_{i=1}^{18} \left| \frac{P(i)-D(i)}{P(i)} \right| \times 100\% \quad (5)$$

where  $P$  is the experimentally determined value and  $D$  is the modelled value for each parameter. This function basically calculates the average standard error. It returns a sum of all percentage deviations of the experimental values  $P(i)$  and the values suggested by the individual model  $D(i,j)$ , where  $i=1 \div 18$  is the number of experiments and  $j=1 \div n$  is the number of individuals in a generation.

To apply a GA-based artificial intelligence tool, several steps must be taken as shown in the figure.

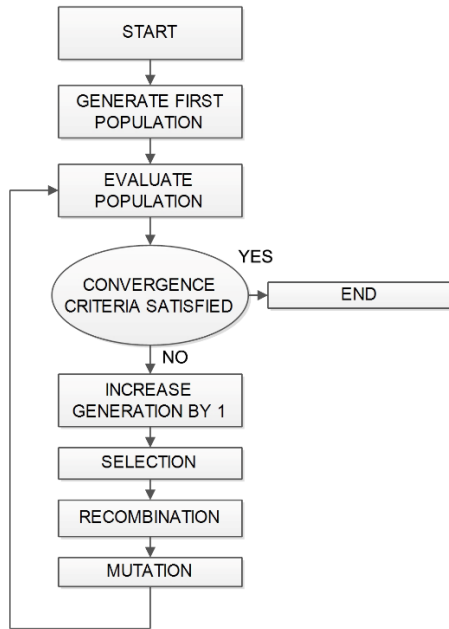


Fig. 3. Genetic algorithm procedure

First, it was necessary to define the number of individuals as the initial population [11]. This is also called Population Initialization. 800 populations were chosen for the torque model and 500 for the thrust force, respectively. Therefore, their coefficients (genes) are randomly generated in the range of 0 to 1. The second step is to evaluate the population, where a population of chromosomes is a set of possible solutions to the optimization problem [12]. Using a uniform distribution as a ranking method, the fitness scaling function was applied. The ideal convergence criterion for a genetic algorithm would be one that guarantees that each and all parameters converge independently. Then the individual with the best score comes first as the fittest individual. All other entities are ranked according to the scaling function. In this method, each individual in a generation is ranked with the best individual from that generation. This method was chosen because the fastest convergence towards the best solution is found.

The selection of individuals for their presence in the mating pool was performed using the roulette wheel method. The size of the wheel area occupied by a single individual is defined by its rank score - the better the score, the larger the area. The wheel is then spun and the individual with the largest area has the most chance of getting a spot in the mating pool. This process is repeated until the two whitest individuals are determined. These individuals are then passed on to the next generation. This process is called elitism and guarantees that the best individuals are passed on to the next generation. By setting such criteria, the genetic difference of the individuals is quickly reduced and leads to a deeper time of convergence. If the criteria are not met, the next step is to increase the generation by 1. Then the individuals undergo selection, recombination again and their mutation takes place. This type of mutation is basically a two-step process. In the first step, the algorithm selects one gene of an individual to mutate, where each gene has the same probability as the mutation rate of the gene to be mutated. In the second step, the algorithm replaces each selected entry with a random number chosen uniformly from the range for that entry.

The best results obtained with GA gave an average absolute deviation for the torque model of 3.26% and the thrust model of 3.43%. After implementing the obtained coefficients, the function now looks like this:

$$\begin{aligned} C_M &= 12,694 \\ x_M &= 2,189 \\ y_M &= 0,719 \end{aligned}$$

The equation for calculating the torque is now as follows equations 6:

$$M = 12,694 \cdot D^{2,189} \cdot f^{0,719} \quad (6)$$

The results shown are for the values of the following variables:

$$\begin{aligned} C_F &= 378,077 \\ x_F &= 1,182 \\ y_F &= 0,613 \end{aligned}$$

The calculation of the thrust force is performed according to the equation 7:

$$F_f = 378,077 \cdot D^{1,182} \cdot f^{0,613} \quad (7)$$

After modeling the torque and thrust force in the module GA, the obtained results were compared. The quantitative possibility of prediction was evaluated in terms of the percentage of deviation (deviation) between the obtained and expected values. Based on the calculation of the relative error of each point of the experiment, the proportionality error of the observed models was calculated. The generated models, based on genetic algorithms, showed good agreement with the experimental data. According to [13] it can be concluded that the models of GA have an acceptable error, that is, they have a good ability to predict results. The figure 4 shows a 3D interpretation of the mathematical models for torque and thrust force. The influence of the drill

diameter and feed rate on the torque shown on figure 4a. It is clear that, increasing the drill diameter and feed rate have a very sensitive effect on the torque. According to Figure 4b, the 3D surface demonstrates that the range of suitable employing feed rates is changed with the variation of diameter. Basically, in the end it can be concluded that both input parameters have the same effect, mostly linear in nature, on the torque and thrust force.

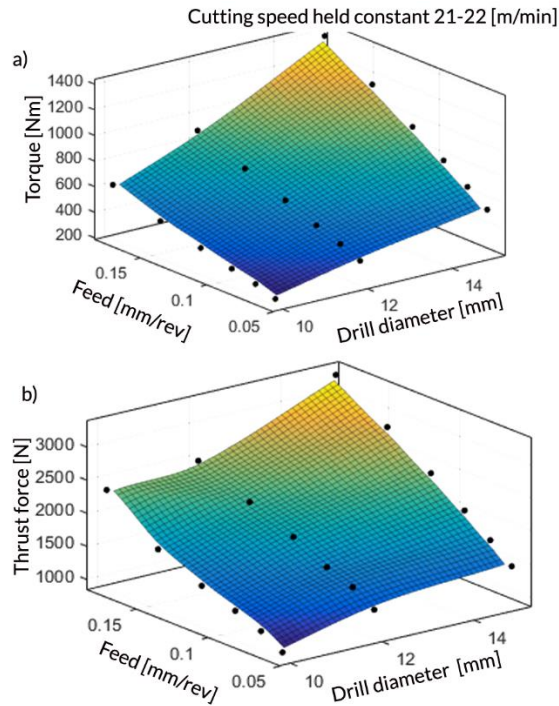


Fig. 4. 3D response surface: (a) torque and (b) thrust force

## 5. CONCLUSION

This paper presents the results of experimental investigations carried out with the aim of modeling torque and thrust force. In order to model these performances, experiments were carried out while machining C15 steel with HSS drills. The modeling was carried out using artificial intelligence tools with a genetic algorithm, all with the aim of better understanding the machining process. The error of the obtained models is acceptable and is 3.26% for the torque model, while it is 3.43% for the thrust force. Through the research conducted in this paper, new questions arise and are mentioned as directions for future research. One of them is the improvement of the modeling of the drilling process with a larger number of measurement points, as well as an additional analysis of the influence of the input parameters on the torque and the thrust force.

## 6. REFERENCES

- [1] Tönshoff, H. K., Spintig, W., König, W.: Machining of Holes - Development in Drilling Technology, Annals of the CIRP, vol. 43, no. 2, pp. 551-561, 1994.
- [2] Merchant, M. E.: Basic mechanics of the metal

cutting process, Journal of Applied Mechanics, pp. A168–A175, 1954.

- [3] Shaw, M.C.: Metal Cutting Principles, Third ed., M.I.T., Cambridge, Mass., 1954.
- [4] Oxford, C. J.: On the drilling of metals I-basic mechanics of the process, Transactions of ASME 77 pp. 103–114, 1954.
- [5] Shaw, M. C., Oxford, C. J.: On the drilling of metals II—the torque and thrust of drilling, Transactions of ASME 79, pp. 139–148, 1957.
- [6] Williams, R. A.: A study of the drilling process, Journal of Engineering for Industry, Vol. 96, pp. 1207–1215, 1974.
- [7] Armarego, E. J. A. Cheng, C. Y.: Drilling with flat rake face and conventional twist drills—I. theoretical investigation, International Journal of Machine Tools and Manufacture, Vol. 12, pp. 17–35, 1972.
- [8] Gostimirovic, M., et al.: Evolutionary optimization of jet lag in the abrasive water jet machining. The International Journal of Advanced Manufacturing Technology. Vol. 101(9), pp. 3131-3141, 2019.
- [9] Kumar, D.R., et al.: Optimization Of Drilling Process On Carbon-Fiber Reinforced Plastics Using Genetic Algorithm. Surface Review and Letters (SRL).Vol. 28(03), pp. 1-13, 2021.
- [10] Pandey, A.K. and G.D. Gautam: Grey relational analysis-based genetic algorithm optimization of electrical discharge drilling of Nimonic-90 superalloy. Journal of the Brazilian Society of Mechanical Sciences and Engineering. Vol. 40(3), pp. 1-16, 2018.
- [11] Suthar, J., U. Bhushi, and S. Teli: Drilling process improvement with genetic algorithm. Materials Today: Proceedings.Vol. 44, pp. 2735-2739, 2021.
- [12] Zolpakar, N.A., et al., Application of multi-objective genetic algorithm (MOGA) optimization in machining processes, in Optimization of Manufacturing Processes. Springer. pp. 185-199, 2020.
- [13] Sekulic, M., et al.: Prediction of surface roughness in the ball-end milling process using response surface methodology, genetic algorithms, and grey wolf optimizer algorithm. Advances in Production Engineering & Management. Vol. 13(1), pp. 18-30, 2018.

**Authors:** Full Prof. Milenko Sekulić, Assist. Prof. Dragan Rodić, Full Prof. Marin Gostimirović, Assoc. Prof. Borislav Savković, M.Sc. Anđelko Aleksić, M.Sc. Nenad Kulundžić, University of Novi Sad, Faculty of Technical Sciences, Department of Production Engineering, Trg Dositeja Obradovića 6, 21000 Novi Sad, Serbia, Phone.: +381 21 485-23-24, Fax: +381 21 454-495.  
E-mail: [milenkos@uns.ac.rs](mailto:milenkos@uns.ac.rs); [rodicdr@uns.ac.rs](mailto:rodicdr@uns.ac.rs); [maring@uns.ac.rs](mailto:maring@uns.ac.rs); [savkovic@uns.ac.rs](mailto:savkovic@uns.ac.rs); [andjelkoa94@uns.ac.rs](mailto:andjelkoa94@uns.ac.rs); [kulundzic@uns.ac.rs](mailto:kulundzic@uns.ac.rs)

**ACKNOWLEDGMENTS:** This paper has been supported by the Ministry of Education, Science and Technological Development through the project no. 451-03-68/2020-14/200156: “Innovative scientific and artistic research from the FTS (activity) domain”.

Nedić, B., Baralić, J.

## EXPERIMENTAL INVESTIGATION OF THE INFLUENCE OF MACHINING PARAMETERS ON CUT QUALITY IN MDF LASER CUTTING

**Abstract:** This paper presents the technological tests conducted on mediapan (MDF) with and without decorative foil, in order to determinate maximum cutting speed and best quality of cut. The main goal was to get high quality of cut surface without damaging the edge or any ignition traces. To prevent any ignition a compressor was used. Tests were conducted using two different air pressures - 1 bar and 3 bars. The aim of this paper was to find the optimal cutting regimes, combining different powers, cutting speeds and air pressure in order to find the optimal one for mediapan with and without decorative foil. Results obtained from these tests, can be used as entry data, when laser cutting is used in furniture industry or in any other industry where cutting these kind of material is necessary in order to manufacture the final product.

**Key words:** laser beam, mediapan MDF, cut quality, optimal cutting parameters.

### 1. INTRODUCTION

Today, laser machining is very common in almost all industries. With this machining procedure, almost all materials - metallic and non-metallic, can be cut, welded or coated on; it is only necessary to select the appropriate type of laser and laser power. Unlike conventional machining procedures, laser beam, as a tool, does not wear out, and material removal is not dependent on its hardness but on the optical properties of the laser and the optical and thermophysical properties of the material. [1] Laser (light amplification by stimulated emission of radiation) is a source of light radiation that emits a coherent beam of photons. As a source, it is stable in frequency, wavelength and power. Unlike light emitted by common sources, such as light bulbs, laser light is mostly monochromatic, ie. only one wavelength (color) and is directed in a narrow beam. The beam is coherent, which means that the electromagnetic waves are in the same phase with each other and propagate in the same direction.

### 2. CUTTING WOOD MATERIALS WITH CO<sub>2</sub> LASER

The nonmetallic materials have low thermal conductivity and thermal diffusion coefficients, but most of these materials have high absorptivity for the 10.6  $\mu\text{m}$  wavelength radiation of CO<sub>2</sub> laser [2]. CO<sub>2</sub> lasers are very often used today for cutting wood materials because wood very well absorbs radiation wavelength of 10.6  $\mu\text{m}$ . The effect of heating, evaporation and combustion of wood occurs rapidly [3].

CO<sub>2</sub> laser is molecular gas laser. On figure 1. is shown CO<sub>2</sub> laser beam machining schematic.

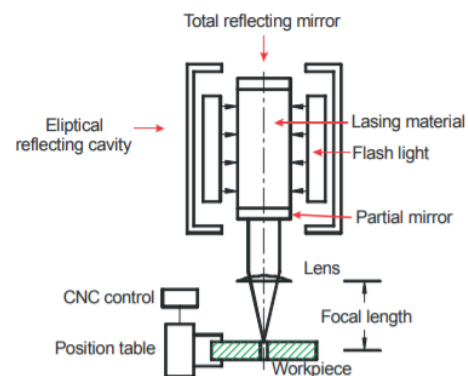


Fig. 1. CO<sub>2</sub> laser beam machining schematic [4]

The laser tube is about 1000 mm long. The diameter of the laser tube is about a few tens of millimeters. A laser beam with 10.6  $\mu\text{m}$  wavelength passes through a partial mirror. Then, the laser beam passes through lenses, which focuses the laser beam on the small spot. This causes an enormous amount of light and thermal energy which leads to the melting and evaporation of machining material.

The cutting of wooden materials was one of the first commercial applications of lasers in the early 1970s. Mass-production of mediapan-MDF began in the 1980s. Mediapan (MDF) is a medium-thick fiberboard made mainly of beech, spruce, fir and wood with the addition of polymer resins. Unlike plywood, MDF has a homogeneous and very fine structure, so it has a higher hardness and is more resistant to moisture, and it can be processed in the traditional way as well as wood.

When cutting wooden materials, several problems usually occur, and they are:

- When cutting foil-coated materials, the foil may melt and stick to the bottom of the workpiece. In order to prevent this phenomenon, it is necessary to process the object during processing elevated from the work table of the machine (place it on the grid during processing, etc.);

- When wood is cut with a laser, traces of ignition often appear on the surface. This phenomenon is most easily eliminated by placing tape or foil on the surface of the workpiece. Also, the supply of compressed air prevents the appearance of traces of ignition.

If traces of ignition still appear, the easiest way to remove it is to sand. Figure 2. shows the samples cut with the applied protective tape and without the protective tape.



Fig. 2. Samples cut with protective tape and without protective tape [5]

Many authors have investigated the influence of laser cutting process parameters on the quality of wood cutting. Among the first studies were those conducted by Lum et al. [6]. In their work, the authors cut MDF with different combinations of laser power, cutting speed and gas pressure in order to determine their impact on the quality of the kerf. They found that, the average kerf width decreases with increasing the cutting speed. They also found that the pressure of the shielding gas had no significant effect on the cut width. The authors observed that increasing the cutting speed leads to an increase in the roughness of the cut surface. As they did not notice the influence of the type of shielding gas, they concluded that it is more economical to use compressed air than nitrogen to laser cut MDF.

Today, many recommendations for cutting and engraving wooden materials can be found in the literature. Modern wood materials are classified into two groups: soft woods and hard woods.

On low power laser cutting machines - 30 ÷ 60 W, soft wood (pine, cedar, alder, basswood, etc.) is mainly machined, while for hard wood cutting (birch, maple, cherry, mahogany, walnut, and oak) need more powerful lasers - 50 ÷ 120 W, because of their density.

### 3. EXPERIMENTAL RESEARCH

In this paper, the cutting of mediapan-MDF, 3 mm thick, with and without decorative foil was examined. The influence of the machining parameters (laser power, cutting speed and shielding gas-air pressure) on the quality of the cut edge was analyzed. The quality of the cutting edge was assessed visually. It was observed

whether there was a complete cut through the MDF board and whether there were visible traces of ignition. The criterion adopted as the boundary between satisfactory and unsatisfactory quality is the good quality of the cut edge-kerf with small traces of ignition on the cutting line.

Air was used as a shielding gas during cutting. Cutting was performed at an air pressure of 1 bar and 3 bars. Before cutting, the beam was focused at the top surface of each piece.

The tests were performed on a CNC laser cutting machine "LaserCut1209". In Figure 3. is shown appearance of the working space and the cutting head of the laser machine.



Fig. 3. CNC machine "LaserCut1209", working space and laser cutting head

The maximum power of the laser is 80W, the maximum speed of the tool is 70mm/min, while the maximum working strokes of the tool are 1000mm x 700mm x 300mm.

The dimensions and shape of the samples cut during the test are shown in Figure 4.

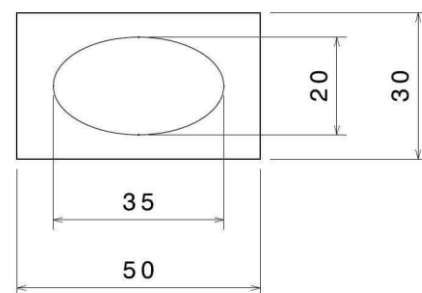


Fig.4. Dimensions and shape of samples

### 3.1 The results obtained by cutting at air pressure of 1 bar

Machining parameters		Comments
P [W]	v [mm/s]	
80	60	Uncut
80	50	Averaged with a slight tearing of the material at the kerf edges and significant burning of the edges
80	40	Good quality kerf edge with traces of ignition
80	30	Good kerf edge quality with traces of ignition to a lesser extent than in the previous case
60	30	Averaged with slight damage at one edge
60	20	Good quality kerf edge with small traces of ignition
40	20	Good quality kerf edge with small traces of ignition
40	15	Good quality kerf edge with small traces of ignition
20	15	Uncut
20	10	Uncut

Table 1. MDF, enriched with decorative foil, ≠3mm

Machining parameters		Comments
P [W]	v [mm/s]	
80	50	Very poor quality of the kerf edge with significant traces of ignition
80	40	Very poor quality of the kerf edge with small traces of ignition
80	30	Good quality kerf edge with small traces of ignition
60	30	Good quality kerf edge with small traces of ignition
60	20	Good quality kerf edge with one spot on the edge of the ellipse
40	30	Good quality kerf edge with small traces of ignition
40	20	Excellent kerf edge quality with almost no traces of ignition
20	20	Uncut
20	10	Uncut
20	5	Uncut

Table 2. MDF, ≠ 3 mm

Figure 5. shows the appearance of the cut samples at air pressure of 1 bar.

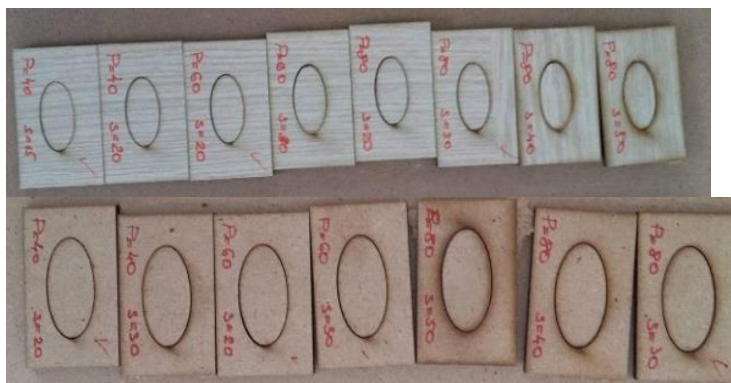


Fig. 5. Samples of MDF enriched with decorative foil ≠ 3 mm and MDF ≠ 3 mm

### 3.2 The results obtained by cutting at air pressure of 3 bars

Machining parameters		Comments
P [W]	v [mm/s]	
80	50	Partly averaged with significant traces of ignition
80	40	Poor quality of the kerf edge with traces of ignition
80	30	Good kerf edge quality with slight traces of ignition
60	30	Good kerf edge quality with slight traces of ignition
40	30	Poor kerf edge quality with slight traces of ignition
40	20	Good kerf edge quality with one spot on the ellipse

20	20	Uncut
20	10	Uncut
20	5	Poor kerf edge quality with one spot on the ellipse

Table 3. MDF, enriched with decorative foil, ≠3mm

Machining parameters		Comments
P[W]	v [mm/s]	
80	70	Poor quality of the kerf edge with traces of ignition
80	60	Good kerf edge quality with slight traces of ignition
80	55	Good kerf edge quality with slight traces of ignition
60	55	Good kerf edge quality with slight traces of ignition
60	50	Good kerf edge quality with slight traces of ignition
40	50	Good kerf edge quality with slight traces of ignition
40	40	Good kerf edge quality with slight traces of ignition
40	30	Good kerf edge quality with slight traces of ignition
20	30	Uncut
20	20	Uncut
20	10	Uncut
20	5	Partly averaged with traces of ignition

Table 4. MDF, ≠ 3 mm

Samples of MDF enriched with decorative foil ≠ 3 mm and MDF ≠ 3 mm are shown in Figure 6.

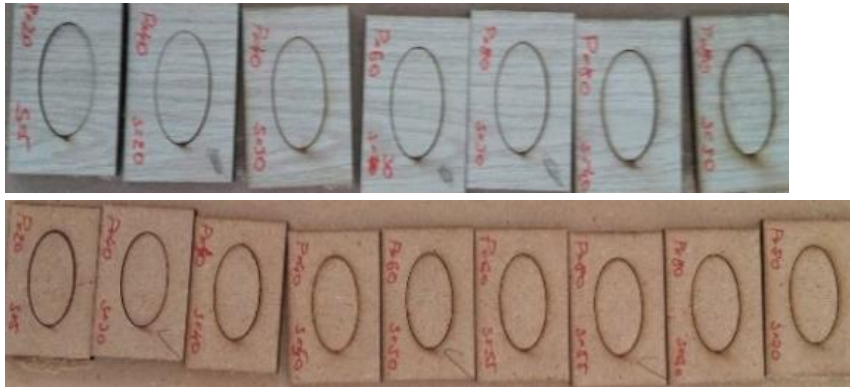
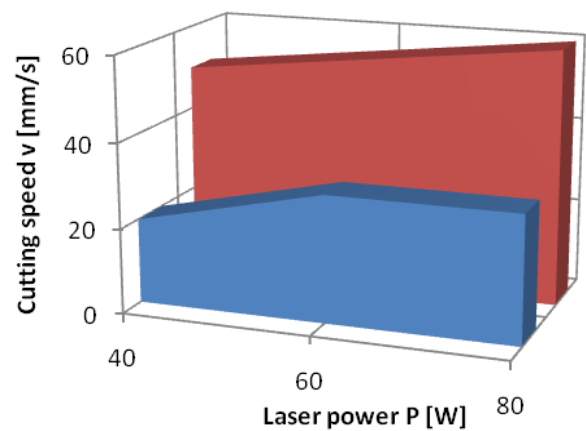
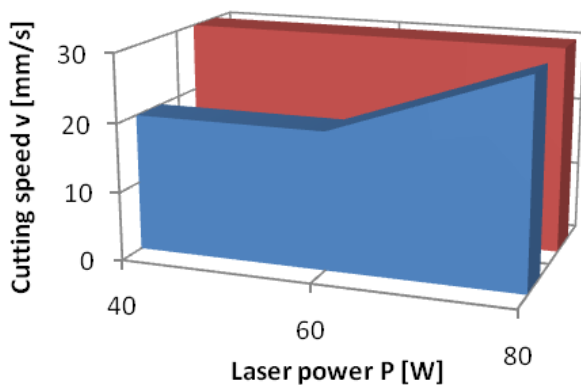


Fig. 6. Samples of MDF enriched with decorative foil ≠ 3 mm and MDF ≠ 3 mm

Figures 7 and 8 show the optimal cutting modes of MDF enriched with decorative foil and ordinary MDF

≠ 3mm, when braking with different air pressures, laser power and different cutting speeds.



■ MDF enriched with decorative foil  
 ■ MDF

Fig. 7. Optimal cutting modes at air pressure of 1 bar

Fig. 8. Optimal cutting modes at air pressure of 3 bars

### 3.3. Analysis of results

From the diagrams shown in Figures 7 and 8. it can be concluded that ordinary MDF can be cut, in satisfactory quality, at higher speeds than MDF enriched with decorative foil regardless of whether the cutting is done with air pressure of 1 bar, or at cutting with an air pressure of 3 bar. Recommendations that can be found in the literature are that the appearance of traces of ignition on the edges of the cut can be prevented by using a protective foil on the boards of wooden material. In this research, ordinary MDF and MDF enriched with decorative foil were used. It can be concluded that the decorative foil is very sensitive to heat, so the MDF enriched with the decorative foil must be cut with lower cutting speeds. When comparing the cutting results with an air pressure of 1 bar and 3 bar, it can be concluded that the cutting speeds at which a satisfactory cutting quality can be achieved are significantly higher when cutting with a higher air pressure.

### 4. CONCLUSION

Cutting speed is one of the most important parameters when cutting, both from the economic aspect and from the aspect of productivity. Laser cutting of flat wood materials has an advantage over traditional cutting methods due to greater precision and significantly narrower cut, as well as higher productivity.

The results of the research showed that the cutting speeds for MDF enriched with decorative foil are significantly lower than the cutting speeds of ordinary MDF. This is due to the high sensitivity of the decorative foil to heat. If it is necessary to cut the MDF enriched with decorative foil at higher cutting speeds, the surfaces to be cut should still be protected with a protective foil. In that way, the traces of ignition will be less pronounced on the edges of the cut. Also, it can be concluded that when cutting with higher laser power, both types of MDF can be cut at higher speeds.

When cutting MDF with higher air pressures, which was used as a shielding gas, it is possible to cut the MDF at significantly higher speeds without the appearance of traces of ignition. It can be seen from the diagrams that the cutting speeds at an air pressure of 3 bars are almost twice as high as when cutting with an air pressure of 1 bar. In the case of MDF enriched with decorative foil, the air pressure did not have a significant effect on the cutting speed. Based on this, it can be concluded that the decorative foil is very sensitive to the heat.

In order to determine the influence of air pressure on the quality of the cut when cutting MDF enriched with decorative foil, additional tests are needed. Also, it is reasonable to perform these tests on the other wooden plate materials. If it proves that an increase in air pressure leads to an increase in the cutting speed, as is the case with MDF, then it is economically justified to reconstruct the laser cutting machine in order to enable the supply of higher pressure air to the cutting zone.

### 5. REFERENCES

- [1] Meijer, J.: *Laser beam machining (LBM), state of the art and new opportunities*, Journal of Materials Processing Technology, Vol. 149, pp. 2–17, 2004
- [2] Zhou, B.H., Mahdavian, S.M.: *Experimental and theoretical analyses of cutting nonmetallic materials by low power CO<sub>2</sub>-laser*, Journal of Materials Processing Technology, Vol. 146(2), pp.188-192, 2004
- [3] Kubovsky, I., Babiak, M., Cipka, Š.: *A determination of specific wood mass removal energy in machining by CO<sub>2</sub> laser*, Acta facultatis xylogologiae Zvolen, Vol. 54(2), pp. 31-37, 2012
- [4] Baralić, J., Nedić, B., Đurić, S.: *The influence of laser milling process parameters on depth of cut and surface roughness*, SERBIATRIB'19, FIN Kragujevac, Kragujevac, 2019
- [5] <https://all3dp.com/1/laser-cut-files-templates/>
- [6] Lum, K. C. P., Ng, S. L., Black, I.: *CO<sub>2</sub> laser cutting of MDF, 1- Determination of process parameter settings*, Journal of Optics and Laser Technology, Vol.32, pp. 67-76, 2000.
- [7] Eltawahnia, H. A., Rossinib, N. S., Dassistib, M., Alrashedc, K., Aldahamc, T., Benyounisd, K. Y., Olabie, A. G.: *Evalaution and optimization of laser cutting parametersfor plywood materials*, Optics and Lasers in Engineering, Volume 51, Issue 9, pp. 1029-1043, September 2013.
- [8] Milikić, D.: *Nekonvencionalni postupci obrade*, Univerzitet u Novom Sadu, Novi Sad, 2002
- [9] Lazić, M.: *Nekonvencionalni postupci obrade*, Mašinski fakultet u Kragujevcu, Kragujevac, 1990

**Authors: Full Prof. Bogdan Nedić, Assist. Prof. Jelena Baralić**

University of Kragujevac, Faculty of Engineering Sciences Kragujevac, Department of Production Engineering, Sestre Janjić, 34000 Kragujevac, +38134 335990, University of Kragujevac, Faculty of Technical Čačak, Department of mechatronics, Svetog Save 65, 32000 Čačak, Serbia, Phone: +381 32302733. E-mail: [nedic@kg.ac.rs](mailto:nedic@kg.ac.rs); [jelena.baralic@ftn.kg.ac.rs](mailto:jelena.baralic@ftn.kg.ac.rs)

**ACKNOWLEDGMENTS:** This study was supported by the Ministry of Education, Science and Technological Development of the Republic of Serbia, and these results are parts of the Grant No. 451 451-03-9/2021-14/200132 with University of Kragujevac - Faculty of Technical Sciences Čačak.





Aleksić, A., Sekulić, M., Gostimirović, M., Rodić, D., Savković, B., Antić, A.

## EFFECT OF CUTTING PARAMETERS ON CUTTING FORCES IN TURNING OF CPM 10V STEEL

**Abstract:** The objective of this paper is to investigate the effect of cutting parameters on cutting forces during turning of CPM 10V steel with coated cutting tool. Machining of CPM 10V steel and finding a suitable tool is very challenging due to its physical and mechanical properties, especially since the machining of this material has not been extensively researched. The experiments were carried out using an Index GU -600 CNC lathe and the cutting forces were measured in process. A three-factorial three-level experimental design was used for the experiments. Statistical method analysis of variance (ANOVA) is applied to study the effects of cutting speed, feed rate, and depth of cut on cutting forces. The results of this study show that depth of cut has the most significant effect on main force and radial force, while feed rate and cutting speed have the most significant effect on feed force. The developed model can be used in the machining industry to predict and analyze cutting parameters for optimal cutting forces.

**Key words:** CPM-10V, powder metallurgy, cutting parameters, ANOVA

### 1. INTRODUCTION

In the recent past, considerable improvements have been made in turning, making it easier to machine materials that are difficult to cut and resulting in better machinability (better surface finish and lower cutting forces). The forces acting on the tool are an important aspect of machining. Knowledge of cutting forces is necessary for estimating power requirements and designing machine tool elements and fixtures that are sufficiently rigid and free from vibration. Most of the energy consumed in metal cutting is converted to heat near the cutting edge of the tool, and many of the economic and technical problems in machining are caused by this heating. Therefore, proper selection of cutting tools and process parameters to achieve high cutting performance in a turning operation is a critical task [1].

Steels with high vanadium content in the tooling industry are used, such as cutting blades, paper cutters, drilling tools, cold forming tools, etc. The main problem with this type of steel is reduced toughness, which is an undesirable consequence of increasing the vanadium content. Powder metallurgy is a technology developed to obtain a fine carbide structure, even when a high content of alloying additions is made. Soon, crucible metallurgists discovered that much higher alloy steels, especially high vanadium steels, were possible with powder metallurgy. In 1978, the "Powder Metallurgy" method was used to develop CPM 10V steel with a high vanadium content (about 10%), which has both good wear resistance and high toughness. Since then, CPM 10V has been widely used in tools that require high wear resistance and have a toughness problem [2].

Figure 2 shows the difference in the microstructure of steels produced by conventional methods and powder metallurgy. The difference in the homogeneity of the microstructure is visible.

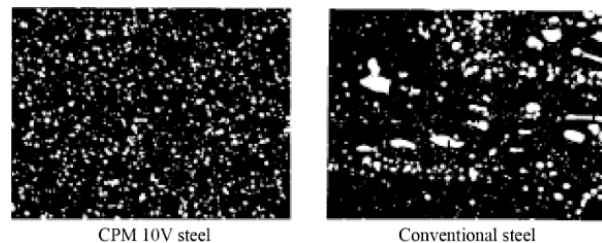


Fig. 1. Microstructure of CPM 10V steel and conventional steel [2]

This paper aims to analyze the parameters of the processing mode (cutting depth, feed rate, and cutting speed) on the cutting forces (The main cutting force -  $F_v$ , radial force -  $F_p$ , and feed force  $F_f$ ), as well as to develop a mathematical model. Minitab 17 software was used to analyze the results.

### 2. MATERIALS AND METHODS

#### 2.1 Experimental setup

Experimental work was carried out at the Faculty of Technical Sciences, in the Laboratory for Conventional Machining.

The conditions for experimental testing are given in this chapter. Conditions apply to:

- The workpiece material,
- machine tool,
- cutting tool and
- cutting conditions,
- measuring technique.

**The workpiece material:** Experimental tests were performed on CPM 10V steel produced by powder metallurgy. Powder metallurgy is a technology developed to obtain a fine carbide structure even when a large amount of alloying additions are used. 10V is the evolution of the earlier 4÷5% vanadium steel. Its combination of toughness, wear resistance, and cutting edge stability predestines it to replace tool steels that are prone to chipping at the tool cutting edge during cold working [3]. The chemical structure is shown in Table 1.

The workpiece had a length of 80 mm (cutting length) and a diameter of 40 mm.

Steel	C	Mn	Si	Cr	V	Mo	S
10V	2,45	0,5	0,9	5,25	9,75	1,30	0,07

Table 1. Chemical structure of CPM 10V steel [4]

**Machine tool:** The experimental work was carried out at the Department of Production Engineering, the Faculty of Technical Sciences in Novi Sad. The machining was conducted on a Index GU-600 CNC lathe in dry condition.

**Cutting tool:** A turning cutter SVLBL2525M16, with cemented carbide inserts („SECO“ type VBMT160408-M5, TP1501) with coated Ti(C,N) + Al<sub>2</sub>O<sub>3</sub>+ Cr (Used edge detection) [5]. Table 2 illustrates the geometrical characteristics of the cutting tool positioned on its tool holder.

Geometrical Characteristics of VBMT160408-M5 insert	Value
Clearance angle major	5°
Insert included angle	35°
Theoretical cutting edge length	16,61 mm
Corner radius	0,80 mm
Insert thickness	4,76 mm

Table 2. Geometrical specifications of VBMT160408-M5 insert [5]

**Cutting conditions:**

- Cutting speed  $v$ ,
- Feed rate  $f$ ,
- Depth of cut  $a$ .

Table 3 is shown machining parameters and their levels based on the material of the workpiece and the recommendations of the tool manufacturer.

Levels	Depth of cut $a$ [mm]	Feed rate $f$ [mm/rev]	Cutting speed $v$ [m/min]
Max. +1	1,6	0,26	600
Midium 0	1,13	0,22	424
Min. -1	0,8	0,18	300

Table 3. Machining parameters and their levels

**Measuring technique:** For the cutting force measurements a Kistler® three-axis piezoelectric type 9257A is used (Figure 2a). The dynamometer is mounted on the machine via a specially designed holder, as shown in Figure 2b.

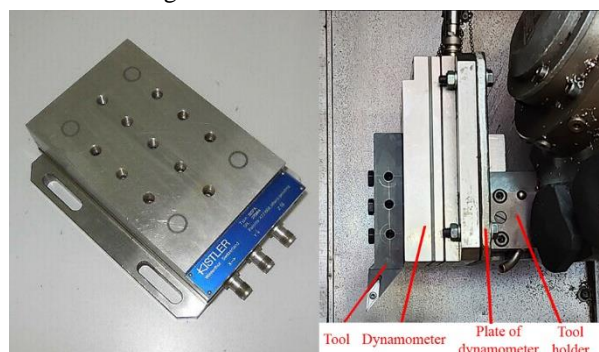


Fig. 2. a) The 3-axis Kistler 9257A dynamometer, b) specially designed holder of dynamometer

The piezoelectric dynamometer is connected to a charge amplifier through 3 coaxial cables shielded, grounded, and waterproof. Further on, the amplifier communicates with a PC across an A/D card, which converts the analog signal to digital. The signal processing is performed by the LabView program. Figure 3 illustrates the layout diagram for the data processing.

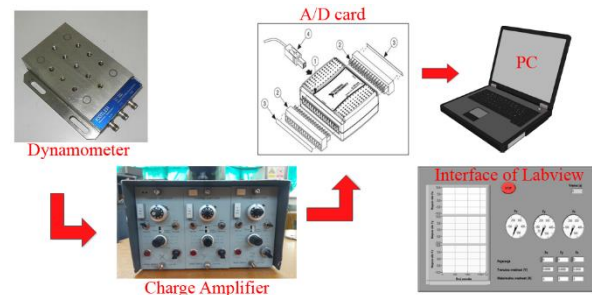


Fig. 3. Layout diagram for signal processing

### 3. RESULTS AND DESCUSSION

In table 4 is shown the setup of experiments and results of cutting forces. All of the experiments were conducted with one insert without coolant.

S. No.	Cutting parameters			$F_v$	$F_p$	$F_f$
	$a$ [mm]	$f$ [mm/rev]	$v$ [m/min]			
1	0,8	0,18	300	880,53	84,02	379,74
2	1,6	0,18	300	1594,42	177,13	339,89
3	0,8	0,26	300	1140,57	86,24	420,45
4	1,6	0,26	300	2154,48	187,84	421,54
5	0,8	0,18	600	784,58	69,42	397,23
6	1,6	0,18	600	1495,42	176,43	419,22
7	0,8	0,26	600	990,89	68,88	422,01
8	1,6	0,26	600	1971,29	175,00	455,99
9	1,13	0,22	424	1250,11	115,37	413,66
10	1,13	0,22	424	1260,04	112,31	397,19
11	1,13	0,22	424	1284,36	115,46	395,42
12	1,13	0,22	424	1287,87	115,28	396,24

Table 4. The setup of experiments and results of cutting forces

#### 3.1 Response surface regression: $F_v$

For regression analysis, analysis of variance (ANOVA), as well as the response surfaces commercially available statistical analysis software, was used. The analysis determined the significance of the model and the flow of the processing parameters on the cutting forces.

Based on Table 4, an analysis of variance was performed. The results of the analysis are shown in Table 5.

Analysis of Variance

Source	DF	Adj SS	Adj MS	F-Value	P-Value
Model	7	1851178	264454	932,06	0,000
Linear	3	1778159	592720	2089,03	0,000
a	1	1461229	1461229	5150,07	0,000
f	1	282106	282106	994,27	0,000
v	1	34824	34824	122,74	0,000
Square	1	4705	4705	16,58	0,015
a*a	1	4705	4705	16,58	0,015
2-Way Interaction	3	43097	14366	50,63	0,001
a*f	1	40553	40553	142,93	0,000
a*v	1	167	167	0,59	0,486
f*v	1	2378	2378	8,38	0,044
Error	4	1135	284		
Lack-of-Fit	1	116	116	0,34	0,600
Pure Error	3	1019	340		
Total	11	1852313			

Model Summary

S	R-sq	R-sq(adj)	R-sq(pred)
16,8443	99,94%	99,83%	99,50%

Table 5. Response Surface Regression:  $F_v$  versus  $a, f, v$

Based on the value of P, a decision is made on the significance of the parameters. If the value of  $P < 0,05$ , the parameter is significant [6]. By reviewing Table 5, it can be concluded that all parameters are significant, except for  $a * v$ .

The adequacy of the model is reflected in the value of "Lack-of-fit" the value of P is 0,600, which means that the model is adequate (the value of P must be higher than 0,05). After analyzing the mathematical model (R-sq and R-sq(adj)), it is concluded that the model is adequate. Since the value of the reduced model is greater than 90% (R-sq (adj) = 99,83%), it is adopted (Equation 1).

$$F_v = 335 - 300 * a + 648 * f + 0,284 * v + 176,6 * a^2 + 4450 * a * f - 2,873 * f * v \quad (1)$$

The significance of parameters can be determined based on ANOVA analysis. Figure 4 shows the strength of the processing parameters for the force  $F_v$ , where it can be seen that the greatest influence on the force  $F_v$  has the depth of cut, followed by a feed rate, and the least important is the cutting speed.

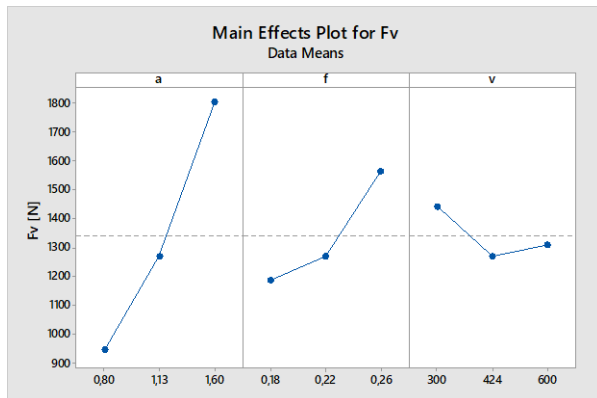


Fig. 4. Effect of cutting parameters on cutting force  $F_v$

### 3.2 Response surface regression: $F_p$

In the same way, as for the force  $F_v$ , an analysis of the force  $F_p$  was performed. The results of the analysis are shown in Table 6.

Analysis of Variance

Source	DF	Adj SS	Adj MS	F-Value	P-Value
Model	7	21629,9	3090,0	685,26	0,000
Linear	3	21065,5	7021,8	1557,21	0,000
a	1	20791,7	20791,7	4610,91	0,000
f	1	15,0	15,0	3,33	0,142
v	1	258,8	258,8	57,39	0,002
Square	1	83,4	83,4	18,49	0,013
a*a	1	83,4	83,4	18,49	0,013
2-Way Interaction	3	77,4	25,8	5,72	0,063
a*f	1	7,2	7,2	1,60	0,274
a*v	1	42,4	42,4	9,41	0,037
f*v	1	27,8	27,8	6,15	0,068
Error	4	18,0	4,5		
Lack-of-Fit	1	11,0	11,0	4,69	0,119
Pure Error	3	7,0	2,3		
Total	11	21648,0			

Model Summary

S	R-sq	R-sq(adj)	R-sq(pred)
2,12350	99,92%	99,77%	96,69%

Table 6. Response Surface Regression:  $F_p$  versus  $a, f, v$

The value of p for the "Lack of fit" function is 0.119, which means that the model is adequate (Equation 2). The feed rate is not significant for the penetration force  $F_p$ , as well as all iterations with it ( $a * f$ , and  $f * v$ ). The reduced mathematical model is shown by Equation 2.

$$F_p = 37 + 9,7 * a - 0,0157 * v + 36,42 * a^2 + 0,0384 * a * v \quad (2)$$

Figure 5 shows the strength of the processing parameters for the force  $F_p$ , where it can be seen that the largest and only influence on the force  $F_p$  has the depth of cut, while the feed rate and cutting speed have almost no effect.

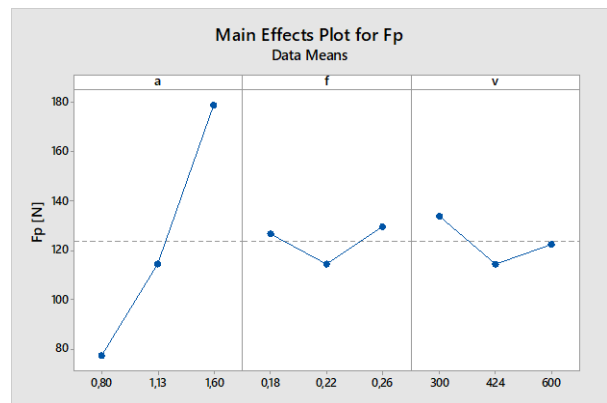


Fig. 5. Effect of cutting parameters on cutting force  $F_p$

### 3.3 Response surface regression: $F_f$

As in previous times, an analysis for the force  $F_f$  was performed. The results of the analysis are shown in Table 7.

The value of p for the "Lack of fit" function is 0,325, which means that the model is adequate (Equation 3). The depth of cut is not significant for the force  $F_f$ , as well iterations  $a * a, a * f$ , and  $f * v$ . In this case, a reduced mathematical model will not be used, because the value of R-sq(adj) is  $< 90\%$ , so the original mathematical model was used, whose accuracy is R-sq = 96,24%.

## Analysis of Variance

Source	DF	Adj SS	Adj MS	F-Value	P-Value
Model	7	8513,10	1216,16	14,62	0,010
Linear	3	6470,36	2156,79	25,92	0,004
a	1	37,02	37,02	0,44	0,541
f	1	4227,86	4227,86	50,82	0,002
v	1	2205,48	2205,48	26,51	0,007
Square	1	31,75	31,75	0,38	0,570
a*a	1	31,75	31,75	0,38	0,570
2-Way Interaction	3	1934,15	644,72	7,75	0,038
a*f	1	350,20	350,20	4,21	0,109
a*v	1	1121,72	1121,72	13,48	0,021
f*v	1	462,23	462,23	5,56	0,078
Error	4	332,79	83,20		
Lack-of-Fit	1	104,76	104,76	1,38	0,325
Pure Error	3	228,03	76,01		
Total	11	8845,89			

## Model Summary

S	R-sq	R-sq(adj)	R-sq(pred)
9,12131	96,24%	89,65%	19,62%

Table 7. Response Surface Regression:  $F_f$  versus  $a, f, v$

$$F_f = 343,4 - 228 * a + 649 * f + 0,153 * v + 22,5 * a^2 + 414 * a * f + 0,1974 a * v - 1,267 f * v \quad (3)$$

Figure 6 shows the strength of the processing parameters for the force  $F_f$ , where it can be seen that the largest influence on the force  $F_f$  has the feed rate and cutting speed, while the depth of cut has no effect.

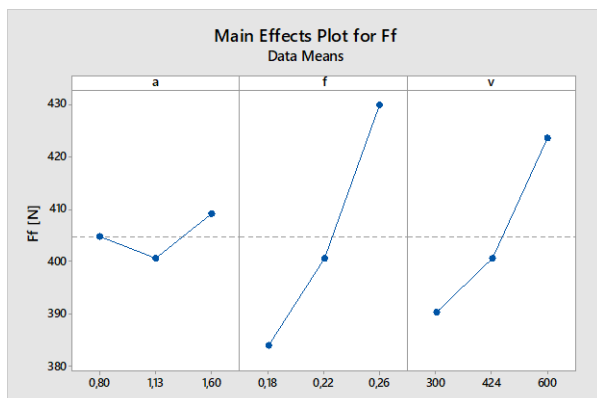


Fig. 6. Effect of cutting parameters on cutting force  $F_f$

## 4. CONCLUSION

Based on the theoretical and experimental studies carried out and the analyzes performed, the following conclusions can be drawn:

- Collecting data on forces in the cutting zone is a complicated process and depends on a variety of factors as well as on the accuracy of the measurement and acquisition system. A properly tuned measurement and acquisition system is a prerequisite for a good experiment.
- Design of experiments and analysis of variance contributes greatly to accurately represent the adequacy and significance of models and parameters, thus facilitating the work of researchers.

- The machinability of CPM 10V tool steel in terms of cutting forces is better with increasing cutting speed (as cutting speed values increase, forces decrease).
- The major influence on the main cutting force is the depth of cut followed by feed rate and the least important is cutting speed.
- Radial cutting force: depth of cut has the greatest influence, while feed rate and cutting speed have no influence.
- Feed rate and cutting speed have a similar influence on feed force while the depth of cut has no influence.

Continuing research in the field of machining CPM 10V tool steel with carbide inserts can go in the direction of expanding the factors influencing the cutting forces in turning. Optimization of the process is also the way to be followed in further research.

## 5. REFERENCES

- [1] Vaxevanidis, N.M., Kechagias, J.D., Fountas, N., Manolakos D.E.: *Influence of cutting parameters on the machinability of AISI D6 tool steel in turning*, Chapter 9 in: J.P. Davim (ed.) *Machining: Operations, technology and management*, Nova Publishers, USA, 2013.
- [2] Haswell, T.W., Kasak, A.L: *Powder metallurgy steel article with high vanadium-carbide content*, Crucible Inc., Pittsburgh, Pa, 1978.
- [3] Haswell, W. T., Kasak, A.: *Powder-Metallurgy steel article with high vanadium-carbide content*, US Patent US4249945A, 1981.
- [4] Larrin, T.: *CPM 10V Steel – History, properties, and how to heat treat*, Knife engineering, Pittsburgh, Pa, 2020.
- [5] “Secotools.com”  
[https://www.secotools.com/article/p\\_02959792](https://www.secotools.com/article/p_02959792).
- [6] Montgomery, C.D.: *Design and analysis of experiments*, Library of congress, Hoboken NJ, 2017.

**Authors:** M.Sc. Anđelko Aleksić, Full Prof. Milenko Sekulić, Full Prof. Marin Gostimirović, Assist. Prof. Dragan Rodić, Assoc. Prof. Borislav Savković, Full Prof. Aco Antić, University of Novi Sad, Faculty of Technical Sciences, Department of Production Engineering, Trg Dositeja Obradovića 6, 21000 Novi Sad, Serbia, Phone.: +381 21 485-23-24, Fax: +381 21 454-495.  
E-mail: [andjelkoa94@uns.ac.rs](mailto:andjelkoa94@uns.ac.rs); [milenkos@uns.ac.rs](mailto:milenkos@uns.ac.rs); [maring@uns.ac.rs](mailto:maring@uns.ac.rs); [rodicdr@uns.ac.rs](mailto:rodicdr@uns.ac.rs); [savkovic@uns.ac.rs](mailto:savkovic@uns.ac.rs); [antica@uns.ac.rs](mailto:antica@uns.ac.rs);

## ACKNOWLEDGEMENT

This paper has been supported by the Ministry of Education, Science and Technological Development through the project no. 451-03-68/2020-14/200156: “Innovative scientific and artistic research from the FTS (activity) domain”.



Section B:

**MACHINE TOOLS AND AUTOMATIC  
FLEXIBLE TECHNOLOGICAL SYSTEMS,  
CAx AND CIM PROCEDURES AND  
SYSTEMS**



Slavković, N., Vorkapić, N., Živanović, S., Dimić, Z., Kokotović, B.

**VIRTUAL BISCARA ROBOT INTEGRATED WITH OPEN-ARCHITECTURE CONTROL SYSTEM**

**Abstract:** The paper presents the developed control system with open architecture for the BiSCARA robot, based on the robot kinematic model. The control system is realized in the LinuxCNC software environment and includes the virtual robot model configured using several predefined Python classes and OpenGL. Presented methodology for configuring virtual robots could be used for any other robot or machine tool with parallel kinematic. The verification of the robot control system and robot kinematic model has been performed through several examples of drawing of contour on the configured virtual robot.

**Key words:** Kinematic modelling, Virtual robot, Control system, LinuxCNC, Simulation

**1. INTRODUCTION**

The first five-bar robot, i.e. pantograph robot, shown in Fig. 1a, was described in a US patent in 1934 [1, 2]. Much later, in 1978, Prof. Hiroshi Makino invented the well-known SCARA robot [3]. Then, in 1985, Donald C. Fyler came up with the idea of using a five-bar mechanism, shown in Fig. 1b, as a robot [1,4].

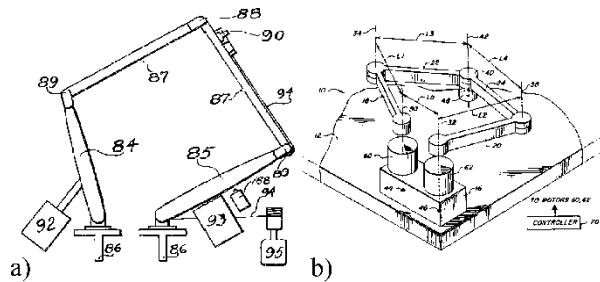


Fig. 1. Concept of five-bar, i.e. dual SCARA or BiSCARA, robot [1]

The first company that construct and commercialize the dual SCARA or BiSCARA robot, known as MELFA RP-1A, was Mitsubishi Electric, Fig. 2a, in 1998 [1].

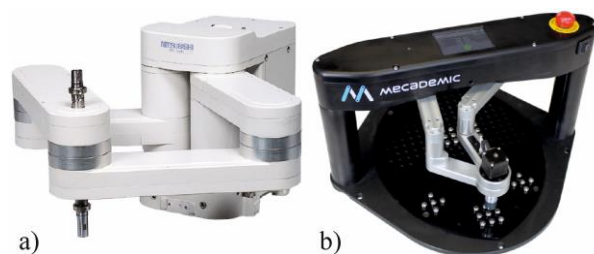


Fig. 2. Industrial BiSCARA robots [1]

An example of a developed industrial prototype, based on such a mechanism, is the DEXSTAR robot (Dextrous Twin-Arm Robot), Fig. 2b, which is developed for manipulation purposes [5].

The BiSCARA robot is very popular and is suitable for education and experimental work. Also, it is useful as a base mechanism that can be improved with the

additional translatory and rotary axis in order to develop four or five-axis robots.

This paper presents the developed control system with open architecture for the adopted model of the BiSCARA robot, according to the kinematic and CAD models [6]. The control system is realized in the LinuxCNC software environment and includes the virtual robot model configured using several predefined Python classes and OpenGL.

**2. KINEMATIC MODELLING**

Parallel BiSCARA robot can be viewed as a planar manipulator with two degrees of freedom, Fig. 1. The kinematic modelling, which is described in detail in [6], is realized in order to develop an open-architecture control system. Figure 3 shows the kinematic model of the BiSCARA robot. The robot consists of a base, a platform, and two kinematic chains with struts lengths  $l_1$  and  $l_2$ . All elements of the mechanism are connected by a joint with one rotary degree of freedom. The frame  $\{B\}$  represents the base frame, while the platform is represented by point P because the struts of length  $l_2$  are connected at the point P.

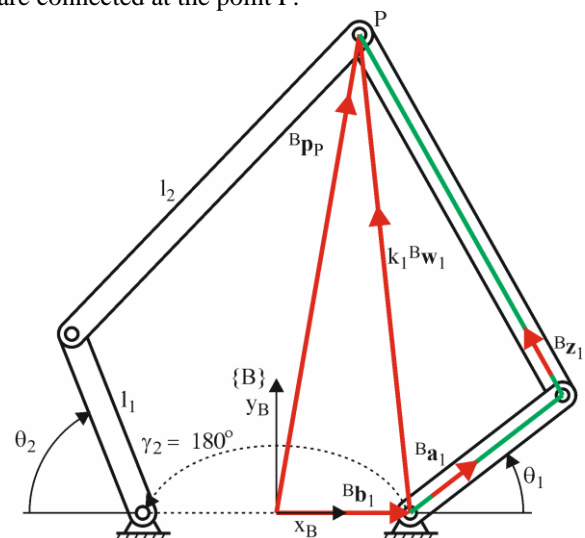


Fig. 3. Kinematic model of BiSCARA robot

As it can be seen from Fig. 3 the world coordinate vector can be represented as

$${}^B \mathbf{p}_P = [x_P \quad y_P]^T \quad (1)$$

while joint coordinate vector can be defined as

$$\boldsymbol{\theta} = [\theta_1 \quad \theta_2]^T \quad (2)$$

As it is said in [6], the vectors defined by the parameters of the mechanism are

- position vectors of the joint centers at the base  ${}^B \mathbf{b}_i = [b_{ix} \quad 0]^T$ ,
- unit vectors  ${}^B \mathbf{a}_i$  and  ${}^B \mathbf{z}_i$  along struts with lengths  $l_1$  and  $l_2$ , and
- unit vectors  ${}^B \mathbf{w}_i$ .

where  $i=1, 2$  represents the number of kinematic chain.

From Fig. 3 it is obvious that unit vector  ${}^B \mathbf{a}_i$  can be defined as

$${}^B \mathbf{a}_i = \begin{bmatrix} \cos(\theta_i) \cos(\gamma_i) \\ \sin(\theta_i) \end{bmatrix} \quad (3)$$

where the angle  $\gamma_i$  represents the angle that defines arrangement of kinematic chains and was introduced in order to generalize the solution of the inverse kinematic problem and parallel determination of joint coordinates during the solving an inverse kinematic problem.

Based on the defined vectors, according to Fig. 3, observing one kinematic chain, the following vector equations can be reported

$$\begin{aligned} {}^B \mathbf{p}_P &= {}^B \mathbf{b}_i + k_i {}^B \mathbf{w}_i \\ k_i {}^B \mathbf{w}_i &= l_1 {}^B \mathbf{a}_i + l_2 {}^B \mathbf{z}_i \end{aligned} \quad (4)$$

from which inverse and direct kinematic problems can be solved in analytic form.

Complete solution of inverse and direct kinematic problems, as the determination of Jacobian matrix and analysis of workspace is represented in authors' previous work [6]. Here is presented only the solutions of inverse kinematic problem that is crucial for development of virtual robot integrated with control system.

The joint coordinates can be determined using following equations

$$\theta_i = 2 \text{Atan}(t_{1/2}) \quad (5)$$

where

$$t_{1/2} = \frac{y_P \pm \sqrt{A_i^2 + y_P^2 - B_i^2}}{(A_i + B_i)} \quad (6)$$

and

$$\begin{aligned} A_i &= (x_P - b_{ix}) \cos(\gamma_i) \\ B_i &= \frac{l_1^2 - l_2^2 + (x_P - b_{ix})^2 + y_P^2}{2l_1} \end{aligned} \quad (7)$$

From equation (6), it is obvious that there are two solutions of the inverse kinematic problem whereby the appropriate solution is adopted according to the part of the workspace necessary to robot perform the task.

### 3. VIRTUAL ROBOT INTEGRATED WITH CONTROL SYSTEM

The open architecture control system is based on the LinuxCNC software system and is a real-time control system for machine tools and robots, whose code can be freely used, modified, and distribute [7, 8, 9]. Software LinuxCNC [10] enables the programming of machine tools and robots according to the RS-274 or

ISO 6983 standard.

The LinuxCNC software structure is shown on Fig. 4. It consists of four basic modules: motion controller (EMCMOT), discrete I/O controller (EMCIO), task coordinating module (EMCTASK), and graphical user interface (GUI). Of these four modules, only EMCMOT is a real-time module.

EMCMOT module performs trajectory planning, direct and inverse kinematics calculations, and computation of desired outputs to motor drivers. All I/O functions that are not directly related to the actual motions of machine axes are handled within the EMCIO module. EMCTASK module is a task-level command handler and program interpreter for the RS-274 NGC machine tool programming language, commonly referred to as a G-code [8].

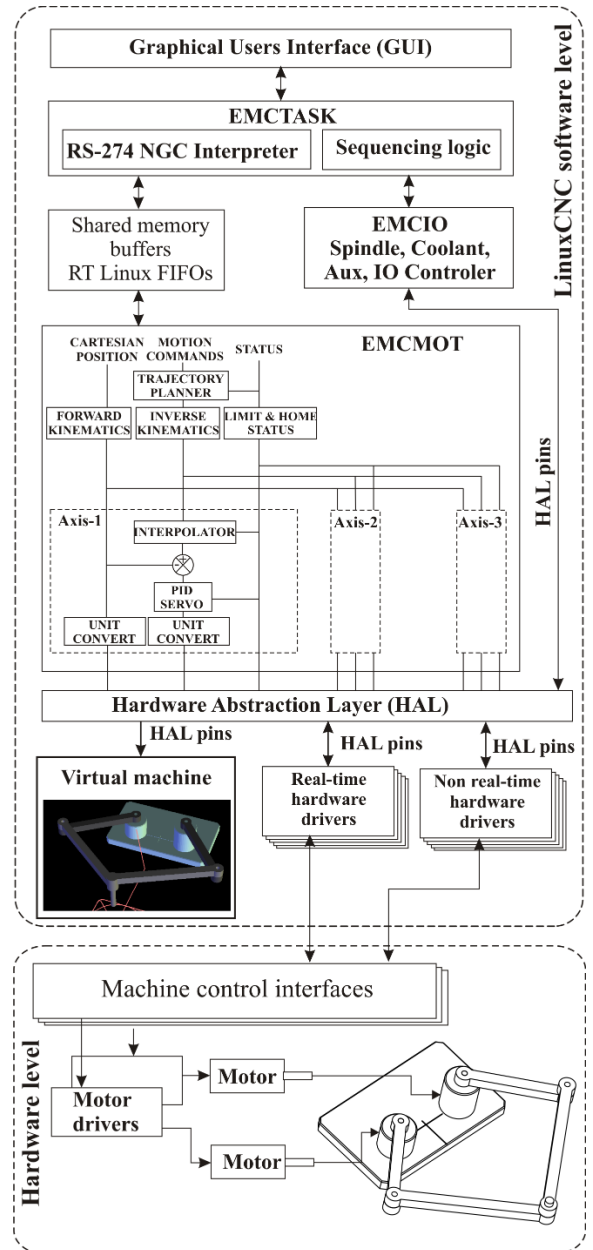


Fig. 4. Software structure of control system based on LinuxCNC

Several user interfaces have been developed for EMC2 software system. AXIS is the most advanced GUI, featuring an interactive G-code previewer. It is



expanded to specific application needs of the proposed robotic machining system.

Based on the equations of inverse and direct kinematics, defined and derived from kinematic model of the BiSCARA robot, the kinematic module is programmed in C language and is integrated into the LinuxCNC software system in the EMC MOT module.

The virtual robot is configured in a Python 3D environment. Python is a programming language that can be used to program graphical user interface and allows programming and connection geometric primitives, as well as their integration with the EMC Axis GUI environment [9].

For virtual machine simulation set of Python functions Vismach is used, which can be used to create and animate the machine tools or robot models. The Vismach shows the machine or robot model in a 3D environment while moving parts of the robot are virtually actuated and they move with changes in the corresponding values signals received via the HAL pin connection.

The basic flow of activities in configuring the virtual robots in a Python 3D environment is to: (1) create HAL connections that control movement and that perform actuated of moving axes; (2) create basic components of robots, which make up its structure. Components can be programmed in the Python languages environment itself and grouped into collections or can be load as finished components; (3) create moving robot elements; (4) create animated components of robots; (5) assembling the robot model by loading and by positioning the components in the appropriate place [9].

Configuring virtual robots, directly in Python language, is practically the programming of the coordinates of geometric primitives, in order to define virtual robot assemblies. The job is getting easier by modeling a simplified model of a machine in some CAD system, from where could get the required coordinates, and then the programming of virtual robot components are approached in the Python program language. Virtual robot components can be significant simplified and described by elementary geometric primitive (Box, Cylinder, Sphere ...). The position of the primitive is programmed relative to the given reference coordinate system. Primitives, which make up one whole, are grouped into collections. Moving elements are connected by appropriate rotary or translatory connections. All parameters of the virtual robot are needed to be correctly placed as on a real robot, and the directions of the axes are set according to the defined kinematic model. During the programming, the errors are noticed immediately, corrected, and then the next component is defined.

The second way allows getting more faithful copies of real robots in the virtual world and consists of loading complete subassemblies of the robot, prepared in a CAD/CAM environment. Components are prepared in Ascii STL or Ascii OBJ format, which Python can load directly into the reference coordinate system, and then the component has to be positioned and oriented appropriately.

The result of any described procedures is a virtual

robot or machine in a Python 3D environment that is integrated with a graphical interface Axis. The virtual robot runs in a Python 3D environment and allows the axis of the robot to move which results in the drawing of the toolpath. The simulation was generated as a result of the execution of G-code in real-time, in the same way as to control a real machine. That way it is possible to complete and verify the control system before the completion of real robots.

According to the second described procedure the virtual BiSCARA robot is generated and integrated with a developed open architecture control system, Fig. 4.

#### 4. EXPERIMENTS

Development of virtual environments, for programming and robots or machine tools simulation is important for several reasons: (1) the need to verify the program, (2) verification of control system during the development of a new generation of robots or machine tools with complex kinematics, and (3) training and education for programming of robots or machine tools [9].

Verification of the developed virtual prototype integrated into the control system was performed through several examples of drawing tool paths. The programming was done by generating a G-code in the CAD/CAM system PTC Creo 5.0 [11].

A CAD virtual BiSCARA robot has also been prepared within a CAD/CAM programming system, Fig.5.

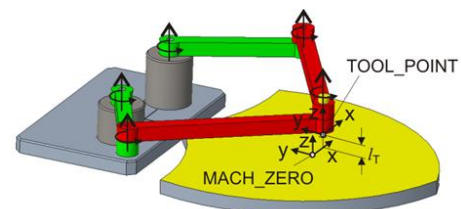


Fig. 5. CAD virtual model of BiSCARA robot [6]

This virtual robot works based on loaded toolpaths (CLF) and precedes the postprocessing of the program, i.e. generating the G-code, and is described in detail in authors' previous work [6].

The developed virtual two-axis mechanism, integrated with control system, is suitable for drawing of tool paths and laser engraving, so the programs generated in the CAD/CAM system are based on the strategy of trajectory milling. The programming itself is completely conventional and the same as for all other machine tools designed to perform these types of tasks.

Figure 6 shows one of the experiments, on virtual robot integrated with control system, which represents the drawing of the programmed tool path in the shape of the Serbian coat of arms. Figure 6a shows the developed virtual robot while drawing a programmed path that is as detail presented in Fig. 6c. Figure 6b shows the environment of the LinuxCNC software system and the loaded programmed path, which is essentially also one of the verifications of the generated G-code.

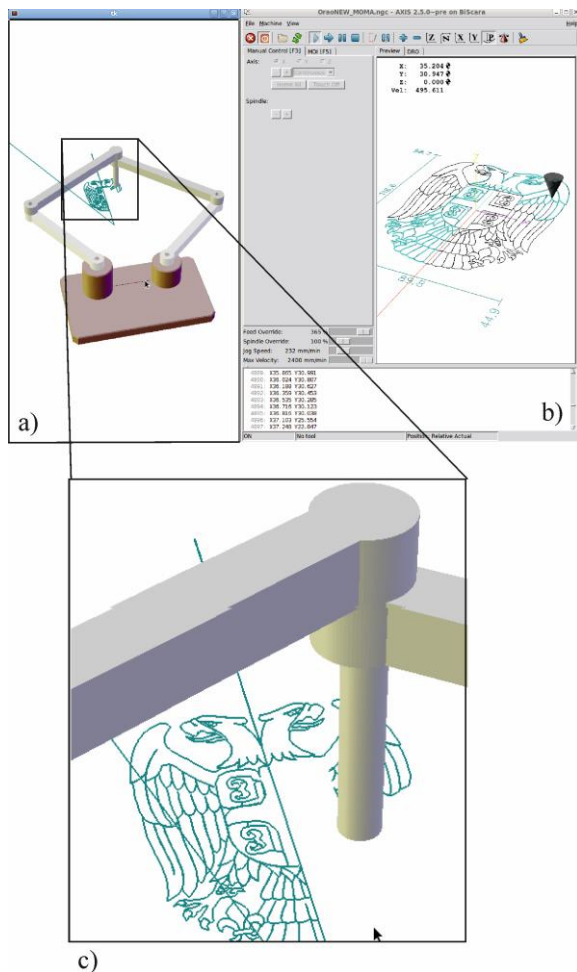


Fig. 6. Drawing of programmed tool path on virtual BiSCARA robot

## 5. CONCLUSION

Configuring of virtual robots or machine tools, among other things is important to verify control systems during the development of a new generation of robots or machine tools with complex kinematics.

The paper presents a developed open-architecture control system for BiSCARA robots. The open architecture control system is based on the LinuxCNC software system and includes the integrated virtual robot in a Python graphical environment.

The virtual prototype of the robot is configured based on the developed complete kinematic model of the robot, and also the CAD model of the robot based on the adopted parameters of the mechanism.

The realization of the laboratory prototype will be covered by further research, which will also include the development of a 4-axis robot by adding on described base mechanism one translatory and one rotary axis.

## 6. REFERENCES

- [1] *DexTAR, User's Manual, Version 1.0*, by Mecademic Inc., 2014–2015.
- [2] Pollard Jr., W.L.G.: *Spray Painting Machine*, US Patent 2,213,108, filed October 29, 1934, issued August 27, 1940.

- [3] Makino, H., Kato, A., and Yamazaki, Y.: *Research and commercialization of SCARA robot*, International Journal of Automation Technology, vol. 1, no. 1, pp. 61–62, 2007.
- [4] Fyler, D.C.: *Control Arm Assembly*, US Patent 4,712,971, filed February 13, 1985, issued December 15, 1987.
- [5] Joubair, A., Slamani, M., Bonev, I. A: *Kinematic calibration of a five-bar planar parallel robot using all working modes*, Robotics and Computer-Integrated Manufacturing, vol. 29, pp. 15–25, 2013.
- [6] Slavkovic, N., Zivanovic, S., Vorkapic, N.: *Configuring a virtual prototype of a BiSCARA robot*, TEHNIKA, Union of Engineers and Technicians of Serbia, vol. 70, no.3, pp. 311-317, 2021. (in Serbian)
- [7] Živanović, S., Dimić, Z., Vasilčić, G., Kokotović, B.: *Configuring a virtual reconfigurable two-axis machine with parallel kinematics integrated with an open architecture CNC system based on EMC2 software*, TEHNIKA, Union of Engineers and Technicians of Serbia, vol.67, no.4, pp. 519-526, 2018. (in Serbian)
- [8] Milutinovic, D., Glavonjic, M, Slavkovic, N., Dimic, Z., Zivanovic, S., Kokotovic, B., Tanovic, Lj.: *Reconfigurable robotic machining system controlled and programmed in a machine tool manner*, International Journal of Advanced Manufacturing Technology, vol. 53, no. 9-12, pp. 1217-1229, 2011.
- [9] Živanović, S., Dimić, Z.: *Virtual five-axis machine tool integrated with programming and control system*, TEHNIKA, Union of Engineers and Technicians of Serbia, vol.68, no.3, pp. 397-404, 2019. (in Serbian)
- [10] *Linux CNC*, Enhanced Machine Control - EMC2, webpage, <http://www.linuxcnc.org/>
- [11] *PTC Creo*, webpage, <https://www.ptc.com/>

**Authors:** Assoc. Prof. Nikola Slavković, Teaching Assistant Nikola Vorkapić, Full Prof. Saša Živanović, Research Associate Dr. Zoran Dimic, Assist. Prof. Branko Kokotović University of Belgrade, Faculty of Mechanical Engineering, Kraljice Marije 16, 11120 Belgrade, Serbia, Phone: +381 11 33-02-423, Fax: +381 11 33-70-364  
Lola Institute, Kneza Višeslava 70a, 11030 Belgrade, Serbia, Phone: +381 11 35-72-990, Fax: +381 11 25-44-096  
E-mail: [nslavkovic@mas.bg.ac.rs](mailto:nslavkovic@mas.bg.ac.rs);  
[nvorkapic@mas.bg.ac.rs](mailto:nvorkapic@mas.bg.ac.rs); [szivanovic@mas.bg.ac.rs](mailto:szivanovic@mas.bg.ac.rs);  
[zoran.dimic@li.rs](mailto:zoran.dimic@li.rs); [bkokotovic@mas.bg.ac.rs](mailto:bkokotovic@mas.bg.ac.rs)

**ACKNOWLEDGMENTS:** This work has been financially supported by the Ministry of Education, Science and Technological Development of the Serbian Government, through the project “Integrated research in macro, micro, and nano mechanical engineering (contract No. 451-03-9/2021-14/200105), and by the Science Fund of the Republic of Serbia, grant No. 6523109, AI - MISSION4.0, 2020-2022.

Nikolić, V., Tabakovic, S.

## DEVELOPMENT OF POST-PROCESSOR FOR CNC MACHINE TOOLS WITH HYBRID DEFINITION OF GEOMETRIC PARAMETERS OF TOOL PATH

**Abstract:** *The development of the aviation industry as well as the improvement of mold making at the beginning of the 21st century has created the need to improve the kinematics of material processing by cutting through the improvement of machine tools. This primarily refers to program movements in which the position of the tool in relation to the machining surface is spatially defined when making surfaces defined by complex geometric expressions. This process primarily included methods of programming CNC machines as well as their implementation in CAM programming systems.*

*The paper describes the development of postprocessors for multi - axis machining centers for milling, which enables the definition of a control program in which the position of the tool in relation to the machining surface is interpreted in different ways in accordance with the technological procedure and technologist requirements.*

**Key words:** *Post-processor, CAM, CNC, toolpath, 5axis machining.*

### 1. INTRODUCTION

The growing demands of the military and aerospace industries, as well as the mold making industry, create a need for further development of the kinematics of material processing by cutting, which requires the improvement of machine tools. This enables the execution of complex and precise multi-axis movements that require a specific approach to programming by CAM programming systems.

In addition to the challenge of forming a quality tool path that is an indicator of the capabilities of programmers and CAM software, there is also the challenge of properly performing these movements on the machine tool, ie. proper post-processing so that the obtained position of the tool and the machining surface is accurate. The most important factors of multi-axis machining are the choice of control parameters and their control. It is necessary to control the position of the tool in relation to the surface to be worked, the rest of the workpiece, clamps, machine elements, etc. The position can be defined in several ways, using the physical angles of the numerically controlled axes of the machine, the tool direction vector, or certain angular sets (Euler angles) of the workpiece in space. In addition to this, the way in which these paths will be interpolated is chosen. All of these factors contribute to the developer having a lot of control options, but also a lot of room for error where the wrong method can damage a machine or a workpiece. Depending on the geometry of the work surface, a different way of defining the position of the tool and the way of its interpolation will be needed. It is already known that certain path definition strategies are more suitable for characteristic surface types.

This paper will present a hybrid definition of geometric parameters of the tool path in the SolidCAM software package.

### 2. CAM SYSTEMS

The role of the CAM system is to be a programming tool that enables the automation of the tool path definition process. The input to this process is the geometry of the workpiece and data on the material, tool, machine tool, accessories, and quality and precision requirements. The programmer then, from the database of available operations and procedures, selects the appropriate ones and defines the machining which he then verifies in search of collisions and unfavorable movements for the needs of correction and optimization. Choosing a CAM system can be crucial for improving productivity because it is necessary to choose software that can process complex models and at the same time based on them creates tool paths suitable for their processing. The verified toolpaths are then post-processed in order for the driver to interpret the corresponding specific machine tool.

The task of the post-processor is to convert the tool path data obtained from the CAM software into machine-readable data while retaining all the limitations and information defined by the programmer. The CAM system delivers information in a neutral form such as information about the machine, the tool, the workpiece, and the paths themselves, which the post-processor translates into the "language" that the machine tool control unit understands.

In this process, the quality of the post-processor comes to the fore, which can describe the same path in many ways. The influence of programmers on post-processing may or may not exist. Depending on the technological procedure and the requirements of the technologist, a different form of control information may be required, and if the post-processor does not deliver it in the desired form or with the desired accuracy, it may result in damage to the workpiece. In the post-processing process, attention should also be paid to physical limitations in the form of axis travel as well as maximum and minimum speeds.

For the purposes of the work, the SolidCAM software package will be used, which supports the creation and post-processing of complex multi-axis paths.

### 3. POST-PROCESSOR

The post-processor, depending on the manufacturer, may consist of one or more files that may be available for modification to the user or be locked and allow changes only by the vendor. How the SolidCAM software package was used for this work will be described in the post-processor structure.

The post-processor consists of two parts, ie. two files. The first is GPP ("General Post-Processor") which defines the appearance of the future NC program, and the second VMID ("Virtual Machine ID") which contains the kinematic structure of the machine tool, the characteristics of the control unit, and all additional parameters necessary for defining the NC code.

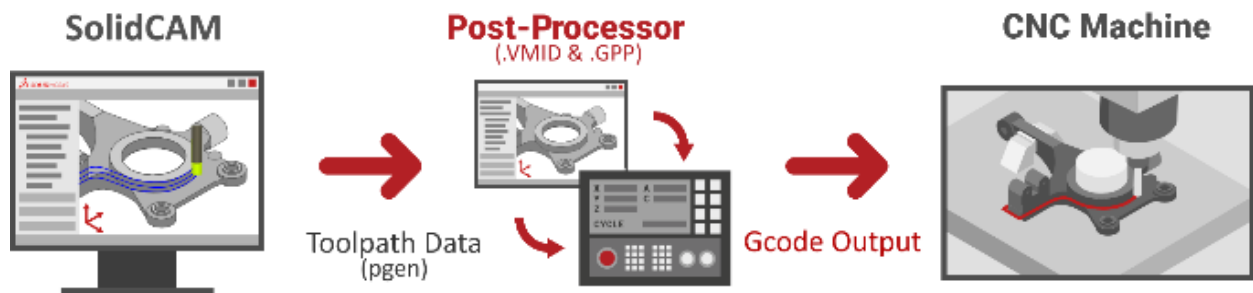


Fig. 1. NC code output process

The **GPP file** defines the procedure for transforming parameters and defined tool paths into NC code. The GPP file consists of a series of procedures, variables, and parameters written according to the rules of GPPL ("General Post Processor Language"), the internal programming language of SolidCAM. This file can be created using a plain text editor.

The GPP file consists of procedures that describe each movement or change in SolidCAM. Within the GPPL, procedures can be systemic or user-defined. Each procedure is defined by a name and begins with the "@" symbol and ends with the "endp" command. Between these two elements is the body of the procedure that determines what will be printed in the NC code and under what conditions.

The **VMID file** represents the virtual twin of the machine. Describes its kinematic structure and control unit. It is defined using the VMID Editor provided in the SolidCAM installation.

The VMID file defines linear and rotational axes and all devices located on them and in the machine. The directions of movement, maximum and minimum positions, speeds of movement, etc., as well as the devices placed on them, are assigned to the axes. Additional options that come on the machine such as a cooling device, a chip evacuation device or other devices are also set in the VMID file.

In addition to the listed options, drilling and probe cycles, control unit parameters related to plane control,

circular interpolation, compensation, etc. are also defined. It is also possible to define a so-called "Working Style" by which the client can correct the NC code to be read correctly on the control unit. In addition to defining all the necessary parameters, there is also the option of adding parameters tailored to the user in order to manage certain parts of post-processing according to his wishes and requirements.

### 4. HYBRID DEFINITION OF GEOMETRIC PARAMETERS OF TOOL PATH

The paper uses the Siemens Sinumerik 840D control unit as an example, for which the definition of 2 types of tool paths is described, ie. ways of describing the position of the tool in relation to the work surface, during multi-axis machining. The method of using the physical angles of the rotational axes and the method of defining the direction vector for each trajectory point were chosen.

In addition, 2 types of interpolation are used, ORIAXES and ORIVECT, which can significantly affect processing. Combinations of both path definition methods with both types of interpolation will be performed.

A self-created model is used as a test work piece, which is modeled so that it contains type surfaces that favor different types of defining tool paths.

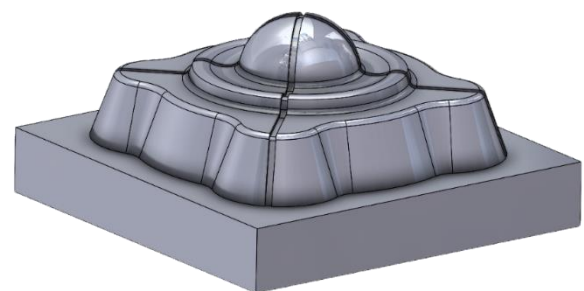


Fig. 2. Test work piece

Parameterization is performed by adding user-defined parameters that will be available for change within the operating window of any milling operation. These parameters must first be defined in the VMID file where it is necessary to give them a name and description that the user will see, and define the name and type of the variable to be used in the GPP file.

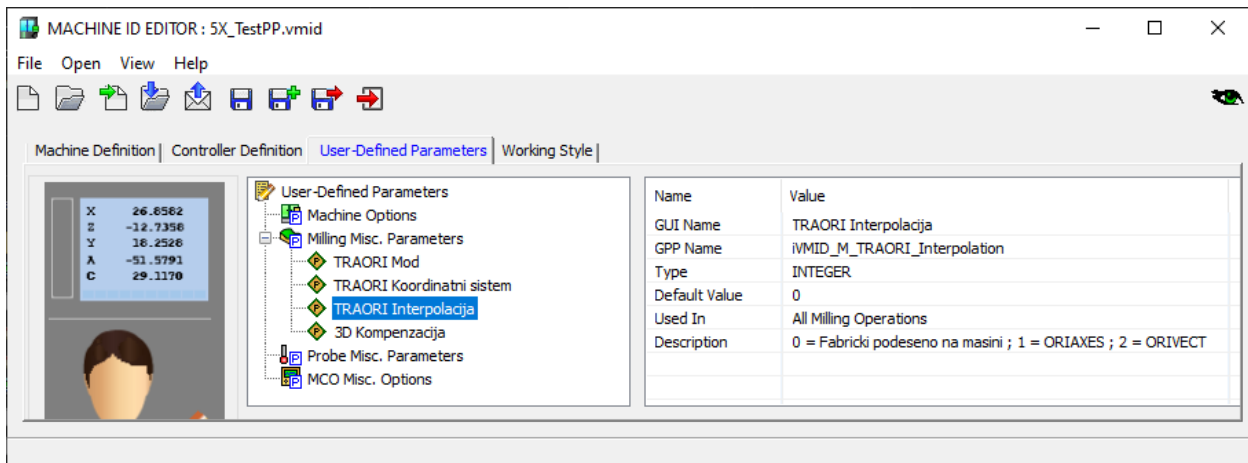


Fig. 3. User-defined parameters inside VMID file

4 variables have been defined that will allow the user to control the appearance of the output NC code in several ways.

The main focus of this paper will be on the "TRAORI Mod" parameter used to define the tool path by physical angles or vectors and on the "TRAORI Interpolation" parameter which will define how the machine control unit interpolates the tool path. These variables are then added to the GPP file to use different tool path data obtained from SolidCAM in post-processing, depending on their value.

After selecting the options in the additional parameters, a clear change in the output NC code can be seen with each change. The figure below shows the difference between "TRAORI Mod" with physical angles and with vectors as well as with ORIAxes and ORIVECT interpolation.

easier to use the angles of the physical axes of the machine.

The figure below shows a test workpiece with toolpaths that have been tested and verified.

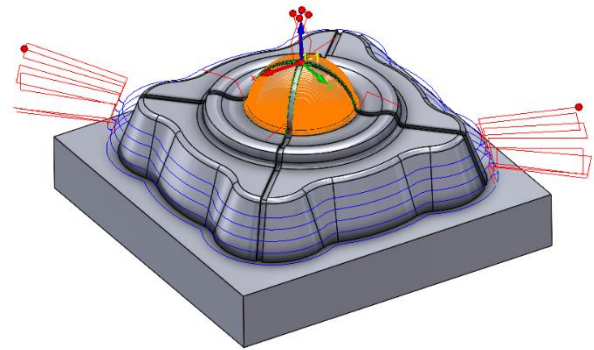


Fig. 5. Test work piece with all tested toolpaths

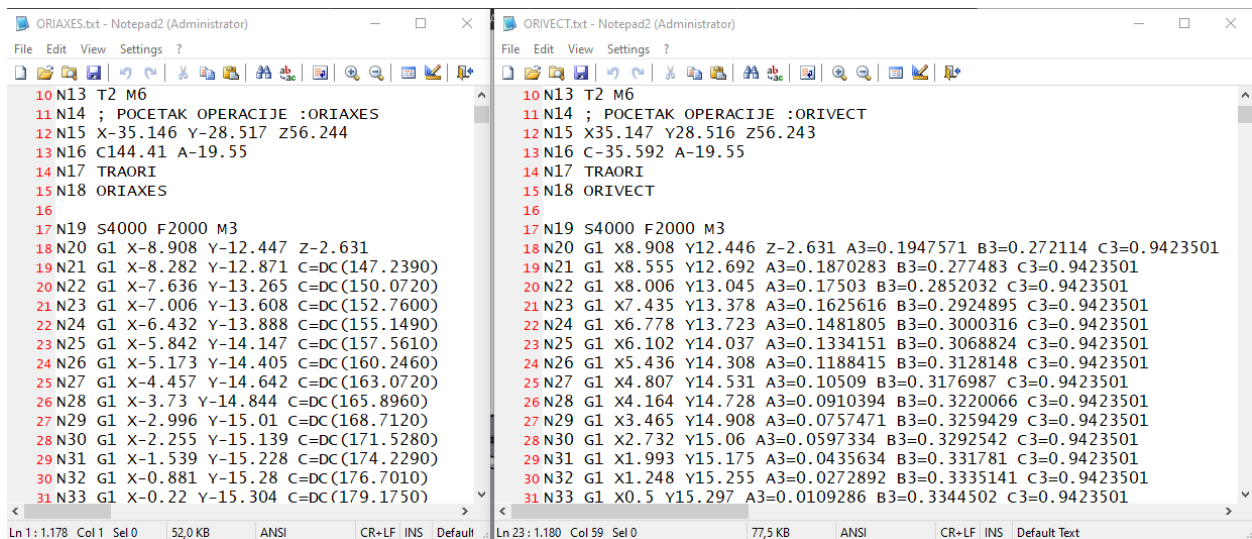


Fig. 4. NC code difference with the change of "TRAORI Mod" parameter

#### 4.1 VERIFICATION AND SIMULATION OF THE OBTAINED RESULTS

As mentioned earlier, surfaces have been selected on the workpiece that will show the advantages of choosing one or another type of tool path definition. For free-formed surfaces, it is more convenient to use the vector type of path description due to the exact relation of the tool direction to the surface, while for surfaces at a certain angle it is more convenient and

The verification was performed in Siemens' Sinutrain software, which is a Sinumerik 840D virtual control unit. The tool paths are post-processed so that all possible combinations of the parameters "TRAORI Mod" and "TRAORI Interpolation" are obtained in order to show and notice the possible difference in the movement of the tool and the obtained quality of the processed surface. The virtual machine is configured as a simultaneous five-axis with three linear axes (X, Y,

Z) and two rotary (A and C).

Inspection of the obtained results in Sinutrain software did not show a visible difference in the quality of the surface in the 3D view, nor a difference in the speed of simulation of any of the types of the defined path.

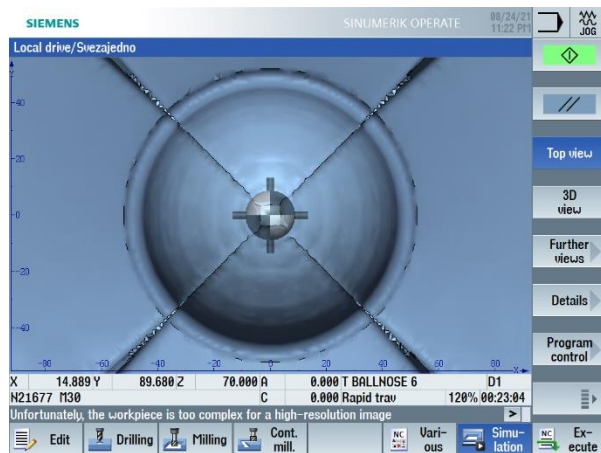


Fig. 6. Results in Sinumerik Sinutrain

Unfortunately, Sinutrain is not able to provide a quality 3D image of the object after processing due to its primary purpose to verify the NC code in the form of syntax errors and possible collisions. Nevertheless, trajectory analysis showed that satisfactory results were obtained.

## 5. CONCLUSION

In order to maximize the use of the machine tool and control unit as well as to optimize the tool path and obtain a satisfactory quality of the machined surface, it is very important to be able to manage the kinematic parameters of the tool path description.

The paper presents dual post-processing, ie. creating a post-processor that allows the formation of a driver with two different kinematic descriptions of the

tool path. The process was realized for the example of a machine with 5 simultaneously controlled axes and Sinumerik 840D control unit, on which testing and verification was performed in the software package for simulation Sinutrain.

NC code verification has proven that both trajectory concepts work and give satisfactory results without obvious differences in surface quality. Further verification and search for differences is possible only when processing a specific workpiece on a machine tool without relying on path verification software.

## 6. REFERENCES

- [1] Zeljković M., Tabaković S., Živković A., Živanović S., Mladenović C., Knežev M.: *Osnove CAD/CAE/CAM tehnologija*, University of Novi Sad, Faculty of Technical Sciences, Novi Sad, 2018.
- [2] Kief, H., Roschiwal, H.: *CNC-Handbook*, Carl Hanser Verlag, Munich, 2013.
- [3] Apro, K.: *Secrets of 5-Axis Machining*, Industrial Press, Inc., New York, 2008.
- [4] Smid, P.: *CNC Control Setup for Milling and Turning*, Industrial Press, Inc., New York, 2010.
- [5] *SolidCAM 2021 GPPTool Help*, Internal SolidCAM documentation, 2021.

**Authors:** Vukašin Nikolić, Full Prof. Slobodan Tabaković, University of Novi Sad, Faculty of Technical Sciences, Department of Production Engineering, Trg Dositeja Obradovića 6, 21000 Novi Sad, Serbia, Phone.: +381 21 485-23-24, Fax: +381 21 454-495.

E-mail: [vuk.nik@hotmail.com](mailto:vuk.nik@hotmail.com); [tabak@uns.ac.rs](mailto:tabak@uns.ac.rs)

**ACKNOWLEDGMENTS:** Authors wishing to acknowledge assistance or encouragement from colleagues, special work by technical staff or financial support from organizations should do so in an unnumbered Acknowledgments section immediately following the last numbered section of the paper.

Tabaković, S., Živanović, S., Dimić, Z., Zeljković, M.

## PROGRAMMING AND PROGRAM VERIFICATION OF 3-AXIS HYBRID KINEMATICS CNC MACHINE FOR RAPID PROTOTYPING

**Abstract:** The paper presents the programming and program verification on 3-axis hybrid kinematics CNC machine for rapid prototyping. The original hybrid (parallel-serial) 3-axis O-X glide mechanism developed for the purpose of building rapid prototyping machine and multifunctional machine tools is presented. The paper analyzes the available programming software, which can be one of the standard CAD/CAM systems or a specialized CAM system. In addition to the analysis and presentation of the programming method procedure, the program verification by material removal simulation and virtual machine simulation according to a given program was also considered. Verification of programming methods was realized by machining several characteristic parts. The paper presents the first prototype of a machine, developed for the purpose of testing characteristics with an open control system based on the LinuxCNC.

**Key words:** programming, CAD/CAM, program verification, virtual machine, O-X glide mechanism

### 1. INTRODUCTION

The improvement of modern society at the beginning of the XXI century is directly conditioned by the development and improvement of production capacities and means that enable their efficient application. An example of this is the constant growth of industrial production encouraged by the improvement of machine tools. Their development in modern conditions implies the improvement of exploitation characteristics (this primarily means increasing the processing mode up to several times) and kinematic structure [1].

As a result, in addition to conventional serial, there is also a parallel as well as a hybrid kinematic structure that provides significant opportunities to improve the characteristics of machine tools in certain areas. The problem of programming such machine tools due to the need to transform the machining path into the movements achieved by the so-called virtual axes of the machine tool can be a significant engineering challenge. Depending on the structure and characteristics of the control system, this problem can be solved within the software that transforms the coordinates of the virtual axis, which is an original technical solution for each individual problem.

The paper presents the programming and program verification on a 3-axis hybrid kinematics CNC machine for rapid prototyping. The presented machine has a kinematic structure based on the original hybrid (parallel-serial) 3-axis O-X glide mechanism [2-5] which was developed to build a rapid prototyping machine and multifunctional machine tools are presented. The paper analyzes the available programming software, programming method procedure, the program verification by material removal simulation and virtual machine simulation. Verification of programming methods was realized by machining several characteristic parts.

### 2. BASIC CONCEPT OF 3-AXIS HYBRID KINEMATICS CNC MACHINE FOR RAPID PROTOTYPING

The O-X glide mechanism with hybrid kinematics was taken as the basis of the mechanical structure of the presented machine tool. This type of machine tool was created by combining a plane parallel mechanism and a supporting structure that enables its translational movement. The planar parallel mechanism is designed so that the executive body of the machine can reach the largest part of the working space in two configurations of the mechanism, which behaves dual as two parallel mechanisms with different characteristics in terms of: working space dimensions, stiffness, speed, etc. Figure 1 shows the initial concepts of a machine with hybrid kinematics in positions with a stretched (O) and crossed (X) O-X structure [1].

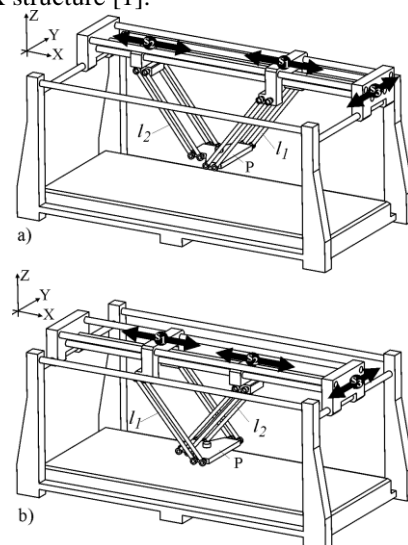


Fig. 1. Initial hybrid O-X glide mechanism

The parallel mechanism consists of a planar structure containing a movable platform, which is connected to rods of constant length via spherical joints. At the other end, the rods are connected to the corresponding sliders by rotating joints (with one degree of freedom), each of which moves according to its own guide. In order to increase the autonomy of the slider movement, they are positioned at different distances, in the direction of the vertical axis, which enables their passing in the plane, as well as the movement of the mechanism, in the extended (O) and crossed (X) position.

### 3. PROGRAMMING AND PROGRAM VERIFICATION

This chapter provides basic information about an established programming environment, which includes a virtual machine for tool path verification in CAD/CAM system PTC Creo, as well as information about programming based on STL files [6].

Generating of model, i.e. STL file, and appropriate toolpath prior to fabrication of the physical models using subtracting technology can be done using any CAD/CAM systems (Creo, Catia,...) or specialized software for the rapid manufacturing (based on STL), which allows pre-machining layer by layer and finally finishing.

#### 3.1 Programming in CAD/CAM system PTC Creo

As a basic programming software for 3-axis hybrid kinematics CNC machine based on O-X glide mechanism can be used available CAD/CAM solutions. For this research is chosen CAD/CAM system PTC Creo or Catia. Figure 2 shows basic structure of programming systems. Verification of program can be realized by: simulation of tool paths, material removal simulation and machine simulation when virtual machine working using program CLF (Cutter Location File). Process of postprocessing of tool path is same as for conventional three axis machine tools, by ISO 6983 standard.

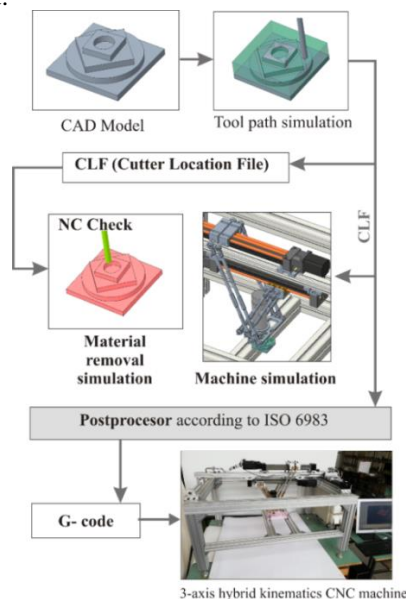


Fig. 2. Basic structure of programming system

#### 3.2 Machine simulation in the CAD/CAM system

PTC Creo software system supports all stages of the programming CNC machine tools, modeling and simulation of virtual machine model. The stages are [6]: (i) modeling the mechanism with defined kinematic connections, (ii) definition of ranges in kinematic connections, (iii) manual interactive inspection of defined virtual kinematic connections, (iv) creating a video file of tool path simulation on a virtual machine.

The configured virtual machine can be used for simulation of tool path which include the possibility of virtual prototype elements movements as a rigid body system [5]. For this possibility need define all kinematic connections between components. The required kinematic connections for the considered 3-axis hybrid kinematic machine are three translations ( $s_1$ ,  $s_2$ , and  $s_3$ ) with slider type of connection, and 16 rotary joints with pin type connection, at the points of connection the parallel mechanism rods with the moving platform and sliders, Fig.3.

After defining the kinematic connections of the moving parts of the machine, it is necessary to make a connection between the coordinate systems on the workpiece and the tool and the virtual machine within the used CAD/CAM system (PTC Creo). Virtual machine tool need defining coordinate system MACH\_ZERO, on machine table and TOOL\_POINT on front of main spindle (Fig. 3). Also, workpiece and tool have the same coordinate systems. By matching of the appropriate coordinate systems of tools and workpieces is possible to prepare set-up for simulation. After that it is possible to run a simulation of the virtual machine tool according to a program by using Machine Play option, Fig.4.

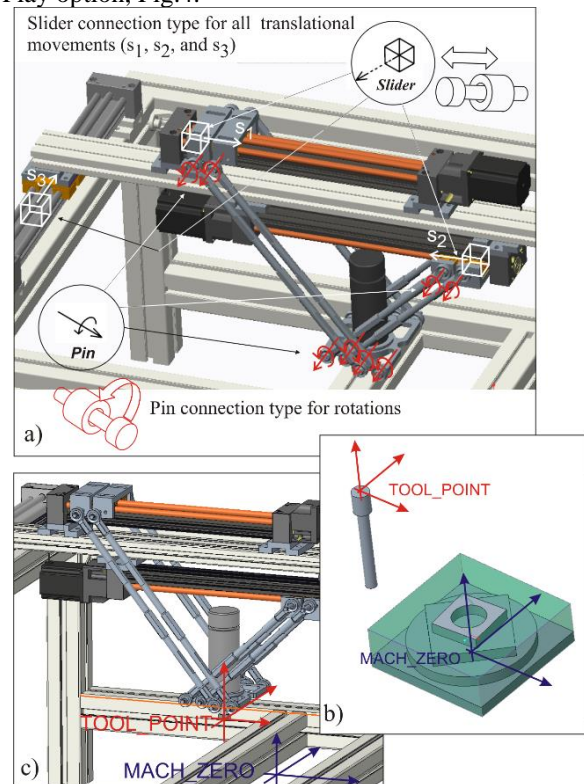


Fig. 3. Virtual machine tool of 3-axis hybrid kinematics CNC machine with defined kinematic links and



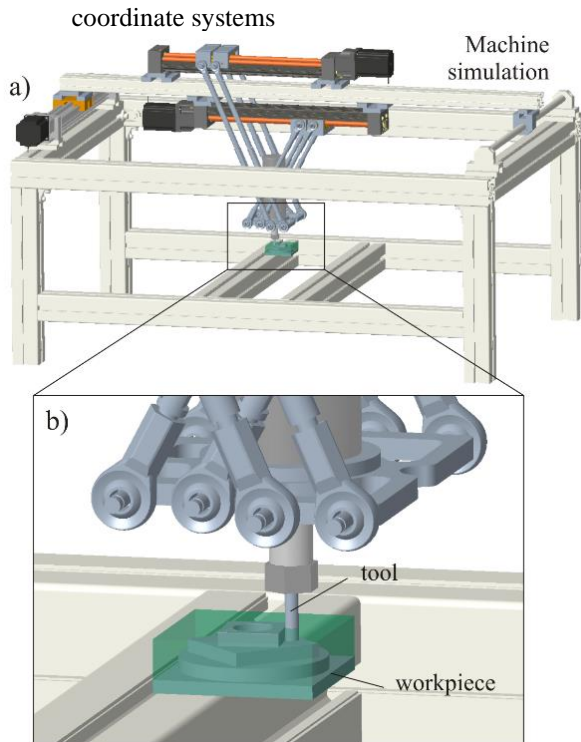


Fig. 4. Virtual machine simulation in CAD/CAM environment

### 3.3 Programming in CAM based on STL files

Typical process for subtractive technology in rapid prototyping also known as desktop milling. This procedure involves the following steps: (1) CAD modeling of prototype; (2) STL conversion; (3) Loading of STL file in CAM system; (4) planning roughing and finishing strategy for milling; (4) generating adequate G-code; (5) G-code verification with material removal simulation; (7) Fabrication of prototype using desktop milling [6].

Specialized software packages for machining based on STL file have many and some of them are CUT3D, Deskproto, MeshCAM, etc. These software packages is characterized by easy use and fast generation of roughing and finishing tool paths. These software packages enable the loading of the model in the STL format, orientating of model for machining, tool selection, choosing machining strategies for roughing and finishing, material removal simulation for different materials, and finally postprocessing the toolpath into G-code.

One example of the application of specialized CAM software that works on the basis of the STL file is shown in Figure 5. The Fig. 5 shows an example of the generated paths for roughing and finishing, as well as the corresponding verification of material removal in the software itself. Postprocessing was then performed to obtain the G code. The postprocessed G code was additionally verified by a material removal simulation in another program such as the CIMCO editor. Based on this example, machining was performed, and results of which are shown in section 4.

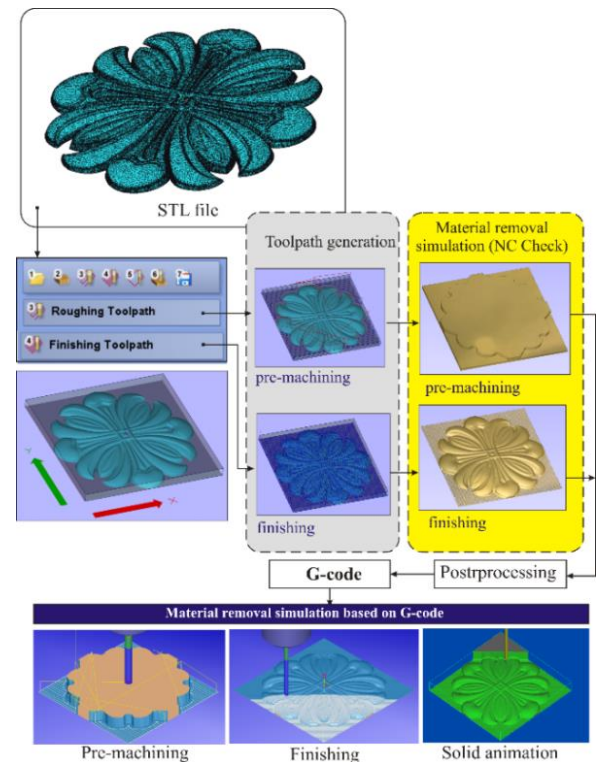
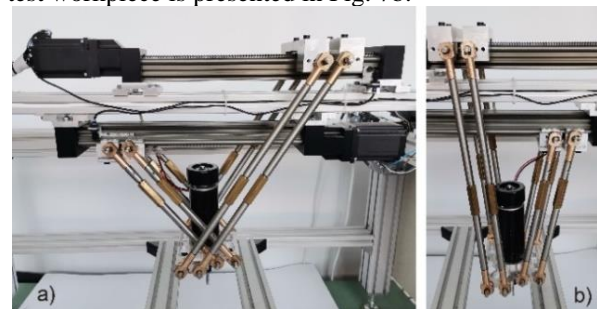


Fig. 5. Rapid prototyping using subtractive technology based on STL files in CUT3D

## 4. MACHINING TEST

First prototype of the machine tool with hybrid kinematics based on O-X glide mechanism has been built in the Laboratory on the base of a customized concept and mechanical characteristics analysis. Linear axes are composed of step motors NEMA 23 and Igus linear axes. Figure 6 shows the realization of both machine variants i.e. with the extended (O) and crossed (X) glide mechanism.

The first tests were performed on a crossed form X configuration the machine by machining the test part. Verification of the machine prototype is realized through machining of several workpieces, where as a material Styrofoam was used. A custom test workpiece which is used for test of the CNC machines work accuracy was used in process of verification of the machine's performance during test work of machine, Fig 7a. This test was performed by machining of the part which is similar to ISO test workpiece. In this case, a flat endmill (diameter 5 mm) was used. The finished test workpiece is presented in Fig. 7b.



a) crossed (X) glide mechanism b) extended (O) glide mechanism  
Fig. 6. Configured prototype of machine with O-X glide hybrid mechanism

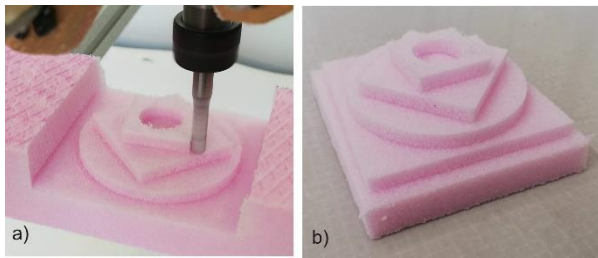


Fig. 7. Machining a custom test workpiece

The second test was performed by machining model of the rosette sculpture, based on STL file, Fig.8. Procedure of programming and program verification, for this example, is shown in Fig.5. This is an illustration of machining using subtractive rapid prototyping technique. In this case, a flat-endmill (diameter 5mm) and ball-endmill (diameter 3mm) was used. Figure 8 displays 3-axis machining where is first executed pre-machining (Fig.8a), and after that finishing (Fig.8b).

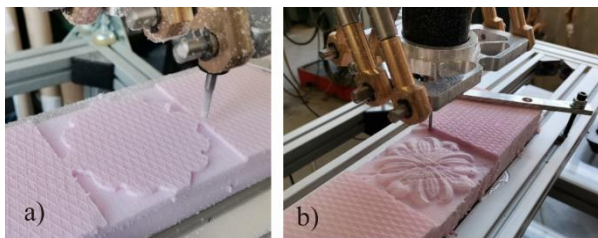


Fig. 8. Machining the rosette sculpture

## 5. CONCLUSION

In this paper presented prototype of of 3-axis hybrid kinematics CNC machine for rapid prototyping, based on O-X glide hybrid mechanism. Developed 3-axis hybrid kinematics CNC machine for rapid prototyping is an educational and research resource that is open to further improvements. This machine is reconfigurable and capable for building of multifunctional machine tool. The paper describes methods for programming and program verification, and experimental verification trough machining test.

During the realization of the first prototype of 3-axis hybrid kinematics CNC machine for rapid prototyping following activities were realized: (i) testing X variant of the mechanism, (ii) configuration of the machine tool control, (iii) configuring of the virtual prototype, (iv) simulation of the virtual prototype, (v) preparing and testing programming environment, (vi) verification of generated toolpath and (vii) testing and trial runs of the machine tool.

The first next steps are further testing and other variants of the O mechanism while providing easy reconfiguration from the X to the O variant and vice versa.

Future research in the field of improvements of the presented concept includes analyzes the applicability of the concept to laser processing machines and additive technology.

## 6. REFERENCES

- [1] Živanovic, S., Tabaković, S., Zeljković, M., Mladjenovic C.: *Machining simulation and verification of tool path for CNC machine tools with serial and hybrid kinematics*, VIII International Conference “Heavy Machinery-HM 2014”, Zlatibor, 25-28 June 2014
- [2] Tabakovic S., Zeljkovic M., Gatalo R., Mladjenovic C.: *Device for manipulating workpieces or tools in machine tools and industrial manipulators*, in: S. Intellectual Property Office (Ed.), Republic of Serbia
- [3] Tabakovic, S, Zivanovic, S, Zeljkovic, M.: *The application of virtual prototype in design of a hybrid mechanism based machine tools*, Journal of Production Engineering Vol.18, pp.77-80, 2015.
- [4] Zivanovic, S., Tabakovic, S., Zeljkovic, M., Milojevic, Z.: *Configuring a machine tool based on hybrid O-X glide mechanism*, Machine Design, Vol.8, pp.141-148, 2016.
- [5] Tabaković, S., Živanović S.: *Simulation of kinematic of virtual prototype of a machine tool based on hybrid O-X mechanism*, Proceedings of 3rd International Scientific Conference Conference on Mechanical Engineering Technologies and Applications COMETA 2016, pp.199-206, University of East Sarajevo, Faculty of Mechanical Engineering, Jahorina, B&H, Republic of Srpska, 2016.
- [6] Zivanovic S., Popovic, M., Vorkapic, N., Pjevic, M., Slavkovic N.: *An Overview of Rapid Prototyping Technologies using Subtractive, Additive and Formative Processes*, FME Transactions Vol.48, No. 1, pp. 246-253, 2020.

**Authors: Full Prof. Slobodan Tabaković, Full Prof. Milan Zeljković,**

University of Novi Sad, Faculty of Technical Sciences, Department of Production Engineering, Trg Dositeja Obradovića 6, 21000 Novi Sad, Serbia, Phone.: +381 21 485-23-24, Fax: +381 21 454-495.

E-mail: [tabak@uns.ac.rs](mailto:tabak@uns.ac.rs); [milanz@uns.ac.rs](mailto:milanz@uns.ac.rs)

**Full Prof. Saša Živanović, PhD Zoran Dimić,**

University of Belgrade, Faculty of Mechanical Engineering, Production Engineering Department, Kraljice Marije 16, 11120 Belgrade, Serbia, Phone.: +381 11 3302-423, Fax: +381 11 3370-364.

Lola Institute, Kneza Visislava 70a, Serbia

E-mail: [szivanovic@mas.bg.ac.rs](mailto:szivanovic@mas.bg.ac.rs); [zoran.dimic@li.rs](mailto:zoran.dimic@li.rs)

## ACKNOWLEDGMENTS:

This paper has been supported by the Ministry of Education, Science and Technological Development of the Republic of Serbia through the project no. 451-03-68/2020-14/200156: “Innovative scientific and artistic research from the Faculty of Technical Sciences, Novi Sad, Serbia, activity domain”

The presented research was supported by the Ministry of Education, Science and Technological Development of the Republic of Serbia by contract No. 451-03-9/2021-14/200105 of 05.02.2021.

Ižol, P., Varga, J., Vrabel', M., Demko, M., Greš, M.

**EVALUATION OF 3-AXIS AND 5-AXIS MILLING STRATEGIES  
WHEN MACHINING FREEFORM SURFACE FEATURES**

**Abstract:** *The article deals with the comparison and evaluation of milling strategies, which are available in CAM systems and are used for the production of components with freeform surfaces. For the purpose of the experiment a test sample with a repeating shape feature was designed. First half of the test sample shape features were machined using 3-Axis milling strategies while second half was performed with strategies available on 5-Axis CNC machining centre. Simulated machining times as well as virtually machined surfaces using color maps with deviation values were evaluated by employed CAM software. Obtained data was used to evaluate the performance of 3-Axis and 5-Axis milling centre both individually and mutually. These results will be used to compare software data with data obtained from real sample production. The main goal is to verify the reliability of the results provided by CAM systems in the production of parts with freeform feature surfaces.*

**Key words:** *CAM system, milling strategies, machined surface*

**1. INTRODUCTION**

At present, most activities in the manufacturing industry are carried out on CNC machines. 3-axis or 5-axis machines of various kinematic principles are most often used in milling applications. Each type has its field of employment according to its advantages and disadvantages. For some activities, the possibilities of machines overlap and the user must decide on which particular machine will carry out the process. The decision is mostly based on the user's experience with similar tasks.

To an increasing number of manufactured products have shaped or free form surfaces, respectively. They very often occur on tools for mass production, such as molds, dies and press tools. However, in many cases it is not necessary to employ 5-axis machine tool. The rule is that if the product (molded plastic part, pressed parts) can be removed from the tool shape in the specified direction, the shape is available for the milling tool in the same direction. This corresponds to the use of 3-axis machine tool. But 5-axis machines also bring a number of benefits. One of them is the changing position of the axis of the milling tool relative to the manufactured shape to ensure suitable cutting conditions [1, 2].

During the production of parts with shaped surfaces, spherical and toroidal milling tools are used. Due to the changing geometry of the tool - workpiece contact, it is not possible to keep the cutting conditions at constant values. The variability of the contact geometry is described in several publications [4, 5, 6]. For this reason, the choice of toolpaths is one of the critical parameters in the design of machining processes. In commercial CAM systems, toolpaths are selected from standard path libraries, and their shape is selected mainly with respect to the geometry of the finished surface [3].

**2. EXPERIMENT METHODOLOGY**

This paper is based on previous investigations [7-10], dealing with the comparison of strategies for 3-axis milling machines. The aim of the experiments was to compare the milling strategies used in the production of components with shaped surfaces. Since the shaped surface is usually manufactured by 3 and 5-axis milling, they were compared to identical strategies for both milling processes. Three strategies were chosen, namely Constant-Z, Radial and Linear. The Linear strategy took the opportunity to automatically generate additional paths rotated 90 ° to improve surface quality.

For the purposes of the experiment, a sample with six hemispherical surfaces on cylindrical protrusions was designed. The purpose of the protrusions is to allow good access of the tool and measuring device to the evaluated surfaces. The dimensions of the base are 100 x 67 mm, the radius of the hemispherical surfaces is 10 mm. The material of the sample is steel 1.2083, often plastic molds. The semi-finished product has the same floor plan dimensions as the sample, its height is 26 mm. The CAM system SolidCAM 2019 was chosen for the creation of NC programs. The advantage of the system is the ability to convert 3-axis milling operations to 5-axis while maintaining the main settings, which was fully utilized during the experiment. A postprocessor for the 5-axis continuous milling machine DMG Mori DMU 60 eVo was used to generate NC programs, on which the sample will be produced.

Fig. 1 illustrates the shape of a sample with the contour of the stock material and the position of the zero point.

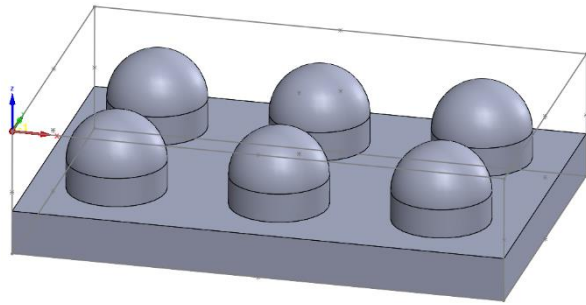


Fig. 1. Sample with the contour of the stock material and the position of the zero point

Software (CAM) data were evaluated, namely simulated machining times and virtually machined surfaces using color maps with deviation values. The acquired data were used to compare strategies for 3- and 5-axis milling as well as to their mutual comparison. The obtained software data will be aligned with data achieved during real sample production. The ultimate goal is to verify the reliability of the results from simulations of CAM system and to compare the advantages and disadvantages of using 3- and 5-axis machines in the production of shaped surfaces..

### 3. EXPERIMENTAL WORK

The NR.RD.10,0.20 °.Z4.HB.L TI400 milling cutter with the manufacturer's recommended cutting speed  $v_c = 150$  m/min and feed per tooth  $f_z = 0.1$  mm was chosen for the production of shaped surfaces. The same parameters were used in the settings of all assessed strategies, the main requirement was the height of the peaks (surface roughness) after machining, set to 0.005 mm

Generated toolpaths for 3-axis milling are shown in Fig. 2.

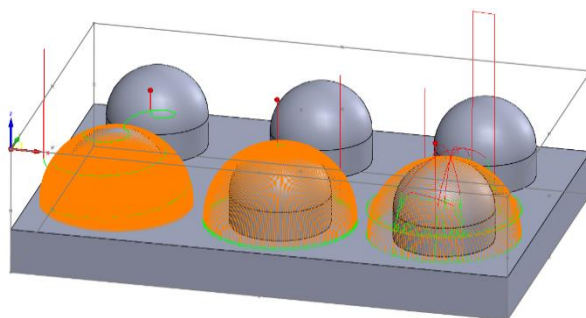


Fig. 2 Toolpaths for 3-axis milling. From the left : Constant-Z, Radial and Linear

By converting 3-axis operations to 5-axes, the monitored settings were kept. The position of the tool axis was controlled by a curve (circle) sketched at a defined distance below the shaped surface. The inclination angle of the tool axis relative to the Z axis is controlled by the size of the circle and distance, respectively. The deflection of the tool axis improves the engagement ratios, because a tool area with a low cutting speed is excluded from cutting. The position of the tool at the top of the shape and at its bottom is shown in Fig. 3. The tool paths for 5-axis milling are shown in Fig. 4.

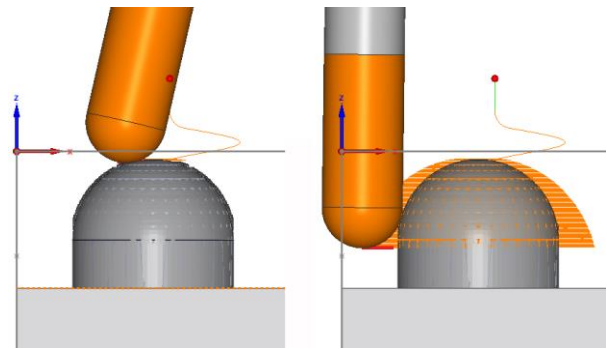


Fig. 3 The tool position at the top and bottom of the workpiece during machining simulation

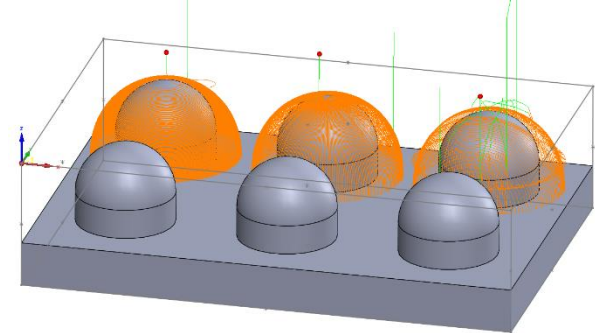


Fig. 4 Toolpaths for 5-axis milling. From the left : Constant-Z, Radial and Linear

The tool paths of the Constant-Z strategy were almost identical in both cases. Significant differences are noticeable in the other two strategies. Within the 5-axis variant, the tool paths are not regularly distributed. Fig. 5 represents a detailed view of the tool paths by employed radial strategy near the apex during 3-axis milling, while Fig. 6 shows the paths in 5-axis milling. The irregularity is caused by plotting tool paths for the cutting tool center (the top of the hemisphere), not for the tool - part touch point.

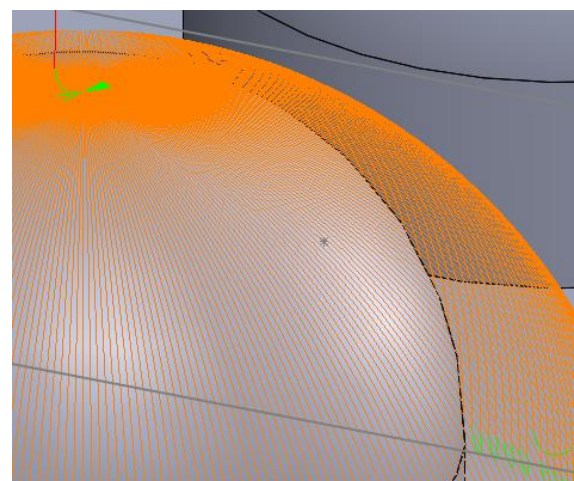


Fig. 5 Toolpaths for 3-axis milling with employed radial strategy

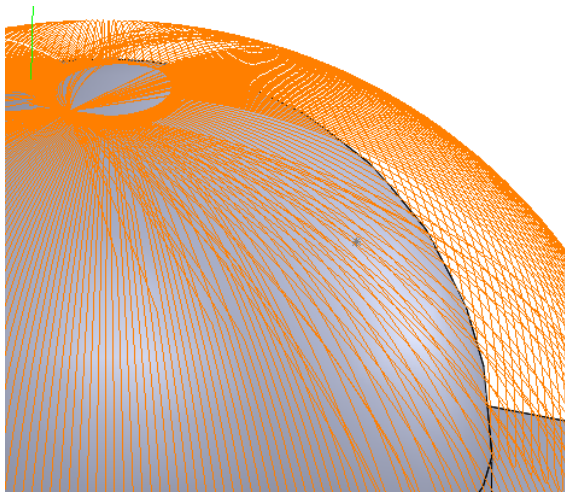


Fig. 6 Toolpaths for 5-axis milling with employed radial strategy

#### 4. RESULTS

Machining times were also obtained when generating the tool paths. Their comparison is shown in the graph in Fig. 7. During 5-axis milling, the machining time was slightly extended. It is about 3% for the Constant-Z strategy, 6% for the Radial strategy and 12% for the Linear strategy.

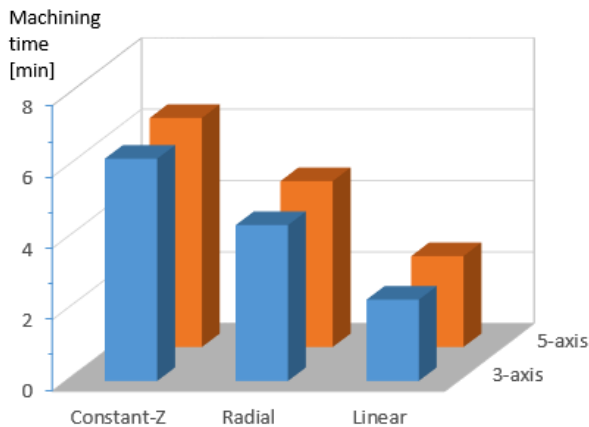


Fig. 7 Comparison of the machining times

Used CAM system allows an analysis of the virtual surface finish using color maps. It is possible to assign a value to colors and to determine the share of undercut or uncut areas in the total area of the produced shape by their gradual change.

In Fig. 8 is an overall view of the sample after simulation in a CAM system. The assignment of undercut and undercut values to the individual colors is shown in Fig. 9.

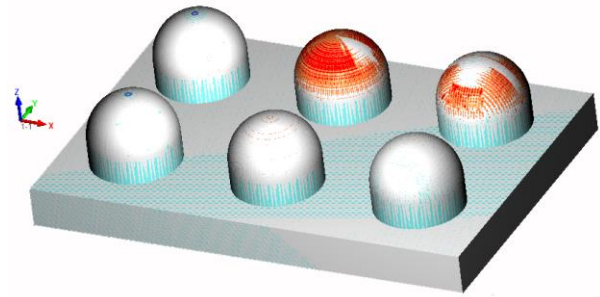


Fig. 8 Surface finish of the samples after simulated machining

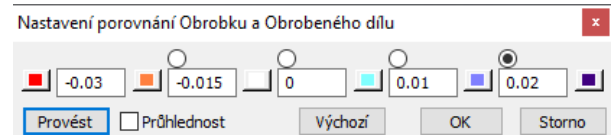


Fig. 9 Assigned values to colors for undercut and undercut analysis

When machining with Constant-Z strategy, almost identical surfaces were obtained, in the 5-axis variant, slightly higher undercut values were observed.

The Radial strategy showed only undercut deviations. In the 3-axis variant, the undercut occurred only locally near the apex; in the 5-axis variant, almost the entire surface of the sample was undercut. The maximum value of the deviation was also significantly higher. A visual comparison is shown in Fig. 10.

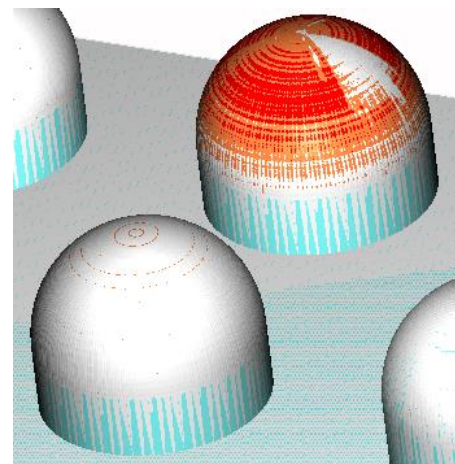


Fig. 10 Comparison of the machined surfaces made by Radial strategy - bottom 3-axis, top 5-axis milling

Within employed Linear strategy, identical deviations of uncuts were achieved; the 5-axis variants had a significantly higher maximum deviation value.

An overview of the maximum values of deviations for the assessed strategies and milling methods is given in Tab. 1. The comparison in the form of a graph is shown in Fig. 11.

Strategy		Undercut values max. [mm]	Uncut values max. [mm]
Constant-Z	3-axis	-0,012	0,03
	5-axis	-0,015	0,03
Radial	3-axis	-0,015	0
	5-axis	-0,039	0
Linear	3-axis	-0,014	0,015
	5-axis	-0,05	0,015

Tab. 1 Maximum values of undercut and uncut for evaluated strategies

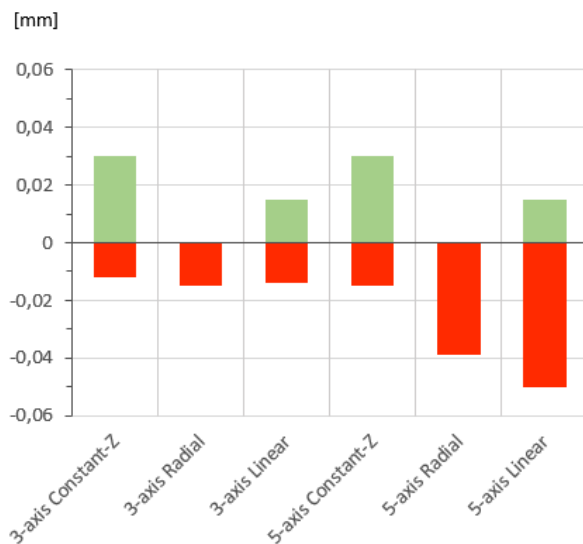


Fig. 11 Comparison of machined surface deviations (red – undercut, green - uncut)

## 5. CONCLUSIONS

The tool paths obtained by 3-axis milling were arranged regularly for all strategies. During 5-axis milling, with the exception of the Constant-Z strategy, the tool paths are irregularly arranged with obvious compaction and/or omission of some areas. The reason is above described way of plotting tool paths by the CAM software.

Simulated machining showed an increase in machining time of 3 to 12% in all 5-axis milling strategies, which was least pronounced in the Constant-Z strategy with regularly arranged paths.

Surface analyzes after simulated sample machining indicate higher undercut values in 5-axis milling. At the same time, undercutting affects a significantly larger area of the machined surface than with 3-axis milling. The smallest differences were achieved with the Constant-Z strategy.

Described results will be used for comparison with the results obtained during real production of the samples. The aim is to verify the reliability of the results from simulations and analyzes available in CAM systems during the production of parts with shaped surfaces.

## 6. REFERENCES

- [1] Bologa, O., Breaz, R.-E., Racz, S.-G., Crenganiş, M.: *Decision-making tool for moving from 3-axes to 5-axes CNC machine-tool*, Procedia Computer Science, 91, pp. 184-192, 2016.
- [2] Sadílek, M., Poruba, Z., Čepová, L., Šajgalík, M.: *Increasing the Accuracy of Free-Form Surface Multiaxis Milling*, Materials, 14, 2021.
- [3] Altintas, Y., Kersting, P., Biermann, D., Budak, E., Denkena, B., Lazoglu, I.: *Virtual process systems for part machining operations*, CIRP Annals - Manufacturing Technology, 63, pp. 585–605, 2014.
- [4] Kaymakci, M., Lazoglu, I.: *Tool path selection strategies for complex sculptured surface machining*, Machining Science and Technology, 12, pp. 119–132, 2008.
- [5] Kim, S.-J., Lee, H.-U., Cho, D.-W.: *Feedrate scheduling for indexable end milling process based on an improved cutting force model*, International Journal of Machine Tools & Manufacture, 46, pp. 1589–1597, 2006.
- [6] Diciuc, V., Lobontiu, M., Nasui, V.: *The modeling of the ball nose end milling process by using cad methods*, Academic Journal of Manufacturing Engineering, 9, pp. 42-47, 2011.
- [7] Ižol, P., Tomáš, M., Beňo, J.: *Milling strategies evaluation when simulating the forming dies' functional surfaces production*, Open Engineering, 6, 8 pp, 2016.
- [8] Ižol, P., Vrabel', M., Maňková, I.: *Comparison of Milling Strategies when Machining Freeform Surfaces*, Materials Science Forum - Novel Trends in Production Devices and Systems, 3, pp. 18-25, 2016.
- [9] Beňo, J., Maňková, I., Draganovská, D., Ižol, P.: *Sampling Based Assessment of the Free-Form Milling Strategies*, Key Engineering Materials, 686, pp. 51-56, 2016.
- [10] Varga, J., Spišák, E.: *Influence of the milling strategies on roundness of machined surfaces*, Acta Mechanica Slovaca 24(3), pp. 20-27, 2020.

**Authors:** Assoc. Prof. Peter Ižol, Assist. Prof. Ján Varga, Assoc. Prof. Marek Vrabel', PhD Stud. Michal Demko, Res. Assist. Prof. Miroslav Greš, Technical University of Košice, Faculty of Mechanical Engineering, Prototyping and Innovation Centre, Park Komenského 12A, 042 00 Košice, Slovakia, Phone: +421 55 602 3361.

E-mail: [peter.izol@tuke.sk](mailto:peter.izol@tuke.sk); [jan.varga@tuke.sk](mailto:jan.varga@tuke.sk); [marek.vrabel@tuke.sk](mailto:marek.vrabel@tuke.sk); [michal.demko@tuke.sk](mailto:michal.demko@tuke.sk); [miroslav.gres@tuke.sk](mailto:miroslav.gres@tuke.sk)

**ACKNOWLEDGMENTS:** This work was elaborated with support of the grant projects KEGA 048TUKE-4/2020 “Web base training to support experimental skills in engineering testing” and VEGA „Efficiency improvement in machining nickel based super alloys by texturing cutting tools and utilization of solid lubricants.“ supported by Scientific Grant Agency of the Ministry of Education, Science and Research of Slovakia.

Grešová, Z., Ižol, P., Maňková, I. Vrabel', M.

## THE EFFECT OF CUTTER PATH STRATEGIES ON SURFACE ROUGHNESS WHEN MACHINING TITANIUM ALLOY

**Abstract:** The article deals with the comparison and evaluation of finishing cutter path strategies when applied to one of the difficult to cut material such as Ti-alloy. The titanium alloy has been increasingly used for high performance application for oil and gas, aerospace, energy, medical and automotive industries. The importance of milling strategies outgoing from their impact on the economic aspects of production, realized using CNC machines. A planar sample was designed for the purposes of the experiment, enabling finishing cutter path strategies for shaped surfaces. Three cutting strategies were involved and compared- spiral, constant Z and line feed. For assessment of the effect of the cutting strategies three different feed rate were used. Comparison of simulated cutter path strategies and machined surface were visually inspected as well as measured surface roughness were evaluated. The constant Z cutting path strategy was found as suitable cutting strategy from point of view of surface roughness.

**Key words:** 3 Cutting path strategy, surface roughness, titanium alloy

### 1. INTRODUCTION

Research on cutter path generation techniques has been plentiful over the past decade. Nevertheless, the implementation of the cutter path techniques has been strictly limited to machining the so-called easy-to-machine workpiece materials. Proper selection of cutter path strategy is crucial for achieving desired machined surfaces [1].

One of the fundamental metal cutting processes is end milling which is very often utilized in various industry.

Surface roughness is one of the most important quality characteristics in the machining. However, surface roughness is also affected by the cutter path strategies. For minimizing the surface roughness, the proper selection of cutter path strategies is very important. Machining with optimum parameters and path strategies will contribute to lower energy consumptions and hence, will lead to lower production costs. This leads to the widespread of applying specific pre-determined machining strategy and product design mainly in the automotive and aerospace industry [2].

One of the current trends is utilization high-strength and metal materials in different designs. A common feature of these materials is difficult to machine. Materials that are difficult to machine and advanced materials such as Ti6Al4V have been increasingly used for high-performance applications in industries such as oil and gas, aerospace, energy, medical, and automotive. These types of material are characterised by factors such as limited tool life, high generated forces, torque, and temperature in the cutting zone caused by low thermal conductivity, as well as chemical reactivity with the cutting tool. In this study different cutting path strategy were chosen and surface roughness were measured and compared for various feed per tooth and tool path strategy, as well as simulated and machined surface topography were compared.

### 2. METHODOLOGY

#### 2.1 Workpiece and machining process

The machining process was performed on titanium alloy TiAl6V4 due to its widespread application for oil and gas, aerospace, energy, medical and automotive industries. Solid block of Ti alloy with a dimension of 70x70x28 mm was used as the stock was machined into shape as shown in Fig 1 for each cutting path strategy.

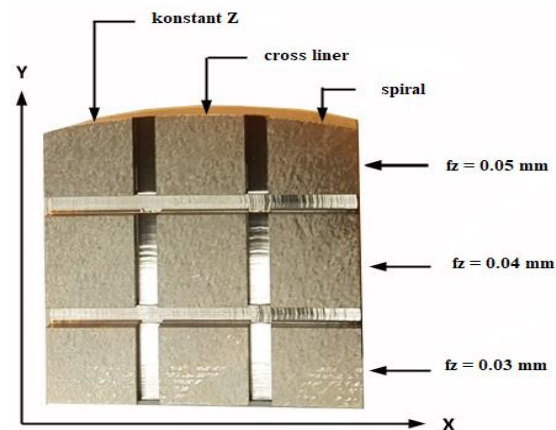


Fig. 1. View on work-piece with used cutter path strategies and feed per tooth

Solid Works software was used to model the block and assign the cutting path strategies. SolidCAM software was used to generate cutting tool path and the appropriate codes which were compatible with the CNC machine controller. Grooves were made by milling on the semi-finished product, creating nine surfaces for the application of finishing cutting path strategies. The cutting path strategies chosen were constant Z, cross linear and spiral. The cutting path strategies that were used for this study were chosen the available strategies from the software commonly used in industry SolidCAM. Machining operation were done by a DMG Mori EcoMill 50 equipped with Sinumerik 840D

controller. Cutting fluid with 6% of oil content was supplied with high pressure, which helped to remove the chips from the cutting lip and avoid built-up edge formation as well as minimise heat generation in the shear zone (cutting tool/work piece interface), where high mechanical and thermal loading occurs. When machining Ti and its alloys, the contact length between the chip and tool is extremely short (less than one-third of the contact length of steel with the same feed rate and depth of cut [3]). This implies that the high cutting temperature and stress are simultaneously concentrated near the cutting edge (within 0.5 mm) [4].

Cutting tools – a 3-fluted ball-nose end-mills - applied in experiments with diameter of 8 mm were from tungsten carbide type WC/Co, S type, suitable for machining of titanium alloys, Fig. 2.



Fig. 2. Ball-nose end mill cutter used in machining

Experiment were performed using constant cutting speed 100 m/min, depth of cut 0.3 mm and three feed per tooth 0.03 mm, 0.04 mm and 0.05 mm. Cutting parameters were chosen according to cutting tool producer recommendation.

**2.2 Cutting path strategies design**

Figures 3, 4 and 5 show schematic of cutting path strategies used in this study. The cutting path strategies chosen were constant Z, cross liner and spiral. These strategies are recommended for shaped surface finishing (concave or convex). Flat work piece was inclined by 45 degrees around the X axis of the machine tool coordinate system. To avoid that ball-nose end mill center will not be in contact with the work piece at a zero resp. low cutting speed. Fig. 3 shows cutting path strategy constant Z.

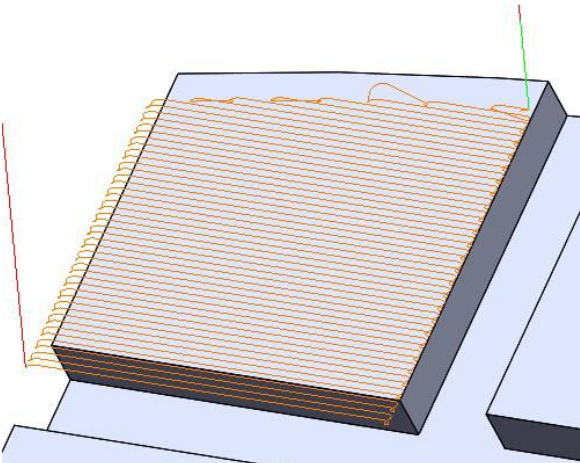


Fig. 3. The cutting path strategy: constant Z

The path is parallel with the X axis of machine tool coordinate system and the minimal occurrence of non-productive pathways without cutting is detectable. Fig. 4 shows cutting path strategy cross liner. In this strategy, liner was chosen with the additional option completion to cross. The basic strategy generates parallel paths in the selected direction and the choice to cross will ensure the generation of the second set of tracks in a direction rotated by 90°. The surface is in this case, passed the tool twice. Even with this strategy, the occurrence of non-productive tool path is minimized.

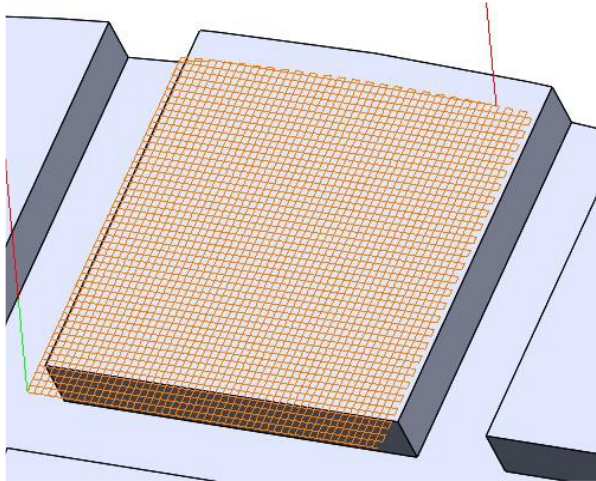


Fig. 4. Cutting path strategy: cross liner

The third strategy considered is the spiral, see Fig 5. Its advantage is a continuous uninterrupted cut at suitable shape of the machined surface. Usually spiral milling is a strategy where the cutter may start at the center of the surface and then proceeds spirally outwards. The cuter recurs to the starting point in each cycle and then cuts outwards to the next outer cycle. On the other hand, at rectangular shape, the cut is interrupted at the edge of the surface, then the tool is raised above the surface, it is moved and starts at the beginning of the next path element. The consequence is a high incidence of non-productive tool pathways.

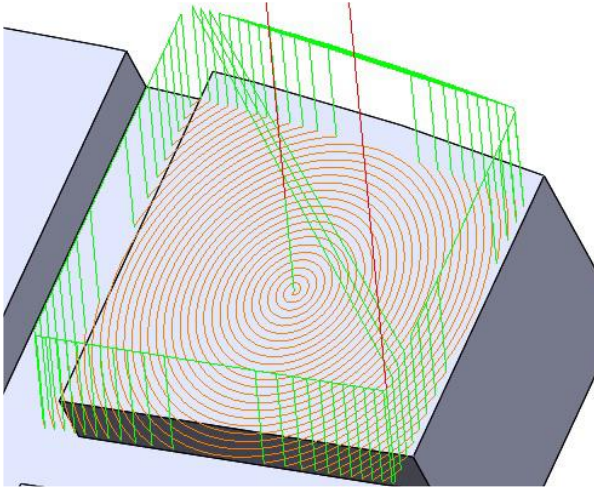


Fig. 5. The cutting path strategy: spiral



The high of scallops (SH) defined by the CAM programmer controlling was set constant: SH = 0.005 mm for all used strategies.

**3. RESULTS AND DISCUSSION**

**3.1 Comparison of simulated and machined surface**

The surface texture was documented using an optical microscope. Surface texture was visually compared to the virtual machined surface simulated in the system SolidCAM. The comparison for the Constant Z strategy is Fig. 6a. Traces of the tool are visible in the distance selected by the programming system based on the specified SH. Fig- 6b and 6c show simulated and real machined surface for cross liner strategy and spiral, respectively.

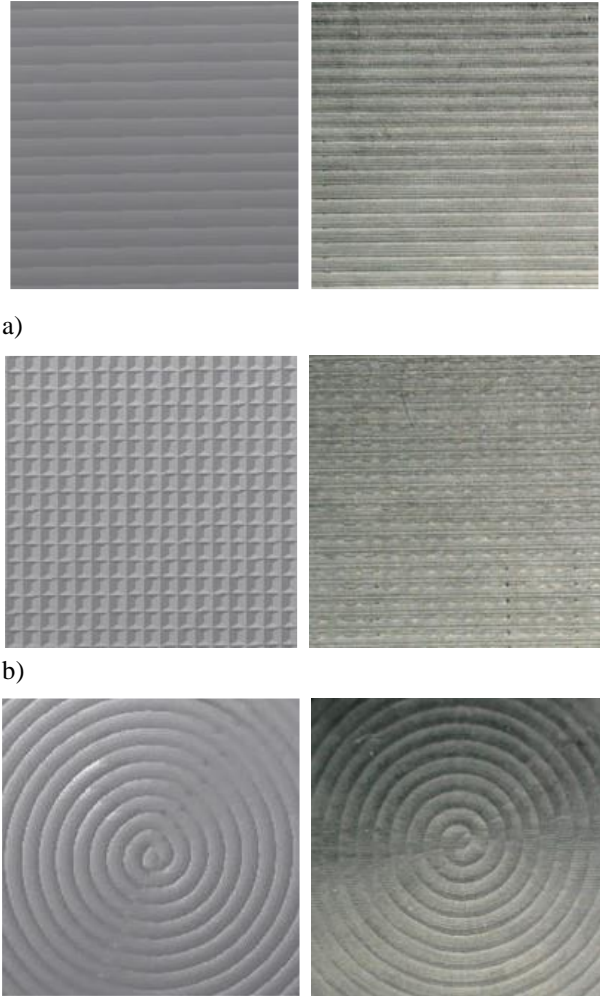


Fig. 6. Comparison of simulated (left side) and machined surface texture for cutting path a) constant Z b) cross liner and c) spiral

**3.2 Measuring surface roughness**

All machined surfaces were tested using Mitutoyo SJ-301 SurfTest surface roughness testing equipment. The test includes testing the surface roughness travelling distance direction along both x-axis and y-axis of the surface, see Fig.1. The surface profile of each test was compared and the average surface profile Ra and Rz for each cutting path strategy was obtained and compared.

Influence of feed per tooth was compared. Average

Ra and Rz was calculated from 3 measurements in each direction. Fig. 7, 8, 9 and 10 show relation among tool path strategy and feed per tooth in x and y directions. In Fig. 7 the Ra value in y-axis direction for spiral strategy is smaller than for constant Z for all used feed. However, comparing with x-axis direction measurement the best roughness Ra is for constant Z strategy against spiral one, Fig 8. Again, the clear dependence of the feed on roughness was not confirmed.

The same results can be concluded for surface roughness Rz, see Fig. 9 and 10. Again, the best Rz was for constant Z strategy in x-axis directions on the other hand, in y-axis direction the spiral strategy show better result than other two strategies.

Comparing influence of feed per tooth on surface roughness quality the lowest Ra was observed for feed 0.4 mm for each used tool path strategy.

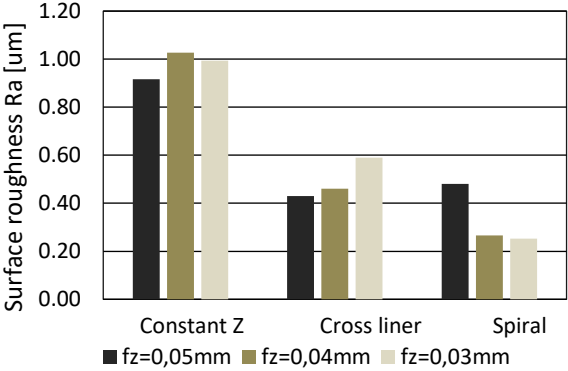


Fig. 7. The roughness Ra for each cutting strategy and various feed per tooth in Y-axis direction

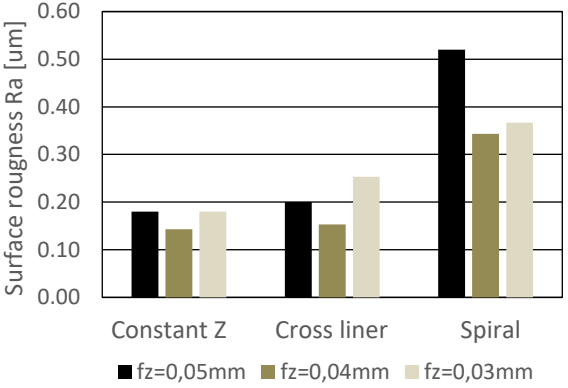


Fig. 8. The roughness Ra for each cutting strategy and various feed per tooth in X-axis direction

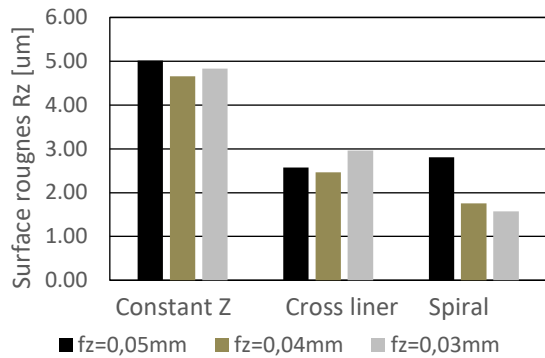


Fig. 9. The roughness Rz for each cutting strategy and various feed per tooth in Y-axis direction

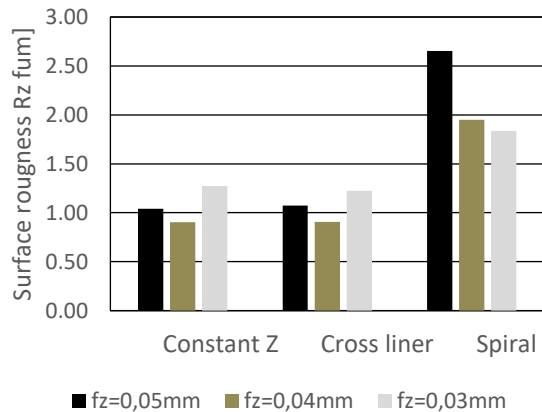


Fig. 10. The roughness Rz for each cutting strategy and various feed per tooth in X-axis direction

#### 4. CONCLUSIONS

The effect of cutting path strategies on surface finish roughness when milling Ti alloy were investigated. In this study, the following points can be concluded:

- Cutting path strategies do influence the surface finish of the surface of titanium alloy.
- Evaluations of surface roughness were not confirmed clear rule that with decreasing of feed surface roughness decrease too.
- The lowest value of Ra roughness was observed for feed 0.4 mm for each used tool path strategy.
- From the above results, it is not possible to state clearly the advantages of the used strategies from the point of view of achieving surface roughness.

#### 5. REFERENCES

- [1] Toh, C.K: A study of the effects of cutter path strategies and orientations in milling *Journal of Materials Processing Technology* 152 (2004) 346–356
- [2] Ali Akhavan Farid, Mohammad Asyraf Zulkif Mohd Yusoff: Effect of cutting path strategy on the quality of convexly curved surface and its energy consumption. *International Journal of Lightweight Materials and Manufacture* 3 (2020) 338-343

- [3] ARRAZOLA, P. J, GARAY, A., IRIARTE, L. M, ARMENDIA, M.: at all. Machinability of titanium alloys (Ti6Al4V and Ti555.3), *J. Mater. Process. Technol.* 209 (2009) 2223-2230.
- [4] SHARIF, S. et al.: Machinability of titanium alloys in drilling. *InTech* ISBN 978-953-51-0354-7, (2012) pp.117-138

**Authors:** Ing. Zuzana Grešová, doc. Ing. Peter Ižol, PhD., prof. Ing. Ildikó Maňková, CSc. doc. Ing. Marek Vrabel', PhD. Technical University of Košice, Faculty of Mechanical Engineering, Letná 9, 04012 Košice, Slovakia Phone.: +421 55 602 3513  
E-mail: [ingzgresova@gmail.com](mailto:ingzgresova@gmail.com); [peter.izol@tuke.sk](mailto:peter.izol@tuke.sk); [ildiko.mankova@tuke.sk](mailto:ildiko.mankova@tuke.sk); [marek.vrabel@tuke.sk](mailto:marek.vrabel@tuke.sk)

**ACKNOWLEDGMENTS:** This work was supported by the granted research project VEGA 1/0457/21" and partly by project KEGA 048TUKE-4/2020.

Bojanić Šejat, M., Rackov, M., Knežević, I., Živković, A.

**MODAL ANALYSIS OF BALL BEARINGS USING FINITE ELEMENT METHOD**

**Abstract:** *Dynamic behavior of roller bearings under the loads can be described by a mathematical model. The dynamic bearing model is modeled using the finite element method. Analysis of the dynamic behavior of the radial bearing refers to the modal analysis, ie. the determination of the natural frequencies, the main forms of oscillation and damping for the considered bearing, with different values of the clearance. This analysis is based on the simultaneous analysis of excitation and response signals in the time domain or more often in the frequency domain. In addition to FEM, it was also performed the experimental test on a FKL 6006 bearing with different clearance values.*

*Within this paper, a comparison of the results of the modal analysis performed experimentally with the results obtained by the finite element method was performed. The compared results show a satisfactory deviation.*

**Key words:** *frequency, FEM, modal analysis, modal parameters, oscillation modes*

**1. INTRODUCTION**

Rolling bearings are one of the most widely used machine elements, whose task is to serve as supports for shafts with simultaneous transmission of radial and axial forces, as well as ensuring the accuracy of their position. Ball bearings are a complex modeling system with a large number of input and output parameters and complex physical and chemical processes that occur during their exploitation. For these reasons, it is practically impossible to form a comprehensive mathematical model for the analysis of ball bearing behavior.

Based on Hertz's theory of contact and raceway control theory, Jones [1] and Harris [2] proposed a classical model for rolling bearing analysis, which is still used in bearing simulation. In analyzes, the contact angle is often considered constant, but in reality it is not. Liao [3] proposed a new model for the analysis of displacement and load in a ball bearing with a variable contact angle. Wang [4] developed a new quasi-static model for the calculation of ball bearings, which are exposed to the combined load of radial forces, axial forces and moment. Stribeck [5] was the first to investigate the load distribution for the radial load of ball bearings with zero clearance, and later extended the research to different clearances in ball bearings. Based on Stribeck's research, Sjoval et al. [6] investigated the load distribution on ball and the state of contact between the ball and the raceway under a given radial and axial preload. The clearance affects the dynamic behavior of the ball bearings. the clearance affects the creation of disturbing forces that cause oscillatory movement and vibrations of the bearing elements. The size of the radial clearance does not affect the natural frequency of the bearing [7, 8] and the clearance does not affect the frequency of rotation of the bearing elements[9].

The effects of static and dynamic bearing behavior must be predicted with great certainty at the design phase. As already mentioned, in order to obtain the most favorable construction, the defined static and

dynamic model must take into account a large number of parameters that affect the behavior of the corresponding bearing [10]. Therefore, in practical application when establishing a mathematical model, more attention is paid to the parameters that affect the behavior of bearings in exploitation.

In this paper, the procedure for determining modal parameters, experimental testing and FEM model is presented. Experimental tests are one of the methods of determining modal parameters that are, for the most part, simple, fast and very importantly, non-destructive method. Based on the identified modal parameters, it is possible to obtain a mathematical model of dynamic behavior that describes the dynamic behavior of ball bearings under the action of external loads.

**2. EXPERIMENTAL MODAL ANALYSIS**

Experimental modal analysis is an experimental definition of the modal parameters of a linear, time-invariant system that represent a significant basis for the analysis of the dynamic behavior of roller bearings. This analysis is based on the simultaneous analysis of excitation and response signals in the time domain or more often in the frequency domain.

In order to determine the modal parameters of the observed ball bearings, ie. natural frequency, modal stiffness and damping coefficient, it is necessary to experimentally define the function of the frequency response of the ball bearing signal based on the input signal (excitation) and the output signal (in this case acceleration). Figure 1 shows an experimental model for determining the bearing frequency response function, which consists of an acceleration sensor (1), which measures the oscillation on the outer bearing ring, and an excitation hammer (2), which excites the bearing.

The excitation hammer and the acceleration sensor are connected to the A/D card (3), which sends the collected data directly to the computer (4).

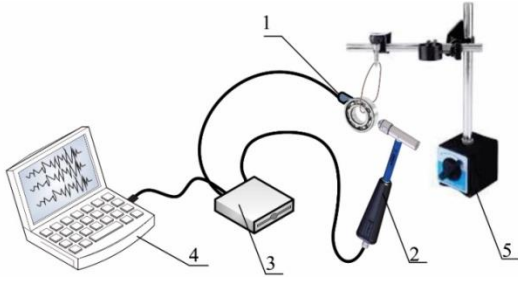


Fig. 1. Schematic of the experiment to determine the FRF bearings

The signal collected by the acceleration sensor and the hammer signal are sent via A/D card to a PC, where they are stored in tabular form using a specific software system. By creating an algorithm in the program system, fast Fourier transform (FFT) of the obtained signals and determination of the frequency response function of the observed system are enabled. The system frequency response function is displayed as a real and an imaginary part. It should be noted that when defining the real and imaginary part of the bearing frequency response function, signal filtering below 50 Hz and above 10 kHz was applied in order to remove unnecessary noise from the recorded signals, and to obtain as clear diagrams as possible.

## 2.1 Experimental determination of frequency response function and modal parameters of ball bearings

Experimental modal analysis with impulse excitation force is the simplest method for determining the frequency response function, and as such is most often used to define the modal parameters of the bearing. The transfer function determined by measuring for one mode of oscillation, for the "real" and "imaginary part". The maximum value of the amplitude is not at  $\omega/\omega_n = 1$ , but at lower values, and the attenuated natural frequency has a value  $\omega_d = \omega_n \sqrt{1 - \xi^2}$ . The same applies to the minimum value of the transfer function  $\omega_d = \omega_n \sqrt{1 + \xi^2}$ .

According to [11], the modal damping coefficient can be determined from the real part of the transfer function as:

$$2\xi = \frac{\left(\frac{\omega_2}{\omega_1}\right)^2 - 1}{\left(\frac{\omega_2}{\omega_1}\right)^2 + 1} \quad (1)$$

When the recorded data in the time domain is transformed into a frequency domain using fast Fourier transform, the Frequency Response Function (FRF) is obtained between the point where the response of the system (i) was measured and the point where the excitation force (j) acted, which can be shown as follows:

$$FRF_{ij}(\omega) = \frac{X_i(\omega)}{F_j(\omega)} \quad (2)$$

Also, it should be noted that in most cases it is necessary to obtain the displacement  $X$  as the response of the system. However, if the measurement is performed with acceleration sensors, the previous equation has the form [12]:

$$FRF(\omega) = \frac{\ddot{x}}{F(\omega)} = \frac{A(\omega)}{F(\omega)} \quad (3)$$

The conversion of acceleration into displacement can be performed by dividing the signal collected by the accelerometer by  $(i\omega)^2$  and  $-\omega^2$ , respectively.

The frequency response function of the system, obtained in the previously described way, is complex, ie it consists of a real  $G$  and an imaginary  $H$  part:

$$FRF(\omega) = G + iH \quad (4)$$

The real and imaginary part of its frequency response function can be calculated based on the following expressions:

$$\text{Re}\left(\frac{X}{F}\right) = \frac{1}{k} \left( \frac{1-r^2}{(1-r^2)^2 + (2 \cdot \zeta \cdot r)^2} \right) \quad (5)$$

$$\text{Im}\left(\frac{X}{F}\right) = \frac{1}{k} \left( \frac{-2 \cdot \zeta \cdot r}{(1-r^2)^2 + (2 \cdot \zeta \cdot r)^2} \right) \quad (6)$$

where is:  $r = \frac{\omega}{\omega_n}$ , at  $\omega = \omega_n$  (the moment when

resonance occurs) the imaginary part of the transfer function has value  $H = -1/(2\xi k)$ , then is

$$k = \frac{-1}{2\xi H} \quad (7)$$

Forasmuch it is its own frequency  $\omega^2 = k/m$ , modal mass  $m$  can be expressed as:

$$m = \frac{k}{\omega_n^2} \quad (8)$$

where is:  $\xi$  - damping coefficient;  $k$  - modal stiffness, where  $H$  is the minimum of the imaginary part FRF;  $m$  - modal mass.

## 2.2 Experimental modal analysis for ball bearing 6006

Experimental modal analysis is performed by measuring the bearing response to the excitation force generated by the excitation hammer at a point located in the middle of the outer surface of the outer ring for the bearing, which is supported on a magnetic holder, by means of an elastic rubber band. The measurement is performed using an acceleration sensor. Figure 2 shows the procedure of experimental modal analysis.

Modal analysis was performed for bearings 6006 with clearance values of 10, 20, 30 and 40  $\mu\text{m}$ . Figure 3 shows the appearance of the real and imaginary part of the FRF for the tested bearing and the gap values of 20  $\mu\text{m}$ . It can be seen from the figures that the tested bearing has only one dominant mode in the observed frequency range, so the modal parameters of the bearing are determined only for that mode, based on relations (7) and (8). The calculated results are shown

in Table 1.



Fig. 2. Experimental modal analysis of ball bearings

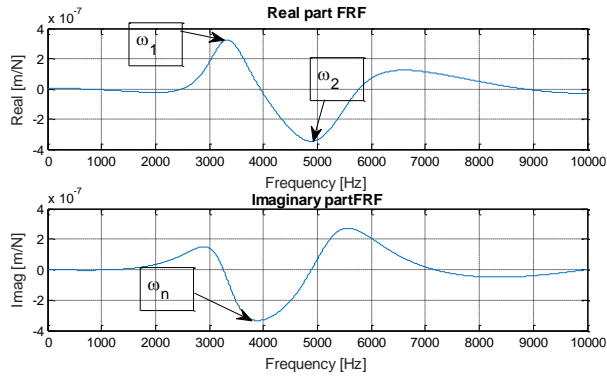


Fig. 3. Real and imaginary part of FRF for ball bearing

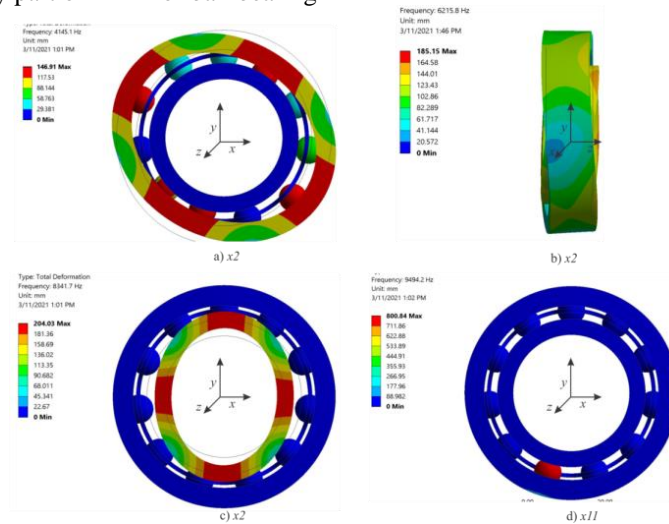


Fig. 4. Radial bearing oscillation modes

In this case, the modal mass is approximately equal to the mass of the outer ring. The next two modes are the modes of tilt of the ring around the Z axis, ie the bearing moves from the radial plane (Figure 5b), where both frequencies coincide, too. In any case, the amplitude of the natural frequency (observed on the outer ring) is very small due to the small angular stiffness, so this natural frequency can hardly be registered in the experimental measurement. The next two modes are the oscillations of the inner ring along the X and Y axes (Figure 5c), with a very small difference between the natural frequencies (less than 2%). In this case, the amplitude of the outer ring is almost equal to 0, which indicates that these modes will be difficult to detect during experimental tests. The next eleven modes are the so-called rolling body oscillation modes. Each individual mode of rolling elements has corresponding natural frequencies that differ very little (about 1%) (Figure 5d). Also, in this

6006 and clearance value  $G_r = 20 \mu\text{m}$

Clearance	$\omega_1$	$\omega_2$	$\omega_n$	$\zeta$	$k$ [N/m]	$m$ [kg]
10	3296	4853	4267	0,36	$0,22 \times 10^7$	0,119
20	3337	4866	3919	0,38	$0,19 \times 10^7$	0,123
30	3384	4889	4121	0,35	$0,20 \times 10^7$	0,117
40	3323	4708	3995	0,33	$0,18 \times 10^7$	0,113

Table 1. Modal parameters calculated based on experiment and FRF application

### 3. MODAL ANALYSIS OF BEARING OBTAINED BY FEM MODEL

In order to examine the modal parameters, a numerical model of ball bearings was developed, modeled in a general purpose software system, based on the finite element method (FEM). Modal analysis was performed for different clearance values (0, 10, 20, 30 and 40  $\mu\text{m}$ ) for the case of a freely suspended bearing, in order to compare the results with the experimental tests. Figure 4 shows the main forms of vibrations of the observed bearing for a radial clearance of 20  $\mu\text{m}$ .

case, the amplitude of the outer ring is equal to 0, so these modes will be difficult to notice when measuring. Figure 5 shows the amplitude-frequency diagram obtained during FEM modeling of a radial bearing, where it is seen that the dominant natural frequency that occurs due to the oscillation of the outer ring of the bearing. Also, the natural frequencies of the second mode can be observed on the diagram, the amplitude of the vibration of the rings lies around the Z axis ( $\omega_{02} = 6348 \text{ Hz}$ ), as well as the amplitude of the vibration of the rolling bodies ( $\omega_{03} = 9284 \text{ Hz}$ ). The modal parameters of bearings based on FEM modeling were determined by the frequency response function, as in the experimental test, as shown in the previous section. Since the considered bearings have one dominant mode in the observed frequency range, regardless of the clearance, the modal parameters are determined only for that one mode. Figure 6 shows the real and imaginary part of the frequency response functions for

considering bearings with a clearance of 20  $\mu\text{m}$ . The comparison of natural frequencies for the first three modes of oscillation determined by experimental testing and FEM modeling is shown in Table 2.

Table 3 shows the calculated modal parameters for the observed bearings with a clearance of 20  $\mu\text{m}$  and their comparison with experimentally determined data.

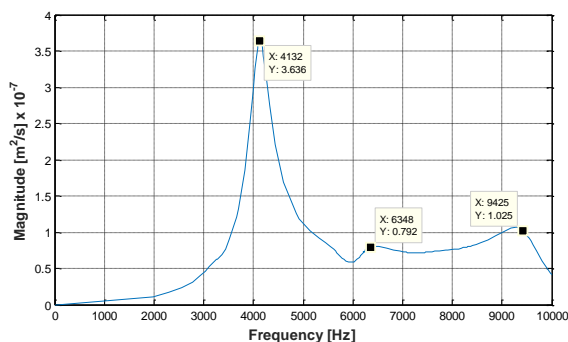


Fig. 5. Amplitude-frequency characteristic of radial bearing determined by FEM model

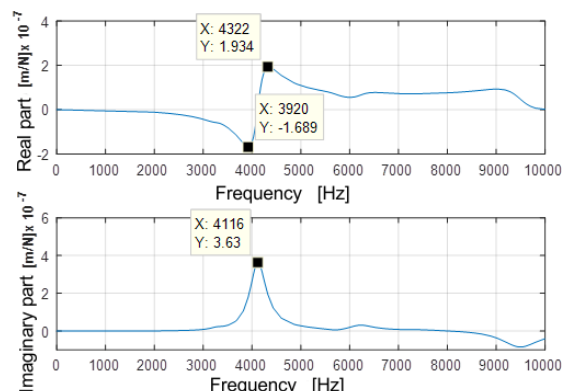


Fig. 6. Real and imaginary part of the frequency response function

Natural frequencies	Experiment [Hz]	FEM model [Hz]	Deviation
$\omega_1$	3450	4132	-16,51 %
$\omega_2$	6379	6348	0,49 %
$\omega_3$	9146	9284	-1,49%

Table 2. Comparison of natural frequencies determined experimentally in relation to the obtained by FEM modeling for  $G_r = 20 \mu\text{m}$

Modal parameters	Experiment	FEM model	Deviation
$\omega_n$ [Hz]	3919	4116	-4,79%
$Kx$ [N/ $\mu\text{m}$ ]	19	21	-9,52%

Table 3. Comparison of modal parameters determined by experiment and by FEM model

#### 4. DISCUSSION AND CONCLUSIONS

By comparing the values of the characteristic frequencies from Table 2, it can be seen that the largest deviation between the frequencies determined by FEM modeling and experimentally, are on the first mode, which is also the largest. However, as the maximum deviation is about -16%, it can be concluded that FEM modeling gives satisfactory results, especially since the difference between FEM modeling and experimental testing at the frequency  $f_n$  (Table 3) is only -4.79%. A

comprehensive analysis of the results also revealed that the change in clearance in this way of testing (free support bearing) has a negligible impact on the change of natural frequencies, as well as on the change of modal parameters.

Based on the previous diagrams and Table 6.2, it can be concluded that the clearance does not affect the natural frequencies, as well as the modal parameters of the radial bearing.

#### 5. REFERENCES

- [1] Jones, A., *A general theory for elastically constrained ball and radial roller bearings under arbitrary load and speed conditions*. 1960.
- [2] Harris, T.A., *Rolling bearing analysis*. 2001: John Wiley and sons.
- [3] Liao, N.T. and J.F. Lin, *A new method for the analysis of deformation and load in a ball bearing with variable contact angle*. J. Mech. Des., 2001. **123**(2): p. 304-312.
- [4] Wang, W.-z., et al., *Modeling angular contact ball bearing without raceway control hypothesis*. Mechanism and Machine Theory, 2014. **82**: p. 154-172.
- [5] Stribeck, R., *Ball bearings for various loads*. Trans. ASME, 1907. **29**: p. 420-463.
- [6] Sjovald, H., *The load distribution within ball and roller bearings under given external radial and axial load*. Teknisk Tidskrift Mek., 1933(9).
- [7] Harsha, S., *Nonlinear dynamic response of a balanced rotor supported by rolling element bearings due to radial internal clearance effect*. Mechanism and Machine Theory, 2006. **41**(6): p. 688-706.
- [8] Upadhyay, S., S. Harsha, and S. Jain, *Analysis of nonlinear phenomena in high speed ball bearings due to radial clearance and unbalanced rotor effects*. Journal of Vibration and Control, 2010. **16**(1): p. 65-88.
- [9] Tomovic, R., et al., *Vibration response of rigid rotor in unloaded rolling element bearing*. International Journal of Mechanical Sciences, 2010. **52**(9): p. 1176-1185.
- [10] Živković, A., *Računarska i eksperimentalna analiza ponašanja kugličnih ležaja za specijalne namene*, 2013, Doktorska disertacija, Univerzitet u Novom Sadu, Fakultet tehničkih nauka.
- [11] Wensing, J.A., *On the dynamics of ball bearings*. Twente University, 1998.
- [12] Mladenović, C., *Dinamičko ponašanje obradnih sistema za mikroobradu*, 2020, Doktorska disertacija, Univerzitet u Novom Sadu, Fakultet tehničkih nauka.

**Authors:** M.Sc. Mirjana Bojanić Šejat, Assoc. Prof. Milan Rackov, Teach. Assist. with Phd Ivan Knežević, Assoc. Prof. Aleksandar Živković

University of Novi Sad, Faculty of Technical Sciences, Trg Dositeja Obradovića 6, 21000 Novi Sad, Serbia, Phone: +381 21 485-23-72

E-mail: [bojanicm@uns.ac.rs](mailto:bojanicm@uns.ac.rs); [racmil@uns.ac.rs](mailto:racmil@uns.ac.rs); [ivanknezevic@uns.ac.rs](mailto:ivanknezevic@uns.ac.rs); [acozy@uns.ac.rs](mailto:acozy@uns.ac.rs)

**ACKNOWLEDGMENTS:** This paper has been supported by the Ministry of Education, Science and Technological Development through the project no. 451-03-9/2021-14/200156: "Innovative scientific and artistic research from the FTS (activity) domain".

Santoši, Ž., Šokac, M., Budak, I., Vukelić, Đ.

## INVESTIGATION OF DIFFERENT CIRCULAR IMAGE ACQUISITION METHODS IN CLOSE-RANGE PHOTOGRAMMETRY - VIRTUAL APPROACH

**Abstract:** Image acquisition strategy and image quality itself are significant parameters in 3D reconstruction using close-range photogrammetry. The basic principle of this 3D digitization method is to capture images of the object from several different positions to cover the object's surfaces. This paper is dedicated to investigation of three circular image acquisition methods using the virtual approach. The box, cylinder and freeform 3D geometric models were created using specialized 3D software. The visual texture was applied to these 3D models, and then virtual photographs were taken using different circular strategies. Virtual photographs with different angles, concerning the axis of rotation of the object, were captured and with the same increment in each of four rings. All tested circular strategies in terms of 3D digitization quality has proven effective.

**Key words:** close-range, image acquisition, photogrammetry, sfm, virtual

### 1. INTRODUCTION

Close-range photogrammetry based on Structure from motion is attractive method of 3D digitization. It encompasses methods of image measurement and interpretation in order to derive the shape and location of an object from one or more photographs of that object.

The primary purpose of a photogrammetric measurement is the three-dimensional reconstruction of an object in digital form or graphical form [1]. A prerequisite for using this method is that the 3D object has a stochastic visual texture.

Taking photos can be completely arbitrary, but in order to achieve the best possible result of 3D reconstruction, it is necessary to make a shooting plan. With photogrammetry, from the aspect of overall dimensions, it is possible to digitize objects in a very wide range, which enables its wide application. It is present in various fields, from mechanical engineering, architecture, animation, biomedicine, geodetic surveying, etc. [2–5]. The virtual approach to photogrammetry is still insufficiently researched, but there are also advances in this field [6–8].

### 2. IMAGE ACQUISITION METHODS

Capturing photos presents a very sophisticated procedure because the 3D digitization of many different objects has an individual approach. Overall dimensions, geometrical complexity, lighting conditions, accessibility of the object and the state of the visual texture of the object are the main factors in choosing the strategy of photo acquisition [9]. The number of photos, their resolutions and positions from which they will be taken depends on these factors. In general, in close-range photogrammetry, two types of objects can be distinguished, namely planar (facade)-2.5D and isolated 3D objects. The difference between these two types of objects is that 2.5D objects do not have a pronounced third dimension, unlike 3D isolated objects. Isolated objects can also be convergent or divergent [10].

#### 2.1 Planar image acquisition method

Planar methods of photo acquisition are predominant methods when it comes to surveying terrain topography using unmanned aerial vehicles (UAVs), and also in relief monitoring and climate change research. In this method, photographs are taken in parallel with the 3D digitization object (Fig. 1). The level of overlap with this acquisition method should be from 60% to 80% [10].

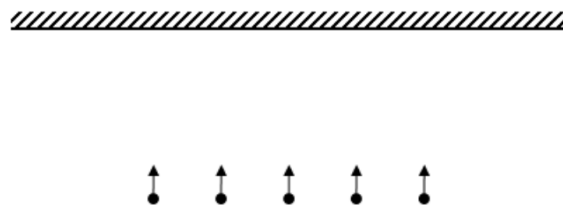


Fig. 1. Planar (facade) image acquisition method [10].

#### 2.2 Circular image acquisition method

Another very common method of photo acquisition is the circular image acquisition method. This method is applied for isolated objects (Fig. 2).

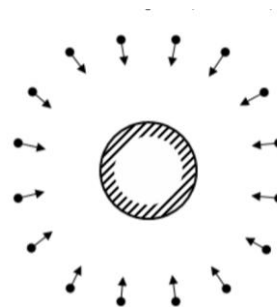


Fig. 2. Image acquisition method – isolated object [10].

The 3D digitization object is surrounded by

photographs that converge towards it. The values taken for incremental displacement range from  $10\pm 30^\circ$  depending on the complexity of the 3D digitization object, but they can also exceed these limits [7, 11].

### 3. METHODOLOGY

On Fig. 6. the methodology is presented, i.e. a block diagram that contains the basic steps in examining different strategies of photo acquisition in a virtual approach. In the first place in this methodology is the setting of the virtual environment (scene).

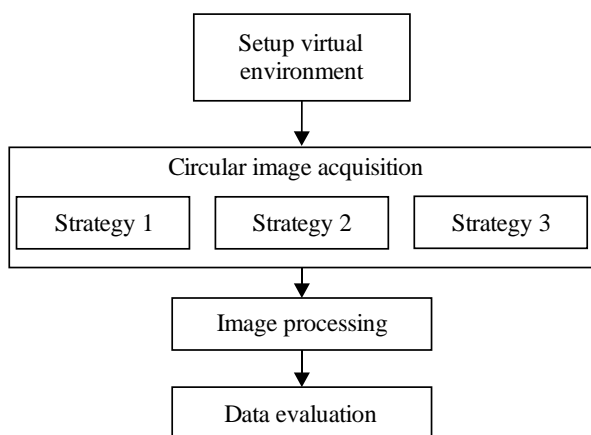


Fig. 3. The flowchart of the proposed methodology

After setting up the scene, the acquisition of photos follows for each specific setting, which are defined by three strategies. The captured images in each of the strategies are processed separately by software and as a result, point clouds are obtained, which are evaluated in the last phase.

#### 3.1 Setup of the virtual environment

The creation of the virtual environment was done using *Blender* software. *Blender* is a free and open source 3D creation suite. It supports the entirety of the 3D pipeline — modeling, rigging, animation, simulation, rendering, compositing and motion tracking, video editing and 2D animation pipeline [12]. On Fig. 4. a virtual scene is shown in which the basic elements are defined: lighting, camera and 3D digitization object.

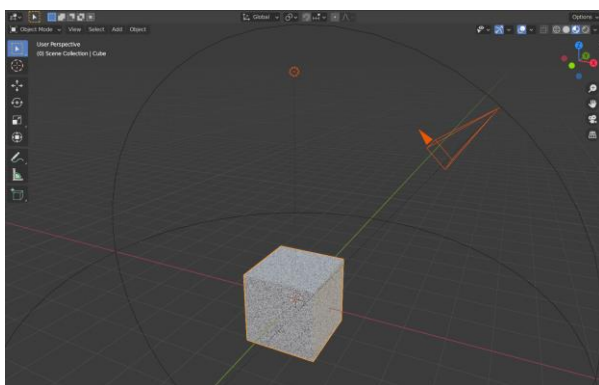


Fig. 4. *Blender* virtual environment with basic elements  
When setting up a virtual scene, it should be taken

care to make the scene as true as possible. In this step, the selection and positioning of the physical object is performed. Three 3D models were created: a cube, a cylinder and one object with freeform surfaces (Fig. 5). Since 3D models were created without visual texture, it was necessary to apply the texture before acquisition. To apply the texture, the synthetic texture *pi\_I* [8] was used, which belongs to the group of stochastic textures. After that the adjustment or positioning of the lighting is performed. It is possible to install one or more spot light sources. The lighting is placed above the 3D digitization object in order to reduce or, at least, even out the resulting shadows on the 3D model.

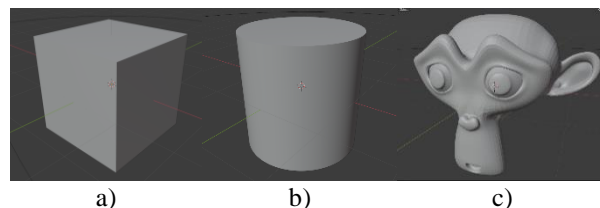


Fig. 5. 3D models of a) a) box, b) cylinder and c) freeform object

Each of the 3D models was captured with the same virtual camera settings. The camera was set to a 50 mm focal length and a defined full frame sensor with an output resolution of 1920x1080.

#### 3.2 Image strategies and image acquisition

Acquisition of photos with photogrammetric 3D digitization can be performed in two cases, when the object is stationary, so the camera moves relatively around the object, or when the camera is static and the object of 3D digitization is rotated using a turntable. The strategies used in this study have four circular rings ranging from  $0^\circ$  to  $90^\circ$  in relation to the axis of rotation of the 3D digitization object. Observing the first ring, which is at  $0^\circ$ , i.e. it covers an angle of  $90^\circ$  with the axis of rotation, virtual photos with an increment of  $10^\circ$  were taken and as a result 36 photos were taken in the first ring. The second ring was recorded with an increment of  $15^\circ$ , the third ring with  $20^\circ$  increment and the last fourth ring with an increment of  $30^\circ$ .

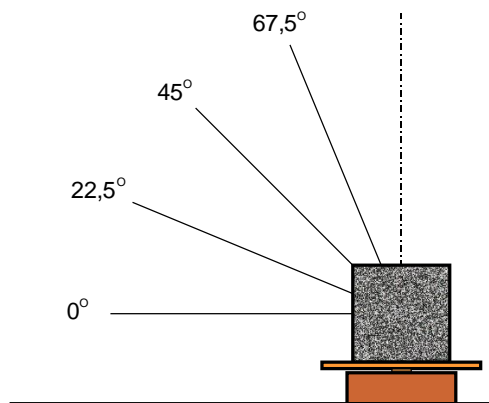


Fig. 6. Basic image acquisition with equal angle - strategy 1

This distribution allows the acquisition of fewer photos than if a constant increment were used in all



circular rings. The smallest increment is located in the first circular ring due to the fact that the photographs make the largest angle with the rotation axis of the 3D digitization object, and thus there is the greatest chance that there will be occlusion, i.e. self-shielding of the object. On Fig.6. strategy 1 used in this research is presented. The photographs in this strategy have an equal distribution of circular rings ranging from  $0^\circ$  to  $90^\circ$  with respect to the rotation axis, so that the circular rings are located at  $0^\circ$ ,  $22.5^\circ$ ,  $45^\circ$  and  $67.5^\circ$ , respectively.

Strategy 2 is shown in Fig. 7. which does not have a uniform distribution. The distribution was created by squaring a series of odd numbers 3, 5, 7, and 9, so that the circular rings are formed at  $9^\circ$ ,  $25^\circ$ ,  $49^\circ$  and  $81^\circ$ . The first ring with a slight slope of  $9^\circ$  aims to make a good coverage with the second ring (which is at  $25^\circ$ ), in order to create a good coverage for the other rings that follow, and which are at a greater distance.

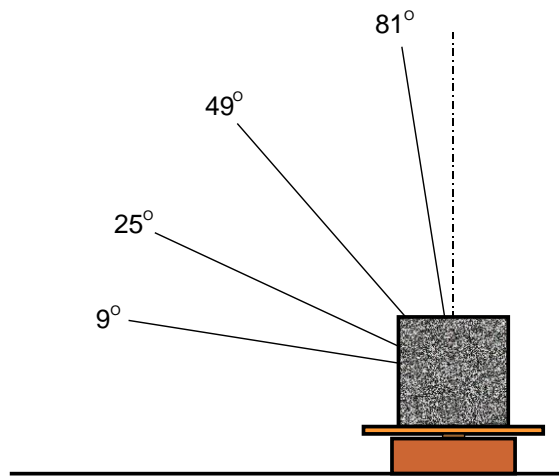


Fig. 7. Square function image acquisition - strategy 2

The third strategy shown in Fig. 8. is a modification of the previous strategy number 2.

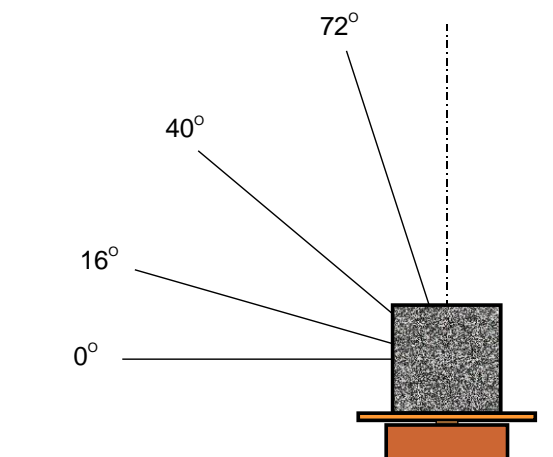


Fig. 8. Modified square images acquisition - strategy 3

The goal of this strategy is to keep the distances between the circular rings, but to keep the first circular ring at  $0^\circ$ , i.e. to match a  $90^\circ$  with the objects rotation

axis, so the circular rings are arranged at  $0^\circ$ ,  $16^\circ$ ,  $40^\circ$  and  $72^\circ$ , respectively.

#### 4. RESULTS AND DISCUSSION

After image acquisition, sets of photographs with 90 photographs for each strategy were obtained. Examples of captured photographs are shown in Fig. 9.

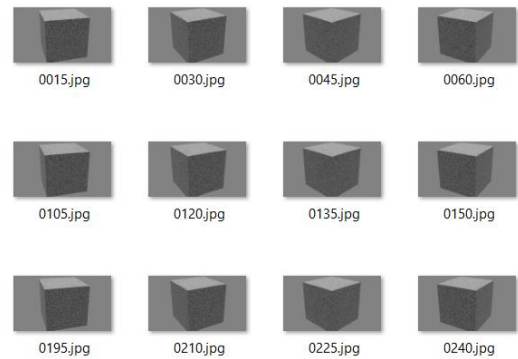


Fig. 9. Example of extracted images at specific increment

The only exception is the freeform model, since for its complete reconstruction it was necessary to expand the acquisition to the other half, which led to an increase in the number of photos. So, there were needed a total of 144 photos for strategy 1 and 3, and 180 photos for strategy 2. Photos were processed using *Agisoft Metashape* software, where the same software setup parameters were used for reconstruction. An example of the appearance of the reconstructed point cloud and the positions from which the photographs were taken is shown in Fig. 10. where the correct distribution of photographs around the 3D digitizing object can be observed.

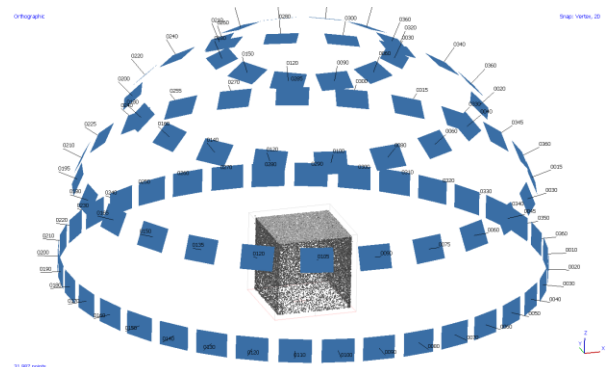


Fig. 10. Sparse point cloud and image distribution for strategy 1

The results of 3D digitization are presented in Table 1 where the parameters for monitoring the quality of 3D digitization can be observed. Quality evaluation of 3D digitization was performed by comparing the parameter "Q" presented in [8] and which is a combined quality indicator that combines the number of reconstructed points, RMS reprojection error and Max reprojection error expressed in pixels.

Strategy	Box			Cylinder			Free form		
	1	2	3	1	2	3	1	2*	3
Reconstructed tie points	31987	30036	32786	17530	17628	17539	18331	21905	17292
RMS reprojection error pix	0.23583	0.23128	0.194345	0.228013	0.205684	0.198674	0.314692	0.305952	0.289073
Max reprojection error pix	7.48666	6.14595	6.91457	7.98671	4.92748	6.39904	11.5229	8.55061	11.7444
“Q” %	85	90	100	74	99	88	99	140	96

Table 1. 3D digitalization results for three different 3D models: box, cylinder and freeform

According to Table 1, there is a slight difference between the used strategies for all measurable parameters. For example, with 3D digitization of the cube, the best result was achieved with strategy 3, then with the cylinder it was strategy 2, as well as with freeform 3D model, noting that twice as many virtual photos were used for 3D digitization of freeform model.

## 5. CONCLUSIONS

This paper presents a comparison of three different types of circular acquisition methods of photographs in close-range photogrammetry based on the SfM approach in a virtual environment. The virtual approach has a number of advantages over real experiments, namely:

- Easier scene setting,
- Faster photo acquisition,
- Managed control of lighting components, camera and object.

As a direction of future research, the examination of strategies with regard to the group of objects should be singled out, and the acquisition system should be optimized in order to achieve the best possible results of 3D digitization.

## 6. REFERENCES

- [1] Luhmann, T., Robson, S. Kyle, S. Harley, I.: *Close Range Photogrammetry*, Whittles Publishing, Dunbeath, 2006.
- [2] Firzal, Y.: *Architectural Photogrammetry: a Low-Cost Image Acquisition Method in Documenting Built Environment*, International Journal of Geomate, Vol. 20, No. 81, pp. 100–105, 2021.
- [3] Iglhaut, J. Cabo, C. Puliti, S. Piermattei, L. O’Connor, J. Rosette, J.: *Structure from Motion Photogrammetry in Forestry: a Review*, Current Forestry Reports, Vol. 5, No. 3, pp. 155–168, 2019.
- [4] Saovana, N. Yabuki, N. Fukuda, T.: *A Performance Evaluation of Feature Detectors and Descriptors for Unmodified Infrastructure Site Digital Images*, 4th International Conference on Civil and Building Engineering Informatics (ICBEI2019). pp. 113–120, Sendai, Miyagi, Japan 7-8 November, 2019.
- [5] Costa, C. M., Veiga, G., Sousa, A., Rocha, L., Sousa, A. A., Rodrigues, R., Thomas, U., *Modeling of video projectors in OpenGL for implementing a spatial augmented reality teaching system for assembly operations*, 19th IEEE International Conference on Autonomous Robot Systems and Competitions (ICARSC) pp. 1-8, 24-26 April 2019
- [6] Esmaeili, H. Thwaites, H.: *Virtual photogrammetry*, 22nd International Conference on Virtual System & Multimedia (VSMM), pp. 1–6, 17-21, October 2016
- [7] Gajic, D. B., Mihic, S., Dragan, D., Petrovic, V., Anisic, Z.: *Simulation of Photogrammetry-Based 3D Data Acquisition*, International Journal of Simulation Modelling, Vol. 18, No. 1, pp. 59–71, 2019
- [8] Santoši, Ž., Budak, I., Stojaković, V., Šokac, M., Vukelić, Đ.: *Evaluation of synthetically generated patterns for image-based 3D reconstruction of texture-less objects*, Measurement, Vol. 147, p. 106883, 2019
- [9] Budak, I., Santosi, Z., Stojakovic, V., Korolija Crkvenjakov, D., Obradovic, R., Milosevic, M., Sokac, M.: *Development of expert system for the selection of 3D digitization method in tangible cultural heritage*, Technical gazette, Vol. 26, No. 3, pp. 837-844, 2019.
- [10] Agisoft LLC, *Agisoft Metashape User Manual*, Agisoft Metashape, 2020, [Online]. Available: [https://www.agisoft.com/pdf/metashape-pro\\_1\\_5\\_en.pdf](https://www.agisoft.com/pdf/metashape-pro_1_5_en.pdf). (accessed Jun. 24, 2020)
- [11] Kaufman, J., Rennie, A. E., Clement, M.: *Single Camera Photogrammetry for Reverse Engineering and Fabrication of Ancient and Modern Artifacts*, Procedia CIRP, Vol. 36, pp. 223–229, 2015
- [12] “blender.org - Home of the Blender project - Free and Open 3D Creation Software.” Available: <https://www.blender.org/> (accessed Jun. 24, 2020).

**Authors:** Assist. with PhD **Željko Santoši**, Assist. Prof. **Mario Šokac**, Full Prof. **Igor Budak**, Full Prof. **Đorđe Vukelić**, University of Novi Sad, Faculty of Technical Sciences, Department of Production Engineering, Trg Dositeja Obradovića 6, 21000 Novi Sad, Serbia, Phone.: +381 21 485-23-24, Fax: +381 21 454-495.  
E-mail: [zeljkos@uns.ac.rs](mailto:zeljkos@uns.ac.rs); [marios@uns.ac.rs](mailto:marios@uns.ac.rs); [budaki@uns.ac.rs](mailto:budaki@uns.ac.rs); [vukelic@uns.ac.rs](mailto:vukelic@uns.ac.rs)

## ACKNOWLEDGMENTS:

This paper presents the results achieved in the framework of the project 142-451-2316/202 funded by the Provincial Secretariat for Higher Education and Scientific Research

Dekić, P., Milutinović, B., Ristić, M., Pavlović, M., Kostić, N., Nikolić, M., Jovković, S.

**REENGINEERING OF BRAKE TRIANGLE BY USING CAD/CAM APPLICATIONS**

**Abstract:** This paper presents the concept of simultaneous design of an innovated product works increasing the competitiveness of the company on the example of manufacturing of a brake triangle. An analysis of the existing product and production process were performed and identified all the shortcomings of the existing concept. It is also shown and application of the Solid Works software package for virtual 3D model analysis. Based on the conclusions from the stress-strain analysis, the technology of product production is determined in accordance with the modern manufacturing technologies and with the application of QForm and Feature CAM software's.

**Key words:** reengineering, brake triangle, Solid Works, QForm, Feature CAM

**1. INTRODUCTION**

By applying of modern manufacturing technologies, productivity increases, product development time is shorten and the competitiveness of companies increases. The combination of modern technologies with computer product development achieves maximum productivity and competitiveness in the global market with optimal engagement of production capacities. [1]

During product development process, the first step is a product model creation in order to eliminate the shortcomings of the final product. However, the creation of a physical model can be very complicated and expensive, so in recent times, the creation of a virtual product model is performed, that is, the creation of a product model in a virtual environment. By applying reverse engineering, product improvement starts from the final product and through the process of designing in the opposite direction, an improved product is obtained. Variant solutions are also sought in similar products from competing companies.

Also, due to frequent changes in the model, it is necessary to make more physical models, which requires additional time during product development, but also additional financial costs. By creating a 3D model of the product in the appropriate software package, you get a model in a virtual environment, which can be changed, customized and analyzed without additional financial and time costs. Any change in the model can be done very simply and without the need to create a new prototype, which makes the product development process cheaper and significantly time consuming shorter.

The simulation procedure, i.e. stress-strain analysis, gives answers as to whether the product meets the required characteristics, but the main word is its behaviour in operation. Prototyping is supported by the application of rapid prototyping. Nowadays, in addition to product quality, a significant role is played by the production time, which primarily depends on the choice of production technology, so it is necessary to perform a reengineering of the production process. [2,3].

This paper presents the process of reengineering for

the product itself and the manufacturing process on the example of a brake triangle using modern software packages. SolidWorks application was used for modeling and stress-strain analysis for two different variations. QForm application was used for simulating of forging process and Feature CAM application was used for simulating of machining processes.

**2. REENGINEERING OF BRAKE TRIANGLE**

In most rail freight wagons of the older generation, brake inserts are used, whereby braking is realized on the principle of traction braking, i.e. creating friction between the wheels of the wagon and the brake insert. An integral part of such a braking system is the brake triangular shown in Figure 1 (white arrows.)



Fig. 1. Brake triangle

At the ends of the brake triangular there is a brake insert figure 2 (white arrows). The task of the triangular rod is to make contact between the steel wheel and the brake insert by pulling it, which creates friction and brakes.



Fig. 2. Brake inserts

The reengineering procedure is based on the following procedure:

- Analysis of possibilities for improvement of product
- Analysis of the existing manufacturing technology for improvement.

First, the product and the process of its production are analyzed, the shortcomings of the product itself are sought and new 3D models are developed using the appropriate CAD application. Then stress-strain simulations are also performed and the optimal solution is sought. For such selected solution, the manufacturing technology is chosen by using appropriate CAM applications.

### 2.1. Analysis of product improvement opportunities

The parts of the brake triangle are made by various machining procedures, whereby the parts are also thermal treated. Their connection into the final product is done by electric arc welding. At the end of the technological process, the surface protection of the product is performed. The 3D model of brake triangle together with components and manufacturing technologies is shown in Table 1.

	<b>1. Sleeve</b>
	-turning -welding
	<b>2. Pipe</b>
	-turning -welding
	<b>3. Profile</b>
-grinding -welding	
<b>4. Fastening</b>	
-milling -welding	
<b>5. Ear</b>	
-milling -welding	

Table 1. 3D model of brake triangle

Based on the described technological procedure shown in table 1, it can be concluded that the current production technology of a brake triangle, on the one hand, is very complex and demanding, while on the other hand it is poorly cost-effective. When it comes to machining, a number of different machine tools are required (saws; lathe (conventional or CNC lathe/machining centre; milling machines) (conventional/CNC milling machine/machining centre) and CNC plasma/laser. It should be noted that in case the parts are made on conventional machines, it would be necessary to provide highly qualified employees. In case the parts are made on CNC machines, it is necessary to organize the work with the help of the CNC machine operator, while the G-code would be made by a CNC machine engineer-programmer. The most demanding part is the sleeve of brake triangle.

This part requires high manufacturing accuracy, as well as the brake triangle itself, so it is necessary that each part in the production process is controlled before the joining process. After machining, the parts are thermal treated. After the welding process, it is also necessary to perform a final control of each product. The welding process requires a certified welder and appropriate equipment. At the end of the production

process, it is necessary to perform surface protection of the finished product, so appropriate equipment is needed here as well. In addition to the engagement of a large number of machine tools, the engagement of a large number of employees of various expertise is also necessary: auxiliary workers, toolmakers (turners and mills); CNC machine operator, CNC programmer; welder and shift controller. Also, productivity is very low.

A more detailed analysis shows that two procedures are mandatory and cannot be improved or replaced by current technologies, namely thermal treatment and surface protection.

### 2.2. Developing of a new product model with Solid Works application

The improvement of the production technology was done in the direction of modifying the existing solution so that the parts of the sleeve, profile and pipe are united in assembly 1 (sleeve), and the parts ear and fastening in assembly 2 (ear of brake triangle) as shown in figure 3.

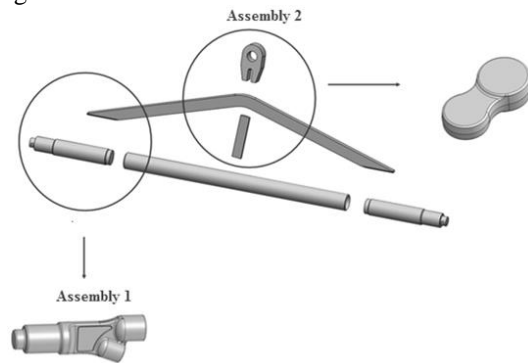


Fig. 3. Improved parts of old model

The Solid Works software package was used to create a 3D virtual model of a sleeve and ear of brake triangle. In order to perform an analysis of product functionality and selection of the optimal solution, two variants were created, which are shown in Table 2.

Variant solution	Appearance of solution
<b>1<sup>st</sup> variantion</b> -sleeve 12,2 kg, -ear 2,9 kg	
<b>2<sup>nd</sup> variantion</b> - sleeve 6,7 kg, - ear 2,6 kg	

Table 2. Variant solutions with characteristics

By comparing the variant solutions, it can be concluded that less material is needed to make the second variant solution, which reduces the time and costs of production. Simulations, i.e. analysis of stress-strain states were performed with 3D models of the sleeve due to a very important role within the brake triangle, for both variant solutions with the same load -

torque (160 kN), in order to compare their results. For these simulations, the SolidWorks Simulation module and the finite element method were used. As a basic element in the application of the finite element method, a triangular element was used. Due to the complex geometry of the work, the correction of the basic elements needed to be performed, i.e. the elements were reduced. The results of the stress-strain analysis are shown in figure 4.

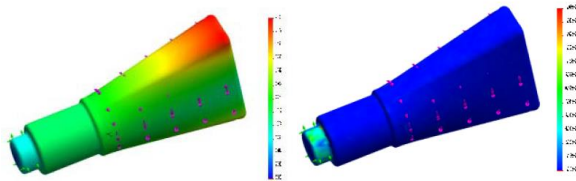


Fig. 4. Stress-strain state of the sleeve under a given load – 1<sup>st</sup> variation

In the stress diagram, the lower stress is shown in blue, which shows that the stress distribution for a given model is quite satisfactory. In the strain diagram, the largest strain occurs at the end, which is expected according to the given limit and load. The simulation results showed that the product of the presented geometry and material meets the given requirements.

Constraints and loads were set for the second variant solution as well, and meshing was performed same as for 1<sup>st</sup> variation. Due to the even more complex geometry in relation to the first variant solution, meshing control was done here as well. Then, according to the given parameters, a simulation was performed. The simulation results are shown in figure 5, i.e. stress-strain diagrams.

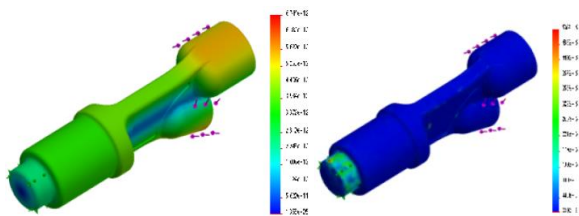


Fig. 5. Stress-strain state of the sleeve under a given load – 2<sup>nd</sup> variation

Compared to the first variant solution, it can be concluded that in the middle there are places where higher stress values occur, which is quite expected, similar to the reduction of the sleeve wall, which does not affect the functionality of the part in the complete assembly. However, in the strain diagram, the strain differs in relation to the first variant solution, which is a consequence of a partial change in geometry, and the strain is distributed differently along the entire part. The simulation results showed that the second variant solution satisfies the given requirements, whereby the mass of the sleeve is significantly smaller compared to the first variant solution. This improved product is shown in figure 6.

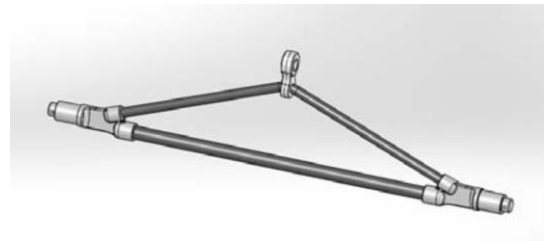


Fig. 6. 3D model of the improved product

### 3. IMPROVING OF MANUFACTURING TECHNOLOGIES

The analysis of the shortcomings of the existing technology of manufacturing of a brake triangle from the aspect of technological process, production costs and production time showed that the current technology of manufacturing of a brake triangle has many shortcomings:

- Requires the engagement of a larger number of machine tools.
- There are many prescribed processing operations of different nominal quality, which increases the possibility of production errors.
- Requires the employment of a larger number of workers, which is significantly increasing the impact of the human factor on post-production.

The solution to these problems can be found in the production of sleeves and ears by forging technology and subsequent processing on a CNC machine. Joining the parts of the product would be done mechanically. The forging technology was chosen because the parts obtained with this technology have excellent mechanical properties and can withstand high dynamic loads that occur during braking and a large number of cycle changes. The simulation of the forging process was performed by a QForm application [4].

During the simulation of the forging process, both variant solutions were also considered, due to the fear that the complex geometry of 2<sup>nd</sup> variation would be difficult to forge. The ear is not considered because it is easy to forge due to its size and simple geometry. For the purposes of this analysis, it was necessary to create a model of the forging dies in Solid Works, which is shown in the figure 7.

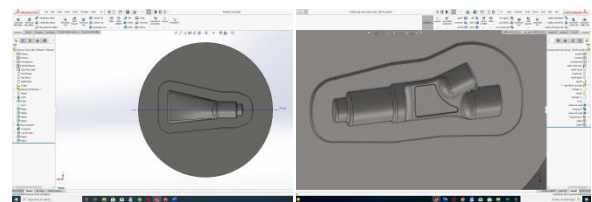


Fig. 7. 3D model of forging dies

As it was determined that both variants can be made with the same forging force of 600 kN, the forging analysis of the 2<sup>nd</sup> variation was approached. The biggest challenge was to determine the size of the starting piece. three cases were considered: Ø75x270mm, Ø70x280mm and Ø65x280mm, where the closing of the die was 2mm. The appearance of the starting piece in die is shown in the figure 8.

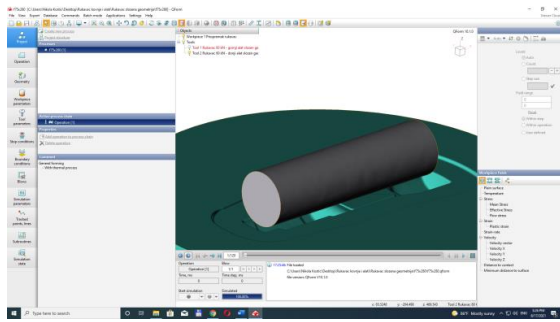


Fig. 8. Circular preparation in die

It was determined by simulation that the best forging was obtained with a preparation of size  $\text{Ø}70 \times 280 \text{mm}$ . This is shown in the figures 9.

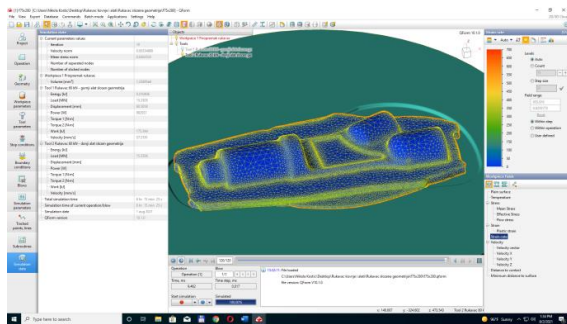


Fig. 9. Forging with preparation  $\text{Ø}70 \times 280 \text{mm}$

After the forging procedure, it is necessary to perform furrowing and shot blasting procedures.

The last phase in reengineering is the machining of the sleeve, making holes and tightening the bearing for the brake insert. This procedure was simulated using Feature CAM. The simulation of the sleeve turning process is shown in the figure 10.

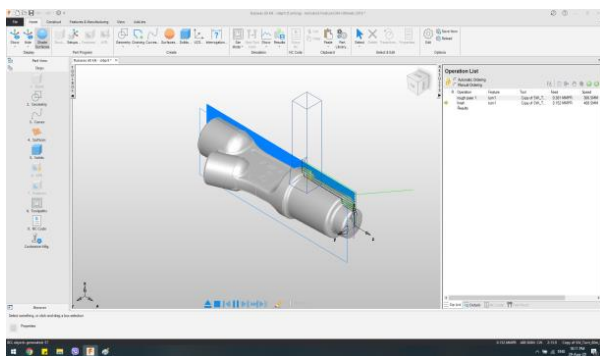


Fig. 10. Simulation of the turning process

The simulation of the process of holes making in the sleeve is shown in the figure 11.

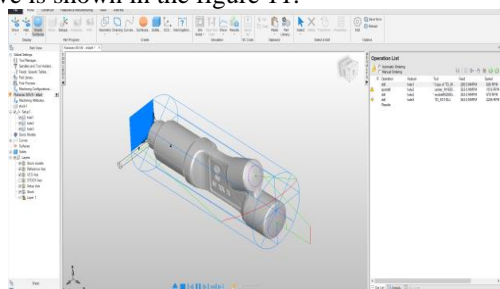


Fig. 11. Simulation of the hole making process

## 4. CONCLUSIONS

In this paper it is shown that by combining the appropriate production technology in accordance with the simulation results, productivity is significantly affected, because, on the one hand, the development time is shortened, while, on the other hand, the technological process is optimized. The main result is faster and cheaper production.

The process of reengineering on the example of the brake triangle with the help of appropriate CAD / CAM applications has shown that it is possible to create and analyze a large number of variant solutions without physically creating any model.

## 5. REFERENCES

- [1] Wego, W. *Reverse engineering -technology of re invention*, CRC Press Taylor & Francis Group, Usa., 2011
- [2] Irani, Z., Hlupic, V., Baldwin, L. P., & Love, P. E. *Re-engineering manufacturing processes through simulation modeling*, Logistics Information Management 13(1): pp7-13, 2011.
- [3] N. M. Tahir, U. I. Bature, K. A. Abubakar, M. A. Baba, S. M., *Engineering and Manufacturing*, Yarima, International Journal of Engineering and Manufacturing, Vol.10, No.6, 2020.
- [4] Alran T., Ngaile G., Shen G.: *Cold and hot forging: fundamentate and applications*. ASM PiiMicatinn. 2004.

**Authors:** Senior Lectu. Petar Đekić, Senior Lectu. Biljana Milutinović, Full Prof. Miloš Ristić, Lectu. Milan Pavlović, M.Sc. Nikola Kostić, M.Sc. Milan Nikolić, Full Prof. Srđan Jovković, The Academy of Applied Technical and Preschool Studies-Niš, Aleksandra Medvedeva 20, Niš, 18000 Serbia. Phone: +381 18 588 211, Fax: +381 18 588 210.

E-mail: [petar.djekic@akademijanis.edu.rs](mailto:petar.djekic@akademijanis.edu.rs);  
[biljana.milutinovic@akademijanis.edu.rs](mailto:biljana.milutinovic@akademijanis.edu.rs);  
[milos.ristic@akademijanis.edu.rs](mailto:milos.ristic@akademijanis.edu.rs);  
[milan.pavlovic@akademijanis.edu.rs](mailto:milan.pavlovic@akademijanis.edu.rs);  
[nikola.kostic@akademijanis.edu.rs](mailto:nikola.kostic@akademijanis.edu.rs);  
[milan.nikolic.ni@akademijanis.edu.rs](mailto:milan.nikolic.ni@akademijanis.edu.rs);  
[srdjan.jovkovic@akademijanis.edu.rs](mailto:srdjan.jovkovic@akademijanis.edu.rs)

**ACKNOWLEDGMENTS:** The research presented in this paper was realized within the project "**Simultaneous design of an innovative product to improve the competitiveness of enterprises**" Support measures for MSMEs, for projects of cooperation with scientific and educational institutions, innovation organizations and associations funded by the Office for Local Economic Development and Niš.

# **MMA 2021**

---

**FLEXIBLE TECHNOLOGIES**

**Section C:**  
**METROLOGY, QUALITY, FIXTURES,**  
**CUTTING TOOLS AND TRIBOLOGY**





Ranisavljev, M., Štrbac, B., Janković, P., Lanc, Z., Matin, I., Hadžistević, M.

## THE IMPORTANCE OF MEASURING SYSTEM ANALYSIS IN PROCESS CAPABILITY ASSESSMENT

**Abstract:** *The implementation of statistical methods in the product development phases has become an unavoidable part of engineering practice. Monitoring of the condition of the process or production equipment is performed using established methodologies, which include the analysis of process capabilities. This analysis involves identifying the need to evaluate the production process or system, data collection, analysis, and interpretation of data. Data acquisition is performed using a measuring system, which with its characteristics in terms of accuracy and precision must meet certain criteria. This paper aims to determine the capability of the process, calculating the capability indices  $C_p$  and  $C_{pk}$ , with special reference to the measurement system. Before using the data in the analysis of abilities, an analysis of the measurement system was previously performed to determine its variation in the total variation of the study. The variation of the measuring system proved to be acceptable, which gave the author a sufficient reason to further exploit that measuring system. The process capability study was conducted on a sample of 125 parts, where it was concluded that the observed process is within the statistical control limits and can produce most of the workpieces within the specification limits.*

**Key words:** *Measurement system analysis, bias, GR&R, process capability*

### 1. Introduction

Statistical monitoring of processes in engineering activities is the basis for achieving the quality of the production process, reducing the number of defective products, and maximizing profits [1]. Each production process has its imperfections that are the cause of variations in the quality characteristics of workpieces. Sometimes it is difficult to identify and quantify all the causes of variation, but it is necessary to determine their impact on the observed process. Insight into the state of the process is obtained by measuring the quality characteristics of the workpiece with a certain measuring system. If the measuring system does not give reliable results, the interpretation of the data and the state of the process will lead to inaccurate conclusions [2].

The process capability analysis study is a statistical tool that uses the normal distribution curve and control charts to determine the extent to which the observed process meets the requirements set by the specification. According to Kotz and Montgomery, several key assumptions need to be tested before assessing process capability: the process must be in a state of statistical control; the quality characteristic must have a normal distribution; in case the specification has a lower and upper limit; the mean value of the process must be in the middle between the limits of the specification; observations must be random and independent.

Several papers have addressed the issue of process capability analysis based on measured quality characteristics. Pawar et al. [3] used this to monitor and improve its processes in the automotive industry by changing process parameters for boring operations and conducting and comparing results from both sets of experiments. They conclude that after changing machine parameters such as spindle speed, feed rate, and depth of cut and analyzing process capability, they can achieve comparatively better process performances. Research in

the field of additive technologies has been improved by the methodology of statistical process control, especially in the application of new composite materials in the Fused Deposition Modeling method. Sharma et al. performed multi-response optimization and process capability analysis for surface properties of 3D printed functional prototypes of polyvinyl chloride (PVC) reinforced with polypropylene (PP) and hydroxyapatite (HAp) for possible bio-sensing applications. process capability indices ( $C_p$  and  $C_{pk}$ ) were calculated to ensure the statistical nature of the process [4]. Ketan and Nassir improved the process of extrusion of aluminum profiles through the DMAIC methodology and calculations and interpretation of process capability indices. In that manner, they are able to accomplish decrease in the dispersion of the production process, and as a result, a significant reduction in the number of bad pieces was achieved, resulting in increased earnings from 127,000 monetary units per 1000 kg of product to 223,000 monetary units [5].

Measurement data are used more often and, in more ways, than ever before. For instance, the decision to adjust a manufacturing process is now commonly based on measurement data. The input data for conducting any type of process analysis are the measured data obtained by a measuring system. The quality of measurement data is defined by the statistical properties of multiple measurements obtained from a measurement system operating under stable conditions. The statistical properties most used to characterize the quality of data are the bias and variance of the measurement system. The property called bias refers to the location of the data relative to a reference (master) value, and the property called variance refers to the spread of the data. The test procedure which should be used to understand a measurement system and to quantify its variability depends on the sources of variation which may affect the measurement system. In many situations, the major

sources of variation are due to the instrument (gage/equipment), person (appraiser), and method (measurement procedure) [6]. The prevalence of this methodology is most pronounced in the automotive industry, where are parts like ball bearings frequently inspected. The crucial piece of measuring equipment such as for measuring the performances of ball bearings is submitted to verification through measurement system analysis. Measurement system analysis (MSA) was used to assess the vibration measurement system of rolling bearings [7]. This methodology is so important that could be, in some case, supplement to the various standards, such as VDI / DGQ 3442 standard for the assessment of the accuracy of numerical machine tools [8].

In this paper, attention was paid to the measurement system and its impact on the obtained results, so that before the analysis of the process capability, the analysis of the measurement system was performed using Gage Repeatability and Reproducibility Study (GR&R). The Gage Repeatability and Reproducibility of measuring instruments breaks down the total variation in the study into variation due to workpieces (processes) and variation due to the measuring system. The results from



Fig. 1. Checking the bias of the measuring device by measuring the gauge block

GR&R study should be evaluated to determine if the measurement device is acceptable for its intended application. A measurement system should be stable before any additional analysis is valid.

## 2. Experimental research

To better understand the observed production process in a real production environment, there is a need to investigate how well that process can meet customer requirements and how well the measuring system can describe the process through the evaluation of the quality characteristics. Knowing this information can help engineers to optimize and upgrade any given process, thus reducing the costs of production many times over.

First, we must look carefully at the measuring system. All measurement processes conducted in this paper were performed with a flat measuring plate micrometer with 50 ÷ 75 mm measuring range, and 0.01 mm resolution.

To check the bias of the measurement results, a block gauge with a length of 50 mm was measured. (Fig. 1.).



Fig. 2. Acquisition of measurement data for process capability analysis

The gage block was measured 25 times under the same conditions. Bias is calculated from the following equations [10]:

$$\text{bias}_i = x_i - \text{reference value} \quad (2.1)$$

$$\text{avg bias} = \frac{\sum_{i=1}^n \text{bias}_i}{n} \quad (2.2)$$

From the available sample, it is calculated that the Bias has the average value of 0.002 mm, where the reference value is 50 mm from gage block, and the  $x_i$  values are results of the measurement obtained by micrometer.

Following the guidelines in literature [13], for the study of process capability, 125 samples were randomly selected. The quality characteristic being measured (Fig. 2.) is the simple distance between two parallel planes on the workpiece. Parallel planes on the workpiece were machined on the vertical milling machine. The dimension stated by technical documentation is  $50 \pm 0,1$  mm.

## 3. Results and discussion

After performing the bias test on the selected gage, the gage repeatability and reproducibility study is conducted. Repeatability is described as variation in measurements obtained with one measuring instrument when used several times by an appraiser while measuring the identical characteristic on the same part. It is commonly referred to as E.V. – Equipment Variation. Reproducibility is described as variation in the average of the measurements made by different appraisers using the same gage when measuring a characteristic on one part. It is commonly referred to as A.V. – Appraiser Variation. Method used to calculate variations in measurement system and in manufacturing process is Analysis of variance (ANOVA). Analysis of variance is a standard statistical technique and can be used to analyze the measurement error and other sources of variability of data in a measurement systems study. In the analysis of variance, the variance can be decomposed into four categories: parts, appraisers (operator), interaction between parts and appraisers, and replication error due to the gage [10].

Goal of the Gage R&R study is to show that E.V. or Equipment Variation does not play a significant role in overall variation. Most of the total variation must be attributed to process variation (part-to-part variation) [4]. MINITAB® statistical software is used for all calculations and graphical displays. Results according to ANOVA method are given in Table 1 and Table 2. and graphical representation in Fig. 3.

Gage R&R Study – ANOVA Method					
Two-way ANOVA table with interaction					
Source	DF	SS	MS	F	P
Part	9	0,0166900	0,0018544	172,655	0,000
Operator	2	0,0000067	0,0000033	0,310	0,737
Part * Operator	18	0,0001933	0,0000107	1,074	0,399
Repeatability	60	0,0006000	0,0000100		
Total	89	0,0174900			
$\alpha$ to remove interaction term = 0,05					

Table 1. Gage R&R Study – ANOVA Method

Source	VarCo.	%Con. of VarCo.	SD	Study Var (6 x SD)	%Stud. Var (%SV)
Total GRR	0,0000102	4,73	0,0031892	0,0191351	21,75
Repeat.	0,0000102	4,73	0,0031892	0,0191351	21,75
Repr.	0,0000000	0,00	0,0000000	0,0000000	0,00
Operator	0,0000000	0,00	0,0000000	0,0000000	0,00
Part-to-part	0,0002049	95,27	0,0143150	0,0858900	97,61
Total var.	0,0002151	100,00	0,0146660	0,0879957	100,00
Number of Distinct Categories = 6					

Table 2. Gage R&R Study

According to ANOVA, workpieces have statistical significance ( $p$ -value = 0.000  $<$   $\alpha$  = 0.05), while operators and the interaction of operators with workpieces do not have statistical significance.

The contribution of the variation of the measurement system in the study is 4.73%, while the contribution of the variation between workpieces in the overall study is significant and amounts to 95.27%. The histogram of the variation components shows that most of the variations in the study can be attributed to variation due to the manufacturing process (workpieces). Metrologists have achieved satisfactory repeatability and reproducibility. On the range map and Xbar map, most points go beyond the control limits, which in this case is good, the measuring instrument is chosen correctly. The

measuring system recognized 6 different categories of workpieces, which is a satisfactory case (NDC should be 5 or more). Since the variation of the measuring system is 27.75%  $<$  30% in the %StudyVar column and based on the criteria given in the literature [10], we can conclude that the selected measuring system is conditionally acceptable.

As for the study of process capability, the observed process has an upper (USL) and lower (LSL) limit of the specification. The values of the specification limit are 50.1 mm, while the value of the lower limit is 49.9 mm. Based on that, ideally, the mean value of the measured result should be in the middle between the upper and lower limit of the specification. Analysis of the obtained results shows a minuscule difference between the index  $C_p = 2.67$  and  $C_{pk} = 2.59$  (in Fig. 4. Pp and Ppk). The difference between these two indices confirms that the observed process is not centered. The values of both capability indices exceed the value of 1.33, considered the limit below which these indices should not have values. The observed process has a small scatter of results, which is shown by the index  $C_p$ .

The number of defective parts per million produced, in this case, is equal to 0, i.e., the PPM index (Parts per million = 0.00).

#### 4. Conclusion

The conducted study shows the importance of the analysis of process capabilities as a statistical tool for monitoring and quality assurance of manufactured workpieces that will meet the prescribed specifications. Reducing variations from the set value (target T) affects the reduction of losses in the production process. This is the desired goal according to today's modern theories of quality improvement. Before conducting the process capability study, special attention was paid to the measurement system, as an essential link in the measurement process chain. A crossed study of repeatability and reproducibility of measuring instruments was conducted to determine the variation of the measuring system. The reference standard (gauge block) used in the study has a nominal length of 50 mm. The analysis of the measuring system showed that the observed measuring device has all the necessary features to be used with certainty for data acquisition in the process capability study. The analysis of the obtained results from the process capability study showed that the observed process has good stability, i.e., the range of 6 $\sigma$  is within the specification limits, and good centricity because the value of the  $C_{pk}$  index is approximately equal to the  $C_p$  index value. Based on this, the estimated number of workpieces that do not meet the specification, presented as a PPM index, is minimized.

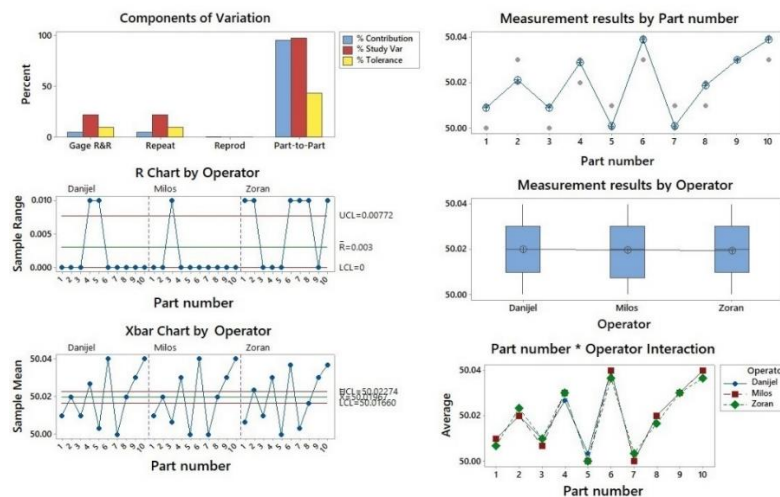


Fig. 3. Graphical representation of the results of the ANOVA method

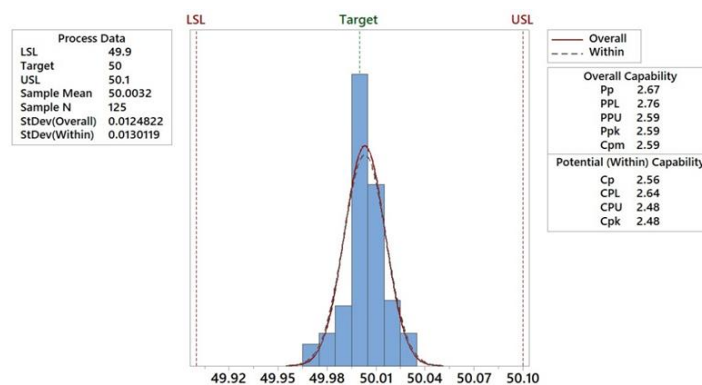


Fig. 4. Process capability analysis for measured results

## 5. REFERENCES

- [1] Stepenhurst, T.: *Mastering statistical process control A Handbook for Performance Improvement Using Cases*, Elsevier Butterworth-Heinemann, 2005.
- [2] Saikaew, C.: *An implementation of measurement system analysis for assessment of machine and part variations in turning operation*, Measurement, 118, 2018
- [3] H. U. Pawar, S. K. Bagga, and D. K. Dubey: *Investigation of production parameters for process capability analysis: A case study*, Mater. Today Proc., vol. 43, pp. 196–202, 2021.
- [4] R. Sharma, R. Singh, and A. Batish.: *On multi response optimization and process capability analysis for surface properties of 3D printed functional prototypes of PVC reinforced with PP and HAp*, Mater. Today Proc., vol. 28, pp. 1115–1122, 2019.
- [5] Ketan, H., Nassir, M.: *Aluminium hot extrusion process capability improvement using Six Sigma*, Adv. Prod. Eng. Manag., vol. 11, no. 1, pp. 59–69, 2016.
- [6] Down, M., et al.: *Measurement system analysis reference manual*, Chrysler Group LLC, Ford Motor Company, General Motors Corporation, 2010.
- [7] M. Wrzochal and S. Adamczak.: *Application of a Gage R&R study in evaluation of rolling bearing measurement system accuracy*, Transp. Res. Procedia, vol. 40, pp. 934–939
- [8] Štrbac, B., et al: *Supplement to the Standard VDI/DGQ 3442 with Gage R&R Study*, New Technologies, Development and Application IV, Sarajevo, 2021.

**Authors:** B.Sc. Miloš Ranisavljev, Assist. Prof. Branko Štrbac, M.Sc. Zorana Lanc, PhD Matin Ivan Full Prof. Miodrag Hadžistević, University of Novi Sad, Faculty of Technical Sciences, Department of Production Engineering, Trg Dositeja Obradovića 6, 21000 Novi Sad, Serbia, Phone.: +381 21 485-23-24. E-mail: [ranisavljev@uns.ac.rs](mailto:ranisavljev@uns.ac.rs); [strbacb@uns.ac.rs](mailto:strbacb@uns.ac.rs); [zoranalanc@uns.ac.rs](mailto:zoranalanc@uns.ac.rs); [matini@uns.ac.rs](mailto:matini@uns.ac.rs); [miodrags@uns.ac.rs](mailto:miodrags@uns.ac.rs)

**Full Prof. Predrag Janković**, Faculty of Mechanical Engineering in Niš, University of Niš, Aleksandra Medvedeva 14, 18106 Niš, Serbia E-mail: [predrag.jankovic@masfak.ni.ac.rs](mailto:predrag.jankovic@masfak.ni.ac.rs)

**ACKNOWLEDGMENT:** The results presented in this paper are obtained in the framework of the project entitled “Innovative scientific and artistic research from FTS (activity) domain” funded by the Ministry of Education, Sciences and Technological Development of Republic of Serbia”

Janković P., Madić M., Štrbac B., Hadžistević M., Mladenović P.

## APPLICATION OF GAGE R&R FOR EVALUATION MEASUREMENT SYSTEM PRECISION: CASE STUDY

**Abstract:** *In order to effectively control and improve production processes and the quality of products, modern production systems require reliable measurement results. Measurement system analysis (MSA) is a set of useful tools used for the assessment of the quality of the measurement systems. While the accuracy of the used measurement system is estimated based on linearity, bias, stability, conducting gage repeatability and reproducibility (Gage R&R) analyses is inevitable for the assessment of measurement system precision. Gage R&R studies are an essential part of a Quality Management System (QMS) aimed to measure the variation amount in the measurement system which arise from the measurement device and operators responsible for measurement. The present study illustrates the application of the GR&R study for evaluating a measurement system used in the industry for measuring the contact height of the automotive relay.*

**Key words:** *measurement system analysis, gage R&R analysis, precision, automotive industry*

### 1. INTRODUCTION

According to the ISO 10012 standard, the measurement process - (measurement process, measurement) is: "a set of operations for determining the value of a quantity". Following the same standard, a measurement management system is "a set of interconnected or interacting elements that are needed to achieve metrological validation and continuous management of measurement processes".

Measurements occupy a special place among different types of quantitative evaluation, and they are characterized by the establishment of an unambiguous connection between the measured physical quantities and their numerical expression. It is almost impossible to describe any phenomenon without relying on measurement results. Furthermore, without measurement, product quality control cannot be imagined as a condition for its placing on the market.

Manufacturing companies use different types of measuring systems based on the measurement results of which conclusions are made about whether the production process or product quality characteristics meet the set technological requirements and specifications. In addition, the measurement results are the basis for statistical control, improvement, and optimization of production processes and product quality. In this regard, the quality and reliability of the measurement results of the measuring system are crucial.

Since all components of the measurement system in a particular application, to a greater or lesser extent, cause variation in measurement results, which may ultimately lead to increased costs, it is necessary to analyze the measurement system to isolate and quantify all components of measurement variation, system, as well as to assess the ability of the measuring system for a given purpose. Montgomery [1] defines the analysis of measuring systems as an experimental and statistical method that identifies variations in the measuring

system. Having in mind that the variation of the measuring system directly contributes to the total measured variation, continuous measurement, analysis of measuring systems, and validation of the adequacy of the measuring system are essential for improving production processes and product quality.

In general, the analysis of measuring systems enables the analysis of the accuracy and precision of measuring systems (measurements, control, testing).

### 2. MEASUREMENTS SYSTEM ANALYSIS

To effectively control and improve production processes and product quality, modern production systems require reliable measurement results. The quality of measurement results is defined by the statistical characteristics of repeated measurements by the measuring system, where the systematic error and variation of the measuring system are most often taken into account. Therefore, in order to ensure reliable results of the measuring system, it is necessary to monitor and control the measuring system, which in the analysis of measuring systems means the analysis of measuring devices, measuring procedures, meters, measuring conditions, etc. [2].

Due to its significance, measurement system analysis (MSA) is one of the most important quality tools that is widely used in manufacturing companies, especially in the automotive industry. Within the DMAIC (Define, Measure, Analyze, Improve, Control) methodology of continuous quality improvement, analysis of measurement systems is the first key step that precedes and is the basis for the application of other quality tools such as statistical process control, correlation analysis, regression analysis, statistical hypothesis testing, experimental planning theory, etc.

If the measurement system is not adequate, it is almost impossible to monitor, control, improve or manage the process [1]. Its application in real production conditions can ultimately lead to wrong

conclusions regarding the quality of the process or product. As a result, type I and II errors occur [3]:

- Non-acceptance of products that meet the prescribed requirements ("good" products) which negatively affects the internal flow of products, increases waste, finishing costs.
- Acceptance of products that do not meet the prescribed requirements ("bad" products) which reduce the quality of the product/process, the reliability of the production process, and can also negatively affect customer relations.

MSA is a collection of experiments and analyses performed to evaluate a measurement system's capability, performance and quantifies location and width variation.

### 2.1 Variation in measurement systems

The capability of the measuring system is based on the estimation of the combined variation of measurement errors (random and systematic) based on the short-term estimation (series of measuring cycles, given time period of production, ...) of the measuring system including analysis of the following components [1]:

- systematic error and linearity,
- repeatability and reproducibility (gage R&R, GRR)

The sources of variation in a measurement process can include the following:

- Process,
- Personnel,
- Tools / Equipment,
- Items to be measured and
- Environmental factors.

All of these possible sources of variation should be considered during measurement system analysis. Most MSA activities examine two primary sources of variation – the parts and the measurement of those parts. The sum of these two values represents the total variation in a measurement system.

Various factors, to a greater or lesser extent, without or in interaction, affect the variation of the measurement system. Variation of the measuring system can be represented by variation of position (accuracy) and variation of scattering (precision). The variation of the position shows the accuracy of the measuring system, ie the closeness of the agreement between the measurement results and the actual value of the measured quantity. The variation of scattering shows the precision of the measuring system, ie the closeness of the matching of the measurement results from repeated measurements under unchanged measurement conditions. The components of position variation and scattering are shown in Figure 1 The components of variation in the measuring system are also called the parameters of the analysis of measuring systems. The analysis of measuring systems aims to quantify these parameters.

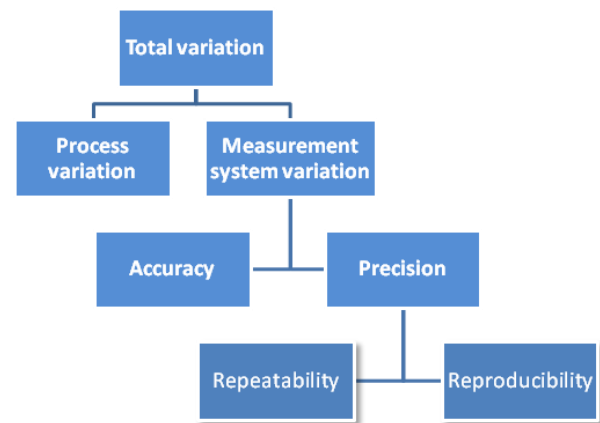


Fig. 1. Components of the variation of measurement (measuring system)

### 2.2 Gage Repeatability and Reproducibility analysis

As we have seen, measurement system analysis is a tool for analyzing the variation present in each measurement process and test equipment. A gage, in this context, is a measurement tool.

Gage R&R analysis focuses on two key aspects of measurements:

- **Repeatability**, which is the variation between successive measurements of the same part, same characteristic, by the same person using the same gage,
- **Reproducibility** which is the difference in the average of the measurements made by different people using the same instrument when measuring the identical characteristic on the same part.

According to Breifoglu [4], possible causes of measurement system variation can be identified and quantified by analysis of linearity, stability, repeatability, and reproducibility. To perform a comprehensive analysis of the measurement system, it is necessary to know all the influencing factors, as well as their influence on the measurement result [5]. For this purpose, experiments with randomized experiments are planned and realized in which, depending on the purpose, standards, reference measuring objects, or workpieces from production are measured one or more times by one or more meters in unchanged measuring conditions [6].

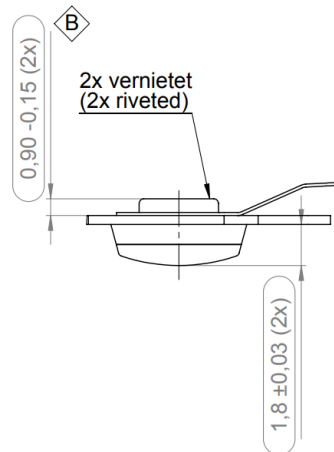
In industrial practice, various methods of selection and evaluation of measuring systems can be found, most of which are based on determining the percentage of measuring system parameters (eg systematic error, scatter variation, linearity ...) concerning process variation or tolerance field of product characteristics [7].

## 3. CASE STUDY – MEASUREMENT STUDY DEFINITION

MSA study, i.e. gage R&R study related to the precision of the measurement system was performed in a company "GRUNER Serbian" d.o.o. from Vlasotince (Serbia), a foreign company working mainly for the automotive industry. Its main products include car relays, smart meter relays, actuators, and its components. Their products are assembled in well-

known OEMs.

The goal of the MSA was related to the company's goal to check whether the measurement system, which is used for the riveting process, is reliable. In the measurement process, a comparator with a resolution of 0.001mm, was independent of the measurement of the rivet height on the contact spring (Fig. 2a). The specification for the rivet height is  $1.8 \pm 0.03$  mm. The measurement method of the rivet height on the contact spring is given in Figure 2b.



a)



b)

Fig. 2. Measurement of the rivet height on the contact spring

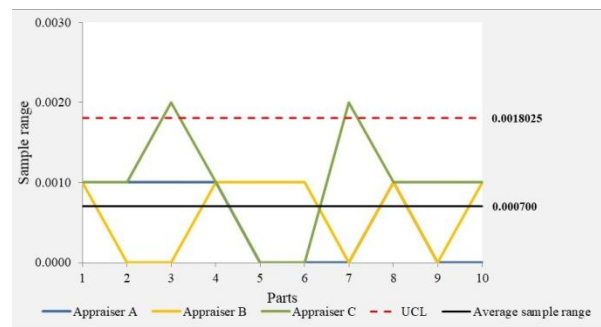
Measurement of the rivet heights was performed on contact springs which were collected from each production shift to cover the full manufacturing tolerances (covering different process variations such as machine, operator, time, shift). In sum 10 contact springs were randomly selected to conduct MSA. The measurement process was conducted in the company's metrological laboratory with a calibrated comparator. Three appraisers (A, B, and C), who are trained and regularly conduct measurements of this type, were selected. All measurements by appraisers were conducted in random order and to the statistical

measurement independence by hiding the measured part number [8].

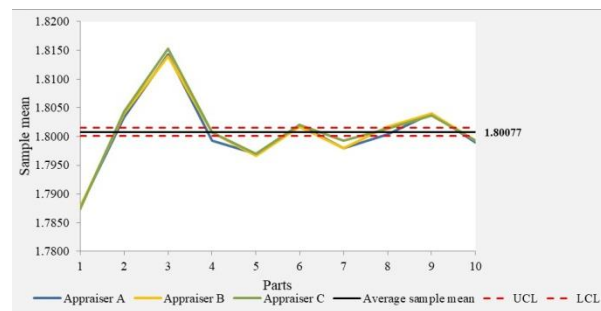
In the present study, measurement system evaluation was performed with the application of the average and range methods. Unlike the ANOVA method, this method can distribute the total measurement system variability into process variation (part-to-part variation), gage variability (repeatability), and operators' variability (reproducibility), without the possibility to determine appraiser by part variability [9].

#### 4. RESULTS AND DISCUSSION

Based on the obtained measurement results, for confirmation of the statistical process stability, R and  $\bar{X}$  charts were generated (Figure 3).



a) R chart by appraiser



b)  $\bar{X}$  chart by appraiser

Fig. 3. R and  $\bar{X}$  charts for the present MSA study

The application of R chart enables the visualization of the range of repeated measurements for each part and each appraiser individually. As could be observed, the R chart shows that appraiser C is having problems measuring parts consistently. On the other hand, appraisers A and B measure consistently which is indicated by the small range values and the fact that all points fall within the control limits. Any observations outside the control limits may indicate the existence of special sources of variation, such as e.g., error in the measurement procedure and the like. As could be observed from Figure 3, control limits are narrow and a majority of points are out of the control limits indicating that the measurement system has low variation and that majority of variation is due to the differences between parts.

Based on the obtained measurements, the results of the GRR analysis are computed based on mathematical expressions given in [10] and are given in Table 1.

Variability component	Value	% of variability component	Value
Equipment variability (EV) - repeatability	0.00041	%EV	0.69%
Appraiser variability (AV) - reproducibility	0.00027	%AV	0.45%
Repeatability and reproducibility (GRR)	0.00049	%GRR	0.82%
Part variability (PV)	0.00849	%PV	99.81%
Total variability (TV)	0.00851	<i>ndc</i>	24

Table 1. Results of conducted GRR analysis by the average and range method

Based on two criteria [11], i.e. %GRR (percentage of total repeatability and reproducibility divided by total variability or tolerance and multiplied by 100) and *ndc* (number of distinct categories) parameter, showing how many different categories of measuring objects can be reliably recognized by the applied measuring system, the application of the average and range method helps in decision making whether the applied measurement system is acceptable, conditionally acceptable or not acceptable [8].

The results from Table 1 suggest that the measurement system can be considered acceptable because the %GRR is less than 10%. Thus, the applied measurement system with a comparator can provide reliable data about the process, i.e., measurement of the rivet height on the contact spring. In addition, *ndc* parameter has the value of 24, which is significantly higher than then limit value of 5 [11], which indicates that the applied measurement system with comparator is precise and can reliably distinguish one part from others.

When one compares the % contribution from part variability (99.81%) and %GRR (0.82%) it could be noticed that the first one is significantly higher. Thus, one can conclude that most of the variability is due to differences between parts and only negligible contribution from the applied measurement system.

## 5. CONCLUSIONS

Whether it is about process control, process optimization or quality assurance adequate, capable and reliable measurement systems are inevitable. In order to perform comprehensive analyses of the measurement systems, under the MSA different specially designed experiments are planned and implemented depending on the purpose.

This study presented the use of MSA to evaluate the performance of the measurement system with a comparator for measurement of the rivet height on the contact spring. The performed Gage R&R study was realized upon the application of the average and range method. From the obtained results and analysis it was observed that the applied measurement system is acceptable. Still, further training of the appraiser C may be suggested in order to improve the consistency of the measurements.

## 6. REFERENCES

- [1] Montgomery, D. C.: *Introduction to Statistical Quality Control*, John Wiley & Sons, 2007.
- [2] Automotive Industry Action Group.: *Measurement Systems Analysis Reference Manual*, 2010.
- [3] Mottonen, M., Belt, P., Harkonen, J., Haapasalo, H., Kess, P.: *Manufacturing process capability and specification limits*, The Open Industrial and Manufacturing Engineering Journal, Vol. 1, pp. 29-36, 2008.
- [4] Breyfogle, F. W.: *Implementing Six Sigma: Smarter Solutions Using Statistical Methods*, John Wiley & Sons, 2013.
- [5] Bantleon, M.: *Einführung in die Messsystemanalyse (MSA)*, Steinbeis-transferzentrum Produktion und Qualität, Duravit, 2017.
- [6] Keferstein, C. P., Marxer, M.: *Fertigungsmesstechnik Fertigungsmesstechnik Praxisorientierte Grundlagen, moderne Messverfahren*, Springer, 2014.
- [7] Tabisz, R.: *The capability evaluating of industrial measurement systems*, Proceedings of the XVII IMEKO World Congress, Dubrovnik, Croatia, pp. 2185-2188, 2003.
- [8] Čepová, L., Kováčiková, A., Čep, R., Klaput, P., Mizera, O.: *Measurement system analyses-gauge repeatability and reproducibility methods*, 2018.
- [9] Simion, C.: *A Case Study on Gage R&R In Automotive Industry*, Academic Journal of Manufacturing Engineering, 13(3), 2015.
- [10] Janković, P., Madić, M.: *Fundamentals of metrology and analysis of measuring systems, (title in Serbian)*, University of Niš, Faculty of Mechanical Engineering., 2020.
- [11] Chrysler Corporation, Ford Motor Company, General Motors Corporation (AIAG): *MSA - Measurement Systems Analysis (MSA) Fourth Edition*. AIAG., 2010.

**Authors:** Full Prof. Predrag Janković, Assist. Prof. Miloš Madić, Assist. Prof. Branko Štrbac, Full Prof. Miodrag Hadžistević, M.Sc. Predrag Mladenović, Faculty of Mechanical Engineering in Niš, University of Niš, Aleksandra Medvedeva 14, 18106 Niš, Serbia Faculty of Technical Sciences, University of Novi Sad, Trg Dositeja Obradovića 6, 21102 Novi Sad, Serbia GRUNER Serbian d.o.o., Vlasotince, Serbia  
E-mail: [predrag.jankovic@masfak.ni.ac.rs](mailto:predrag.jankovic@masfak.ni.ac.rs); [milos.madic@masfak.ni.ac.rs](mailto:milos.madic@masfak.ni.ac.rs); [strbacb@uns.ac.rs](mailto:strbacb@uns.ac.rs); [miodrags@uns.ac.rs](mailto:miodrags@uns.ac.rs); [Predrag.Mladenovic@gruner.de](mailto:Predrag.Mladenovic@gruner.de)

**ACKNOWLEDGMENTS:** This research was financially supported by the Ministry of Education, Science and Technological Development of the Republic of Serbia (Contract No. 451-03-9/2021-14/200109).



Terek, V., Miletić, A., Kovačević, L., Škorić, B., Kukuruzović, D., Drnovšek, A., Panjan, P., Terek, P.

## COMPARISON OF TWO METHODS USED FOR EVALUATION OF HIGH TEMPERATURE TRIBOLOGICAL PERFORMANCE OF PROTECTIVE COATINGS

**Abstract:** In this study, TiAlN coating was deposited on hot-working tool steel, using cathodic arc deposition. Two approaches used for high temperature tribological evaluation were compared, the tests conducted directly at high temperature (HT) and on previously annealed (PA) samples. Coatings were tested against Al<sub>2</sub>O<sub>3</sub> ball at room temperature (RT), 300, 500, 600 and 700 °C in air, using high temperature pin-on-disk tribometer. Tribo-tracks were evaluated using stylus profilometry, confocal microscopy, focused ion beam and energy dispersive spectroscopy. Apart from pronounced oscillations observed in PA tests, coefficient of friction was quite similar for RT and PA tests, while those obtained in HT tests were not comparable. Coatings wear mechanism at RT and in PA tests can be characterized as both abrasive and adhesive, while wear mechanisms observed at HT should be regarded as abrasive and oxidative. It is indicated that tribological tests performed on PA samples are not adequate for simplifying the high temperature tribological investigations.

**Key words:** PVD coatings, TiAlN, high temperature tribology, COF, wear

### 1. INTRODUCTION

During the last three decades, ternary hard coatings such as TiAlN have found widespread use for many cutting applications at high working temperatures. Such high interest in these coatings comes from their high hardness and resistance against wear and oxidation [1]. There are many papers reporting on microstructure and mechanical properties of TiAlN coatings [2,3]. However, far less attention is given to their tribological behavior, especially at high temperatures. Therefore, there is a constant need to contribute to better understanding of tribological behavior of hard coatings at elevated temperatures.

Evaluations of coatings' tribological behavior at high temperature are the most commonly performed directly on high temperature [4]. However, to simplify these evaluations, the usual approach is to heat coated samples to desired temperature and conduct tribological tests after samples cool down to room temperature [5]. Both these methods of high temperature tribological evaluations are equally important for practical use of coatings and for their tribological behavior, but different results were observed. Therefore, a motivation for this investigation was to point out differences in high temperature tribological behavior between these two approaches.

### 2. MATERIAL AND METHODS

In this investigation, TiAlN coating was prepared using cathodic arc deposition. Before deposition, disk-shaped samples made of hot-working tool steel (EN X38CrMoV5) were grinded (P2000 sandpaper) and fine polished (3µm diamond paste). Measured thickness and hardness of coating was 3 µm and 3050 HV<sub>0.05</sub>, respectively. Tribological behavior of coating was evaluated in air atmosphere, using high temperature pin-on-disk tribometer (Anton Paar, THT). Tribological

tests of coated samples were conducted at room temperature (RT), 500, 600 and 700 °C, and on samples previously annealed (PA) at the same temperatures. The following parameters were chosen for all tribological tests: velocity of 5 cm/s, normal load of 5 N and number of cycles of 2000. Alumina (Al<sub>2</sub>O<sub>3</sub>) ball with diameter of 6 mm was used as a counterpart.

After the tribological tests, wear tracks were evaluated by stylus profilometry (Taylor Hobson, Talysurf), confocal microscopy (CFM) (Zeiss, Axio CSM700) and focused ion beam (FIB) (Fei, Helios Nanolab 650i) equipped with energy dispersive spectroscopy (EDS).

The wear rate of coated samples was evaluated using wear track profile measurements. Coating wear volume was calculated using the average value of six evenly distributed profiles measured on each wear track. The wear rate was calculated as the worn material volume per sliding distance and normal load, as shown in Eq.(1)

$$\text{wear rate} = \frac{V}{F \cdot s} \left[ \frac{\text{mm}^3}{\text{Nm}} \right] \quad (1)$$

where  $V$  is wear volume (mm<sup>3</sup>),  $F$  is the load (N) and  $s$  is the sliding distance (m).

### 3. RESULTS AND DISCUSSION

#### 3.1 Tribological tests at RT and on PA samples

Typical coefficient of friction (COF) values, of the TiAlN coating tested at different temperatures, are presented in Figure 1.

The steady-state coefficient of friction obtained from tribological test conducted at room temperature was 0.72. Value of COF for tribo-test at RT was mostly steady with only a slight increase after an approximately 1500 cycles. Quite similar values of steady-state COF were obtained from tribological tests on previously annealed samples. However, unlike RT tests, each test

on the PA samples was characterized by pronounced oscillations of COF.

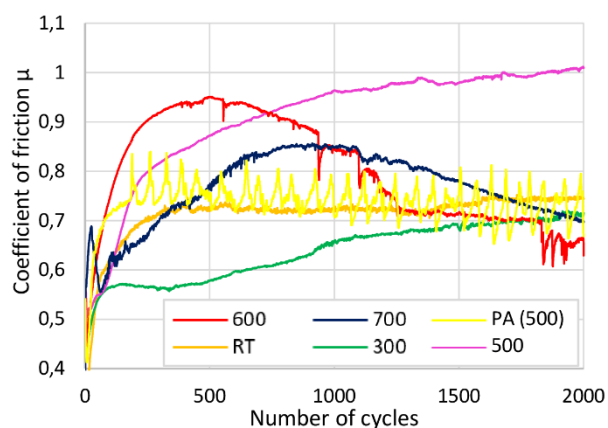


Fig. 1. COF of  $\text{Al}_2\text{O}_3$  ball on TiAlN in different testing conditions.

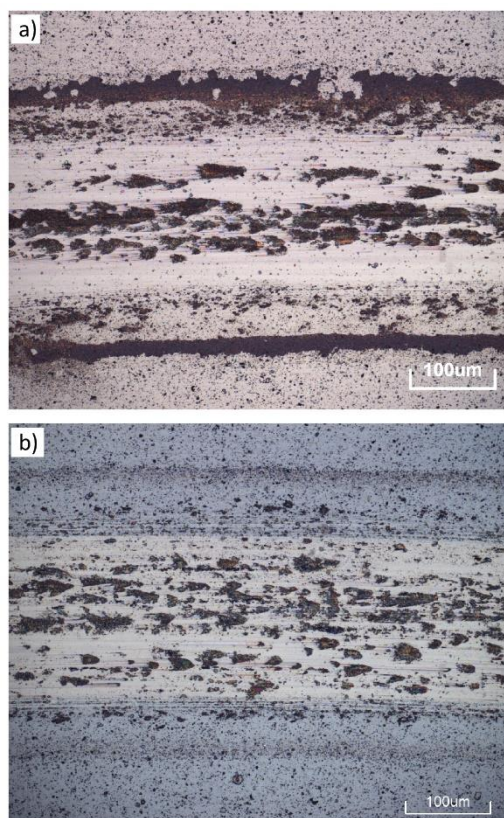


Fig. 2. Wear track surface morphology image obtained by CFM for tribo-test: a) at RT; b) on sample previously annealed at 500 °C

In order to better understand wear behavior of investigated coating, wear tracks were analyzed by confocal microscopy. Figure 2 presents surface morphologies of wear tracks generated in tribological tests at RT and on PA samples. Apart from having similar steady-state COF, visual analysis of wear tracks revealed also quite similar wear mechanism at RT and in PA tests and led us to several findings. First, both wear tracks are of same width. Second, they are both characterized with smooth areas, which is characteristic of abrasive wear mechanism. Third, both wear tracks are partially covered with small protrusions, mostly

concentrated in the middle of wear track, which is characteristic of adhesive wear mechanism. Therefore, judging by the visual analysis of wear tracks, it can be concluded that both abrasive and adhesive wear mechanisms are present in tribological tests at RT and on PA samples.

Annealing of TiAlN coatings, of various chemical composition, has been widely covered in literature. Results of these investigations show that exposure of TiAlN to high temperature results in formation of aluminum oxide and titanium oxide on the surface of the coating [6,7]. Contact between alumina counterpart and oxide of the same material that formed during annealing, may lead to observed adhesive wear [5]. Therefore, pronounced oscillations of COF on PA samples are suggested to be the consequence of adhesive wear of coatings.

### 3.2 Tribological tests at 300 and 500 °C

Coefficient of friction values obtained at 300 and 500 °C are not comparable with those at RT and on PA samples. For these tests COF is steady, and it slightly increases to a maximum value of 0.7 and 1 for 300 and 500 °C, respectively. It can be observed that COF value at 300 °C is lower than at room temperature. However, inclining trend of COF value suggests that COF at 300 °C in later stages can outgrow room temperature COF.

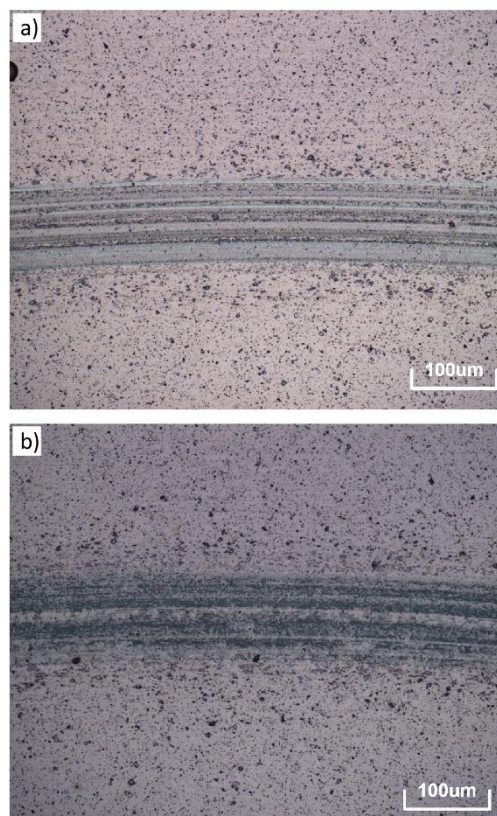


Fig. 3. Wear track surface morphology image obtained by CFM for tribo-tests: a) at 300 °C; b) at 500 °C.

Some authors reported increased friction coefficient when  $\text{TiO}_2$  and  $\text{Al}_2\text{O}_3$  were present in tribological contact [8–10]. It is suggested that the most common

stoichiometric forms of TiO<sub>2</sub>, rutile and anatase, increase coefficient of friction, while non-stoichiometric phases of titanium oxide, so-called Magnéli phases, are known to possess easy shear characteristic and hence low friction. However, Shum et al [10] showed that for TiAlN films only stoichiometric rutile titanium oxide is found. Therefore, it is believed that high friction at 500 °C is a result of alumina counterpart sliding against titanium and alumina oxides that formed on coating's surface.

Figure 3 presents surface morphologies of wear tracks generated in tribological tests at 300 and 500 °C. Width of wear tracks is similar and considerably smaller than at RT and on PA samples. No observable adhesive wear is present, however, smooth surface found inside of wear tracks at 300 and 500 °C corresponds to abrasive wear mechanism. Additionally, since these tests are conducted at temperatures at which oxides form, oxidative wear mechanism is also present. Therefore, it can be observed that there is a significant difference in wear mechanisms between tribological tests at high temperature and on PA samples.

The observed difference between tribological tests at high temperature and on PA samples is suggested to be due to difference in contact between Al<sub>2</sub>O<sub>3</sub> counterpart and the oxides on surface. In tribological tests on PA samples, alumina counterpart is in contact with thick oxide that formed on the surface of coating during annealing. On the other side, in high temperature tribological tests, alumina counterpart is in contact with thin, newly formed, oxide which is constantly being removed.

### 3.3 Tribological tests at 600 and 700 °C

Coefficient of friction at 600 and 700 °C reached maximum values of 0.95 and 0.85, respectively, after which it declined. As already mentioned for tests at 300 and 500 °C, high values of COF are the consequence of counterpart sliding on alumina and titanium oxide. However, in order to understand the reason for decrease of COF after a certain number of cycles, wear tracks obtained at 600 and 700 °C were analyzed by FIB and EDS. It was found that degradation of coating inside the wear track started at 600 °C. At 700 °C coating was completely damaged by Fe-O and Cr-O that formed underneath the coating and filled the wear tracks. Therefore, it is suggested that declining COF in tests at 600 and 700 °C is a result of alumina counterpart sliding on Fe-O and Cr-O that formed inside of wear tracks. Additionally, it is evident that coating degradation inside of wear tracks is a consequence of substrate material oxidation. Figure 4 shows EDS line analysis and wear track of coating tested at 700 °C.

In order to determine the mechanism of substrate oxidation inside of wear tracks, detailed analysis of wear track at 600 °C was performed by FIB and EDS (Figure 5). Apart from Fe - O and Cr - O in the center of the wear track, it was found that oxidation initiates through micro cracks formed inside of the wear track as a consequence of material fatigue. Fatigue micro cracks are more pronounced at high temperature due to degradation of substrate mechanical properties and consequently its

load-bearing capacity. However, in order to better understand formation and influence of fatigue micro cracks on high temperature tribological behavior, an additional comprehensive investigation is required.

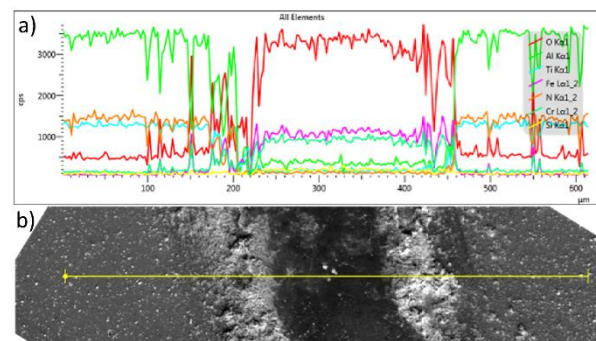


Fig. 4. TiAlN coating tested at 700 °C: a) EDS line analysis of chemical composition; b) wear track.

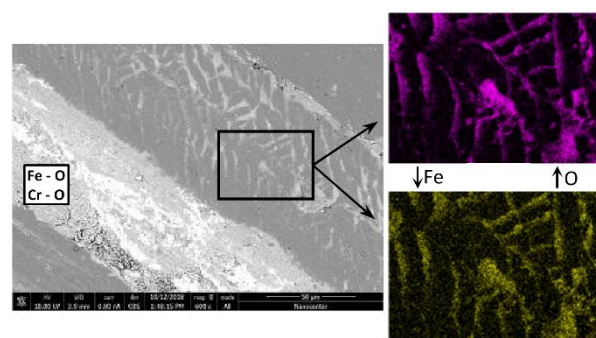


Fig. 5. EDS mapping of TiAlN coating's wear track obtained at 600 °C.

### 3.4 Wear rate

Wear rate of TiAlN coating tested in different conditions was analyzed, and results are presented in Figure 6. It is important to mention that coatings were not worn through during tribological tests.

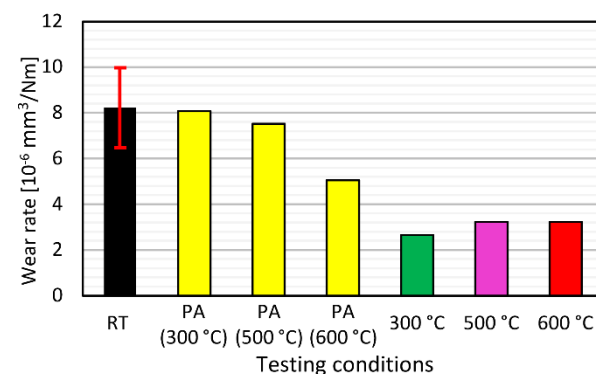


Fig. 6. Wear rate of TiAlN coating for tests without total coating failure and/or oxidation.

It was found that tribological tests at RT and on PA samples show similar wear rate that decreased with increase in testing temperature. On the other side, tribological tests at high temperature (300, 500 and 600 °C) displayed significantly lower wear rates. Additionally, increase in wear rate with increase in testing temperature was observed, which is in agreement with pronounced oxidation of wear tracks at high

temperatures. Wear rate at 700 °C is not relevant due to extensive oxidation, therefore it is not presented.

#### 4. CONCLUSIONS

Detailed analysis of COF values and wear tracks revealed that tribological tests on PA samples are quite similar to RT tests. However, COF values and wear tracks, observed for these tests, are significantly different than those obtained from high temperature tribological test. Therefore, it can be concluded that tribological tests performed on previously annealed samples are different than high temperature tests and not suitable for simulating high temperature tribological behavior of TiAlN coating.

Judging by the results, it is postulated that oxides formed on surface of TiAlN exhibit different microstructure, morphology and mechanical properties when tested on high temperature.

Oxidation process is very complex and it highly varies with the chemical composition of coatings, annealing time and temperature, etc [7]. Therefore, in order to confirm the presence and composition of oxide layer, it is suggested that chemical analysis of coatings' surface is performed. Additionally, in order to successfully evaluate coating high temperature tribological behavior, it is necessary to exclude the effects of substrate oxidation on results of tribological tests by using substrate materials that do not oxidize at testing temperatures.

#### 5. REFERENCES

- [1] PalDey S., Deevi S.C.: *Single layer and multilayer wear resistant coatings of (Ti,Al)N: A review*, Material Science & Engineering: A, 342, pp. 58–79, 2003.
- [2] Huang H., Li Z., Wang M., Xie C.: *Microstructural and mechanical properties of TiAlN and Ti<sub>3</sub>AlN films deposited by reactive magnetron sputtering*, Material Science Forum, 816, pp. 283–288, 2015.
- [3] Walczak M., Pasierbiewicz K., Szala M.: *Adhesion and mechanical properties of TiAlN and AlTiN magnetron sputtered coatings deposited on the DMSL titanium alloy substrate*, Proceedings of the 12th International Conference “Ion Implantation and Other Applications of Ions and Electrons”, ION 2018, pp. 294–298, Poland, Kazimierz Dolny, June 18–21, 2018.
- [4] Qi Z.B., Sun P., Zhu F.P., Wu Z.T., Liu B., Wang C., Peng D.L., Wu C.H.: *Relationship between tribological properties and oxidation behavior of Ti 0.34 Al 0.66 N coatings at elevated temperature up to 900 °C*, Surface and Coatings Technology, 231, pp. 267–272, 2013.
- [5] Wang L., Nie X.: *Effect of annealing temperature on tribological properties and material transfer phenomena of CrN and CrAlN coatings*, Journal of Materials Engineering and Performance, 23, pp. 560–571, 2014.
- [6] Hofmann S.: *Formation and diffusion properties of oxide films on metals and on nitride coatings studied with Auger electron spectroscopy and X-ray photoelectron spectroscopy*, Thin Solid Films, 193-194, pp. 648–664, 1990.
- [7] Joshi A., Hu H.S.: *Oxidation behavior of titanium-aluminium nitrides*, Surface and Coatings Technology, 76–77, pp. 499–507, 1995.
- [8] Öztürk A., Ezirmik K.V., Kazmanli K., Ürgen M., Eryilmaz O.L., Erdemir A.: *Comparative tribological behaviors of TiN-, CrN- and MoN-Cu nanocomposite coatings*, Tribology International, 41, pp. 49–59, 2008.
- [9] Cho C.W., Lee Y.Z.: *Tribological characteristics of oxide layer formed on TiN coated silicon wafer*, Tribology Letters, 16, pp. 259–263, 2004.
- [10] Shum P.W., Tam W.C., Li K.Y., Zhou Z.F., Shen G.: *Mechanical and tribological properties of titanium-aluminium-nitride films deposited by reactive close-field unbalanced magnetron sputtering*, Wear, 257, pp. 1030–1040, 2004.

**Authors:** M.Sc. Vladimir Terek, Aleksandar Miletić Ph.D., Assoc. Prof. Lazar Kovačević, Full Prof. Branko Škorić, M.Sc. Dragan Kukuruzović, Assist. Prof. Pal Terek, University of Novi Sad, Faculty of Technical Sciences, Department of Production Engineering, Trg Dositeja Obradovića 6, 21000 Novi Sad, Serbia, Phone.: +381 21 450 810, Fax: +381 21 458 133.

E-mail: [vladimirterek@uns.ac.rs](mailto:vladimirterek@uns.ac.rs); [miletic@uns.ac.rs](mailto:miletic@uns.ac.rs); [lazarkov@uns.ac.rs](mailto:lazarkov@uns.ac.rs); [skoricb@uns.ac.rs](mailto:skoricb@uns.ac.rs); [kukuruzovic@uns.ac.rs](mailto:kukuruzovic@uns.ac.rs); [palterek@uns.ac.rs](mailto:palterek@uns.ac.rs)

**Researcher Aleksandar Miletić**, Polytechnique Montreal, Department of Engineering Physics, Quebec H3T 1J4, Canada, Phone.: +1 514 340 4711.

E-mail: [aleksandar.miletic@polymtl.ca](mailto:aleksandar.miletic@polymtl.ca)

**Young Researcher Aljaž Drnovšek**, **Research Counselor Peter Panjan**, Jožef Stefan Institute, Department of Thin Films and Surfaces, Jamova 39, Ljubljana, 1000, Slovenia, Phone.: +386 1 477 39 00, Fax: +386 1 251 93 85.

E-mail: [Aljaz.Drnovsek@ijs.si](mailto:Aljaz.Drnovsek@ijs.si); [peter.panjan@ijs.si](mailto:peter.panjan@ijs.si)

**ACKNOWLEDGMENTS:** This research was funded by Serbian-Slovenian bilateral project (2018-2019) grant 48. This work was also funded by the Slovenian Research Agency (program P2-0082) and European Regional Development Funds (CENN Nanocenter, OP13.1.1.2.02.006).

Anania, F. D., Bisu, C. F., But, A., Canarache, M. R.

## STUDY CONCERNING THE STIFFNESS EVALUATION FOR A MODULAR CLAMPING DEVICES

**Abstract:** In this paper is presented a way of stiffness evaluation for a modular clamping system used in milling application. Modular clamping device systems allow to increase the productivity in machining process by decreasing the set-up time. The study is made on a self-centering vice with four contact points mounted on two beryl's. For positioning on machine table is used a steel plate with a grid of accurate holes M16. The method for stiffness evaluation use the calculus based on self-frequencies of the system with and without stock mounted on it.

**Key words:** modular clamping systems, self-frequencies, stiffness, machining

### 1. INTRODUCTION

In the current context, the field of manufacturing industry imposes increasingly high requirements in terms of product quality and delivery times.

From the point of view of the evolution of the manufacturing technology, the limits are reached in terms of the individual development of each components involved: machine tools, tools and tool holders, devices, CAD-CAM software.

The next step in the evolution of technological manufacturing systems is to integrate technologies and equipment's by digitizing all aspects that influence the machining process.

Thus, in the context of Industry 4.0, digitalization does not only involve graphical representation and implementation in dedicated software, but also the exact copy of the behavior of each component in the process to optimize all machining parameters.

Until 2015-2016, the equipment and technologies that compete in the manufacturing processes were developed individually by different type of companies.

From a digital point of view, databases of components, machines, devices, tools and tools holders have been created with more or less link between technologies.

In the 2020s the focus is on integrating technologies and developing cyber physical systems that faithfully replicate in real systems. Basically, a digital twin is created that copies and communicates with the physical system in real time.

A digital system simulates a real system through a mathematical model. The more complex the real system, the more complicated the mathematical model will be because it must abstract and consider all the variables that define the behavior of the real system.

In machining systems, the number of such variables is relatively finite (industrial systems are essentially man-made artificial environments, dedicated to a certain activity), but it is still necessary to reduce them. A small number of variables used in the mathematical modeling of an industrial system will reduce the number of possible errors and will increase the efficiency and safety of the system.

For the milling process the real system is composed of:

- Milling machine center
- Clamping device
- Tools + tools holders subassemblies
- Stock / Part
- NC program.

A digital system for milling = Software's CAD-CAM-NC that involve

- 3D Digital Twin of the machining center with NC controller and postprocessors
- 3D Digital Twin of clamping devices
- 3D Digital Twin of tool and tools holders
- 3D model of part and stock

In this context, each component of the digital model must be identical in all aspects, with the equivalent component in the real system.

To achieve this, advanced techniques and methods must be used to measure, evaluate and digitizing different features of the real component.

The study presented in this paper is focused on the clamping system used in milling application and presents a way of qualitative and quantitative evaluation. These results can be used to establish parameters for linking the digital model with the real one.

A classic clamping system (fig.1) used for complex or simple parts requires a relatively high set-up time, but more than that will input a set of random, at first side, variables in both real and digital machining process. This can negatively influence the milling process due to mismatch between the digital and real machining process. For example, the calculus of machining parameters assumes ideal cutting condition which are not respected in the real process. There are two ways to take it into account these conditions:

1. By adjusting machining parameters based on machining tests (expensive and time losing)
2. By adjusting/changing machining components to respect the ideal cutting condition (take into account for example the stiffness of the clamping system, of tools and tool holders etc.)



Fig. 1. Workpiece fixed with brackets in the tool shop by machine operators [3]

In practice, the variable that is empirically controlled in terms of the operator and engineer experience is given by the stiffness of the real system. In digital systems the way of considering the clamping system stiffness is through the machining parameters calculus if this stiffness can be quantified.

The clamping system stiffness is very important in the machining process and has direct influence over:

- Surface quality
- Wear of cutting tools
- Wear of machining center
- Machining time.

To have control over the system stiffness to use it in machining parameters calculus in order to create a twin machining system digital and real, the clamping systems must be designed in a different way.

The solution consists in the use of modular systems, specially designed so that the stiffness can be set-up, by controlling the support points and the tightening from the CAD phase. (fig.2).

In this way the information sent to machine operator has a digital correspondence in the CAM

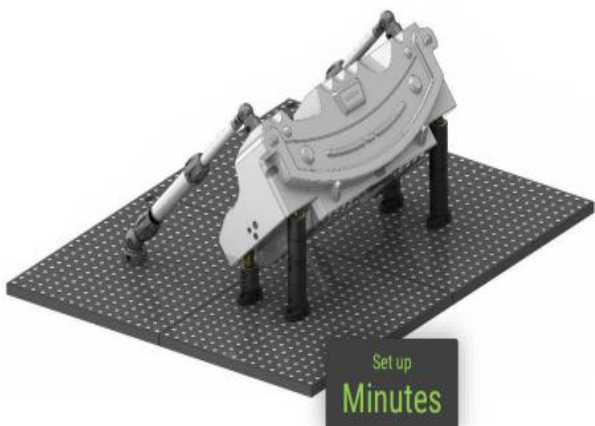


Fig. 2. Standardized & modular clamping provided in the design stage [3]

In practice we can achieve this using modular, standardized systems for which tightening torque is imposed for maximum rigidity.

## 2. EXPERIMENTAL DEVICE FOR STIFFNESS EVALUATION OF MODULAR CLAMPING SYSTEM

In this paper is proposed a method for calculating the static stiffness of a modular clamping system based on its own frequencies.

The components of the modular system are developed by FCS (a company specialized in modular systems).

The system is composed from a self-centering vice mounted on two modular breyls on a based plate with D16 H7 holes. The holes are used for accurate center and fixe the breyls. All assembly is mounted on a milling machining center MCV300 from Machine tool laboratory of University Politehnica from Bucharest.

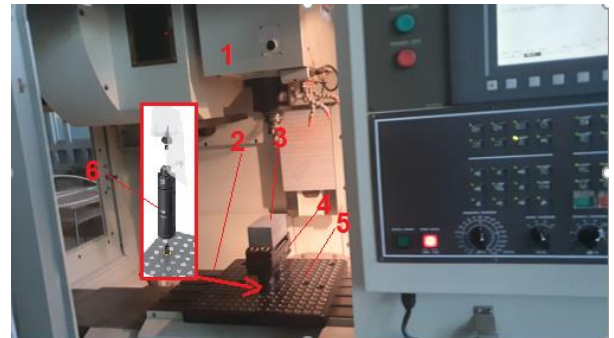


Fig. 3. machining set-up : 1-machine tool, 2-machine table, 3-stock, 4-self-centering vice, 5-base plate, 6-breyl assembly.

For data acquisition a National Instrument device was used(fig.4). Two accelerometers mounted on X and Y direction (according with machine axis) and an impact hammer were connected. (fig.5).



Fig. 4. Measuring system: 1- National Instrument device, 2- Laptop, 3- Accelerometers, 4- Impact hammer

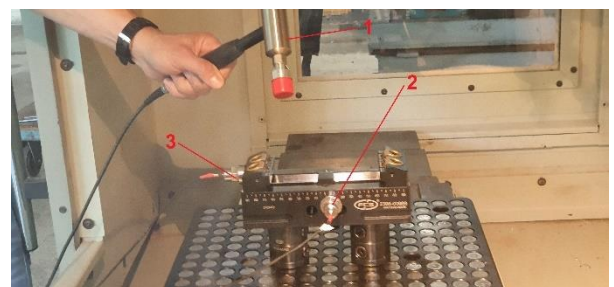


Fig. 5. Measuring components: 1-Impact hammer, 2 -X

### 2.1 Data acquisition

The measurements were made for two scenarios:

1. For the system mounted on machine table without stock (fig.5) and open jaw.
2. For the system mounted with stock clamped as follow: vice jaw tightened with 20 Nm torque (from 40Nm maximum) and glows tightened with 10 Nm torque (from 15 Nm maximum) (fig.6)

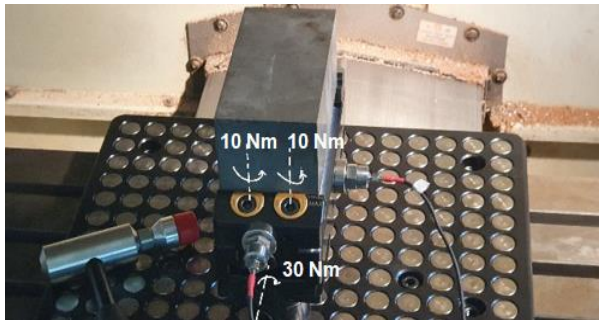


Fig. 6. Double clamping torque on the vice

The measurements were made for two direction in XY machining plane. For this study the measurements from X direction were used.

The measurements from the device without stock were used for filtering the signal in the case of stock mounted.

Figure 7 shows the waveform for the data measured at impact on the X-axis direction for the stockless system.

Figure 8 shows the data acquisition for the system with sock mounted

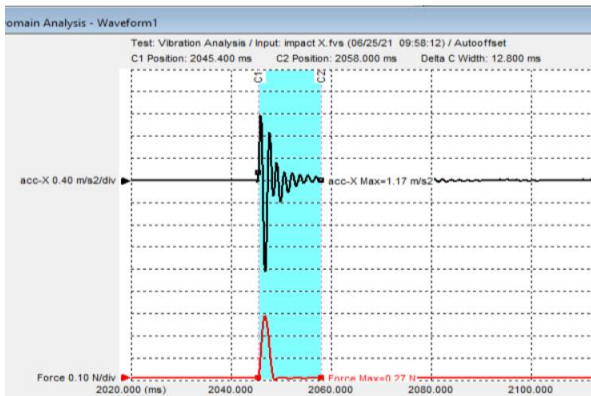


Fig. 7. Waveform data for sockless system.

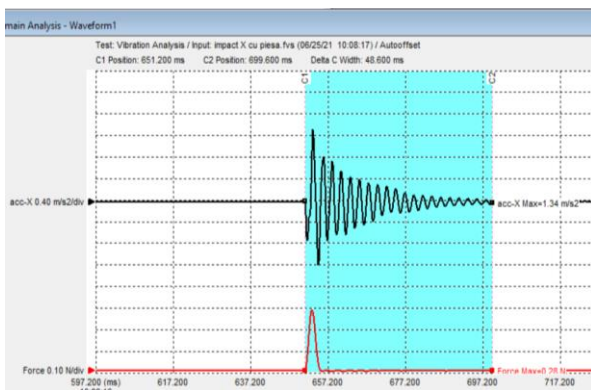


Fig. 8. Waveform data for system with stock mounted.

To obtain the frequency spectrum, the Fast Fourier transform or FFT is applied. In order to obtain the highest possible accuracy, a specific filter -pass band- is applied on the waveform signal.

For the system without stock (fig.9) it is observed that in the frequency spectrum there is a low frequency of 64Hz, but which is attributed to the fact that the part clamping system is open. Thus, the stiffness of the whole assembly is reduced.

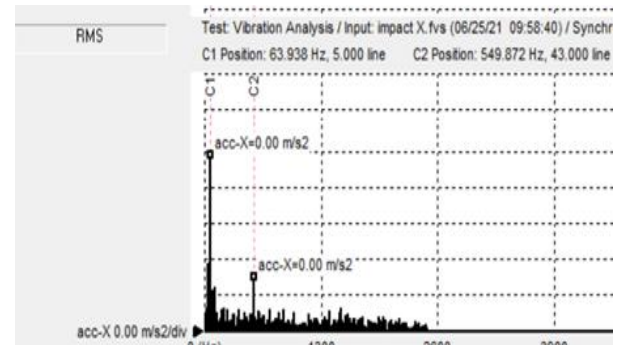


Fig.9 Frequency spectrum for stockless assembly

The purpose of this determination is to perform a comparison but also to validate the testing procedure. At the same time, the existence of high frequencies can be identified.

In the case of the stock mounted assembly by applying the Fourier transform, the frequency spectrum is obtained for the machining configuration(fig.10).

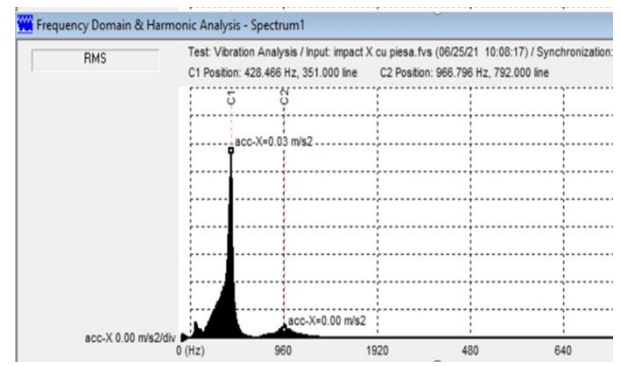


Fig. 10. Frequency spectrum for stock mounted assembly

It is observed from the analysis of the frequency spectrum, the existence of 428Hz high frequency components, which represents a high stiffness of the assembly (stock+clamping device).

### 2.2 Stiffness calculus

Based on the measurements, it was possible to determine the stiffness of the system related to the X direction.

$$\omega = 2 \cdot \pi \cdot f \quad (1)$$

$$Kx = \frac{Fx}{x} \quad (2)$$

Where  $f$  (Hz) is the frequency,  $\omega$  (rad/sec) is the angular speed,  $Kx$  is the stiffness parameter (N/m) on x direction,  $Fx$  is the impact force on x direction (N) and

$x$  is the displacement ( $m$ ).

High stiffness has been obtained as part of the range of stiffness that is attributed to machine tools with high stability [12, 13].

$$K_x = 6.5 \cdot 10^8 \text{ N/m} \quad (4)$$

This stiffness is obtained due to the superior quality of clamping systems, due to high quality materials, geometry design and clamping torque control.

### 3. FINAL REMARKS

Following these determinations, it is possible to precisely know the level of stiffness (which must correspond to the ISO standards) necessary to optimize the processing parameters and to know the state of fixing the part.

To obtain optimal conditions of use, the tightening of the part in the device must be done with the controlled torque, respectively with the torque wrench.

The research will continue with new sets of measurements and determinations in dynamic regime, during the machining, aiming to obtain dynamic stiffness.

At the same time a comparative study between a conventional clamping device and a modular clamping device will be performed in order to determine the static and dynamic stiffness.

The industry 4.0 demands must apply to all components involved in a industrial process. For metal cutting machining all elements must be defined with high accuracy from geometry and technology point of view.

For clamping system, one of the most important components of high-quality machining process, the solution is standardization of geometries and clamping torque starting from design phases. FCS company comes with solution in this way.

### 4. REFERENCES

- [1] Marinescu I., Ispas C., Boboc D. – Handbook of Machine Tool Analysis, United States of America, ISBN 0-8247-0704-4, 002, 2002
- [2] Modeling of the Pc MILL100 machine tool and milling process using DELMIA V5R17, Anania, F.D., Zapciu M., Mohora C., DAAAM ISSN 1726-9679, ISI proceedings, <http://worldses.org/indexes/>
- [3] The future of manufacturing in the era of INDUSTRY 4.0. <https://support.fcssystem.com/content/38/download?download=false>
- [4] Anania D. Research concerning the dynamics of high speed manufacturing systems – doctorate thesis, university Politehnica of Bucharest, 2006, Romania.
- [5] Savković, B., Rodić, D.: Paper title in italic, Proceedings title, pp. 25-27, place of the Conference, Publisher, City, Date.
- [6] L.N. López de Lacalle, A. Lamikiz, J.A. Sánchez, M.A. Salgado, Effects of tool deflection in the high speed milling of inclined surfaces, International

Journal of Advanced Manufacturing Technology (2004) (On-line first published, DOI 10.1007/s00170-003-1723-x)

- [7] Yu K (2019) Robust fixture design of compliant assembly process based on a support vector regression model. Int J Adv Manuf Technol 103:111–126
- [8] Fei J, Lin B, Xiao J (2018) Investigation of moving fixture on deformation suppression during milling process of thin-walled structures. J Manuf Process 32:403–411
- [9] Dong ZH, Jiao L, Wang XB, Liang ZQ, Liu ZB, Yi J (2016) FEA-based prediction of machined surface errors for dynamic fixture-workpiece system during milling process. Int J Adv Manuf Technol 85(1–4):299–315
- [10] Wang, M. Y. , and Liu, Y. H. , 2003, “Force Passivity in Fixturing and Grasping,” Proceedings of IEEE International Conference on Robotics and Automation, Taipei, Taiwan, September 14–19, pp. 2236–2241.
- [11] Dessi, C., G. D. Tsibidis, D. Vlassopoulos, M. De Corato, M. Trofa, G. D'Avino, P. L. Maffettone, and S. Coppola, “Analysis of dynamic mechanical response in torsion,” J. Rheol. 60, 275–287 (2016).
- [12] C.F. Bisu, J-Y Knevez, P. Darnis, R. Laheurte, A. Gerard, “New method to characterize a machining system: application in turning”, International Journal of Material Forming, Springer, Vol.2, No. 2, June 2009, pages 93-105
- [13] Majda Pawel, Jastrzebska Joanna, “Measurement uncertainty of generalized stiffness of machine tools”, Measurement, Vol.170, 2021

**Authors:** Asoci. Prof. Anania Florea Dorel, Asoc. Prof. Bisu Claudiu Florinel, University Politehnica from Bucharest, Faculty of Industrial Engineering and Robotics, Department of Robots and Manufacturing Systems, Spl. Independentei nr.313, Bucharest, Romania, tel: +40 21 402 9420.

E-mail: [dorel.anania@upb.ro](mailto:dorel.anania@upb.ro) ; [Claudiu\\_bisu@upb.ro](mailto:Claudiu_bisu@upb.ro),

**Full Prof. But Adrian**, University Politehnica of Timisoara, Faculty of Mechanical engineer, Piața Victoriei 2, Timișoara 300006, Romania, tel 0256 403 000

E-mail: [adi.but@gmail.com](mailto:adi.but@gmail.com)

**Phd. Canarache Marian Radu**, INICAD Design Srl, str Popa tatu no 20. Bucharest Romania,

E-mail: [radu.canarache@inicad.ro](mailto:radu.canarache@inicad.ro)





Section D:  
**PROCESS PLANNING,  
OPTIMIZATION, LOGISTICS AND  
INTERNET TECHNOLOGIES IN  
PRODUCTION ENGINEERING**



Majstorović, V., Stojadinović, S.

**RELATIONS BETWEEN ERP AND INDUSTRY 4.0 MODEL**

**Abstract:** Industry 4.0 is new model of manufacturing systems automation, based on the concept of cyber-physical system (CPS), integrated with information and communication technologies that have been applied in advanced way (cloud computing, big data analytics and AI), and based on distributed control. This approach has becoming more flexible, responsive to customer demands, and product quality is without defects. On the other hand, planning and control manufacturing in this model must have a specific concept that defines it. Also, model (ERP) has its own development, and the subject of this paper is the analysis and synthesis of the follow two models: Industry 4.0 (I4.0) and enterprise resource planning (ERP). The paper also provides a research model for the ERP model in SMEs developing the Industry 4.0 concept.

**Key words:** ERP, Industry 4.0, SME

**1. INTRODUCTION FACTS AND FIGURES**

Production Management refers to the application of management principles to the production function in a factory - involves application of planning, organizing, directing and controlling the production process.

Digitized and networked technology systems, with Internet of Things as per Industry 4.0 concept, have the ability to assign production control tasks to "intelligent" objects: machines, products and parts [1]. In this way, greater flexibility and adaptability of the manufacturing system itself, through the ERP model, is achieved. This approach defines new paradigms of production planning and control, which is based on a hybrid model of transition at centralized to a decentralized management concept. On the other hand, the optimization of ERP parameters is performed at a centralized (supply chain) and / or distributed (part) control level, which means that decisions regarding production planning and control are made globally or locally, according to Kanban (pull) or holon model.

Data became the key elements in planning, control and executing all activities along supply chain in I4.0 model. For these reasons, an organization must carefully treat and properly use all data to create an effective basis for decision making [2]. The main challenge is innovative data management on the Industry 4.0 platform, which includes storage, exchange and use of data. The development and implementation of such concepts must be stimulated because only data that is error-free, up-to-date, accessible and usable can contribute to the success of the company [2].

The Industry 4.0 model allows us to build a smart factory in four dimensions [3-5]: (i) smart manufacturing based on advanced digital-oriented technologies (additive manufacturing, cloud computing and Internet of things). It has automated flexible lines

that adapt production processes with changed conditions to the type of product, while sometime maintaining high quality, high productivity and flexibility, as well as production volume, with optimal consumption of resources; (ii) smart products (advanced production mode and new characteristics). They generate and send to the manufacturer exploitation feedback information, which is used primarily in the field of customer service. On this way increases the value added of the product, and the manufacturer develops a new business model (product + service); (iii) new ways workers perform their activities, based on advanced digital-oriented technologies (smart working), and (iv) smart supply-chain (procurement of raw materials and de-livery of finished products). Bidirectional exchange of information in collaborative production, using it exchange also for digital platforms of design of the innovative products, figures 2 [3].

This framework of a smart factory is also based on four dimensions of basic technologies for Industry 4.0: (i) cloud manufacturing, (ii) internet of things for manufacturing, (iii) big data (for manufacturing), and (iv) analytics (for manufacturing).

Based on our analyses, relate to the ERP model, the dashed line marks elements of both structures. On the other hand, the smart supply chain in the I4.0 concept has a special function - to create added value for the customer, which gives them digital platforms for planning and designing of product and production, procurement and sales, creating a management framework product over the life of the product. This creates a new business model for the organization in the circular economy - eco sustainable smart production [6,7]. In this concept, the ERP model is a key element of the vertical integration model, but is also whole part of the smart chains and core technologies of Industry 4.0, as it shown in Figure 2.

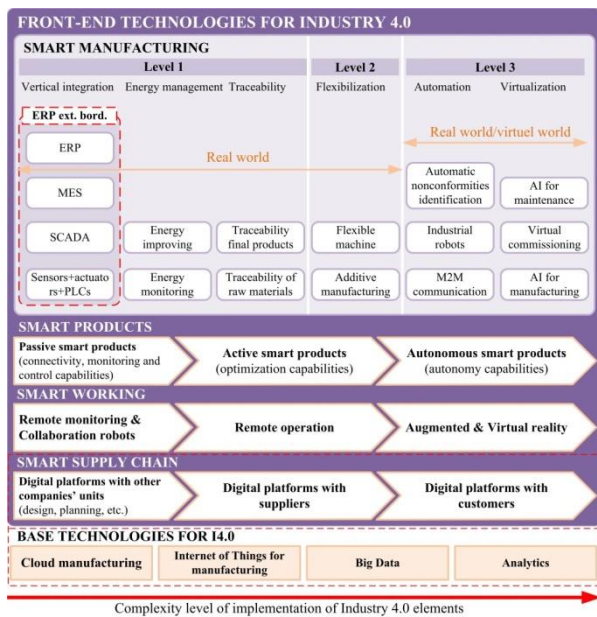


Fig. 2. Framework for Industry 4.0 model (adopted according [3]).

There are three integration concepts in the Industry 4.0 model that apply [8,9]: (i) vertical integration (from process - sensor, to organization (corporate planning) - ERP). The center of integration at this level is the cyber-physical system (CPS), which production is realized; (ii) horizontal - from request for offer to delivery note of finished product (marketing, designing, production, delivery). Integration center is an intelligent product, with added value; and (iii) supply chains and sustainable production with a customer relationship management (CRM) integration center. Thus the organization builds a new business model of its Industry 4.0 concept, the center of which is a large database and its reporting, where the ERP model plays a key role in this.

### 3. RESEARCH AND DEVELOPMENT OF ERP MODEL FOR SMES IN INDUSTRY 4.0 CONTEXT

The Industry 4.0 model currently has forty five elements that make up its full structure applicable in large organizations. Our research shows that this model for SMEs should have between fourteen and twenty two elements depending on the type of production that the SME is engaged. But one of the basic elements without this model cannot be applied is modelling - the virtual part.

Modelling is one of the most important elements of the I4.0 model, especially for the digital twin. This aspect is particularly expressive in the smart manufacturing model, where knowledge modelling is the most important element. In the digital era, the management of technological systems including their elements, encountered in the following forms [10-12]: (i) centralized hierarchical model, where we have an integrated computer system of production and management; (ii) distributed hierarchical model, which builds the symbiosis of the two models (computer-aided manufacturing and management) on the

principles of biologically inspired models; (iii) CPS based distributed control [13], and (iv) IoT based distributed control [14,15]. The last two models are important for our research, and they are realized in the I4.0 concepts through the models: agent based, multi-agent based and holonic based, type of control.

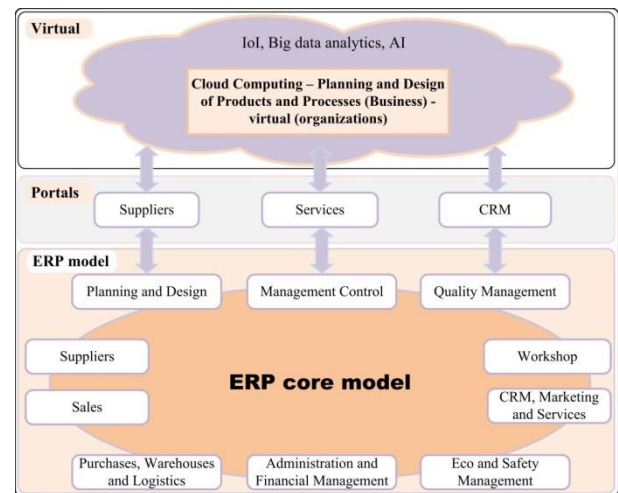


Fig. 3. ERP Industry 4.0 model (adopted according [16])

The ERP model in these concepts builds as an innovative model on new paradigms, such as collaborative control, product-driven agents, IoT and agents, makes the infrastructure of the model itself. The ERP model for smart factories is used to manage all business and technology processes in real time across the whole supply chain, based on a fast and flexible response to its customers' requirements. For the first time the Industry 4.0 model allows us do this, and the ERP model permeates the infrastructure of the entire model shown on Figure 3 [17].

The model has three parts: (i) virtual whole, which is based on the cloud computing (SaaS) model. It contains a virtual model of an ERP system, linked through IoT all business (procurement, sales, management, finance), production (workshop) and technological (designing) processes, with large databases that are generating. Their analysis, optimization and decision making are perform using AI and machine learning techniques; (ii) interfaces (suppliers, services and CRM). Their function is to provide to user the on-line user necessary information related to procurement, sales and other services (for example maintenance) that help us track the dynamics of smart manufacturing, and (iii) core model, which includes the business-technological and managerial functions of the organization as well as the production itself, a total of ten units.

In the smart factory model, the following functions are realized using an intelligent ERP system [16-20]: (i) management of customer requirements. Real time creating the information content of request or offer using: Electronic Data Interchange (EDI) tools, web portals, forecasts and customer MRPs. Also managing the "Master Production Schedule" (MPS), with open orders and framework agreements, the procurement

activities can be scheduled (purchases and production of finished or semi-finished goods); (ii) production planning (MRP 1). The model calculates the needed quantities of raw materials to be procured for the accepted requirements from the previous point, taking into account: accepted offers, existing stock, quantities reserved for production orders in progress and sales plans; (iii) manufacturing scheduling (MRP 2). Production resource planning for MRP 1 orders, taking into account: machines capacity, labor force, maintenance plans, delivery times. Technology documentation (machining operations, tools and controls plans) are elements of this module; (iv) management production (Manufacturing Execution System – MES). Monitoring and managing the complete work order at all stages of production, both at the manufacturing plant and at the subcontractors, including planned maintenance orders; (v) integration and communication between technical departments and customers. This is related for connecting and integrating about a product (in the factory) – PDM (Product Data Management) and product (along lifecycle) – PLM (Product Lifecycle Management), for all stages of product planning and designing (bills of products) from all aspects of defining and reconsidering; (vi) Quality Management System (QMS), EMS and OH&S. These models manage quality information (quality management and traceability), ecology and health protection; (vii) management warehouses and stock, logistics management. All changes to the storage are monitored online via bar code or RFID, and the ERP model takes care about required / planned quantities. Likewise, internal transport as well as all shipments of finished products, are monitored in the same way, and (viii) administration and financial management. Production accounting management to determined all costs and productivity parameters, by different areas and bases.

In Serbia, intensive work is being done to develop and implement ERP models for SMEs (Majstorovic et al. 2019), through the national Platform for Industry 4.0 [20], Figure 4. On the smart workshop where real production takes place as the creating point of manufacturing data. Virtual shop floor of a physical one using agent technology, where each agent has: identification, authorization, configuration, capability, operation and status data, and transmits them and their metadata. Data warehouse is an information hub that stores and exchanges manufacturing data. Data analytics center is the model creation, storage, retrieval and uncertainty which provides machine learning, statistical, or stochastic based models that build on mathematical functions needed to create data driven models. Each agent retrieves such models through a broker agent and decides predictive operations and controls, based on the results that models output. Manufacturing application include applications, such as CAD, CAM, CAQ, ERP systems. These applications communicate with the platform through their application interfaces because they eventually supervise and manage all activities and events occurring on the physical workshop. Agent manager searches adequate agents, and manages them during

their lifecycles. Data governor manages master data as well as the lifecycle and quality of raw data. Workflow manager controls workflows to automate the tasks performed on the platform, manages the rules designed to handle workflow appropriately, and engages in model representation.

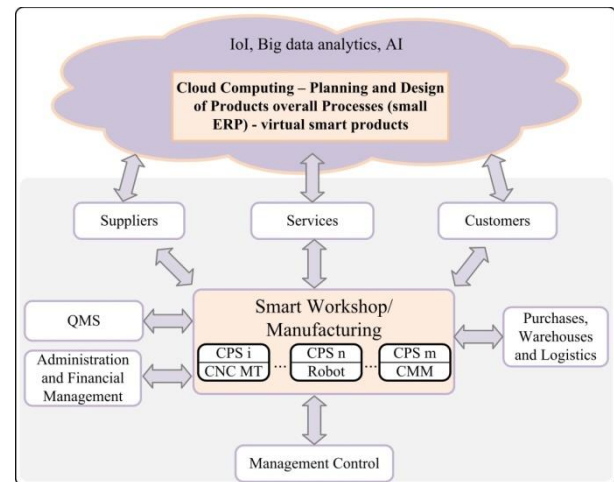


Fig. 4. Framework of a smart manufacturing system for Industry 4.0 in SMEs.

Security controller protects against computer viruses and hacking, and controls electronic authorization and authentication, because data and models that incorporate manufacturing experience and knowledge are valuable and, thus, must be protected. For SMEs, the integral model of smart manufacturing and ERP is researched and defined, based on the base elements of Industry 4.0: Cyber physical systems (CPS), M2M – Man-machine communication / MMI – Man-machine interaction, Operation management for I4.0, Digital Twins, Horizontal & Vertical Integration, Using Light Signals, Smart / Mobile Maintenance, Condition Monitoring, VR - Virtual Reality, QR Code, Data Security, Open Communication Protocols (OPC-UA), IoT - Internet of Things (IIoT - Industrial Internet of Things) ), Real-Time Communication, Big Data, Cloud, Automation Pyramid, Resource Planning (ERP), Work Order Management (MES), Supplier Relationships, Intelligent Logistics, Customer Relationships, WWW [21,22]. The SMEs for which this project is implemented are from the field of metal industry and produce parts, subassemblies and assemblies for factories from Italy, Switzerland, Austria, Germany and the Netherlands.

#### 4. CONCLUSIONS

The concept of Industry 4.0 has a special place and role for the design engineer and production planner, which is still irreplaceable, but now has a different role, namely a new paradigm. It is particularly reflected in the construction and management of the digital twin model of the smart factory, and thus of the ERP module. In [21,22], this approach is explored in detail, and a five-level model of the pyramid of the industrial internet is proposed: (i) smart object (physical objects and embedded intelligence), (ii) industrial internet of

things (level 1 and network, (iii) cyber-physical production system (level 2 and integration previous levels), (iv) service-oriented digital twin (ubiquitous knowledge and level 3), and (v) smart factory (manufacturing employees and level 4). From an ERP perspective, the specificities of executives monitoring CPSs, facility managers and engineer resource planners are specifically referenced and used here, as outlined in Levels 4 and 5. One of the future directions of ERP development is the open source model.

Research on the project [20] in the forthcoming period will focus on the development of demonstration models for individual I4.0 segments for SMEs (designing - digital twin, procurement, customers, MES, etc.).

## 5. REFERENCES

- [1] Bendul, J., Blunck, H.: (2019) *The design space of production planning and control for Industry 4.0*, Computers in Industry, 105, 260-272.
- [2] Hochmuth, A. C., Bartodziej, C., Schwägler, C.: (2017) *Industry 4.0 Is your ERP system ready for the digital era?* ([https://www2.deloitte.com/content/dam/Deloitte/de/Documents/technology/Deloitte\\_ERP\\_Industrie-4-0\\_Whitepaper.pdf](https://www2.deloitte.com/content/dam/Deloitte/de/Documents/technology/Deloitte_ERP_Industrie-4-0_Whitepaper.pdf) – Accessed of Feb. 2020).
- [3] Frank, A., Dalenogare, L., Ayala, N.: (2019) *Industry 4.0 technologies: Implementation patterns in manufacturing*, International Journal of Production Economics, 210, 15–26.
- [4] Emmanouilidis, C., Pistofidis, P., Bertonecelj, L., Katsouros, V., Fournaris, A., Koulamas, C., Ruiz-Carcel, C.: (2019) *Enabling the human in the loop: Linked data and knowledge in industrial cyber-physical systems*, Annual Reviews in Control, 47, 249–265.
- [5] Dassisti, M., Giovannini, A., Merla, P., Chimienti, M., Panetto, H.: (2019) *An approach to support Industry 4.0 adoption in SMEs using a core-metamodel*, Annual Reviews in Control, 47, 266–274.
- [6] Fallera, C., Feldmüllera, D.: (2015) *Industry 4.0 Learning Factory for regional SMEs*, Procedia CIRP, 32, 88 – 91.
- [7] Erola, S., Sihna, W.: (2017) *Intelligent production planning and control in the cloud – towards a scalable software architecture*, Procedia CIRP, 62, 571 – 576.
- [8] Xua, D. L., Xu, L. E., Lia, L.: (2018) *Industry 4.0: state of the art and future trends*, International Journal of Production Research, 56 (8) 2941–2962.
- [9] Ivanov, D., Sethi, S., Dolgui, A., Sokolov, B.: (2018) *A survey on control theory applications to operational systems, supply chain management, and Industry 4.0*, Annual Reviews in Control, 46, 134–147.
- [10] Morel, G., Pereira, E. C., Nof, Y. S.: (2019) *Historical survey and emerging challenges of manufacturing automation modeling and control: A systems architecting perspective*, Annual Reviews in Control, 47, 21–34.
- [11] Zuehlke, D.: (2010) *Smart Factory - Towards a factory-of-things*, Annual Reviews in Control, 34, 129–138.
- [12] Industry 4.0 – Opportunities and Challenges of the Industrial Internet, 2019. (<https://www.pwc.nl/en/assets/documents/pwc-industrie-4-0.pdf>, - Accessed of March 2020).
- [13] Rodič, B.: (2017) *Industry 4.0 and the new simulation modelling paradigm*, Organizacija, 50 (3), 193–207.
- [14] Lim, K.Y.H., Zheng, P., Chen, C.: (2020) *A state-of-the-art survey of Digital Twin: techniques, engineering product lifecycle management and business innovation perspectives*, J Intell Manuf., 31, 1313–1337.
- [15] Barber, P.: *Industry 4.0 and the Digital Factory*, <https://www.weforum.org/agenda/2019/07/factories-lead-fourth-industrial-revolution-automation-jobs/> (Accessed of March 2020).
- [16] Panetto, P., Iung, B., Ivanov, D., Weichhart, G., Wang, X.: (2019) *Challenges for the cyber-physical manufacturing enterprises of the future*, Annual Reviews in Control, 47, 200–213.
- [17] ERP and Industry 4.0, <https://www.centrossoftware.com/en/erp-and-industry-4.0>, Accessed of March 2020).
- [18] Ahmad, M., Cuenca, R.: (2013) *Critical success factors for ERP implementation in SMEs*, Robotics and Computer-Integrated Manufacturing, 29, 104–111.
- [19] Usuga, C.J.P., Lamouri, S., Grabot, B. et al.: (2020) *Machine learning applied in production planning and control: a state-of-the-art in the era of industry 4.0*, J Intell Manuf, 31,1531–1558.
- [20] Majstorovic, V, et al.: *I4.0 for SMEs*, Project, Faculty of Mechanical Engineering, Belgrade, 2019.
- [21] Olson, D., Johansson, B., Carvalho, R.: (2018) *Open source ERP business model framework*, Robotics and Computer-Integrated Manufacturing, 50, 30–36.
- [22] Longo, F., Nicoletti, L., Padovano, A.: (2019) *Ubiquitous knowledge empowers the Smart Factory: The impacts of a Service-oriented Digital Twin on enterprises' performance*, Annual Reviews in Control, 47, 2019, 221-236.

**Authors: Full Prof. Vidosav D. Majstorović, Assist. Prof. Slavenko M. Stojadinović,**  
 University of Belgrade, Faculty of Mechanical Engineering, Department of Production Engineering, Kraljice Marije 16, 11120 Beograd 35, Serbia, Phone.: +381 11 3370-341, Fax: +381 11 3370-364.  
 E-mail: [vidosav.majstorovic@sbb.rs](mailto:vidosav.majstorovic@sbb.rs);  
[sstojadinovic@mas.bg.ac.rs](mailto:sstojadinovic@mas.bg.ac.rs)

Tomov, M., Velkoska, C.

## ANALYSIS AND TRENDS OF THE CHANGES IN THE GRAPHIC INTERPRETATION OF THE QUALITY COSTS MODELS

**Abstract:** This paper presents four approaches to the graphic interpretation of the quality costs structure definition models: classical, modern, modified, and visionary approach. These give rise to theoretical graphic quality costs models and illustrate the relationship between the quality costs categories, as well as the relationship between the quality costs categories and the total quality costs and the quality level. The paper comparatively analyzes the underlying assumptions, existing knowledge, and principles characteristic of each approach. This contributes to the shaping of the quality costs categories curves and the overall quality cost curve in the theoretical models. The conducted analysis in the paper will enable forecasting the trend of development of theoretical graphic models and identification of potential stakeholders that contribute to changes in the structure and the behavior of the quality costs categories, and thus the behavior of the overall quality costs.

**Key words:** quality costs, PAF model, trade-off model, graphic models

### 1. INTRODUCTION

The quality costs, viewed through the prism of the added value of quality represent a key indicator to measuring the performance of the company work processes and activities [1], especially having in mind that they represent 5-25% of the sales revenues [2]. However, since the quality costs category model element's structure depends on the nature of the company, its size, the type of product, the requirements of the users, the quality maturity, the objectives [3], this contributes to the development of different approaches to understanding quality costs.

In general, the quality costs entail the sum of all costs that would disappear if we do not have any quality issues (Joseph M. Juran, 1974) [4]. In practice, the quality costs quantify the overall efforts related to the achievement and maintenance of quality compliance and repair of quality noncompliance [5]. In this regard, Armand V. Feigenbaum (1956) presented the traditional four faceted structure of the quality cost – PAF model (prevention activities costs, appraisal activities costs, internal and external failure costs) [6]. However, a dichotomous structure is also frequently applied – categorization of quality compliance costs (prevention costs and appraisal costs) and quality noncompliance costs (internal and external failures costs) [6].

The literature presents a descriptive interpretation of the quality costs models, which describes the categories in the models [7], a graphical interpretation which explains the interdependence between the quality costs categories, as well as the relationship between the categories and quality levels (including the total quality costs) [8], and a mathematical interpretation, representing mathematical expressions for calculating of the quality costs elements, categories, and total quality costs [9].

This paper aims to analyze the changes that occur in the graphical interpretation models of the quality costs and to anticipate their trends in the future.

### 2. GRAPHICAL INTERPRETATION OF THE QUALITY COSTS MODELS

Theoretical research suggests four approaches to the graphical interpretation of the quality costs models: classical (traditional), modern, modified, and a visionary approach which give rise to the graphical theoretic quality costs models [1, 10].

The first graphical quality cost model interpretation reflects the scientific approach of Joseph M. Juran (1951), also known as “The Economics of Quality”. This interpretation suggests the existence of an economic quality level, where one achieves the highest quality level with lowest quality costs [1, 5]. Joseph M. Juran, Gryna F. M. and Bingham R. (1962), unify this graphic model and the already affirmed PAF categorization and present the classical (traditional) quality cost tradeoff model, which juxtapositions the prevention and appraisal costs with the failure costs, also known as Juran's classical model (figure 1.) [5, 9], a representative of the models developed in the 20<sup>th</sup> century [1]. According to this approach, as the prevention and appraisal costs increase, the failure costs decrease which leads to the point of the economic quality level (under 100% quality compliance) with lowest total quality costs [1, 2].

The presented inverse relationship represents a universally accepted principle which explains the balance between the two categories, a matter of concern in the operational management of companies [4], because it accepts less than 100% compliance, i.e. that one should invest in compliance activities until the increase of the compliance costs is less than the benefits [11]. This may be acceptable for a lower level of quality maturity in the initial stages of the quality systems program implementation.

The inverse relationship is pronounced more when one considers external failure costs as opposed to internal failure costs [1].

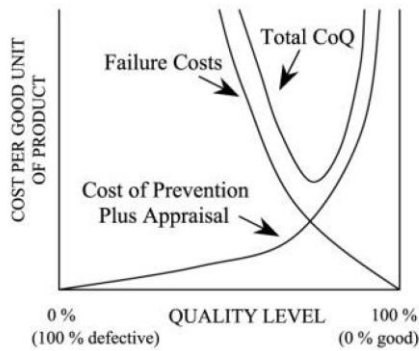


Fig. 1. Traditional COQ trade off model [5].

The assumptions about the imperfection of the prevention and appraisal activities, not considering the effects from quality improvements, as well as the effects from the increased effectiveness and efficiency controls, justify the continuous investments in prevention and appraisal in the classical approach [1].

The evolution of the classical quality cost model is marked by the model for optimal quality level developed by Lundvall, D. M. and Joseph M. Juran (1974) [12], the PAF model by Armand V. Feigenbaum (1991) [13], and the integrated profit model by Miller J. R. and Morris J. S. (2000) [8].

The research of Samir K. Srivastava (2008) presented managerial recommendations for the three quality zones from the model of Joseph M. Juran and Gryna F. M. (1988) (figure 2.) [14]. It is of particular importance, in the zone of indifference – optimal quality level, to continue the efforts to continuously improve and alleviate the investments in prevention [14].

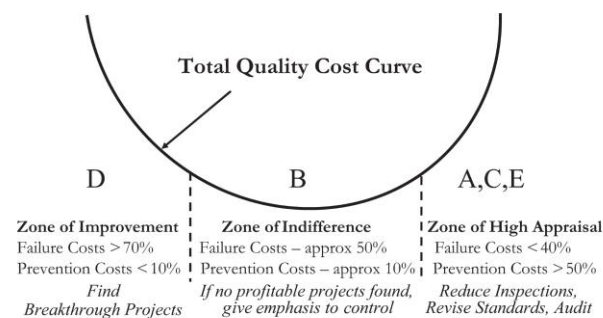


Fig. 2. Categorization of sites and recommendations [14].

The research of Plunkett J. J. and Dale B. G. (1988), Visawan D. and Tannock J. (2004), as well as Burgess T. F. (1996) showed that the classical approach features inaccuracies and fails to consider the effect of quality delivered to users, while Philip B. Crosby (1979) suggests that the approach fails to motivate the companies to commit to quality [11].

The transition from the classical to the modern approach is reflected in the quality-based learning model, developed by Fine C. H. (1986). There, due to the improved knowledge effect, the compliance cost curve bends downward, thereby reflecting a reduction in the total quality costs and an increase of the quality level [1, 15]. Lorente A. R. M., Rodriguez A. G. and Rawlins

L., (1998) published the cumulative effect of the preventive activities and concluded that continuous prevention leads to a higher level of quality and lower costs necessary to maintain the quality level [12], which makes prevention the most cost-effective category for quality spending [11].

According to the research of Ittner C. D., (1996), and Omar M. K. and Murgan S. (2014), who support the continuous improvement approach, reduction of failure costs can be achieved at low or no-subsequent increase in the conformance costs [6, 15, 16]. Moreover, according to Gemal S. Weheba and Ahmad K. Elshennawy (2004), one should distinguish between the prevention costs and quality improvement costs [16].

The robust quality standard theory of Genichi Taguchi also contributes to the understanding of the modern approach. It focuses on incorporating quality in the design phase, i.e., a robust design, a design resilient to external influences, would preclude deviations from the target quality value and “losses to society” [11, 17]. Taguchi’s Quality Loss Function measures the loss due to variability when quality deviates from a target value even if the actual value falls within the specification limits, as well to estimate the hidden quality costs [17]. Unlike the compliance-oriented quality feature of the classical approach, the presented target-oriented quality is a much more sensitive method for measuring quality [17].

The modern approach (model) originated from Arthur M. Schneiderman (1986) and Joseph M. Juran and Gryna F. M. (1988, 1993). They reviewed the classical model by assuming that the compliance costs convergence trend to infinity had an exponential trend which, at a level of 100% perfection reaches a finite value, for achieving zero failures with finite total quality costs, also known as the zero-failure approach (figure 3.) [1, 5, 7, 8, 9]. Philip B. Crosby, Plunkett J. J., Dale B. G., and Freiesleben J., also suggest that the continuous quality improvement and investments in prevention are economically justified and that the level of perfection is in the point of least total quality costs [9, 12].

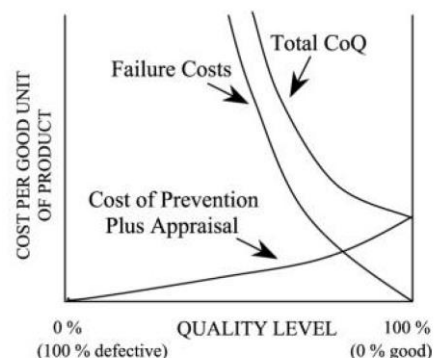


Fig. 3. Modern model of quality cost [5].

Joseph M. Juran and Gryna F. M. (1993) thought that perfection is an economic goal, but only in the long run [8].

According to Arthur M. Schneiderman (1986), this can be done only on the basis of incremental economics [9] and with sufficient investments in prevention



activities since that also leads to a reduction of the appraisal costs [7].

Freiesleben J. (2004) also suggests that the picture swift achievement of perfection is unrealistic and therefore suggests a dynamic model which illustrates the continuous quality improvement through technological progress, the lessons learned, and identifying the roots and resolving the reasons for failures, which is in line with the modern approach (figure 4.) [8]. Ittner C. D. (1996), with an empirical study, validated the revised model [15] and emphasized the need to consider the prevention costs and the appraisal costs separately which, according to Oakland J. S., (1993) is difficult to achieve [14].

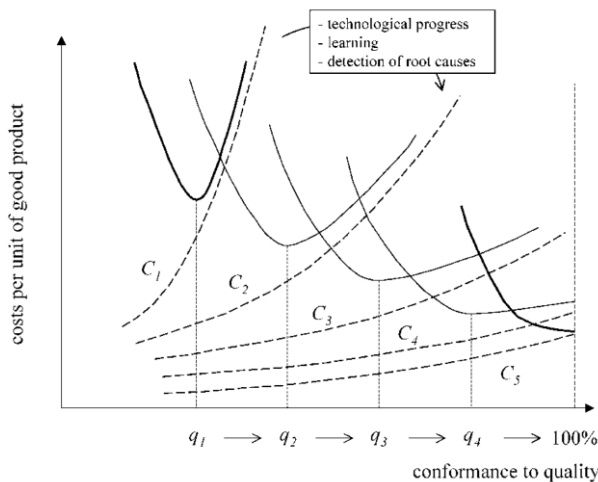


Fig. 4. Model of Freiesleben [8]  
( $C_i$  – costs of achieving good quality,  $q_i$  – quality level)

The behavior of the modern approach curves is expected with the development of automatics and robotics in the new technologies, which facilitate a reduction of human error, and automatic quality inspection and control, which leads to a less steep increase of the compliance costs curve [1]. From a practical viewpoint, modern management helps move the responsibility of quality from the quality assurance and control department to the corporate level which sets the quality objectives which, in turn, raises the overall level of quality [11].

The comparison between the classical and the modern approach, according to Burgess T. F. (1996) showed that the revised model is sustainable in the long run and the traditional model is applicable in the short term [5]. The researchers Fine C. H. (1986), Dawes E. W. (1989), Marcellus R. L. and Dada M. (1991), and Love (1995) think that the traditional model reflects a static snapshot of the quality costs, while the revised model creates a picture in a dynamic environment [5]. Other researchers, such as Porter L. J. and Rayner P. (1992), Cole R. E. (1992), Shank J. K. and Govindarajan V. (1994), explain that they represent two conflicting views on the cost-effectiveness of quality [5].

The critiques of Dale B. G. and Plunkett J. J. (1988) suggest that both approaches are considered under the assumption of a perfect quality design due to zero failures on 100% quality level, which would be expected for the costs for internal failures, but not for the costs of

external failures [16]. From a different viewpoint, both approaches create confusion and do not foster continuous improvement since they present a level of quality for which the prevention and appraisal costs exceed the failure costs [16].

Freiesleben J. (2004) disputes the compliance cost behavioral trend in the classical model because if quality has an upward trend, then we should not expect an increase of the compliance costs. Furthermore, as the level of quality increases and the preventive costs have an upward trend, then the appraisal costs should have a downward trend, because as the level of quality increases, the failures reduce [8], which is corroborated by empirical research [2]. Moreover, neither approach considers the hidden quality costs which, according to Joseph M. Juran and Gryna F. M. (1993), should also contain the sale losses, especially in the modern approach [8]. Research shows that the correlation between the prevention costs and the internal failure costs in real time is not possible and therefore it is necessary to consider the time delays when considering the trade-off relationships within quality costs [4].

The empirical research of Plewa M., Kaiser G., and Hartmann E. (2016) suggests a modification of the modern approach (figure 5) with an elaboration that there exists a highest point of the compliance costs, after which the compliance costs reduce and positively correlate with the failure costs and the total quality costs, provided that the levels of quality are equal to or greater than 90% quality compliance [2].

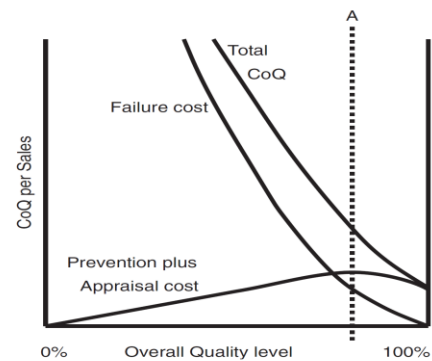


Fig.5. Modification of the modern model [2].

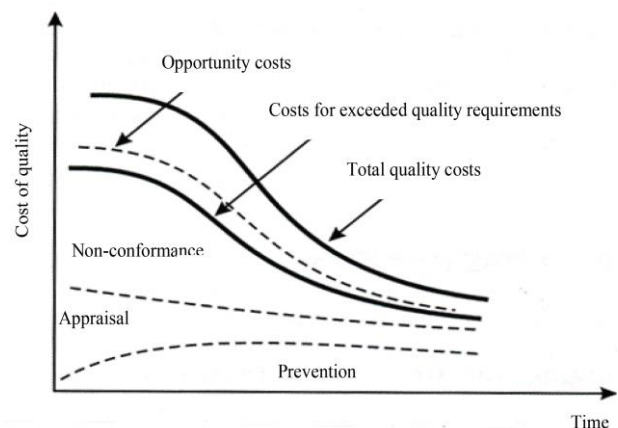


Fig.6. Visionary approach of quality cost model [10].

The visionary approach to the graphical interpretation refers to continuous organizational quality

improvement (figure 6) [10], which rests of the thesis of Philip B. Crosby (1979) that quality is free [2]. The correlation between the quality costs categories is positive. The research of Sturm S., Kaiser G., and Hartmann E. (2019) showed that higher levels of quality and lower total quality costs are noticeable in the long run and that the categories of the quality costs exhibit the same behavioral trend in the long run, and they are expected to disappear [6].

In addition, the empirical research of Glogovac M., and Filipovic J., (2018) showed that companies committed to substantively fulfilling the requirements of ISO 9001:2015, focusing on the user, corrective measures, leadership, competences, awareness, knowledge, and continuous improvement with a view to their adequacy for the quality cost system, do achieve better results [3].

### 3. CONCLUSION

The presented graphic interpretations represent a static snapshot of the current status of the quality costs categories (and the total quality costs) for a particular level of quality.

Future graphic interpretation should be expected to present the behavior of the prevention costs separately from the appraisal costs and to present their correlation with the costs of internal failures, external failures and the opportunity costs for different conditions and quality maturity phases. In addition, it is necessary to analyze and order the influence cost quality elements, which will stimulate thinking about analyzing and discovering the reasons for such influences. One should especially study the influence of the effect of enhanced knowledge and the application of the quality management tools, techniques, and methods, to the performance of the prevention activities and appraisal activities in relation to the time factor.

### 4. REFERENCES

- [1] Omurgonulsen, M.: *A research on the measurement of quality costs in the Turkish food manufacturing industry*, Total Quality Management, Vol. 20, No. 5, pp. 547-562, 2009.
- [2] Plewa, M., Kaiser G., Hartmann, E.: *Is quality still free? Empirical evidence on quality cost in modern manufacturing*, International Journal of Quality & Reliability Management, Vol. 33, No. 9, pp. 1270-1285, 2016.
- [3] Glogovac, M., Filipovic, J.: *Quality costs in practice and an analysis of the factors affecting quality cost management*, Total Quality Management, Vol. 29, No. 13, pp. 1521-1544, 2018.
- [4] Su, Q., Shi, J.-H., Lai, S.-J.: *Research on the trade-off relationship within quality costs: A case study*, Total Quality Management, Vol. 20, No. 12, pp. 1395-1405, 2009.
- [5] Schiffauerova, A., Thomson, V.: *A Review of Research on Cost of Quality Models and Best Practices*, International Journal of Quality & Reliability Management, Vol 23, No 6, pp. 647-669, 2006.
- [6] Sturm, S., Kaiser G., Hartmann, E.: *Long-run dynamics between cost of quality and quality performance*, International Journal of Quality & Reliability Management Vol. 36 No. 8, pp. 1438-1453, 2019.
- [7] Porter, L. J., Rayner, P.: *Quality costing for total quality management*, International Journal of Production Economics, Vol. 27, pp. 69-81, 1992.
- [8] Freiesleben, J.: *On the Limited Value of Cost of Quality Models*, Total Quality Management, Vol. 15, No. 7, pp. 959-969, 2004.
- [9] Castillo-Villar, K. K., Smith, N. R., Simonton, J. L.: *A model for supply chain design considering the cost of quality*, Applied Mathematical Modelling Vol. 36, pp. 5920-5935, 2012.
- [10] Szczepanska, K.: *Koszty jakosci dla inzenierow*, Wydawnictwo Placet, Warszawa, 2009.
- [11] Cheah, S.-J., Md. Shahbudin, A. S., Md. Taib, F.: *Tracking hidden quality costs in a manufacturing company: an action research*, International Journal of Quality & Reliability Management, Vol. 28, No. 4, pp. 405-425, 2011.
- [12] Lorente, A. R. M., Rodriguez, A. G., Rawlins, L.: *The cumulative effect of prevention*, International Journal of Operations & Production Management, Vo. 18, No. 8, pp. 727-739, 1998.
- [13] Holota, T., Hrubec, J., Kotus, M., Holiencinova, M., Caposova, E.: *The management of quality costs analysis model*, Serbian Journal of Management Vol. 11, No. 1, pp. 119-127, 2016.
- [14] Srivastava, C. K.: *Towards estimating Cost of Quality in supply chains*, Total Quality Management, Vol. 19, No. 3, pp. 193-208, 2008.
- [15] Ittner, C. D.: *Exploratory Evidence on the Behavior of Quality Costs*, Operations Research, Vol. 44, No. 1, pp. 114-130, 1996.
- [16] Weheba, G. S., Elshennawy, A. K.: *A revised model for the cost of quality*, International Journal of Quality & Reliability Management, Vol. 21, No. 3, pp. 291-308, 2004.
- [17] Albright, T. L., Roth, H. P.: *The Measurement of Quality Costs: An Alternative Paradigm*, Accounting Horizons, pp.15-27, June 1992.

**Authors: Assoc. Prof. Dr. sc. Mite Tomov**, Ss. Cyril and Methodius" University in Skopje, Faculty of Mechanical Engineering, 1000 Skopje, North Macedonia. Phone: +389 02 30 99 298; E-mail: [mite.tomov@mf.edu.mk](mailto:mite.tomov@mf.edu.mk)  
**Assist. Prof. Dr. sc. Cvetanka Velkoska**, International Vision University in Gostivar, Faculty of Engineering and Architecture, 1230, Gostivar, North Macedonia, Phone: +389 42 222 325. E-mail: [cvetanka.velkoska@vizyon.edu.mk](mailto:cvetanka.velkoska@vizyon.edu.mk)

Nedeljković, D., Jakovljević, Ž.

## IMPLEMENTATION OF CNN BASED ALGORITHM FOR CYBER-ATTACKS DETECTION ON A REAL-WORLD CONTROL SYSTEM

**Abstract:** The emergence of the Industry 4.0 concept leads to crucial changes in manufacturing by building advanced industrial systems and applications based on Cyber-Physical Systems (CPS), as the core of this approach. Using CPS, manufacturing assets are designed in the form of systems of systems through interconnection of smart devices with integrated computation and communication capabilities. System control logic is distributed over a large number of resources, and its performance is achieved through their coordinated work and ubiquitous communication raising the issue of cyber-attacks by malicious adversaries. Since cybersecurity within industrial control systems is safety related, it is necessary to timely detect cyber-attacks on industrial assets; for these purposes a number of different approaches have been developed. As a technique of choice, deep learning (DL) based methods emerge, providing good online performances. In this work, we focus on the implementation of a DL based cyber-attack detection algorithm on an electro-pneumatic positioning system containing smart sensor and smart actuator. In particular, we employ cyber-attack detection procedure based on 1D Convolutional Neural Network (CNN) at the local controller of the smart actuator. The implemented algorithm can successfully detect cyber-attacks in real-time, as will be experimentally demonstrated.

**Keywords:** Industrial Control Systems, Cyber-Physical Systems, Convolutional Neural Network, Cybersecurity

### 1. INTRODUCTION

Cyber-Physical Systems (CPS) become the core components of the Industrial Control Systems (ICS) not only at manufacturing shop floors, but also in power systems, water treatment plants, and other critical infrastructures [1]. CPS based smart devices (sensors, actuators...) integrate computational and communication capabilities into physical processes and enable distribution of control tasks, where the control system is realized through their intensive communication and interoperability. In this way Industrial Internet of Things (IIoT) is introduced, and consequently smart devices are often connected to the internet, instead of communication only within the industrial plant [2]. Widespread communication opens up various security related concerns such as the occurrence of malicious cyber-attacks that can compromise system operation or even endanger human life. Creating an intrusion detection method that provides ICS operation in a safe manner is a challenging task. Due to the inherent differences in IT systems and ICS, traditional IT detection mechanisms cannot successfully handle all security issues of ICS. For instance, noisy behavior of a physical process can result in a high rate of false positive and/or low rate of true positive attack detections [3].

A basic control loop of ICS employs SCADA (Supervisory Control and Data Acquisition) systems, controllers (PLCs, microcontrollers), sensors, and actuators to manage some physical process (Fig. 1). The controller interprets the sensor measurements  $x_i$ , and based on the control task transmits the commands  $y_i$  to the actuator. The actuator executes corresponding action and closes the control loop.

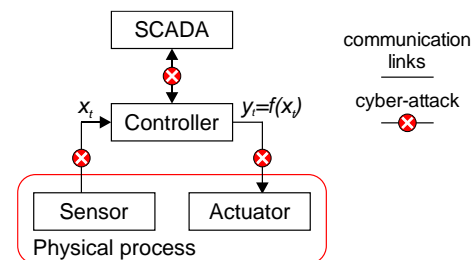


Fig. 1. Simplified scheme of ICS

Communication links sensor/controller and controller/actuator represent vulnerable points for cyber-attacks by different adversaries. To reach the desired goal, attackers maliciously modify the sensor output and/or actuator input signal through communication channels.

For the design of Intrusion Detection Systems (IDS) within ICS, data centric approaches are most frequently employed. Within these approaches, the behavior of the system in normal operation (without attacks) is modeled based on the data acquired from the system operating in isolated conditions. Once the model is generated, it is integrated in ICS on the receiving side and the attacks on the communication links that alter transmitted data are detected based on the discrepancy between modeled and received signal values. The model in normal operation can be created using different techniques such as dynamic neural network combined with integral sliding-mode attack compensator [4], support vector machines [5], recurrent neural networks [6], multi-layer perceptron [7], timed automata [8], Convolutional Neural Networks (CNN) [9].

In this paper we present a procedure and results of the implementation of a cyber-attack detection algorithm on ICS. In particular, we show how CNN

based algorithm for intrusion detection can be applied on a low level controller of CPS as a part of the electro-pneumatic positioning system. We chose 1D CNN as a suitable technique for IDS design due to its relatively simple configuration and real-time applicability.

The rest of the paper is organized as follows. In Section 2, electro-pneumatic positioning system is briefly described. Section 3 presents the developed 1D CNN based cyber-attack detection algorithm. The implementation of the algorithm on a real-world installation is presented in Section 4. Finally, conclusions and future work guidelines are provided in Section 5.

## 2. ELECTRO-PNEUMATIC POSITIONING SYSTEM

Electro-pneumatic positioning system DisEPP that we will consider in this paper consists of two CPS (Fig. 2): 1) a smart actuator (pneumatic cylinder controlled by electro-pneumatic air pressure regulator on one, and mechanically controlled air pressure regulator on the other side that enable the desired motion of the cylinder) augmented with local controller LC1 and 2) smart sensor (magnetic linear encoder placed along cylinder) augmented with LC2. Both LCs are based on ARM Cortex-M3 running at 96 MHz [10], extended with IEEE 802.15.4-compliant wireless transceiver Microchip MRF24J40MA [11]. The control task is distributed between LC1 and LC2, where LC1 has the desired trajectory at input and implements PID controller to compute the required motion of the cylinder based on the sensory signal. The information regarding desired motion is transferred to LC2 using IEEE 802.15.4 protocol, and this communication link represents a vulnerable point for cyber-attacks by different adversaries. The details regarding this system can be found in [12].

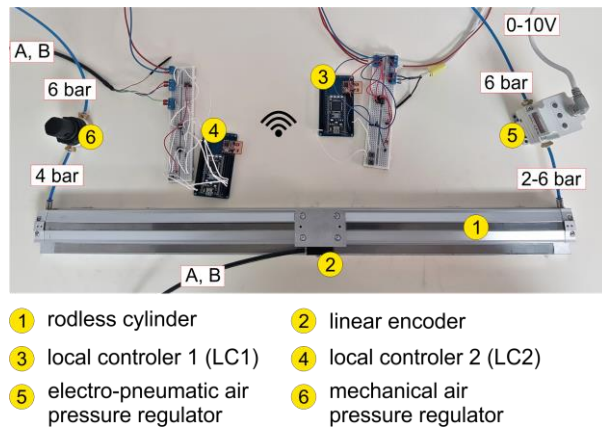


Fig. 2. Experimental setup of DisEPP

## 3. CYBER-ATTACKS DETECTION ALGORITHM

Our 1D CNN based IDS employs auto-regression, where the prediction of the current signal value  $x_i$  is obtained taking into account the buffer of previous  $z$  values  $x_{i-z}, \dots, x_{i-1}$ ; in particular we use the buffer size of  $z=16$ . For model generation, the transmitted signal

between LC1 and LC2 during normal operation was recorded using piston trajectory with positions of 50, 400, 250, 400, and 100 mm that was cyclically repeated. A total of 406,230 records were acquired. To mitigate the negative effects of abrupt changes in the signal, it is filtered using low-pass FIR filter. The whole dataset is divided into training, validation, and test part, with a ratio of 80/10/10%.

A number of different 1D CNN architectures for auto-regression were explored and the architecture consisting of nine layers presented in Figure 3 was chosen as appropriate. Network starts with two blocks containing two convolution layers, followed by a max pooling layer. The output from the max pooling layer is unrolled by flattening layer, which is connected with a dense layer. The final result is generated through the second dense layer at the end of the network. The number of filters in convolution layers is 8-16-16-32, where the filter size  $m$  for all layers is 2. The downsampling rate  $p$  for both max pooling layers is set to 2, with a stride  $s=2$ . The first dense layer involves 30 neurons, whereas the number of neurons in the second layer is determined by the network's output shape (in our case 1). Rectified linear unit (ReLU) activation function was employed in all convolutional layers. The model was trained in Python v3.8.5 using a Spyder with TensorFlow v2.3.0 in the background.

Online attack detection is done according to the following procedure. If a discrepancy between measured and estimated value exceeds the threshold ( $T$ ) consecutively 15 times, the attack is present. The threshold value was experimentally determined and it is equal to 0.0051.

## 4. ALGORITHM IMPLEMENTATION ON A REAL-WORLD INSTALLATION

Before presenting the procedure for transformation of CNN based algorithm from TensorFlow platform to the local controller environment, we will briefly discuss the general structure of layers used in architecture from Fig. 3.

*Convolution layer*, as the basis of the CNN, performs 1D convolution utilizing a certain number of finite length filters. Output from the convolutional layer is calculated in the following way:

$$y_{i,j} = \sigma(\mathbf{w}_i * \mathbf{x}_j + b_i) \quad (1)$$

where  $\mathbf{w}_i$  represents a matrix of filter coefficients and  $b_i$  denotes bias of the  $i$ -th filter,  $y_{i,j}$  is layer output and  $\mathbf{x}_j$  its input vector. Operator  $*$  denotes convolution of two vectors - signal  $h$  and filter  $g$  and it is defined by:

$$(h * g)(k) = \sum_{k=0}^m h(k)g(m-k) \quad (2)$$

where  $m$  denotes the size of filter. If the size of signal is  $z$  with a filter length of  $m$ , after convolution an output vector of length  $z+m-1$  is obtained. Nonlinear transformation and extraction of representative features from data in the convolution layer are performed using the activation function  $\sigma$ , usually ReLU.

*Pooling layer* downsamples the signal for a predefined number of samples by choosing one of  $p$  samples according to the selected criterion (maximum, average value, etc.). Maximum pooling layer used in

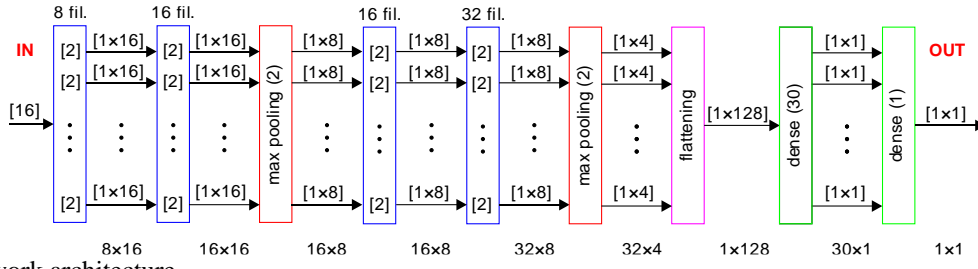


Fig. 3. Network architecture

our network can be described in the following form:

$$y_i = \max(x_{i-s-s+1}, \dots, x_{i-s+p}), i \in \{1, \dots, n/s\} \quad (3)$$

where  $s$  represents stride.

*Flattening layer* converts the data of any format  $x_{i,j}$  into a one-dimensional array  $y_k$  and it is usually placed before a dense layer.

*Dense layer* learns nonlinear dependencies of data by connecting every neuron in one layer to all neurons in the next layer. The general form of the dense layer is written as follows:

$$y_i = \sigma \left( \sum_j W_{i,j} x_j + b_i \right) \quad (4)$$

where  $W_{i,j}$  represents weight coefficient between  $i$ -th neuron of the current and  $j$ -th neuron of the previous layer.  $x_j$  and  $y_i$  denote layer input and output,  $b_i$  is bias of the  $i$ -th neuron, whereas  $\sigma$  is the activation function.

Since the program implementation of max pooling, flattening and dense layers is straightforward, we will focus on the implementation of convolutional layers. The output from TensorFlow is a trained model composed of a certain number of parameters arranged in the predefined format. The parameters of the convolution layer  $c$  are placed in a structure  $\mathbf{S}$  with two members: (1) three-dimensional matrix  $\mathbf{W}_c$  that includes weight coefficients and (2) bias vector  $\mathbf{b}_c$ .

$$\mathbf{s} = \begin{bmatrix} \mathbf{W}_c[m_c][i_c][f_c] \\ \mathbf{b}_c[f_c] \end{bmatrix} \quad (5)$$

The size of  $\mathbf{W}_c$  is  $m_c \times i_c \times f_c$  where  $m_c$  represents filter size,  $i_c$  is the number of input vectors, and  $f_c$  denotes the number of filters in the current layer  $c$ . The order of the values in the filters is reversed (the last value is entered first), which must be taken into consideration during convolution calculation using (2).

The implementation of convolution layer that has one vector at input (such as the first layer in Fig. 3) is straightforward. However, when the input is not in the form of a single vector, the procedure becomes more complex and it is not easily observed from (1). In this case, one filter convolves all input vectors, sums the obtained values column by column, and makes one output vector. The same procedure is repeated for each filter in the layer and the output of the size  $f_c \times z_c$  is created ( $z_c$  is the length of input and  $f_c$  the number of filters in the layer  $c$ ). For example, for the second convolutional layer from Fig. 3 with 16 filters, the input consisting of 8 vectors of length 16 is transformed into an output of shape 16x16. Details regarding the implementation of the described procedure are given in Pseudocode 1.

The control task of both local controllers is implemented in C++ using Keil uVision5 environment [13]. Therefore, to apply the CNN based intrusion

detection algorithm on LC1, we programmed every layer from the network with the elementary C++ functions.

Pseudocode 1: Convolutional layer implementation (the notation is explained in Table 2)

```

for  $i=1$  to  $f_c$  do // for all filters
  for  $j=1$  to  $\text{len}(\mathbf{O}_{c-1}[1])$  do // for all input vectors
     $\mathbf{w} = \{\mathbf{W}_c[m_c][j][i] : \mathbf{W}_c[1][j][i]\}$  // current filter
    // convolution start
    for  $v=1$  to  $z_c$  do
       $\mathbf{c}[v-1] = \mathbf{w}[m_c] * \mathbf{x}_c[j][v-m_c] + \dots + \mathbf{w}[1] * \mathbf{x}_c[j][v]$ 
    end for
     $\mathbf{c} = \mathbf{c}[m_c : \text{end}]$  // exclusion of the first  $m_c - 1$  values
    // convolution end
    // putting convolution of input vector into matrix  $\mathbf{I}_c$ 
    for  $k=1$  to  $\text{len}(\mathbf{O}_{c-1}[2])$  do
       $\mathbf{I}_c[j][k] = \mathbf{c}[k]$ 
    end for
  end for
  // column-wise summing of the inputs filtered by  $\mathbf{w}$ 
  for  $q=1$  to  $\text{len}(\mathbf{O}_{c-1}[2])$  do
    for  $h=1$  to  $\text{len}(\mathbf{O}_{c-1}[1])$  do
       $\mathbf{p}[q] += \mathbf{I}_c[h][q]$ 
    end for
     $\mathbf{p}[q] += \mathbf{b}_c[i]$  // addition of the bias value
     $\mathbf{p}[q] = \mathbf{p}[q] * (\mathbf{p}[q] > 0)$  // ReLU
     $\mathbf{O}_c[i][q] = \mathbf{p}[q]$ 
  end for // one output vector is obtained
end for

```

Label	Description	Label	Description
$\mathbf{W}_c$	weight matrix for layer $c$	$m_c$	filter size in layer $c$
$\mathbf{b}_c$	bias vector for layer $c$	$\mathbf{w}$	current filter
$\mathbf{O}_c$	output matrix from conv. layer $c$	$\mathbf{c}$	convolution vector
$f_c$	no. of filters in layer $c$	$\mathbf{x}_c$	input vector
$z_c$	input length in layer $c$	$\mathbf{p}$	current sum

Table 2. Notation used in Pseudocode 1

The performances of the implemented IDS were validated using a number of attacks. Namely, after a time period in which the system operated in normal conditions, the real data on the LC2 were replaced with false data and transmitted to the LC1. The implemented algorithm successfully detected all attacks, without false positives. In this paper, we present the results of the detection of two attacks ( $A_1$  and  $A_2$ ), as shown in Fig. 4. In  $A_1$  the signal value is sequentially fixed to 0.5-0.7-0.5-0.7 for certain time periods. On the other hand,  $A_2$  presents a sequence of linear increase of signal values by 0.0025 followed by its decrease by 0.002, and another increase by 0.001; the signal is also contaminated with random noise in the range [0, 0.001] per sample, respectively. The moments of attack

detection are marked green dashed line in Fig. 4.

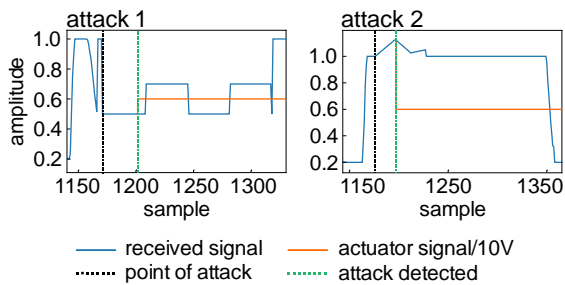


Fig. 4. The detected attacks on DisEPP

Certain actions should be taken to protect the system at the moment of attack detection. In our experiments, regardless the data received from LC2, LC1 sends a value of 0.6 to the actuator (orange line in Fig. 4), stopping the piston immediately. The application of the IDS algorithm did not cause any disturbances during normal system's functioning.

## 5. CONCLUSION

In this paper we have presented the implementation of 1D CNN based algorithm for detection of attacks on smart devices within ICS. In particular, we applied IDS on the low level controller of CPS in the electro-pneumatic positioning system. The procedure for transformation of CNN from the TensorFlow platform to the local controller environment is presented. Namely, built-in functions in TensorFlow have been replaced by elementary functions supported by C++.

The real-time detection performances of the implemented IDS were illustrated using examples of two attacks. The algorithm proved effective in detecting both attacks without false positives. The implementation of the attack detection mechanism did not generate any disturbances on the normal system operation. Our future research efforts will be directed to applying new methods for attack detection based on different deep learning techniques on DisEPP. Furthermore, a CNN-based algorithm will be implemented on more complex systems.

## 6. REFERENCES

- [1] Monostori, L., Kádár, B., Bauernhansl, T., Kondoh, S., Kumara, S., Reinhart, G., Sauer, O., Schuh, G., Sihn, W., Ueda, K.: *Cyber-physical systems in manufacturing*, CIRP Annals, vol. 65, no. 2, pp. 621-641, 2016.
- [2] Atzori, L., Iera, A., Morabito, G.: *The Internet of Things: A survey*, Computer Networks, vol. 54, no. 15, pp. 2787-2805, 2010.
- [3] Khan, I. A., Pi, D., Khan, Z. U., Hussain, Y., Nawaz, A.: *HML-IDS: A hybrid-multilevel anomaly prediction approach for intrusion detection in SCADA systems*, IEEE Access, vol. 7, pp. 89507-89521, 2019.
- [4] Huang, X., Dong, J.: *Reliable control of cyber-physical systems under sensor and actuator attacks: An identifier-critic based integral sliding-*

*mode control approach*, Neurocomputing, vol. 361, pp. 229-242, 2019.

- [5] Nedeljković, D., Jakovljević, Ž., Miljković, Z.: *The detection of sensor signal attacks in industrial control systems*, FME Transactions, vol. 48, no. 1, pp. 7-12, 2020.
- [6] Inoue, J., Yamagata, Y., Chen, Y., Poskitt, C. M., Sun, J.: *Anomaly detection for a water treatment system using unsupervised machine learning*, 2017 IEEE International Conference on Data Mining Workshops (ICDMW), pp. 1058-1065, IEEE, New Orleans, 2017.
- [7] MR, G. R., Somu, N., Mathur, A. P.: *A multilayer perceptron model for anomaly detection in water treatment plants*, International Journal of Critical Infrastructure Protection, vol. 31, art. no.100393, 2020.
- [8] Mercaldo, F., Martinelli, F., Santone, A.: *Real-Time SCADA attack detection by means of formal methods*, 28th intern. conf. on enab. techn.: infrastr. for collab. enterp. (WETICE), pp. 231-236, IEEE, Napoli, 2019.
- [9] Kravchik, M., Shabtai, A.: *Detecting cyber attacks in industrial control systems using convolutional neural networks*, 2018 Workshop on Cyber-Physical Systems Security and PrivaCy, pp. 72-83, ACM, New York, 2018.
- [10] NXP Semiconductors N.V., 2009. LPC1769/68/66/65/64/63 32-bit ARM Cortex-M3 microcontroller. URL: [https://www.nxp.com/docs/en/data-sheet/LPC1769\\_68\\_67\\_66\\_65\\_64\\_63.pdf](https://www.nxp.com/docs/en/data-sheet/LPC1769_68_67_66_65_64_63.pdf)
- [11] Microchip Technology Inc. (2008, Jan.), "MRF24J40MA 2.4 GHz IEEE Std. 802.15.4TMRP Transceiver Module," [Online]. Available: <http://ww1.microchip.com/downloads/en/DeviceDoc/70329b.pdf>
- [12] Nedeljkovic, D. M., Jakovljevic, Z. B., Miljkovic, Z. D., Pajic, M.: *Detection of cyber-attacks in electro-pneumatic positioning system with distributed control*: 27th Telecommunications Forum (TELFOR), art. no. 8971062, IEEE, Belgrade, 2019.
- [13] <https://www.keil.com/download/>, Accessed on: July, 2021.

**Authors: Teach. assist. Dušan Nedeljković, Full Dr. Živana Jakovljević**, University of Belgrade, Faculty of Mechanical Engineering, Department of Production Engineering, Kraljice Marije 16, 11120 Belgrade, Serbia, Phone.: +381 11 3302-200, Fax: +381 11 3370364.

E-mail: [dnedeljkovic@mas.bg.ac.rs](mailto:dnedeljkovic@mas.bg.ac.rs);  
[zjakovljevic@mas.bg.ac.rs](mailto:zjakovljevic@mas.bg.ac.rs)

**ACKNOWLEDGMENTS:** This research was supported by the Science Fund of the Republic of Serbia, grant No. 6523109, AI-MISSION 4.0.

The research in this paper was supported by the Ministry of Education, Science and Technological Development of the Serbian Government, 451-03-68/2020-14/200105.

Banciu F.V., Pamintas E., Feier A. I.

## THE APPLICATION OF NEW INDUSTRIAL MAINTENANCE CONCEPTS - AN EASY WAY TO SAVING MONEY

**Abstract:** Since the beginning of the current millennium, various professional organizations, research institutes, scientific papers in journals and various conferences around the world, address the issue of maintenance, generically speaking, both theoretically, directly or tangentially and by examples of benefits in industry for various production processes, machines and installations. However, recent studies and reports reveal that even in highly industrially developed countries, company management aims to improve maintenance in only about 15% of cases for the next plan year. Why, this is the question? This paper will try to provide answers and even propose possible solutions to increase the applicability in industry of new concepts and theories of maintenance. The arguments used are less oriented on the technical side, they are mainly focused on the “money” indicator, close to the understanding of the company's senior management, i.e. on how huge material benefits can be obtained compared to the insignificant investment expenses.

**Key words:** maintenance concepts, total productive maintenance, managerial decisions, implementation guides, productive efficiency, benefits

### 1. PRODUCTION LOSSES – HEAVY BURDEN – WHAT/WHO CAN REDUCE THEM?

There is no company, especially the new ones, that has not raised the issue of reducing all or some of the 8 categories of losses defined by T. Ohno [1] and maximizing productive efficiency. Failures in the attempts of firms to be more competitive are related to misapplication or non-compliance with application stages of more than 25 methods or tools dedicated to this purpose.

The multi-step regression model showed that Total Productive Maintenance, Poka – Yoke, Kaizen, 5S, Kanban, Six Big Losses, Heijunka, Takt Time, Andon, OEE, SMED and KPIs are the best tools for loss management, and of these, it has been shown that 5S, Kaizen, Kanban, Poka - Yoke and TPM are highly recommended for starting each initiative to make efficient a company [2].

This is how things stand, as in any enterprise and especially in the companies producing goods, maintenance or rather its lack is mentioned among the major categories of losses, we will focus on it.

#### 1.1 WHAT?

It is widely known that industrial maintenance is a knowledge intensive field based on different disciplines covering a wide range of technical sciences involved in the various technologies included in modern industrial equipment. Therefore, until recently, the complexity of the equipment and the need to have a knowledge bag corresponding to a very large area of science and technology was the main limitation of substantial improvements to the discipline of maintenance. In fact, innovative advances in support technologies are needed to enable maintenance engineering to fully develop its potential. In this respect, new ICT-based and microelectronic technologies - such as intelligent data

capture, advanced viewing, wireless, IoT (internet of things) and intelligent sensors - provide maintenance with the environmental intelligence needed to renew the way forward maintenance [3].

The evolution of the field to which the task of preserving machinery and installations has come to be seen, in a general picture in figure 1, as having three well-defined areas: management and management of activities (Underground), workers maintenance and repair work (First Level) and Maintenance Intervention Objects (Workshop).

<b>Workshop</b>	Machinist
	Machine tool operator Worker
<b>First Level</b>	Maintenance operator in:
	- Pneumatics
	- Hydraulics
	- Electronic
	- Computer
	- Chemistry
	- Mechanics
	- Technolgy
	- Electrical
	- Materials
- Phisics	
- Math	
<b>Underground</b>	* Head of the Maintenance Department
	* Material Basis,
	* Endowments, * Support Services

Fig. 1. The way of maintenance running in a company

The results of the company from the operation of

machinery and installations are linked to the hopes of those who have their eyes and ears at every moment on how they "fight the productive but also the related and support sector, the administrative management compartments but more chosen patronage.

## 1.2 WHO?

As you can see in figure 1, the maintenance operator, the one who had to repair and re-install the fallen equipment, has accumulated constant knowledge, has acquired skills and has perfected his technique continuously. This happened until he has not dealt with the constructive and functional complexity of the subject of its activity. The need to carry out the tasks led to the transition from a worker to a team of workers. Then he continued with qualifications centred on the types of actuation and control (mechanical, electrical, hydro-pneumatic, electronics) and more rarely on machine type and their subassemblies (gearboxes, transport systems and tracks, frames and elements of the resistance structure, spindles etc.).

At the same time, there has also been a change in the role of the teams: intervention, maintenance and supervision, repairs, etc. The coordination of the work of the teams has gone from the task of maintenance and repair to the maintenance department, which, with the change of name, has also received new tasks: planning, management, monitoring, control, prediction, design and development strategies modernization, etc.

## 2. MAINTENANCE –A NECESSITY!

Over time, the usual wear of technical equipment makes their efficiency significantly decrease. The compensation brought by the amounts accumulated from the payment of depreciation must be supported by an adequate maintenance strategy, rational investments in advanced technological solutions for monitoring the technical condition of the equipment.

Even if the latter seem initially for the management of the company as an expense at least unproductive, if not useless, the long-term benefits far outweigh the risks of having a maintenance "by ear", eliminate stress and chaos from the maintenance activity.

At the same time, the advanced technique of real-time monitoring of equipment and digital management of maintenance activities is able to help managers organize the company, automate production lines, streamline routine maintenance operations, reduce consistent bills for the energy consumed and improve the operational safety standards of the company. There is no other way to increase your revenue and stay competitive! Performing according to the schedules of the maintenance activities on the production equipment ensures their operation at the set parameters throughout the production cycle.

Carrying out maintenance late or superficially is an appealing strategy for a firm, because in the short term it will lead to financial savings. In the long run, however, this managerial decision will inevitably lead, in a first phase, to the operation of the equipment under parameters and then even to their failure. In both cases,

the company will be negatively affected, on the one hand, by significant production losses, directly and visibly and on the other hand by additional indirect, hidden costs. In addition to the two components of losses, quantifiable in money, there is also the disruption of the way production is organized in the company, which leads to a poor mental state of the employees, an increased insecurity at work.

## 3. WHAT IS NOT SPENT, IS A SAVING, SO MONEY OBTAINED EASILY

One way to make money, honestly and unspeculative, is to produce and sell, so to do productive work, in short, to work. One way to save money is not to spend it, so not to take the money out of your pocket unnecessarily or, if it really is needed, not to pay faster than at maturity and in no case more than it does. The first way is a gregarious description of the work of a firm producing material goods. The other way is to present maintenance as a conservative activity of money and to stop unnecessary expenses.

Among the most important goals of any productive company is to ensure its own sustainability by continuously resuming production cycles, while recovering the initial investment costs, including those with the installation of equipment and additional ones to cover inflation, fiscal adjustments and the increase in prices of raw materials and energy.

The causes that generate a hidden amount of costs for productive companies, so we will be able to better understand the size of the savings that can be made only by rigorously complying with the maintenance prescriptions:

a) The quantitative decrease of the production – the non-operation to the optimal parameters, the unscheduled non-operational times for the production equipment, the frequent shutdown for carrying out unscheduled or accidental repairs seriously encumber the quantity of finished parts, disrupts the supply / shipping chain and the efficiency of the activity and the productivity of the operator decreases dramatically. The company's diminished revenues decrease even more due to the addition of additional costs with materials, spare parts and overtime paid to maintenance technicians or to a third party; so seriously diminished income!

b) Reducing the quality of production – a large part of the products no longer fall within the allowable tolerances or the prescriptions of the quality standards. Therefore, they are either scrapped, turning into waste that must be disposed of from the productive space, or they require reshuffles with additional expenses of time and workmanship or in the best case they are sold below the pre-calculated price. Whatever the case may be, the company's revenues are falling. The decrease in the quality of production has another adverse effect, namely, it affects the reputation of a company, which in the medium term can lead to the loss of customers; therefore, money wasted here too!

c) Failure to comply with schedules and schedules – due to the operating gaps of the equipment, both the



production schedules and those of the related activities of preparing the production / dispatch of the finished products, etc. can no longer be carried out. The availability of equipment being subject to chance, there is no certainty of the correct realization of the schedules and the rescheduling are unpredictable, as uncertain become the supply programs established with the suppliers and the dispatching programs negotiated with the customers; So, the firm appears unserious and money wasted!

d) The decrease in the safety of the operator of the production equipment – the lack of specialized maintenance for long periods of time, the accumulation of bug fixes of the defects ("to turn the wheel") in conjunction with the normal deterioration in operation of the equipment can culminate in an accidental failure of major gravity both for the equipment and, unfortunately, for the human operator. The bills for repairing the equipment increase vertiginously and the medical, insurance and compensation ones for the injured operator become exorbitant. All these costs could be avoided by simple routine maintenance operations; so, other unplanned high costs and possible unwanted responsibilities!

e) The increase in the amount of penalties, fines and retraining - the failure of the economic operator to comply with the various prescriptions regulated by different authorities and national agencies or professional associations regarding the emissions of toxic substances, pollutants, the safety of the working environment, the protection of the human operator, the noise level, prohibitive consumers of, etc. is severely penalized. The inspectors entitled to check the compliance of the companies, for the lack of adequate maintenance measures of the facilities, order, in case of serious violations of the rules, the cessation of the company's activity. Most of the time, however, in case of non-compliances, the agents order important penalties and fines, in addition to obliging the company to carry out costly corrective measures before resuming production; So, not the small expense and danger of closing the firm!

f) Increased investment costs – an improperly maintained equipment will go out of the parameters faster, suffering, most often, irreparable damage and therefore requiring its premature replacement, before the end of the preconized life cycle. The more expensive the equipment in question or is in a critical position on the production line, the greater the financial losses of the firm will be. In addition, the decommissioned equipment, until its disposal, will occupy spaces in the company that do not produce but for which locations, rents and other expenses are paid. Because the equipment was not professionally monitored and no maintenance works were performed at the time, the damage of the company becomes consistent!

From the above it is clear that the adoption of a crash strategy or the postponement of maintenance, both

seemingly very little expensive, in fact leads to an increase in operational costs, depreciates the quality of finished products, increases safety risks and can make the equipment irreparable, significantly shortening its life cycle and ultimately significantly increasing the damage of the company.

#### **4. WHICH MAINTENANCE STRATEGY IS THE BEST?**

The amount of money that companies spent yearly on maintenance can be as large as the net income earned [4]. Modern manufacturing systems generally consist of automated and flexible machines, which operate at much higher rates than the traditional or conventional machines. As a result of this higher utilization rates, automated manufacturing systems may incur four times more wear and tear than traditional manufacturing systems. The effect of such an accelerated usage consists in higher failure rates, which in turn would increase the importance of maintenance and maintenance-related activities as well as effective maintenance management.

While maintenance actions can reduce the effects of breakdowns due to wear-outs, random failures are still unavoidable. Therefore, it is important to understand the implications of a given maintenance plan on a system before the implementation of such a plan. In any case, the importance of maintenance function has increased due to its role in keeping and improving the equipment availability, product quality, safety requirements, and plant cost-effectiveness levels since maintenance costs constitute an important part of the operating budget of manufacturing company [5].

Most of the previous studies, which deal with maintenance modeling and optimization [6, 7], have concentrated on finding an optimum balance between the costs and benefits of preventive maintenance. In this paper, procedures that combine analytical and simulation models to analyze the effects of corrective, preventive, opportunistic, and other maintenance strategies on performance of modern manufacturing systems are only mentioned in order to serve the best choice for the concrete company

So, returning to the question in the subchapter, the answer is not an easy one, nor can it be obtained without taking into account the size and specifics of the production in the company, the degree of automation, the state of the equipment, the qualification of the operating staff, etc. It is not the time, nor the place, nor does it correspond to the dese-so-stated purpose of this study, to try an answer of this kind. But we can make arguments to answer the question, which is the least expensive maintenance strategy and which at the same time, is suitable for most all firms, firms from the smallest to the largest.

Total Productive Maintenance – known by the acronym TPM – is the name of the maintenance concept that can easily bring money to any company, even if it only applies the 5S measures in the concept. Putting the TPM strategy into practice requires a minimum investment effort and a substantial managerial commitment to achieve amazingly good economic results in the end.

In order to substantiate the above statement, we present below only the result after one year of such an implementation of the TPM in an SME-type enterprise, completed in 2010. In the graph in Figure 2, the clues that were chosen to be designed and then monitored, measured and finally subjected to analysis are as follows:

- Ivy-Inventory;
- Wmp-Work in machining process;
- Mte-Machine tool efficiency;
- Lpt-Lead time order to product;
- Mst-Machine tool set time;
- Mlt-Manufacturing lead time;
- Ert-Equipment running time;
- Tsm-Time of materials cycle;
- Cpw-Cost of product warranty;
- Cdi-Cost of direct & indirect labor;
- Pcs-Product cost;
- Opc-Overall productivity of entire capital

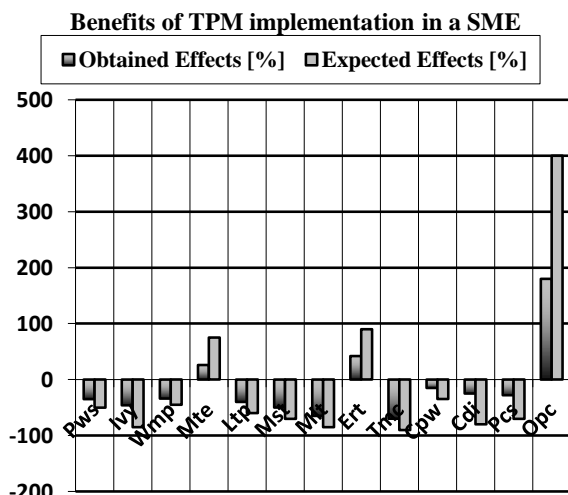


Fig. 2. The way of TPM running in a company

Briefly, the results shows in figure 2 contain both, the estimated benefits and the real one. In connection with this chart it can be easy to observe at a glance that for all compared indexes, the expectations are greater than the real results, be they above or below the horizontal axis.

The method of application, even if it is recently cited and characterized by the authors of a larger study (8) as a "conservative", it could not be challenged in terms of financial results – global savings of about 20% for the applicant company. It's like buying the dollar for 80 cents. Easy money, isn't it?

#### 4. CONCLUSIONS

It is understandable the optics of the top managers, oriented on the profit of the company's activity, but it is incomprehensible that they do not pay due attention to the hidden costs (related to the decrease or stagnation of the production and its quality) and very hidden (related to the satisfaction of customers but also of their own employees). A simple analysis of the sources of loss only on the maintenance side and their elimination or at least their mitigation by implementing the appropriate

maintenance strategy, is certainly bringing savings. The investment is minimal if the strategy is based on the TPM conceptually or at least on an important part of it – the 5S measures. The result is not immediate, but after about a year it will be seen – money obtained easily! The experience of the practical activity in the field has shown us abundantly that in order to achieve good results, so easy money; there must first be a little sweat and patience. No stage of implementation should be skipped, no measure should be rushed, the procedures must be followed exactly and consultation with specialists is absolutely necessary – J.A. Comenius advised us that "the clairvoyance of a single person, no matter how penetrating it may be, gives the possibility of sneaking a mistake", therefore, teamwork is a sine qua non condition in such situations.

#### 5. REFERENCES

- [1] Ohno, T.: *Toyota production system – Beyond large-scale production*, 1st edition, Productivity Press, New, doi: 10.4324/9780429273018, 1988.
- [2] Leksic, I.A, Stefanic, N.A, Veza, I.: *The impact of using different lean manufacturing tools on waste reduction*, Advances in Production Engineering & Management, Volume 15, Number 1, p 84, <https://doi.org/10.14743/apem2020.1.351>, 2020.
- [3] Fumagalli, L., Elefante, D., Macchi, M, Iung, B.: *Evaluating the role of maintenancematurity in adoption of new ICT in the process industry*, in: In IMS'08: 9th IFAC Workshop on IMS, Szczecin, Poland, October 9–10, 2008.
- [4] McKone, K., Wiess, E.: *TPM. Planned and Autonomous Maintenance: Bridging the Gap Between Practice and Research*, Production and Operations Management, Vol. 7, No. 4, 1988.
- [5] Al-Najjar, B., Alsayouf, I.: *Selecting the Most Efficient Maintenance Approach Using Fuzzy Multiple Criteria Decision Making*, International Journal of Production Economics, Vol. 84, No. 1, 2003.
- [6] Chan, F. T. S., Lau, H. C. R., Ip, R. W. L., Chan, H. K., Kong, S. *Implementation of Total Productive Maintenance: A Case Study*. International Journal of Production Economics, Vol. 95, No. 1, 2005.
- [7] Savsar, M.: *Simulation Analysis of Maintenance Policies in Just-In-Time Production Systems*, International Journal of Operations & Production Management, Vol. 17, No. 3, 1997.
- [8] Xiang, Z.T., Feng, C. J.: *Implementing Total Productive Maintenance in a Manufacturing Small or Medium-Sized Enterprise*, Journal of Industrial Engineering and Management, number 14(2) (<https://doi.org/10.3926/jiem.3286>) pp 156 and 167, 2021.

**Authors: Lecturer Felicia Veronica Banciu, Assoc. Prof. Eugen Pamintas, Lecturer Anamaria Ioana Feier**, Politehnica University of Timișoara, Mechanical Faculty, Department of Materials and Manufacturing Engineering, No 1 M. Viteazul Av., Timișoara, Romania, Phone.: +40 2564009, Fax: +40 2563521.  
E-mail: [felicia.banciu@upt.ro](mailto:felicia.banciu@upt.ro); [eugen.pamintas@upt.ro](mailto:eugen.pamintas@upt.ro); [anamaria.feier@upt.ro](mailto:anamaria.feier@upt.ro)

Turudija, R., Arandelović, J., Stojković, M., Korunović, N.

## ASSAY ON CLOUD BASED PRODUCT LIFECYCLE MANAGEMENT – OPEN PRODUCT AND TECHNOLOGY DEVELOPMENT WITHIN EDUCATION

**Abstract:** *The growing relevance of Open Product Development paradigm moves the whole toolset related to Product Lifecycle Management into the cloud. To teach upcoming mechanical engineers for such a working environment, but also to identify gains and challenges of using current Cloud PLM tools, an assay on usage of Cloud PLM was performed. A kind of test Cloud PLM framework was prepared and implemented for four subjects' courses of Mechanical Engineering studies that are related to CAD, CAE, CAPP and CAM and which are interconnected. The framework, which is built on Dassault Systemes 3DEXperience platform, is designed to simulate the application of Cloud PLM toolset as a student goes through a series of project assignments on these courses. The applicability of the framework was analyzed concerning the teachers- who assign, monitor, and evaluate project tasks, and concerning the students- who use PLM tools for the realization of project tasks.*

**Key words:** *Cloud PLM, Process Planning, Collaborative engineering, Open Product Development*

### 1. INTRODUCTION

For a long time, there has been a trend of digitalizing the tools that engineers use in their daily work. This is becoming more pronounced with the rapid development of computers and especially with the development of software solutions based on the Cloud. Because of this, the education of engineers cannot be limited to the time spent on university studies. But this is not the only challenge facing the process of educating new generations of engineers. The educational system intended for engineers must always be up to date with the latest techniques and innovation's, which are constantly adapting to the needs of the market.

Product lifecycle management (PLM) systems are comprehensive software packages that are used throughout the entire life cycle of a product - from its conception, through production, exploitation and finally recycling. PLM systems are described as systems, since they comprise of multiple components, such as databases and data management software, project planning software, Computer-aided design (CAD), Computer-aided engineering (CAE), Computer-aided manufacturing (CAM), Computer-aided process planning (CAPP), etc. By themselves, PLM systems have been present in engineering practice since the early 2000s [1], but as we mentioned earlier, a novelty that is now becoming increasingly relevant is the application of these systems with additional benefits provided by their integration with the Cloud. The domain of a standard PLM system was limited to the scope of a single "company", which means that it facilitated collaboration and the process within one organizational unit. Cloud PLM offers an even broader application that keeps pace with globalization and increasing cooperation between different units within a company and beyond to other stake holders in the process [2]. Moreover, Cloud PLM systems offer greater collaboration, integration, and quick

reachability, which is why a growing number of companies are considering such systems [2]. *De facto*, with a greater interest in cloud PLM, there will be a demand for employees who can immediately start using these systems, without additional training. Accordingly, our goal is to create a conceptual solution (framework) within a Cloud PLM system that can be applied to existing courses at the Faculty of Mechanical Engineering in Nis, in order to prepare future engineers for the needs of the market. Naturally, this endeavor also has its challenges. For example, it is necessary to organize the system interface so that the student can intuitively get accustomed to use the new software, but at the same time it has to maintain a satisfactory level of functionality.

Recently, we are experience the growth of Open science paradigm. It promotes a specific approach to science that, among other things, implies openness of intellectual products like scientific publications, data, software, or educational resources. The development of classical products can be expected to follow a similar trend. This approach is known as Open Product Development or Open Design, and it is defined by openness / accessibility and the possibility to reuse a design, or a process developed by someone else (using already developed and published design as a basis for further development of a new solution or as a final product). Clearly, this goes hand in hand with Cloud PLM systems that can provide an excellent platform for further implementation of the open product development concept and thus allow for optimal use of our collective resources [3].

All of this additionally emphasizes the necessity to prepare students for future work in Cloud PLM systems. Given that we have been using Dassault Systemes software packages for student education in CAD, CAM, etc., clearly in the case of the Faculty of Mechanical Engineering in Nis it would be a natural transition to start using the Dassault Systemes 3DEXperience platform. Here, we used this platform to

simulate an engineers' working environment through courses at the faculty, with the goal to determine its advantages and disadvantages. It is important to notice that the framework, which will be discussed later, is based on the experience of professors and assistants who work on these subjects and thus are familiar with the needs of students. This paper did not accidentally omit the analysis of the presented framework based on students using it. This was left for future work, so that an appropriate amount of attention could be paid to that topic.

## 2. CURRENT SOLUTIONS AND EXAMPLES

There are currently several cloud PLM solutions available on the market, such as: Siemens Teamcenter, Fusion 360 Manage, PTC Windchill, Arena PLM, Dassault Systemes 3DEXperience platform, etc. Companies that develop PLM systems provide descriptions of varying details on their websites. Even though it is important to compare these systems according to their characteristics, a comparison based on data from developer websites would not be objective and should be left to separate studies that primarily deal with benchmarking. An example of this is the use case comparison of the Fusion 360 and 3DEXperience platform in which functionalities of each system have been noted and displayed side by side allowing for an expeditious comparison of this software depending on the users' needs, when comparing the number of functional advantages in this study the 3DEXperience platform can be seen as the more functional choice [4]. Another interesting example is given by Saorín, J. L., et al [5] which considers the process of developing a product with a realistic engineering approach. Their approach has one very interesting idea: the students who participate in the projects are divided into groups and they are also assigned roles within those groups. This is very useful because it gives different students the opportunity to experience different rolls within a PLM system.

Fradl, B. et al [6] showcase a specific scenario that uses a pick-and-place robot which can sort "packages" based on their RFID tags to educate student about PLM systems [6]. This approach has the benefit of a practical example, but on the other hand it does not cover education of PLM systems in a broader sense due to the fact that it is limited to one exercise, and not the continuous study of multiple courses, which can emulate the working conditions off an engineer.

In order to overcome the complexity of PLM systems and for students to be able to understand the presented material, it is very important that the PLM systems are applied during all 4 years of study [7]. By dividing the complex topic of cloud PLM into smaller parts, it can be easier for students to not only learn, but embrace this system as the default norm [7].

In order for education in the field of cloud PLM to be complete and in line with the knowledge that students will need in the workplace, it is necessary for the project not only to deal with the design, but also with simulation and manufacturing of a product. Due to the fact that this kind of project would be

overwhelming to a student encountering cloud PLM for the first time, we propose a framework that is distributed through multiple courses, ideally spanning the entire duration of studies in order to create a collaborative environment that is present on the everyday basis.

## 3. OUR SOLUTION

As was said hereinbefore, Cloud PLM systems have a tendency to be difficult to learn because of their complexity. This is why we wanted to construct a relatively easy to use and understand environment, on an existing Cloud PLM platform. The Faculty of Mechanical Engineering in Nis has been using Catia and SolidWorks software in education for many years now. Thus, we decided on using the Dassault Systemes 3DEXperience platform, which contains both mentioned CAD programs as its integrated parts. The goal that we eventually want to achieve is to implement the 3DEXperience platform in four courses that already exist on the Faculty of Mechanical Engineering in Nis (the courses can be seen in the Fig. 1.).

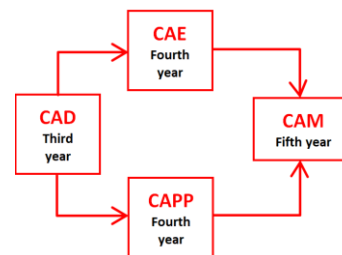


Fig. 1. Scheme of existing courses for which the framework is being developed

Students will be divided into groups of three (every year there will be no more than four or five groups). When students encounter CAD in their third year of studies, which is the first of these four courses, every group will be given a project - to design a relatively complex assembly. Through the 3DEXperience platform, they will collaborate, exchange ideas, adhere to the defined schedule, and complete assigned projects. Project outcomes, like 3D models, textual documents, pictures, technical drawings, etc. will be stored on the 3DEXperience platform. In their fourth year, students will encounter CAE and CAPP courses, and will be given projects based on outcomes from the CAD course. The outcomes of CAE and CAPP projects will also be stored on the 3DEXperience platform and will be used for CAM course in the fifth year. At the end, all the outcomes will be used to form a library for future generations of students to learn from.

For now, we constructed a framework for CAD and CAM courses, which will serve as a base for making the rest of the framework. The framework is made from the dashboard called 'Faculty of Mechanical Engineering in Nis', that has four tabs meant for collaboration and structured view of documents, projects and tasks, social group tab where different ideas, questions and surveys can be posted, and a tab for defining issues and special approval/review routes.

In order to avoid allocating too much time during courses to explain the functioning of the created framework to students, we wanted the framework to be as intuitive and easy to use as possible. Because of this, the framework is mostly accessed by ‘dashboard apps’ (widgets is a commonly used term for dashboard apps, and will be used in the text below), which are easier, simpler and more intuitive than web apps. Furthermore, the 3DEXperience platform is linked to Dassault’s native apps (like Catia), which are used primarily for product design, analysis and manufacture planning. Widgets can be set up on dashboards tabs and their location and size is fully customizable (Fig. 2.), so working with and transferring different documents between widgets, with the ‘drag-and-drop’ method, is faster and easier than with web apps. On the other hand, web apps, which open in new browser tab, possess more options and more details, so experienced users can take advantages and benefit from them. We believe that, for the purpose of teaching users that do not have prior experience with Cloud PLM environments, widgets strike a fine balance between learning PLM environments and intuitive use.

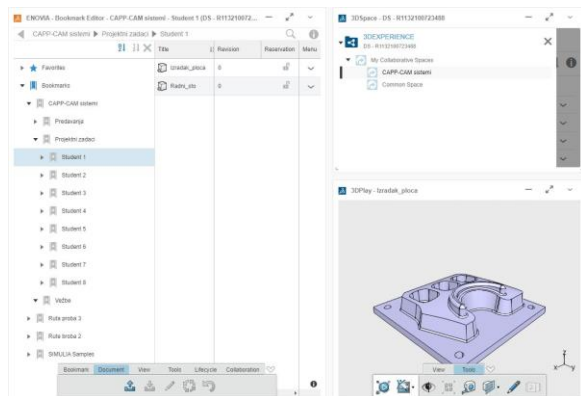


Fig. 2. Example of customized widgets on a tab

Every user that logs on the 3DEXperience platform has credentials. Credentials are composed of organization that the user is part of (for us, the organization is Faculty of Mechanical Engineering in Nis), Collaborative Spaces that the user is part of, and access role within the Collaborative Space that determines what the user can do in the Collaborative Spaces that he or she is assigned to. In our framework, students have ‘Author’ roles that gives them access to read any content that is stored on Collaborative Spaces that they are a part of, access to create evaluation content, such as reviews, simulations, etc., and access to create definition content such as physical products, CAD parts, systems, manufacturing, etc. Professors and teaching assistants have ‘Leader’ roles, which gives them all the access that ‘Author’ role has, plus the access to create resource content, such as libraries, project templates, etc. Students will be a part of four different Collaborative Spaces during their studies, which are named after already existing courses.

All the documents that are uploaded to the platform have a lifecycle, which is defined by documents’ maturity states: Private – In Work – Frozen – Released

– Obsolete. Maturity state defines if the document is being drafted, worked on, waiting on review and approval, finished, or not relevant anymore. All the Collaborative Spaces from this framework are set to be ‘Protected’, which means that only documents in Released or Obsolete maturity state are visible to other members of the Collaborative Space. This is made so not to bother users with unnecessary documents and information. Because documents are stored in non-structured way on Collaborative Spaces, ‘Bookmark Editor’ widget is used to structure them. For every course there are 3 bookmarks, ‘Lectures’, ‘Exercises’ and ‘Project Assignments’ with different number of sub-bookmarks, dependent on how many are needed. In addition to ‘3DSpace’ widget, which provides a view of all Collaborative Spaces that the user is a part of, and ‘Bookmark Editor’ widget, ‘3DPlay’ is also located in the first tab of our framework dashboard. ‘3DPlay’ is a widget that provides a fast and easy view of 2D/3D models or textual documents. This widget provides different options for writing comments, questions and taking screen captures that can then be published in ‘3DSwim’ widget that is located in the third tab of our dashboard framework (Fig. 3.), which is meant for discussions in different communities (every course has its own community). Through 3DSwim widget, audio and video calls can be made with up to 14 users through private conversations, where users can share their screens and exchange ideas.

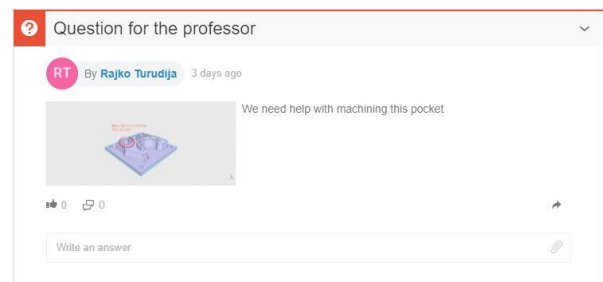


Fig. 3. Question posted to the 3DSwim widget

In the second tab, through ‘Project Planning’ (Fig. 4.) widget, projects and project tasks can be defined, scheduled and assigned to students. This way students can have a clear view of everything that they need to do. In addition, professors can assign tasks that are not a part of any student project through ‘Collaboration Tasks’ widget. All users can see maturity state of documents through ‘Collaborative Lifecycle’ widget, which is also located in the second tab of our framework dashboard.

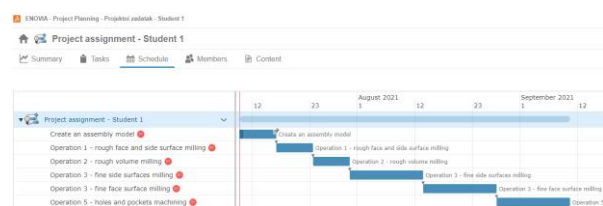


Fig. 4. Schedule defined in Project Planning widget



Fig. 5. Route example for student project monitoring and approval

In the fourth and final tab, professors can create issues through ‘Issue Management’ widget. When professors find a mistake in a student project, they can assign students to fix the issue, give them instructions on how to solve the said mistake, and set dates by when the issue has to be resolved. On this tab, through ‘Route Management’ widget, specific routes for approving or reviewing project assignments can be created (Fig. 5.). This is meant for teaching assistants, so that professors have an insight into how far the assistants have come with reviewing student projects. This widget can also be used in situations where there is a group leader (one of the students) who needs to approve every step of the project. As mentioned before, Cloud PLM platform we used can be unintuitive, but there are other shortcomings. Some of them are listed below:

- ‘Route Management’ widget does not possess the option to create template routes, so web app ‘Collaboration and Approvals’ needs to be used. But when route templates are created in this web app, they can’t be used in widget ‘Route Management’;
- Deletion of the documents from the platform is strenuous. Documents can’t be deleted if they are not in ‘Draft’ maturity state, and have any kind of relation with anything on the platform;
- If Collaborative Space needs to be deleted, all the documents inside it firstly have to be deleted manually;
- Platform sometimes needs a lot of time to process the deleted, updated, edited documents through all the apps on the platform;

#### 4. CONCLUSION

Although we believe that the framework is a good base from which we can build on and help students understand Cloud PLM solutions, collaboration environments, and even open-market and open-design concepts, we still need to test it with our students, and see some tangible results that we are on the right way. From what we have experienced while creating this framework, Cloud PLM solutions can be very complicated, especially for new users. It takes time to get used to this kind of management, and to constantly keep colleagues and superiors apprised about what has been done, and what needs to be done. Even though use of Cloud PLM systems is inevitable because of their benefits, the question arises whether such concepts need to be introduced in small businesses and manufacturing environments due to their current complexity. For our future work, first we need to build upon what we have created and expand the framework to all four already existing courses. Then we would like to come up with some guidelines for developers and vendors of such PLM systems, to help them improve their products. For this, we will need to create a new

framework and implement it in already existing businesses and manufacturing environments, to further test the capabilities of Cloud PLM platforms such as 3DExperience.

#### 5. REFERENCES

- [1] Segonds, F., Mantelet, F., Nelson, J., & Gaillard, S.: Proposition of a PLM tool to support textile design: A case study applied to the definition of the early stages of design requirements. *Computers in Industry*, 66, 21–30, 2015.
- [2] Singh, S., & Misra, S. C.: Significance of Cloud PLM in Industry 4.0. *Product Lifecycle Management (Volume 4): The Case Studies*, 249–255, 2019.
- [3] Boisseau, É., Omhover, J.-F., & Bouchard, C.: Open-design: A state of the art review. *Design Science*, 4, 2018.
- [4] Vila, C., Ugarte, D., Ríos, J., & Abellán, J. V.: Project-based collaborative engineering learning to develop Industry 4.0 skills within a PLM framework. *Procedia Manufacturing*, 13, 1269–1276, 2017.
- [5] Saorín, J. L., de la Torre-Cantero, J., Melián Díaz, D., & López-Chao, V.: Cloud-Based Collaborative 3D Modeling to Train Engineers for the Industry 4.0. *Applied Sciences*, 9(21), 4559, 2019.
- [6] Fradl, B., Sohrweide, A., & Nyffenegger, F.: PLM in Education – The Escape from Boredom. *IFIP Advances in Information and Communication Technology*, 297–307, 2017.
- [7] Vuksanovich, B., Wallace, D., & Costarell, M.: *Mechanical Engineering Curriculum Improvement Using Product Lifecycle Management (PLM). Volume 7: Engineering Education and Professional Development*, 2009.

**Authors:** Teach. Assist. **Rajko Turudija**, Teach. Assist. **Jovan Arandjelović**, Assoc. Prof. **Miloš Stojković**, Assoc. Prof. **Nikola Korunović**, University of Niš, Faculty of Mechanical Engineering, Department of Production Information Technologies, Aleksandra Medvedeva 14, 18000 Niš, Serbia, Phone.: +381 18 588 255, Fax: +381 18 588 244  
E-mail: [rajko.turudija@masfak.ni.ac.rs](mailto:rajko.turudija@masfak.ni.ac.rs);  
[jovan.arandjelovic@masfak.ni.ac.rs](mailto:jovan.arandjelovic@masfak.ni.ac.rs);  
[milos.stojkovic@masfak.ni.ac.rs](mailto:milos.stojkovic@masfak.ni.ac.rs);  
[nikola.korunovic@masfak.ni.ac.rs](mailto:nikola.korunovic@masfak.ni.ac.rs)

**ACKNOWLEDGMENTS:** This research was financially supported by the Ministry of Education, Science and Technological Development of the Republic of Serbia (Contract No. 451-03-9/2021-14/200109). We also must emphasize our gratitude to the company CAD CAM DATA d.o.o. for helping us take our first steps on the 3DExperience platform.

Trstenjak, M., Opetuk, T., Cajner, H., Đukić, G.

## PROCESS PLANNING AND INDUSTRY 4.0 – THE IMPORTANCE OF STRATEGICALLY DEFINED TRANSITION TOWARDS DIGITAL WORK ENVIRONMENT

**Abstract:** *Current level of education, skills available on the market and undefined strategic plan are often referred as the biggest barriers towards Industry 4.0 implementation. The strategically defined transitional period avoids unnecessary costs and minimizes the risks regarding the very high investments and dynamic, unpredictable market. In this paper, the emphasis will be put on digitization of the process planning department and its strategic transition towards Industry 4.0 concept. The models of process planning within the smart factory from the literature will be examined, as well as the frameworks for their strategic transformation. A novel method based on statistical ranking of data collected from the expert group is proposed, as well as the distinction of the Industry 4.0 elements to be implemented specifically for process planning, so that the general framework for the strategic transformation of process planning can be given.*

**Key words:** *process planning, industry 4.0, smart factory*

### 1. INTRODUCTION

Process planning, as one of the main phases in the product lifecycle, also has to go through radical changes to achieve the state of digital manufacturing, by the concept of Industry 4.0. Ten years after the introduction of the digital working environment, the concept isn't omnipresent and a standard in the manufacturing industry both in Europe and the rest of the world. The demand of high flexibility and personalized product placement is one of the key components of the new system, which is why the process planning plays one of the key roles in the value chain [1]. The accurate and optimal process plan enables the cost reduction in the next stages of the product lifecycle, such as manufacturing or exploitation. Mass customization demands the high level of flexibility and the definition of many process plans variants [2]. The digitization of process planning sector enables the quick and accurate transition between the different product variants and definition of personalized products by the market demand. This is how it is possible to remain competitiveness level on the market, but the transition to digital concept requires certain challenges. The reason why many companies haven't yet been completely digitized is the level of investment in the new digital system required and the unpredictable character of the future consequences, such as return of investment time [3]. To minimize the risk of the transition, the optimal strategic plan has to be defined, so that the implementation of the elements can be optimal and personalized for the certain industrial needs [4]. Besides that, the goals of the implementation of the digital concept have to be defined as well as the vision for the ideal future digital environment.

### 2. TRANSITION TO INDUSTRY 4.0

The transitional period for a company can be most

challenging. Traditionalists who aren't aware of the benefits of the new concept are very hard to convince to even make the decision to start the transformation process towards Industry 4.0. Those who are familiar with the concept and are willing to accept the change and make digital improvements within their company are aware of the very high risk of the radical changes followed by very high investments on the unpredictable and dynamic market [5]. This is the mostly case with SMEs who are very careful with every new investment and don't have space for high risks and dealing with consequences of it [6]. That is why the correct strategic plan for the transition has to be defined, also personalized and unique, but by the general framework available from the literature and from the case studies available. For the accurate strategy plan definition the following phases must be included: definition of wanted ideal state to be achieved, recognition of current biggest challenges and barriers in Industry 4.0 implementation, readiness factor calculation and education of the workers [7].

#### 2.1. Definition of ideal state of the company by the Industry 4.0 concept – process planning

The first stage before the strategic plan definition is to definition of the ideal future state of the company. In terms of process planning this is the upgrade of CAPP system with artificial intelligence (machine learning), advanced and predictive big data analytics, placed on the cloud and connected to other parts of the value chain. It has enhanced direct connection with manufacturing planning (scheduling) department. Automatic definition of process plans also depends on the currently available machines and other available resources which, in the end, shortens not only planning, but also time of the physical manufacturing, increases the product quality and lowers the costs because of the combination of quality and quantity of data available and its analysis. Apart from that, it is connected to every other department within the manufacturing

system, which enables an easy communication and continuous improvement with direct feedback from the various sides so that process can be optimized as often as possible. With the current trends on the market, which is aimed at personalized products, this kind of process planning system enables quick and efficient adjustment to the new needs with the direct customer feedback available so that the product quality and functionality connected to the technological process design can be defined without any barriers of time and additional cost. [8]

## **2.2. Challenges and barriers in Industry 4.0 implementation**

Since the concept of Industry 4.0 is known for a decade already and yet it hasn't been implemented on the expected level and to the fullest in most of the companies, especially in the SMEs it can be concluded that there are certain challenges and barriers present which overcome the perception of its benefits. The most common that can be found in the most relevant research are education and workforce skills, local legislation, local infrastructure, human resistance to change and lack of optimal strategy [9].

The skills needed for the new digital manufacturing concept are different from the traditional ones. Due high level of automation human role within the system changes and is more control-oriented rather than physical work which is now conducted by robots. New technologies such as big data analytics or digital twin and the work principles such as real-time optimization demand new kinds of knowledge and personalized approach to every production system as a single unit, so the theoretical knowledge must be adapted to the needs of a real and currently existing system. Workers must also be aware of the benefits of the new digital environment while the digital skills aren't yet incorporated completely in the general educational system so it could produce the workforce with appropriate skills and specific knowledge [10]. Without the knowledge, workers might think that the change might cause the loss of their jobs, so there is high amount of resistance to change still present in every company which has decided to implement the Industry 4.0 concept. Especially if the traditional work methods have proven to be successful so far, the resistance can be very high, but the dynamic trends on the market will soon cause the inability for the adaption to the new needs, because the traditional systems aren't as flexible as the digital. Resistance to change can be lowered by education and explanation of benefits which new work environment will bring to the currently available workforce, but also to the management [11].

Local legislation is another most common barrier and challenge to overcome while implementing Industry 4.0 into the traditional manufacturing system. The local governance must also be aware of the benefits which the transition to Industry 4.0 brings, so that the bureaucracy level can be decreased but also the financial support can be given. Level of interventions needed for the transition from traditional to digital system varies from company to company, but it usually demands very high financial investments into

hardware, software and education and the support and approval of the local government plays here a key role in the support and acceleration of the transition [12]. Related with that is the infrastructure, in this case most important one is the availability of the high-speed internet connection. In every digital system the big amount of data should be transmitted in the real time, while the most of the processes of the analysis, communication and control is provided online. Concept of Internet of things, which is one of the most common elements of Industry 4.0 demands stable and high-speed internet which is closely related to the local infrastructure available in the area. If there is not such yet present, the local government should be aware of the possible interventions so that the local companies would achieve their goal, which would, in the end, have big financial benefits for the entire area and its level of sustainable future development [13].

Transition towards Industry 4.0 cannot be provided in optimal manners without proper strategy. The good strategy minimizes the risks and eliminates the possibilities of the future loss. It leads the company towards the implementation of the optimal system that will generate the high revenue and will be flexible so it can adapt to the market needs as quick as possible. Also, the transitional period which includes very high investments with optimal strategy can minimize the unnecessary tasks or Industry 4.0 element implementation, wrong adaption of the digital system and reduce the time needed for the complete implementation.

## **3. MODEL FOR OF STRATEGIC PLAN DEFINITION – PROCESS PLANNING IN INDUSTRY 4.0**

Strategic plan of transformation into Industry 4.0 is most commonly defined by readiness factor calculation. There are many methods available in the literature, while most of them are based on the questionnaire by which the current level of development by certain elements of Industry 4.0 is recognized. Therefore the strategic plan is defined by the level of change needed for a certain element, compared with ideal model. More advanced methods include decision support systems and give importance ponders of certain elements with subjective judgment of a represent of company.

In this research the expert group was formed, with 15 professionals from the industry and 15 from the academia. In order to get a general overview of the optimal transformation strategy, they were asked to rate the process planning in Industry 4.0 elements by following goals:

1. Readiness for financial investment
2. Implementation and exploitation complexity
3. Return of investment (ROI) time

The elements that were evaluated are following:

*CAD – E1*

*CAM – E2*

*Automatic recognition of geometrical features – E3*

*Automatic definition of technologies and operation sequencing- E4*



*Automatic definition of tools, machines, fixtures etc.- E5*

*Automatic definition of machining time and cost – E6*

*Tool usability optimization – E7*

*Machine usability optimization – E8*

*Automatic definition of process plan – E9*

*Planning activities standardization – E10*

*Human subjectivity minimization – E11*

*Continuous control, improvement and system optimization – E12*

The elements were rated on the scale 1 to 9 where 1 is least and 9 most important element. In the Implementation and exploitation complexity and return of investment time goals the ranks were transformed so that those with highest complexity have given the least priority and those with longer ROI time were also given lowest priority in implementation. The ranking was provided by ranking method included in Friedman test, and the data were analyzed in the Statistica software. The results are shown in Table 1.

	Financial investment readiness	Implementation and exploitation complexity	Return of investment time
Element	Rank	Rank	Rank
E1	8,5333	7,75	7,1
E2	7,7667	7,9333	6,4333
E3	4,9333	4,2667	5,7333
E4	5,3667	6,05	5,5167
E5	6,6167	5,4833	5,7167
E6	6,8833	6,5667	6,2667
E7	4,7333	6,7333	7,1667
E8	7,0333	7,3	6,1667
E9	6,8667	6,1	6,35
E10	6,8167	6,7667	6,7833
E11	4,95	6,85	7,65
E12	7,5	6,2	7,1167

Table 1. Ranks of process planning in Industry 4.0 elements

Expert group has estimated that the CAD (E1) is first element to be implemented if the most important goal for the company is financial investment readiness. CAD software is very commonly used so this kind of result was expected and it doesn't demand very high financial investments for its implementation. Similar is with CAM software (E2), which is second element to be implemented. Those two elements were also given highest priority when the goal is implementation and exploitation complexity. When the goal is return of investment time, then it is estimated that this would be firstly achieved by minimization of human subjectivity (E11). Second is implementation of culture of continuous control, improvement and system optimization (E12) and tool usability optimization (E7).

Culture of continuous improvement is estimated with the third highest rank when the goal is financial investment readiness. This is expected and logical, because the transition that happens in this case should

be in human workforce mindset and therefore it doesn't require as high investments as other elements. The elements that is ranked with the lowest importance when the goal is financial investment readiness are Automatic recognition of geometrical features (E3) and Tool usability optimization (E7). Automatic recognition of geometrical features is one of the most demanding challenges in the process planning automation, especially with the very high variety of the products, therefore the development of this kind of system would be very expensive. When the goal is implementation and exploitation complexity, element that are ranked with least priority is automatic definition of technologies and operation sequencing (E3). Similar to automatic recognition of geometrical features and directly related to it, this is the core of the automated (smart) process planning and is very complicated to implement because it requires the development of a very complex software system with specific knowledge and procedures. When the goal is return of investment time, the lowest rank was given to Automatic definition of technologies and operation sequencing (E4), Automatic recognition of geometrical features (E3) and Automatic definition of tools, machines, fixtures etc. (E5). As the most complex and expensive elements, the return of investment in those elements is the longest.

### 3.1. Transitional strategy plan definition

In order to define an optimal transitional strategy plan, the companies must define goals of their transformation firstly. This means that they should give certain importance to each of three goals: financial investment readiness, implementation and exploitation complexity and return of investment time. The goal definition is understood as what is their priority, what is the expected result that they want to achieve while implementing the Industry 4.0 elements. The ranks of the elements defined by expert group are transformed into ponders by normalized vector method and goals are also ranked but by the representative person from the company for which the strategy plan is to be defined. They are also transformed into ponders and by multiplication of elements and goal ponders, similar to AHP method the final element implementation priorities are defined. The strategy is defined by the ranks and therefore its implementation is suggested to be done according to the priorities in order to achieve optimal transition towards ideal Industry 4.0 environment in the company. In example, if the company has given high priorities to return of investment time (priority importance rank 7) and financial investment readiness goals (priority importance rank 9), then the order of elements that should be implemented by its priorities is as shown in Table 2.

Rank	Element	Ponder
1	CAD	0,0493
2	Continuous control, improvement and system optimization	0,0463
3	CAM	0,0455
4	Planning activities standardization	0,0433
5	Human subjectivity minimization	0,0422
6	Automatic definition of machining time and cost	0,0418
7	Automatic definition of process plan	0,041
8	Tool usability optimization	0,0406
9	Machine usability optimization	0,0393
10	Automatic definition of tools, machines, fixtures etc.	0,0386
11	Automatic definition of technologies and operation sequencing	0,0359
12	Automatic recognition of geometrical features	0,0351

Table 2. Ranks of process planning in Industry 4.0 elements with high importance of ROI time and financial investment readiness

#### 4. CONCLUSION

Industry 4.0 as a concept of digital (smart) factory has been present on the market for a decade, but yet it hasn't been implemented into the manufacturing companies on the expected levels. Many yet perceive the transition as a very challenging and risky task and try to avoid the changes. There are many barriers like skills of workers, local legislation, infrastructure, human resistance to change and lack of strategy for the future development. Strategy of transition must be personalized for each case and usually it was based on the rough estimation of current state in the company compared to the ideal state. In this paper the elements of smart process planning were defined and prioritized by expert group by three goals: Readiness for financial investment, Implementation and exploitation complexity, Return of investment time. The strategy plan is when ranks of elements are transformed into ponders by normalized vector method combined with goal priorities. Priority list of elements is given which is the strategy for their future optimal implementation. For the future work the Industry 4.0 elements can be extended so this method can be used to evaluate the company as a whole. Also, more goals could be defined to get more accurate results for each company.

#### 5. REFERENCES

[1] Meindl B, Ayala NF, Mendonsa J, Frank AG. The four smarts of Industry 4.0: *Evolution of ten years of research and future perspectives*. Technological Forecasting and Social Change, 168, Elsevier, 2021  
[2] Wang, Y., Ma, HS., Yang, JH. et al.: Industry 4.0: a way from mass customization to mass personalization production. *Adv. Manuf.*, 5, pp.

311–320, 2017  
[3] Zhang, C., Chen, Y., Chen, H. et al.: Industry 4.0 and its Implementation: a Review, *Inf Syst Front*, 2021  
[4] Mahdiraji, H.A., Zavadskas, E.K., Skare, M., Kafshgar, F.Z.R., Arab, A: Evaluating strategies for implementing industry 4.0: a hybrid expert oriented approach of BWM and interval valued intuitionistic fuzzy TODIM, *Economic Research-Ekonomska Istraživanja*, 33 (1), pp. 1600-1620, 2020  
[5] Trstenjak, M., Opetuk, T., Cajner, H., Tosanovic, N.: Process Planning in Industry 4.0—Current State, Potential and Management of Transformation, *Sustainability*. 2020; 12(15), 5878, 2020  
[6] Sriram, R.M., Vinodh, S.: Analysis of readiness factors for Industry 4.0 implementation in SMEs using COPRAS, *International Journal of Quality & Reliability Management*, 38 (5), pp. 1178-1192, 2021  
[7] Sony, M. Naik, S.: Key ingredients for evaluating Industry 4.0 readiness for organizations: a literature review, *Benchmarking: An International Journal*, 27(7), pp. 2213-2232, 2020  
[8] Trstenjak, M., Cosic, P.: Process Planning in Industry 4.0 Environment, *Procedia Manufacturing*, 11, pp. 1744-1750, 2017  
[9] Vuksanović Herceg I., Kuč V., Mijušković V.M., Herceg T.: Challenges and Driving Forces for Industry 4.0 Implementation, *Sustainability*, 2020; 12(10), 4208, 2020  
[10] Kaasinen, E., Schmalfuß, F., Öztürk, C., Aromaa, S., Boubekeur, M., Heilala, J., Heikkilä, P., Kuula, T., Liinasuo, M., Mach, S., Mehta, R., Petäjä, E., Walter, T.: Empowering and engaging industrial workers with Operator 4.0 solutions, *Computers & Industrial* 139, 105678, 2020  
[11] Xing F., Peng G., Liang T., Zuo S., Li S.: Managing Changes Initiated by Industrial Big Data Technologies: A Technochange Management Model. In: Streitz N., Konomi S. (eds) *Distributed, Ambient and Pervasive Interactions. HCII 2019*, 11587. Springer, Cham, 2019  
[12] Rao, Y., Yang, F.: Strategic Research for Talent Cultivation of Strategic Emerging Industries under Industry 4.0, *Proceedings of the 2018 8th International Conference on Management, Education and Information (MEICI 2018)*, 2018  
[13] Grusho, A.A., Zabezhalo, M.I., Piskovski, V.O. et al.: Industry 4.0: Opportunities and Risks in the Context of Information Security Problems, *Autom. Doc. Math. Linguist.* 54, pp. 55–63, 2020

**Authors:** Asist. Maja Trstenjak, Assist. Prof. Tihomir Opetuk, Assoc. Prof. Hrvoje Cajner, Full. Prof. Goran Đukić,  
University of Zagreb, Faculty of Mechanical Engineering and Naval Architecture, Department of Industrial Engineering, Ivana Lučića 5, 10 000 Zagreb, Croatia,  
Phone.: +385 1 6168 222, Fax: +385 1 6156 940.  
E-mail: [maja.trstenjak@fsb.hr](mailto:maja.trstenjak@fsb.hr); [tihomir.opetuk@fsb.hr](mailto:tihomir.opetuk@fsb.hr); [hrvoje.cajner@fsb.hr](mailto:hrvoje.cajner@fsb.hr); [goran.dukic@fsb.hr](mailto:goran.dukic@fsb.hr)

Randelović, S., Milutinović, M., Movrin, D., Blagojević, V., Kostić, N.

## NEW GENERATION OF PRODUCTION SYSTEM ACCORDING TO THE CONCEPT OF I4.0

**Abstract:** *At the beginning of this millennium, modern production systems in the physical, mechanical, material, and computer sense may not offer a chance for a major technical breakthrough. What we have in terms of technology has long been tested, confirmed and is already widely exploited in the production facilities of the world's most powerful companies. But one area that has not been mentioned captures the attention of everyone at the beginning of this millennium with the belief that there will be room to make a new step forward and a competitive advantage in the global market. These are information technologies that have long supported production, but now in the context of complete digitalization and exchange of much larger amounts of data generated in production systems and its environment. Based on these data, it is already possible to monitor and analyze production systems in much more detail in real time with the possibility of optimization in order to achieve global success.*

**Key words:** *Production systems, Information technology, I4.0*

### 1. INTRODUCTION

The latest developments in the global market are rapidly being transferred to production systems and require the voice of the customer to be transformed into a new product. All the facts that are collected on the market are very quickly transmitted to the level of production that throws out different products according to customer requirements. It is still a mass production, but now there are no more exactly the same products in unlimited series because everyone wants to show their commitment to the customer and his requirements.

Industry 4.0 is a term often used to refer the fourth industrial revolution and to the developmental process in the management of manufacturing and production process [1].

The term Industry 4.0 was first publicly introduced in 2011 as "Industrie 4.0" by a group of representatives from different fields (such as business, politics, and academia) under an initiative to enhance the German competitiveness in the manufacturing industry. The German federal government adopted the idea in its High-Tech Strategy for 2020.

In 2003, they developed and published their first set of recommendations. Their vision entailed that these Cyber-Physical Systems comprise smart machines, storage systems and production facilities capable of autonomously exchanging information, triggering actions and controlling each other independently. This facilitates fundamental improvements to the industrial processes involved in manufacturing, engineering, material usage and supply chain and life cycle management [2].

Industry 4.0 remains a term well-known in German-speaking areas. Consequently, this guide will aim at attempting to define the term, exploring the design principles, the advantages and the challenges facing such an approach, and try to quantify the potential lying underneath.

Giving you the immediate insights and broader global picture you need to improve your manufacturing operations.

### 2. CHANGE IN THE SOFTWARE PLATFORMS AND DIGITAL CONECTIONS

In addition to integration, communication and information exchange are crucial issues for the implementation of I4.0 technologies [4]. Namely, by adding sensors, actuators and other types of intelligent components to physical objects and devices we create integrated systems, but only if enable network communication between such systems they will be upgraded to cyber-physical systems - intelligent, networked systems with built-in sensors, actuators and processors that interact with the physical world (including humans as users) and support real-time operations. They represent the integration of local "intelligence" and communication capacities, and thanks to the built-in microcontroller these systems are "smart" to be able to make independent decisions. However, although their decisions are autonomous and decentralized, they are still in line with the process plan defined at higher levels of decision-making [3].

Cloud technology is a set of networked computing resources that provide IT infrastructure and services, including operating systems, applications, internal and external data storage space. Appropriate services are accessed over networks without the need to install software on the user's computer. The provision and use of IT services is enabled through different types of interface, protocols and web browsers. By switching to cloud technology, significant savings are achieved in terms of hardware, labor and energy. In this way, companies can reduce annual operating IT costs by over 80% [3].

In industrial plants and processes, real-time data of large volume and various formats are generated at high speed. Big data technology enables continuous

collection of information from various sources with the capacity of search and analysis in order to optimize production processes and workflows. The data obtained from the sensors are analyzed using algorithms for the so-called data mining. These algorithms are based on intelligent mathematical and statistical models and machine learning methods. The goal is to find behavioral patterns by revealing hidden connections between collected data.

### 3.0 NEW PRODUCTION SYSTEM AND THEIR MAIN CHARACTERISTICS

Modern production systems in the broadest sense imply:

- predictive analytics
- process optimization
- smart factory
- environmental control
- quality assurance and
- worker health and safety



Fig. 1. Requirements for production system today

Each of these concepts has been asking numerous questions for many years and opens new ways in which direction the future development of production systems should go.

#### 3.1 Predictive analytics

Based on a large number of collected data from production processes, it is possible to make a prediction of events in the future. There is nothing new here that it is not about online data of various types, from text messages, numerical values but also images, which are used for planning, design and implementation of production processes [4]. Based on the current situation, their analysis and comparison can predict the near and distant future and thus plan their processes according to customer requirements. Analytical approach and analysis of a large amount of data requires powerful software resources for their storage, exchange, but also fast processing in order to obtain the right information to predict the behavior of the system and future work.

#### 3.2 Process optimization

A large amount of data, big data, is only the basis for optimizing process parameters and finding optimal values in terms of repeatability and continuous

measurement. As market conditions change rapidly, extensively collected data from the production process do not provide the right answer unless they are optimized according to different criteria. Depending on the type of production process, key parameters are identified, they are continuously monitored, collected and their values are optimized in order to obtain a product for the global market.



Fig. 2. Optimization for all parameters of process

Energy consumption comes to the fore more than ever. Moreover, energy consumption per unit of product is the basic criterion for classifying a process and assessing its impact on the environment both in the short and long term.



Fig. 3. Energy consumption on the level of basic process

#### 3.3 Smart Factory

The digitized industrial revolution, it's transforming everything, from the factories where products are made throughout the journey when products are shipped and across the entire supply chain driven by data and connectivity. Embracing artificial intelligence and 5G, powering cognitive systems, launching new business models improving cost efficiency, increasing yields and quality improving worker safety and skills make a smart factory [5].

The safety and reliability of production processes is increasing every day based on the large amount of data collected and enormous experience. This rich experience is passed from generation to generation through various methods and analyzes in order to use the observed omissions and mistakes in the right way.

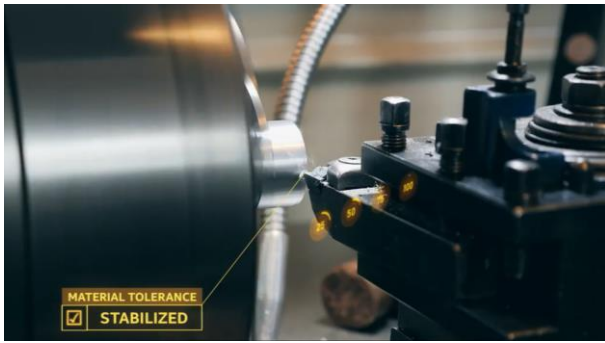


Fig. 4. Parameters of process collect and smart analysis in real time

### 3.4 Environmental control

Today's trends and changes in the near and far environment of people are the subject of increasing research and analysis while meeting strict international standards. It is necessary that the production process has zero effect on the environment, but despite everything, the consequences are felt all around us. Experience shows that small changes in the level of parameters, in the production process itself, bring great savings and reduced impact on a much wider global scale. The fact that a large number of production processes, which interact with nature, leaves an indelible mark only warns that control must be even more effective in order to preserve the planet in its current state. It has long been clear that there is no going back and that the natural balances are permanently disturbed so that we are left with a struggle for its survival [4].

### 3.5 Quality assurance

Achieving the level of quality by applying local and international standards is just a guarantee that there is no going back. Continuous PDCA cycles of production processes push and pull forward, but without ensuring the achieved quality, everything would return to the initial level. Realistic parameters indicate that the path to the top is increasingly difficult and that without the application of global standards there is no assurance of the achieved level of business [3,4].

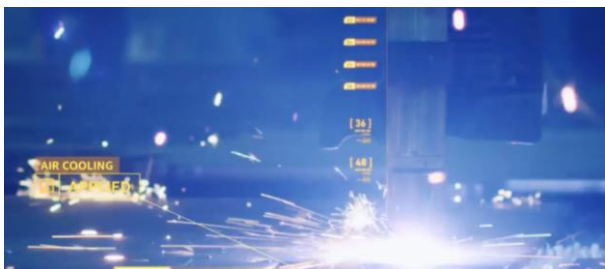


Fig. 5. Environmental control and top quality as basic conditions

### 3.6 Worker health and safety

The greatest wealth of production processes is man, as its initiator, creator, designer and executor. For these reasons, the value of production processes is reflected in the fact that people are safe in its implementation. Occupational safety, health care, application of protective measures and equipment are today an

integral part of production processes and business policy of the company. A large number of companies put this in the foreground in order to raise the quality level of employees to the highest level. In addition to all indicators, they represent an important criterion for attracting young people to be their active factor.



Fig. 6. Human resource and team work is imperative

Although the technological level of production processes has been significantly raised, it is inevitable that errors occur both on individual components and their assemblies. The FMEA method represent early identification of the place of occurrence of the error, determination of its severity according to the consequences, frequency of occurrence and assessment of the possibility of detection are the basis for determining the priority value of the risk [5].



Fig. 7. The real product and implementation FMEA

The goal is for the observed error to be evaluated, recorded and unrepeatable so that the customer receives a product without error with the projected level of quality. The digital twin represents a big step forward where the real product and potential places of its failure are monitored on a virtual model. In a large number of samples, the occurrence of individual errors is minimized, but if this error is repeated, without its processing and the opportunity to change the process parameters based on it, then this is a problem [4,5].

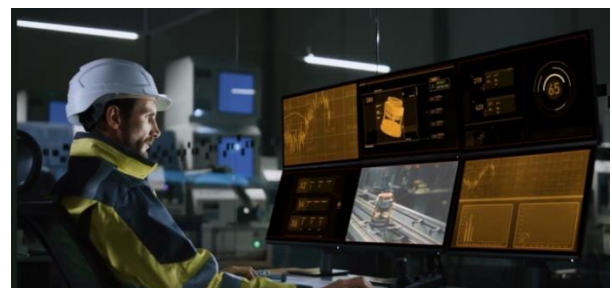


Fig. 8. Monitoring and comparison of real process and key parameters on real and virtual model

#### 4.0 CONCLUSION

Industry 4.0 is definitely a revolutionary approach to manufacturing techniques. The concept will push global manufacturers to a new level of optimization and productivity. Not only that, but customers will also enjoy a new level of personally customized products that may have never been available before. As mentioned above, the economic rewards are immense.

However, there are still many challenges that need to be tackled systematically to ensure a smooth transition. This needs to be the focus of large corporations and governments alike. Pushing research and experimentation in such fields are essential.

#### 5.0 REFERENCES

- [1] Drath, R. & Horch, A. (2014). Industrie 4.0: Hit or Hype? *IEEE Industrial Electronics Magazine*, 8, 56-58. <https://doi.org/10.1109/MIE.2014.2312079>
- [2] Pfeiffer, S. (2017). The Vision of "Industrie 4.0" in the Making a Case of Future Told, Tamed, and Traded. *Nanoethics*, 11, 107-121. <https://doi.org/10.1007/s11569-016-0280-3>
- [3] Qin, J., Liu Y., & Grosvenor, R. (2016). A *Categorical Framework of Manufacturing for Industry 4.0 and Beyond*. *Procedia CIRP*, 52, 173-178. <https://doi.org/10.1016/j.procir.2016.08.005>
- [4] Kagermann H., Wahlster W., Helbig J., "Recommendations for Implementing the Strategic Initiative Industrie 4.0" 2013.
- [5] Kagermann, H. Anderl, R. Gausemeier, J. Schuch, G. Wahlster, W., "Industrie 4.0 in a Global Context" ACATECH 2016.

**Authors: Full Prof. Sasa Randelović, Full Prof. Vladislav Blagojević, M.Sc.Nikola Kostić,** University of Nis, Faculty of Mechanical Engineering, Chair of Production and Information Technology, Aleksandra Medvedeva, 14, 18000 Nis,

E-mail: [sassa@masfak.ni.ac.rs](mailto:sassa@masfak.ni.ac.rs);

[vlada@masfak.ni.ac.rs](mailto:vlada@masfak.ni.ac.rs); [kostic94nikola@gmail.com](mailto:kostic94nikola@gmail.com)

Phone.: +381 18 500-702, Fax: +381 18 500-699.

**Assoc. Prof. Mladomir Milutinović, Assist. Prof. Dejan Movrin,** University of Novi Sad, Faculty of Technical Sciences, Department of Production Engineering, Trg Dositeja Obradovića 6, 21000 Novi Sad, Serbia,

E-mail: [mladomil@uns.ac.rs](mailto:mladomil@uns.ac.rs); [movrin@uns.ac.rs](mailto:movrin@uns.ac.rs)

**ACKNOWLEDGMENTS:** This research was financially supported by the Ministry of Education, Science and Technological Development of the Republic of Serbia (Contract No. 451-03-9/2021-14/200109).

Milosavljević, M., Morača, S., Fajsi, A.

**INDUSTRY 4.0: A REVIEW OF TECHNOLOGY INFLUENCE ON BUSINESS MODELS**

**Abstract:** *In today's business environment, companies must be able to quickly readapt, remodel and adjust their business models to be able to respond to volatile market demands. In that sense collecting data from various sensors and devices, analyzing and applying algorithms to facilitate process control, and machine learning plays a significant role in the process of digital transformation as well as reaching higher levels of productivity, flexibility, and the delivery of business benefits. The purpose of this study is to present a brief literature review with special emphasis on companies' agility from adopting Industry 4.0 technologies, while simultaneously examining their influence on companies' business model innovation. Although technological advancements are seen as the crucial operation key points (OKPs), to maximize their advantages, companies' focus on their adequate technological, organizational, and business environment mustn't be put aside in the process of digital transformation.*

**Key words:** *Industry 4.0, digital transformation, business model, information communication technologies*

**1. INTRODUCTION**

Concepts of Industry 4.0, especially the influence of advanced information and communication technologies (ICT) that come along, are being carefully analyzed in both research and business communities. These technologies aided by software, sensors, processors as well as different communication mediums [1] enable interconnectedness between people, information, and objects due to the convergence of physical and virtual worlds [2]. It is noteworthy that these technologies boost companies' overall efficiency, increase productivity and enhance optimization and simulation abilities [3], consequently changing the traditional business models and encouraging the development of the new digital-based market models [4]. The usage of these technologies in industrial systems and their increased implementation into daily operations will affect job profiles, as well as the decision-making, and planning processes. Therefore, Industry 4.0 will continue to change future doing business and jobs, which will prompt new business models, and will further affect both on industry and markets, eventually influencing the entire product lifecycle, yielding new production methods and business strategies, while simultaneously empowering optimization of workflow and gaining competitive advantages [4]. This paper will pinpoint how some of the novel technologies drive and influence changes in the business environment, as well as the key advantages from their deployment into companies' daily operations.

**2. INDUSTRY 4.0 TECHNOLOGIES**

Sketchy, unstructured, and incomplete information, can severely affect both management and engineering within the company. Furthermore, constantly changing business environment, novel technologies and new ways of doing business influence organizational changes and require internal processes reengineering.

The Industry 4.0 technologies are supposed to make companies' structures and processes more flexible, and furthermore to enable an analysis of large amounts of real-time data, as well as improvement of strategic and operational decision-making activities [5]. However, in order to leverage this information, companies need to make significant investments in adequate types of technologies and equipment to be able to gather, process, analyze and use in their decision-making processes. With the aid of the new technologies companies have the potential to achieve higher levels of automation, interoperability, actionable insights, and information transparency [6]. According to some authors [7, 8], Industry 4.0 technologies are based on the usage of the Internet of things (IoT), Big Data Analytics (BDA), Cloud Computing, Artificial Intelligence (AI). In the following sections, we will showcase, potential benefits and obstacles from utilizing the aforementioned technologies, as well as related challenges and issues that follow.

**2.1. Internet of Things (IoT)**

Research [9] refer to IoT as the resulting global network of interconnected smart objects aided by Internet technologies; the set of supporting technologies required to fulfill such a vision (e.g., RFIDs, sensor, actuators, M2M communication, mobile phones, etc.) and; the group of services and applications supporting these technologies to create new market opportunities and business models. Its rapid development and increasing use are believed to help different industries to enhance their process accuracy, precision, optimize their cost structure and leverage from real-time information, and monitoring of key performance indicators (KPIs) which will facilitate the decision-making process [10], making it more data-centric. Given its complexity and broad means of use, to fully leverage and benefit from IoT, there are many technological challenges facing its utilization. Some of the main challenges are presented in [11], where

security and privacy issues are pinpointed as the main challenges to overcome in the future. Besides these problems, due to its broad means of use, IoT has found its application in different areas such as supply chain, logistics, transportation, healthcare, smart cities, environmental monitoring and management, automation, traffic management, etc.

## **2.2. Big Data and Analytics (BDA).**

Collected data, most commonly are not in a format that is analysis-ready. Effective processing of big data can be related to several issues such as capturing, transferring, storing, cleaning, analyzing, filtering, searching, securing, visualizing, etc. which resulted in the emergence of an array of novel systems to address these and other potential big data issues [12]. This process requires the usage of different tools and techniques such as correlations, cluster analysis, filtering, decision trees, Bayesian analysis, neural network analysis, regression analysis, textual analysis [13]. In this regard, another issue related to lack of coordination between database systems that host the data and provide SQL querying, with analytics packages that perform various forms of non-SQL processing, such as data mining and statistical analyses. Besides, there are plenty of possible error sources such as computer systems troubleshooting, models which always have certain assumptions, and eventually analysis output based on inaccurate or incorrect data [14], which can seriously affect decision-making processes and result in business underperformance.

## **2.3. Cloud Computing**

According to the National Institute of Standard and Technologies [15], cloud computing can be defined as: “a model for enabling ubiquitous, convenient, on-demand network access to a shared pool of configurable computing resources (e.g., networks, servers, storage, applications, and services) that can be rapidly provisioned and released with minimal management effort or service provider interaction.” As stated by Hwang et al. [16], within the cloud computing environment, the service content such as the amount of storage, transmission speed, degree of data encryption, etc., can be modified by service providers following the needs of end-users. Advantages of using these services refer to energy efficiency, optimization of hardware and software resource utilization, elasticity, performance isolation, and flexibility [17]. Main challenges regarding cloud computing are thoroughly analyzed [18], where the author states, that additional issues can be related to data placement and content distribution, privacy, network setup, billing, applications’ requirements, flexibility, usability, and data flow. Some of the main cloud computing services providers are Amazon Web Services (AWS), Google Cloud, SAP, IBM Cloud, Salesforce, Microsoft Azure, etc.

## **2.4. Artificial Intelligence (AI).**

AI researchers have identified several fields of its use, varying from education, healthcare, manufacturing, supply chain management, etc., whilst

indicating its potential to eventually replace human labor. In that sense, it is said, that AI aided technologies, would control real-time processes, while simultaneously making manual processes more efficient [19]. Therefore, AI along with machine learning (ML) is continuing to transform the existing managerial practices used for performance analysis, development of new approaches, and decoding of the ever-changing business environment [20]. On the other hand, information companies such as Amazon, are able to forecast future purchases of their customers, before they even make a purchase and use this data to enhance their inventory management. Be that as it may, the degree of AI well-functioning is highly dependent on collected and processed data, which requires a lot of resources and lacks flexibility in case of minor changes.

## **3. TECHNOLOGY INFLUENCE ON BUSINESS MODELS**

Industry 4.0 keeps remodeling the existing ways of doing business and value creation, streaming it towards the digital era whilst emphasizing companies’ agility as one of the main elements responsible for enhanced relationships with its customers, more collaborative environments, or new products and services development. In this spirit, the improvement of companies’ capabilities, in addition, requires an increase of manager's cognitive agility which enhances imagination of newly established business patterns for creating and comprehending new sorts of value-creating products and services [21]. Accordingly, the value chain is becoming more reactive, given the fact that Industry advocates the integration between customers and manufacturers, and therefore empowering their relationship allowing the creation of flexible business models in accordance with market requirements [22] (Fig. 1) [23]. Considering that

Industry 4.0 relates to “networked manufacturing”, “self-organizing adaptive logistics” and “customer integrated engineering”, appropriate business models will primarily be associated with particularly dynamic business networks than solely on one company [24]. The systems integration adjacent to the growing digitization of industrial production is likely to result in the creation of newly established digital market models [25]. In that sense, prediction models, have to be based on interconnected parameters (varying from different sources), but with clear, distinctive, and the mutual influence on process efficiency and fulfillment of market demands. This is possible to achieve with the aid of the aforementioned technologies, but on the other hand, it is questionable whether investments in these types of technologies will enable the development of usable and realistic predictive models. Besides that, swift changes also need to be taken into consideration, since they will require the development of the new models, which is both expensive and time-consuming due to additional training and preparation of adequate AI data. In order to secure achieving of competitive advantages, regarding the shortage of delivery times, boosting organizational productivity, and optimal



quality, despite the changes in the business environment, companies have to thrive towards increasing the overall flexibility of their business processes referring to their supply chain management, equipment, and comprehensive employees' strategy. This also depends on the company's partners' abilities to establish a mutual connection and adequately deploy novel technologies in both supply chain management and distribution network.

• **Supply chain management.** According to Swaford

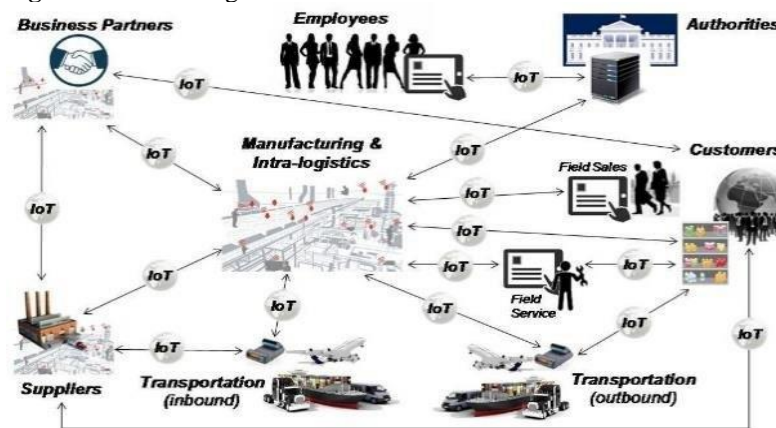


Fig. 1. Running business – Industry 4.0 [23].

- **Equipment.** The usage of modern manufacturing technologies, such as advanced software and sensors have increased the reliability and flexibility of manufacturing organization by cost reduction and product creation utilizing less input (energy, resources, human work, etc.) followed by the ability to quickly respond novel customer demands regarding products' top quality, customization and personalization, time to market reduction, as well as reduced product delivery time [27].
- **Employees.** Novel technologies significantly contribute to the increase of process automation and operations complexity, and hence impose both the necessity for employees' higher level of competencies and adequate training programs from different areas to enhance their multi-tasking skills. Consequently, a new model of work organization emerges and imposes the transformation of communication patterns and business processes which lead to customization or in some cases creation of new IT structures, new ways of employees' management, etc.

#### 4. FINAL REMARKS

It can be concluded that Industry 4.0, comes along with different types of technologies, which are proven to have a positive effect on companies' performance. These technologies allow companies to better organize their workflow processes, collect various information throughout an entire product's lifecycle, to better understand their customers' needs and demands, as well as better data management. Although information and data management are seen as crucial elements in today's business environment, some of the questions arising are related to filtering the right kind of data,

et al. [26], an agile supply chain helps companies to quickly adapt to new marketplace circumstances and therefore ensuring the achievement of competitive advantages. Apart from that, more flexible supply chain management, allows companies to be more customer-centric as well as to better synchronize their supply with their current demand which is of utmost importance for heterogenous and volatile marketplaces.

data credibility, differentiation of valid and spam data, etc. Therefore, data analysis can be considered more demanding than its simple identification and collection, since it requires highly skilled employees to deploy and incorporate the analysis results into the decision-making processes. Rapid changes in the business environment, require more agile structures, which allow companies to more easily adapt to new market circumstances. The formation of comprehensive and homogeneous IT and AI structures, in business network environments, allows the integration of different companies, as well as different departments which eventually leads to better communication and collaboration. Horizontal integration empowers the formulation of a structure which allows manufacturers, suppliers, and end consumers to actively collaborate and exchange information in the real-time context, thanks to the interconnectedness among process, machines, and systems. Vertical integration, on the other hand, requires ICT infrastructure within a company, which allows collected data by different actuators and sensors to be available and visible both to management and manufacturing, which enhances the real-time decision-making processes. Due to changes in an entire value chain, companies have to be able to timely readapt their business models in order to stay competitive, especially in volatile markets.

#### 5. REFERENCES

- [1] Bahrin, M. A. K., Othman, M. F., Azli, N. H. N., & Talib, M. F.: *Industry 4.0: A review on industrial automation and robotic*. Jurnal Teknologi, 78, pp. 6-13, 2016.
- [2] Thoben, K. D., Wiesner, S., & Wuest, T.: "*Industrie 4.0*" and smart manufacturing-a review of research

- issues and application examples, International journal of automation technology, 11(1), pp. 4-16, 2017.
- [3] Wollschlaeger, M., Sauter, T., & Jasperneite, J.: *The future of industrial communication: Automation networks in the era of the internet of things and industry 4.0*, IEEE industrial electronics magazine, 11(1), pp. 17-27, 2017.
- [4] Pereira, A. C., Romero, F.: *A review of the meanings and the implications of the Industry 4.0 concept*, Procedia Manufacturing, 13, pp. 1206-1214, 2017.
- [5] Porter, M. E., Heppelmann, J. E.: *How smart, connected products are transforming competition*, Harvard business review, 92(11), pp. 64-88, 2014.
- [6] Haleem, A., Javaid, M.: *Additive manufacturing applications in industry 4.0: a review*, Journal of Industrial Integration and Management, 4(04), 2019.
- [7] Tao, F., Cheng, J., Qi, Q., Zhang, M., Zhang, H., & Sui, F.: *Digital twin-driven product design, manufacturing and service with big data*, The International Journal of Advanced Manufacturing Technology, 94(9), pp. 3563-3576, 2018.
- [8] Wang, S., Wan, J., Li, D., & Zhang, C.: *Implementing smart factory of industrie 4.0: an outlook*, International journal of distributed sensor networks, 12(1), pp. 1-10, 2016.
- [9] Atzori, L., Iera, A., Morabito, G.: *The internet of things: A survey*. Computer networks, 54(15), pp. 2787-2805, 2010.
- [10] Rajput, S., & Singh, S. P.: *Identifying Industry 4.0 IoT enablers by integrated PCA-ISM-DEMATEL approach*, Management Decision, 2019.
- [11] Hossain, M. M., Fotouhi, M., Hasan, R.: *Towards an analysis of security issues, challenges, and open problems in the internet of things*. In 2015 IEEE world congress on services pp. 21-28, IEEE, 2015.
- [12] Baeza-Yates, R.: *Big data or right data?*. In AMW, 2013.
- [13] Davis, C. K.: *Beyond data and analysis*, Communications of the ACM, 57(6), pp. 39-41, 2014.
- [14] Labrinidis, A., Jagadish, H. V.: *Challenges and opportunities with big data*, Proceedings of the VLDB Endowment, 5(12), pp. 2032-2033, 2012.
- [15] *NIST Cloud Computing Program – NCCP*. (20, November 2015). NIST. Retrieved June 18, 2021 from <https://www.nist.gov/programs-projects/nist-cloud-computing-program-nccp>
- [16] Hwang, J. J., Chuang, H. K., Hsu, Y. C., & Wu, C. H.: *A business model for cloud computing based on a separate encryption and decryption service*, In 2011 International Conference on Information Science and Applications, pp. 1-7, Jeju Island, IEEE, 26 April, 2011.
- [17] Botta, A., De Donato, W., Persico, V., & Pescapé, A.: *Integration of cloud computing and internet of things: a survey*. Future generation computer systems, 56, pp. 684-700, 2016.
- [18] Shamsi, J., Khojaye, M. A., Qasmi, M. A.: *Data-intensive cloud computing: requirements, expectations, challenges, and solutions*, Journal of grid computing, 11(2), pp. 281-310, 2013.
- [19] Zhong, R. Y., Xun X., E., Klotz, Stephen T. Newman: *Intelligent manufacturing in the context of industry 4.0: a review*, Engineering 3(5), pp. 616-630, 2017.
- [20] Kaplan, A., & Haenlein, M.: *Rulers of the world, unite! The challenges and opportunities of artificial intelligence*, Business Horizons, 63(1), pp. 37-50, 2020.
- [21] Ruohomaa, H., Kantola, J., & Salminen, V. (2017, July). *Value network development in Industry 4.0 environment*, In International Conference on Applied Human Factors and Ergonomics, pp. 28-39, Springer, Cham, 2017, July.
- [22] Geissbauer, R., Vedsø, J., & Schrauf, S. (2016, May 09). *A strategist's guide to Industry 4.0*, Retrieved June 28, 2021, from <https://www.strategy-business.com/article/A-Strategists-Guide-to-Industry-4.0>
- [23] *The Transition Towards Industry 4.0: Business Opportunities and Expected Impacts for Suppliers and Manufacturers - Scientific Figure on ResearchGate*. Available from: [https://www.researchgate.net/figure/Business-scenario-of-Industry-40-17\\_fig1\\_319389171](https://www.researchgate.net/figure/Business-scenario-of-Industry-40-17_fig1_319389171) (accessed 19 Jun, 2021)
- [24] Prause, G.: *Sustainable business models and structures for Industry 4.0*, Journal of Security & Sustainability Issues, 5(2), pp. 160-169, 2015.
- [25] Zezulka, F., Marcon, P., Vesely, I., & Sajdl, O.: *Industry 4.0—An Introduction in the phenomenon*, IFAC-PapersOnLine, 49(25), pp. 8-12, 2016.
- [26] Swafford, P. M., Soumen G., & Nagesh M.: *The antecedents of supply chain agility of a firm: scale development and model testing*, Journal of Operations management 24(2), pp. 170-188, 2006.
- [27] Edwards, David K.: *Practical guidelines for lean manufacturing equipment*, Production and Inventory Management Journal 37(2), 1996.

**Authors: M.Sc. Marko Milosavljević, Full Prof. Slobodan Morača, Teach. Assist. Angela Fajsi**, University of Novi Sad, Faculty of Technical Sciences, Department of Industrial Engineering and Management, Trg Dositeja Obradovića 6, 21000 Novi Sad, Serbia, Phone.: +381 21 485-23-24, Fax: +381 21 454-495.  
E-mail: [marko.milosavljevic073@gmail.com](mailto:marko.milosavljevic073@gmail.com); [moraca@uns.ac.rs](mailto:moraca@uns.ac.rs); [angela.fajsi@gmail.com](mailto:angela.fajsi@gmail.com)

But, A., Canarache, R., Gal, L.

## IMPROVE PRODUCTIVITY THROUGH DIGITAL MANUFACTURING

**Abstract:** *In the future the digitalization and "Industry 4.0" will be in every step of the product lifecycle from design to the manufacture, service, and maintenance.*

*Through digitalization, the companies will be able to operate and program the complex CNC machine tools that will be ready to respond more flexibly to the market demands and at the same time to boost their productivity.*

*Work preparation and production can be breaking down further into additional process steps, ranging from tendering to quality assurance.*

*The demand for digitalization solution can be illustrated thru the following targets and questions what every production company must define and establish:*

*1. How long time will be the part on the machine to be manufacturing*

*2. Is that CNC machine tools (what is able and have the technical characteristics) available*

*3. Are necessary new cutting tools for this new job*

*4. The CNC operator is familiar with the CNC control equipment*

*5. Does the workpiece tolerance correspond with the customer specifications*

*Is not so easy to link up all this requests and to find the best solutions in time and to have high productivity. Digital manufacturing will give us the preliminary units costs and delivery deadline that must be determined to be able to tender for a job correctly.*

*Today, the amount of time a workpiece will require for machining can be calculated quickly reliably and very important, without trial runs, using CNC simulation solutions.*

*This recommendations from our paper can be an answer at the production companies and the advantage of this implementations is that can be made step by step.*

*The solution of this implementation should be in concordance with the company's requirements and resources.*

**Key words:** *digitalisation, Industry 4.0, cnc*

### 1. INTRODUCTION

Digitalization -about used terminology Industrial Internet,[2] is a term and refers to the integration of complex physical machinery with networked sensors and software.

The industrial Internet draws together fields such as machine learning, big data, the Internet of things and machine-to-machine communication to ingest data from machines, analyze it (often in real-time), and use it to adjust operations.

Industry 4.0 [2] is a project in the high-tech strategy, which promotes the computerization of traditional industries such as manufacturing. The goal is the intelligent factory (Smart Factory), which is characterized by adaptability, resource efficiency and ergonomics as well as the integration of customers and business partners in business and value processes.

Technological basis are cyber-physical systems and the internet of things. Experts believe that Industry 4.0 or the fourth industrial revolution, could be a reality in about 10 to 20 years. Meanwhile, in the United States, an initiative known as the Smart Manufacturing Leadership Coalition is also working on the future of manufacturing.

Industry 4.0 as part of networked world business networks smart products supporting actively manufacturing process network of human beings,

machines and resources factory interfaces with smart mobility, smart logistics and smart grid.

It is about collaboration productivity!

Industrial internet in the future next natural development step is to expand from virtualization of manufacturing to virtualize the whole company and its ecosystem. Snapshot from current company performance can be basis for simulation. Through simulations can be tested different future scenarios: raw material price, energy price, production machinery capacity and productivity, transportation cost, etc. As a result, best fit can be played in production.

### 2. EXPLANATIONS AND HOW TO WORK

Digitalization is fundamentally changing our working environment and society (Fig. 1). Billions of intelligent devices and machines generate massive amounts of data, creating a bridge between real and virtual worlds. Turning these vast amounts of data into value is a real source of competitive advantage for both businesses and economies. However, the level of preparedness for this change varies widely from country to country.

Upswing for Romania trough digitalization:

1. Can't build a house without foundation. Foundation would be great education. Industry professionals are needed. The ones who can play the virtual factory simulations (Smart Factory Game).

2. Part of foundation is virtual factory builders. Could there even be synergies with game industry? Finally, it's only a question of building a strategy game linked to parameters from real business.



Fig. 1. Digitalization changing our working environment.

3. Romania is fertile soil for implementation, pioneers can be found in industry.

Industry 4.0 in products workshop products, parts, assemblies, and end user products will benefit from in all its varieties and applications. New engines carry a lot of digital information as well monitoring of the machine condition is one of the approaches where information technology is widely used. Collecting this data from several engines gives valuable information for further development of the engine itself and above all new value adding services.

New technologies - like Industry 4.0- enable new products and new services interaction.

New world order generates new needs for products and to create new business opportunities.

Today, Digitalization drives the evolution of demand:

1. Artificial Intelligence- Purpose,
2. Digital-Agility,
3. Industry -Efficiency,
4. Trade- Scale,
5. Agriculture-Survival. Fig. [2]

### 3. THE TARGETS

Technologies that shape the digital age. The breadth and depth of these changes herald the transformation of entire systems of production, management, and governance. The targets are:

I. VELOCITY Mobile Internet, cloud Technology, Processing power, Big Data, New energy supplies and technology. 3 Internet of things 4. Sharing economy, crowd sourcing.

II. SCOPE: Robotics, autonomous transport, artificial intelligence, advance manufacturing, 3D printing, advance materials, biotechnology,

III. SYTEMS IMPACT: Future of jobs survey, World Economic Forum.

Why is everyone talking about digital? Digital developments are disrupting almost every industry in every country Top mature industry by 2020 Top new industries by VELOCITY Aerospace & Defense Chemical, Materials & Food Electronics Oil & Gas Engineering & Construction, Pharmaceuticals &

Healthcare Auto mobile ICT Energy & Power Urban Logistics Alternative energy 3D printing Cyber security Big Data Managed services Virtual commerce Cloud computing 1.

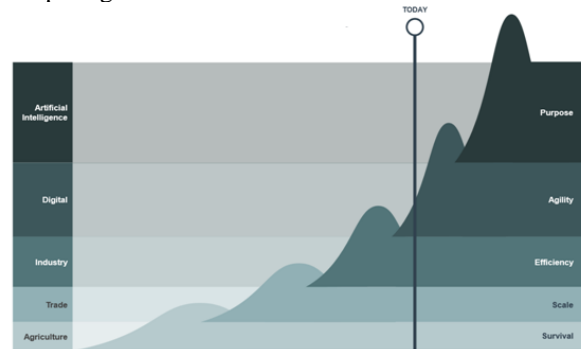


Fig.2 Digitalization drives the evolution of demand.

SCOPE Metals & Mining Waste management Wellness industry 1. SYSTEMS IMPACT Market size potential

(Source: [3] Frost & Sullivan, Mega trends (2015); Bloomberg industry data)

The two important data's who must take in consideration in production are: the unit costs and the delivery deadline.

Digitalization is very competitive in this area. Now the time of manufacturing can be calculated reliably and very fast. For this is not necessary to have any trial run, only to use the CNC simulation capabilities of the CAM software. Together with the time of preparation (who at every workshop is different but know by every CNC operator particular) we can establish the time for delivery.

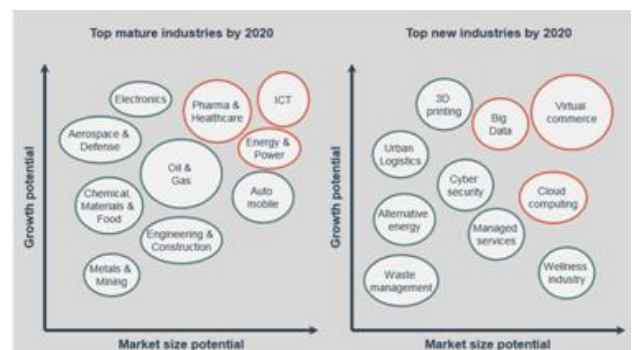


Fig.3. Industrial's area and new branch of digitalization

To gain an overview of machine performance and utilization, operators can consult the overall equipment efficiency indicators, which are read out from the CNC. Machine utilization can be displayed on a PC or a mobile data device using the software from the modern CNC equipment.

Production managers can use these data to assess the availability of the relevant machine.

It allows to find out the exact status of an order online during a shift.

Thanks to this transparency can respond quickly to machine malfunctions and shift the production of urgently needed part to another machine.

G code and graphical programming is an option for simpler individual work pieces.

The best and more advantages will be obtained to use the offline programming for more complex workpieces or to increase the output of the machinery and make production more flexible.

But the solution with an integrated CAD/CAM -CNC process chain is even more efficient.

One most important factor in resource planning for CNC production is tool availability. Today are programs who can provide a real -time overview of availability and prevent time-consuming searching during production. With this option, the user can immediately see the required tools are in the desired machine. More than that, are software (yet integrated in the numerical control) who can quick and reliable compare tool requirements for specific manufacturing jobs with stocks of tools throughout the factory. The tool requirement list is then automatically sent to the tool setting device, and the identified geometric data are sent to the CNC's tool offset memory. If there are any tool shortages, the data are immediately forwarded to higher-level ordering systems.

Users have long become used to the digital word when it comes to private means of communication. A similar look and feel in the control system make for easy CNC operation. The new numerical control equipment's have a user-friendly operator interface that is based heavily on the operating philosophy of PCs and the gesture-based operation that users are familiar with from Smartphone's and tablets is now available on the machine.

#### 4. CONCLUSION

If the machine manufacturer's service staff need to access data on the machine or CNC externally, this immediately raises the question of data security. Now the digitalization maintenance allows the monitoring of machine status, with the machine raising the alarm in the event of a fault. This shortens the times required for diagnostics and minimize serious consequences such unforeseen machine downtimes and major damage. It also means that maintenance work can be carried out proactively, eliminating unnecessary periods of machine downtime.

Collaboration has never been easy, and companies have long struggled to solve collaboration challenges. However, as products and development ecosystems continue to get more complex, collaboration needs have increased. Unfortunately, poor collaboration comes at a high price. It results in delays, errors, and increased costs, all of which have an impact on profitability. The good news is that digitalization technologies, such as the cloud and innovation platforms, can help to significantly overcome barriers and improve design collaboration across the enterprise.

Recommendations and the steps based on industry experience are:

- Understand the true cost of poor collaboration on both engineers and the entire company.
- Invest in digitalization improvements to increase engineering efficiency.
- Recognize the significance of collaboration requirements on engineers from the number of people involved, different departments, and processes impacted.
- Ensure excellent collaboration between engineering and manufacturing to overcome knowledge gaps and support seamless hand-offs.
- Support effective collaboration between design engineers and simulation analysts to empower engineers to catch problems and design more competitive products.
- Considered digitalization technologies, such as cloud and an innovation platform, to support and enable better collaboration processes

#### 5. REFERENCES

- [1] But Adrian-(2009) "Advanced machine-tools and manufacturing systems." Editura Politehnica-Timisoara 2009
- [2] Metal Cutting Technology (2016) Training Handbook Sandvik Coromant
- [3] Frost & Sullivan, Mega trends (2015); Bloomberg industry data

**Authors: Ph.D. Eng. Adrian BUT**

POLITEHNICA University of Timișoara, Mechanical Faculty, Department of Materials and Manufacturing Engineering, B-dul Mihai Viteazu nr.1, Timișoara 300222, Romania,

E-mails: [adrian.but@upt.ro](mailto:adrian.but@upt.ro); [adi.but@gmail.com](mailto:adi.but@gmail.com)

**Ph.D. Eng. Radu CANARACHE**

INICAD DESIGN, Bucharest, Str. Popa Tatu nr.27, Romania

E-mails: [radu.canarache@yahoo.com](mailto:radu.canarache@yahoo.com)

**Ph.D. Eng. Lucian GAL**

AUREL VLAICU" University of Arad, B-dul Revolutiei nr 1.Arad, Romania

E-mails: [lucian.gal@gmail.com](mailto:lucian.gal@gmail.com)



Tešić, Z., Kuzmanović, B., Tasić, N., Škorić, B.

**KEY DIMENSIONS FOR SUCCESSFUL APPLICATION OF BUSINESS PROCESS MANAGEMENT MODEL**

**Abstract:** *Business Process Management (BPM) is an approach to change management through business process improvement, encompassing the cycle, from analysis and design to implementation, and control of business processes. Having in mind the focus on business processes, the subject approach can be defined as the achievement of business strategies through the improvement, management and control of essential business [1]. Accepting the idea of the need for further research in this area, a research was conducted, and the results are presented in this article. The offered model is the result of the analysis of theoretical knowledge, experimentally obtained information, as well as the knowledge of competent respondents. The model includes five dimensions (factors) for successful design, implementation and control of business and manufacturing processes. The results of the research show that the selected dimensions of the BPM model are important for the management of the industrial enterprise.*

**Key words:** *Business process, Key Factors, Process Improvement, Model*

**1. INTRODUCTION**

BPM is a structural approach for the analysis and continuous improvement of business processes of the company such as marketing, production, communications and other components. The management of business processes of the organization also refers to many "intangible" factors of business: intellectual property/intellectual capital of the organization, relations with consumers, etc. On the other hand, human capital can be understood as a necessary condition for quality business process management. Process Orientation (PO) includes the focus of managers and employees on business processes, business process mapping and process standardization, which significantly affects process performance and customer-focused performance [1]. Many authors believe that there are challenges and limitations in applying the principle of process orientation to an operational organization. Total Quality Management (TQM), Process Improvement (PI) and Business Process Reengineering (BPR) are some of the most commonly used approaches in increasing the application of business process orientation. The most important role is played by the BPM approach which has managed to incorporate many positive aspects of previous approaches.

BPM is more than business process improvement and reengineering, more than process design and more than software applications. It is an integral part of management that includes the implementation, execution and analysis of business processes [simulation]. BPM is a field of knowledge that contains methods, techniques and tools for the design, execution, control and analysis of business processes [2]. This research provides several important theoretical and managerial contributions that lead to better understanding of the essence of process orientation and business process management approaches. The basic dimensions of the BPM

approach are set, and then the empirical research determines the importance of certain individual dimensions, their relationship and the impact on the maturity of BPM [simulation]. The presented model and the obtained results contribute to the understanding of the role of design, standardization and continuous process improvement as well as improving the efficiency of business processes and improving the effectiveness of industrial and service enterprises.

**2. THEORETICAL FUNDAMENTALS**

BPM brings more capability than ever before to align operational activities with *strategies and goals*. This helps us to focus our enterprise resources on the creation and improvement of customer value. In this way, BPM is set in the center of business processes as critical organisational asset that must be recognized, and developed to deliver value-added products and services to customer.

Most authors that research problems of applying the process approach agree that the BPM approach allows organisations to implement strategies that were set, to design business processes, to implement business process models and to control business processes. When it comes to the choice of dimensions (key factors) for the successful implementation of BPM and PO, there are different opinions, but they do not differ much. The dimensions of BPM approach that are highlighted by notable authors and which are the fundamental basis for the selection of the five dimensions that are key factors for successful design, implementation and control of business processes in accordance with the strategies are shown below:

1. De Bruin in [3]: Strategic approach, Process management (methods), Information technology and standards, Employee management, Business culture;
2. Onega and Ravesteyn in [4]: Processes awareness, Process description, Process

measurement, Process control, Process improvement, Resources and knowledge, Information technology;

3. Vom Brocke at all in [5]: Goal-dimension, Process-dimension, Organisation and Environment-dimension;
4. Kohlbacker and Gruenwald in [6]: Process design and documentation, Process performance measurement, Corporate culture, Organisational structure, Process-oriented HR systems, Coordination and integration;
5. Vom Brocke and Rosemann in [7]: Strategic Alignment, Governance, Methods, Information Technology, People, Culture;
6. Wong at all in [8]: Manager commitment, Employee involvement, IT infrastructure, Strategic alignment, Organisation culture, Organisation performance

The model is made out of five dimensions that are based on business process orientation and which can be a starting point for determining the significance, use and maturity of the BPM approach [simulation]. The selected dimensions are described below.

### **2.1. Strategies and goals**

The set business strategies of the company are the basis of BPM's approach. The strategy of the enterprise in the descriptive approach is understood as planned or actual coordination of main goals and actions of the organisation, in time and space, which constantly connects the organisation with its environment. A mature organisation must be harmoniously connected horizontally and vertically. The goal and performance of a certain assignment must be consistent with the goals and performance of the process, and the goals and performance of the process must be consistent with the strategic goals and performance of the enterprise [8]. The organisations strategy describes how the organisation intends to create sustainable value growth for its owners, consumers, and employees in work processes. Business and production processes will not automatically achieve strategies, they require continuous and efficient management - process-oriented management. Business processes play a key role in achieving strategic, tactical and operational goals using modern technologies and highly educated human resources.

### **2.2. Process design**

Process design includes development of business process models through the company, which should contain detailed descriptions of processes (inputs, activities, outputs). Business and production process models must contain a clearly defined organisational structure of the company, human resources engaged in the execution of processes as well as technical support, primarily information technology, which are used in the execution of enterprise business processes. The models contain designed new business process specifications, detailed views of all activities and tasks, rules and definitions for the exchange of information between organisational units, physical design and IT infrastructure. Designing processes, among other

techniques, contributes to determining the feasibility of projects to improve processes. This enables consolidation of knowledge, identification and formulation of changes, in accordance with future goals and needs of the current situation.

### **2.3. Process measurement**

Process measurement includes continuous observations, monitoring, tracking activities of the organisation and its processes and activities, as well as the effects of these activities in order to gain insight into the amount and speed of progress made while achieving the goals that have been set. The performance of the processes needs to be measured in order to be able to compare the planned values with the realized output values, which gives the possibility to evaluate the strategies and goals of the enterprise. Information obtained through measurement, analysis and evaluation is a necessary condition for sound decision-making for strategic management purposes. Performance measurement consists of a systematic definition and selection (quantitative or qualitative) of measurable indicators, as well as obtaining their measures at certain intervals, the tracking of which enables monitoring achievements and progress in the process of achieving previously set goals.

### **2.4. Process improvement and employee management**

Process improvement represents the stages in which customer requirements are accepted, requirements are realized, success is assessed and customer requirements are constantly checked in order to discover possible improvement activities. The enterprises should focus on eliminating wastes and identifying new areas of improvement. The enablers within the model are the foundation that must be in place if continuous improvement is to be achieved or commenced in the first place. The enablers include: (a) the culture that promotes continuous improvement and innovation; (b) employee focus; (c) integration of continuous improvement; (d) focus on key processes and standardization of best practices [9].

Employee management is a key factor for establishing process flows at an optimal level. Continuous education, training, empowerment, acquisition of knowledge and skills of employees affect the achievement and maintenance of the state of optimization [4]. The participation of the entire company, manager motivation and proper training policies for employees are just some human resource practices necessary to develop a continuous improvement program [9].

### **2.5. Standardized processes and information technologies**

When standardizing its business processes, the enterprise exploits the best practices throughout the company. Standardized business processes in an organisation provide a base for their improvement. Business process models show how they are currently executed and represent the basis for quality repetition of process execution in a future period. A standardized



process includes the knowledge and experience of employees and thus provides a basis for educating and introducing new executors in the realization of the process, and at the same time forms the basis for innovating the process.

Information technology is a significant dimension of the BPM model that provides the basis for the successful introduction of process organization in the enterprise. Information technologies provide identical measurements, which contributes to the preparation of unified reviews and reports that managers need at the level of strategic decision-making, as well as in making decisions at the operational level [9].

### 3. RESEARCH METHOD

To develop a questionnaire, BPM dimensions were operationalized, following the literature sources. Face validity of the questionnaire was conducted with academics, scholars and practitioners, followed by the pilot test, in a small number of companies. Some minor corrections were made, however, there were no major complaints, regarding the instruments length and clarity. Respondent's subjective estimates were collected with a five-point Likert scale. The sample structure consisted of medium and large organisations in the manufacturing industry, the telecommunications industry, and banks. as shown in Table 1.

	Country			Total
	B&H	Croatia	Serbia	
Manufacturing sector	39	58	48	145
Telecommunic. sector	16	16	14	46
Financial sector	22	70	32	124
Total	77	144	94	315

Table 1. Respondent composition by the country

Due to its exploratory nature, this study was based on the variance-based method. Although previously used in numerous studies, to the best of our knowledge, empirical validation of research constructs was rarely the case in the context of the research population. Also, the variance-based method (PLS-SEM) works better in the case of small sample sizes, where, it is unreasonable to presume normality in the underlying data.

### 4. THE MEASUREMENT MODEL

The construct constitution by its respectful manifest variables and reflective nature of research constructs was assessed under confirmatory factor analysis (CFA). According to literature recommendations, the analysis of following factors was conducted: construct reliability (Cronbach's  $\alpha$ ), composite reliability (CR), convergent (CV), and discriminate validity (DV). Path coefficients were tested under the bootstrapping technique, with 5000 subsamples. Determination coefficients ( $R^2$  values) were found to be acceptable, speaking in favour of the research models predictive

power [8]. Validated research model is shown in Fig. 1.

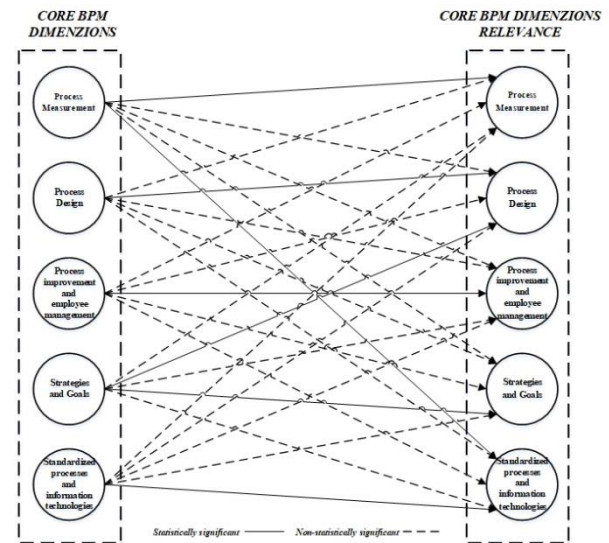


Fig. 1. The structural model results

### 5. DISCUSSION

The result of the analysis of the data is the evidence that all dimensions identified in the literature were accepted as real critical factors according to the tacit knowledge of the experts. The dimensions of the BPM model are important for the establishment of process orientation and are key factors for the successful design, implementation, control and improvement of business processes in accordance with the adopted business strategies of the company. Research has shown that *strategies and goals* is a quite important dimension, which is in line with many studies cited in this article. Strategy planning, strategy implementation, strategic performance management system design are the macro-level factors impacting the BPM effectiveness in measuring and managing business processes.

*Standardized processes and information technologies* is the second most important dimension, which shows that managers are aware of the need to apply information technology as a tool for successful business process management. The need for standardization of business processes is specifically considered in the LEAN concept of business improvement as a key factor for repeating the success in the execution of processes and their continuous improvement. Information technology has a great influence on communication, process execution and acquisition of knowledge from employees, but at the same time employees must have the necessary knowledge and skills to use complex information systems [7].

*Employee management and process improvement* is also a very important dimension, which ensures that the organisation has human resources that have the appropriate knowledge, skills, experience and ability to manage processes under the set strategies and continuously improve business processes. All employees must know what their role is in the process, how their work affects others and how they contribute

to achieving organisational goals. Further, they should understand how individual processes contribute to the overall goals of the organisation. The structural model results show that *Process measurement* is also a significant dimension of BPM. Successful process measurement enables reviewing achieved results as well as it creates the basis for adjusting business processes. Through the measurement of the process, employees are constantly informed about the results in terms of achieving the set goals.

The result of applying the Kruskal-Wallis analysis of variance shows that there are statistically significant differences between the three sectors of activity in terms of deviations (differences, gaps) between assessments of the significance of claims in scale items and the application-representation of these claims in observed process management practice. The results of the Kolmogorov-Smirnov test show that there are no statistically significant differences between the telecommunications sector and the financial sector in terms of deviations (differences, gaps) between estimates of the significance of claims in scale items and the applicability of these claims in the observed process management practice. Differences between the manufacturing sector on the one hand and the telecommunications sector and the financial sector on the other. The results of the Mann-Witney test show that there are statistically significant differences between the manufacturing sector and the telecommunications sector and the manufacturing sector and the financial sector, but that there are no statistically significant differences between the telecommunications sector and the financial sector. These results are consistent with the results of the Kolmogorov-Smirnov test [9].

## 6. CONCLUSION

BPM approach is a collection of methods and tools that allow us to answer questions: what are our processes, how do we design processes, how do we ensure their performance, how do we manage processes and how technologies and human resources should support processes. The importance of BPM for the organisation is the reason for conducting the research presented in this paper. The choice of dimensions as key factors was made based on knowledge collected from theoretical and empirical research of many authors. The identified and analyzed dimensions can be considered as a starting point for organisations and managers who want to successfully implement BPM approach. The results of the research show that in most companies in countries that make up the sample of the survey, the situation is positive in terms of understanding the impact of the BPM approach to the organisation and management of business processes. The selected dimensions of the BPM model were recognized by the surveyed participants and it is shown which dimensions have a greater impact on business process management and which dimensions are more important for the success of process orientation. Future research should focus on determining the importance of business process models in implementing business

process performance management systems.

## 7. REFERENCES

- [1] Van Assen, M.: *Process orientation and the impact on operational performance and customer-focused performance*, Business Process Management Journal, Vol. 24, No. 2, pp. 446-458, 2018
- [2] Lindsay, A., Downs, D., Lunn, K.: *Business processes-attempts to find a definition*, Information and Software Technology, Vol. 45, No. 15, pp. 1015-1019, 2003.
- [3] De Bruin, T.: *Insights into the Evolution of BPM in Organizations*, Proceedings of the 18<sup>th</sup> Australasian Conference, pp. 1-10, AIS Electronic Library (AISeL). Toowoomba, 5-7 Dec 2007.
- [4] Onega, G., Ravesteyn, P.; *Business process management maturity and performance*, Business Process Management Journal, Vol. 26, No. 1, pp. 132-149, 2020.
- [5] VomBrocke, J., Zelt, S., Schmiedel, T.: *On the role of context in business process management*, International Journal of Information Management, Vol. 36, No. 3, 486-495, 2016.
- [6] Kohlbacker, M., Gruenwald, S.: *Process orientation: conceptualization and measurement*, Business Process Management Journal, Vol. 17, No. 2, pp. 267-283, 2011.
- [7] VomBrocke, J.; Rosemann, M. (2010). *Handbook of Business process Management*, Springer-Verlag Berlin, Heidelberg, 2010.
- [8] Wong, W. P., Tseng, M. L., Tan, K. H.: *A business process management capabilities perspective on organisation performance*, Total Quality Management, Vol. 25, No. 6, pp. 602-617, 2014.
- [9] Gudelj, M., Delic, M., Kuzmanovic, B., Tesic, Z., Tasić, N.: *Business Process Management Model as an approach to process orientation*, Int j simul model, Vol. 22, No. 2, 2021.

**Authors: Full Prof. Zdravko Tešić, Assoc. Prof. Bogdan Kuzmanović, Assist. Prof. Nemanja Tasić, Full Prof. Branko Škorić**, University of Novi Sad, Faculty of Technical Sciences, Department of Industrial Engineering and Management, Department of Production Engineering, Trg Dositeja Obradovića 6, 21000 Novi Sad, Serbia, Phone.: +381 21 485-23-24, Fax: +381 21 454-495.  
E-mail: [ztesic@uns.ac.rs](mailto:ztesic@uns.ac.rs); [kbogdan@uns.ac.rs](mailto:kbogdan@uns.ac.rs); [nemanja.tasic@uns.ac.rs](mailto:nemanja.tasic@uns.ac.rs); [skoricb@uns.ac.rs](mailto:skoricb@uns.ac.rs)

**ACKNOWLEDGMENTS:** The results presented in this paper are part of the research within the project "Research of the possibility of applying artificial intelligence in industrial engineering, management and teaching process at DIIM", at the Department of Industrial Engineering and Management, Faculty of Technical Sciences in Novi Sad, University of Novi Sad, Republic of Serbia"

Milošević, M., Lukić, D., Ostojić, G., Lazarević, M., Antić, A.

## APPLICATION OF CLOUD-BASED MACHINE LEARNING IN CUTTING TOOL CONDITION MONITORING

**Abstract:** One of the primary technologies in the Industry 4.0 concept refers to Smart maintenance or predictive maintenance that includes continuous or periodic sensor monitoring of physical changes in the condition of manufacturing resources (Condition monitoring). In this way, production delays or failures are timely prevented or minimized. In this context, the paper present a developed cloud-based system for monitoring the condition of cutting tool wear by measuring vibration. This system applies a machine learning method that is integrated within the MS Azure cloud system. The verification was performed on the data of the calculated central moments during the turning process, for cutting tool inserts with different degrees of wear.

**Key words:** Cloud manufacturing, Machine learning, I4.0, Smart maintenance, Condition monitoring

### 1. INTRODUCTION

A necessary step in achieving the main goal of Industry 4.0 - the creation of smart factories, is the application of smart manufacturing methods, intelligent tools and smart services [1]. For this purpose, the basic task is to conceptualize efficient smart maintenance system as one of the basic technologies that will be applied in smart manufacturing and which bases its functions on monitoring the physical parameters of condition in a manufacturing process. The final goal is to increase the flexibility of manufacturing companies in the direction of developing sustainable manufacturing driven by intelligent services, as well as predict, prevent or minimize delays and potential failures in production.

Novel research in this area has focused on creating a framework for an intelligent manufacturing environment to be used in the implementation of the Industry 4.0 concept [1]. Smart manufacturing uses various methods based on artificial intelligence. Therefore, a number of intelligent tools and services related to monitoring the condition of a production are introduced and applied in a manufacturing process. For this purpose, it is necessary to improve the system for monitoring cutting tool wear in the workspace of the machine tool, i.e. to create a framework for intelligent predictive cutting tool maintenance. This system includes monitoring the condition of cutting tool wear with the vibration measuring equipment. The data collected by measuring the vibration of the tool are analyzed using machine learning methods, which make the base of Smart maintenance technology. In this way, cutting tool failures and unplanned, costly delays in a manufacturing process are timely prevent, remove and eliminate.

### 2. CLOUD-BASED MACHINE LEARNING

Azure Machine Learning Studio allows create and test different machine learning models for a some data set. This is a platform for managing a machine learning system in the cloud. Software, platform, and infrastructure are provided by Microsoft Azure,

supporting numerous programming languages and cloud-based tools and frameworks. By applying ML Studio it is possible:

- Develop a machine learning model using data from one or more sources.
- Transform and analyze data with statistical functions in order to determine the set of results (it is an iterative process in which the correction of parameters changes the results until a efficient trained model is obtained).

Fig.1 shows the basic procedure for applying machine learning for one experiment.

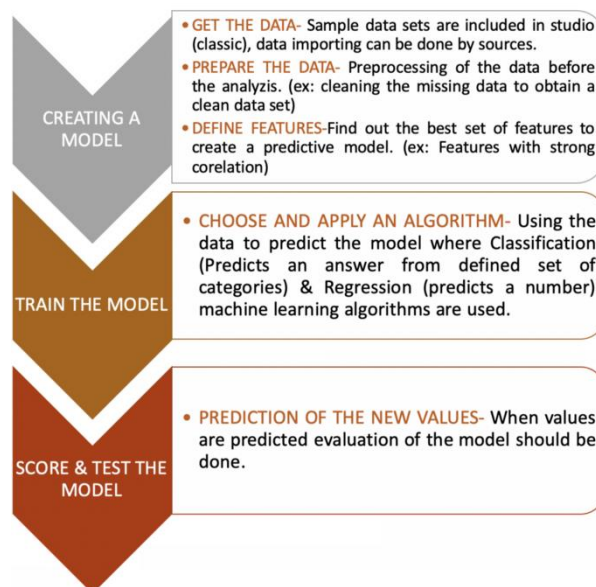


Fig. 1. Azure ML workflow of a machine learning predictive model create [2]

In order to develop a model of predictive analysis, data from one or more sources are used, transformed and analyzed, and a set of results is generated by applying statistical functions. By modifying the different functions and their parameters, the obtained results converge until a trained, efficient model is created. ML Studio provides an interactive, visual workspace for easy

creation, testing, and iterations on a predictive analysis model, Fig.2.

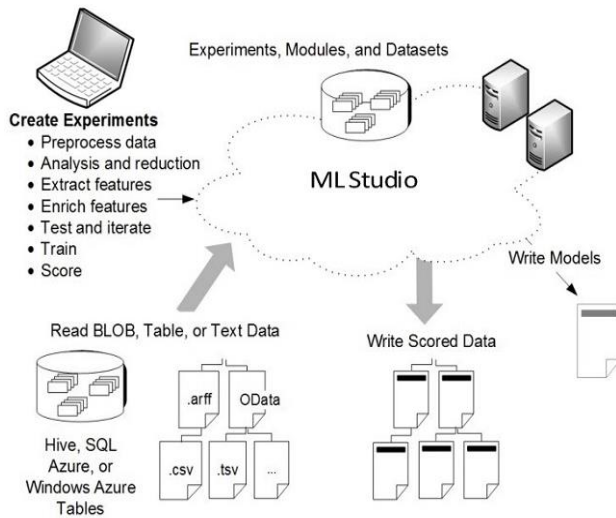


Fig. 2. ML Studio interactive workspace [2]

The user combines datasets and modules for analysis in an interactive workspace, linking them into a machine learning training experiment. When the results are satisfying then the training experiment is translated into a predictive experiment in the form of a web service, so that other users can access to the created model.

The metrics for regression models are generally designed to estimate the amount of error. A model is considered to fit the data well if the difference between observed and predicted values is small. The pattern of the residuals (the difference between any one predicted point and its corresponding actual value) can indicate potential bias in the model [2].

To estimate regression models in the ML Studio, the following metrics are used [2,3]:

- **Mean absolute error (MAE)** measures how close the predictions are to the actual outcomes; thus, a lower score is better.
- **Root mean squared error (RMSE)** creates a single value that summarizes the error in the model. By squaring the difference, the metric disregards the difference between over-prediction and under-prediction.
- **Relative absolute error (RAE)** is the relative absolute difference between expected and actual values; relative because the mean difference is divided by the arithmetic mean.
- **Relative squared error (RSE)** similarly normalizes the total squared error of the predicted values by dividing by the total squared error of the actual values.
- **Coefficient of determination**, often referred to as  $R^2$ , represents the predictive power of the model as a value between 0 and 1. Zero means the model is random (explains nothing); 1 means there is a perfect fit. However, caution should be used in interpreting  $R^2$  values, as low values can be entirely normal and high values can be suspect.

### 3. SENSOR SYSTEM FOR MONITORING OF CUTTING TOOL VIBRATION

The sensor system for monitoring of the cutting tool vibration has the following characteristics:

- Uses adequate sensors to measure vibration acceleration in order to better detect the dynamic characteristics of the cutting process and implement it in the monitoring system.
- Uses algorithms based on artificial intelligence in the field of cutting tool wear monitoring, which are based on the application of a priori knowledge about the condition of cutting tool wear.
- Finds a satisfying model of extracting vectors of input characteristics by applying transformations in the time-frequency domain.

The sensor part of the data pre-processing module consists of an accelerometer for measuring the vibration acceleration mounted on the tool handle, Fig.3. A part of the subsystem for data pre-processing also includes an A/D converter card which receives analog information from the sensor, converts it into digital information and forwards it to the measurement database.

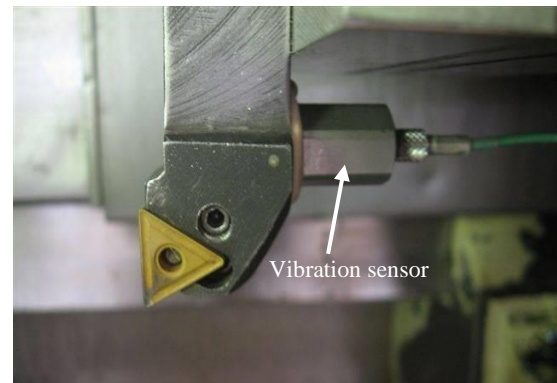


Fig. 3. Installation of sensor for measuring cutting tool vibration

The structure of the preprocessing subsystem can be observed through the three phases shown in Fig.4.

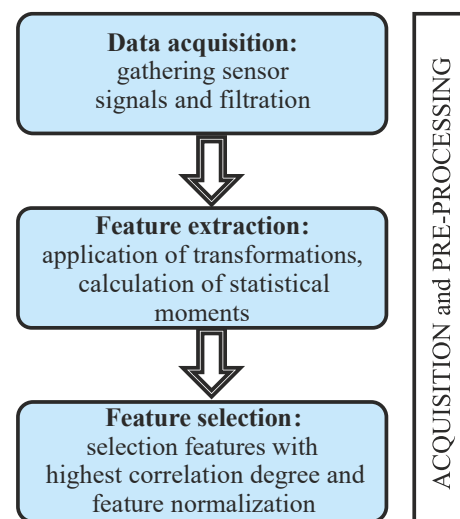


Fig. 4. Pre-processing data collected from sensor

In the first phase, data is collected from the sensor and the filter band is selected.

The second phase is the extraction of the features. The main goal of feature extraction is to significantly reduce the amount of “raw” data collected from sensor in the time and frequency domain. At the same time, relevant tool status information is retained in the selected features. It should be known that different extraction methods have different possibilities for obtaining a set of information about the cutting tool condition by processing the sensor signal.

Nowadays, numerous of industrial measuring systems, which are used to monitoring the wear of cutting tools, are supplied with a built-in signal filter (analog pre-signal processing). With such filters, the frequency band is usually limited to the area that the sensor covers the best. Additional signal filtering (digital pre-signal processing) within the operating range of the sensor is required to attenuate the frequencies of those signals that are an integrative part of the machining process and are not related to tool wear (machine vibration, deformation and material break, friction of material on the sides of the tool...).

The recorded signal was initially processed by a low-pass filter, where the frequency range up to 50 kHz was analyzed due to the characteristics of the applied sensor. A discrete Fourier transform was applied on the filtered signal and the spectral filtered signal shown in Fig.5 was obtained. For further analysis, the upper part of the signal spectrum, the high-frequency part, was separated from the obtained signal spectrogram because in that part of the spectrum there are discriminant features that characterize the condition of the cutting tool wear [4].

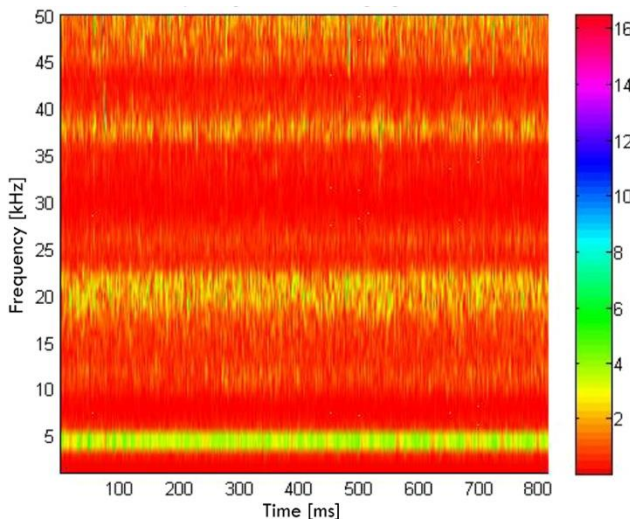


Fig. 5. Filtered signal spectrogram

From the measured results, the orientation of the central moments can be observed by the frequency of formation of chips lamellae, which are obtained by machining with a tool with different degrees of wear of the cutting insert according to individual filter sizes. The exception is the deviation from the orientation of the tool insert with the highest wear, which can be justified by the fact that the cutting insert is full degraded and that this insert has changed the type of chips.

#### 4. ANALYSIS OF CENTRAL MOMENTS OF CUTTING TOOL WEAR IN ML STUDIO

The final output from the data acquisition and pre-processing module are the calculated central moments for the defined scales. The dataset part of the central moments values is shown in Table 1.

Central moments	New tool insert	Wear band (VB) 0,25mm	Wear band (VB) 0,55mm	Full degraded tool insert
<b>Scale I</b>				
Mean	-0.13794819926	-0.12472823415	-0.11436530596	-0.12541743628
Variance	4.33004452633	1.61527765463	0.59496679855	1.00174617608
Skewness	-1.47780598530	-0.96825146333	-0.41422192202	-1.21663428609
Kurtosis	0.11382051257	0.06486639025	0.04587497758	0.12541445114
<b>Scale II</b>				
Mean	-0.22383778716	-0.18795982515	-0.16372339460	-0.18678597239
Variance	3.06549712564	1.23954201485	0.36939617833	0.63390553200
Skewness	-1.17290133182	-0.77377167145	-0.48294701146	-1.06014195154
Kurtosis	0.08259091746	0.05210368214	0.04575176375	0.08659298047
<b>Scale III</b>				
Mean	-0.30352420900	-0.23958936267	-0.20836828770	-0.24357300170
Variance	1.56893965739	0.75401003960	0.17995614785	0.33778890834
Skewness	-1.07040434106	-0.63626635922	-0.57505774822	-1.13331518583
Kurtosis	0.06757675981	0.04609144501	0.04589097543	0.07824611322

Table 1. Segment of calculated central moments at particular scales for various stages of cutting tool wear

The values of the calculated central moments were applied as discriminant features: variance, skewness and kurtosis. These features were chosen because their values have a more pronounced change with the change in the cutting tool wear, i.e. have a better correlation with cutting tool wear compared to other features. By applying the classification in only one scale, a quality classification of the cutting tool wear condition can be performed, especially because there is only one physical source of information, i.e. vibrations.

Dataset on the central moments generated by processing and calculation after analysis of the tool vibration spectrum were recorded and as such were transferred to the ML Studio, Fig.6.

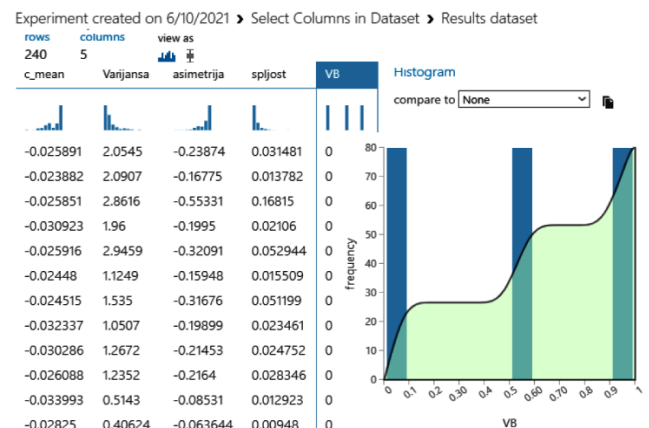


Fig. 6. Segment of calculated central moments imported in ML Studio

The project, actually an experiment was formed in the ML Studio environment, in which the steps of the algorithm for machine learning were defined, also include the metrics of the regression model. Finally, the project was started, after which the validation, training, scoring and evaluation were executed over the dataset on central moments related to the estimation of cutting tool wear, Fig.7.

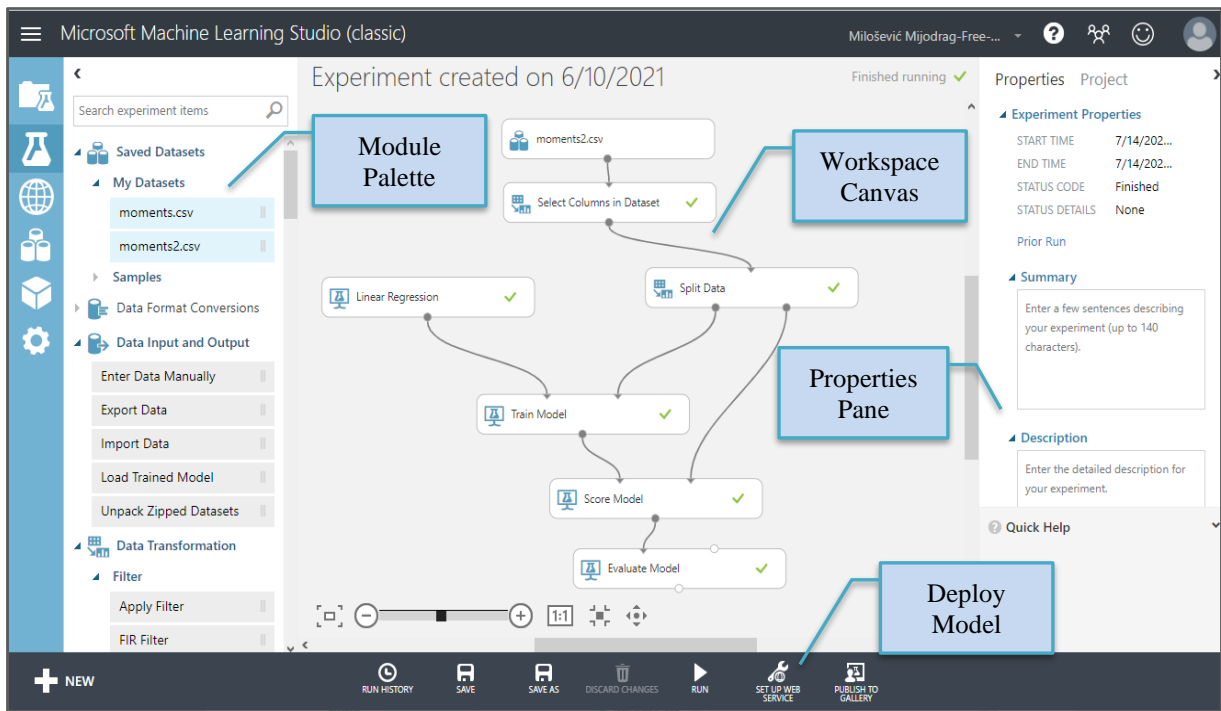


Fig. 7. Validation and evaluation of the machine learning experiment

The developed model of machine learning enables width estimate of the wear band on the cutting tool back surface, depending on the intensity of vibrations. Based on this model, it is possible to generate an intelligent web service that can exist within the system of smart manufacturing and manufacturing based on cloud technologies, Fig.8.

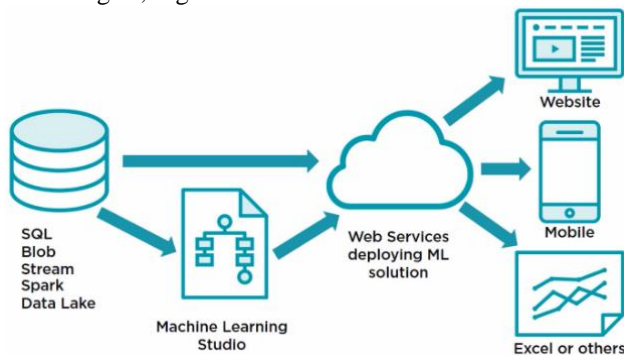


Fig. 8. Web service deployment in Azure ML Studio environment [2]

## 5. CONCLUSION

The presented system for predictive monitoring of the cutting tool wear is classified in the domain of smart predictive maintenance. Continuous sensor monitoring of the cutting tool vibrations in manufacturing process results in the extraction of statistical features and the calculation of central moments. Using the cloud-based machine learning technique, the degree of wear on the back surface of the cutting tool can be estimated on the basis of these features.

The defined framework present the basis for development of intelligent services and methods that are applied in a smart manufacturing environment.

## 6. REFERENCES

- [1] Zhong, R. Y., Xun X., E., Klotz, Stephen T. Newman: *Intelligent manufacturing in the context of Industry 4.0: a review*, Engineering, Vol.3, No.5, pp. 616-630, 2017.
- [2] <https://docs.microsoft.com/en-us/azure/machine-learning>, August 2021.
- [3] Barnes, J.: *Microsoft Azure Essentials - Azure Machine Learning*, The Microsoft Press Store, ISBN:978-0-7356-9817-8, 2015.
- [4] Antić, A., Popović, B., Krstanović, L., Obradović, R., Milošević, M.: *Novel texture-based descriptors for tool wear condition monitoring*, Mechanical Systems and Signal Processing, Vol. 98, pp.1-15, 2018.

**Authors:** Assoc. Prof. Mijodrag Milošević, Assoc. Prof. Dejan Lukić, Full Prof. Gordana Ostojić, Full Prof. Milovan Lazarević, Full Prof. Aco Antić, University of Novi Sad, Faculty of Technical Sciences, Department of Production Engineering, Trg Dositeja Obradovića 6, 21000 Novi Sad, Serbia, Phone: +381 21 485-2346.

E-mail: [mido@uns.ac.rs](mailto:mido@uns.ac.rs); [lukicd@uns.ac.rs](mailto:lukicd@uns.ac.rs); [goca@uns.ac.rs](mailto:goca@uns.ac.rs); [laza@uns.ac.rs](mailto:laza@uns.ac.rs); [antica@uns.ac.rs](mailto:antica@uns.ac.rs)

**ACKNOWLEDGMENTS:** This paper is part of a research on the projects: "Application of smart manufacturing methods in Industry 4.0", No.142-451-3173/2020 and "Application of edge computing and artificial intelligence methods in smart products", No. 142-451-2312/2021, supported by Provincial Secretariat for Higher Education and Scientific Research of the Autonomous Province of Vojvodina.



Section E:  
**MATERIALS, METAL FORMING,  
CASTING AND WELDING**





Bobić, Z., Petrović, B., Kojić, S., Terek, V., Škorić, B., Kovačević, L., Stojanović, G., Terek, P.

## A PRELIMINARY STUDY OF VARIOUS MOUTHWASH INFLUENCE ON NiTi ALLOY CORROSION

**Abstract:** In this study, we examined the behavior of NiTi alloy archwires exposed for 21 days to different corrosive media: artificial saliva, Eludril®, Aquafresh®, and Listerine®. Corrosion was characterized by changes in surface topography. Each specimen was scanned by atomic force microscopy, at 5 locations of 100x100 μm areas, before and after the corrosion tests. Image analysis software was utilized for the analysis of topographic images and calculations of surface roughness parameters. Changes in the surface topography of specimens for all treatments are hardly noticeable. Using the paired T-test, it was revealed that changes in roughness parameters are insignificant. However, on the smooth areas between the scratches, small changes in the surface topography can be noticed. Therefore, quantification and characterization of the corrosion effects, for non-accelerated tests, should be performed on the surface areas smaller than areas used in this study.

**Key words:** NiTi, Corrosion, Atomic force microscopy, Surface topography, Biomaterial

### 1. INTRODUCTION

Nickel-Titanium alloy is a biomaterial that is widely applied for dental orthodontic applications. During orthodontic treatment, practitioners recommended that their patients used various mouthwashes to prevent caries and dental enamel [1]. Through the application Ni-Ti alloy, Ni-Ti wires are exposed to a different environment that could lead to corrosion and release of metal ions into the body. The release of metal ions from dental alloys may have an adverse biological effect, depending on the ion species and its concentrations [2]. The corrosion resistance of biomaterials is very important property because it is one of the factors that directly affect the material biocompatibility. It has been shown that Ni ion release caused by corrosion process, can lead to allergenicity, toxicity, and carcinogenicity [1,3].

Evaluation of NiTi alloy corrosion in conditions that exist in human oral cavity remain a great characterization challenge. Difficulties in the characterization of nanostructures and nano topographic changes of the surface are avoided in many investigations [4–7] by employing accelerated corrosion tests. However, these tests do not sufficiently reassemble the real situations.

Therefore, the aim of this work was to perform non accelerated corrosion test of Ni-Ti wires in various corrosive media, characterize and quantify the occurred changes in topography. In order to achieve this objective, atomic force microscopy (AFM) measurements were performed before and after the corrosion tests.

### 2. MATERIALS AND METHODS

The corrosion performance of NiTi orthodontic wires (Denaturum, Germany) was evaluated in this study. Four prismatic specimens were prepared of the wire in as-received condition. Before corrosion tests, 6

scan locations were marked on each specimen. In order to easily locate the same area after the corrosion tests, these were marked by scratches on the specimen surface. A return to the same location (area) after the corrosion test provides a possibility to characterize the nano topographic changes induced by corrosion processes with a relatively low number of measurements. On the other side, detection of nano topographic changes on the surface requires numerous measurements at randomly selected locations, before and after the corrosion test. Each specimen was exposed to one of four corrosive media of interest (saliva or mouthwash).

Specimen denotations and the corresponding corrosive media are shown in Table. 1.

Specimen	Corrosive medium
Specimen 1	Artificial saliva
Specimen 2	Aquafresh® Mouthwash
Specimen 3	Eludril® Mouthwash
Specimen 4	Listerine® Mouthwash

Table 1. Specimens' denotation and employed mediums.

Corrosion was characterized by means of changes in surface topography. For these purposes, each specimen was analyzed in 6 predefined locations before and after the corrosion test by employing AFM (CP-II di, Veeco). AFM measurements were performed in contact mode, using symmetrically etched Silicon-Nitride tip. The scanning parameters were as follows: fast scanning direction X-axis, scanning area 100x100 μm, setpoint 225 nN, scanning rate 0.5 Hz and gain 0.5.

In order to return to a predefined location after the corrosion test, a procedure was developed. Before and after the corrosion test, the probe was positioned in the same position relative to the specimen. In other words, the probe/sample relative position was set at the predefined probe elevation. However, during the probe approach to the sample a deviation from the ideal path was observed. Such deviation can cause a mismatch scanning location, before and after the test.

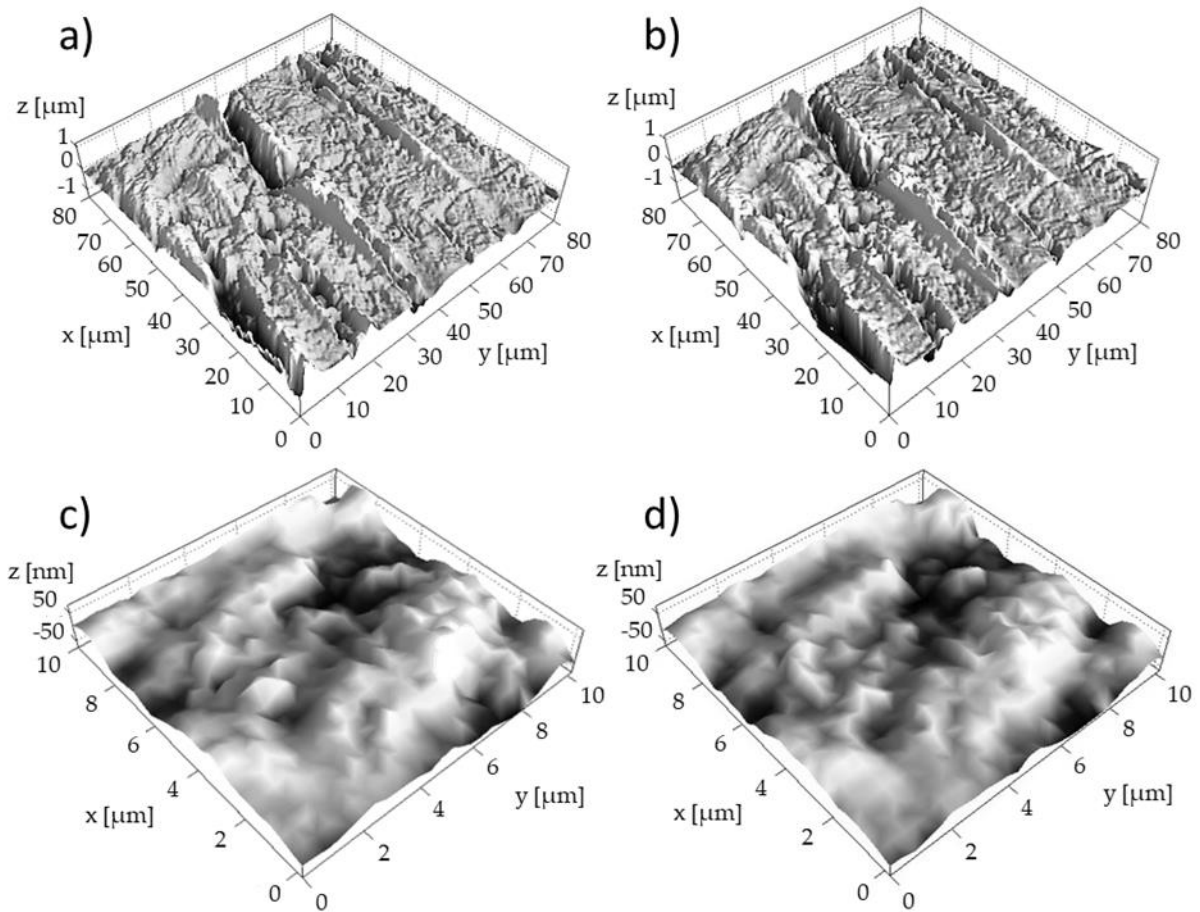


Fig. 1. Representative AFM images before and after corrosion test: (a) 80x80  $\mu\text{m}$  AFM topography image of initial surface before corrosion test; (b) 80x80  $\mu\text{m}$  AFM topography image of surface after corrosion test; (c) 10x10  $\mu\text{m}$  AFM topography image of initial surface before corrosion test; (d) 10x10  $\mu\text{m}$  AFM topography image of surface after corrosion test

Therefore, before and after the corrosion test, the exact probe path was determined. Based on differences in probe trajectories and differences in specimen heights the probe positions correction was calculated. However, not even this procedure can provide return of the probe to the identical locations after the corrosion test. Therefore, 80x80  $\mu\text{m}$  and 10x10  $\mu\text{m}$  areas were extracted from measurements performed on the areas of 100x100  $\mu\text{m}$ . The effects of corrosion were evaluated on these extracted areas.

SIIP (Image Metrology) image analysis software was employed for the analysis of topographic images, extracting areas 80x80  $\mu\text{m}$  and 10x10  $\mu\text{m}$  and the calculation of surface roughness parameters.

All values of quantitative parameters, obtained by AFM, were submitted to normality test (Anderson–Darling test,  $p > .05$ ), and subsequently to paired T-test. All statistics analyses were performed with Minitab 16 software at a significance level of 5%.

### 3. RESULTS

Representative AFM topographic images, of the same location before and after the corrosion test, are presented in Figure 1a and Figure 1b. The initial surface of specimens is characterized by irregular parallel deep

grooves, higher peaks, and smoother areas between the grooves. The height of the peaks and depth of the grooves are in order of micrometer. Changes caused by corrosion were not observed by comparison of topographic images before and after the corrosion tests.

Representative topographic images of 10x10  $\mu\text{m}$  the areas between the grooves are presented in Figure 1c and Figure 1d. In such small areas changes in surfaces topography, caused by corrosion, are clearly noticeable. In these cases surfaces become much smoother.

Surface roughness parameters ( $S_a$  and  $S_{10z}$ ) determined before and after the corrosion tests for the areas of 80x80  $\mu\text{m}$ , are for all specimens presented in Figure 2. It has to be noted that the average values of  $S_a$  parameter, are in the scale of nanometers. On the other side, the average values of  $S_{10z}$  parameter are in the scale of micrometers which indicates the existence of deep grooves and high peaks on the specimen surface. Although, all specimens were produced of one archwire, differences of ~15% in surface roughness parameters, are observed. The changes of  $S_a$  and  $S_{10z}$  parameters are not so pronounced. Also, it can be seen that the values of confidence interval have a minor change after the tests. Confidence intervals of the values determined before and after the test overlap for all investigated cases.

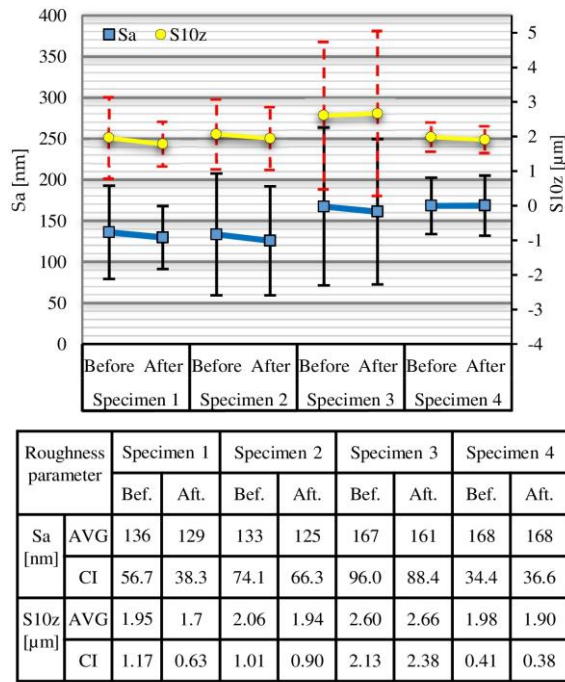


Fig. 2. Average values (AVG) of surface roughness parameters Sa and S10z and corresponding confidence intervals (CI), before (Bef.) and after (Aft.) corrosion test, of 80x80 μm areas.

Statistical analysis of Sa and S10z surface roughness parameters, are for the areas of 80x80 μm presented in Figure 3. It was determined that data distribution complies normality standard.

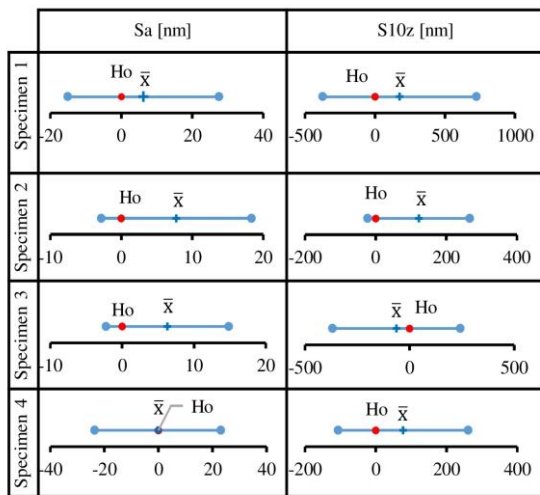
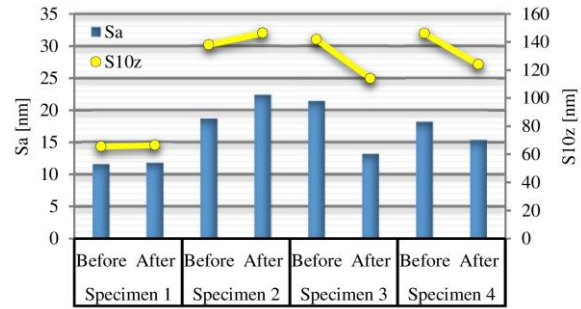


Fig. 3. Results of T-test: statistical analysis of the changes in Sa and S10z surface roughness parameters determined on the areas of 80x80 μm before and after the tests for all specimens on surface.

Results of paired T-test determined for Sa and S10z surface roughness parameters, are for the areas of 80x80 μm presented in Figure 3. T-test revealed that corrosive media, on observed area, did not cause a significant change of considered surface roughness parameters.

Surface roughness parameters (Sa and S10z) determined before and after the corrosion tests for the

areas of 10x10 μm, are for all specimens presented in Figure 4. The changes in surface roughness parameters Sa and S10z are pronounced for all specimens exposed to mouthwashes. While specimen exposed to artificial saliva did not display a pronounced change of considered parameters.



Roughness parameter		Specimen 1		Specimen 2		Specimen 3		Specimen 4	
		Bef.	Aft.	Bef.	Aft.	Bef.	Aft.	Bef.	Aft.
Sa [nm]		11.57	11.81	18.63	22.37	21.36	13.15	18.15	15.31
S10z [nm]		65.45	66.39	137.9	146.2	141.6	113.9	146	124

Fig. 4. Values of surface roughness parameters Sa and S10z, before (Bef.) and after (Aft.) corrosion test, of surface areas 10x10 μm areas.

#### 4. DISCUSSION

It is evident that corrosion processes did not induce a noticeable changes of surfaces. At least this is the case for topography acquired at areas of 80x80 μm. The initial surface roughness parameters Sa and S10z for scanning areas of 80x80 μm displayed a slight difference between the specimens (Figure 2). Differences in the initial average values of surface roughness Sa and S10z parameters between specimens are less than 10%. Variation in these parameters is probably a consequence of different amount of grooves and their different depths.

Considering the results of the T-test it is evident that all corrosive media did not cause significant change in surface topography. These results lead us to the following findings. First, the specimen 1 exposed to artificial saliva did not significantly changed the surface topography. Huang et al. [8] came to the same finding that artificial saliva, with a pH value less than 3.5, does not induce a significant corrosion of Ni-Ti alloy. Second, the specimen 3 exposed to a solution with 0.1% chlorhexidine gluconate and 0.5% chlorobutanol did not significantly changed the surface topography. The investigation of P. Osak et al. [6], reported that solution with 0.1% chlorhexidine gluconate and 0.5% chlorobutanol causes corrosion effects of NiTi wires. Third, specimens 2 and 4 exposed to a solution with 0.05% NaF (fluoride ions :250 ppm and 220 ppm) did not significantly change the surface topography. In investigation of Huang et al. [9], it has been reported that the protectiveness of TiO<sub>2</sub> formed on Ti alloy is degraded by fluoride ions when the NaF concentration exceeds 0.1% (fluoride ion: close to 500 ppm). This

occurs due to the formation of a Ti-F complex compound. However, in investigations [1,4,5], it has been reported that Ni-Ti alloy can corrode in solution with concentration of NaF less than 0.1%.

The analysis of the changes that occurred on specimen topography (Figure 1) and changes in surface roughness parameters (Figure 4), lead us to the following findings. First, the occurred nano changes on the surface indicate the low intensity of corrosive processes. Second, considering the changes in surface roughness parameter (Figure 4), it can be noticed that the type of changes in surface topography depends on the type of corrosive medium. employed medium has an influence on the type of changes that occurred on the surface. Third, corrosion processes induced changes in surface roughness parameters only when areas of 10x10 µm are compared. Variations in roughness parameters, caused by deep grooves are much larger than the changes caused by the low intensity of considered corrosion processes. Therefore, further investigation should be performed on surface areas smaller than 80x80 µm. Results obtained on the areas of 10x10 µm should be analysed with caution. The changes in surface topography and changes in surface roughness parameters are considered as the changes that occurred as a consequence of corrosion processes. However, it has to be noted that the observed changes in surface roughness parameters may also be a consequence of the low resolution of topographic images.

## 5. CONCLUSIONS

The corrosion behavior of NiTi alloy in artificial saliva, chloride solution, and fluoride solution was investigated. Analysis of the results of surface roughness parameters and changes in surface topography leads to the following conclusions:

- Chloride containing solutions with the concentration of 0.1% chlorhexidine gluconate and 0.5% chlorobutanol, and fluoride containing solutions with concentration of 0.05% NaF caused changes in surface topography on a nano level.
- Changes that occurred on the surface caused by corrosion processes in a non-accelerated test can be observed only on small areas such as a 10x10 µm.
- It is proposed that in further investigations of NiTi alloy that concern the changes in topography caused by corrosion, surfaces should be evaluated on the areas smaller than 80x80 µm.

## 6. REFERENCES

[1] N. Schiff, B. Grosgeat, M. Lissac, F. Dalard, *Influence of fluoridated mouthwashes on corrosion resistance of orthodontic wires*, *Biomaterials*. 25 (2004) 4535–4542.

[2] M.R. Grimsdottir, A. Hensten-Petersen, A. Kullmann, *Cytotoxic effect of orthodontic appliances*, *Eur. J. Orthod.* 14 (1992) 47–53.

[3] R. Köster, D. Vieluf, M. Kiehn, M. Sommerauer, J. Kahler, S. Baldus, T. Meinertz, C.W. Hamm, *Nickel and molybdenum contact allergies in patients with coronary in-stent restenosis*, *Lancet*. 356 (2000) 1895–1897.

[4] X. Li, J. Wang, E. Hou Han, W. Ke, *Influence of fluoride and chloride on corrosion behavior of NiTi orthodontic wires*, *Acta Biomater.* 3 (2007) 807–815.

[5] H.H. Huang, T.H. Lee, T.K. Huang, S.Y. Lin, L.K. Chen, M.Y. Chou, *Corrosion resistance of different nickel-titanium archwires in acidic fluoride-containing artificial saliva*, *Angle Orthod.* 80 (2010) 547–553.

[6] P. Osak, B. Łosiewicz, *EIS Study on Interfacial Properties of Passivated Nitinol Orthodontic Wire in Saliva Modified with Eludril® Mouthwash 1*, 54 (2018) 680–688.

[7] G. Perinetti, L. Contardo, M. Ceschi, F. Antonioli, L. Franchi, T. Baccetti, R. Di Lenarda, *Surface corrosion and fracture resistance of two nickel-titanium-based archwires induced by fluoride, pH, and thermocycling. An in vitro comparative study*, *Eur. J. Orthod.* 34 (2012) 1–9.

[8] H.H. Huang, Y.H. Chiu, T.H. Lee, S.C. Wu, H.W. Yang, K.H. Su, C.C. Hsu, *Ion release from NiTi orthodontic wires in artificial saliva with various acidities*, *Biomaterials*. 24 (2003) 3585–3592.

[9] H.-H. Huang, *Effects of fluoride concentration and elastic tensile strain on the corrosion resistance of commercially pure titanium*, *Biomaterials*. 23 (2002) 59–63.

**Authors:** M.Sc. Zoran Bobić, M.Sc. Sanja Kojić, M.Sc. Vladimir Terek, Full Prof. Branko Škorić, Associate Prof. Lazar Kovačević, Full Prof. Goran Stojanović, Assist. Prof. Pal Terek,

University of Novi Sad, Faculty of Technical Sciences, Department of Production Engineering, Trg Dositeja Obradovića 6, 21000 Novi Sad, Serbia, Phone.: +381 21 485-23-30

E-mail: [zoranbobic@uns.ac.rs](mailto:zoranbobic@uns.ac.rs); [sanjakojic@uns.ac.rs](mailto:sanjakojic@uns.ac.rs); [vladimirterek@uns.ac.rs](mailto:vladimirterek@uns.ac.rs); [skoricb@uns.ac.rs](mailto:skoricb@uns.ac.rs); [lazarkov@uns.ac.rs](mailto:lazarkov@uns.ac.rs); [sgoran@uns.ac.rs](mailto:sgoran@uns.ac.rs); [palterek@uns.ac.rs](mailto:palterek@uns.ac.rs)

**Assist. Prof. Bojan Petrović**

University of Novi Sad, Faculty of Medicine, Hajduk Veljkova 3, 21000 Novi Sad, Serbia.

E-mail: [bojan.petrovic@mf.uns.ac.rs](mailto:bojan.petrovic@mf.uns.ac.rs);

**ACKNOWLEDGMENTS:** This project has received funding from the European Union's Horizon 2020 research and innovation program under the Marie Skłodowska-Curie grant agreement No.872370

Kukuruzović, D., Kovačević, L., Terek, P., Terek, V., Škorić, B., Miletić, A., Panjan, P., Čekada, M.

## THE INFLUENCE OF CrAlN COATING DEFECTS AND CHEMICAL COMPOSITION ON DELAMINATION CAUSED BY AL CAST ALLOY SOLDERING

**Abstract:** A nanolayered CrAlN coating with three different chemical compositions was deposited on samples made of hot working steel. Those samples were used for simulating the HPDC process in aluminum die casting. Soldering and detachment forces of the coating were evaluated by using a detachment test. The influence of period of contact between the molten alloy and the sample surface were examined by using prolonged solidification. Contact surfaces off the sample and the casted aluminium were analysed by a 3D profilometer and a Scanning Electron Microscope (SEM). The amount of coating delamination and soldered material correlated with the number of coating defects. Higher detachment forces were found on samples with a higher number of coating defects. It was found that the amount of coating delamination and soldering increased with the increase of the number of coating defects. In order to increase tool life in HPDC-processes we need to decrease the number of coating defects.

**Key words:** Coating defects, CrAlN, HPDC, soldering, SEM

### 1. INTRODUCTION

The goal of surface engineering is to enhance tool performance. Common application of this methods is in High pressure die casting (HPDC) process. During this process, die (tool) surface is exposed to extreme conditions which lead to thermal fatigue, erosion, corrosion, cast alloy soldering, and abrasion wear [1]. Cast alloy soldering is a process in which the molten alloy reacts with die material and forms strong intermetallic bonds between the casting and die material. As a result of soldering, during the ejection of the casting, those bonds can lead to sticking of casting material to the sample surface. That in return leads to the increase of the ejection forces [2]. Soldering reduces casting quality and increases machine downtime. As a result, there is a shortening of die life [3–6].

In order to reduce tool maintenance and extend tool life and improve the casting ejection performance, die lubricant was sprayed on the die surface. Due to the large amount of lubricant used during HPDC process, there is increase in production cost. In order to make this process more economical and reduce the use of die lubricant, hard ceramic PVD coatings are deposited [7–9]. Ceramic coatings are used because of their high hardness, oxidation resistance, chemical inertness, and thermal stability[10–12]. These properties ensure high corrosion, soldering, and erosion resistance of die surfaces.

A detachment test was used to investigate the soldering performance of duplex nanolayer CrAlN coating in contact with Al-Si-Cu cast alloy. Soldering was evaluated by using delayed solidification for three different time periods.

### 2. MATERIALS AND METHODS

Sample material that was used for this study was a EN X27CrMoV51 hot-working tool steel in a quenched

and double tempered condition. In this experiment a disc shaped sample  $\Phi 30 \times 5$  mm was used. Samples (contact) surfaces were submitted to grinding. After surface preparation, plasma nitriding was carried out, and the compound layer was removed by diamond paste polishing technique using  $3 \mu\text{m}$  paste granulation. After the polishing process, a nanolayered CrAlN coating with three different chemical composition was deposited using a CC800/9 (CemeCon) industrial DC-magnetron sputtering system.

The sample surface roughness was measured using a profilometer, while coating thickness was defined using a standard ball cratering test. The coatings adhesion was evaluated by Rockwell C test. The test was conducted by applying a force of 150 N. All coatings exhibited very high adhesion. The number and size of coating defect and area covered by the defects was obtained by MountainsMap software. Obtained values are given in table 1.

The detachment test was used for simulating the HPDC process. In this test, molten aluminum that was heated to  $750 \text{ }^\circ\text{C}$  was poured into a preheated mold. The mold that was made from a thermal insulating material was preheated to  $650 \text{ }^\circ\text{C}$ . To prevent instant solidification of the molten aluminum when coming in contact with the sample surface, the samples was preheated to  $300 \text{ }^\circ\text{C}$ . In order to simulate more casting cycles, the assembly (mold, sample, molten aluminum) was kept in a furnace that was heated to  $700 \text{ }^\circ\text{C}$  for a defined time period. After the delayed period, the assembly was taken out the furnace and allowed to cool in ambient air. The selected periods were defined as continues solidification (CS), delayed solidification for 10 min (DS10) and 30 min (DS30).

After solidification, a ZGIM 500 tensile tester was used to separate the casting from the sample surface and to measure the force needed for the detachment of the casting. Both sample and casting surfaces were analyzed using light optical microscope (LOM), confocal microscope (CFM) and a Scanning Electron Microscope (SEM).

### 3. RESULTS AND DISCUSSION

By analyzing the samples contact surface, it was found that the number of coating defects varied from sample to sample. The results are given in table 1. They represent the average values of the surface roughness, number of coating defects and area covered by the defects for the examined samples.

Sample	Sa [ $\mu\text{m}$ ]	Coating defects density [num/mm <sup>2</sup> ]	Area of coating defects [ $\mu\text{m}^2$ ]	Coating thickens [ $\mu\text{m}$ ]
CrAlN	0,075	91	59	5,7
CrAlN-Al	0,065	72	84	4,9
CrAlN-Cr	0,097	101	78	7,1

Table 1. Sample topographic properties and coating thickness. Average values are given for nine samples of each group

From table 1, it can be seen that the CrAlN-Al samples, which had a higher amount of Al, had the lowest average surface roughness and a smaller amount of coating defects, but the area that was covered whit coating defects was the largest. The larger area covered by coating defects can be explained by the different sizes and types of coating defects that were created during coating deposition [13–16]. Opposed to CrAlN-Al coating, the CrAlN-Cr coating exhibited the highest average surface roughness and a higher amount of coating defects.

Forces obtained using the detachment test are given in Figure 1. It shows that the CrAlN-Al and CrAlN-Cr samples exhibited similar values of detachment forces, while the CrAlN coating showed the smallest detachment forces for all three periods of solidification. These forces correlate with the area covered by coating defects. The CrAlN coating exhibited the smallest area covered by coating defects, hence the lowest detachment force.

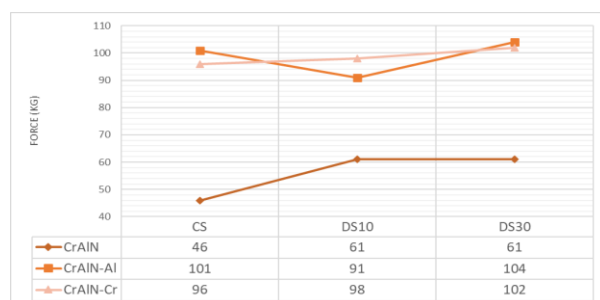


Fig. 1. Sample detachment forces (CS - continues solidification, DS10 - delayed solidification for 10 min and DS30 - delayed solidification for 30 min)

A LOM image of the sample and casting after the detachment test is given in figure 2. It can be seen that the contact surfaces of the sample and casting are a mirror like image. This enables us to easier determine the amount of soldering and coating delamination, that

occurred during the detachment of the casting from the sample surface. Looking at Figure 2a it becomes obvious that there existed a high amount of soldering in the contact area of the casting and the CrAlN-Al sample.

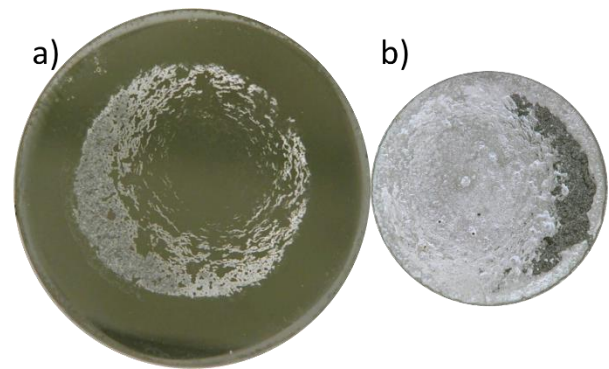


Fig. 2. LOM Image of the CrAlN-Al a) sample and b) casting contact surfaces after the detachment test

By analyzing the sample surface by SEM, distinctive forms of soldering were found on the contact surface. The investigated sample surface was mapped by four arrows (Figure 3a). The green arrow indicated the nodular defect that was found on the sample surface. It can be seen that the defect broke in two, where one part of the defect staid on the sample surface, while the other part detached with the casting. The black arrow showed the substrate material, while the blue arrow represented the coating that didn't delaminate from the sample surface. EDX spectrum showed (figure 3b) that the defect consisted of 59,75 % Al, 13,05 % Cr, 10,28 % N. The cracked coating that didn't fully detach from the sample surface was indicated with the red arrow.

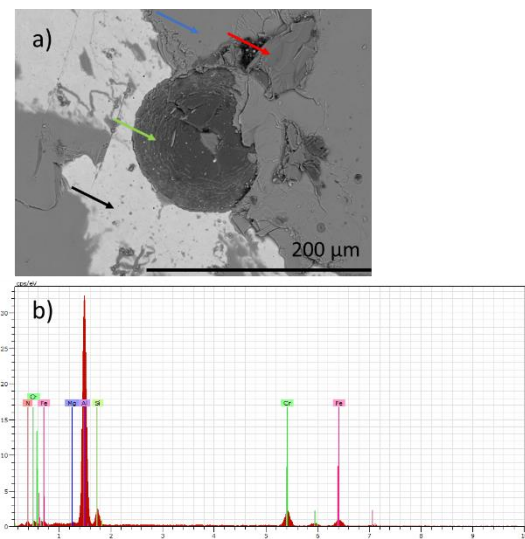


Fig. 3. SEM image of the CrAlN-Al a) sample and b) EDX spectrum

By knowing that ceramics don't corrode in contact with molten aluminum [17], the assumption is that intermetallic phases formed between the substrate material and the casted aluminum through and around the coating defects. This led to the decay of the contact

surface of the substrate material and the coating. As a result, the adhesion forces between the two materials decreased. This led to coating delamination from the sample surface and the rise of the detachment forces. From these results it can be seen that the detachment forces are defined by the forces of the intermetallic phase and coating adhesion. Comparing the detachment forces whit area covered by soldered aluminum and delaminated coating (Figure 4), it can be seen that the forces increase whit the increase of soldering and coating delamination.

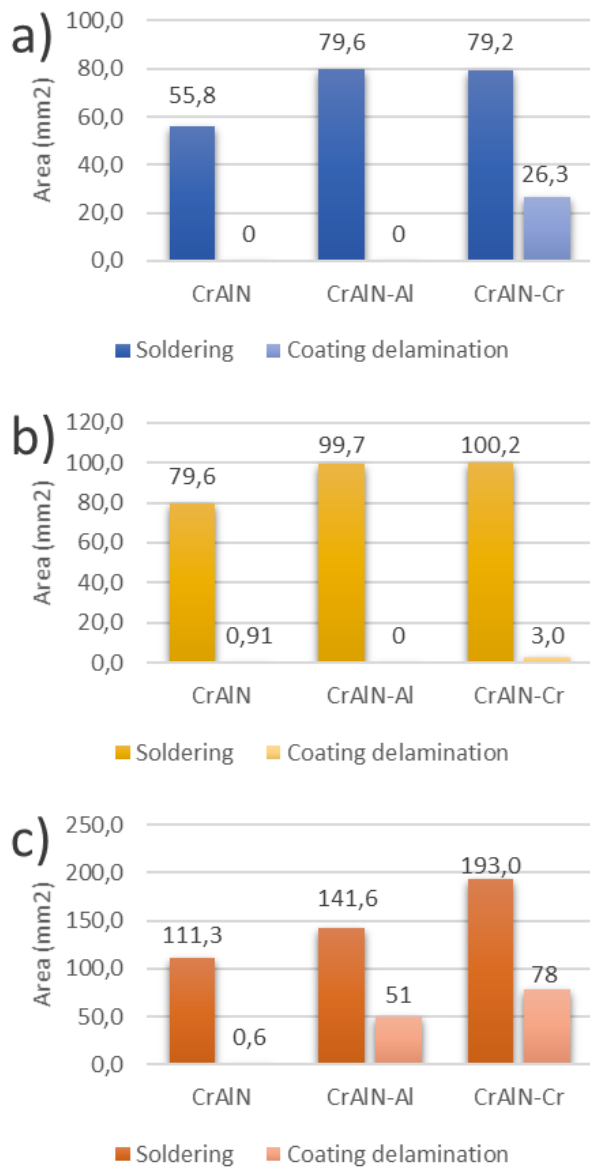


Fig. 4. Sample surface area covered by soldered aluminum and coating delamination for defined time of solidification, a) CS - continues solidification, b) DS10 - delayed solidification for 10 min, c) DS30 - delayed solidification for 30 min

Figure 4 shows that soldering and coating delamination gradually increased whit the increase of the period of solidification. It is noticeable that all three chemical compositions exhibited the increase of soldered area. The CrAlN-Al coating exhibited a

decrease in the detachment force for the DS10 time frame (Figure 1). This can be associated whit the fact that there was no coating delamination (Figure 4b) during the detachment of the casting from the sample surface. By analyzing Figure 4 it can be noticed that coating delamination had a higher influence on detachment forces, due to the high adhesion forces.

#### 4. CONCLUSIONS

By controlling the number and density of coating defects we can affect the bonding of the casting to the coated die surfaces, hence increase the durability and resistance of the coating.

It was found that the chemical composition of the CrAlN coating had a smaller influence on the formation of intermetallic compounds. These phases formed through coating defects. The samples with a higher amount of coating delamination also had a larger amount of coating defects and higher detachment forces. The number of coating defects was not given for every sample, but the average value of nine samples for each chemical composition.

It was found that CrAlN coatings whit more Al and Cr exhibited higher detachment forces than the CrAlN coating.

Future research will be based on finding ways to reduce the number of coating defects that occur during the production of protective coatings. There will also be a researcher on finding new materials that can enhance HPDC tool life.

#### 5. REFERENCES

- [1] Persson, A., Hogmark, S., Bergström, J.: *Failure modes in field-tested brass die casting dies*, J. Mater. Process. Technol., 148, pp. 108–118., 2004.
- [2] Gobber, F., Pisa, A., Ugues, D., Lombardo, S., Fracchia, E., Rosso, M.: *Study of the Effect of Surface—Roughness of Dies and Tooling for HPDC on Soldering*, in: Light Met. 2018, pp. 977–981, 2018.
- [3] Zhu, H., Guo, J., Jia, J.: *Experimental study and theoretical analysis on die soldering in aluminum die casting*, J. Mater. Process. Technol., 123, pp. 229–235, 2002.
- [4] Terek, P., Kovačević, L., Miletić, A., Panjan, P., Baloš, S., Škorić, B., Kakaš, D.: *Effects of die core treatments and surface finishes on the sticking and galling tendency of Al–Si alloy casting during ejection*, Wear., 356–357, pp. 122–134, 2016.
- [5] Han, Q.Y.: *Mechanism of die soldering during aluminum die casting*, China Foundry., 12, pp. 136–143, (2015).
- [6] Chen, Z.W.: *Formation and progression of die soldering during high pressure die casting*, Mater. Sci. Eng. A., 397, pp. 356–369, 2005. <https://doi.org/10.1016/j.msea.2005.02.057>.
- [7] Peter, I., Rosso, M., Gobber, F.S.: *Study of protective coatings for aluminum die casting molds*, Appl. Surf. Sci., 358, pp. 563–571, 2015..
- [8] Paiva, J., Fox-Rabinovich, G., Locks Junior, E., Stolf, P., Seid Ahmed, Y., Matos Martins, M.,

- Bork, C., Veldhuis, S.: *Tribological and Wear Performance of Nanocomposite PVD Hard Coatings Deposited on Aluminum Die Casting Tool*, Materials (Basel), 11, pp. 358, 2018.
- [9] Lorusso, M., Ugues, D., Oliva, C., Ghisleni, R.: *Failure modes of PVD coatings in molten Al-alloy contact*, Acta Metall. Slovaca., 19, pp. 30-42, 2013.
- [10] Tentardini, E.K., Aharanov, A., Chellapilla, R., Shivpuri, S., Lakare, R., Castro, M., Kunrath, A.O., Moore, J.J., Kwietniewski, C., Baumvol, I.J.R.: *Reactivity between aluminum and (Ti,Al)N coatings for casting dies*, Thin Solid Films., 516, pp. 3062–3069, 2008.
- [11] Bobzin, K., Brögelmann, T., Hartmann, U., Kruppe, N.C.: *Analysis of CrN/AlN/Al<sub>2</sub>O<sub>3</sub> and two industrially used coatings deposited on die casting cores after application in an aluminum die casting machine*, Surf. Coatings Technol., 308, pp. 374–382, 2016.
- [12] Lin, J., Carrera, S., Kunrath, A.O., Myers, S., Mishra, B., Ried, P., Moore, J.J., Zhong, D.: *Design methodology for optimized die coatings: The case for aluminum pressure die-casting*, Surf. Coatings Technol., 201, pp. 2930–2941, 2006.
- [13] Panjan, P., Čekada, M., Panjan, M., Kek-Merl, D., Zupanič, F., Čurković, L., Paskvale, S.: *Surface density of growth defects in different PVD hard coatings prepared by sputtering*, Vacuum., 86, pp. 794–798, 2012.
- [14] Čekada, M., Panjan, P., Kek-Merl, D., Panjan, M., Kapun, G.: *SEM study of defects in PVD hard coatings*, Vacuum., 82, pp. 252–256, 2007.
- [15] Drnovšek, A., Panjan, P., Panjan, M., Čekada, M.: *The influence of growth defects in sputter-deposited TiAlN hard coatings on their tribological behavior*, Surf. Coatings Technol., 288, pp. 171–178, 2016.
- [16] Münz, W.D., Lewis, D., Creasey, S., Hurkmans, T., Trinh, T., Ijzendor, W.: *Defects in TiN and TiAlN coatings grown by combined cathodic arc/unbalanced magnetron technology*, Vacuum., 46, pp. 323–330, 1995.
- [17] Salman, A., Gabbitas, B.L., Cao, P., Zhang, D.L.: *The performance of thermally sprayed titanium based composite coatings in molten aluminium*, Surf. Coatings Technol., 205, pp. 5000–5008, 2011..

**Authors: Teach. Assist. Dragan Kukuruzović, Assoc. Prof. Lazar Kovacević, Assist. Prof. Pal Terek, Teach. Assist. Vladimir Terek, Full Prof. Branko Škorić, Aleksandar Miletić Ph.D.,**

University of Novi Sad, Faculty of Technical Sciences, Department of Production Engineering, Trg Dositeja Obradovića 6, 21000 Novi Sad, Serbia, Phone.: +381 21 485-23-13.

E-mail: [kukuruzovic@uns.ac.rs](mailto:kukuruzovic@uns.ac.rs); [lazarkov@uns.ac.rs](mailto:lazarkov@uns.ac.rs); [palterek@uns.ac.rs](mailto:palterek@uns.ac.rs); [vladimirterek@uns.ac.rs](mailto:vladimirterek@uns.ac.rs); [skoricb@uns.ac.rs](mailto:skoricb@uns.ac.rs)

**Researcher Aleksandar Miletić**

Polytechnique Montreal, Department of Engineering Physics, Quebec H3T 1J4, Canada, Phone.: +1 514 340 4711.

E-mail: [aleksandar.miletic@polymtl.ca](mailto:aleksandar.miletic@polymtl.ca)

**Research Counselor Peter Panjan, Assoc. Prof. Miha Čekada**

Jožef Stefan Institute, Jamova 39, 1000 Ljubljana, Slovenia, Phone.: +386 01 477-389, Fax: +386 01 251-9385.

E-mail: [peter.panjan@ijs.si](mailto:peter.panjan@ijs.si); [miha.cekada@ijs.si](mailto:miha.cekada@ijs.si)

**ACKNOWLEDGMENTS:** The results presented in this paper are part of the research within the project "Interdisciplinarity of technologies in production engineering", at the Department of Production Engineering, Faculty of Technical Sciences, University of Novi Sad, Serbia.

Special thanks to the colleges from Department of Thin films and surfaces, Institute "Jožef Stefan" (Ljubljana, Slovenia) and BioSense Institute (Novi Sad, Serbia) who helped with samples characterization. We acknowledge GasTeh d.o.o. (Indjia, Serbia) for samples fabrication and Termometal d.o.o. (Ada, Serbia) for heat treatment.



Milutinović, M., Konjović, Z., Randelović, S., Movrin, D., Vilotić, M.,  
Stefanović, Lj., Krašnik, M.

## RECENT ACHIEVEMENTS IN THE PRODUCTION OF BI AND MULTI-METAL COMPONENTS BY METAL FORMING TECHNOLOGIES

**Abstract:** *Bimetals / multimetals offer distinctive properties that monolithic metals alone could not provide and therefore, bimetallic / multimetallic products are increasingly used and built into different devices. The properties (mechanical, technical, electrical, etc.) of products made from two or more laminated metals joined together can be adjusted in wide range by proper composition of constitutive components as well as by lamination (manufacturing) process itself. The creation and manufacturing of multilayer materials is a complex issue that requires a multidisciplinary approach. Today, different technological procedures and techniques are applied to obtain these components among which, traditional manufacturing methods like casting and welding are still dominant. This paper deals with research trends and recent achievements in the field of bimetals/multimetal production using conventional metal forming technologies. These technologies exhibit many advantages, particularly in term of time and cost reduction.*

**Key words:** *Metal forming, bimetals, deformation bonding*

### 1. INTRODUCTION

Bimetal is an integral, layered structure (form) consisting of two different metals or alloys joined together using different technologies. Similarly, multimetal refers to an inseparable assembly in which three or more metal-based materials are joined together with discrete interfaces. It worth to note that joining of constitutive materials is done while, at least, one of the components is in the solid state. Since bimetals/multimetals are composed of two or more layers of separate metals/alloys they significantly differ from alloys that are a mixture of two or more metals. Therefore, bimetals/multimetals are also referred to as laminated metal composite (LMC).

It is considered that the first bimetallic/multimetallic composite was created in the ancient Greece [1]. Namely, according to some interpretations of Homer's epic poem "The Iliad" Achilles's shield, which demonstrated superior performance during combats, was made of five layers: 2 bronze, 2 tin, and 1 gold. Famous Japanese sword Katana is also a multimetallic product. Three types of steel are used for the blade - a very low carbon steel is used for the core of the blade while the high carbon steel and the remelted pig iron are combined to form the outer skin of the blade [2]. Today, due to their overall excellent properties, bimetallic components are widely used in various fields of industry (automobile, aerospace, chemical, food etc [3]).

The properties (mechanical, electrical, thermal, magnetic, frictional etc.) of the materials in a bimetallic/multimetallic assembly work together to provide advantages over a product manufactured from either of these materials alone. For example, bimetallic parts composed of steel and aluminium combine the strength of steel with electrical conductivity and corrosion resistance of aluminium (TEAM Slavonki brod). An intelligent material combination also ensures the cost

and weight reduction of a bimetal/multimetal product. In this regard, it was shown that introduction of lightweight bimetal gears (Al-6082/Carbon Steel,) to vehicle transmission system can result in weight savings of 30-50% relative to traditional steel gears [4]. This, in turn, results in improved transmission performance: rotational inertia of the automotive transmission system and fuel consumption are reduced while acceleration speed is increased. Further, bimetallic/multimetallic assembly could have different properties at different sections that allows for flexible part design and optimal utilization of material. Thus, it could be said that bimetals/multimetals exhibits unique characteristics that monolithic metals alone could not provide. In general, the properties of a bimetal/multimetal can be adjusted in wide range by proper composition of constitutive components as well as by lamination manufacturing process itself.

Different technologies and techniques are employed in production of bimetals/multimetals. According to the method of joining layers, these technique are classified into three main groups - bonding, deposition, and spray forming [1]. Bonding technique could be also divided into several subgroups such as: adhesive bonding, melt bonding, infiltration, diffusion bonding, reaction bonding, and deformation bonding (joining by forming). The main difference between deformation bonding and other bonding processes is whether obvious plastic deformation occurs during the joining process.

The formation of metal-metal bond between layers in a bimetal joint lead to the microstructure evolution near the interface. The microstructure as well as bond strength are influenced by several factors: surface preparation of the component materials, bonding temperature and pressure, interdiffusion, and chemical reactions between the components. The performance and quality of a bimetallic/multimetallic joint are commonly characterized by two geometric parameters: thickness of the diffusion layer and interfacial bonding

rate, which is mainly influenced by the mutual diffusion behavior of elements between the components [5]. In this paper, recent advances as well as the challenges in the production of bimetals/multimetals by metal forming methods will be discussed.

## 2. JOINING BY PLASTIC DEFORMATION

Joining by plastic deformation is the most efficient technique for industrial production of bimetallic and multimetallic products [5]. In general, this technique can be divided into two sub-categories: metallurgical joining and mechanical joining. In metallurgical joining, which is also known as cold welding, deformation bonding or solid-state welding, constitutive materials are joined together through a metallurgical bond created by large plastic deformation and without external heating. In another words, during cold welding no metal is liquified or even heated to a notable degree. The bonding mechanism is based on a well-known physic phenomenon: two clean, flat surfaces of similar metal would strongly adhere if brought into contact and pressed together while in a vacuum. However, almost all metals in normal conditions are covered with a thin layer of oxide or other contaminants that may prevents the metal atoms on the contact surface from being pressed together and bonded with one another. According to the film theory [6], which is commonly used to explain the bonding mechanism of cold welding, large plastic strain removes the oxide/impurity films at the interface between layers (Fig.1) allowing clean surfaces to come into contact so that atoms are able to join with one another i.e., to establish a metallurgical bonding. In addition, heat generated due to plastic deformation and interfacial slipping results in materials softening that speeds up the joining process and strength of the bond. Forming technologies commonly employed for deformation bonding includes upsetting, cold forging, rolling, extrusion and explosive forming.

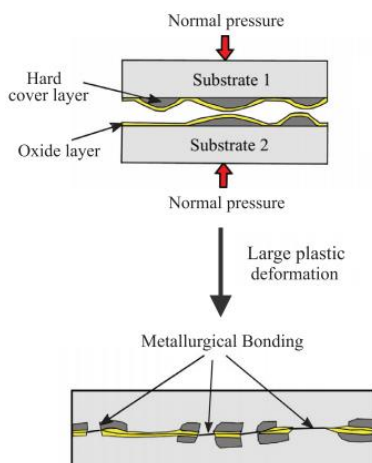


Fig. 1. The scheme of deformation bonding [6]

On the other hand, mechanical joining by plastic deformation is based on a difference in geometry of two coupling parts (before assembly) i.e., a difference in the elastic recovery of the assembled components that leads to interference pressure between the components after

deformation [7, 8]. This contact pressure holds the two parts together by friction creating a mechanical joint also known as interference-fit joint. Strength of this joint depends mainly on the coefficient of friction and the size contact area as well as contact pressure, which could be controlled by plastic strain and the amount of the interference. It worth to note that in the mechanical joining processes the contact surfaces are not bonded so the breaking up of the oxide films is not required like in case of the metallurgical joining. This type of joint is met in case of tubular components joined together either by expansion or compression of the constitutive parts (Fig.2).

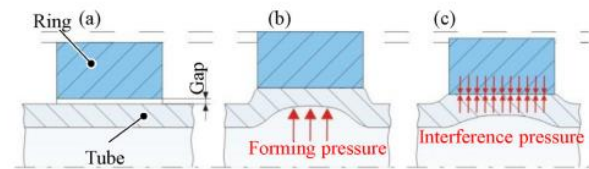


Fig. 2. Principle of interference-fit joint manufactured by expansion (a) positioning, (b) maximum expansion under forming pressure and (c) elastic recovery [7]

The main advantages and disadvantages of joining by plastic deformation compared to other bonding process are [7]:  
Advantages:

- Wide range of materials, including dissimilar ones (metallic/non-metallic) can be joined in this manner
- Less distortion and lower tensile residual stress
- High process reliability, robustness and simple quality control
- Environmental friendly procedures
- High rate of production

Disadvantages:

- Overlap joints - alignment may be a problem
- Geometrical unevenness of joining
- More difficult correction and repair
- Lack of standardization and calculation methods
- Materials should clean (deformation bonding)
- One material in the joint must be somewhat ductile

## 3. BI AND MULTI METALLIC COMPONENTS PRODUCED BY JOINING BY PLASTIC DEFORMATION

Certainly, the most widespread bimetallic /multimetallic products obtained by joining by forming are coins, medals and similar products. Bimetallic coins are used primarily to help prevent counterfeiting as they are more expensive and challenging to produce compared to conventional one-metal coins. Therefore, bimetallic and multimetallic coins (Fig.3) are now produced by over 150 countries [9].



Fig. 3. Examples of the various kinds of bimetallic and multimetallic coins [9]

There are several methods of producing bimetallic/multimetallic coins but today, ring and foil

technology (Fig.4) are mostly employed [10]. In ring technology two elements to be joined (external and inner) are of the similar thickness. The external ring is manufactured in a multi-stage sequence consisting of the following metal forming operations: piecing, blanking and rimming. The outer edge of the ring is raised (rimming operation) in order to reduce the coining pressure. The inner part is an ordinary coin blank, except for the special milling applied to the edge. Joining of two elements or minting operation is realized by a closed die. During compression the outer ring deforms to flow inside the milled indentations, providing efficient anti-twist locking and increasing the strength of the bond. With other hand, the bimetallic foil technology uses two discs of different materials and different thickness - first is very thin (foil) while second one is "normal" disc. Closed die for joining the two discs is shown in Fig.5

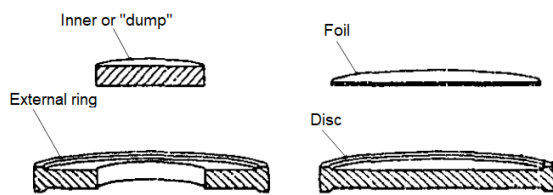


Fig. 4. Ring (left) and foil (right) technology [10]

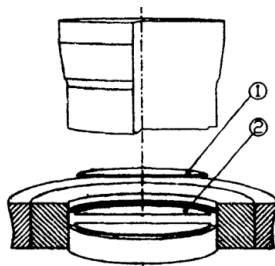


Fig. 5. Tolling for foil (1) and disc (2) assembling [10]

Another popular group of bimetallic and multimetallic products are rods, tubes/pipes, profiles and related multi-layered components, which are commonly produced by multicomponent billet extrusion in cold and hot conditions. Due to superior properties, the market for these components is large and includes applications in food, chemical, petrochemical, aero-space and power-generation industries [11]. Depending on the geometry of die and billet, there are three basic forms of bimetallic extrusion: forward extrusion, backward extrusion and tube extrusion. In all cases the bimetallic billet is composed of outer sleeve and inner core which are combined in accordance to requirements of final product: hard sleeve material - soft core material and vice versa. Conventional forward extrusion tooling is used for producing bimetallic rods from a bimetallic billet (Fig.6a). With other hand, there are two extrusion methods to obtain bimetallic tubes and tube-like components: forward tube extrusion by a special designed punch (punch with an integrated mandrel - Fig.6b) and extrusion-piercing in a profiled die using the punch and a separate mandrel (Fig.6c) [12]. Forward extrusion can be also used to join two tubes from different materials (Fig.7). In this way, tube transition joints of aluminium–stainless steel, aluminium–titanium and zirconium–mild steel are produced for nuclear

power and space technology [8]. The tube from harder material is placed first in the conical die opening while the punch is provided with a mandrel fitting the tube holes to prevent inwards flow.

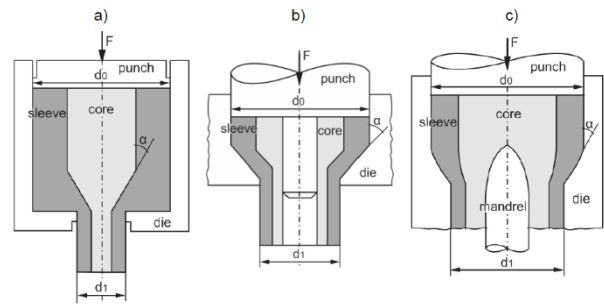


Fig. 6. Different variants of bi-metallic extrusion a.) forward extrusion b, c.) tube extrusion [12].

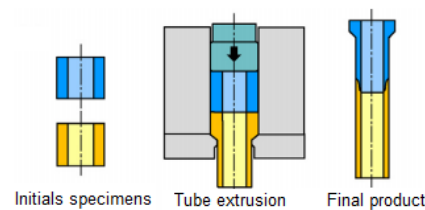


Fig. 7. Forward extrusion of tube transition joint [7]

In addition to challenges associated with the mono-material extrusion, several additional ones are present in process of bi-material extrusion, such as: bonding of materials, concurrent flow of materials and uniform thickness of the layers. The last two items are directly related to differences in geometry and mechanical properties of billet materials (initial heterogeneity), i.e., non-uniform deformation of materials during deformation. Therefore, the inner material (core) that is usually softer may be extruded prior the outer material (sleeve) and vice versa, causing a "balloon" defect at the front of the extrudate and "pinch-off" defect (a lack of core material at the back) [11]. This can be avoided by making core diameter the same as that of the punch. Further, the thickness of inner material may varies along the die, where two extreme cases are possible: zero thickness (rupture of the inner layer) or thickness equal to the outer wall (rupture of outer layers).

Many factors influence bi-metallic extrusion: reduction in area, semi-cone angle, load, friction factors, ratio of core and sleeve radius and ratio of core and sleeve flow stress. In forward extrusion ratio of the core / sleeve length is also important [12].

Bimetallic drawing, which scheme is given in Fig.8, can be also used for manufacturing bimetal tubes/pipes. During the process, large plastic deformation is generated in both the inner and the outer tube and metallurgical bonding between two metals occurs along the interface. The greater the differences in the elastic modulus the greater the strength of the joint. It worth to note that diffusion annealing is often applied in order to improve the bonding strength. With increasing annealing temperature and time, the diffusion process is more intensive and bonding section increase. In some cases (Copper–Steel tube), the bonding strength can reach 220 MPa [13].

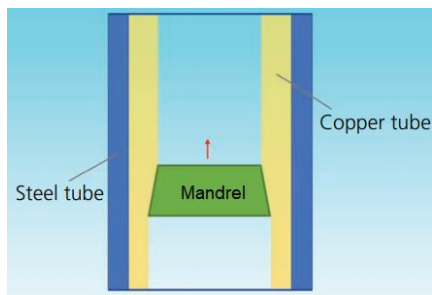


Fig. 8. Drawing of bimetallic tube [13]

As it mentioned before, bimetal gears provide many benefits over mono-metal gears and thus, production of bimetal gears is one of the main trends in the gear industry. Bimetal gears obtained by forming are of particular interest due to numerous advantages of this technology compared to other methods used in gear production (cutting, sintering, and casting). In order to produce bimetal gears of high accuracy, near-net shaping forming (NNSF) and net shape forming (NSF) technologies should be employed. Shown in Fig.9 is a die set for precision cold forging (NSF) of a bimetal gear. The bimetallic billets consists of an inner core of a lower performance material (Lead) and an outer ring from higher performance material (Cooper). Another combination of materials, such as Steel ring and Aliminium core, are also possible.

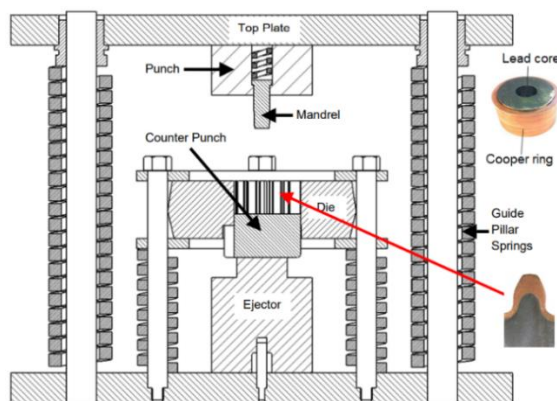


Fig. 9. Die for precision forging of bimetallic gear with cylindrical teeth [14]

#### 4. CONCLUSION

Metal forming technologies enable fast and low cost production of bi and multi metallic components and therefore their industrial application is constantly expanding. In this paper some forming procedures as well as recent trends and achievements in the field of bimetal/multimetal forming are presented, which promises broader implementation of this technology in near future.

#### 5. REFERENCES

- [1] Lesuer D. R., Syn C., et al. *Mechanical behaviour of laminated metal composites*, International Materials Reviews, 41:5, 169-197, 1996.
- [2] [https://en.wikipedia.org/wiki/Japanese\\_swordsmithing#cite\\_note-samuraisword2-10](https://en.wikipedia.org/wiki/Japanese_swordsmithing#cite_note-samuraisword2-10). Accessed on

- 12.08. 2021.
- [3] Li Z., Zhao J., et al. *Numerical and experimental investigation on the forming behaviour of stainless/carbon steel bimetal composite*. Int J Adv Manuf Technol., 101, 1075–1083, 2019.
- [4] <http://www.nicholaspolitis.com/forging-bimetal-lightweight-gears>. Accessed on 12.08.2021
- [5] Zhang Q. Li S.; et al. *Study of a Bimetallic Interfacial Bonding Process Based on Ultrasonic Quantitative Evaluation*. Metals, 8, 329, 2018.
- [6] Khaledi K., Rezaei S., et al. *Modeling of joining by plastic deformation using a bonding interface finite element*. International Journal of Solids and Structures, 160, 68-79, 2019.
- [7] Mori K., Bay N., et al. *Joining by plastic deformation* CIRP Ann. Manuf. Technol., 62 (2), 673-694, 2013.
- [8] Hüyük H, Music O., et al. *Analysis of Elastic-plastic Interference-fit Joints*, Procedia Engineering, 81, 2030-2035, 2014.
- [9] <http://www.bimetallic-coins.com/historia/historia.html>. Accessed on 14.08.2021.
- [10] Barata M., Martins P.A.F. *A study of bimetal coins by the finite element method*, Journal of Material Processing Technology, 26, 337-348, 1991.
- [11] Misiolok W. Z., Sikka V. K. *Physical and Numerical Analysis of Extrusion Process for Production of Bimetallic Tubes*. United States: N.p., 2006. Web. doi:10.2172/889030.
- [12] Plančak, M., Movrin, et al. *Bi-metallic cold backward extrusion - numerical simulation with experimental verification*. International Conference on Innovative Technologies, IN-TECH 2012, Rijeka, 26.-28.09.2012
- [13] Wang .Y, Gao Y., et al. *Review of preparation and application of copper–steel bimetal composites*. Emerging Materials Research 8(4), 538–551, 2019.
- [14] Politis D.J., Lina J., Deanb T.A., Balinta D.S., *An investigation into the forging of Bi-metal gears*, Journal of Materials Processing Technology, 214, 2248–2260, 2014.

**Authors:** Assoc. Prof. Mladomir Milutinović, M.Sc. Zoran Konjović, Assist. Prof. Dejan Movrin, Assist. Prof. Marko Vilotić, M.Sc. Ljiljana Stefanović, University of Novi Sad, Faculty of Technical Sciences, Department of Production Engineering, Trg Dositeja Obradovića 6, 21000 Novi Sad, Serbia

E-mail: [mladomil@uns.ac.rs](mailto:mladomil@uns.ac.rs);

[zoran.konjovic@uns.ac.rs](mailto:zoran.konjovic@uns.ac.rs); [movrin@uns.ac.rs](mailto:movrin@uns.ac.rs);

[markovil@uns.ac.rs](mailto:markovil@uns.ac.rs); [ljiljanastefanovic@uns.ac.rs](mailto:ljiljanastefanovic@uns.ac.rs);

**Full Prof. Saša Randelović**, University of Niš, Faculty of Mechanical engineering, Aleksandra Medvedeva 14, 18000 Niš, Serbia

E-mail: [sasa.randjelovic@masfak.ni.ac.rs](mailto:sasa.randjelovic@masfak.ni.ac.rs);

**Assoc. Prof. Milija Krašnik**. University of East Sarajevo, Faculty of Mechanical engineering, Vuka Karadžića 30, Lukavica, Istočno Sarajevo, Republic of Srpska, Bosnia and Herzegovina.

E-mail: [milija.krasnik@ues.rs.ba](mailto:milija.krasnik@ues.rs.ba).

Janjatović, P., Rajnović, D., Erić Čekić, O., Baloš, S., Dramićanin, M., Šidanin, L.

## THE PROPERTIES AND APPLICATION OF DUAL PHASE AUSTEMPERED DUCTILE IRONS

**Abstract:** The development of the industry shows the continuous need for improving existing material characteristics. In recent years, it has been found that austempered ductile iron (ADI) and dual-phase austempered ductile iron (DP-ADI), which are obtained by the austempering process, have excellent mechanical properties, greater than the starting as-cast ductile cast irons. Special attention is given to the dual-phase austempered ductile iron (DP-ADI). The DP-ADI has a microstructure that consists ausferrite and free (proeutectoid) allotriomorphic ferrite. The heat treatment parameters affect the percentage of these phases which allows the design of the mechanical properties. Therefore, the DP-ADI has improved ductility and machinability, when compared to conventional (fully ausferritic) ADI material. In this work, an overview of DP-ADI material production procedures, its properties, advantages, and possible applications will be presented.

**Key words:** ductile iron, austempered ductile iron, dual-phase austempered ductile iron.

### 1. INTRODUCTION

Heavy vehicles industry and auto industry has reflected a steady growth over the last decade by constantly trying to upgrade their technology and production processes. The economically viable ways to upgrade vehicle components is to improve the mechanical properties of existing materials. One such material is ductile iron. Ductile iron (DI) exhibits a wide range of properties which are obtained through microstructure control [1]. The most important and distinguishing microstructural feature of the ductile irons is the presence of graphite nodules (spheroidal graphite) which give ductility and toughness superior to all other cast irons, and equal to many cast and forged steels.

The mechanical properties of ductile iron can be significantly improved through an austempering heat treatment. In this way, austempered ductile iron (ADI) with a unique microstructure is formed. The unique microstructure consists of graphite nodules in an ausferrite matrix. The ausferrite matrix is a mixture of ausferritic ferrite and carbon enriched retained austenite [1]. The ADI materials have an outstanding combination of fatigue resistance, high strength, machinability, ductility and toughness together with good wear [2–3].

By further improvement of ADI materials, in order to improved ductility and machinability, a dual-phase austempered ductile iron (DP-ADI) was created [4,5]. The dual phase microstructure is obtained by intercritical annealing in the  $\alpha+\gamma$ +graphite region, whereby colonies of free (proeutectoid) ferrite are introduced into fully ausferrite microstructure. After intercritical annealing, quenching to austempering temperature is performed. The final properties of dual-phase ADI depend on the volume amount of free ferrite, which provides ductility and machinability, and the amount and morphology of ausferrite, which grants strength and ductility [4].

### 2. PROPERTIES OF DUAL PHASE AUSTEMPERED DUCTILE IRON

#### 2.1. Microstructure

The method to obtain dual phase microstructure in austempered ductile iron consists of an incomplete austenitization stage at temperatures within the intercritical interval, generally between 750–860 °C. The different heat treatments are used to obtain dual-phase microstructures with different percentages of microconstituents. The scheme of pseudo binary Fe-C phase diagram with marked intercritical interval is shown in Fig. 1.

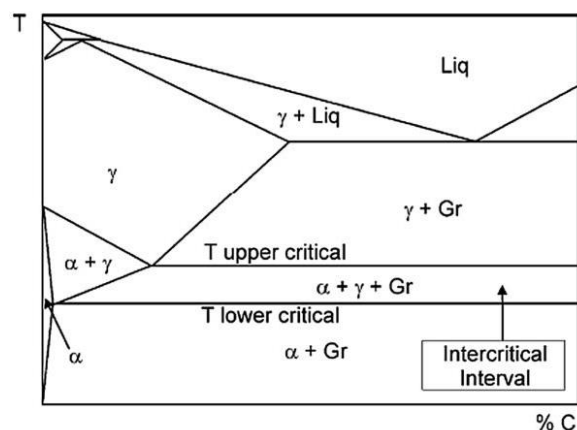


Fig. 1. Schematic pseudo binary Fe-C phase diagram [6]

The upper and lower critical temperatures define the starting point at which ferrite transforms into austenite in heating and respectively in cooling processes. After intercritical annealing, quenching is performed in the usual temperature range 250–400 °C in a salt bath, which is carried out to transform the austenite into ausferrite.

The dual-phase austempered ductile iron has a mixed microstructure, which is consisted of free (proeutectoid)

allotriomorphic ferrite and different amounts and morphologies of ausferrite. The typical microstructure of dual-phase austempered ductile iron, which is obtained after austenitization at 800 °C and austempering at 300 °C is shown in Fig. 2.

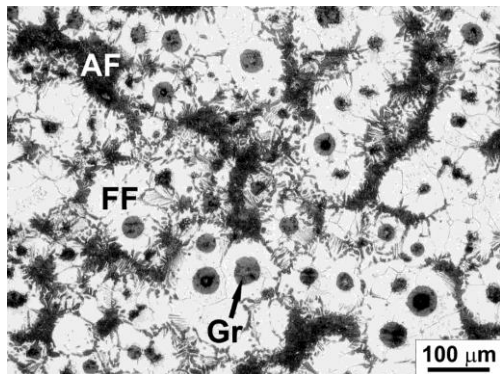


Fig. 2. Microstructure of a dual-phase austempered ductile iron; AF – ausferrite, FF – free ferrite, Gr – graphite nodules

## 2.2. Mechanical Properties

The dual-phase ADI can offer a wide range of the mechanical properties as yield stress, tensile strength, elongation and hardness. Those mechanical properties depend on the relative percentage of free ferrite and ausferrite present in the microstructure [5, 7, 8]. For example, the presence of 20% ausferrite in the microstructure increases yield and tensile strength approx. 30% as compared to fully ferritic ductile iron [9].

Investigations of Basso et al. [6, 9], showed that as the amount of ausferrite increases, the yield and tensile strength increases also, while the elongation decreases for all the austempered temperatures used. The best combination of strength and elongation (UTS=690 MPa, YS=550 MPa, E=22%) was obtained for samples austenitized at 820 °C for one hour and subsequently austempered at 350 °C for one and half hours [6].

The example of microstructure influence on the yield strength (yield stress), tensile strength, and elongation as a function of the amount of ausferrite for 300, 330 and 350 °C austempering temperatures are shown in Fig. 3 [6]. The optimal tensile strength, yield stress and elongation of dual-phase ADI material can be achieved if the austempering process is performed at 350 °C.

## 3. APPLICATION OF DUAL PHASE AUSTEMPERED DUCTILE IRONS

Austempered Ductile Iron has found successful applications across many industries, including construction and mining, agriculture, automotive, heavy truck, and railroad. In some cases, the ADI has replaced aluminium as a weight saving. The ADI components are competitive with steel forgings, castings, weldments, and aluminium forgings and castings [1].

For an illustration, increased mechanical properties of dual-phase ADI allowed for the change of the steering knuckle geometry [10]. The Fig. 4 shows the steering knuckle fabricated from cast iron (a) and a redesigned

steering knuckle produced from dual-phase ADI materials (b). From the Table 1 it can be seen that the steering knuckle produced of dual-phase ADI results in dramatically increased strength and considerable weight savings compared to cast iron. The benefits of reduction in weight have an influence on lower fuel costs, on the whole product weight savings and lower costs of the finished product [8].

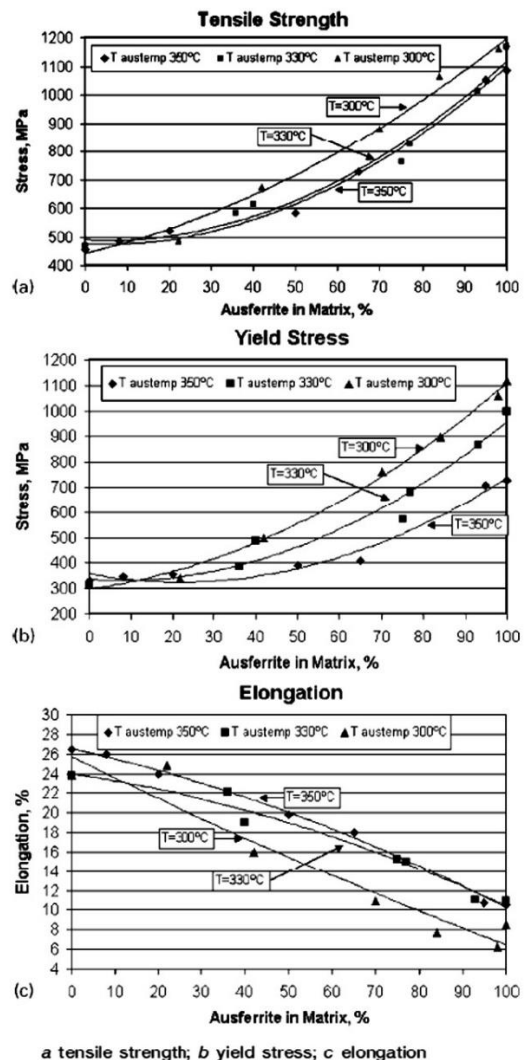


Fig. 3. Relation between amounts of ausferrite in the matrix and mechanical properties [6]

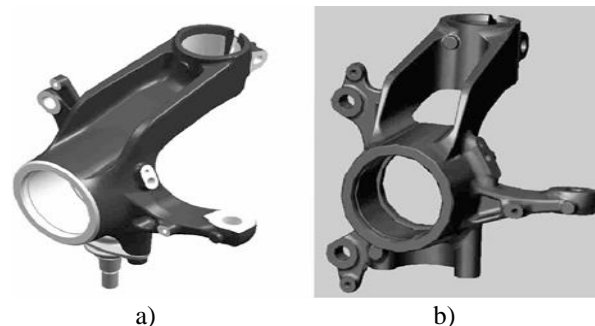


Fig. 4. Steering knuckle produced from a) cast iron, b) dual-phase ADI [10]

Materials	GH 60-38-10 Pearlitic-Ferritic cast iron	ISO 17804/ JS/900-8
R <sub>p0.2</sub> [MPa]	370	600
R <sub>m</sub> [MPa]	590	900
A [%]	10	8
Machined weight [kg]	9.5	7.5
Raw weight [kg]	10.7	8.7

Table 1. Mechanical properties and knuckle weights of cast iron and dual-phase ADI [10]

#### 4. EXPERIMENTAL WORK

Test specimens were cut from 25 mm-thick Y-block-shaped. Y-block were produced of unalloyed ductile iron with a chemical composition in wt%: 3.53C; 2.53Si; 0.347Mn; 0.045Cu; 0.069Ni; 0.055Mg; 0.031P; 0.015S.

Test specimens were differently heat-treated, and 8 different dual phase ADI specimens were obtained. Heat treatment consisted of a partial austenitization and austempering. Austenitization is performed by holding test specimens in the furnace with a protective argon atmosphere. Temperatures of austenitization were in the intercritical interval, that is, austenitization is performed at 840, 820, 800 and 780 °C for 2 hours. The austempering was performed in a salt bath at 300 or 400 °C for 1 h.

The samples which were prepared by standard metallographic preparation techniques, consisted of mechanical grinding, polishing and etching surface with Nital (3%); have been further examined on a "Leitz-Orthoplan" light microscope (LM).

The average volume amount (in %) of ausferrite (AF), free ferrite (FF), and graphite (Gr) in DP-ADI microstructures was quantified by JMicroVision software at the five fields of view.

The Vickers hardness HV10 (ISO 6507) was determined on a hardness testing machine HPO 250, WEB Leipzig, with a test load of 98.07 N (10 kgf) and a dwell time of 15 s.

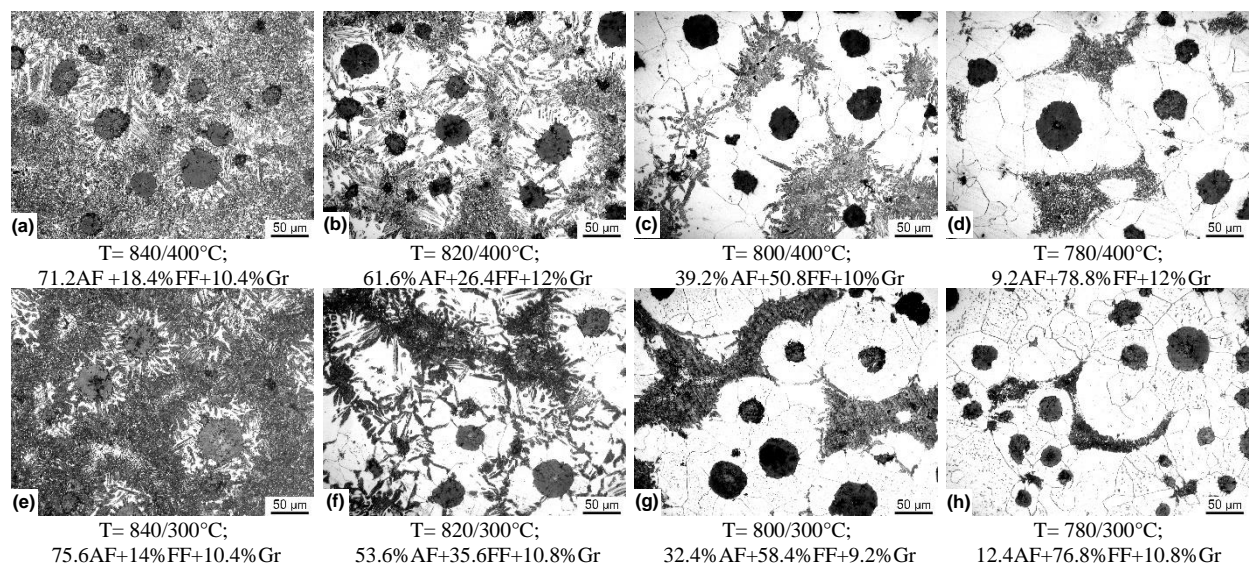


Fig. 6. Microstructure for all samples austenitized and austempered at different temperatures with the percentage fraction of the phases

#### 5. RESULTS

As-cast ductile iron had the graphite spheroidization of more than 90%, and the average graphite volume fraction of  $12 \pm 1.6\%$ , Fig 5a. Nodule size was from 15 to 30  $\mu\text{m}$  and nodule count distribution was from 150 to 200 mm. The starting microstructure was predominantly ferritic (over 90%), Fig. 5b.

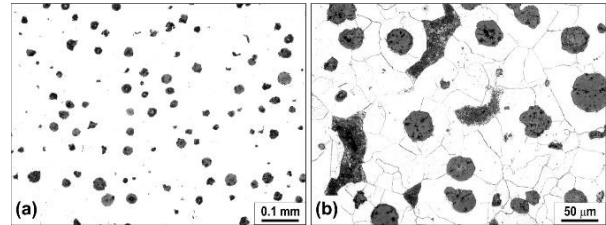


Fig. 5. Microstructure of as-cast ductile iron: (a) polished; (b) etched

The microstructures obtained for all DP-ADI samples is illustrated on Fig. 6. Furthermore, at the Fig. 6 the volume amount (in %) of ausferrite (AF), free ferrite (FF), and graphite (Gr) in microstructures is also given. The graphical representation of microstructure influence on hardness is given in Fig. 7.

The different austenitization temperatures allowed the attainment of different percentages of ausferrite and free ferrite in all samples, Fig 6. With increase of austenitization temp. percentage of ausferrite also increases, while the amount of free ferrite has opposite trend, i.e. decreases. Additionally, the austenitization temp. influence the morphology of the AF microstructure. At the higher austenitization temp. the transformation process is slower producing a larger and broader AF appearance. Contrary, at lower austenitization temp. the transformation is faster, producing finer ausferritic ferrite plates. However, the overall appearance of ausferrite is primarily influenced by the austempering temperature. That is, at 400 °C a plate like morphology of AF is present, while at 300°C the AF have acicular appearance.

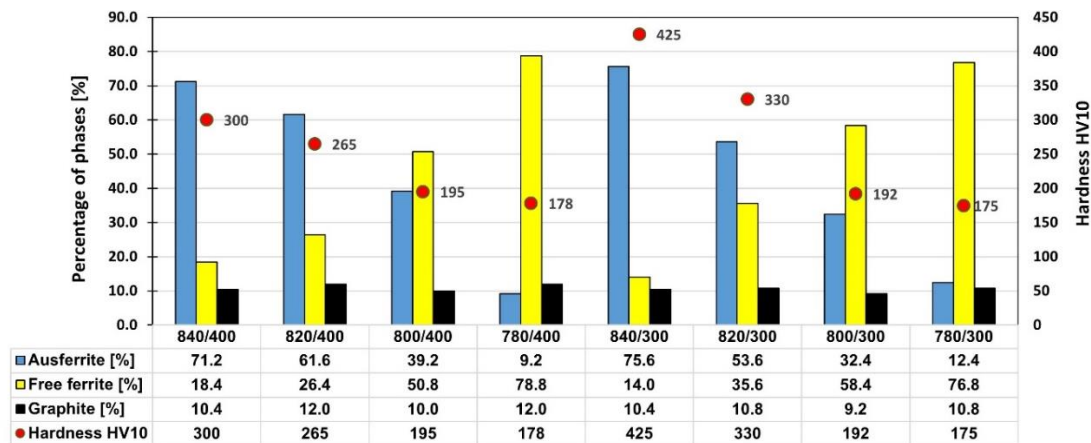


Fig. 7. Effect of microconstituents percentages on the hardness values of dual-phase austempered ductile iron

Achieved different morphology of the AF directly affects the hardness. When the amount of the FF is less than ~50%, the samples that were austempered at 400 °C have a lower level of hardness than samples heat treated at 300°C. When amount of free ferrite is greater than ~50%, hardness is similar for both austempering temperatures, as in this case the hardness is dominated by large amount of free ferrite.

## 6. CONCLUSION

The dual-phase ADI is promising new material, where desired mechanical properties could be easily achieved in a wide range by appropriate austenitization in intercritical range and subsequent austempering.

The change in mechanical properties depends on a microconstituent volume amount in DP-ADI microstructure and on microstructure morphology. This is clearly reflected on the hardness values.

The plate like morphology of AF at 400°C yields lower hardness values, while the acicular appearance of AF at 300°C gives higher hardness values.

## 7. REFERENCES

- [1] Harding R.A: *The production, properties and automotive applications of austempered ductile iron*, Kovove Materials, 45, pp. 1–16 A, (2007).
- [2] Eric, O., Rajnovic, D., Sidjanin, L., Zec, S., Jovanovic, T.: *An austempering study of ductile iron alloyed with copper*, J. Serb. Chem. Soc. 70(7), pp. 1015–1022, (2005).
- [3] Sidjanin, L., Rajnovic, D., Eric, O., Smallman, R.E.: *Austempering study of unalloyed and alloyed ductile irons*. Mater. Sci. Technol. 26(5), pp. 567-571 (2010).
- [4] Basso, A., Sikora, J.: *Review on production processes and mechanical properties of dual phase austempered ductile iron*, Int. J of Metal casting, 6/1, pp. 7-14, (2012).
- [5] Kilicli, V., Erdogan, M.: *Tensile properties of partially austenitised and austempered ductile irons with dual matrix structures*, Materials Science and Technology, 22/8, pp. 919-928, (2006).
- [6] Basso, A.D., Martinez, R.A., Sikora, J.: *Influence of austenitising and austempering temperatures on*

*microstructure and properties of dual phase ADI*, Mater. Sci. Technol. 23 (11), pp. 1321–1326, (2007).

- [7] Sahin, Y., Erdogan, M., Kilicli, V.: *Wear behaviour of austempered ductile irons with dual matrix structures*. Mater. Sci. Eng., A 444, pp. 31–38, (2007).
- [8] Aranzabal, J., Serramoglia, G., Rousiere, D.: *Development of a new mixed (ferritic/ausferritic) ductile iron for automotive suspension parts*, Int. J. Cast Metals Res. 16(1–3), pp. 185–190, (2003).
- [9] Basso, A., Martinez, R., Sikora, J.: *Influence of section size on dual phase ADI microstructure and properties: comparison with fully ferritic and fully ausferritic matrices*. Mater. Sci. Technol. 25(10), pp. 1271-1278, (2009).
- [10] E Eric, O., Rajnovic, D., Sidjanin, L., Janjatović, P., Balos, S.: *Dual Phase Austempered Ductile Iron - The Material Revolution and Its Engineering Applications*, CNNTech 2019, pp. 22-38, Zlatibor, Springer, 3-5 July 2019.

**Authors:** M.Sc. Petar Janjatović, Assoc. Prof. Dragan Rajnović, Full Prof. Sebastian Baloš, Assist. Prof. Miroslav Dramićanin, Full Prof. Leposava Šidanin, University of Novi Sad, Faculty of Technical Sciences, Department of Production Engineering, Trg Dositeja Obradovića 6, 21000 Novi Sad, Serbia, Phone.: +381 21 485-23-23.

E-mail: [janjatovic@uns.ac.rs](mailto:janjatovic@uns.ac.rs); [draganr@uns.ac.rs](mailto:draganr@uns.ac.rs); [sebab@uns.ac.rs](mailto:sebab@uns.ac.rs); [dramicanin@uns.ac.rs](mailto:dramicanin@uns.ac.rs); [lepas@uns.ac.rs](mailto:lepas@uns.ac.rs)

**Assoc. Prof. Olivera Erić Cekić**, University of Kragujevac, Faculty of Mechanical and Civil Engineering in Kraljevo, Department of General Engineering Education, Dositejeva 19, 36000 Kraljevo, Serbia.

E-mail: [olivera66eric@gmail.com](mailto:olivera66eric@gmail.com)

**ACKNOWLEDGMENTS:** The authors gratefully acknowledge research funding by the project "Modern technologies in materials science and welding technology" on the Department of Production Engineering, Faculty of Technical Sciences, Novi Sad, Serbia



Čabrilo, A.

## INFLUENCE OF HEAT INPUT ON THE BALLISTIC PERFORMANCE OF ARMOR STEEL WELDMENTS

**Abstract:** The purpose of this study is to examine the projectile penetration resistance of the base metal and heat-affected zones of armor steel weldments. To ensure the proper quality of armor steel welded joints and associated ballistic protection, it is important to find the optimum heat input for armor steel welding. A total of two armor steel weldments made at heat inputs of 1.29 kJ/mm and 1.55 kJ/mm were tested for ballistic protection performance. The GMAW welding carried out employing a robot controlled process. Owing to a higher ballistic limit, the heat affected zone (HAZ) of the 1.29 kJ/mm weldment was found to be more resistant to projectile penetration than that of the 1.55 kJ/mm weldment. The result showed that the ballistic resistance of heat affected zone exist as the heat input was decreased on 1.29 kJ/mm. It was found that 1.55 kJ/mm does not have ballistic resistance.

**Key words:** armor steel, weldment, projectile penetration, hardness level

### 1. INTRODUCTION

Armor grade steels possessing high strength and hardness are widely used in the production of military armored vehicles such as Lazar III [1]. High hardness armor steel requires carefully controlled welding procedures to avoid hardness losses in heat affected zones [2]. Heat input is the crucial factor associated with the toughness of fusion zones in shielded metal arc-welding weldments [3]. The hardness of armor steel is greatly dependent on the welding temperature history.

Heat affected zone (HAZ) softening occurring during welding of high hardness armor (HHA) steel and the degree of softening in the HAZ is a function of the weld thermal cycle, which depends on the welding process [4]. Gas metal arc welding (GMAW) process has a higher deposition rate, compared to the Shield metal arc welding [5]. In application of the GMAW process, the consumable is continuously added and frequent stops are not happening. As a result, the GMAW process has superior productivity compared to shield metal arc welding (SMAW) [6, 7].

Previous studies have shown that a heat input of 1.2 kJ/mm is safe for the ballistic protection of military armored vehicles, whereas a heat input of 1.9 kJ/mm has been found ballistically unsafe for the armor protection of military vehicles. However, a heat input of 1.2 kJ/mm was found herein to be insufficient to ensure the proper quality of armor steel welded joints, so it was of paramount importance to find the optimum heat input for obtaining the best ballistic protection of the welded joints. Appropriate welding parameters are essential for the ballistic resistance of weld joints [8] in military vehicles, as well as their toughness when the vehicles are moving over uneven terrains.

This paper presents a comparison of the ballistic performance of quenched armor steel weldments made at heat inputs of 1.29 kJ/mm and 1.55 kJ/mm, which form a 100% martensitic structure at a cooling rate of 7 °C/s.

### 2. MATERIALS AND EXPERIMENTAL PROCEDURE

#### 2.1. Base and Filler Material

Armor steels are well established as projectile-resistant materials. The commercially available Protac 500 armor steel was used in this study for its high strength ( $\sigma_y = 1206$  MPa and UTS = 1536 MPa) [9].

The chemical composition (wt. %) of the base metal, armor steel, was 0.27 C, 1.07 Si, 0.706 Mn, 0.637 Cr, 1.09 Ni, 0.3 Mo, 0.039 V, 0.01 S, and 0.02 P. The chemical composition (wt. %) of the filler material, Mn type stainless steel, was 17.76 Cr, 8.24 Ni, 6.29 Mn, 0.89 Si, and 0.08 C. The chemical composition of the welded joint was obtained by Optical emission spectrometer (OES), ARL 2460 (Thermo Fisher Scientific).

#### 2.2. Welding Process

GMAW was performed at heat inputs of 1.29 kJ/mm and 1.55 kJ/mm, using the same welding configuration (Figure 1). A 55 degree single V groove edge with a 4 mm root face gap was employed before welding. Each weld was produced by four pass welding with preheating. The plate dimensions were 500 mm × 250 mm × 11 mm. A water jet cutter was employed for plate cutting and edge preparing.

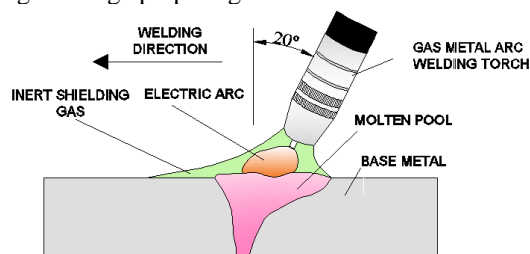


Fig. 1. Schematic drawing of welding process.

The Protac 500 welding parameters are shown in Table 1. Welding heat input calculated in accordance with EN 1011-1, using equation 1. Where heat transfer efficiency was 0.8 for GMAW.

$$Hi = \frac{U * I * K}{v} \quad (1)$$

Where are: Hi - Heat input (kJ/mm), U - Welding voltage (V), I - Welding current (A), v - Welding speed (mm/min) and k - Welding heat efficiency.

The automated welding for both heat inputs considered was performed using the Kuka robot, Augsburg, Germany and the Citronix 400A GMAW welding machine.

Heat Input	Preheat Temp. [°C]	Current [A]	Voltage [V]	Welding Speed [m/min]	Shielding Gas
1.29	150	193	25	0.18	Ar. + 2.5% CO <sub>2</sub>
1.55	150	215	25.5	0.17	Ar. + 2.5% CO <sub>2</sub>

Table 1. Welding parameters of the Protac 500 armor steel welding.

### 2.3. Microhardness testing

According to the EN ISO 9015-1 standard [10], the hardness of welded joints is measured for their complete characterization. The hardness of the Protac 500 welded joints was herein tested 2 mm under the upper welding surface at heat inputs of 1.29 kJ/mm and 1.55 kJ/mm. The hardness of both heat input samples considered was measured along the fusion line for achieving optimum hardness in this critical zone and along the edge of the weld metal. The Digital Micro Vickers Hardness Tester HVS1000 (Laizhou Huayin Testing Instrument Co., Laizhou City, China) was used for microhardness testing, applying a load of 500 g. Each microhardness value represents the mean value of three measurements performed.

### 2.4. Ballistic Testing

The ballistic resistance testing in this study was accomplished in accordance with the VPAM APR 2007 standard [11], which stipulates placing the ballistic pipe at a distance of 10 m from the target [12]. The ballistic test scheme and the 7.62 × 51 mm projectile used are shown in Figure 2 a, b). The projectile speed was measured prior to the experiment at a distance of 7 m from the position of the ballistic pipe mouth. The projectile speed measurements were performed on three projectiles to obtain a representative mean value of the projectile speed.

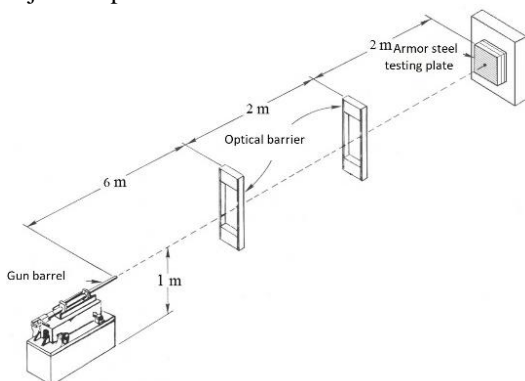


Fig. 2. Ballistic testing scheme.

## 3. RESULTS

### 3.1. Microhardness

Hardness is one of the most important aspects of armored vehicle crew protection and the quality of welded joints. The hardness profiles obtained for heat inputs of 1.29 kJ/mm and 1.55 kJ/mm are shown in Figure 3.

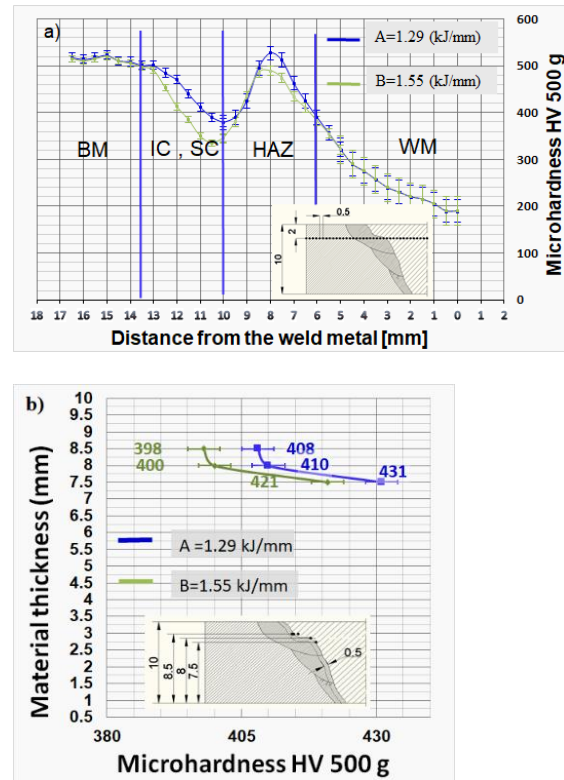


Fig. 3. (a) Hardness distribution of the automated welding at heat inputs of 1.29 kJ/mm (A) and 1.55 kJ/mm (B). (b) Hardness distribution along the fusion line of the automated welding at heat inputs of 1.29 kJ/mm (A) and 1.55 kJ/mm (B). Each hardness value represents the mean value of three measurements performed.

Figure 3 a) shows the hardness of the welded joints preheated at 150 °C, using an inter-pass temperature of 160 °C. The welded joint zones were marked accordingly with the following abbreviations: WM (weld metal), FL (fusion line), HAZ (heat affected zone), IC (inter critical zone), SC (sub critical zone) and BM (base metal).

The hardness profile obtained for a heat input of 1.29 kJ/mm Figure 3 a) indicates hardness variations in the WM, FL, HAZ and BM zones. The hardness values increased from the middle of the WM zone (190 HV) towards the fusion line, along which a value of 339 HV was recorded on the WM side. The FL hardness value was 410 HV. The hardness values increased in the HAZ zone and reached a maximum value of 521 HV at a distance of 8 mm from the weld axis. The values decreased thereafter and a minimum hardness of 378 HV was recorded at a distance of 10 mm from the weld axis.

Upon another subsequent increase, the hardness values eventually leveled off at 509 HV recorded at a

distance of 14 mm from the weld axis, which also marked the limit of the HAZ and OM zones. The average BM hardness value was 509 HV.

The hardness profile obtained for a heat input of 1.55 kJ/mm [Figure 3 b\)](#) also suggests hardness variations in the WM, FL, HAZ and BM zones. The hardness values increased from the middle of the WM (192 HV) towards the fusion line, along which a value of 350 HV was recorded on the WM side. The FL hardness was 400 HV.

The hardness values decreased in the HAZ zone and reached a minimum value of 325 HV at a distance of 10.5 mm from the seam axis. Upon another subsequent increase, the hardness values eventually leveled off at 509 HV recorded at a distance of 14 mm from the seam axis, which also marked the limit of the HAZ and BM zones. The average BM hardness value was 509 HV.

The hardness of the 1.29 kJ/mm and 1.55 kJ/mm weldments was measured along the fusion line [Figure 3 b\)](#). The results obtained show that the fusion line hardness of the 1.29 kJ/mm weldment ranged between 408 HV and 431 HV, whereas the fusion line hardness of the 1.55 kJ/mm weldment ranged between 398 HV and 421 HV. The hardness values were found to be associated with heat effects: the heat effect was more significant in the zones closer to the cover pass, whereas the already cooled additional and base material reduced the heat effect in the more remote zones.

### 3.2. Microstructure

The microstructure of the coarse-grained HAZ region of the 1.29 kJ/mm weldment [Figure 4 a\)](#) indicates martensite and the formation of smaller volume fractions of softer constituents, i.e., lower and upper bainite. The 1.55 kJ/mm weldment [Figure 4 b\)](#) consisted of a mixture of lath martensite and upper and lower bainite. The martensite to bainite (upper + lower) ratio determined was approximately 40:60. With an increase in heat input to 1.55 kJ/mm, an increasing amount of bainite was observed. However, the martensite content diminished in the microstructure of the coarse-grained region near to the fusion line. Such conditions favored the formation of bainite with a predominant amount of upper bainite in the microstructure of the 1.55 kJ/mm welded joints.

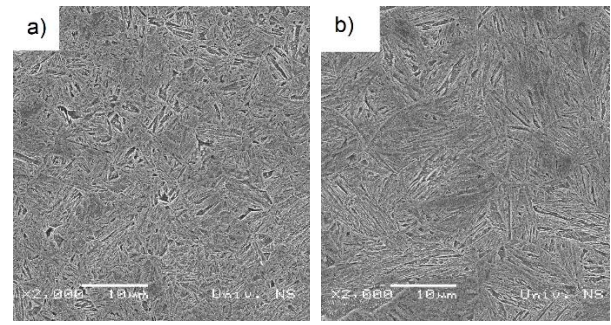


Fig. 4. SEM microstructures of the coarse-grained HAZ (a) of the 1.29 kJ/mm weldment. SEM microstructure of the coarse-grained HAZ (b) of the 1.55 kJ/mm weldment.

### 3.3. Ballistic Test Results

The results of ballistic resistance testing of the welded Protac 500 joints made at a heat input of 1.55 kJ/mm are given in [Table 2\)](#). The results obtained show that the initial velocities of the  $7.62 \times 51$  mm projectile ranged from 854.896 m/s to 848.881 m/s. The equivalent shooting distance was 10 m. Two holes normal were made in this zone in the first two shootings, whereas a bulge with a protrusion was made in the third shooting.

The damaged HAZ area was in the range of 70.24–90.6 mm<sup>2</sup>. The damage on the inside of the heat-affected zone indicates intense plastic deformation in the direction of the projectile's passage.

The initial projectile velocities recorded in the HAZ area of the 1.29 kJ/mm weldment ranged from 850.231 m/s to 852.142 m/s [Table 2\)](#). The equivalent shooting distance was 10 m. Two plastic flows were made in this zone in the first two shootings, whereas a protruding bulge was made in the third shooting. The damaged HAZ area was in the range of 60.9–80.6 mm<sup>2</sup>. The hardness of the HAZ zone ranged from 358 HV to 521 HV.

The initial projectile velocities recorded in base metal of the 1.29 kJ/mm weldment ranged from 849.116 m/s to 852.213 m/s. The equivalent shooting distance was 10 m. Three bulges were made in this zone in three shootings. The damaged base metal area was in the range of 30.9–40.6 mm.

Serial Number	Heat Input	Position	Initial Speed V10	Equivalent Shooting Distance	Angle of Impact Relative to the Projectile Trajectory	Type of Damage
	[kJ/mm]					
4	1.55	HAZ	852.142	10	90	hole normal
5	1.55	HAZ	851.321	10	90	hole normal
6	1.55	HAZ	850.231	10	90	bulge
7	1.55	Base metal	849.116	10	90	plastic flow
8	1.55	Base metal	850.212	10	90	plastic flow
9	1.55	Base metal	852.313	10	90	plastic flow
10	1.29	HAZ	852.048	10	90	bulge
11	1.29	HAZ	851.254	10	90	bulge
12	1.29	HAZ	850.358	10	90	bulge
13	1.29	Base metal	849.742	10	90	plastic flow
14	1.29	Base metal	850.343	10	90	plastic flow
15	1.29	Base metal	852.259	10	90	plastic flow

Table 2. Results of ballistic resistance testing of the welded Protac 500 joint, made at a heat inputs of 1.29 and 1.55 kJ/mm

## 4. DISCUSSION

The microstructure formed in the HAZ is a function of the chemical composition of the steel considered and the weld thermal cycle. The main concern when employing higher heat inputs in the HHA steel welding (namely a heat input of 1.55 kJ/mm) is the formation of wide extensively softened areas in the over-tempered region that could compromise the ballistic performance of the welded structure. Conversely, the resulting prolonged cooling times temper its rehardened HAZ areas, thus reducing the risk of heat affected cold cracking (HACC). These effects could compensate for employing the proposed low level preheating in multi-pass joint welding.

The microhardness HAZ values of the 1.29 kJ/mm weldment ranged from 390 HV to 523 HV, whereas the microhardness HAZ values of the 1.55 kJ/mm weldment ranged from 325 to 490 HV. It is concluded that as heat input decreases, the hardness of the weld metal increases, which leads to ballistic protection.

Changes in the base material hardness of the 1.29 kJ/mm and 1.55 kJ/mm weldments occurred at distances of 13.5 mm and 14.2 mm from the weld axis, respectively. From a perspective of armor protection and ballistic resistance to small arms projectiles, the selection of a heat input is important because it greatly affects the hardness of the HAZ coarse-grained area. A previous study reported that coarse-grained zone hardness values of 541 HV and 502 HV were recorded in the 0.8 kJ/mm and 1.6 kJ/mm weldments [13]. These results are similar to the results obtained in the present study. A hardness value of 523 HV was recorded in the 1.29 kJ/mm weldment. This slightly higher hardness was achieved due to the increased hardenability of Protac 500. With a heat input of 2.37–1.33 kJ/mm, the AISI 4340 was found to have a coarse-grained zone hardness of 403–430 HV [14]. The maximum coarse-grained hardness of 443 HV was achieved with a heat input of 2.37 kJ/mm [15].

The hardness results obtained show that lower heat inputs practically improve the hardness in the coarse-grained HAZ subzone. Moreover, little to no softening was observed in the over-tempered area of the optimized welds, with the hardness values exceeding the lowest hardness value of 509 HV permitted by MIL-STD-1185 at a distance of 15.9 mm from the weld.

The results of the HAZ ballistic resistance testing for the 1.29 kJ/mm and 1.55 kJ/mm weldments, using 10 mm metal sheets, are given in Table 2. None of the three 7.62 × 51 mm projectiles fired made a hole normal in the 1.29 kJ/mm weldment. However, one of the projectiles punched through the HAZ zone of the 1.55 kJ/mm weldment. This can be explained by the diminished hardness of this zone compared to that of the 1.29 kJ/mm weldment.

The results of ballistic resistance testing in the base material zone of the 10 mm thick Protac 500 plates considered are presented in Table 3. None of the three 7.62 × 51 mm projectiles fired made a hole normal in this zone, which can be accounted for by the optimal ductility of the zone (reflected also in the low plastic deformation sustained). Therefore, the 10 mm thick Protac 500 plate was found to provide the required

degree of the base material ballistic protection. The results of ballistic resistance testing in the base material zone show unequivocally that hardness is the predominant mechanical property of high and ultra high strength materials compared to tensile strength, yield stress and impact energy. Bulge was observed in the 1.29 kJ/mm weldment HAZ whereas no grain penetration was recorded in the 1.55 kJ/mm weldment HAZ.

The ballistic results obtained indicate that a heat input of 1.29 kJ/mm was found to be the limit for achieving the desirable armor protection and HAZ ballistic resistance of armor steels forming a 100% martensitic structure at a cooling rate of 25 °C/s. A higher heat input would impair the HAZ ballistic resistance of such steels. In the case of Protac 500, the limit for preventing grain penetration is a heat input of 1.55 kJ/mm. A heat input greater than 1.55 kJ/mm would impair the ballistic resistance of the Protac 500 HAZ.

## 5. CONCLUSIONS

Two armor steel GMAW weldments made at heat inputs of 1.29 kJ/mm and 1.55 kJ/mm were tested for ballistic protection performance.

On the basis of the results obtained, the following conclusions can be drawn:

- The hardness of the HAZ fusion zone diminished at a heat input of 1.55 kJ/mm, resulting in the reduced ballistic protection of armored vehicles. Welded metal hardness is increased with the decrease in heat input.
- The microstructure in the CGHAZ changes from lath bainite / martensite to coarse granular bainite with increasing heat input.
- An increase in heat input leads to a ductile domain, thus reducing the ballistic performance of the 1.55 kJ/mm weldment. In the case of the 7.62 mm AP projectile, hardness and strength of the material are important for ballistic performance. Therefore, the 1.55 kJ/mm weldment was found not to be resistant to the 7.62 × 51 mm projectile penetration.

## 6. REFERENCES

- [1] Jo, M. C., Kim, S., Suh, D. W., Hong, S. S., Kim, H. K., Sohn, S. S., Lee, S.: *Effect of tempering conditions on adiabatic shear banding during dynamic compression and ballistic impact tests of ultra-high-strength armor steel*, Materials Science and Engineering: A, 792, pp. 139818, 2020.
- [2] Saxena, A., Kumaraswamy, A., Sethi, S., Reddy, G. M., Madhu, V.: *Microstructural characterization and high strain rate plastic flow behavior of SMAW Armax 500T steel joints from spherical indentation experiments*, Journal of Materials Engineering and Performance, 27, pp. 4261–4269, 2018.
- [3] Reddy, G. M., Mohandas, T., Tagore, G. R. N.: *Weldability studies of high-strength lowalloy steel using austenitic fillers*, Journal of Materials Engineering and Performance, 49, pp. 213–228, 1995.
- [4] Magudeeswaran, G., Balasubramanian, V., Reddy, G. M., Balasubramanian, T. S.: *Effect of welding process consumables on tensile and impact*

- properties of High Strength Quenched and Tempered steel Joints*, Journal of Iron and Steel Research International, 15, pp. 87–94, 2008.
- [5] Magudeeswaran, G., Balsubramanian, V., Ready, G. M.: *Effect of welding processes and consumables on high cycle fatigue life of high strength quenched and tempered steel joints*, Materials & Design, 29, pp. 1821–1827, 2008.
- [6] Kuzmikova, L.: *An investigation of the weldability of high hardness armor steel*. Ph.D. Thesis, Faculty of Engineering, University of Wollongong, Wollongong, Australia, 2013.
- [7] Teresa, F., Christian, R., Dirk, M.: *Fracture of high-strength armor steel under impact loading*, International Journal of Impact Engineering, 111, pp. 147–164, 2018.
- [8] Cabrilo, A., Geric, K.: *Weldability of High Hardness armor steel*, Advanced Materials Research, 1138, pp. 79-84, 2016.
- [9] Rajkumar, G.B., Murugan, N.: *Development of regression models and optimization of FCAW process parameter of 2205 duplex stainless steel*, Indian Journal of Engineering and Materials Sciences, 21, pp. 149-154, 2014.
- [10] Unfried, J., Garzon, S., Giraldo, J.: *Numerical and experimental analysis of microstructure evolution during arc welding in armor plate steels*, Journal of Materials Processing Technology, 209, pp. 1688–1700, 2009.
- [11] Namkug, K., Sol, H., Myung, R.: *Design of controller for mobile robot in welding process of shipbuilding engineering*, Journal of Computational Design and Engineering, 4, pp. 243–255, 2014.
- [12] Cabrilo, A., Sedmak, A., Burzic, Z., Perkovic, S.: *Fracture mechanics and fatigue crack propagation in armor steel welds*, Engineering Failure Analysis, 106, pp. 104–155, 2019.
- [13] VPAM Association. VPAM Association of Test Laboratories for Bullet Resistant Materials and Constructions. VPAM AMPR 2006-General Basis for Ballistic Material, Construcion and Product Testing. Muenster; VPAM Association of Test Laboratories for Bullet Resistant Materials and Constructions, 2009.
- [14] Madhusudhan, R. G., Mohandas, T.: *Ballistic performance of high-strength low alloy steel weldments*, Journal of Materials Processing Technology, 57, pp. 23–30, 1996.
- [15] Bernetic, J.: *Development of Model for Predicting Hardenability of High Strength Low Alloy Steels*. Ph.D. Thesis, University of Ljubljana Faculty of Natural sciences and engineering department of materials and metallurgy, Slovenia, 2013.

**Author: Ph.D. Prof. Aleksandar Čabrilo**, The Higher Education Technical School of Professional Studies, University of Novi Sad, Skolska 1, 21000 Novi Sad, Serbia, Phone.: +381 21 4892-511, Fax: +381 21 4892-515.

E-mail: [cabrilo@uns.ac.rs](mailto:cabrilo@uns.ac.rs)

#### ACKNOWLEDGMENTS:

The authors would like to thank Aleksandar Mladenovic and Zastava arms for ballistic testing.



Dramićanin, M., Janjatović, P., Adamović, S., Kulundžić, N., Zabunov, I., Rajnović, D., Baloš, S.

## INFLUENCE OF MICRO AND NANO PARTICLES ON THE PERFORMANCE OF ACTIVATED TUNGSTEN INERT GAS WELDING

**Abstract:** The aim of this paper was to study the influence of the submicron and nanoparticle sized  $TiO_2$  particles in the flux and affect the Tungsten inert gas welding (TIG). Microhardness, penetration depth, depth to width (D/W) ratio and microstructures were investigated. The model illustrating material flow was created based on the results. Weld metal surface area could not be positively correlated to the application of flux. Nanoparticles, on the other hand, were shown to be more efficient than submicron particles in improving penetration depth and D/W ratio, while mixtures of submicron and nanoparticles was being the most effective.

**Key words:** submicron particles, nano particles, oxides, penetration depth

### 1. INTRODUCTION

Tungsten inert gas (TIG), also known as Gas tungsten arc welding (GTAW) is a well established welding process that can produce high quality welds on various materials, including various stainless steels, and a number non-ferrous alloys. However, because of its poor productivity, its application has typically been limited to relatively thin sections in different welding positions [1]. The low productivity is due to a low deposition rate as well as low penetration [2]. As the solution to this problem, the flux has developed to increase the penetration depth, and this process was called Activated TIG (A-TIG). Fluxes were produced as a mixture of metallic oxide powders and solvents, most frequently acetone and ethanol [3,4]. The application of flux in TIG/GTAW was proposed for the first time by Paton Welding Institute of National Academy of Sciences, Ukraine, back in the 1960s, when part of USSR, by Gurevich et al. [5]. In this welding process, flux is sprayed or applied with a brush over the cleaned and prepared surface to be welded, resulting in increased penetration depths, weld without the need for groove preparation, no usage consumable material, no multipass weld, decreased application of shielding gas, lower cost, and time-saving [6,7,8].

In this study, nano, micro and a mix of the two types of oxide particles were used in the flux. The influence of different types of oxides was correlated to the molten metal flow was established.

### 2. EXPERIMENTAL PART

Welding, or more accurately, remelting was done on six stainless steel plates with applied flux and one plate without the flux as a control specimen. The arc was established by a  $\varnothing$  2.4 mm tungsten - 2% thorium electrode with a blunt tip. The welding current was 200 A DCEN (direct current electrode negative), while the argon protective gas flow rate was 12 l/min. The arc length was 2 mm, and the welding speed was 100 mm/min. The welding-remelting was done using an EWM Tetrix 300 device with a nozzle diameter of 12.7 mm. The plate material was AISI 304L (X2CrNi18-10)

stainless steel. Its chemical composition is shown in Table 1.

C	Si	Mn	Cr
0.02	0.042	1.55	18.63
Ni	P	S	Fe
8.23	0.032	0.0004	balance

Table 1. Chemical composition of the base metal wt. %.

Six different mixtures were prepared, containing 5 wt. % of particles in acetone ( $(CH_3)_2CO$ ):

1. all-micro (5M)
2. 1 % nano and 4 % micro particles(4M1N)
3. 2 % nano and 3 % micro particles (3M2N)
4. 3 % nano and 2 % micro particles (2M3N)
5. 4 % nano and 1 % micro particles (1M4N)
6. all-nano (designated as 5N)
7. control sample without the flux (0)

The oxide particles were weighed on an analytic balance, and the carrier solvent was mixed with a magnetic stirrer for 10 minutes. The Zetasizer Nano ZS device was used to determine the particle size in the solvent.

A 10 mm brush was used to apply the coating to the base material in a 20 mm wide layer.

Macro testing, microstructure analysis, and microhardness were all used in the post-weld characterization. Cutting, grinding, and polishing on Struers equipment was used to examine macro and microstructures, which were then etched with aqua regia.

Microstructures were examined by a Leitz Orthoplan light microscope in several common locations such as the weld bead (WB), heat affected zone (HAZ), and base metal (BM) were also studied. The light microscope was also used for the measurement of the width and depth of the weld beam, while depth to width ratios (D/W) were calculated.

Vickers microhardness was measured on a Wilson Tukon device with an indentation force of 1 kgf, in a line, 1 mm below the surface and 1 mm above the bottom

of the WB through BM, HAZ, WB, HAZ, and WB, as well as along the center of the WB through the same zones from 1 mm below the surface to the bottom of the WB, with a 0.5 mm distance between the indentations, as shown in Figure 1.

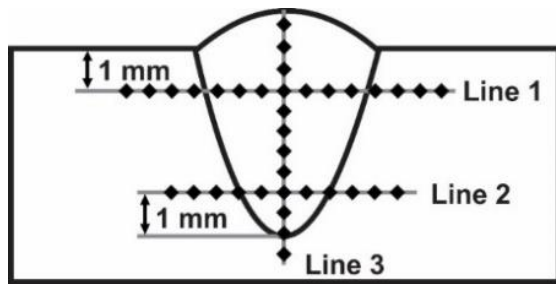


Fig. 1. Microhardness measurement map

### 3. RESULTS

#### 3.1. Particle size distribution in the flux

The particle number and size in the coating are shown in Figure 2. The smallest particles identified were 0.25  $\mu\text{m}$  while the largest particles were in the range 16-17  $\mu\text{m}$ . As can be seen, all solutions had a significant agglomeration of particles, the most particles were in the up to 1  $\mu\text{m}$ . The highest number of the smallest particles were found in solutions 3M2N and 2M3N.

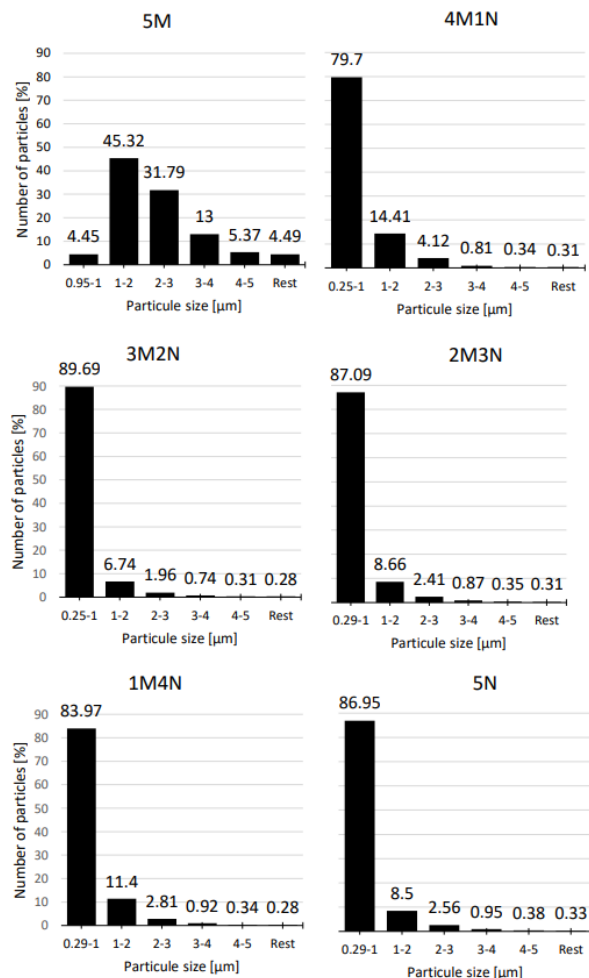


Fig. 2. Particle size distribution

#### 3.2. Macro and Weld bead dimension

Figure 3 shows the macro of the obtained weld beads of the conventionally welded-remelted specimen (0) and the specimens welded with the coating, as well as the width (W), depth (D), and depth to width ratios (D/W). There was a decrease in the width of the seam in some samples, but the most significant change was an increase in the depth of the weld beads in all specimens, except specimen obtained with the 4M1N flux. The highest penetration was achieved when a mixture of micro and nanoparticles, such as 1M4N, 2M3N, and 3M2N, was used. As the penetration depth is increased, the weld's width narrows.

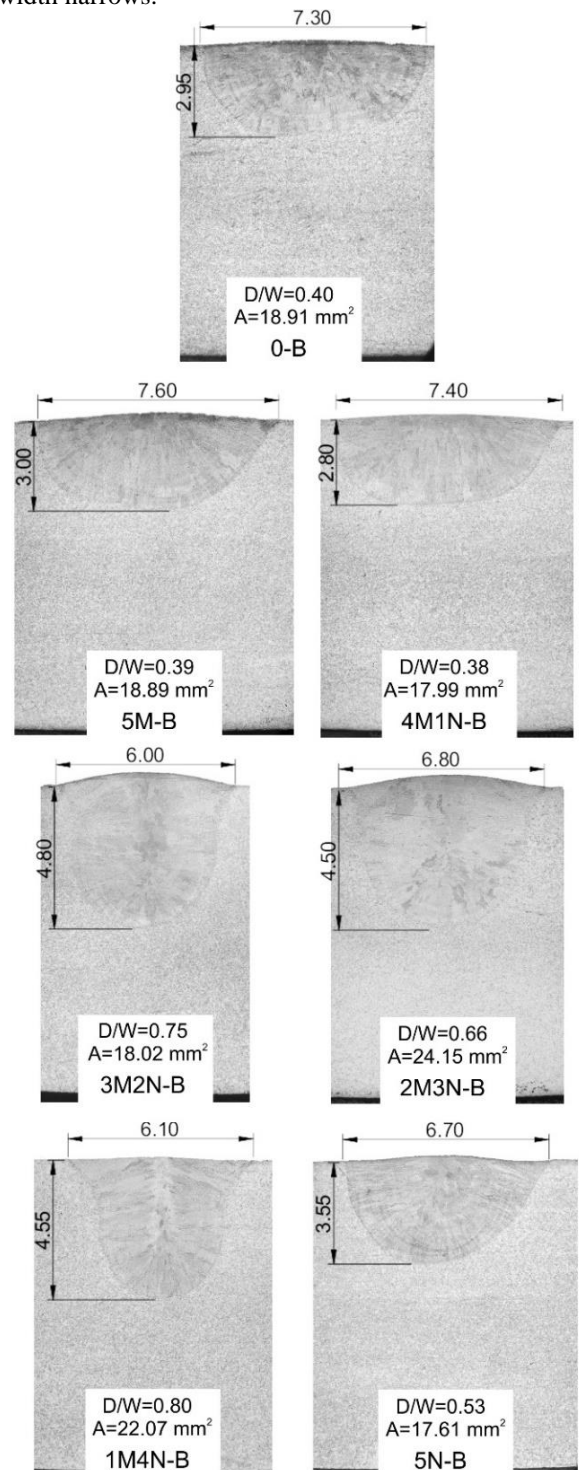


Fig. 3. Macro images of weld cross section



### 3.3. Microstructures

The microstructure of the samples with the most obvious differences is shown in in Figures 4 and 5. Figure 4 shows the microstructure near the fusion line at the bottom of the weld, while in Figure 5 fusion line at the surface of the weld is presented. All microstructures had the typical dendritic morphology in weld metal for austenitic stainless steels.

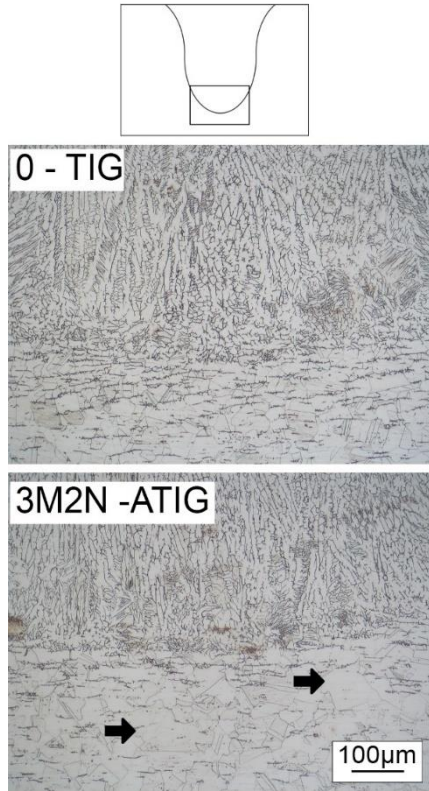


Fig. 4. Fusion line at the bottom of the weld

Figure 4 shows the most obvious change in the base metal under the seam, where significantly larger austenite polygonal grains growth is observed in the specimen welded with the coating. Grain growth can also be seen in Figure 5, although it is placed along the fusion line at the surface of the specimen which is remelted without coating.

### 3.4. Microhardness

Figures 6 and 7 show the results of hardness measurements for representative samples. The minimal drop in hardness in the specimen welded without a coating was measured near the fusing line. In this location, an increase in austenitic grain was observed (Figure 5).

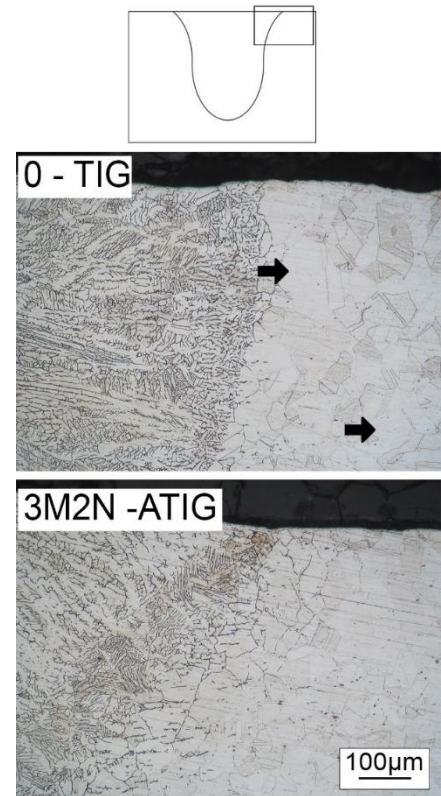


Fig. 5. Fusion line at the surface of the weld

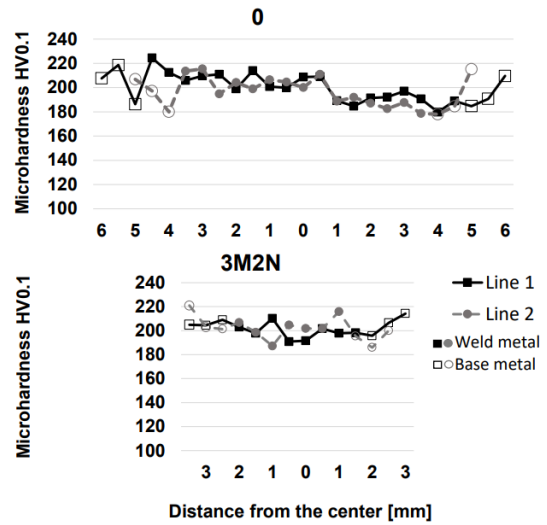


Fig. 6. Microhardness results for line 1 and 2

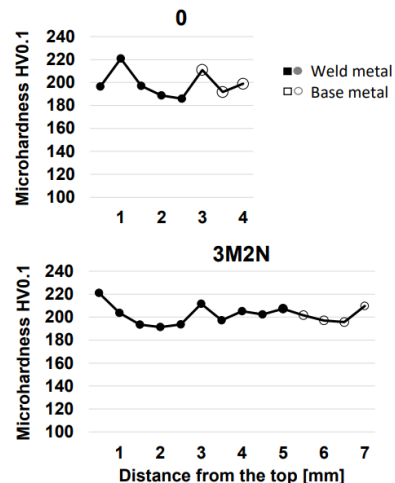


Fig. 7. Microhardness results for line 3

#### 4. DISCUSSION

TiO<sub>2</sub> nanoparticles were found to be more effective than submicron particles in this study, but a combination of the two was found to be the most effective. A similar pattern was observed in the D/W ratio. In the flux, nanoparticles revealed to be more effective than submicron particles. This is consistent with the findings in the study by Tseng and Lin [2], as the thermal dissociation and disintegration of smaller particles occurs considerably more rapidly than the thermal dissociation and decomposition of larger particles during arc heating. Because of agglomeration, the nominal size of the particles used in the flux does not accurately reflect their performance. As a result, zeta sizer values were a considerably more accurate indicator in terms of enhanced penetration in TIG welding.

The application of 3M2N flux provides the maximum weld depth. That means fluxes with a combination of particles are more effective than fluxes containing only nano or submicron particles. This could be due to the existence of submicron and nano particle agglomerates and their random collisions. Agglomerates, in particular, have a low cohesive strength due to the presence of weak secondary bonds between individual nanoparticles, as opposed to the ionic bonds found in submicron TiO<sub>2</sub>.

The growth of austenitic grains suggests that hot fluid flows from the surface towards the fusion boundary of the melt pool in specimens obtained without the flux flow, transferring heat into the base metal. The heat causes the austenite grains to increase, resulting in coarser grains under the surface near the fusion line, while the austenite grains under the weld remain unchanged. In contrast, in specimens obtained with the flux, reversed Marangoni convection causes a hot melt to flow inwards, pushing into the base material. As a result, there is more penetration, but a more intense heat transfer towards the weld as a side effect. This would be minimized in welding with full penetration, where no material is under the weld bead. That means, ceramic backing plates are mandatory, to contain the molten metal at high temperatures. However, ceramic backing plates are mandatory even if no flux is applied, that is, if V-preparation and multipass would have been used.

#### 5. CONCLUSIONS

The following conclusions may be drawn based on the results presented in this study:

- Nanoparticles are more successful in increasing penetration than submicron particles, but a combination of submicron and nanoparticles proved to be the most effective.
- Specimens welded without the flux increased grain size near the fusion line in base metal under the surface, resulting in a decreased hardness in this zone.
- Specimens welded with the flux have increased grain size near the fusion line in base metal under the weld metal, resulting in a decreased hardness in this zone.

- Material flow direction in the weld pool is the result of Marangoni convection in TIG and reversed Marangoni convection in A-TIG.

#### 6. REFERENCES

- [1] K.-H. Tseng, C.-Y. Hsu, *Performance of activated TIG process in austenitic stainless steel welds*, J. Mater. Process. Tech. 211, pp. 503–512, 2011
- [2] K.-H. Tseng, P.-Y. Lin, *UNS S31603 Stainless Steel Tungsten Inert Gas Welds Made with Microparticle and Nanoparticle Oxides*, Mater. 7, pp. 4755–4772, 2014.
- [3] Huang H.-Y., *Argon–hydrogen shielding gas mixtures for activating flux-assisted gas tungsten arc welding*, Metall. Mater. Trans. A Phys. Metall. Mater. Sci. 41 (2010)
- [4] K.-H. Tseng, N.-S. Wang, *Welding activated flux for structural alloy steels*, US Patent 20160167178A1, 2016.
- [5] S.M. Gurevich, V.N. Zamkov, N.A. Kushnirenko, N.A., *Improving the penetration of titanium alloys when they are welded by argon tungsten arc process*, Avtom. Svarka. 9 pp. 1-4, 1965
- [6] P.J. Modenesi, E.R. Apolinário, I.M. Pereira, *TIG welding with single-component fluxes*, J. Mater. Process. Technol. 99, pp. 260–265, 2000.
- [7] N. Chandrasekhar, M. Vasudevan, *Intelligent modeling for optimization of A-TIG welding process*, Mater. Manuf. Process. 25, pp. 1341–1550, 2010
- [8] Balos S, Dramicanin M, Janjatovic P, Zabunov I, Klobcar D, Basic M, Grilli ML. *Metal Oxide Nanoparticle-Based Coating as a Catalyzer for A-TIG Welding: Critical Raw Material Perspective*. Metals. 9(5), pp. 567-578, 2019.

**Authors: Assist. Prof. Miroslav Dramićanin, M.Sc Petar Janjatović, Assist. Prof. Savka Adamović, M.Sc Nenad Kulundžić, Assoc. Prof. Dragan Rajnović, Full Prof. Sebastian Baloš,**

University of Novi Sad, Faculty of Technical Sciences, Trg Dositeja Obradovića 6, 21000 Novi Sad, Serbia, Phone.: +381 21 485-23-24, Fax: +381 21 454-495.

E-mail: [dramicanin@uns.ac.rs](mailto:dramicanin@uns.ac.rs); [janjatovic@uns.ac.rs](mailto:janjatovic@uns.ac.rs);

[adamovicsavka@uns.ac.rs](mailto:adamovicsavka@uns.ac.rs); [kulundzic@uns.ac.rs](mailto:kulundzic@uns.ac.rs);

[draganr@uns.ac.rs](mailto:draganr@uns.ac.rs); [sebab@uns.ac.rs](mailto:sebab@uns.ac.rs)

**Dr Ivan Zabunov**, Proficut, Ruda Hrubika 6, 21470

Bački Petrovac

E-mail: [zabunov@proficut.rs](mailto:zabunov@proficut.rs)

**ACKNOWLEDGMENTS:** This research was supported by the Department of Production Engineering, Faculty of Technical Sciences Novi Sad Serbia, entitled “Interdisciplinary technologies in production engineering”.

Lanc, Z., Zeljković, M., Hadžistević, M., Štrbac, B., Labus Zlatanović, D., Baloš, S.

## EMISSIVITY OF METAL SURFACE COATINGS

**Abstract:** As it is known, emissivity is paramount for accurate temperature measurement using IR thermography. The emissivity of metals is particularly interesting due to its variability in relation to surface conditions (surface roughness and oxidation state), viewing angle, temperature, and wavelength. In the frame of this paper, knowledge regarding metal surface coatings and its effect on emissivity has been gained in an effort to improve risk assessment of workplace burns arising from hot metal surfaces. The present study examined the emissivity of two-component polyurethane metal covering coat on steel and grey cast iron depending on temperature and coating thickness. It was concluded that metal coating leads to moderated metal heating and increases constancy of emissivity compared to uncoated metal surfaces.

**Keywords:** IR thermography, metal coating, burn risk assessment

### 1. INTRODUCTION

Infrared measuring devices record infrared radiation emitted by an object and convert it into an electronic signal. Unlike pyrometer, as the most basic infrared device, which produces a single output using a single sensor, infrared (IR) cameras include an array of sensors to generate a detailed color image of the scene called thermogram [1]. Computation of temperature from data acquired with an IR camera is highly dependable on the emissivity of the target object [2]. The emissivity represents the ratio of the energy emitted by an object to that of a perfect absorber (blackbody) at the same temperature. It depends on both the properties of the substance and the frequency [3]. In addition to temperature and wavelength, emissivity can also be a function of emission angle [4].

The emissivity of metals is particularly interesting due to its variability in relation to surface conditions (surface roughness and oxidation state), viewing angle, temperature, and wavelength. Concerning this issue, it is suggested to use high emissivity coatings to significantly improve the thermal efficiency of metals prior to IR temperature measurement. Metal coatings are often used as one of the engineering control measure recommended by OSH as the most effective means of reducing excessive heat exposure when it comes to working near hot surfaces. Reducing the radiant heat emission from hot surfaces is usually achieved by covering hot surfaces with sheets of low emissivity material such as aluminum or using paint that reduces the amount of heat radiated from this hot surface into the workplace [5].

In regards to this international standard ISO 13732-1:2006 *Ergonomics of the thermal environment — Methods for the assessment of human responses to contact with surfaces — Part 1: Hot surfaces*, provides temperature threshold values for burns that occur during the contact between unprotected human skin and a hot surface. It deals with contact periods of 0.5 s and longer, and it is not applicable for a large area of the skin (10 % or more of the body skin surface or 10 % or more of the head skin surface), due to risk of burns of vital areas of

the face. ISO 13732-1:2006 also describes methods for the assessment of the risks of burning using thermocouples for the temperature measurements of hot surfaces.

Keeping in mind that hot surfaces could be a large area, using IR camera for both measuring and monitoring temperature development of the entire surface, makes these devices an excellent replacement for the thermocouples. The problem arises from the lack of relevant data in terms of emissivity of coated and uncoated metals and its variability with temperature and coating thickness which contributes to a challenging application of IR cameras.

In the frame of this paper, knowledge regarding metal surface coatings and its effect on emissivity has been gained in an effort to improve risk assessment of workplace burns arising from hot metal surfaces. The present paper examined the emissivity of two-component polyurethane metal covering coat on steel and grey cast iron depending on temperature and coating thickness.

### 2. MATERIALS AND METHODS

For the experiment, four workpieces of GJL-200 grey cast iron and four workpieces of the S235 structural steel were fabricated in dimensions 30×30×10 mm. Chemical compositions of the chosen materials are given in Table 1 and Table 2. Six workpieces were coated with a two-component polyurethane covering coat TOP PUR AY, manufactured by PITURA. The coating is characterized by high chemical resistance and excellent mechanical and esthetic properties. TOP PUR AY is resistant to the effect of solutions of certain acids, bases, salts and organic solvents, weathering factors and temperatures up to 150°C and it is mainly used as a covering coat for protection of buses, trucks, delivery vehicles, containers, wagons, etc. Prior to the application of TOP PUR AY, the workpieces were adequately prepared according to the requirements specified in the technical sheet. Each workpiece was previously cleaned of corrosion, oil, grease, dirt and polished.

% C	0.096
% Si	0.015
% Mn	0.800
% S	0.010
% Cr	0.021
% P	0.009
% Cu	0.013
% Ni	0.007
% Mo	0.002
% V	0.002
% W	0.002

Table 1. Chemical composition of the S235 structural steel

% C	3.050
% Si	2.580
% Mn	0.420
% S	0.100
% Cr	0.050
% P	0.068
% Cu	0.07
% Ni	0.020
% Mo	0.005

Table 2. Chemical composition of the GJL-200 grey cast iron

The roughness of the workpieces was measured with a contact method using a MarSurf PS1 device (Table 3). Grey cast iron and steel workpieces were coated in one, then in two and finally in three layers of coating in colure RAL 5010 (Gentian blue), in order to examine the influence of the type of material and layer thickness on the emissivity of coated metals during heating. Coating layers were applied using air spray painting technique where paint is applied to a surface via a spray gun, which is air pressurized. As can be seen from Table 3 with the number of coating layers, the surface roughness Ra decreases, except in the case where only one coating layer was applied. During air spraying of only one coating layer, it was noted that the covering power of the TOP PUR AY was very small. As the number of coating layers increased, the coating more evenly filled the surface of the workpieces, thus reducing the surface roughness. Coating thicknesses of workpieces were measured using Leitz Orthoplan light microscope. Prior to microscopy testing, the common metallographic preparation was conducted. It consisted of cutting, grinding (using a set abrasive papers from the coarsest to the finest) and polishing (diamond suspensions). Coating thicknesses are given in Table 4, while specimen sections showing coating layers are presented in Fig. 1 and Fig. 2, respectively, at 100x magnification.

The emissivity of eight workpieces, two workpieces of steel and grey cast iron without coating and six workpieces with three different coating layers, was determined using experimental setup shown in Fig. 3. Methodology is based on simultaneous heating of a single workpiece, measuring the temperature using an IR camera and type-K thermocouples. Thermocouples were placed in the center of the workpiece.

For the purpose of this paper, a heat-treat furnace was used for heating the workpieces. For obtaining and achieving a uniform temperature distribution on the surface of workpieces during the experiment, workpieces were placed upright in the center of the furnace in the special fireclay block.

Type of material	Ra [ $\mu\text{m}$ ] without coating	Ra [ $\mu\text{m}$ ] with coating
S235 structural steel	0.112	0.278 (1)*
	0.295	0.095 (2)
	0.232	0.106 (3)
GJL-200 grey cast iron	0.412	0.549 (1)
	1.563	0.474 (2)
	0.296	0.189 (3)

\*number in bracket denotes the number of coating layers

Table 3. Surface roughness of the workpieces

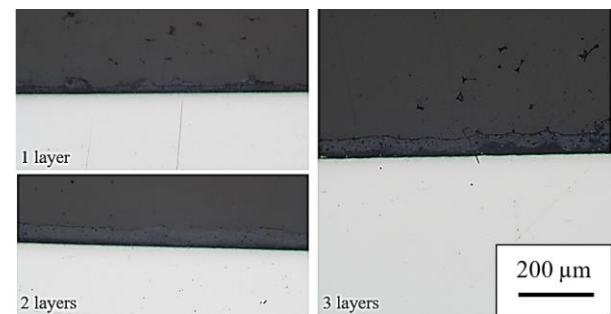


Fig. 1. Specimen sections of the S235 structural steel coating layers

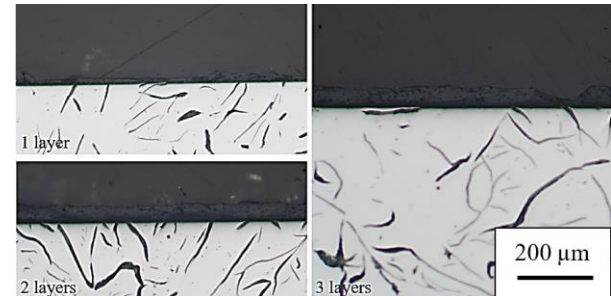


Fig. 2. Specimen sections of the GJL-200 grey cast iron coating layers

Type of material	Average coating thickness [ $\mu\text{m}$ ]		
	1 layer	2 layers	3 layers
S235 structural steel	20	40	50
GJL-200 grey cast iron	20	35	45

Table 4. Coating thicknesses of workpieces

The infrared camera used for thermal imaging was ThermoPro TP8S with a spectral range of 8–14  $\mu\text{m}$  and temperature accuracy of  $\pm 1^\circ\text{C}$ . After installing the thermocouples and setting the IR camera, a workpiece was heated up to  $100^\circ\text{C}$ . During the heating IR camera recorded an IR image of the workpiece for each temperature increase by  $10^\circ\text{C}$ . Afterward, obtained IR images were processed using the Guide Ir Analyzer program where the emissivity of a workpiece was adjusted until the temperature on the IR image became equal to the thermocouple temperature.

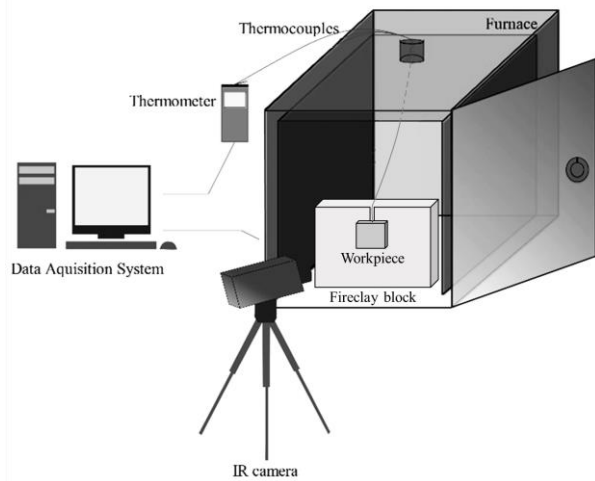


Fig. 3. Experimental setup

### 3. RESULTS AND DISCUSSION

The experimental data show that the emissivity ( $\epsilon$ ) of uncoated workpieces of the S235 structural steel and the GJL-200 grey cast iron slightly increases with temperature (T). The emissivity of the S235 structural steel ranges from 0.17 to 0.22, whereas the emissivity of the GJL-200 grey cast iron is higher and it ranges from 0.3 to 0.32 (Fig. 4). The differences in emissivity are due to the higher surfaces roughness of the GJL-200 grey cast iron workpieces as can be seen in Table 3.

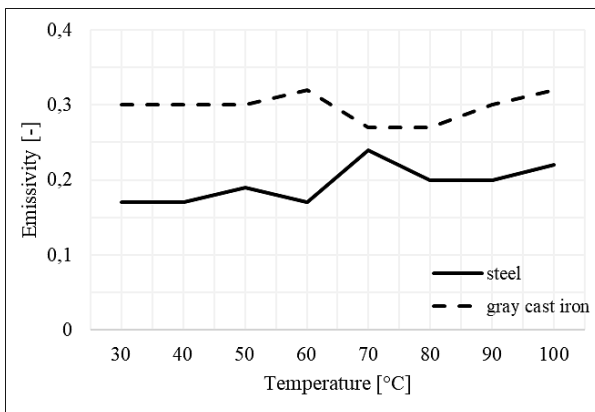


Fig. 4. Emissivity of the S235 structural steel and the GJL-200 grey cast iron without coating

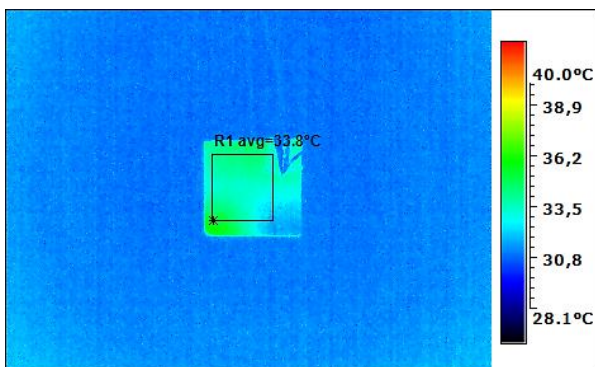


Fig. 5. IR images of the S235 structural steel workpiece without coating on 33.8°C ( $\epsilon = 0.17$ )

IR images of the uncoated S235 structural steel

workpiece presented in Fig. 5 shown highly reflective surface typical for metals that make it difficult to perform IR temperature measurement without using thermocouples as a temperature reference value. Oppositely, coated workpieces presented in Fig. 6 and Fig. 7 show a more uniform temperature distribution and no differences in the emissivity when it comes to type of material were noted.

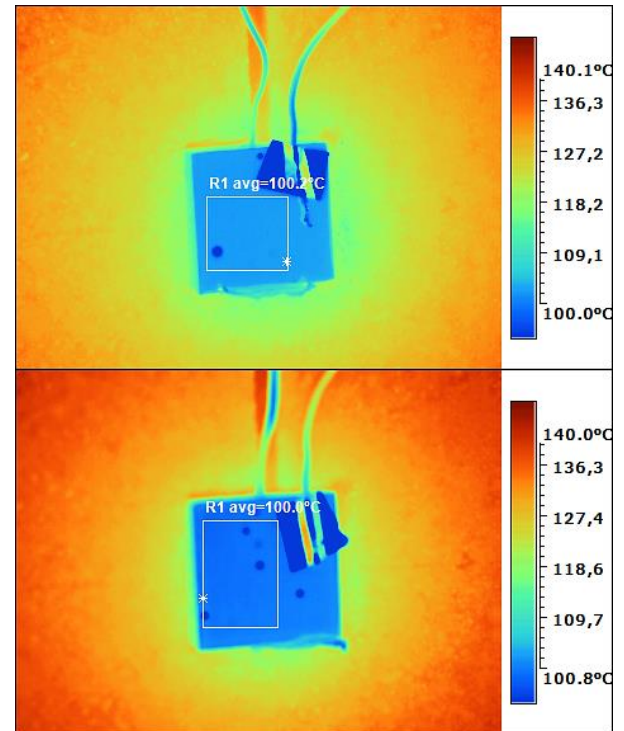


Fig. 6. IR images of the S235 structural steel workpieces with one and three coating layers at  $\sim 100^\circ\text{C}$  ( $\epsilon = 0.95$ )

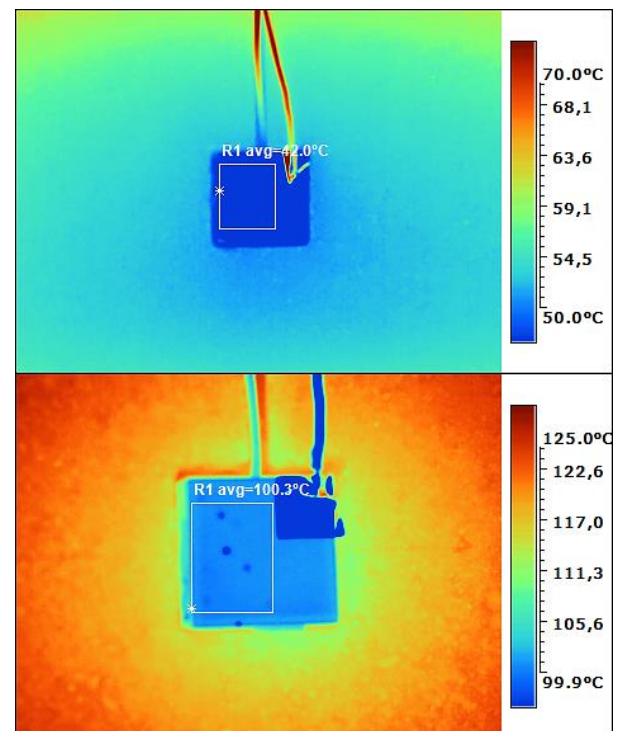


Fig. 7. IR images of the GJL-200 grey cast iron workpieces with three coating layers on 42°C and 100.3°C ( $\epsilon = 0.95$ )

Moreover, the emissivity for coated workpieces was set to be 0.95 and remained constant during the whole experiment. The only difference between IR images of coated workpieces is that at higher temperatures the dust that settled on the coating during the drying is more noticeable. Dust particles can be seen on IR images in the circular form because of their contrast with the heated background. Due to their small size, they do not lead to significant changes in the average temperature of workpieces on IR images, leaving them corresponded to the temperatures measured by thermocouples. Interestingly, there is an evident difference in the temperature distribution on the fireclay block between S235 structural steel workpieces with one and three coating layers at  $\sim 100^{\circ}\text{C}$  (Fig. 6). During the experiment, it was noted that the heating of workpiece with three coating layers required a longer time than heating of workpiece with one coating layer. This explains why the fireclay block is more heated in the first case, even when both workpieces are at the same temperature. Although the heating time is not accurately measured, it could be said with certainty that the tested coating leads to moderate heating of the metal.

Results show that the emissivity of coated workpieces doesn't change with surface roughness, coating thickness (Fig. 6), nor does it depend on the type of material. Additionally, there was no increase in emissivity with a rise in temperature (Fig. 7). Unlike uncoated metals, IR temperature measurement can be performed on coated metals without using thermocouples.

#### 4. CONCLUSION

In the frame of this paper, knowledge regarding metal surface coatings and its effect on emissivity has been gained in an effort to improve risk assessment of workplace burns arising from hot metal surfaces of machines by using IR camera. The present paper examined the emissivity of two-component polyurethane metal covering coat TOP PUR AY on steel and grey cast iron depending on temperature and coating thickness and it is concluded that:

- the emissivity of uncoated S235 structural steel and GJL-200 grey cast iron is changeable and increases with temperature and surface roughness;
- the emissivity of the S235 structural steel ranges from 0.17 to 0.22, whereas the emissivity of the GJL-200 grey cast iron is higher and it ranges from 0.3 to 0.32 for temperatures up to  $100^{\circ}\text{C}$ ;
- the heating of workpieces with three coating layers requires a longer time than heating of workpieces with one coating layer;
- coating leads to moderated metal heating compared to uncoated metal surfaces;
- coating increases emissivity of metal and keeps it constant during heating;
- the emissivity of coated examined metals is 0.95 and does not depend on surface roughness, coating thickness or type of metal.

These findings are valuable for the accurate IR temperature measurement which can be performed from a safe distance prior to burn risk assessment of hot metal surfaces of machines at the workplace. Keeping in mind that metal coatings are often used as one of the most effective means of reducing excessive heat exposure when it comes to working near hot surfaces, it is necessary to obtain certain knowledge regarding their emissivity. Considering that recommended emissivity values for metals are rarely given in relation to temperature and surface roughness, not to mention coating thickness, these results are helpful and much needed for improving burn risk assessment by means of IR thermography. Without having to use thermocouples to experimentally determine the emissivity, temperature measurement can be performed quickly on the entire surface of machine, not just on particular parts. On the other hand, temperature of uncoated metals can also be measured by IR camera, whether using it simultaneously with thermocouples during the burn risk assessment or by determining the emissivity, as described above, before the IR temperature measurement.

#### 5. REFERENCES

- [1] Usamentiaga, R., Venegas, P., Guerediaga, J., Vega, L., Molleda, J., Bulnes, F.: *Infrared Thermography for Temperature Measurement and Non-Destructive Testing*, Sensors, Vol. 14, pp. 12305-12348, 2014
- [2] Mohr, G., Nowakowski, S., Altenburg, S., Maierhofer, C., Hilgenberg, K.: *Experimental Determination of the Emissivity of Powder Layers and Bulk Material in Laser Powder Bed Fusion Using Infrared Thermography and Thermocouples*, Metals, Vol. 10, pp. 1546, 2020
- [3] Vallero, D.: *Fundamentals of Air Pollution* 4th Edition, Academic Press, 2007
- [4] Zhao, W., Chellappa, R.: *Face Processing: Advanced Modeling and Methods*, Academic Press, Orlando, 2005
- [5] [https://www.ccohs.ca/oshanswers/phys\\_agents/heat\\_control.html](https://www.ccohs.ca/oshanswers/phys_agents/heat_control.html)

**Authors:** Res. Assit. Zorana Lanc, Full Prof. Milan Zeljković, Full Prof. Miodrag Hadžistević, Assit. Prof. Branko Štrbac, Assit. Prof. Danka Labus Zlatanović, Full Prof. Sebastian Baloš, University of Novi Sad, Faculty of Technical Sciences, Department of Production Engineering, Trg Dositeja Obradovića 6, 21000 Novi Sad, Serbia, Phone.: +381 21 485-23-24, Fax: +381 21 454-495.

E-mail: [zoranalanc@uns.ac.rs](mailto:zoranalanc@uns.ac.rs); [milanz@uns.ac.rs](mailto:milanz@uns.ac.rs); [miodrags@uns.ac.rs](mailto:miodrags@uns.ac.rs); [strbacb@uns.ac.rs](mailto:strbacb@uns.ac.rs); [danlabus@uns.ac.rs](mailto:danlabus@uns.ac.rs); [sebab@uns.ac.rs](mailto:sebab@uns.ac.rs)

**ACKNOWLEDGMENTS:** Results of the investigation presented in this paper are a part of the research realized in the framework of the project: "Innovative scientific and artistic research from FTS (activity) domain", funded by the Ministry of Education, Sciences and Technological Development of Republic of Serbia.



Section F:  
**MECHANICAL ENGINEERING AND  
ENVIRONMENTAL PROTECTION**





Plavac., F., Pavković, D., Trstenjak, M., Cipek, M., BeniĆ, J., Lisjak, D.

**SPEED CONTROL OF A SERIES DC DRIVE FOR DRILLING APPLICATIONS WITH VIBRATION DAMPING TORQUE FEEDBACK LOOP**

**Abstract:** The paper presents the speed control system design and simulation verification of a petroleum drilling system aimed at effective suppression of drill-string torsional vibrations in legacy drilling drives featuring mature series-wound direct-current motor drive technology. The vibration suppression system is based on the external damping feedback loop using a straightforward low-pass filter-based drill-string torque estimator and a reference correction term in the motor speed target path, with the motor speed feedback control system featuring a proportional-integral controller tuned for stiff disturbance rejection. The control system design is based on the damping optimum criterion, which results in straightforward analytical expressions for controller parameters. The effectiveness of the proposed control strategy is verified by means of comprehensive simulations.

**Key words:** Petroleum drilling; drill-string; vibration suppression; series DC motor drive, simulation

**1. INTRODUCTION**

Mature drilling rigs used in deep drilling operations are still equipped with legacy drilling hardware and control systems, utilizing DC electrical drive technology, whose embedded control units may not possess drill-string torsional vibrations damping features [1]. Since these torsional vibrations have adverse effects to drilling facility operational safety [1], drilling rig retrofitting with active damping features is recognized as a prerequisite for profitable drilling rig operation [2].

Torsional vibration active damping strategies may either be realized with the aim of passive absorber behavior emulation [3], which may lead to drilling electrical drive speed controller retuning [4]. Advanced controller structures have also been considered [5], but they may be subject to realistic limitations on industrial control hardware encountered in field operations.

This has motivated a different approach, i.e. using an external drill-string vibrations suppression system [6]. Its main advantage is that it does not require any changes to the main drilling drive speed controller. Thus, it may be suitable for legacy DC drilling electrical drives, typically configured for stiff speed control [3], which may be important if a highly-nonlinear series-excitation DC machine is used for the main drilling drive.

Having the above facts in mind, this paper proposes a systematic design of an external torsional vibrations compensation system based on drill-string torque feedback obtained from available measurements using a suitable observer. The control system design is based on damping optimum criterion, and its effectiveness is verified by means of computer simulations.

**2. PROCESS MODELS**

**2.1. Drill-string model**

Figure 1a shows a schematic layout of a typical deep drilling rig. Drilling is performed by means of drill-bit rotation using a top-drive drilling motor (characterized by its inertia  $J_1$  and output gearbox transmission ratio  $i$ )

and vertical force on the drill-bit, whose combination results in pulverizing the rock bed material. The drill-string primarily consists of regular thin-walled drill pipes, with transitional (HWDP) pipes and drill collars used within the bottom-hole assembly (BHA) to weigh down the drill-bit [3].

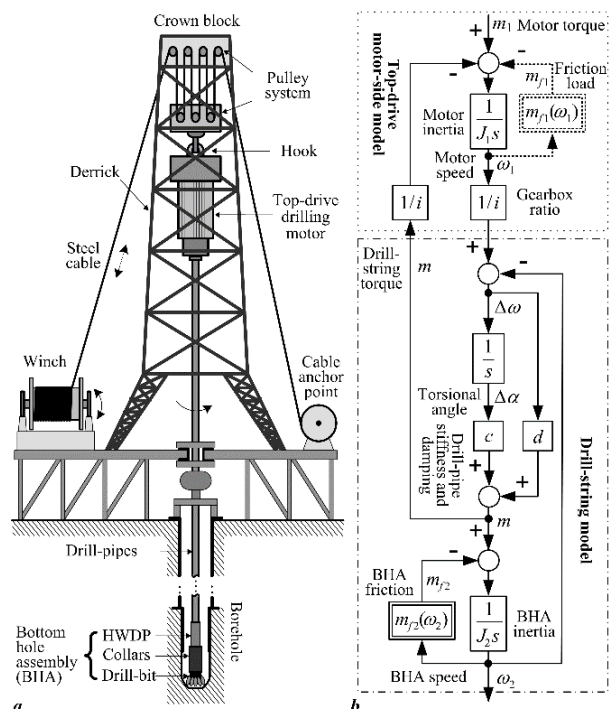


Fig. 1. Schematic layout of drilling rig (a) and related drill-string rotational dynamics model (b).

The drill-string drive rotational dynamics are modeled as the two-mass elastic system (Fig. 1b), with drill-pipes representing a torsional spring characterized by its stiffness  $c$  and damping  $d$  coefficients [4]. The motor and gearbox inertias are lumped into the motor-side inertia  $J_1$ , while the inertias of HWDPs, collars and drill-pipes and the drill-bit inertia are lumped into the inertia at the drill-bit side  $J_2$  [3].

The two-mass elastic model is also characterized by the following resonance frequencies related to stuck tool case ( $\omega_2 = 0$ ), “stiff” motor speed control ( $\omega_1 \approx \text{const.}$ ), and freely-oscillating drill-string, respectively [3]:

$$\Omega_{01} = \sqrt{\frac{c}{J_1 i^2}}, \quad \Omega_{02} = \sqrt{\frac{c}{J_2}}, \quad \Omega_0 = \sqrt{\Omega_{01}^2 + \Omega_{02}^2}. \quad (1)$$

The BHA-side friction torque  $m_{f2}$  can be described by the generalized Stribeck static curve [7]:

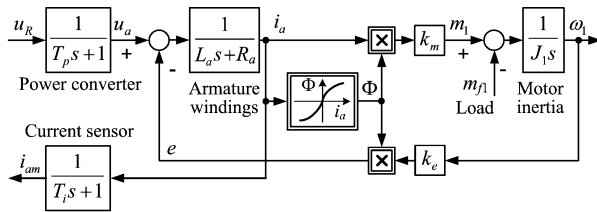
$$m_{f2}(\omega_2) = \left[ M_C + (M_S - M_C) e^{-|\omega_2 / \omega_s|^\delta} \right] \text{sgn}(\omega_2). \quad (2)$$

where  $M_C$  is the Coulomb or kinetic friction torque,  $M_S$  is the maximum static friction torque (breakaway torque),  $\omega_s$  is the Stribeck speed, and  $\delta$  is the so-called Stribeck coefficient [7].

The motor-side load torque, which is related to gearbox losses, can be modeled by using a Coulomb friction model ( $m_{f1} = M_{Cm} \text{sgn}(\omega_1)$ ).

## 2.2. Series DC machine model

Figure 2 shows the equivalent block diagram of a series-excitation DC machine, whose dynamic behavior is described by a system of differential and nonlinear algebraic equations (see [8]), with the parameters of the process model listed in the figure legend in Fig. 2.



**Legend:**  $u_a$ ,  $u_R$  – armature voltage and power converter reference;  $i_a$ ,  $i_{am}$  – armature current and current measurement;  $\Phi$  – magnetic field flux;  $e$  – back electromotive force (back EMF);  $\omega_1$  – motor speed;  $m_1$ ,  $m_{f1}$  – motor and load torque;  $J_1$  – motor inertia;  $k_m$ ,  $k_e$  – torque and EMF constants;  $L_a$ ,  $R_a$  – armature inductance and resistance;  $T_p$ ,  $T_i$  – power converter and current sensor time lag.

Fig. 2. Block diagram of series-excitation DC drive dynamic model.

## 3. CONTROL SYSTEM DESIGN

### 3.1. Damping optimum criterion

The damping optimum criterion [9] is an analytical method of designing of linear continuous-time closed-loop systems, wherein closed-loop poles are assigned based on the purely algebraic approach. The controller tuning procedure is based on the following closed-loop characteristic polynomial:

$$A(s) = D_2^{n-1} D_3^{n-2} \dots D_n T_e^n s^n + \dots + D_2 T_e^2 s^2 + T_e s + 1. \quad (3)$$

where  $T_e$  is the closed-loop system equivalent time constant, and  $D_i$  ( $i = 2 \dots n$ ) are the damping optimum characteristic ratios, which are typically set to 0.5 in order to obtain closed-loop step response with overshoot of approximately 6% and rise time of  $(1.8 - 2.1) \cdot T_e$ .

### 3.2. Series DC machine current and speed control

Figure 3 shows the simplified block diagram of the DC machine current control loop, with the power converter lag ( $T_p$ ) and current sensor lag ( $T_i$ ) lumped together in a single first-order lag term with time constant  $T_{\Sigma i}$  (which may also include the time-

discretization lag in the case of digital current PI controller). It is assumed that motor back EMF is slowly changing (i.e. due to large motor inertia), and it can be compensated for by the current controller action. To obtain fast closed-loop response, zero-pole cancelling is typically used, wherein the dominant armature lag ( $L_a/R_a$ ) is cancelled out by the PI controller zero (integral time constant  $T_{ci}$ ) [8]:

$$T_{ci} = L_a/R_a, \quad (4)$$

while the controller gain  $K_{ci}$  is calculated as follows according to the damping optimum criterion [8]:

$$K_{ci} = \frac{T_{ci}}{T_{ei}} R_a, \quad (5)$$

$$T_{ei} = \frac{T_{\Sigma i}}{D_{2i}}, \quad (6)$$

with  $T_{ei}$  being the current control system closed-loop lag.

Figure 4 shows the method of static linearization of the torque characteristic of a series DC machine used in this work which can be easily implemented in modern power converters. By compensating the nonlinear torque vs. current characteristic, the developed torque  $m_1$  vs. torque reference  $m_R$  dependence may be approximated by a first-order lag term:

$$G_m(s) = \frac{m_1(s)}{m_R(s)} = \frac{1}{T_{ei} s + 1}. \quad (7)$$

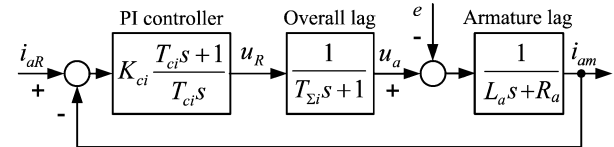


Fig. 3. Block diagram of DC drive current control loop.

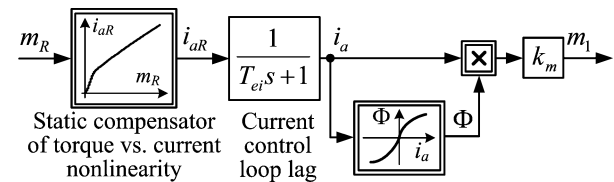


Fig. 4. Block diagram of series-excitation DC machine torque nonlinearity compensation.

By using the above torque vs. current linearization approach, the superimposed speed control system can also be treated as a linear closed-loop system, whose block diagram is shown in Fig. 5. It also features a PI controller whose reference is low-pass filtered to avoid excessive speed reference-related torque commands.

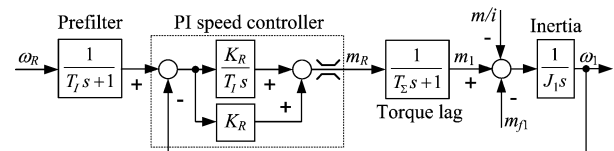


Fig. 5. Block diagram of DC drive speed control loop.

The speed control loop is typically default-tuned to achieve fast suppression of load disturbances at the motor output shaft (in this case the combined effect of motor-side friction  $m_{f1}$  and drill-string torque  $m/i$ ). A fast and well-damped tuning of the speed control loop in the

“default” case of DC drive disconnected from the drill-string can be obtained according to the symmetrical optimum tuning approach [8]:

$$K_R = \frac{J_2/i^2 + J_1}{2T_\Sigma}, \quad (8)$$

$$T_I = T_{e\omega} = 4T_\Sigma, \quad (9)$$

with  $T_\Sigma$  being the equivalent parasitic lag of the speed control loop (Fig. 5) comprising the current loop lag  $T_{ei}$ .

The “stiff” disturbance rejection of the speed control loop results in its “speed source” approximation [10]:

$$G_c(s) = \frac{\omega_1(s)}{\omega_{1R}(s)} = \frac{1}{T_{e\omega}s + 1}. \quad (10)$$

The above tuning is not well suited for drill-string drive characterized by non-negligible compliance, because it may lead to poorly-damped torsional vibrations of the motor torque reference  $m_{1R}$  and BHA speed  $\omega_2$  [10].

### 3.3. Torque-feedback active damping control

To attenuate the drill-string torsional vibrations occurring due to “stiff” speed controller tuning based on (8)-(10), an external control loop based on drill-string torque estimation can be used, as shown in Fig. 6. The drill-string torque is estimated by using a state variable filtering approach [10], as shown in Fig. 6a, whereas the overall control system structure is illustrated in Fig. 6b for the idealized case of “speed source” representation of the speed control loop, negligible drill-string damping ( $d = 0$ ) and BHA rotation ( $\omega_2 > 0$  and  $m_{f2} \approx \text{constant}$ ).

In the above case, the damping optimum-based tuning of the external control loop yields [10]:

$$T_{ed} = \frac{1}{D_{2d}\sqrt{D_{3d}D_{02}}}, \quad (11)$$

$$T_{IR} = T_{ed} - T_{e\omega} - T_{e\omega}, \quad (12)$$

$$K_{md} = \frac{i^2 D_{2d} T_{ed}^2 - (T_{ed} - T_{e\omega} - T_{e\omega})(T_{e\omega} + T_{e\omega}) - D_{02}^2}{J_2 T_{ed} - T_{e\omega} - T_{e\omega}}, \quad (13)$$

with the following feasibility condition imposed on the drill-string torque estimator time constant  $T_{e\omega}$  aimed at obtaining a well-damped closed-loop response [10]:

$$T_{e\omega} \geq \frac{T_{ed}}{2} (1 - \sqrt{1 - 2D_{2d}D_{3d}}) - T_{e\omega}. \quad (14)$$

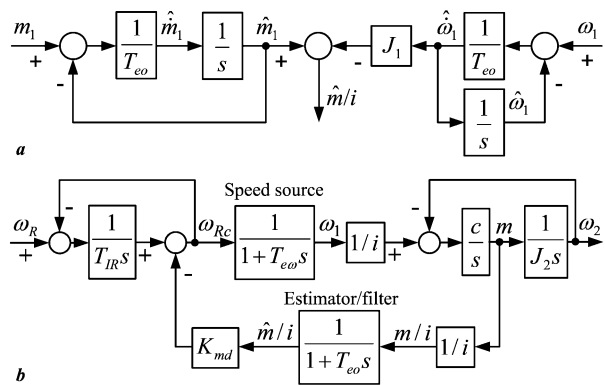


Fig. 6. Block diagram of drill-string torque estimator (a), and external control system (b).

## 4. SIMULATION RESULTS

The overall drill-string control system has been verified by means of comparative simulations for a characteristic drill-string drive configuration whose

parameters are given in Table 1, while Fig. 7 shows the normalized magnetization characteristic of the series DC motor with magnetic field flux  $\Phi$  and armature current given in per unit [p.u.] representation. These parameters are used for the purpose of building the simulation model of the series DC machine-based drill-string drive.

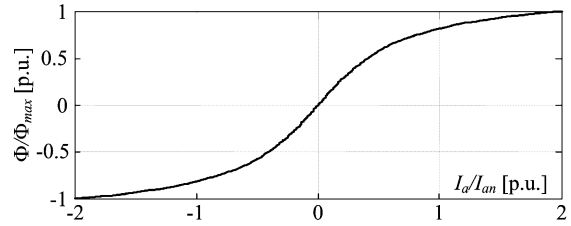


Fig. 7. Series DC motor flux vs. current curve.

Symbol	Description	Value
$M_n$	Rated top-drive motor torque	7900 Nm
$\omega_n$	Rated top-drive motor speed	100 rad/s
$I_{an}$	Rated top-drive motor current	1050 A
$i$	Gearbox ratio	3.2
$k_e\Phi(I_{an})$	Motor EMF constant at rated current	7.54 Vs/rad
$k_m\Phi(I_{an})$	Motor torque constant at rated current	7.24 Nm/A
$R_a$	Total armature + excitation resistance	18 m $\Omega$
$L_a$	Total armature + excitation inductance	2.7 mH
$T_p$	Power converter equivalent lag	2.78 ms
$T_i$	Current sensor equivalent lag	3 ms
$T_\Sigma$	Speed control loop parasitic lag	15 ms
$J_1$	Top-drive motor-side inertia	25 kgm <sup>2</sup>
$J_2$	Drill-string drive BHA-side inertia	301.1 kgm <sup>2</sup>
$c$	Drill-string stiffness coefficient	618.3 Nm/rad
$d$	Drill-string damping coefficient	15.3 Nms/rad
$M_S$	BHA-side static friction torque	4000 Nm
$M_C$	BHA-side Coulomb friction torque	2500 Nm
$\omega_s$	Stribeck speed	0.1 rad/s
$\delta$	Stribeck coefficient	1.0

Table 1. Parameters of drill-string drive.

Figure 8 shows the results of series DC drive speed control system (see Figs. 3 – 6) and designed according to equations (4) – (9). Results show that the “fast” PI speed controller is capable of achieving the so-called “speed source” behavior of the motor speed, being capable of maintaining the motor speed close to the target value regardless of the load at the motor side.

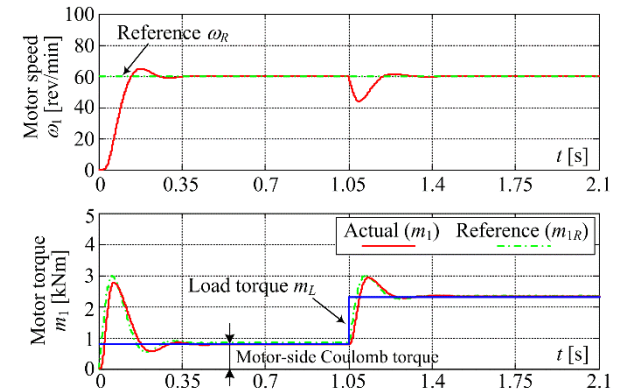


Fig. 8. Series DC drive speed control results.

Figure 9a shows the results for the case of drill-string speed control system based on PI speed controller tuned for fast response (see (8) and (9)), subject to drill-string

compliance and variable drill-bit friction. The fast controller tuning, which does not account for the BHA-characteristic resonant mode at the frequency  $\Omega_{02}$  results in sustained (limit-cycle) oscillations of the motor torque and drill-bit (BHA) speed in the presence of drill-string compliance and tool stick-slip friction. By including the external active damping control based on the drill-string torque reconstruction (Fig. 6) and which accounts for the BHA resonance frequency  $\Omega_{02}$ , the overall drill-string control system performance is notably improved, as shown in Fig. 9b. In particular, the torsional vibrations of both the motor-side and BHA-side speed are effectively attenuated, and satisfactory response speed and settling time are obtained, while also achieving zero steady-state speed reference tracking error.

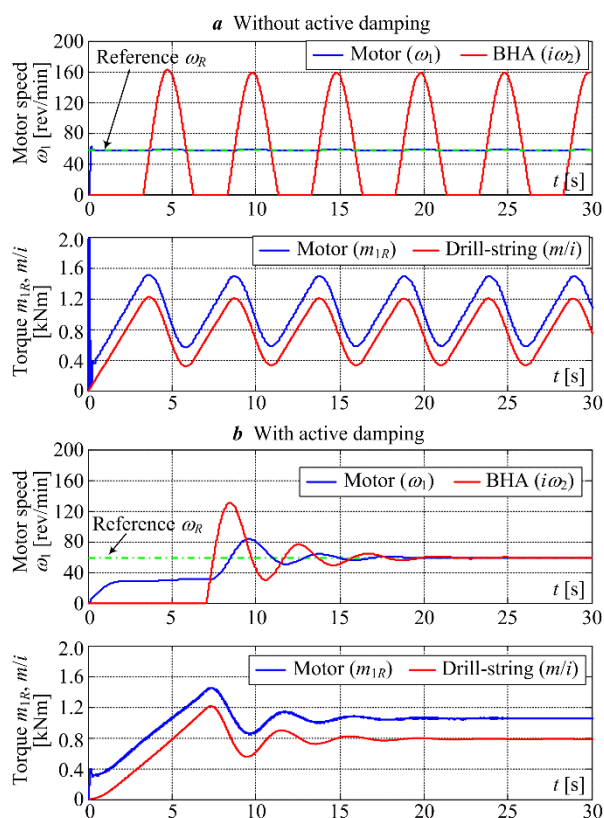


Fig. 9. Simulation results of series DC drive-based control of drill-string system.

## 5. CONCLUSION

The paper has presented the design drill-string drive torsional vibrations active damping system based on external drill-string torque feedback applied to the speed-controlled drilling electrical drive based on series DC motor equipped with fast PI speed controller. The proposed active damping control strategy tuning has been based on the damping optimum criterion, resulting in analytical expressions for controller parameters.

The effectiveness of the proposed control strategy is verified by means of simulations. Simulation results have shown that the “stiff” (fast) PI speed controller tuning, although well-suited for motor speed control without the drill-string attached, results in sustained (limit-cycle) oscillations when drill-string is driven by

such speed control system. On the other hand, the proposed active damping control system results in substantial attenuation of drill-slip compliance and tool friction stick-slip related torsional vibrations under realistic operating conditions, while also resulting in accurate steady-state speed target tracking.

Future work may involve building a suitable test bed for the purpose of experimental verification of the proposed active damping control system design.

## 6. REFERENCES

- [1] Pavković, D.: *Current Trends in Oil Drilling Systems R&D with Emphasis on Croatian Oil Drilling Sector – A Review*, Proceedings of 9<sup>th</sup> Intl. Conf. on Management of Technology - Step to Sustainable Production (MOTSP 2017), Dubrovnik, Croatia, April 2017.
- [2] Kaiser, M. J., Snyder, B. F.: *The Offshore Drilling Industry and Rig Construction in the Gulf of Mexico*, Lecture Notes in Energy, Vol 8, Springer-Verlag, London, UK, 2013.
- [3] Jansen, J. D. van den Steen, L.: *Active Damping of Self-Excited Torsional Vibrations in Oil Well Drillstrings*, Journal of Sound and Vibration, Vol. 179, No. 4, pp. 647 – 668, 1995.
- [4] Runia, D. J., Grauwman, R., Stulemeijer, I.: *A Brief History of the Shell "Soft Torque Rotary System" and Some Recent Case Studies*, Proceedings of SPE/IADC Drilling Conference (SPE-163548-MS), Amsterdam, Netherlands, March 2013.
- [5] Serrarens, A. F. A., van de Molengraft, M. J. G., Kok, J. J., van den Steen, L.: *H-infinity Control for Suppressing Stick-Slip in Oil Well Drillstrings*, IEEE Control Systems Magazine, Vol. 18, No. 2, pp. 19 – 30, 1998.
- [6] Dwars, S.: *Recent Advances in Soft Torque Rotary Systems*, Proceedings of the 3<sup>rd</sup> Intl. Colloquium on Nonlinear Dynamics and Control of Deep Drilling Systems (pp. 29 – 44), Minneapolis, Minnesota, US, 2014.
- [7] Armstrong-Hélouvy, B., Dupont, P., Canudas-de-Wit, C.: *A Survey of Models, Analysis Tools and Compensation Methods for the Control of Machines with Friction*, Automatica, Vol. 30, No. 7, pp. 1083-1138, 1994.
- [8] Leonhard, W.: *Control of Electrical Drives*, Springer-Verlag, Berlin, 1985.
- [9] Naslin, P.: *Essentials of Optimal Control*, Illife Books Ltd., London, UK, 1968.
- [10] Pavković, D., Šprljan, P., Cipek, M., Krznar, M.: *Cross-Axis Control System Design for Borehole Drilling based on Damping Optimum Criterion and utilization of Proportional-Integral Controllers*, Optimization and engineering, Vol. 22, No. 1, pp. 51-81, 2021.

**Authors:** Mag. ing. Filip Plavac, Assoc. Prof. Danijel Pavković, Dr. sc. Maja Trstenjak, Assist. Prof. Mihael Cipek, Mag. ing. Juraj Benić, Prof. Dragutin Lisjak, University of Zagreb, Faculty of Mechanical Engineering and Naval Architecture, Ivana Lučića 5, 10002 Zagreb, Croatia, Phone.: +385 01 616-83-25.  
E-mail: [fplavac1@gmail.com](mailto:fplavac1@gmail.com);  
[daniyel.pavkovic@fsb.hr](mailto:daniyel.pavkovic@fsb.hr); [maja.trstenjak@fsb.hr](mailto:maja.trstenjak@fsb.hr);  
[mihael.cipek@fsb.hr](mailto:mihael.cipek@fsb.hr); [juraj.benic@fsb.hr](mailto:juraj.benic@fsb.hr);  
[dragutin.lisjak@fsb.hr](mailto:dragutin.lisjak@fsb.hr)

**ACKNOWLEDGMENTS:** This research has been supported by the European Regional Development Fund under the grant KK.01.1.1.01.0009 (DATACROSS).

Miljković, Z., Jevtić, Đ., Svorcan, J.

**REINFORCEMENT LEARNING APPROACH FOR  
AUTONOMOUS UAV NAVIGATION IN 3D SPACE**

**Abstract:** *In the last two decades, the rapid development of unmanned aerial vehicles (UAVs) resulted in their usage for a wide range of applications. Miniaturization and cost reduction of electrical components have led to their commercialization, and today they can be utilized for various tasks in an unknown environment. Finding the optimal path based on the start and target pose information is one of the most complex demands for any intelligent UAV system. As this problem requires a high level of adaptability and learning capability of the UAV, the framework based on reinforcement learning is proposed for the localization and navigation tasks. In this paper, Q-learning algorithm for the autonomous navigation of the UAV in 3D space is implemented. To test the proposed methodology for UAV intelligent control, the simulation is conducted in ROS-Gazebo environment. The obtained simulation results have shown that the UAV can reach the target pose autonomously in an efficient way.*

**Key words:** *unmanned aerial vehicles, autonomous localization and navigation, reinforcement learning, Q-learning*

**1. INTRODUCTION**

In the last decades, Unmanned Aerial Vehicles (UAVs) are among the most used mobile robots that find increasing applications due to their longer flight time, increased payload capability, and drop in the cost of electrical components. Also, the technological development of sensor equipment and onboard processing units as well as the advancement in artificial intelligence based approaches, have enabled them to perform more challenging tasks such as remote delivery, surveillance, maintenance, inspection, search and rescue, wildlife tracking, etc. These tasks mainly include missions that are conducted in unstructured and unknown environments with unpredictable weather conditions. On the other side, when it comes to emergency situations such as disaster search, firefighting, or rescuing, mission time plays a vital role in saving somebody's life. Therefore, the ability to navigate autonomously and efficiently in such environments is considered a necessary feature of any intelligent flying mobile robot today.

Navigation is a process during which the robot has to move safely from the start pose to the desired pose along the efficient path avoiding collisions with other objects. In literature, this process is presented using the following components: (i) perception, (ii) localization, (iii) cognition and path planning, and (iv) motion intelligent control, where cognition and path planning raise the most interest by the researchers [1]. Therefore, it could be said that navigation represents the specific aspect of a robot's cognition because it requires the ability to make decisions at the highest level in order to achieve high-order goals [2].

Unlike ground mobile robots, UAVs have a higher dimensional operating space, which is certainly their comparative advantage. However, this also means that navigation task becomes more difficult. In addition, to achieve a high level of autonomy, the UAV controller should rely on the *a priori* information about the

environment, accurate dynamics model, and also must be able to adapt to unforeseen circumstances such as variable payloads, voltage sag, wind loads, etc. [3]. However, the data about the environment is usually limited or doesn't even exist, while modeling the UAV's dynamics is very difficult in practice. Therefore, in order to accomplish missions successfully, autonomous mobile robots should be capable to learn in real-time without, or with limited, human intervention. For such purposes, reinforcement learning (RL) has proven as a promising framework.

RL, also called learning from interaction, represents one of the significant approaches of machine learning today. The concept of this learning method could be described as the goal-seeking agent's trial-and-error search for an optimal solution, which is achieved by exploring the environment and exploiting the past experience [4]. Recent advancements in the field have shown that this learning technique is already deployed in complex tasks, such as autonomous navigation, path tracking, obstacle avoidance, intelligent control, manipulation, or object recognition. Even though significant progress has been made by researchers, autonomous navigation of the UAV operating in real-world space is still considered an open research topic.

Utilizing RL methods for training UAVs in the real-world space brings a new set of technological challenges. Firstly, there is a need for computationally intensive onboard processing, which is usually an energy demanding task [5]. Therefore, it makes it difficult to use it with UAVs since they have limited battery capacity. Secondly, to develop a robust navigation system that could effectively work in the real-world scenario, an UAV must experience a large number of trial-and-error flights, which might be time-consuming, expensive, and very dangerous [5]. The possible solution addressing these challenges is to train the UAV in a simulation environment.

Autonomous navigation of UAVs is an active area of research. In reference [6], Pham et al. implemented a

function approximation-based Q-learning algorithm in conjunction with a PID controller to solve the problem of navigating UAV in 2D space. Even though results have shown that UAV can successfully learn localization and navigation tasks without previous knowledge about the environment, it has been stated that it is necessary to consider the influence of unpredictable wind loads and other uncertainties for application in the real-world space. In paper [7] Wang et al. proposed a deep reinforcement learning approach for UAV navigation tasks in a virtual large-scale continuous space, crowded with high-rise buildings. The main aim of this paper was to train an intelligent agent to perform navigating tasks without the need for path planning and map reconstruction. For such purpose, the authors modeled their problem as a partially observable Markov decision process, enabling the agent to perform high-level tasks under uncertain conditions. The problem of learning an efficient route without running out of electrical energy was analyzed in reference [8]. In order to solve this problem, the authors implemented a model-based RL algorithm called TEXPLORE.

In this paper, the authors have tested the proposed methodology for the autonomous navigation of the UAV in 3D space. In order to complete this intelligent task, a model-free RL algorithm known as Q-learning is applied. To test the algorithm's convergence capability, different trade-off functions for exploration/exploitation problem were analyzed. Finally, the animation is conducted using the Parrot ARDrone as a robotic platform in the ROS-Gazebo environment.

The paper has the following structure. In Section 2 the UAV navigation problem in 3D space is described in detail. The reinforcement learning approach and its mathematical representation are given in Section 3. Implementation of the Q-learning algorithm is presented in Section 4. The proposed algorithm is simulated, and obtained results are shown in Section 5. Concluding remarks are outlined in Section 6.

## 2. PROBLEM DEFINITION

A flying mobile robot, which was designed at the Faculty of Mechanical Engineering in Belgrade within the Laboratory for Industrial Robotics and Artificial Intelligence (ROBOTICS & AI), has the task of cleaning exterior glass surfaces on high-rise buildings (Fig. 1). It uses wires instead of rechargeable batteries. Besides the cleaning system, it has the vision sensor that enables detection of whether the surface is glass or not. High-level decisions about which surfaces should be cleaned, or how to create a mobile robot path based on the external geometry of the building, or when to stop the cleaning task are made by the intelligent agent. Two of the intelligent tasks for the flying mobile robot are localization and navigation, where it has to learn an optimal path based on the start and target pose information.

Suppose the flying mobile robot is placed in the arbitrary pose near the object whose exterior glass surfaces need to be cleaned. To start the cleaning task, the UAV must explore the environment in order to find the target pose detected by the external sensors. We

assume the robot's working area is confined and discretized into a certain number of equal squares. Also, we suppose that the UAV can localize itself within the environment at all times, and that the system is fully observable. The entire learning process could be broken into a certain number of episodes, during which the robot tries to reach the pre-described goal. Each episode consists of a sequence of translational motions, and it ends only once the robot is within the goal state. The intelligent agent selects one of six possible actions at every time step (forward, backward, left, right, up, down). This is always true except when the agent is located on the border of the environment. In such cases, if the selected action will take the UAV out of the confined space, it should keep its current pose. For the considered task, the time steps do not represent the fixed intervals of time; they refer to actions made by the agent.

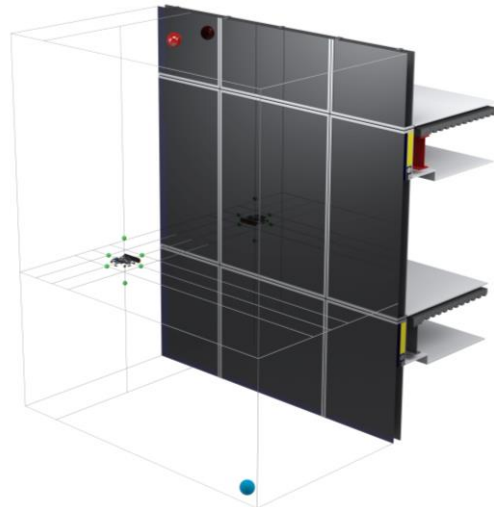


Fig. 1. Flying mobile robot at time step  $t$  during the learning process. Blue sphere represents the start pose while the red one denotes the target pose. All possible next states at time step  $t+1$  are denoted by green spheres.

## 3. REINFORCEMENT LEARNING AND Q-LEARNING

The main elements of the RL model are the intelligent agent and the environment. The intelligent agent, also called the decision-maker, is the entity that has to be able to sense aspects of its environment, act according to the obtained information, and learn from its own experience. In other words, the agent has to map all situations it faces during the learning process to actions, in order to achieve its optimal behavior [4]. Roughly speaking, the environment represents everything outside the agent, i.e., it can be said that the environment is a set of all possible states and rewards. The state represents the basis on which the choice about action selection is being made [4], while the reward is a numerical value representing the next state's desirability based on the current state and action applied in that state. Considering previously mentioned, the agent's overall objective is to maximize the total reward in the long run.

To fully understand the RL problem, one must know how the agent decides which action from the finite collection of actions it should select at every time step.

To answer this question, we have to introduce the core aspect of the RL framework – the policy. The policy gives learning capability to the intelligent agent, i.e., it represents the rule on which actions are taken by the agent at every time step.

Besides trial-and-error search, another important feature of reinforcement learning is delayed reward, which relates to how action applied in the current state may also affect all subsequent rewards. In that manner, the assumption based on the Markov property is fundamental to all reinforcement learning problems. A process is said to have the Markov property, if the current state only depends on the previous state and action applied in that state. Furthermore, since our problem has a finite number of states and rewards, it can be modeled as a finite Markov decision process (finite MDP). The mathematical formulation of the Markov property is shown in Eq. 1:

$$\mathbf{s}_{t+1} = f(\mathbf{s}_t, a_t, \dots, z_t) \quad (1)$$

where:  $\mathbf{s}_{t+1}$  denotes the next state,  $\mathbf{s}_t$  is the current state,  $a_t$  is the action taken at the current state, and  $z_t$  is the disturbance which is usually represented as a probability of each possible next state.

Within the considered problem, the Q-learning algorithm is applied. This algorithm exploits the state-value function at every time step in order to calculate the optimal policy. In every iteration, the optimal state-value function can be updated using the Bellman equation 2:

$$Q_{t+1}(\mathbf{s}_t, a_t) = (1 - \alpha)Q_t(\mathbf{s}_t, a_t) + \alpha \left[ r_{t+1} + \gamma \max_a Q_t(\mathbf{s}_{t+1}, a) \right] \quad (2)$$

where:  $Q_{t+1}(\mathbf{s}_t, a_t)$  denotes state-value function at time step  $t+1$ ;  $r_{t+1}$  is the reward that agent receives after taking action  $a_t$  at the state  $\mathbf{s}_t$ ;  $\gamma$  is the discount factor ( $0 \leq \gamma \leq 1$ ); and  $\alpha$  is the learning rate ( $0 \leq \alpha \leq 1$ ). To create better behavior over time, an agent should exploit actions that it has found to be the most effective in creating total reward. But, in order to find such actions, an agent needs to explore actions that it did not select in the past. In this paper, the trade-off between exploitation and exploration is done by using  $\varepsilon$  greedy policy, which is defined by the following equation 3:

$$\pi(\mathbf{s}) = \begin{cases} \text{a random action } a, \text{ with prob. } \varepsilon; \\ a \in \arg \max_a Q_t(\mathbf{s}_t, a), \text{ otherwise.} \end{cases} \quad (3)$$

where  $\varepsilon$  is a parameter which defines the ratio between exploration and exploitation ( $0 \leq \varepsilon \leq 1$ ).

The state at time step  $t$  is the vector  $\mathbf{s}_t = (x_c, y_c, z_c)$  which represents the pose of the UAV's center of gravity when it is in the hover flight regime. As mentioned earlier, the UAV operating space is discretized into a certain number of squares which vertices represent all possible states during the learning process.

#### 4. Q-LEARNING ALGORITHM

In the beginning, the number of total states, number of total actions that agent can take, start and target pose, learning rate, discount factor, the number of learning episodes, and a trade-off function between exploration and exploitation should be set. These are input

parameters considering the working principle of the algorithm depicted in Table 1. To speed up the simulation process, learning and navigation tasks are separated and performed using different computer engines. Firstly, the Q-table is calculated on a workstation within the ROBOTICS & AI lab, and afterwards, the animation is conducted on the platform called The Construct [9].

1	build Q-table (number_of_states, total_actions) as
2	zero matrix
3	<b>while</b> <i>current_episode</i> < <i>max_episodes</i> <b>do</b>
4	Get initial state
5	<b>while</b> <i>current_state</i> not <i>goal_state</i> <b>do</b>
6	Choose action using (3)
7	Take action that leads to new state and
8	observe reward
9	Update Q-value using (2)
10	<b>end</b>
11	Update $\varepsilon$ parameter (Table 2)
12	<b>end</b>

Table 1. Implemented Q-learning algorithm

#### 5. SIMULATION

In this paper, the simulation environment is defined as a cube with the following dimensions:  $6 \times 11 \times 17$  m, which gives 1122 possible states. At the beginning of the training process, the UAV is given a task to navigate from the start pose at  $(0, -5, 1)$  to the target pose at  $(5, 5, 17)$  in the shortest possible route. The reward function is defined in the same way as in the reference [6]. Therefore, the agent will get +100 if it reaches the goal state. Otherwise, it will take a penalty of  $-1$ , except if it is positioned on the environment boundaries and chooses the action that will lead to a collision with the borders. In that case, it will get a penalty of  $-10$ . The learning rate and discount factor are set to 0.1 and 0.9, respectively.

At the very beginning of the algorithm testing, the intelligent agent was set to explore the environment during the entire training process ( $\varepsilon=1$ ). The obtained results have shown that the agent can learn an optimal path after training for 300 episodes.

Since few recommendations exist in the literature on how to adjust the  $\varepsilon$  parameter, the authors made an analysis in order to explore a suitable trade-off function. Therefore, during the second phase, functions presented in Fig. 2 were used with the intent to analyze the convergence of the RL algorithm during 600 episodes.

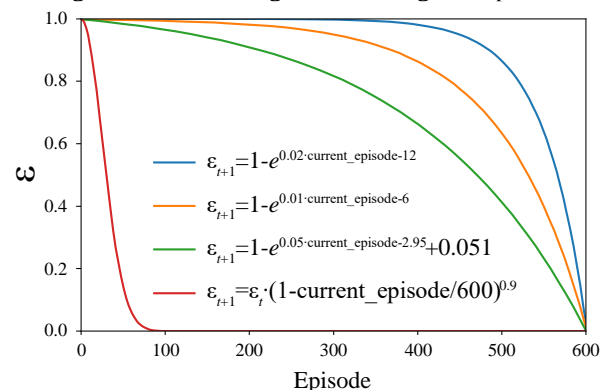


Fig. 2. Tested functions for  $\varepsilon$  parameter generation

It is noted that the algorithm only converged successfully when the function colored blue (Fig. 2) was implemented in it, and the agent took about 570 episodes to find the optimal sequence of actions (Fig. 3 - up). However, since the initial results have shown that the agent could learn the optimal path after reaching 300th episode, in the next phase the agent is forced to exploit the obtained experience every ten episodes. This strategy shows the episode in which the agent learned the optimal behavior more precisely. It could be seen that the optimal number of steps is obtained in the 220th episode and that the UAV has to take 31 steps in order to reach the target pose (Fig. 3 - down).

To achieve statistically significant results, the algorithm is run multiple times with two different scenarios. In the second scenario, the UAV had to navigate from (0, 5, 1) to (5, -5, 17). The algorithm was run ten times per scenario and the obtained results have shown that the UAV can reach the target pose autonomously by taking a minimal number of steps in every run. Even though initial values of the parameters were not changed during the repeated learning process, the paths that the agent learned were different, due to stochastic nature of learning process in conjunction with  $\epsilon$  parameter.

The flight animation of the UAV generated by the proposed RL algorithm could be seen at the link: <https://www.youtube.com/watch?v=F67Wor7WEw0>.

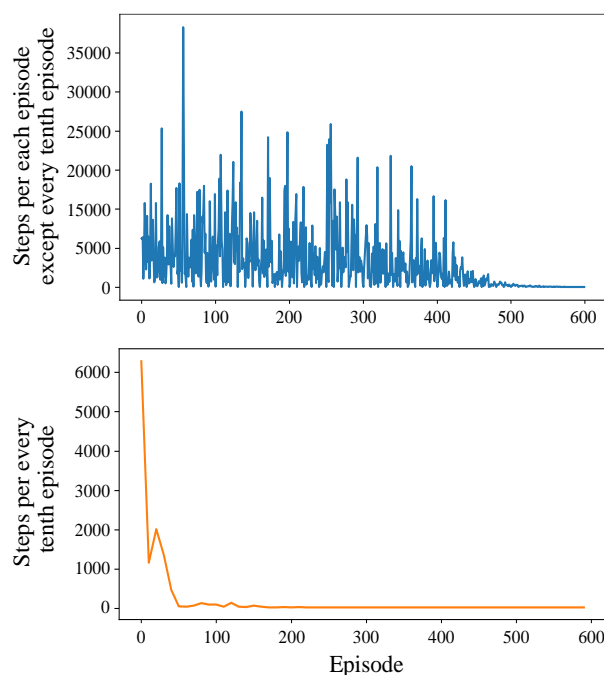


Fig. 3. Number of steps taken by the agent to reach the target pose in each episode except every tenth episode (up), and number of steps taken every ten episodes (down).

## 6. CONCLUSION

In this paper, the implementation of a Q-learning algorithm for realizing intelligent tasks such as searching for the optimal sequence of actions by the UAV in order to navigate to the goal state (target pose) is presented. Since one of the distinctive technological

challenges in RL is the trade-off between exploration and exploitation, the authors conducted research in order to find the adequate trade-off function. Also, compared to previous approaches, the new strategy for finding the episode, with the optimal number of steps, is properly achieved. The performance of the proposed RL algorithm is tested for two different scenarios, and results have demonstrated that the UAV successfully learned the optimal path in every experimental run.

## 7. REFERENCES

- [1] Mac, T. T., Copot, C., Tran, D. T., De Keyser, R.: *Heuristic approaches in robot path planning: A survey*, Robotics and Autonomous Systems, 86, pp. 13-28, December 2016.
- [2] Siegwart, R., Nourbakhsh, I. R., Scaramuzza, D.: *Introduction to autonomous mobile robots*, MIT press, Cambridge, 2011.
- [3] Koch, W., Mancuso, R., West, R., Bestavros, A.: *Reinforcement learning for UAV attitude control*, ACM Transactions on Cyber-Physical Systems, 3(2), pp. 1-21, February 2019.
- [4] Sutton, R. S., Barto, A. G.: *Introduction to reinforcement learning*, MIT press, Cambridge, 1998.
- [5] Sadeghi, F., Levine, S.: *Cad2rl: Real single-image flight without a single real image*, arXiv preprint arXiv:1611.04201, Jun 2017.
- [6] Pham, H. X., La, H. M., Feil-Seifer, D., Van Nguyen, L.: *Reinforcement Learning for Autonomous UAV Navigation Using Function Approximation*, 2018 IEEE International Symposium on Safety, Security, and Rescue Robotics, pp. 1-6, IEEE, Philadelphia, August 2018.
- [7] Wang, C., Wang, J., Shen, Y., Zhang, X.: *Autonomous navigation of UAVs in large-scale complex environments: A deep reinforcement learning approach*, IEEE Transactions on Vehicular Technology, 68(3), pp. 2124-2136, January 2019.
- [8] Imanberdiyev, N., Fu, C., Kayacan, E., Chen, I. M.: *Autonomous navigation of UAV by using real-time model-based reinforcement learning*. 2016 14th international conference on control, automation, robotics and vision (ICARCV), pp. 1-6, IEEE, Phuket, November 2016.
- [9] <https://www.theconstructsim.com/>, Accessed on: August 2021.

**Authors:** Full Prof. Dr. Zoran Miljković<sup>1</sup>, M.Sc. Đorđe Jevtić<sup>2</sup>, Assos. Prof. Dr. Jelena Svorcan<sup>3,1,2,3</sup> University of Belgrade - Faculty of Mechanical Engineering, <sup>1,2</sup>Department of Production Engineering, <sup>3</sup>Department of Aerospace Engineering, Kraljice Marije 16, 11120 Belgrade 35, Serbia, Phone.: +381 11 3302-468, Fax: +381 11 3370-364. E-mail: [zmiljkovic@mas.bg.ac.rs](mailto:zmiljkovic@mas.bg.ac.rs); [drjevtic@mas.bg.ac.rs](mailto:drjevtic@mas.bg.ac.rs); [jsvorcan@mas.bg.ac.rs](mailto:jsvorcan@mas.bg.ac.rs);

**ACKNOWLEDGMENTS:** This research work has been financially supported by the Science Fund of the Republic of Serbia, grant No. 6523109, AI - MISSION4.0, 2020-2022.



Ilić Mićunović, M., Novaković, T., Agarski, B., Čepić, Z., Vukelić, Đ., Budak, I.

## ECO-LABELS AS A TOOL FOR CIRCULAR ECONOMY AND CIRCULAR PACKAGING

**Abstract:** *Circular economy is changing the ways of thinking, business models and habits for producers and consumers. The philosophy of circular economy implies the implementation of eco-design in a product design with the extension of its lifespan through repair, reusability, upgrade, disassemble, remodeling or recycling. Additional goal of circular economy and eco-design is to include use of renewable energy sources in all processes in products lifespan. This represents an ideology that is also supported, in a certain way, through all three types of eco-labels. In Republic of Serbia only 5-7% of total municipal waste is recycled. In the near future, there will be an increase in resource price and energy costs, so developing countries like Serbia must be ready and must have an answer for the future. The circular economy offers a new "product-waste-product" model. So green marketing, which includes eco-labeling, is also significant tool in the market.*

*This study examines the role of eco-labels in the circular economy, through a systematic review of the literature and a review of the current market situation in the Republic of Serbia. We also investigated the role of eco-labels in circular packaging, and how eco-labels can help in promotion of circular packaging model and end of life waste management. We researched the Republic of Serbia market and the presence of various eco-labels that are in the service of the circular economy and packaging.*

*The results indicate that environmental labels and schemes have some support in the circular economy and packaging, but at the same time eco-labels have bigger potential. The Republic of Serbia market was dominated by one type of eco-labeling, so there should be improvements in that area as well.*

**Key words:** *Circular economy, Eco-labeling, circular packaging.*

### 1. INTRODUCTION

Given that resources on planet Earth are limited, the current economic model with valid principles of production, consumption and trade is unsustainable. If this continues, by 2030, global energy consumption is expected to increase by an additional 50%, and water demand is projected to grow by 50% more than current situation [1].

The management of resources and materials will play an important role in the fight for sustainable development and stable life on the planet in the coming period. In such a context, waste management acquires special significance. Waste is today seen as a resource and a development opportunity for a country through a concept called the circular economy [2].

Industrial production, based on term "linear economy" is clearly becoming one of the main polluters of the environment. Whether it is an increasing amount of different types of waste and even hazardous substances as a result of the production process, or it is a matter of used finished products that end up as waste in landfills in increasing quantities [3]. Linear economy is based on the concept of "take - make - use - dispose", i.e. to exploit natural resources, which are necessary for the production of new products. After the production of the product, consumption follows and after a certain time, the product loses its lifespan and ends up as waste. This type of economy has led to the generation of a large amount of waste, which has begun to have negative impacts on the quality of the human environment. A large amount of generated waste requires the

construction of large landfills, which disrupts the flora and fauna, as well as the quality of the land [3].

The current economic model of most (if not all) countries and companies involves using the resources of our planet to produce as many products as possible, most of which, unfortunately, will end up as waste. In the case of Serbia - the waste ends up in the landfill. This concept of resource use is called linear in theory. It goes without saying that this is unsustainable from an environmental point of view and it is an approach that is also economically unprofitable [3].

The model of circular economy is in complete contrast to the currently dominant linear economy that promotes the concept of production called "take (from nature), make (in the process of production), use and dispose (waste)" [3].

This study is based on the examination of the support of ecolabeling in the circular economy and circular packaging. Analysis of products on the market of the Republic of Serbia was performed, in order to examine the presence of eco labels that support the circular concept. The main shortcomings in this symbiosis were concluded literally.

### 2. PRINCIPLES OF CIRCULAR ECONOMY

The circular economy is an approach that transforms the function of resources in the economy. Waste from the production process becomes a valuable raw material in another production process, and the products themselves can be repaired, reused or improved, instead of being discarded. It is based on the maximum

utilization of the used resources, i.e. that the product, instead of being discarded before the full utilization of value, is used again and again [4].

Circular economy is a regenerative economic system in which the environment is taken into account, natural resources are saved and the amount of waste for disposal is reduced. In production processes attention is also paid to energy consumption and emphasis the use of renewable energy sources [5].

When it comes to principles, there are three basic on which the circular economy is based. According to the leading international foundation (Ellen MacArthur Foundation) for research and policy making in the field of circular economy, these are [3]:

1. Elimination of waste and pollution through product design improvement;
2. Keeping products and materials in use for as long as possible and
3. Regeneration of natural systems.

The circular economy should not be equated with the waste management hierarchy. Namely, the hierarchy of waste management was created in the linear economy as a measure of reducing the amount of waste generated and returning one part of raw materials to production processes through recycling. The circular economy is above the process of waste management because it starts primarily from a new way of thinking about the use of resources – 6R process [6] (Figure 1).



Fig. 1. 6R concept of circular economy [6].

On the way to a circular economy, recycling is a leading instrument. Recycling is the process of separating material from waste and reusing it for the same or similar purposes. The process includes the collection, separation, processing and production of new products from used items and materials. It is important to sort waste by type, because many waste materials can be reused if they are collected separately. Anything that can be reused, not thrown away, is recycling.

### 2.1. Circular packaging

Packaging plays a key role in the modern way of life. Without it, most products would break down or be damaged before they reach the store. However, it is often cited as one of the main problems in our planet's battle for environmental sustainability, as it turns into waste after each use. Therefore, companies from different industries are looking for a way to close the circle and reduce the negative impact of packaging on the environment, while still using its positive properties [7].

The biggest problem with packaging is that it usually becomes waste as soon as the customer finishes using the product. That's why smart packaging experts focus on creating a design that is optimized for recycling. By making existing packaging easier to recycle - and by using more and more recycled materials in new packaging - companies can help keep materials in the value chain longer.

This idea is at the heart of the circular economy model: a way of thinking that seeks to collect materials after they are used and to process them so that they can be reused and recycled again. In this way, waste is eliminated and the impact of packaging on the environment is reduced - as long as there are good systems for recycling and waste management [7].

## 3. ASPECTS OF ECOLABELING

Consumers and suppliers, especially in industrialized countries, are increasingly making product purchasing decisions based not only on key quality, price and availability factors, but also on environmental aspects. This includes environmental impacts that may occur before, during and after the production of a particular product. Eco-certification or "eco-labeling", as it is generally called, is finding ways to reduce the destruction of the environment in all areas caused by human activity [8].

An eco-label is defined as a label that is awarded to products that are considered to be less harmful to the environment than other products in the same category [9]. One of the important indirect instruments in environmental protection, on a global level today, is certainly environmental labeling. The mechanism of action of this instrument can, in short, be explained as follows: a label on a product/service that shows that the product/service is less harmful to the environment should, on the one hand, motivate an environmentally conscious consumer to buy it, while growth consumption of such products should, on the other hand, motivate producers to develop and produce more suitable products from the environmental aspect [8].

The reasons for the introduction of environmental labeling are the following:

- Promoting the development, production, advertising and use of products that, as little as possible, endanger the environment;
- Stimulating production in which natural resources are maximally saved with the use of materials subject to recycling;
- Providing customers with complete and reliable information on the impact of a particular product or service on the environment, making it easier for customers interested in protecting the environment [9].

## 4. THE ROLE OF ECO-LABELING IN CIRCULAR ECONOMY

The transition to a circular economy depends on a change in the behavior of producers and consumers. Product labeling schemes are regularly offered as a solution to support these changes. Although there are

numerous labeling schemes and related research on the effectiveness of individual schemes, it remains unclear how influential labeling is in supporting the outcomes of the circular economy.

The transition to a circular economy depends on manufacturers designing products for durability, reusability, repair, upgrade, disassembly or recycling, and consumers - changing the way they buy, use, care for, share and dispose of products. Understanding how eco labeling can encourage businesses to offer more sustainable products and services and help consumers make more sustainable purchasing decisions is a critical issue for progress toward the circular economy. Circular economy can be defined as an economic system that replaces the concept of "end of life" with reduction, alternative reuse, recycling and recovery of materials in the processes of production/distribution and consumption. The goal is to achieve sustainable development by enabling economic growth without compromising the social and environmental well-being of present and future generations. Circular economy policies are advancing globally thanks to Europe introducing a comprehensive European circular package, China announcing the Chinese circular economy Promotion Act and government agencies in Australia developing and/or implementing circular economy policies.

The success of these policies depends to a large extent on consumers making informed purchasing decisions that support outcomes. Consumers are often reluctant to pay more for "green" products and want clearer, easily comparable information on the product's impact on the environment. Consumers are not the only ones playing a central role in the successful implementation of circular economy policy, however - manufacturers are equally important. Although companies are increasingly aware of the possibilities promised by circular economy, product innovations and shifts towards true business models remain limited [10] (Figure 2.).



Fig. 2. Circular economy business model [11]

If eco-labels are observed in more detail, the circular economy is supported in every type of eco-label. Type I (national and regional labels), supported by LCA studies, rely on strict criteria for obtaining licenses for use. These criteria are based on reduced consumption of both natural resources and material savings. Procedures

to develop eco-label criteria for a product category is a complex and long path. The complex system of "EU flower" stands out, as recognizable regional labels. On the other hand, the Type II eco-label, although a much simpler system, which does not require an LCA study and is based on self-declaration of environmental claims, also shows support for the circular economy system. This type is specifically geared towards circular packaging, through support for reuse, reduction, recycling, as well as safe degradation and composting of packaging waste. Within ISO 14021, which supports type II eco-labeling, there are 16 claims that are most commonly applied and that lead to the promotion of reuse and recycling, as well as renewable energy sources and materials. Type III (for specific aspects of products using a life-cycle approach), is based on the entire life cycle of products or services. Although this type does not certify any specific quality of a product/service, it provides the most detailed information to customers themselves with the availability of an LCA study.

However, even if eco labels and schemes support the circular economy in theory, there are a number of problems in the interpretation and credibility of the eco-labels themselves that can be seen in the analysis of literature sources.

## 5. RESULTS AND DISCUSSIONS

The results of the research of products with eco-labels that support the concept of circular economy in the territory of the Republic of Serbia have shown that type II eco-labels dominate. The Mobius loop, in the form of a generic code that indicates the type of material from which the product packaging is made, and thus facilitates waste management, which is in line with the principles of circular economy, is certainly the most present type of label. This recycling code per 100 products tested was present on 91% of the products.

Also one of the most present is the label "Green Dot", with 88%. The "Green Dot" system is based on the principle that the producer pays per kilogram of packaging waste, forming the price by type of material, and by paying the license of the company under whose jurisdiction is the "Green Dot" license (in Serbia Sekopak company). Packaging manufacturers actually pay for collecting, sorting and recycling packaging waste.

In a much smaller percentage (18%), but also present label in our market is FSC, which promotes responsible management of natural resources, specifically forests. It also refers to the production of furniture, as well as wood products in general, but also to the production of paper products and packaging. FSC Italy is the contact for FSC holders for Serbia, Bosnia and Herzegovina, Croatia and Slovenia.

Below 10% of the present regional mark EU flower and Nordic swan. The EU flower is under the jurisdiction of the European Union, while the Nordic swan is from the Nordic region (Norway, Sweden, Finland, Denmark and Iceland). Both of these labels not only support the circular economy, it also stimulates a company's resource efficiency and strengthens its competitiveness - creating new business models and

innovative solutions.

## 6. CONCLUSION

Although most eco labels to a greater or lesser extent support the philosophy of the circular economy, through different models, by examining the market and literature and regarding eco labels, there are several critical points concerning the eco labels themselves. For example concrete evidence of measurable improvements in the environment resulting from the adoption of eco labeling schemes is scarce (with the possible exception of specific products or groups of products). Several reviews indicate a lack of research and empirical data in this area (e.g. on sales volume or market share), which makes it difficult to assess the improvement of environmental impact [8,10,12]. Instead, studies focus on changing attitudes and behaviors, probably because measuring the environmental benefits of labels and distinguishing them from a range of other possible impacts remains a significant challenge. Overall, limited evidence of environmental impacts broadly supports the conclusion of Marrucci et al (2019) [12] that further research is needed to demonstrate the contribution to the results of eco labeling schemes to circular economy. Also one of the biggest problems since the development of eco labels is the existence of knowledge and awareness that can result from a combination of information and communication about the label, the ability of consumers to understand the environmental benefits of buying environmentally friendly products, as well as visibility (e.g. on products, in stores, business or government policies). It is important to educate and understand the labels themselves, so that e.g. in Denmark demonstrated effective campaigns aimed at increasing the recognition and knowledge of eco labels, which should be taken as a model in other countries as well.

## 7. REFERENCES

- [1] European Commission: Closing the Loop - an EU Action Plan for the Circular Economy. Communication from the Commission to the European Parliament, the Council, the European Economic and Social Committee and the Committee of the Regions, 2015.
- [2] European Commission: Behavioural Study on Consumers' Engagement in the Circular Economy - Final Report. Directorate-General for Justice and Consumers, Brussels, 2018.
- [3] Ellen MacArthur Foundation: Towards the Circular Economy Opportunities for the Consumer Goods Sector, 2013.
- [4] Ewert, B.: Moving beyond the obsession with nudging individual behaviour: towards a broader understanding of behavioural public policy. *Publ. Pol. Adm.* 35 (3), 337e360, 2020.
- [5] Corona, B., Shen, L., Reike, D., Rosales Carreon, J., Worrell, E.: Towards sustainable development through the circular economy-a review and critical assessment on current circularity metrics. *Resour. Conserv. Recycl.* 151, 104498, 2019.
- [6] Gluščević, M, Kaluđerović, Lj.: Analiza kapaciteta

jedinica lokalne samouprave u pogledu stvaranja uslova za prelazak na cirkularnu ekonomiju. Beograd: Deutsche Gesellschaft für Internationale Zusammenarbeit (GIZ) GmbH, 2019.

- [7] Rex, E., Baumann, H.: Beyond ecolabels: what green marketing can learn from conventional marketing. *J. Clean. Prod.* 15 (6), 567e576, 2007.
- [8] Yokessa, M., Marette, S.: A review of eco-labels and their economic impact. *Int. Rev. Environ. Resour. Econ.* 13 (1e2), 119e163, 2019.
- [9] Budak, I., Vukelic, Dj., Agarski, A., Ilić Mićunović, M.: Life cycle design and assessment tools, University of Novi Sad, Faculty of technical sciences, Novi Sad, 2020.
- [10] Meis-Harris Julia, Klemm Celine, Kaufman S, Curtis J, Borg Kim, Bragge P.: What is the role of eco-labels for a circular economy? A rapid review of the literature. *J. Clean. Prod.* 306, 1e16, 2021.
- [11] <https://ec.europa.eu/jrc/en/news/research-helps-europe-advance-towards-circular-economy>, 15.07.2021.
- [12] Marrucci, L., Daddi, T., Iraldo, F.: The integration of circular economy with sustainable consumption and production tools: systematic review and future research agenda. *J. Clean. Prod.* 240, 118268, 2019.

**Authors: Assist. Prof. Milana Ilić Mićunović, Assoc. Prof. Boris Agarski, Full Prof. Đorđe Vukelić, Full Prof. Igor Budak**, University of Novi Sad, Faculty of Technical Sciences, Department of Production Engineering, Trg Dositeja Obradovića 6, 21000 Novi Sad, Serbia, Phone.: +381 21 485-23-50, Fax: +381 21 454-495.

E-mail: [milanai@uns.ac.rs](mailto:milanai@uns.ac.rs); [agarski@uns.ac.rs](mailto:agarski@uns.ac.rs); [vukelic@uns.ac.rs](mailto:vukelic@uns.ac.rs); [budaki@uns.ac.rs](mailto:budaki@uns.ac.rs);

**B.S.E. Tamara Novaković**, student of master academic studies, University of Novi Sad, Faculty of Technical Sciences, Department of Environmental Engineering and Occupational Safety and Health, Trg Dositeja Obradovića 6, 21000 Novi Sad, Serbia.

E-mail: [tamara.novakovic.97@gmail.com](mailto:tamara.novakovic.97@gmail.com)

**Assist. Prof. Zoran Čepić**, University of Novi Sad, Faculty of Technical Sciences, Department of Environmental Engineering and Occupational Safety and Health, Trg Dositeja Obradovića 6, 21000 Novi Sad, Serbia, Phone.: +381 21 485-24-10

E-mail: [zorancepic@uns.ac.rs](mailto:zorancepic@uns.ac.rs)

**ACKNOWLEDGMENTS:** The project is co-financed by the Governments of Czechia, Hungary, Poland and Slovakia through Visegrad Grants from International Visegrad Fund. The mission of the fund is to advance ideas for sustainable regional cooperation in Central Europe.

Kosec, B., Cigić, L., Ilić Mićunović, M., Klobčar, D., Nagode, A.

## DUST PARTICLES EMISSIONS AT STEEL CUTTING PROCESSES

**Abstract:** *Oxyfuel cutting and plasma cutting are material processing technologies that are strongly associated with particulate matter emissions.*

*These particles have a negative impact on the health of the operator because they penetrate deep into the lungs due to their small size. The impact is determined by measuring the amount of particulate matter emissions, particles morphology, particles chemical composition, and particles size and their size distribution. The methods for measuring and evaluating these parameters are regulated in the standard ISO 13322-1: 2014.*

*In the presented study, the emitted particles generated during flame cutting and plasma cutting of S460 grade structural steel were analysed. The collection of the particles was performed with the personal particle sampler, the weighing of the particles was performed on an electronic balance, while particle size, their morphology and chemical composition were determined with a field emission scanning electron microscope.*

*By comparing the measurement results, it was determined how the processing technology, the processed material and the use of the extraction filter device affect the emission of fine dust to which the operators are exposed.*

**Key words:** *dust particles, emissions, steel, cutting, analysis.*

### 1. INTRODUCTION

To achieve the desired shape of the product, it is necessary to choose the most suitable machining process. If we want to separate two metal parts, the easiest way to do this is to use thermal cutting. Flame cutting is most commonly used, where an exothermic metal oxidation reaction is used to melt and cut the material [1]. We also know plasma cutting, which allows the cutting of materials that conduct electricity well, because here the material melts due to the electric arc.

In the frame of our investigation work, we chose both the flame and plasma cutting process for cutting S460 structural steel. Both the flame and plasma cutting process apply to machining technologies that are strongly related to dust particle emissions. These particles are dangerous from a health point of view as they can penetrate deep into the lungs of the operator performing these processes. Therefore, it is very important to determine the level of risk to the human respiratory system that is related to the nature, shape and size of the particles. The resulting particles can be of different sizes, the most dangerous being particles with a diameter of less than 10  $\mu\text{m}$ , which are respiratory particles and due to their small size are most easily dispersed in the working environment [2].

### 2. PARTICLES FORMED DURING CUTTING PROCESSES

For cutting processes, the resulting particles can be divided into two groups. Namely, these are particles larger than 20  $\mu\text{m}$ . These are caused by metal injection. Another type of particle is represented by particles with a size of about 1  $\mu\text{m}$ , which are the result of condensation of metal vapors. Upon closer analysis, it was found that ultrafine particles (less than 0.1  $\mu\text{m}$ ) are

also present, representing only about 7% of the total mass of all formed particles.

Chemical analysis of the filters on which the particles were trapped showed that in the welding of aluminum the particles contain organic and elemental carbon, iron and aluminum. In steel welding, however, the particles contained iron, organic carbon, zinc, and copper. The presence of these elements can be attributed to organic coatings on metals, aluminum, galvanized steel or electrodes [3].

Adverse effects on humans can be divided into three categories:

- chemical hazard (caused by particulates and gases),
- mechanical hazard (electricity, heat, noise, vibration), and
- danger due to radiation (electromagnetic radiation in the area of visible, ultraviolet and infrared waves).

Of all the above, the chemical hazard has the greatest impact, as the resulting flue gases and harmful gases have the most negative impact on human health. Epidemiological studies of full-time welders have shown that they developed febrile illness from inhaling metal fumes, respiratory tract irritation, changes in lung function, lung infections, and an increased likelihood of developing lung cancer [4].

#### 2.1. Classification of particles by size

Basically, dust particles are classified as primary particles resulting from emissions from natural or artificial sources and secondary particles formed due to chemical and physical reactions once they are in the atmosphere. To facilitate the determination of the origin of the particles and the influence of the dust particles, we divide them into predetermined size classes. Particles can be quantitatively characterized by determining their geometry. After processing the image with the help of software, we get a set of geometric parameters that describe the size and shape of the

particle [5].

ISO standard 13322, entitled Particle size analysis - Image analysis methods [5], consists of two parts, namely static image analysis and dynamic image analysis. For the purposes of the master's thesis, the first part of the standard describing static analysis will be considered and will be presented below. The purpose of the first part of ISO 13322 is to recommend when captured images can be used for particle size analysis. The aim of this part of the standard is to give a standardized description of the technique used, whereby the obtained measurements correspond to the recommendations of the standard and are traceable.

This section does not describe the devices used to capture images, but the standard is limited to image sections that are relevant to the correctness of the results in the particle size analysis. The first part of the standard contains calibration verification methods and recommendations for using a certified standard as a reference. Throughout the analysis, errors are taken into account that contribute to the final uncertainty of the measurements. This part of ISO 13322 is useful for image analysis to determine the size distribution of stationary particles. The particles are arranged and fixed in the plane observed with the image capture device. The field of view changes by moving the support on which the particles are or by moving the camera, so it is necessary to ensure that there is no distortion of the captured images. The standard focuses on digital images generated by a light or electron detection system and considers only images that are analyzed using pixel counting methods.

### 3. EXPERIMENTAL

The experimental part the work includes the measurement and analysis of particulate emissions produced by the cutting process for structural steel S460 (Tables 1, 2, 3).

Element	C	Si	Mn	Cr	Mo	V
mas %	1,00	1,10	0,30	8,00	2,30	0,30

Table 1. Chemical composition of steel S460

Young's modulus	210 GPa
Density	7640 kg/m <sup>3</sup>
Coefficient of thermal expansion	11,5*10 <sup>-6</sup> m/mK
Specific heat	470 J/kgK
Thermal conductivity	17.6 W/mK

Table 2. Thermal properties of steel S460 at room temperature (20 °C)

Steel	Process	Heat source	Type
S460	Cutting	Flame	Cutter gk TIP200/A
S460	Cutting	Plasma	Cutter Lincoln Electric INVERTEC PC100

Table 3. Cutting process data

All steel cutting operations were carried out for 1

minute, during which time the produced particulate emissions were recorded with the measuring instrument ZAMBELLI EGO PLUS TT (Figure 1), which had to be pre-calibrated. We first weighed the emitted particles that were trapped on the filter of the device and then evaporated them with carbon. With this, we prepared them for observation under a ThermoFisher Scientific Quattro S scanning electron microscope, where we captured images of the particles on the filter and measured their chemical composition. At the very end, we used the computer program ImageJ to process the captured images and determine the geometry and size of the particles.



Fig. 1. Components of measuring instrument ZAMBELLI EGO PLUS TT.

The flame cutting process of S460 steel was performed for 1 minute with a gk TIP200 / A flame cutter on acetylene and oxygen. Plasma cutting of S460 steel was also performed for 1 minute with a Lincoln Electric INVERTEC PC100 plasma cutter connected to direct current and a three-phase voltage of 400 V.

Sampling with this meter can be done spatially or in person. In spatial sampling, the meter is fixed to a specific area in the room, which means that the average amount of dust particles in the measured area is measured. In personal sampling, the meter is located at the operator near his respiratory system. We decided to choose personal sampling as we were interested in the direct impact of particulate emissions on the operator performing the cutting or welding process. To achieve the desired effect, the mouthpiece of the meter was attached under the airway, 30 cm away from the mouth.

Before starting each measurement, it is necessary to calibrate the meter, determine the time of capture of particles and select the filter. Speed, temperature and relative humidity must also be measured during particle capture. The operation of the meter could be compared to the operation of a suction device, as the meter sucks air through a tube attached to a nozzle on which trapped dust particles accumulate that are large enough to trap the filter.

The parameters with the corresponding units and values are shown below and had the same values in all processing operations. Measured constant parameters during measurements:

Room air velocity: 0 m/s.

Room air temperature: 21 °C.

Relative humidity in the room: 50%.

Selected parameters:

Calibration of air flow through the filter: 3 l/min (simulates operators breathing).

Total particle capture time: 1 min.

Filter: Mixed cellulose ester filter (MCE).

The results of dust particle emissions showed that the steel cutting process causes about 7 times more emissions than the manual arc welding process. The highest emission of dust particles is produced by the flame cutting process of S460 structural steel, namely 0.096 g/h.

For particle analysis the ThermoFisher Scientific Quattro S SEM has been used (Figure 2).



Fig 2. Field emission electron microscope (FEG SEM) ThermoFisher Scientific Quattro S.

It is a field emission electron microscope (FEG SEM) that can operate in three different vacuum modes. It operates in low vacuum (up to 200 Pa), in high vacuum ( $<6 \cdot 10^{-4}$  Pa) or in ESEM (Environmental Scanning electron microscope) mode (up to 4000 Pa).

The highest resolution can be achieved in high vacuum mode by scanning electron microscopy (STEM), which in this case is 0.8 nm. With ESEM and low vacuum mode, a resolution of up to 1.3 nm can be achieved. For imaging, the FEG SEM Quattro S is equipped with secondary electron (SE), backscattered electron (PSE) detectors and transmission electron detectors. An energy-dispersive X-ray detector (EDXS) of the new generation Ultim® Max is installed for the analysis of the chemical composition.

In Figure 3 are presented results of dust analysis used field emission electron microscope (FEG SEM).

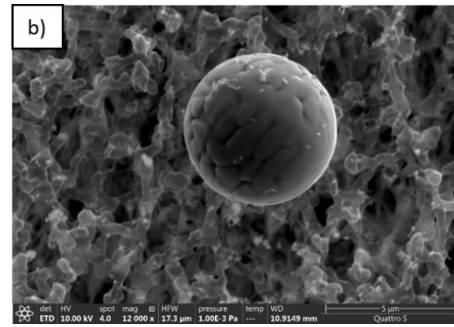
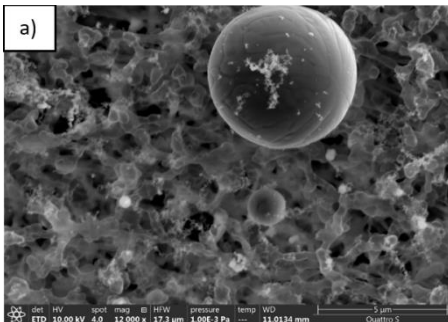


Fig 3. Only emitted dust particles through the use of ETD methods at 12 000 x magnification, for example: a) Oxygen-cutting of steel S460; b) Plasma cutting of steel S460.

By analyzing the obtained images, we came to the conclusion that the individual particles have the correct spherical shape in both the cutting processes. In all cases, clusters of particles or agglomerates were also present, which were composed of individual spherical particles and were clearly visible. Flame cutting produces more particles with an equivalent diameter of less than  $1.75 \mu\text{m}$  than plasma cutting. Plasma cutting produces particles with a diameter greater than  $5.5 \mu\text{m}$  that cannot be detected by flame cutting. This means that, on average, smaller particles are obtained in flame cutting than in plasma cutting. All analyzed particles for both plasma and flame cutting are less than  $10 \mu\text{m}$ , which means that they are classified as respiratory particles, as they reach the lower respiratory tract all the way to the alveoli. Most of the analyzed particles thus do not reach the lower respiratory tract, but the lungs, as they are larger than  $10 \mu\text{m}$ . Such particles are classified in the category of thoracic particles, which are less harmful to humans than respiratory particles.

#### 4. CONCLUSIONS

Prior to sampling (capturing) the emitted dust particles during the cutting processes, care must be taken to ensure that the mixed cellulose ester filter on which the particles are trapped is not moistened. Moisture affects the initial mass of the filter and causes a change in its properties.

The amount of emissions is most influenced by the choice of machining process, which is evident in the case of structural steel S460, where the cutting process causes 7x more emissions than manual arc welding.

In the flame and plasma cutting of S460 steel, all analyzed particles were smaller than  $10 \mu\text{m}$  (respiratory particles), with the particles produced by flame cutting being on average smaller than in plasma cutting. In manual arc welding of S460 steel, as much as 80% of the analyzed particles had a diameter greater than or equal to  $17.3 \mu\text{m}$ , which means that they belong to the category of thoracic particles that reach the lungs and are less harmful than respiratory particles.

## 5. REFERENCES

- [1] Krajcarz, D., *Comparison Metal Water Jet Cutting with Laser and Plasma Cutting*, Procedia Engineering, 6 (2014), 838-843.
- [2] Wahab, M.A., *Comprehensive Materials Processing*, Elsevier Ltd., 6 (2014), 49-76.
- [3] Ilić, M, Budak, I, Kosec, B., Nagode, A., Hodolič, J., *The analysis of particles emission during the process of grinding of steel EN 90MnV8*. Metallurgy, vol. 53, No. 2, pp. 189-192, 2014.
- [4] Dasch, M., *Physical and Chemical Characterization of Airborne Particles from Welding Operations in Automotive Plants*, Journal of Occupational and Environmental Hygiene 5, 2008.
- [5] ISO 13322-1 (2014): *Particle size analysis -- Image analysis methods -- Part 1: Static image analysis methods*, International Standardization Organization.

**Authors: Full Prof. Borut Kosec, Lovro Cigić, Full Prof. Aleš Nagode**, University of Ljubljana, Faculty of Technical Sciences and Engineering, Aškerčeva cesta 12, 1000 Ljubljana, Slovenia, Phone.: +386 1 20 00 410, Fax: +386 1 47 04 560.

E-mail: [borut.kosec@omm.ntf.uni-lj.si](mailto:borut.kosec@omm.ntf.uni-lj.si);

[lb.lovro.cigic@gmail.com](mailto:lb.lovro.cigic@gmail.com);

[ales.nagode@omm.ntf.uni-lj.si](mailto:ales.nagode@omm.ntf.uni-lj.si)

**Assist. Prof. Milana Ilić Mićunović**, University of Novi Sad, Faculty of Technical Sciences, Department of Production Engineering, Trg Dositeja Obradovića 6, 21000 Novi Sad, Serbia, Phone.: +381 21 485-23-50, Fax: +381 21 454-495.

E-mail: [milanai@uns.ac.rs](mailto:milanai@uns.ac.rs)

**Assoc. Prof. Damjan Klobčar**, University of Ljubljana, Faculty Technical Sciences and Engineering, Aškerčeva cesta 6, 1000 Ljubljana, Slovenia, Phone.: +386 1 47 71 205, Fax: +386 1 25 18 567.

E-mail: [damjan.klobcar@fs.uni-lj.si](mailto:damjan.klobcar@fs.uni-lj.si)



Mijanović, K., Kopač, J.

**SUSTAINABLE PRODUCTION TO LONG-TERM ECONOMIC DEVELOPMENT**

**Abstract:** Sustainability of the production plant is an important economic and technical-technological issue of interest for development policy in general, in order to establish long-term economic development. It is a concept that characterizes development with limits to growth and commands all aspects of social life, limiting consumption and production, reduced use of natural resources, and dematerialization of products. Sustainability requires a constant balance between meeting the living needs of current generations and the capacity of natural resources. Therefore, sustainability encompasses at the same time methods for ensuring economic growth, quality of living environment, energy efficiency and waste management, together with health and social equality. Basically, sustainability is the ability to maintain social and economic development that seeks to reduce the exploitation of resources, to harmonize the direction of investment, the orientation of technological development, to ensure long-term development. Sustainable development initiatives are very common at the political level within the UN, OECD, EU and other national levels. The idea of sustainable development is defined and implemented at the production macro level, but there is a serious lack of implementation practice at the applied or practical level.

The paper will show the directions of action of production and integrated environmental management on constant harmonization, interventions from nature with production plans with the application of new technologies and the use of innovations.

**Key words:** Sustainability, long-term economic development, growth limits, pollution, waste management, natural resources, environmental management

**1. INTRODUCTION**

Unplanned use of natural resources can reduce their capacity and disrupt biodiversity. Preservation of the capacity of the spheres of the environment is becoming one of the fundamental principles of sustainable development. Limited resources and consumption based on economic growth do not lead to the line of sustainable development. Preserving the capacity of environmental spheres is an extremely complex issue that depends on many mutual factors, including consumption and production, and a wide range of positive environmental and economic results, with the use of new technologies. Economists typically point to three main macroeconomic goals: full employment, price stability, and economic growth. At the same time, economic growth is directly related to the quality of living environment. Until recently, the theory of general equilibrium and economic growth did not have an environmental aspect. Almost all researchers who have dealt with this so far have been satisfied with the premise that growth means producing more than in the past. This model solves the relations of savings, investment, used capital, labor and the final product, and ensures that everything that is invested is spent. System theory views the production organization as an "open" system, differentiated from the environment by a certain boundary. An open system strives for a state of dynamic equilibrium with its environment through the constant exchange of materials, data and energy. Units within an organization (subsystems) with their own systemic characteristics can be expanded to attract more resources or participants, or narrowed to strengthen existing participation.

This paper will consider such a state of balance of economic forces and action in dynamic conditions when management deals with resources and global spatial constraints, then the purpose of constant increase in production, which leads to the establishment of constant economic growth.

**2. DIRECTIONS OF ACTIVE INTEGRATED ENVIRONMENTAL MANAGEMENT**

Growth theories have not come close to solving the problem from the environmental aspect of the production process. Neoclassical analyzes of resource depletion appeared in the 1930s, and resource economics grew into an economic discipline. The economics of natural resources deal with the harmonization of resources and the need for them indirectly and unsystematically. The analytical apparatus and basic assumptions are the same as in the discipline of welfare economics in which it is argued that the distribution is socially optimal and equitable if the economy is in equilibrium. Environmental economists most often oppose this view, arguing that it is not possible to have an "unlimited" replacement of natural capital with man-made capital as a replacement for natural capital or resources. They see physical laws as the limit to which human capital can replace natural capital. The interaction between population, economic growth and the environment is shown by equation (1)

$$I = P \times A \quad (1)$$

Environmental economics, which has been developing rapidly over the last thirty years or so, is also

unsatisfactory in terms of results and approach. The basic questions he deals with are how to optimize the consumption of resources and what is the social cost of endangering the environment, while the basic postulates of the welfare economy are called for help. Time advantages, social rate of return, other templates that were theoretically justified at one time and cost-benefit analysis are considered. An attempt to monetary value a degraded environment ends in failure because it is something that does not appear on the market and whose consumption cannot be individualized and charged.

Environmental management rules state that there must be no reduction in resource stocks and environmental capacity, ie that this rule can be partially replaced by the replacement of natural capital, man-made capital, or technological progress as a possibility of reducing the use of natural resources. When considering sustainable economic development, "intergenerational equality" must be taken into account, ie the ability of future generations to meet their needs must not be weakened. Sustainability can only be analyzed within the need to maintain natural capital stocks. This need makes it possible to identify the constraints imposed by the functioning of the natural environment on its role in supporting the production system. The extent to which these needs can be reduced depends on what is thought of the degree of sustainability between renewable and non-renewable resources, and between productive capital and natural capital. It also depends on the extent to which technological progress will reduce the amount of resources that enter production in relation to a certain level of living standards, and it also depends on the impact of population growth on the consumption of capital stocks.

### 3. HARMONIZATION OF NATURE INTERVENTIONS WITH PRODUCTION PLANS

Conventional economics usually does not give an accurate picture of the relationship between the

production system and the environment that surrounds the economic system. Simple conventional economic models have completely neglected the relationship between production and the environment. Therefore, production is often considered to be in conflict with the environment, which is why it is necessary to explain the economic functions of the environment, ie the possibility of economic growth and increase the quality of the environment. The environment offers production and business in general: Space for production installations; supply of natural resources that enter the production process (renewable and non-renewable resources); assimilation of unusable residues from production, provided that the environment has a limited capacity for such assimilation; energy sources and energy sources.

In order to be able to determine the interrelationships between production and the environment, as well as the functioning of the model given in Figure 1, the elements of the economic system located in the natural environment are shown. Every quantity of an individual resource that enters the production process must come out of it. The quantitative relationship between the two functions of the environment (resource supply and assimilation of production residues) has a direct or proportional relationship. The more resources used, the more production residues will be generated. The primary resources that the production sector receives from the natural environment are raw materials, ie natural resources (eg wood, water, oxygen, minerals, etc.). Production and consumption create "unusable residues" that are disposed of. The list of these substances is: (sulfur dioxide, organic compounds, toxic solvents, animal waste, fats, pesticides, various particles, construction waste, heavy metals, etc.). The remnants of the production process include energy waste (such as heat, noise, radioactivity). Consumers also generate household wastewater, solid municipal waste from use, used oils, then car emissions and more.

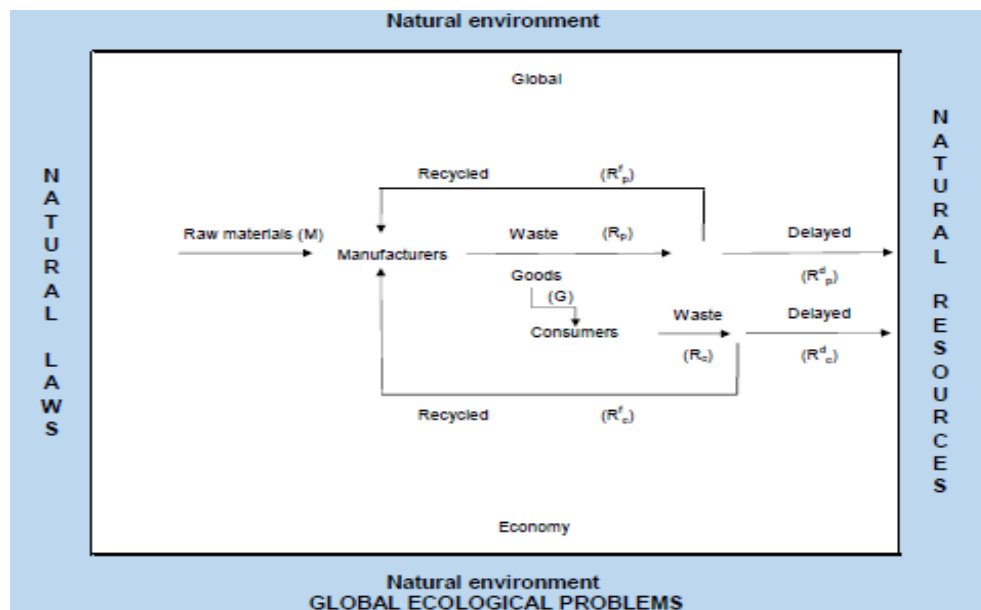


Fig. 1. Economy and Environment (Source: Field, B.C. Environmental Economics, McGraw-Hill International Editions, New York 1994, p. 25).

Figure 1 shows that materials and energy (natural resources) are extracted from nature and that residues from production and consumption are disposed of in the environment. Using the first law of thermodynamics, formula (2) can be derived:

$$M = R_{dp} + R_{dc} \quad (2)$$

M - amount disposed of in the environment

$R_{dp}$  - raw materials that have entered the production process

$R_{dc}$  - raw materials that have entered the consumption process

Formula (2) indicates that the total raw materials that have entered the production and consumption process must be equal to the quantities that are disposed of in the environment. There are three basic ways to reduce the input of raw materials into the production process, and thus reduce residues that need to be disposed of:

1) Reducing the production of goods and services, so that, according to the advocates of "zero growth of production", the amount of disposed waste could be reduced.

2) Reduction of the amount of waste generated in the production process. The way in which the amount of required raw materials, and thus the generated waste, can be reduced, is to reduce the generation of waste in production. Assuming that all other flows remain the same, this implies a fundamental change in the amount of waste generated in the production process for a given amount of goods produced.

3) The third option to reduce waste is to increase the amount that is recycled. Instead of disposing of production and consumption residues in the environment, they can be recycled and used in the production process. The main purpose of recycling is to replace part of the original amount of raw material that enters the production process.

### 3.1. Production planning

The most important task of the environmental manager is to formulate a business policy strategy, ie to determine the direction of the company, and formulate a general business policy. Production planning is the first function and basis of management, which is a guide for other functions. The starting point of planning that always deals with the future, and whose basic determinant is uncertainty, is to predict the future conditions in which the company will operate. Prediction is the result of management's ability to ensure quality information processing and create an appropriate information base for planning. Since it is easier to get information about upcoming events, the reliability of planning is inversely proportional to the time horizon of planning. Plans can be long-term, medium-term or short-term, with certain rules or steps to be achieved.

## 4. CONCLUSION

Proponents of environmental protection have often used the criterion of sustainability lately. Once an activity is judged "unsustainable", it is very difficult to

defend it. Among them, attempts to achieve "sustainability" face several serious problems, the most direct of which is the existence of powerful interests that protect unsustainability. For environmentalists, the existing interest of the present generation is to be placed above the interests of future generations. Those who live in particularly unsustainable ways - wealthy consumers - have a strong interest in resisting change. Moreover, it is common for the poor to want to get rich quick are tempted to ignore the long-term consequences. The second stage that management must face in trying to achieve sustainability is to determine what is meant by that word. The operational definition of sustainability is ultimately based on more or less arbitrary decisions as to the extent to which new knowledge and technology will be able to replace different natural resources. Yet it is basically not possible to accurately predict what future technologies will be available. It is necessary to agree on the distribution key for the use of available natural space.

Trying to achieve sustainability in one country is useful if other countries are working in that direction. The logic of competition and free trade often contradicts sustainability settings. The concept of a production environmentally acceptable system is in line with the broader concept of sustainable development. It promotes the achievement of economic growth without deteriorating the quality of the living environment.

## 5. REFERENCES

- [1] Porrini, D. Environmental policies as an issue of informal efficiency, Working paper, Università degli studi di Milano, Milano, 2005.
- [2] Mijanović, K., Environmental approach to production systems, Cleaner production, Planjaks Tešanj, 2008.
- [3] Črnjar, M. Črnjar, K. Knowledge in the function of sustainable development of PGC, Knowledge - a basic economic resource, Faculty of Economics Rijeka, 2008.

**Authors: Assist. Prof. Krsto Mijanović**, International University of Travnik, Aleja Konzula bb, 72270 Travnik, Bosnia and Herzegovina.

E-mail: [krsto.mijnaovic@unmo.ba](mailto:krsto.mijnaovic@unmo.ba)

**Full Prof. Janez Kopač**, University of Ljubljana, Aškerčeva 2, 1000 Ljubljana, Slovenia

E-mail: [Janez.Kopac@fs.uni-lj.si](mailto:Janez.Kopac@fs.uni-lj.si)



Stanivuk, T., Dujmović, M., Dumanić, N., Barač, M.

## **AUTOMATION OF CONTROL OF ELECTRO-PNEUMATIC (PNEUMATIC) SYSTEM WITH AND WITHOUT PROGRAMMABLE LOGICAL CONTROLLER PLC**

**Abstract:** This paper defines ways of solving practical problems in the field of automation of production processes. It presents different methods of solving the same problem through pneumatics, electro-pneumatics and control of programmable logic controllers. With each method of problem solving, basic guidelines for their implementation have also been given, depending on the complexity of the practical problem. Application of the paper with minor modifications is possible in various fields of mechatronics.

**Key words:** cascade method, stepper (sequential) method, electro-pneumatic method, automation by applying PLC Siemens Logo

### **1. INTRODUCTION**

System automation is an essential precondition for improving the production process. In systems realized by electrical and / or pneumatic elements and devices, programmable logic controllers - PLC, and a combination of the above, automation can be realized in several ways.

This paper presents some of the automation methods, precisely two pneumatic methods (cascade and stepper/(sequential) method), electropneumatic method and PLC control automation, solved for the same given functional (alphanumeric) task. The application of a certain method depends on the given conditions and equipment used for system automation, environmental conditions, as well as on the expertise of employees.

The main feature of these systems is that they are modular and flexible, which means they can be easily adapted to any requirement of today's modern production. The possibility of remote controlling via the PLC interface has become crucial and unavoidable for both process and plant automation. The default functional (alphanumeric) task is solved by using several methods, in such a way that a path-step diagram has been made.

What all the methods have in common is the pneumatic/ electro - pneumatic scheme. All methods have been implemented through simulations of system functionality in the software package Fluid SIM-P, which includes didactic equipment.

### **2. FUNCTIONAL (ALPHANUMERIC) TASK OF THE GIVEN PROBLEM**

**The given functional (alphanumeric) task:**

**B+ (A- C- B-) A+ (C+ A-) A+** (is repeated twice)

Task principle:

By pressing the START push button the following steps are performed:

STEP 1: The piston rod of cylinder B goes into the extracted position.

STEP 2: At the same time, the connecting rods of cylinders A and C go into the retracted position (from the initial extracted position), and the connecting rod of cylinder B returns to the initial retracted position.

STEP 3: The piston rod of cylinder A goes to the extracted position.

STEP 4: At the same time, the connecting rod of cylinder C goes into the extracted position, and the connecting rod of cylinder A into the retracted position.

STEP 5: The connecting rod of cylinder A goes to the extracted position.

The specified cycle (STEP 1 to STEP 5) is automatically repeated once again.

After two repeated cycles have been performed (STEP 1 to STEP 5), further execution of the cycle is possible only after activating the RESET button, which resets the counter and allows the process to be restarted.

#### **2.1. Required parts for the system realization**

Necessary components:

- double-acting cylinders A, B and C (cylinders are indicated with capital letters of the alphabet and if they work simultaneously, we put them in brackets, the sign + means that the cylinder starts from the retracted position);
- 5/2 solenoid double impulse valve for cylinder A
- 5/2 solenoid single valve for cylinders B and C
- limit (make) switches for determining the position of cylinders (A0, A1, B0, B1, C0, C1)
- air service unit and a compressed air supply
- PLC Siemens LOGO;
- DC voltage source – rectifier 24DCV

#### **2.2. Diagram path-step**

Diagram path-step (*Figure 1.*) is the first step in solving automation for this type of system. The diagram serves as a display of changes in the state of the cylinder values, the values of the input signals (limit/make switches and push buttons) and the values of the output signals of the solenoid valves. Through it we check the functionality of the separate steps of the practical part of

the cycle. The diagram shows the states of all elements (inputs and outputs).

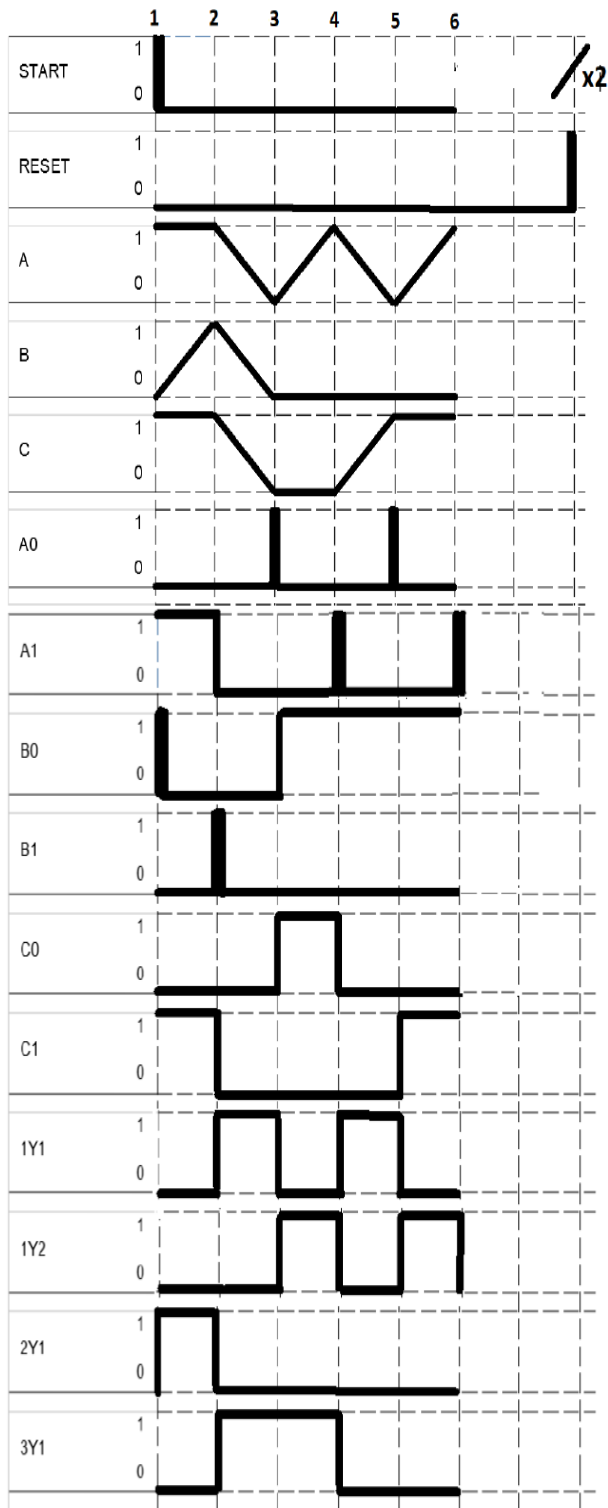


Fig. 1. Diagram path-step

### 3. METHODS OF SOLVING

#### 3.1. Cascade method

Approach:

- A cascade circle (Figure 2. Cascade circle) is drawn according to the functional task of the cylinder motion;

- The cylinders are arranged in cascades in such a way that one cylinder within one cascade may be repeated only once / each section indicates one cascade;

- The cascades are marked in Roman letters, and the direction of the process is clockwise;

- If the cylinders perform simultaneous work, they are drawn next to each other;

- Above the mark of each cylinder, the limit (make) switches on the distance ruler are entered;

- All limit (make) switches are 3/2 roller lever valves located at the end positions of the ruler;

- If the cylinder is extracted (A +), it activates the limit (make) switch a1, and if it is retracted, then it activates a0;

- Thus for (B +) = (b1), a (B-) = (b0);

- The beginning of the cycle is marked with two vertical lines || (START);

- The circle is divided into circular sections, but in a way that one cylinder mustn't appear twice in the same section;

The number of 5/2 impulse valves (n) is 1 less than the number of cascades (c)  $n = c - 1$ ;

- 5/2 impulse valve is in reality 4/2 or 5/2 impulse valve operated pneumatically;

- Impulse valves within the cascade directly start cylinders in the cascade according to the functional task;

- The last impulse valve in the cascade starts the following cascade;

- The cascade directly activates the first cylinder in itself;

- Activation of the next cascade deletes the previous cascade;

- All valves within one cascade have a connected air supply to the output of that cascade (this is the realization of the "AND" function by a passive connection);

- If two distributors in the cascade are activated at the same time, then we connect them in series regardless of whether one of the valves is normally open (or even both);

- If START is the first valve in the cascade, it is activated by that cascade;

- The START pneumatic supply goes to the output of the cascade only if it is the first valve in it;

- At the output of an individual cascade, the following are connected: pneumatic supply of all valves in it and the movement of a cylinder according to the task from the function circuit, connector of actuation when we connect several cascade valves;

- When connecting several cascade valves, there is a prescribed way of connecting them: interconnection of cascade valves (from the working line of the previous (4) to the supply of the next starting from the last cascade), each cascade is activated by the impulse of the last valve in the previous cascade. The

free control outputs are connected to the output (2) of the previous cascade;

- If a cylinder repeats the movement, then a new set of limit (make) switches should be placed on the distance ruler for each repeated movement: B + B- B + B- (b1, b0, b11, b00);

- Repeating of the strokes requires an "OR" condition in front of the main valve of the cylinder that repeats the stroke.

Our problem assignment, in which within one cycle we were given one repeating of strokes, simultaneous operation of three and two cylinders and a start from the drawn position, has been solved with 5 cascades (4 cascade valves) according to the attached scheme (Figure 3. Cascade method scheme):

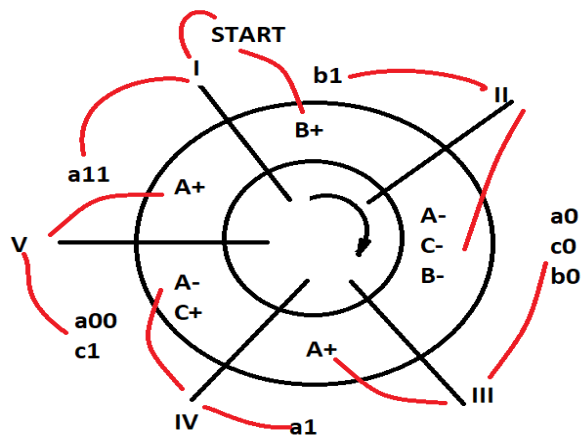


Fig. 2. Cascade circle

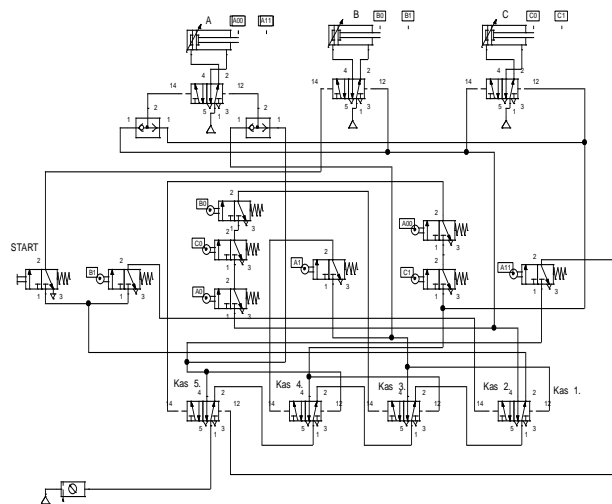


Fig. 3. Cascade method scheme

### 3.2. Stepper method

Approach:

- According to the functional task, we make a division into steps (each working step requires one stepper module Type TAA);

- The existence of one output in each step allows you to easily solve the repetition of the strokes of a cylinder;

- In this case, if a cylinder repeats the movement, it is sufficient to select only two limit/make switches

(for B, b0 and b1), regardless of the number of repetitions;

- All selected make switches are 3/2 roller lever valves, normally closed

- When repeating strokes, the outputs from such a module go to "OR" valves (the number of which depends on the number of repeating strokes);

- Air supply of all 3/2 make switches goes to air-service unit;

- If several cylinders work simultaneously, all of them have one stepper module type TAA in common;

- The stepper module consists of a 3/2 impulse-activated valve, an "AND" function performed with a 3/2 valve in a passive connection and an "OR" valve for switching the output;

- If the "OR" valve shuts off the module output, then it is the type of stepper module TAA;

- If the "OR" valve activates a module output, then it is a type of stepper module TAB;

- We can connect a minimum of 3 modules to the stepper chain;

- Each module has 10 connections: Yn, connected to the starting valve, Zn, Zn + 1 (directly connected – they delete the previous expression) 2 times P (power supply), 2 times L (reset, we can choose not to connect it), X - input, A - output, Yn + 1 (activated by the last activated valve and it goes to the start air supply).

Our problem task in which in one cycle we had one repeated stroke, simultaneous operation of three and two cylinders and a start from the extracted position, was solved with 5 stepper modules according to the attached scheme (Figure 4. Stepper method-scheme):

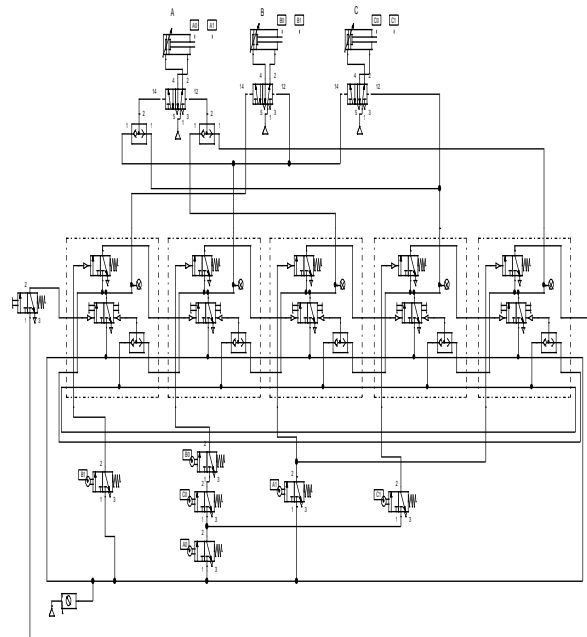


Fig. 4. Stepper method-scheme

### 3.3. Electro-pneumatic method

Approach:

- The number of steps is determined;

- The rule of self-preservation connection (basics of

electropneumatics) is respected, because in order to perform the next stroke, it is necessary that the previous one is performed and that there are no remaining impulses that block the continuation of work;

-Each step has its own relay that connects it to the associated electromagnet on the solenoid valve;  
 -After the START button, there is always a limit make switch in the series with which the process ends, and then in the following branches the switches are arranged according to the functional task;  
 -Relay switches directly activate the associated electromagnets/coil of relay (Figure 5. *Electropneumatic method*);

-In the last step (the RESET key is connected in parallel with the penultimate limit switch);  
 -When repeating strokes, it is not necessary to place "OR" valves next to the cylinder or duplicate limit switches, which greatly simplifies the performance.

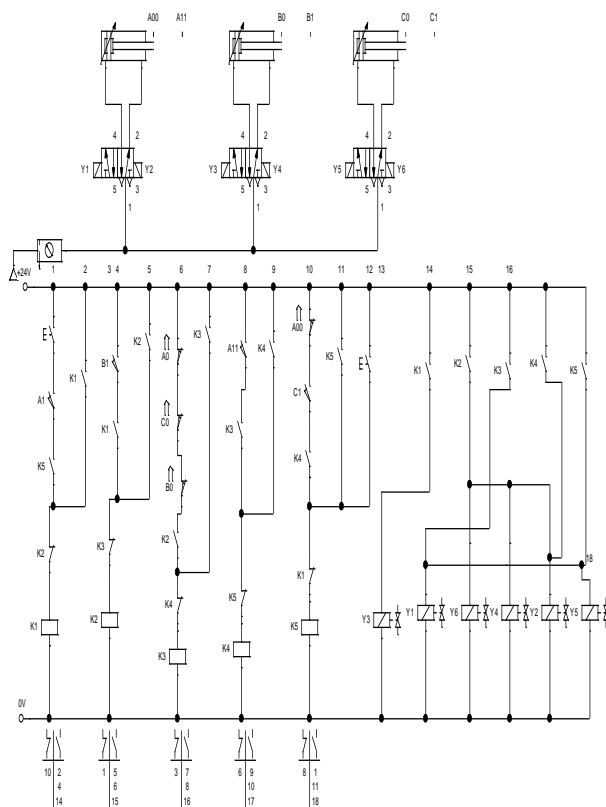


Fig. 5. Electropneumatic method

### 3.4. Automation of PLC control

#### 3.4.1. Address table

The address table (Table 1. Address table) lists all inputs (push buttons and limit/make switches) and all outputs (actuators) that are connected to the PLC.

Each element must have its own unique name in order for the program to distinguish it and successfully perform the given action.

Component name	Address on PLC	Component description
START button	I1	Starts the cycle

Limit/make switch A0	I2	End retracted position of cylinder piston A
Limit/make switch A1	I3	End extracted position of cylinder piston A
Limit/make switch B0	I4	End retracted position of cylinder piston B
Limit/make switch B1	I5	End extracted position of cylinder piston B
Limit/make switch C0	I6	End retracted position of cylinder piston C
Limit/make switch C1	I7	Cylinder piston C end extended position
RESET button	I8	Resets the counter and allows the cycle to be repeated
1Y1 valve solenoid	Q1	Coil 5/2 solenoid impulse valve
1Y2 valve solenoid	Q2	Coil 5/2 solenoid impulse valve
2Y1 valve solenoid	Q3	Coil 5/2 solenoid valve
3Y1 valve solenoid	Q4	Coil 5/2 solenoid valve

Table 1. Address table

#### 3.4.2. Pneumatic scheme

Parts of the pneumatic scheme:

- double-acting cylinders A, B, C;
- 5/2 solenoid double impulse valves for cylinders A;
- 5/2 solenoid single valves for cylinders B and C with return spring;
- limit/make switches A0, A1, B0, B1, C0, C1 (Figure 6. *Pneumatic diagram*);
- pneumatic compressor.

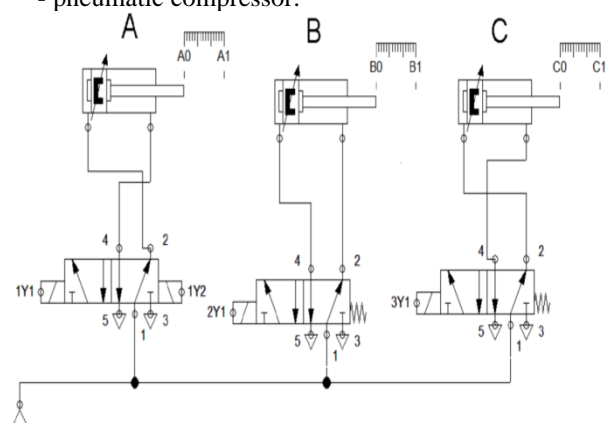


Fig. 6. Pneumatic diagram

#### 3.4.3. Wiring diagram for PLC

The electrical connection diagram to the PLC (Figure 7. *Wiring diagram for PLC*) shows the electrical wiring of all input and output elements to the PLC. The power source is a 24 DCV rectifier.

Eight inputs (I1-I8) and four outputs (Q1-Q4) are connected to the PLC.



**Inputs:**

- START- normally open push button,
- A0, A1, B0, B1, C0, C1 - normally open relay contacts,
- RESET - normally open push button.

**Outputs:**

- 1Y1, 1Y2, 2Y1, 3Y1 – valve solenoids (electromagnetic coils).

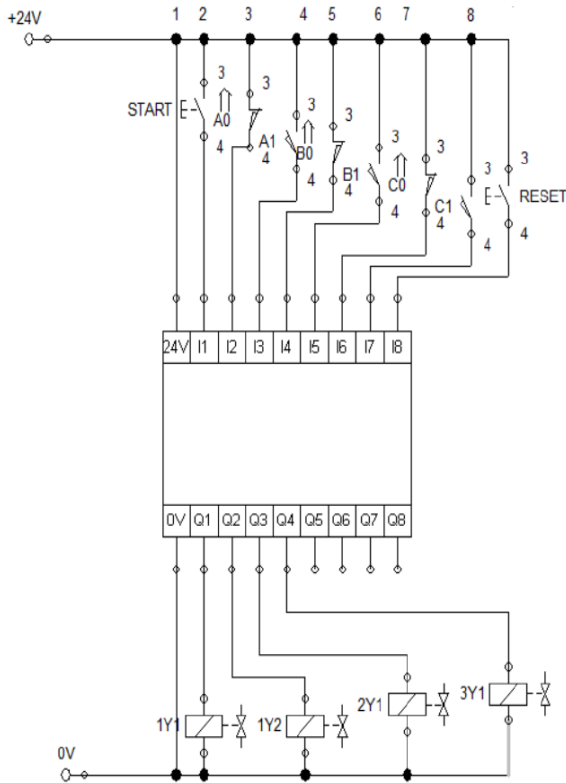


Fig. 7. Wiring diagram for PLC

**3.4.4. Program for PLC - function block diagram**

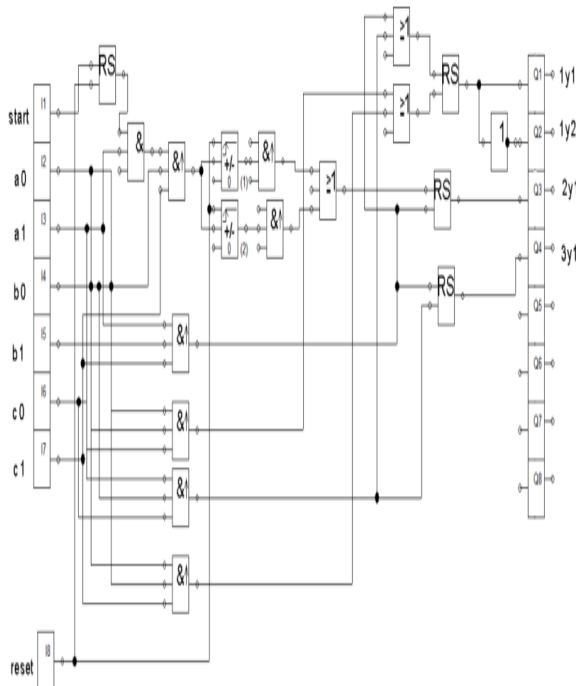


Fig. 8. Function block diagram - FBD

A function block diagram is a program that is written to the PLC for the required functionality. The Siemens LOGO PLC programming software package is LOGO Soft Comfort. It is currently the latest version of the V8. The software package provides two programming modes, programming in a function block diagram (FBD) and programming in a ladder diagram (LAD). The transition from FBD to LAD and vice versa takes place with the click of a mouse in the options, so it is not necessary to know both methods of programming. Program to be entered in the PLC - function block diagram (Figure 8. Function block diagram - FBD) for the required functionality (alphanumeric task):

**B + (A- C- B-) A + (C + A-) A +** (repeated twice) is shown in the following figure.

Blocks used in the program:

Inputs I (1,2,3,4,5,6,7,8,)

- I1 - start push button

- I (2-7) - limit/make switches on cylinders

- I (8) - RESET push button.

Outputs Q (1,2,3,4)

-Q (1,2,3,4) electromagnetic coil (valve solenoid)

- Function AND (AND (&)) - the block passes the signal only after all conditions are fulfilled and does so until at least one condition changes;

- Function AND with edge (AND (Edge)) - the block gives an impulse only after all conditions are fulfilled, repeated impulse can be given only when one of the conditions is reset;

- Up / Down counter - counts how many times it has received an impulse and starts to release signal only when it reaches the required (default) number;

- OR (Or) function - at least one of the conditions must be fulfilled for the block to pass a signal;

- RS (Latching Relay RS) - the block passes the signal when it receives an impulse at the set input, and stops passing when it receives an impulse at the reset input;

- NOT function - the block gives a signal at the output opposite to the input.

**4. CONCLUSION**

On the example of using different methods of solving, we approached the way of realization of a specific practical problem depending on the available equipment, production conditions and staff training. From all the above, it is easy to conclude that PLC control is the best solution for modern automatic systems, because it provides the possibility of easy upgrading and control. Each of the methods can be applied in practice and are necessarily preconditioned by the production process itself and all its peculiarities.

**5. REFERENCES**

[1] Programabilni logički kontroler (PLC) <https://www.manualslib.com/manual/1382742/Siemens-Logo.html> (accessed 10 May 2021)

[2] LOGO!Soft Comfort Online Help - Industry Support Siemens

- <https://support.industry.siemens.com/cs/document/100782807/logo!soft-comfort-online-help?dti=0&pnid=13632&lc=en-US> (accessed 10 May 2021)
- [3] Siemens LOGO Starter Kit – PLC Programming for Beginners  
<https://www.plcademy.com/siemens-logo-starter-kit/> (accessed 10 May 2021)
- [4] Korbar, R: Pneumatika i hidraulika, Veleučilište u Karlovcu, Karlovac, 2007.
- [5] Nikolić, G.: Pneumatika, Školske novine, Zagreb, 1994.
- [6] Koroman, V.; Mirković, R.: Hidraulika i pneumatika, Školska knjiga, Zagreb, 1991.
- [7] Rabie, M.: Fluid Power Engineering, McGraw-Hill, 2009. 2. Lang, R.A. (ed.): Pneumatic Trainer 1;
- [8] Planning and Design of Hydraulic Power Systems, Mannesmann Rexroth AG, 1998.
- [9] [www.vuka.hr/fileadmin/user\\_upload/knjiznica/online\\_izdanja/Pneumatika\\_i\\_hidraulika\\_-\\_skripta.pdf](http://www.vuka.hr/fileadmin/user_upload/knjiznica/online_izdanja/Pneumatika_i_hidraulika_-_skripta.pdf)
- [10] Festo didactic, Fluid Sim P/H (licensed programs for drawing and simulating the operation of schemes)
- Authors: Assoc. Prof. Tatjana Stanivuk,**  
University of Split, Faculty of Maritime Studies, Croatia.  
E-mail: [tstanivu@pfst.hr](mailto:tstanivu@pfst.hr);
- Prof. at High School and Assis. at University FESB Split, Miroslav Dujmović**  
Technical school of mechanical engineering and mechatronics, Split, Croatia.  
University of Split Faculty of Electrical Engineering, Mechanical Engineering and Naval Architecture  
E-mail: [miroslav.dujmovic@gmail.com](mailto:miroslav.dujmovic@gmail.com)
- Prof. at High School and Lecturer at University Department of Professional Studies, Nadan Dumanić**  
Technical school of mechanical engineering and mechatronics, Split, Croatia.  
University of Split, University Department of Professional Studies Croatia.  
E-mail: [nadan.dumanic@gmail.com](mailto:nadan.dumanic@gmail.com)
- Prof. at Highschool, Marina Barač**  
Technical school of mechanical engineering and mechatronics, Split, Croatia.

Dudić, B., Kovač, P., Savković, B.

## INDUSTRIAL ROBOTS APPLICATION

**Abstract:** *To succeed in the world market, companies must invest in the purchase of technology such as industrial robots. Industrial robots have become very important tools that give manufacturers an edge over the competition in an increasingly challenging global market. In the production process, industrial robots are able to perform a given activity better than humans in terms of quality of work. Robots are able to work continuously 24 hours a day, where for comparison, human working time is on average 8-10 hours. We also need to know that robots are flexible, so they are able to respond to a change in production faster than humans. Manufacturers who use this technology are gaining an effective economic tool that allows them to gain an advantage on the world market. Over the last 5 years, the global market has recorded a record in the number of robots delivered and manufactured, where the total robot market is around \$ 45 billion. As for the countries that are the largest customers of robots are China, South Korea, Japan, the USA and Germany. The aim of this work is to point out the very important and significant role of industrial robots, to show the situation on the world market and what are the innovations and investments in this field, also to give guidelines on how the market will behave in the next period and which are the most important companies manufactured by industrial robots.*

**Key words:** *industrial robots, innovation, technology, production, businesses.*

### 1. INTRODUCTION

To succeed in the world market, companies must invest in the purchase of technology such as industrial robots. What is most debated today is that whether industrial robots take over people's work, we can say that robots only take over the most difficult work of production itself where man is not able to do it. This means that industrial robots are an early machine that is taking over a large amount of money, which is feared by people, car production, welding of work and others. All the major machines are used in production, innovation in industrial robotic water and some new into a set of unknown experts. The Czech Republic will also take advantage of all its mechanization, not just the lack of manpower.

The success of the migration of the post office and the improvement of the security of the councilor and the efficiency council. Medicine is an area that helps all of the robot's work, but the development does not in itself detract from it and relieve doctors. A measure of the fact that robots would be implemented in production and the need for capital is needed. The concept of new propellants increases the competition in the market for the production of the robot and thus accompanies the access price of the robot and the machine. The tenders referred to in the code for the production of motor vehicles show that people are substitutable for the workers to carry out this task in a contradictory manner, or that such attitudes are a matter of course for workers who cannot do so at all adequate to replace people. States such as Japan and China are introducing technological innovations and introducing new developments in line with industrial robots. The attitudes of robotic workers to the people in the midst of people are running away from productivity, increasing productivity. The position in the developing

countries is all the same, the situation is in decline, so that the robots confuse people with their activities.

### 2. METHODOLOGY

#### 2.1. Literature Review

Technologies are constantly evolving, with a slower pace and every large amount of demand for certain jobs. Globalization has not limited itself to a single sector or sector, which has overwhelmed them, and has become an indispensable one in order to make the forerunner competitive in this dynamic marketplace. The creation of virtual reality is finding application in the design of simulators for training astronauts, pilots, flight dispatchers, surgeons, and other professionals, as well as in project engineering and architecture (Joseph, 2016) [1].

In the table 1, the author shows the development of the robot in the years to come. The doctrine is only advancing for robots to be more successful with their single people. Developments in the field of medicine and biotechnology will bring significant changes to the market. Mobile robots creating an area of robotics deal with the robots, which are able in capable surroundings to move in the time. Their study, research, design and construction deals robotics. From the perspective of the robot subsystems - mechanical, electronic, control, propulsion and others talk about the robot as a mechatronic system [1].

Ten years ago, companies were opposed to high initial investments in automation and robotics, and while today, robotics is a major factor in holding back the success and concreteness of doing business in the global market. The advantages that the installation of robots brings are increased production productivity, waste reduction or the possibility of facilitating human labor when handling semi-finished products, pallets, or

other components. It can state that by 2025, industrial robots will work up to 52% of the total working time, people only 48% [2, 3].

Year	Expected result	Reference with the year of prognosis
2018	Robot will pass driving permit test	Oleg Varlamov, MIVAR president, 2016
2019	90% of institutions will have a staff member holding the position of chief data officer (CDO)	Cortner, 2016
2020	30 thousand unscrewed civil aerial vehicles will be in use in the USA	US Federal Aviation Administration, 2012
2022	Robots will be capable of understanding human behavior and responding to it	Expert and analytical report of Rosbusinessconsulting (RBC), 2014
2024	Commercially available motorcars will be capable of reacting to changes in the traffic situation and moving autonomously	IHS Automotive, 2014
2025	Application of industrial robots will reduce labor payment expenditures by 16%	Boston Consulting Group, 2015
2028	First autonomous medical microrobots will be capable of independent directional movements in a patient's body	"A Roadmap for US Robotics: From Internet to Robotics", 2013
2029	AI will be capable of self-learning, understanding jokes, and imitating emotional expressions	Ray Kurzweil, Google's director of engineering, 2014
2030	Commercial androids will have an outer appearance and capabilities identical to those of the human	Expert workshop Trends and Prospects of Robotics Development in Russia, 2014
2032	Robots will exceed intellectual potential inherent in humans	Dave Evans, Cisco chief futurist, 2011
2035	In Japan, robots will master 49% of the 600 currently existing professions	Nomura Research Institute, 2015
2040	Law-enforcement robots will exist	Professor Noel Sharkey, University of Sheffield, 2012

Table 1. Prospects of development of robotics engineering for the period up to 2040.

The global market for robots is expected to grow at a compound annual growth rate (CAGR) of around 37.4 % to reach just under 500 billion U.S. dollars by 2025. It is predicted that this market will hit the 100 billion U.S. dollar mark in 2020, Figure 1.

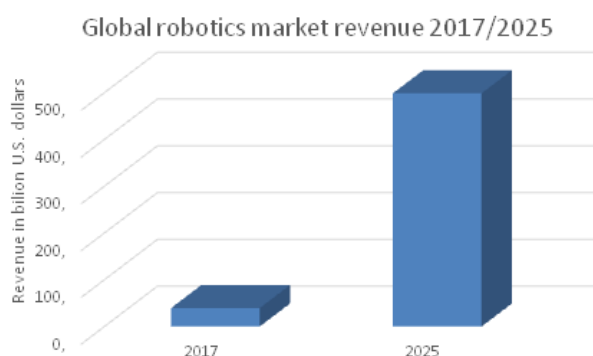


Fig. 1. Size of the global market for industrial and non-industrial robots between 2017 and 2025 (in billion U.S. dollars) [1]

## 2.2. On the road to autonomy

The invention of the world's first robot is credited to George Devol. The Unimate, a material handling robot performing basic welding and carrying tasks, was introduced in 1961. Robots are programmable machines that have the capability to move on at least three axes. They were developed to assist human workers with a wide array of tasks, including heavy lifting, as well as hazardous or repetitive work. Today's robots have a much higher degree of autonomy based

on several technological advancements made in recent years. The industrial robotics market, which has traditionally represented the robotics industry and has been led by Japanese and European robot manufacturers, is giving way to non-industrial robots, such as personal assistant robots, customer service robots, autonomous vehicles, and unmanned aerial vehicles (UAVs).

## 2.3. Industrial robots

The definition of an industrial robot can be explained as an automatically controlled, pre-programmable multi-purpose manipulator with programmable three or more axes, which is fixed in place or moves and consists of a manipulator and a control system. Industrial robots are pre-programmable devices designed for the handling and transport of parts, tools or specialized production tools by means of variable programmed robots on performing specific production tasks. Automation has recently become a key issue in ensuring competitiveness in manufacturing industries of various industries. Increased use of robotics will help improve the position of companies in current world production.

This graph (Figure 2.) shows shipments of multipurpose industrial robots from 2016 to 2020, key by region. In 2017, some 66,000 units were shipped in Europe. Industrial robots are designed for an industrial environment and are used for handling, assembling or modifying workpieces.

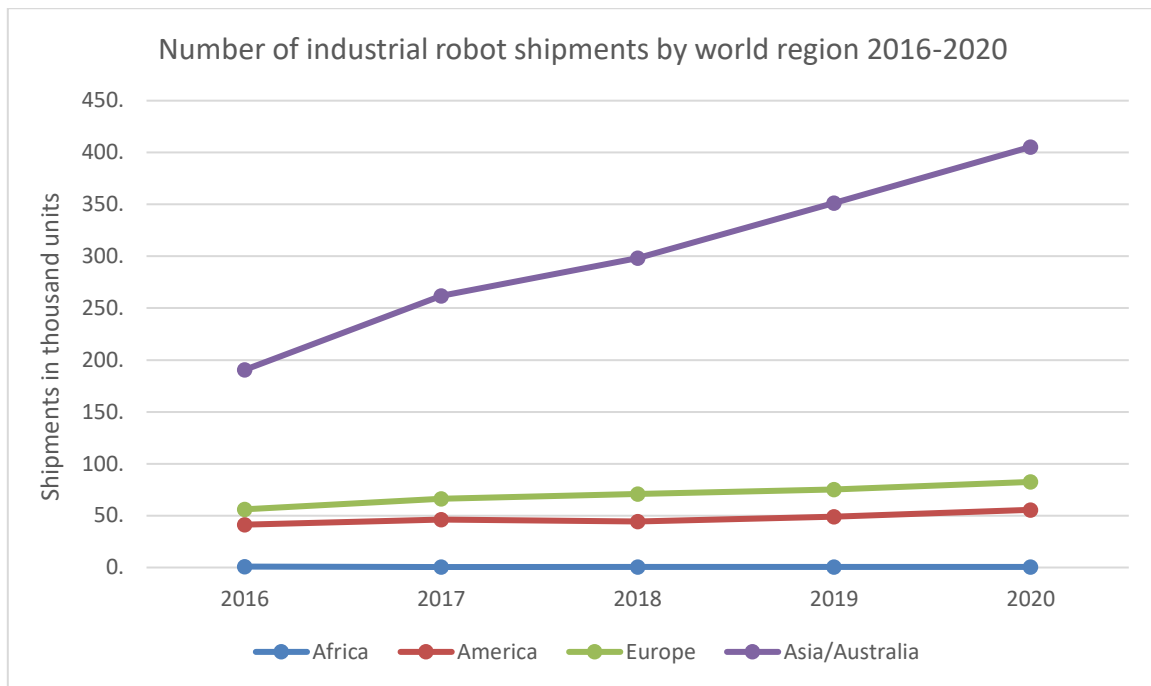


Fig. 2. Estimated annual industrial robot shipments in selected regions worldwide from 2016 to 2020, by region (in 1,000 units) [1]

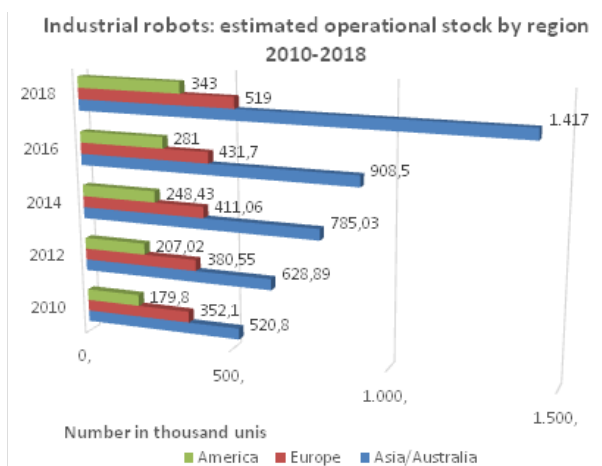


Fig. 3. Projected operational stock of multipurpose industrial robots from 2010 to 2018, by region (in 1,000 units) [1].

This statistic represents the estimated operational stock of multipurpose industrial robots in selected regions worldwide between 2010 and 2018. In 2018, the number of industrial robots in Europe is estimated to come to around 519,000 units, Figure 3.

The basic difference between an industrial robot and a manipulator lies in the flexible programmability of the end member of the robot. It is quite difficult to classify industrial robots as universal handling devices, because they form a very complex mechanism consisting of progressive materials from a constructional point of view. Therefore, we divide them according to various criteria, such as application determination, function, kinematic structures, control method and programmability, etc.

Industrial robots can be divided into 3 generations:

- 1st generation industrial robots - the program does not change during its operation; its change is

simple. The control is often mechanical, this type of robot is very widespread, because they are used for simple operations such as take and place or do and over it.

- 2nd generation industrial robots - have the option of selecting or switching the program according to the requirements in which they are located. An integral part of them is a sensitive subsystem consisting of several sensors. A computer is required for control and they are equipped with an open-ended coordination system.

- 3rd generation industrial robots - also called cognitive robots. They are mechanisms with the possibility of perception and rational thinking, without independent action and emotional perception. If a person gives him a goal, the robot executes it, drawing up a plan for himself to achieve it. They represent a leader in the development of handling equipment.

Division of robots according to application purpose:

- Manipulation robots - its main task is the manipulation of the object (semi-finished products, components, products, tools), change of position, orientation, stopping and clamping, warehouse handling, palletizing, depoliticization.

- Technological robots - have a focused role on the direct performance of technical activities (welding, assembly, coating, grinding, bending, plasma cutting). Special robots - they are equipped with accessories for gripping the manipulated object and a tool that performs a technological operation when gripping the object, such as removing the molding from the press and cutting the sprue at the same time.

### 2.3.1. Global market for thoughtful robots

Today, in the global market, industrial robots play a crucial role in achieving economic benefits. Over the last 5 years, the global market has recorded a record in

the number of robots delivered and manufactured, where the total robot market is around \$ 45 billion. The electronics and electrical engineering industry have become the largest factor in the global sales market. The automotive industry continues to be the largest user of robots, accounting for 35 percent of all robots. Industrial robots have become very important tools that give manufacturers an edge over the competition in an increasingly challenging global market. We can say that robots work 24 hours a day, 7 days a week, without losing their performance in any way. In the workplace, industrial robots offer a higher level of control and productivity and also consistently help to achieve high product quality. We also need to know that robots are flexible, so they are able to respond to a change in production faster than humans [1].

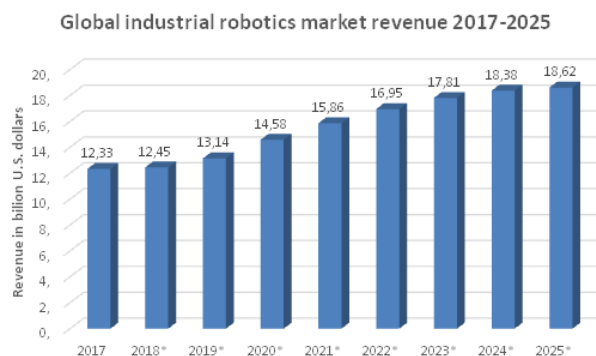


Fig. 4. Size of the industrial robotics market worldwide from 2017 to 2025 (in billion U.S. dollars) [1]

This statistic shows the revenue generated from the industrial robotics market worldwide in 2017, with a forecast through 2025. In 2017, the industrial robotics market amounted to some 12.3 billion U.S. dollars globally, Figure 4. The industrial robotics market has traditionally represented the robotics industry and has been led by Japanese and European robotics manufacturers, but has given way to non-industrial robots, such as personal assistant robots, customer service robots, autonomous vehicles, and unmanned aerial vehicles (UAVs).

In the production process, industrial robots can significantly reduce production costs, improve quality and shorten the time to market for new products. Manufacturers who use this technology are gaining an effective economic tool that allows them to gain an advantage on the world market. Robots can deliver a certain amount of power without interruption and for a long time, in a highly consistent way, while employees cannot maintain such power for a long time.

Mainly industrial robots are represented by various industries in such positions as manual and demanding work, production processes where they are harmful to human health, and especially to physically strenuous work. Workers must be trained and prepared to be able to control the robots and, if necessary, program, operate and understand them.

#### 2.4. The largest robot manufacturers

As for the countries that are the largest customers of robots is China and the second largest market is South

Korea, which thanks to large investments by companies in the electrical industry. We can also rank in the top five markets that buy robots and these are: Japan, USA and Germany.

Among the largest robot manufacturers are: Yaskawa, Kuka Robotics, Fanuc, ABB Swedish-Swiss company, Figure 5 [1].

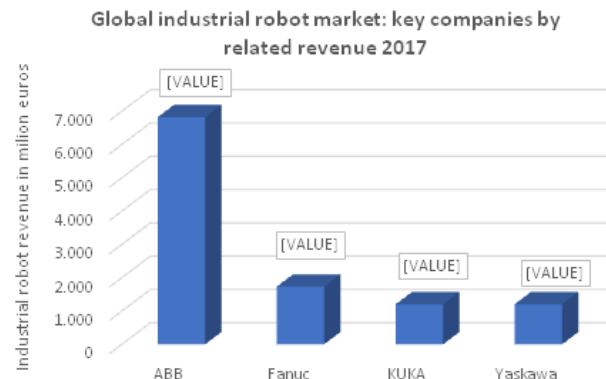


Fig. 5. Leading companies in the global industrial robot market in 2017, based on revenue from industrial robot sales (in million euros) [1].

This statistic represents the leading companies in the global industrial robot market in 2017, based on industrial robot revenue. In that year, Fanuc generated some 1.7 billion euros from industrial robot sales.

### 3. INDUSTRIAL ROBOT MARKET

Although industrial robots have made inroads into a growing number of industries such as the food and beverages industry, the highly automated car manufacturing sector remains the largest area of application for electro-mechanical machines. The robotics industry's growth trend is largely driven by rising wage levels that force manufacturers worldwide to replace human labor with machines. Asia and Europe are home to the key players in the market, including ABB, KUKA, Fanuc and the Yaskawa Electric Corporation. With relevant sales of around 1.2 billion euros, Japan-based Yaskawa was ranked among the largest manufacturers of industrial robots in 2017. The company's heavy duty industrial robots can be used for welding, assembly, coating, materials handling, materials cutting, materials removal and spot welding. In the 2017 fiscal year, Yaskawa generated almost 450 billion Japanese yen in net sales.

The robotics industry is a subsector of the automation industry. This industry is comprised of a variety of products and services, including relays, switches, sensors and drives, machine vision and control systems, as well as industry software development and services. Conglomerates like Siemens, Mitsubishi Electric or General Electric are the major vendors of industrial automation and industry software.

#### 3.1. ABB GROUP

**ABB GROUP (ASEA Brown Boveri)** is a Swiss-Swedish multinational company that operates mainly in

the areas of robotics, power engineering, heavy electrical equipment and automation technology. ABB GROUP is a pioneering technology leader with a comprehensive offering for digital industries. With a history of innovation spanning more than 130 years, ABB is today a leader in digital industries with four customer-focused, globally leading businesses: Electrification, Industrial Automation, Motion, and Robotics & Discrete Automation, supported by its common ABB Ability™ digital platform. ABB's market-leading Power Grids business will be divested to Hitachi in 2020. ABB operates in more than 100 countries with about 147,000 employees.[10] It can also say that ABB has installed more than 400,000 robots worldwide and has a position of 1 in the world of robotics.

The main activity of ABB GROUP is:

**Products:** control room solutions, communication networks, drives, high voltage products, low voltage products and systems, measurement and analytics, mechanical power transmission, medium voltage products, metallurgy products, motors and generators, PLC automation, power converters and inverters, robotics, semiconductors, substation automation, protection and control, transformers.

**Systems:** control systems, distributed energy resources and microgrids, electric vehicle charging infrastructure, enterprise software, FACTS, HVDC, marine vessels, network management, operations management software, power consulting, power electronics, safety, substation automation, protection and control, substations and electrification, turbocharging, UPS and power conditioning [1].

The industrial robots are used in many application areas, such as material handling, loading, and unloading of machines, palletizing and depalletizing, spot and arc welding. They are used in some large companies, predominantly in the automotive industry, but also in other industries such as the aerospace industry. Specific applications include:

- Transport industry: for the transport of heavy loads, where their load capacity and free positioning are used.
- Food and beverage industry: for tasks such as loading and unloading of packaging machines, cutting meat, stacking and palletizing, and quality control.
- Construction industry: e.g., for ensuring an even flow of material.
- Glass industry: used, for instance in the thermal treatment of glass and quartz glass in laboratory glass production, bending and forming operations.
- Foundry and forging industry: the robots' heat and dirt resistance enable them to be used directly before, in and on the casting machines. They can also be used for operations such as deburring, grinding, or drilling, and for quality control.
- Wood industry: for grinding, milling, drilling, sawing, palletizing or sorting applications.

- Metal processing: for operations such as drilling, milling, sawing or bending and punching. Industrial robots are used in welding, assembly, loading and unloading processes.
- Stone processing: the ceramic and stone industries use the industrial robots for bridge sawing

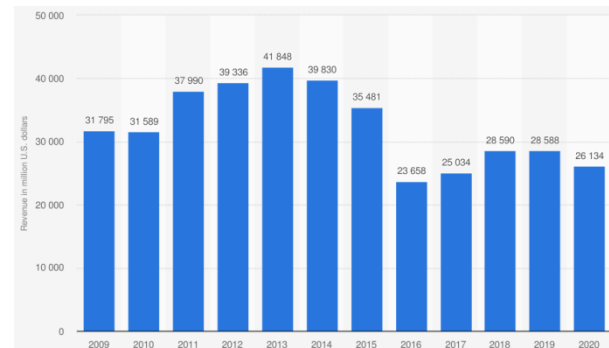


Fig 6. Revenue of the ABB Groupe from FY 2009 to FY 2020 (in the million U.S. dollars) [4]

### 3.2. KUKA Group's

This statistic shows KUKA Group's revenue between the fiscal year of 1999 and the fiscal year of 2018. In the fiscal year of 2018, the Germany-based producer of industrial robots generated around 3.3 billion euros (or about 3.72 billion U.S. dollars, as of March 28, 2019) in revenue.

The KUKA Group is ranked among the leading manufacturers of industrial robots. Its products range from spot welding robots to medical devices and can be deployed in an array of industries, including automotive and aerospace manufacturing. In 2016, KUKA and its largest shareholder at the time, Germany-based Voith GmbH, received a takeover bid from China's Midea Group. The unsolicited offer valued the German robot maker at almost 40 times the firm's expected 2016 earnings. As of March 2017, Midea has acquired around 95 percent of KUKA's stock. As a result of slowing growth in China and widespread unrest among Chinese factory workers, Asian investors are beginning to increase outbound merger and acquisition (M&A) deals. Furthermore, the Industrial Internet of Things (IIoT) revolution is expected to drive consolidation in the automation industry, a growing number of companies in traditional sectors are at a crossroads and are forced to make strategic decisions. In 2015, the highest level of M&A activity in the industrial sector could be attributed to PLM and System Integrators.

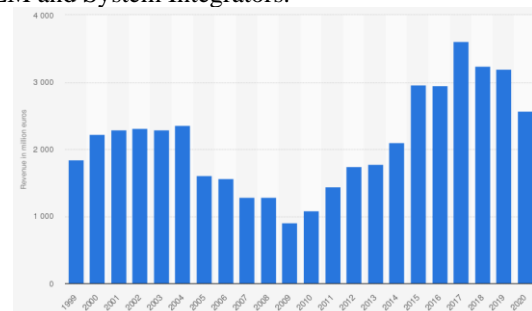


Fig. 7. KUKA Group's revenue from FY 1999 to FY 2018 (in million euros)

### 3.3. Yaskawa

The Yaskawa Electric Corporation is a Japanese company that was founded in 1915. The Yaskawa Electric Corporation is one of the largest manufacturers of servos, motion controllers, AC motor drives, switches and industrial robots. Their Motoman robots are heavy duty industrial robots used in welding, packaging, assembly, coating, cutting, material handling and general automation.

We strengthen our core businesses of servo motor, controller, AC drives and industrial robots using these core technologies to the full, and evolve mechatronics by the use of digital data. We achieve revolutionary industrial automation and are committed to contributing to solve customers' business challenges.

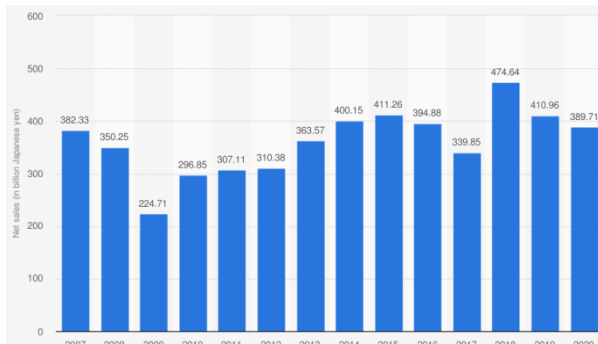


Fig. 8. Yaskawa's net sales from FY 2007 to FY 2018 (in billion Japanese yen) [5]

This statistic depicts Yaskawa's net sales from the fiscal year of 2007 to the fiscal year of 2018. In the fiscal year ending February 28, 2019, the Japanese manufacturer generated net sales of almost 362 billion Japanese yen (about four billion U.S. dollars).

### 3.4. FANUC

The main activity of FANUC is aimed at the following products:

- Servo Drives and Machine Controllers,
- AC Drives
- Robots
- Industrial robots for various industrial processes
- System Engineering.

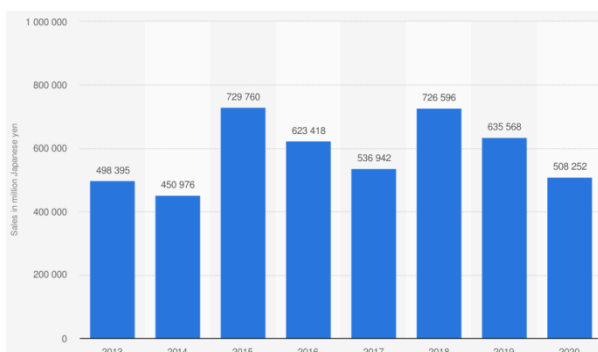


Fig. 9. FANUC's net sales from FY 2013 to FY 2020 (in million Japanese yen)

## 4. CONCLUSIONS

The new possibilities that bring robots fascinate people, or also introduce the fear that they have from them. Fear of the future of the benefits of automation and robots that are less people streamlines the fear of their messengers, not to mention the lack of understanding of technology delivery. The promotion of human technology, the adoption and understanding of new technologies, the new ideas that accompany the transfer of these problems. Understanding the trend of trend and technological development, access prices for advanced and appropriate information technology and robotics in the promotion and positive development of the forerunner and in the development of the economic and economic position of the country and the competition. All of these are preceded by the development and distribution of software and hardware for the research of robots and robotics, which can be found in academic circles, governments or the private sector positively escaping the situation of the government in the marketplace. Many precursors have also come from unprofitable precursors, start-up companies and all young people who offer their innovative ideas, as this is an illicit amount of money and represents the need to address the need for new precursors to the committee.

## 5. REFERENCES

- [1] In Statista - The Statistics Portal. Available online: <https://www.statista.com/statistics/272179/shipment-s-of-industrial-robots-by-world-region/>. (accessed on 05-07-2021)
- [2] Smrček, J., Kárník, L., 2008. Robotics, Service robots, Design, construction, solutions. Košice. P. 534. ISBN 80-7165-713-2.
- [3] Kárník, L., 2004. Service robots. VŠB-TU Ostrava, Ostrava. p. 144. ISBN 80-248-0626-6
- [4] ABB Group. Available online: <https://global.abb/group/en>. (accessed on 05-07-2021)
- [5] Yaskawa Group. Available online: <https://www.yaskawa-global.com/>. (accessed on 05-07-2021)

**Authors:** Assist. Prof. Branislav Dudić PhD, Comenius University in Bratislava, Faculty of Management, Bratislava 82005 Slovakia University Business Academy, Faculty of Economics and Engineering Management, Novi Sad 21000, Serbia. E-mail: [branislav.dudic@fm.uniba.sk](mailto:branislav.dudic@fm.uniba.sk)  
 Prof. Pavel Kovač PhD, Assoc. Prof. Borislav Savković PhD, University of Novi Sad, Faculty of Technical Sciences, Institute for Production Engineering, Trg Dositeja Obradovica 6, 21000 Novi Sad, Serbia, Phone.: +381 21 450-366, Fax: +381 21 454-495.

E-mail: [pkovac@uns.ac.rs](mailto:pkovac@uns.ac.rs)  
[savkovic@uns.ac.rs](mailto:savkovic@uns.ac.rs)



**MMA 2021**  

---

**FLEXIBLE TECHNOLOGIES**

Section **G**:  
**ADDITIVE MANUFACTURING  
TECHNOLOGIES**



Vasileska, E., Demir, A. G., Colosimo, B. M., Gečevska, V., Previtali, B.

## ENERGY INPUT ADAPTATION ACCORDING TO PART GEOMETRY IN SELECTIVE LASER MELTING THROUGH EMPIRICAL MODELLING OF THERMAL EMISSION

**Abstract:** Common practice in Selective Laser Melting (SLM) is employing a series of fixed process parameters throughout the whole build. However, process thermal conditions strongly depend on the local geometry of the part. Formation of some common defects, including swelling regions and elevated zones, emerges in critical corner areas due to excessive heat accumulation when constant parameters are used. Adaptation of energy input according to the geometry of the processed zone is highly desirable for avoiding defect formation. To assess the processing conditions, observation of the melt pool and its variation as a function of the process parameters with a coaxial camera operating in near infrared (NIR) demonstrated to be a feasible option. This work develops an empirical model that gives the correct amount of energy input to achieve stable melt pool depending on the single vector length, hence the part geometry. The model was validated on a prototype SLM system, and the results showed that controlling the process parameters considerably improves the geometrical accuracy of the parts with sharp edges prone to hot spot formation. **Key words:** Additive manufacturing, geometrical accuracy, melt pool monitoring, process modelling, energy input control

### 1. INTRODUCTION AND MOTIVATION

Selective Laser Melting (SLM) is getting broad recognition amongst the metal additive manufacturing processes due to the possibility to produce complex geometries with internal channels and lightweight structures, otherwise impossible with conventional manufacturing methods. However, the lack of process repeatability and product quality diminishes its wide acceptance in highly regulated industries [1]. One of the main factors accountable for the defect occurrence is the inaccurate choice of process parameters [2]. The scanning parameters are commonly set experimentally, calibrated to achieve high density in bulk geometries, and are subsequently employed to produce the whole part. However, a fixed set of parameters do not account for the geometrical variations between and within parts.

The parameters which result with nominal part density in stable regions, may generate defects when scanning critical regions such as overhangs or acute corners where overheating occurs and leads to geometrical and microstructural defects [3][4]. Common geometrical defect occurring in regions with peaked ends due to heat accumulation and buildup of residual thermal stress is the swelling defect, which is the topic investigated in this study. The swelling is defined as elevated ridges of solidified material which warp or curl upwards out of the powder layer [5].

Simulations of the melting and solidification behavior of the SLM process with Finite Element Analysis (FEA) have shown its possibility to optimize the process parameters for theoretically achieving certain part density [6]. Nevertheless, effective simulation tools able to adapt process parameters depending on the part geometry are still to be developed.

To have an insight into the momentary conditions of the process, several works developed different types of

off-axial and coaxial monitoring setups [7]. The thermal conditions and hence the exhibited melt pool during the process is correlated to the final product quality [8].

Real-time monitoring of the melt pool dimensions during the scanning process is feasible with coaxial monitoring setup with camera, which provides high spatial resolution of the observed region. Commercial solutions for coaxial monitoring of the melt pool have also been produced. While these solutions are more widely adapted as a means for quality control during and after the build process [7], their use for process parameter development has not received much attention.

Hence, the present work develops a process model for adapting the laser energy input by modulating the laser power as a function of the part geometry, for generating stable melting conditions and avoiding the swelling defect in critical sharp regions of the part. For the development of the empirical model a coaxial melt pool monitoring system was employed. According to Fox et al. [9], controlling the melt pool dimensions throughout the process can ensure robust part quality. Therefore, the area of the melt pool was selected as a monitoring feature which demonstrates the process conditions.

Demir et al. [10] proved that employing a different set of process parameters in bulk region and in thin structure results in stable melt pool in the whole part geometry.

The developed empirical model in the presented work optimizes the parameters as a function of the length of the scan vectors, hence the part geometry.

### 2. CONTROL OF LASER ENERGY DENSITY BY POWER MODULATION

During SLM, within a given layer several scan vectors are generated, which are then melted with a chosen energy input. The given energy input is required to melt a specific mass of material. To find the laser

energy density delivered at each point of the process, the following equation is used:

$$E[\text{J}/\text{mm}^3] = \frac{P}{h \cdot z \cdot v} \quad (1)$$

where  $h$  [ $\mu\text{m}$ ] is the hatch distance,  $z$  [ $\mu\text{m}$ ] is the layer thickness,  $P$  [W] is the input power and  $v$  [mm/s] is the scan speed of the laser beam.

The laser can be operated in two modes: continuous wave (CW) and pulsed wave (PW) [11]. When scanning in CW mode, the laser source outputs a continuous power profile that interacts with the material at all times. The laser is scanned with a constant speed and constant power equal to  $P_{\text{cw}}$ . In PW mode, the laser intermittently interacts with the powder, meaning that the laser beam is not continuously brought to the material, but only at the instances when there is an active pulse [12]. As a result, the laser power will no longer remain constant with respect to time, but it will be modulated. The scanning speed in PW mode is constant, which implies that the laser beam moves continuously while the laser is emitting and not emitting. The resulting average power of the pulsed beam travelling with constant velocity is calculated as:

$$P_{\text{avg,PW}}[\text{W}] = P_{\text{peak,PW}} \cdot \delta \quad (2)$$

where  $P_{\text{peak,PW}}$  [W] is the peak laser power of the impulse, and  $\delta$  [-] is the duty cycle. The duty cycle  $\delta$  expresses the laser on-time over the whole pulsation period:

$$\delta = \frac{t_{\text{on}}}{t_{\text{on}} + t_{\text{off}}} = \frac{t_{\text{on}}}{t_{\text{tot}}} \quad (3)$$

where  $t_{\text{on}}$  [s] is the period of time when the laser is emitting during one pulse, and  $t_{\text{off}}$  [s] is the period of time the laser is not emitting during one pulse. Therefore, as  $\delta$  increases, the laser moves from PW to CW scanning mode, until reaching value equal to 1 which corresponds to laser scanning in CW mode. The modulation frequency  $f$  describes the temporal behavior of the pulse emission, and is defined as:

$$f[\text{Hz}] = \frac{1}{t_{\text{tot}}} \quad (4)$$

### 3. CONCEPT

The SLM produced object consists of building multiple layers on top of each other, while a layer consists of scanning and fusing multiple scan vectors. The geometrical defect of swelling happens due to excessive energy density delivered at a specific point in the fabricated object, resulting with enlargement of the melt pool above the nominal value at that point. Hence, adaptation of the energy density according to the scanned geometry becomes crucially important.

Scanning a sharp edge implies scanning adjacent scan vectors with small length. Hence when the laser scans a scan vector in the edge, in a short time it passes on scanning the next scan vector. This time between them is so short that it does not allow for the first scan vector to cool down and solidify the molten material, but instead it is merging with the molten material of the next scan vector as the laser beam is passing. This can lead to accumulation of heat in the corner region, leading to melt pool enlargement and swelling on the final workpiece shape.

Therefore, the laser energy input needs to be adapted

to maintain a stable build and optimal workpiece quality. Considering Eq. 1 and the several process parameters which influence the energy density, in this work the duty cycle was selected to adapt the energy input and to control the heat accumulation, hence the occurrence of swelling.

To reveal the heat accumulation zones and construct the process model, coaxial monitoring of the melt pool via a CMOS camera is employed. The reference melt pool area, which corresponds to a stable melting process, is determined through the common practice of producing samples with simple shapes such as cubes with process parameters achieving high part density. Finally, the process model allows the adjustment of the duty cycle as a function of the local part geometry in order to avoid geometrical deviations of the final part.

## 3. EXPERIMENTAL HARDWARE AND SOFTWARE

### 3.1. Open SLM platform

An open and custom-made SLM platform ‘‘Penelope’’ was used to conduct the experimental work [13]. The powder bed is placed in a closed chamber where an inert argon atmosphere is created. The laser source employed in the experiment is a single mode fiber laser (IPG Photonics YLR-150/750-QCW-AC, Cambridge, MA, USA) which can emit in both CW and PW regime by power modulation. The laser optical chain consists of a collimating unit with a focal length of 50 mm, a focus shifting two-lens system (VarioScan 20, Scanlab, Puchheim, Germany), and a 420 mm f-theta lens, while the deflection of the laser beam toward the building platform is achieved using two galvanometric mirrors. The main specifications of the open SLM platform and its optical chain can be found in Table 1.

Parameter	Value
Laser emission wavelength, $\lambda$	1070 nm
Max. laser power, $P_{\text{peak}}$	250 W
Max. laser modulation frequency	10 kHz
Beam quality factor, $M^2$	1.1
Nominal beam diameter at the focal plane, $d_0$ ( $1/e^2$ )	70 $\mu\text{m}$
Working volume	60×60×20 mm <sup>3</sup>

Table 1: Main characteristics of the open SLM system.

### 3.2. Material

In the experimental work, gas-atomized stainless steel AISI 316L (Cogne Acciai, Brescia, Italy) powder was used, with a packing density of 4.07 g/cm<sup>3</sup>, and powder size distribution measured as D10: 22.9  $\mu\text{m}$ , D50: 31.9  $\mu\text{m}$ ; and D90: 44.3  $\mu\text{m}$ .

### 3.3. Coaxial monitoring module

To acquire the thermal emission of the melt pool, a coaxial monitoring system was designed and connected directly onto the machine working head, thus looking through the scan head to observe the zone of interaction of laser beam and powder bed. A scheme of the optical chain is presented in Fig. 1. The NIR range was viewed with an industrial CMOS camera (Ximea xiQ USB

Vision, Münster, Germany) and two optical filters positioned before the camera which limit the acquisition wavelength between 850 and 1000 nm (FEL0850 and FESH1000, Thorlabs, Newton, NJ, USA). A focusing lens (Camera Adapter, Scanlab GmbH, Puchheim, Germany) was used to fix the image plane with a focal length of 120 mm. The employed 8-bit camera sensor has a size of  $1280 \times 1204$  pixel<sup>2</sup>, and pixel size of  $4.8 \times 4.8$   $\mu\text{m}^2$ . The camera field of view was calibrated to  $4.3 \times 4.3$  mm<sup>2</sup> by adapting the region of interest, in order to view the full length of the melt pool in all directions, achieving a spatial resolution of 14  $\mu\text{m}/\text{pixel}$  and an acquisition rate of 1200 fps with an exposure time of 29  $\mu\text{s}$ . As schematically demonstrated in Fig. 1, the process emission travels through the f-theta lens, galvanometric mirrors, and dichroic mirror reflective between 400 and 1000 nm, towards the camera sensor.

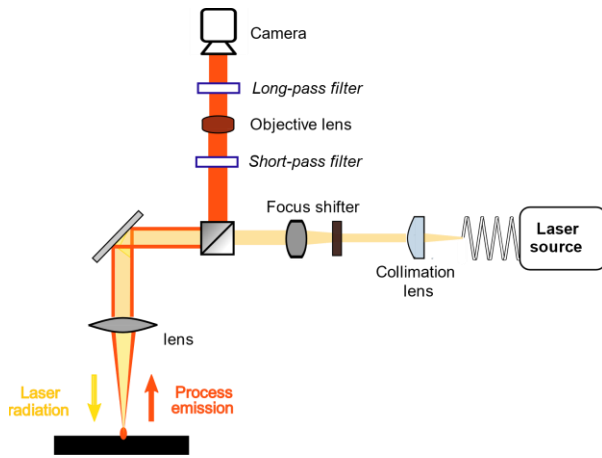


Fig. 1. Optical chain of the coaxial monitoring setup employed in the experiments.

### 3.4. Extraction and measurement of melt pool area

The acquired NIR images were then analyzed with an image processing algorithm for extracting the melt pool area (MPA) from the process emission, as a key indicator for the process stability.

The algorithm consisted of three parts. Firstly, the NIR image was binarized applying static thresholding method, which converts the image into a matrix with elements equal to either 1 (white pixel) or 0 (black pixel) depending on whether the pixel's original value of grey level is higher/equal or lower than a threshold constant  $C$ . This procedure is expressed with the following equation:

$$\mathbf{p}_{f,r,c}^T = \begin{cases} \mathbf{1}, & \mathbf{p}_{f,r,c} \geq C \\ \mathbf{0}, & \mathbf{p}_{f,r,c} < C \end{cases} \quad (5)$$

where  $\mathbf{p}_{f,r,c}$  is the gray level of the pixel in row  $r$  and column  $c$  of the frame  $f$ , and  $\mathbf{p}_{f,r,c}^T$  is the binary value of  $\mathbf{p}_{f,r,c}$  according to the threshold constant  $C$ . The threshold constant  $C$  was evaluated by matching the area computed from the NIR images with the area measured from externally illuminated images [14].

The second part of the algorithm consisted of removing the ejected particles and spatters from the NIR image, such that the algorithm recognizes and extracts only the melt pool.

Finally, the MPA of the frame  $f$  ( $MPA_f$ ) was computed as the sum of all the white pixels found within the boundaries of the extracted melt pool blob:

$$MPA_f[\text{mm}^2] = r^2 \cdot \sum_{r=1}^m \sum_{c=1}^n \mathbf{p}_{f,r,c}^T \quad (6)$$

where  $r$  is the spatial resolution.

Fig. 2 illustrates the algorithm procedure, initializing with the raw image, followed by thresholding, spatter elimination, and finally melt pool area extraction.

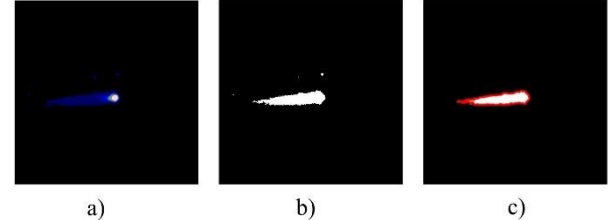


Fig. 2. Image analysis sequence: a) raw image frame acquired during experimentation shown in false colors of intensity, b) binarized image, c) image after spatter removal and melt pool extraction. Each image shows an observation field of  $4.3 \times 4.3$  mm<sup>2</sup>.

## 4. DEVELOPMENT OF THE MODEL FOR ENERGY INPUT ADAPTATION

### 4.1. Experiment design

To develop the process model that estimates the nominal duty cycle ( $\delta$ ) per scan vector corresponding to the part geometry, an equilateral triangle with a side equal to 5 mm is chosen as a printing geometry since it provides continuous change of scan vector length. Each triangle specimen was printed with a constant duty cycle and consisted of 30 layers scanned with the same scanning direction and pattern. Each triangle is scanned starting from the longest scan vector and then continuing to the shortest one at the edge of the shape. The effect of the amount of energy density on the melt pool is investigated by varying the duty cycles from 0.3 to 1, where duty cycle equals to 1 corresponds to CW laser scanning mode. Each condition was replicated twice.

The fixed and varied process parameters employed in the experiment are listed in Table 2. The fixed process parameters are confirmed through preliminary experiments to successfully fabricate a bulky part obtaining high density when the laser is scanning in CW mode.

To find the nominal melt pool area which indicates stable melting process, a square geometry with 5 mm side was scanned in CW mode, with process parameters which were preliminary proven to produce a high-density solid part with  $\rho > 99.5\%$ . A total of 30 layers were printed. Melt pool videos with the coaxial camera setup were acquired throughout the experiments.

Fixed parameters	
Layer thickness, $z$ [ $\mu\text{m}$ ]	50
Hatch distance, $h$ [ $\mu\text{m}$ ]	70
Scan speed, $v$ [mm/s]	400
Peak power, $P_{peak}$ [W]	200

Pulse repetition rate, $PRR$ [kHz]	3
Scan direction [°]	0
Scan strategy	Meander
<b>Varied parameters</b>	
Duty cycle, $\delta$	0.3 – 1.0
Scan vector length, $l_{sv}$ [mm]	0.05 – 5.0

Table 2. Fixed and varied scanning parameters employed during the experiment

#### 4.2. Process modelling

Analyzing the melt pool images of the square sample, the nominal melt pool area indicating stable melting conditions was estimated as  $0.46 \text{ mm}^2$ .

The process emission videos from the scanning process of the triangle samples showed that the melt pool is highly affected by the change of the average laser power and scan vector length. The average MPA per scan vector length ( $l_{sv}$ ) and duty cycle ( $\delta$ ) is shown in Fig. 3. A decreasing trend of the melt pool area can be observed as the duty cycle decreases, while an increasing trend as the scan vector length decreases. This implies that scanning the sharp regions with high energy input results in MPA enlargement due to the lower time for heat dissipation, thus creating a defective region where swelling is observed. Considering the nominal melt pool area, the conditions causing overheating phenomenon can be observed when the MPA is larger than  $0.46 \text{ mm}^2$ , and the conditions of under-melting when MPA is lower than  $0.46 \text{ mm}^2$ . Therefore, it can be concluded that scanning with duty cycle lower than 0.7 always results in insufficient melting even in the small scan vector lengths. Furthermore, it is observed that employing the CW regime on the longer scan vector lengths ( $\geq 4 \text{ mm}$ ) results in stable melting conditions and nominal MPA. Lastly, it is concluded that nominal MPA can be achieved throughout the whole processed geometry if the duty cycle is adapted per scan vector length.

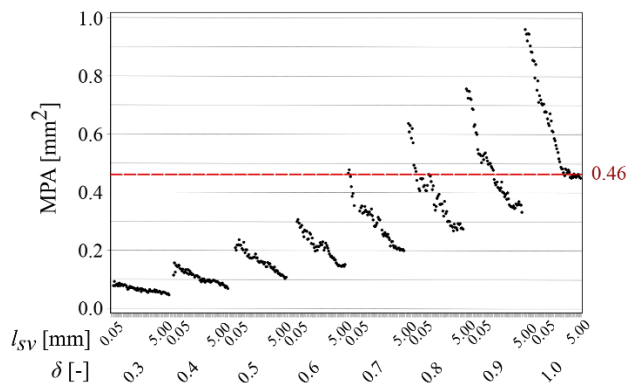


Fig. 3. Average MPA per scan vector length ( $l_{sv}$ ) and duty cycle ( $\delta$ ) in the triangle specimens

A regression model was sought on the measured MPA using the two input variables ( $l_{sv}$  and  $\delta$ ). The following empirical model with  $R_{adj}^2 = 98.61\%$  was fitted:

$$\ln(MPA) = -3.0153 + 3.843 \cdot \delta - 0.2241 \cdot l_{sv} - 0.86 \cdot \delta^2 + 0.00912 \cdot l_{sv}^2 \quad (7)$$

The P-value of the variables and their interaction showed high statistical significance in describing the MPA (p-values were  $<0.05$ ), while the normality and homogeneity of the residuals were verified.

Knowing the nominal MPA, the duty cycle can be easily adapted as function of the scan vector length in order to deliver the optimal amount of energy input and to avoid defect generation in the fabricated part.

Using the regression model, the energy density required to maintain the same MPA with varying scan vector could be calculated. The duty cycle relates to the laser energy density with the relation explained in Chapter 2. Fig. 4 presents the modeled duty cycle and the nominal density of the laser energy input per scan vector length, demonstrating the estimated amount of linear energy density decrease as the scan vector length reduces. The direct linear relationship found was used to modify the energy density by allocating the correct duty cycle as a function of the assigned vector length. Since the vectors are positioned prior to the process initiation, the process parameters could be changed offline similar to a feed forward control scheme.

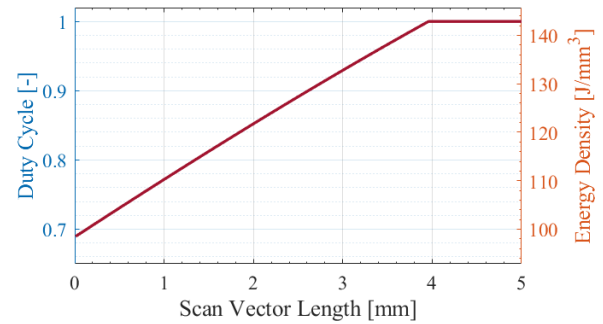


Fig. 4. Optimized duty cycle to achieve nominal MPA per scan vector length and the corresponding adapted laser energy density

## 5. MODEL VALIDATION

### 5.1. Experiment design

To validate the proposed model for energy input adaptation, experiments were carried out on a 4-point star and the already defined triangle, both containing sharp regions where swelling may occur due to extensive energy input. Fig. 5 illustrates schematic of the geometry of the specimens as well as the scanning direction. Specimens without any parameter adaptation, thus scanned entirely in CW mode, were also produced for comparison, whereas the fixed parameters in all validation experiments were equivalent to the ones listed in Table 2. Each print consisted of 30 layers.

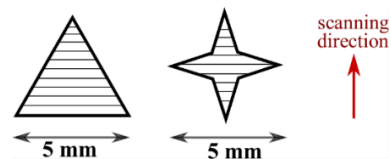


Fig. 5. Model validation geometries and scanning direction

In the specimens fabricated with adapted energy input, each scan vector was scanned with optimized duty cycle for attaining stable MPA.

To inspect the geometrical accuracy of the produced specimens, focus variation microscopy (Alicona Infinite Focus) was used for a three-dimensional reconstruction of the sample surfaces. Images were acquired using 5X magnification with estimated vertical and lateral resolutions of  $1.1\ \mu\text{m}$  and  $7.83\ \mu\text{m}$ , respectively. Mean square error of the surface geometry was calculated from the reconstructions.

## 5.2. Results

The three-dimensional reconstruction of the upper surface of the produced specimens is reported in Fig. 6 and Fig. 7, where the surface comparison of the parts produced with constant and with adapted energy input is visualized. In both parts scanned with CW regime, severe swelling is observed at the sharp regions where an excess of heat accumulation exhibits melt pool area enlargement resulting with faulty part. The mean square error of the surface geometry was lowered from  $8.75$  to  $1.17\ \text{mm}^2$  for the triangle shape, and from  $6.42$  to  $1.15\ \text{mm}^2$  for the 4-point star shape.

The specimens' macrographs are shown in Fig. 8 demonstrating the geometrical defect in the sharp region when employing constant duty cycle for scanning the whole part. Adapting the duty cycle depending on the part geometry proved to considerably improve the melting conditions and avoid the swelling occurrence due to overheating in short scan vectors in both geometries.

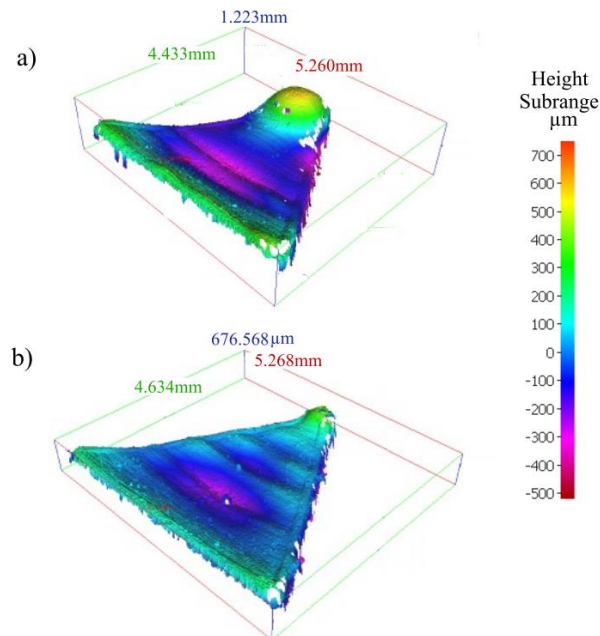


Fig. 6. 3D reconstructions of the produced triangle specimens (a) without ( $\text{MSE} = 8.75\ \text{mm}^2$ ) and (b) with the adapted energy input ( $\text{MSE} = 1.17\ \text{mm}^2$ ).

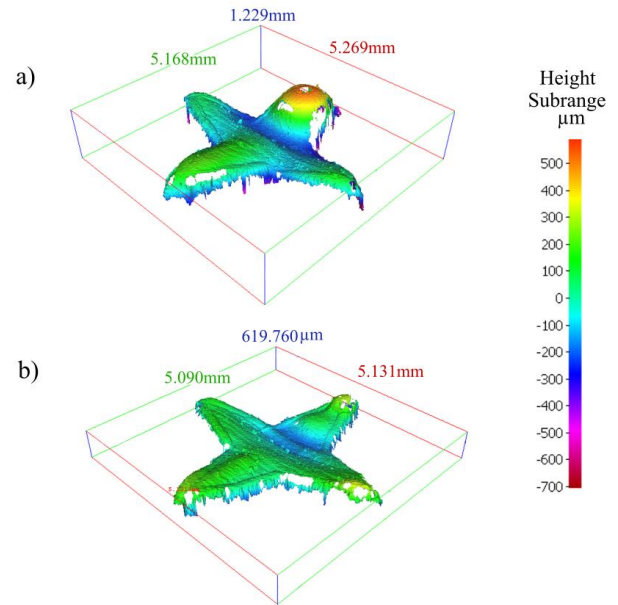


Fig. 7. 3D reconstructions of the produced 4-point star specimens (a) without ( $\text{MSE} = 6.42\ \text{mm}^2$ ) and (b) with the adapted energy input ( $\text{MSE} = 1.15\ \text{mm}^2$ ).

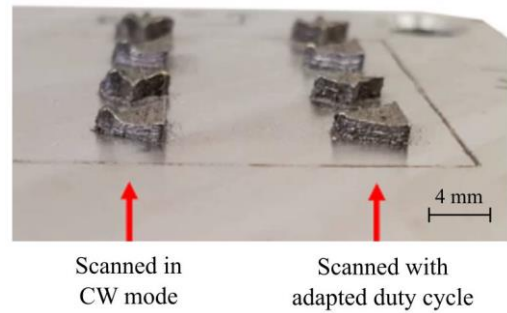


Fig. 8. Comparison of the produced specimens scanned with and without adapting the energy input

## 6. CONCLUSION

The present work demonstrates that adapting the laser energy input by modulating the laser power as a function of the part geometry, can produce stable melting process and avoid the generation of the swelling defect in critical sharp regions of the part. For assessing the melting conditions, a coaxial camera limited to the NIR process emission was employed. An image analysis algorithm for extracting the melt pool and calculating its area was developed.

Experimental campaign showed that the melt pool is highly affected by the energy density input and the scan vector length. To assess the energy input, the duty cycle was selected as a variable process parameter modifying the delivered laser power, since it does not affect the process productivity. It was proven that when high laser energy was delivered in an acute corner constructed of small scan vector lengths, overheating occurred due to excessive heat accumulation resulting with enlargement of melt pool area, and thus surface swelling of the final part. Therefore, an empirical model was developed which estimates the nominal duty cycle to achieve stable melt pool depending on the single vector length, hence the part geometry. The model was validated on two

geometries with critical edges.

This work develops an empirical model that gives the correct amount of energy input. The model was validated on SLM prototype. The results showed that adapting the energy input improves geometrical deviations and avoids overheating phenomena in corner regions consisting of short scan vectors. The presented work does not for the microstructural defects. The developed empirical model has been also used to develop a layer-wise feedback control strategy on critical shapes [15] and overhanging structures [16].

## 7. REFERENCES

- [1] C. Dordlofva, A. Lindwall, P. Törlind, Opportunities and challenges for additive manufacturing in space applications, Proc. Nord. Nord. 2016. 1 (2016).
- [2] J. V. Gordon, S.P. Narra, R.W. Cunningham, H. Liu, H. Chen, R.M. Suter, J.L. Beuth, A.D. Rollett, Defect structure process maps for laser powder bed fusion additive manufacturing, Addit. Manuf. 36 (2020) 101552. doi:10.1016/j.addma.2020.101552.
- [3] A. Charles, A. Elkaseer, L. Thijs, S.G. Scholz, Dimensional errors due to overhanging features in laser powder bed fusion parts made of Ti-6Al-4V, Appl. Sci. 10 (2020). doi:10.3390/app10072416.
- [4] E. Malekipour, H. El-Mounayri, Common defects and contributing parameters in powder bed fusion AM process and their classification for online monitoring and control: a review, Int. J. Adv. Manuf. Technol. 95 (2018) 527–550. doi:10.1007/s00170-017-1172-6.
- [5] J. zur Jacobsmühlen, S. Kleszczynski, G. Witt, D. Merhof, Detection of elevated regions in surface images from laser beam melting processes, in: IECON 2015 - 41st Annu. Conf. IEEE Ind. Electron. Soc., 2015: pp. 1270–1275. doi:10.1109/IECON.2015.7392275.
- [6] I. Baturynska, O. Semeniuta, K. Martinsen, Optimization of Process Parameters for Powder Bed Fusion Additive Manufacturing by Combination of Machine Learning and Finite Element Method: A Conceptual Framework, Procedia CIRP. 67 (2018) 227–232. doi:10.1016/j.procir.2017.12.204.
- [7] M. Grasso, B.M. Colosimo, Process defects and *in situ* monitoring methods in metal powder bed fusion: a review, Meas. Sci. Technol. 28 (2017) 044005. doi:10.1088/1361-6501/aa5c4f.
- [8] L. Scime, J. Beuth, Using machine learning to identify in-situ melt pool signatures indicative of flaw formation in a laser powder bed fusion additive manufacturing process, Addit. Manuf. 25 (2019) 151–165. doi:10.1016/j.addma.2018.11.010.
- [9] J. Fox, F. Lopez, B. Lane, H. Yeung, S. Grantham, On the requirements for model-based thermal control of melt pool geometry in laser powder bed fusion additive manufacturing, Mater. Sci. Technol. Conf. Exhib. 2016, MS T 2016. 1 (2016) 133–140.
- [10] A.G. Demir, L. Mazzoleni, L. Caprio, M. Pacher, B. Previtali, Complementary use of pulsed and continuous wave emission modes to stabilize melt pool geometry in laser powder bed fusion, Opt. Laser Technol. 113 (2019) 15–26. doi:10.1016/j.optlastec.2018.12.005.
- [11] L. Caprio, A.G. Demir, B. Previtali, Comparative study between CW and PW emissions in selective laser melting, J. Laser Appl. 30 (2018) 032305. doi:10.2351/1.5040631.
- [12] L. Caprio, A.G. Demir, B. Previtali, Influence of pulsed and continuous wave emission on melting efficiency in selective laser melting, J. Mater. Process. Technol. 266 (2019). doi:10.1016/j.jmatprotec.2018.11.019.
- [13] B.M. Colosimo, E. Grossi, F. Caltanisetta, M. Grasso, Penelope: A Novel Prototype for In Situ Defect Removal in LPBF, Jom. 72 (2020) 1332–1339. doi:10.1007/s11837-019-03964-0.
- [14] M. Pacher, L. Mazzoleni, L. Caprio, A.G. Demir, B. Previtali, Estimation of melt pool size by complementary use of external illumination and process emission in coaxial monitoring of selective laser melting, J. Laser Appl. 31 (2019) 022305. doi:10.2351/1.5096117.
- [15] E. Vasileska, A.G. Demir, B.M. Colosimo, B. Previtali, Layer-wise control of selective laser melting by means of inline melt pool area measurements, J. Laser Appl. 32 (2020) 022057. doi:10.2351/7.0000108.
- [16] E. Vasileska, A.G. Demir, B.M. Colosimo, B. Previtali (in press), A novel paradigm for feedback control in LPBF: layer-wise correction for overhang structures, Advances in Manufacturing

**Authors:** Ema Vasileska, Valentina Gečevska, Ss. Cyril and Methodius University in Skopje, Faculty of Mechanical Engineering - Skopje, Ul. Ruger Boskovic 18, 1000 Skopje, North Macedonia, Phone: +38923099200, Fax: +38923099298.

E-mail: [ema.vasileska@mf.edu.mk](mailto:ema.vasileska@mf.edu.mk);

[valentina.gecevska@mf.edu.mk](mailto:valentina.gecevska@mf.edu.mk)

**Ali Gökhan Demir, Bianca Maria Colosimo, Barbara Previtali**, Politecnico di Milano, Department of Mechanical Engineering, Via La Masa 1, 20156 Milan, Italy, Phone: +390223998425, Fax: +390223998580.

E-mail: [aligokhan.demir@polimi.it](mailto:aligokhan.demir@polimi.it);

[biancamaria.colosimo@polimi.it](mailto:biancamaria.colosimo@polimi.it);

[barbara.previtali@polimi.it](mailto:barbara.previtali@polimi.it)

## ACKNOWLEDGMENTS:

The authors would like to thank IPG Italy and Optoprim for their technical support. The Italian Ministry of Education, University and Research is acknowledged for the support provided through the Project "Department of Excellence LIS4.0 - Lightweight and Smart Structures for Industry 4.0".



Ignjatović Stupar, D., Chabrol, G. R., Baraze, A. R. I., Lecler S., Tessier, A., Cutard, T., Brendle, J.

## FEASIBILITY OF ADDITIVE MANUFACTURING PROCESSES FOR LUNAR SOIL SIMULANTS

**Abstract:** *Combination of In-situ Resource Utilization (ISRU) and on-site Additive Manufacturing (AM) is one of the “outer space applied technologies” candidates where free shape fabrication from micro (e.g., tools) to mega scale (e.g. lunar habitats) will allow in coming future to settle the Moon or potentially other celestial bodies. Within this research, Selected Laser Melting (SLM) of lunar soil (regolith) simulants (LHS-1 LMS-1 and JSC-2A) using a continuous wave 100 W 1090 nm fiber laser was applied. The resulting samples were mechanically and optically characterized. A numerical multiphysics model was developed to understand the heat transfer and optimize the SLM process. Results obtained are in good agreement with the numerical model. The physical and chemical characteristics of the various materials (granulometry, density, composition, and thermal properties) have a strong impact on the AM parameters.*

**Key words:** *additive manufacturing, laser, Multiphysics modelling, Lunar soil simulant, regolith*

### 1. INTRODUCTION

The lunar regolith is a dust like material that is derived from the degradation of the underlying rocks by the joint action of the impact of meteorites and solar winds on the surface of the Moon [1].

Characterization of lunar soil was done through samples collected during the Apollo and Luna missions. Having real material in hands and experiences gained by astronauts, researchers came with much clearer conclusions on how regolith, the main lunar soil material, behaves under different conditions, such as lack of atmosphere, low gravity, and extreme temperatures. The quantity of returned regolith was insufficient to be used worldwide as a test material in the development of new technological solution for future lunar settlement. One of the solutions was to create simulant materials which will be terrestrially exploited or artificially made to replace the original regolith. Many simulants that mimic Moon soil were terrestrially created according to the chemical and physical characterization of the original lunar samples [2]. For the present research, the test material, simulants LMS-1 and JSC-2A were used in experimental and simulation parts.

Additive Manufacturing (AM) by 3D Printing (3DP), Selective Laser Sintering (SLS) and Selective Laser Melting (SLM) are just a few example of technologies which have given good results in utilization of powder in manufacturing of 3D objects [3]. For that reason, those technologies in combination with lunar raw material will be suited for on-site manufacturing infrastructure on the Moon.

Using in-situ materials and laser technology for construction of the lunar habitats avoids the need to bring significant quantities of resources from the Earth to the Moon.

This paper is introducing the comparative results obtained between simulation done by COMSOL Multiphysics model and from experimental outputs done at ICube laboratory, Illkirch, France. The objective was

to create 2D structures by selected laser melting of diverse lunar simulants by optimizing the sintering process through the simulation.

### 2. MATERIALS AND METHODS

Nano-sized Lunar regolith simulants are materials developed by University of Central Florida (LMS-1) and JSC-2A by NASA.

First things first, information regarding the chemical and physical composition of material has to be known, mainly crystallinity, particles size distribution, shape, and cohesion for the reason to understand its interrelation behavior during the AM procedures [4–7]. Viscosity temperature and wetting behavior are playing important role in parametrization of AM settings [8]. During the heating process, material is passing through several phases to achieve final glassy phase. Geometric shape of melting pool depends on fixed viscosity points and that is where the viscosity temperature and wetting behavior have to be observed and adjust by control of energy intensity and speed.

Behavior of lunar soil in AM process is similar to behavior of metal powder under the same conditions. The norm ISO 7884-2:1987 defines the “workability range” of glassy material which represents the viscosity range between working and Littleton points [9]. Those points are helping to optimize the parameters during the AM process and to better control thermal system. Unfortunately, similar standard for moon dust does not exist but due to similarity between metal powder and lunar simulants this can be applicable until the point when wettability of material starts to affect the consolidation of printed layers due to composition of the lunar soil. Regarding the lunar soil, the analysis of the chemical composition showed that the regolith is predominantly have silica and aluminum oxides but also contains iron, titanium, calcium and magnesium oxides. [1].

The experimental part was done at the ICube

laboratory, Illkirch, France. A RedPower SPI SP-100C continuous wave fiber laser of 100 W with a Gaussian profile, at wavelength of 1090 nm, and with diameter spot of 0.7 mm was used. A Newport motion controller was used for the table displacement in X direction, while the laser power and time exposure were done with LabVIEW software. Displacements in the Y direction were done manually using a micrometer stage installed directly on top of the X stage underneath the laser focusing set up. In this AM procedure only 2D manufacturing was possible.

In parallel a COMSOL Multiphysics model was developed to understand and optimize the experimental process. The multiphysics model was implemented with the thermal conductivity, density, heat capacity and latent heat of fusion of the regolith simulants. The thermal conductivity was based on these two equations [10–12]:

$$K = 0.001561 + 5.426 \cdot 10^{-11} T^3 \quad (1)$$

$$K = 10^{-9.332 + \frac{1.409 \cdot 10^4}{T}} \quad (2)$$

where  $T$  is temperature in K. First equation is representing temperature of material before sintering/melting procedure ( $T < 1500$  K) and second one after melting ( $T > 1500$  K).

Stebbins' model [13] was used to model the evolution of density of material with temperature. The heat capacity was calculated over the three temperature ranges:  $T < 350$  K,  $350$  K  $< T < 1500$  K, and  $T > 1500$  K using the respective equations given by Schreiner *et al.* [14]. A latent heat of fusion of 458 kJ/kg was used

according to the model developed by Kang *et al.* [15]. Thermal conductivity of 0.82 W/(mK) is used due to model proposed by Langseth, Cremers and Kang [10][11][15]. Due to the high absorption of regolith (80% in our case), the laser beam was modelled as a Gaussian surface heating source on the top surface.

Convective heat transfer and thermal radiations were considered as energy losses on the top surface. Insulation and a temperature fixed to 293 K were used as numerical conditions on the other boundaries. A mesh size of 100  $\mu\text{m}$ , typically 7 times smaller than the laser spot waist, is imposed on the top surface.

### 3. RESULTS

The first simulation on COMSOL was done in the static mode what is shown in the Fig. 1. A power of 10 W was fixed, and time exposure of laser was variable from 5 ms to 10 s. The depth propagation of heat is sensitive to the time of the laser exposure. As expected, with increased time exposures, the size of printed spot increases as well.

From the experimental part the task was to observe the behavior of LMS-1 simulant under the different laser powers, from 5 to 20 W in different time exposure from 1 s to 20 s. As can be seen in Fig. 1 and 2, in case of 10 W power and 5 s exposure, the thickness of the melted spot is approximately 1.3 mm. The experimental results were validated by the simulation. It is confirmed that if the power and time are increasing, the size of printed sample increases respectively as represented in Fig. 2.

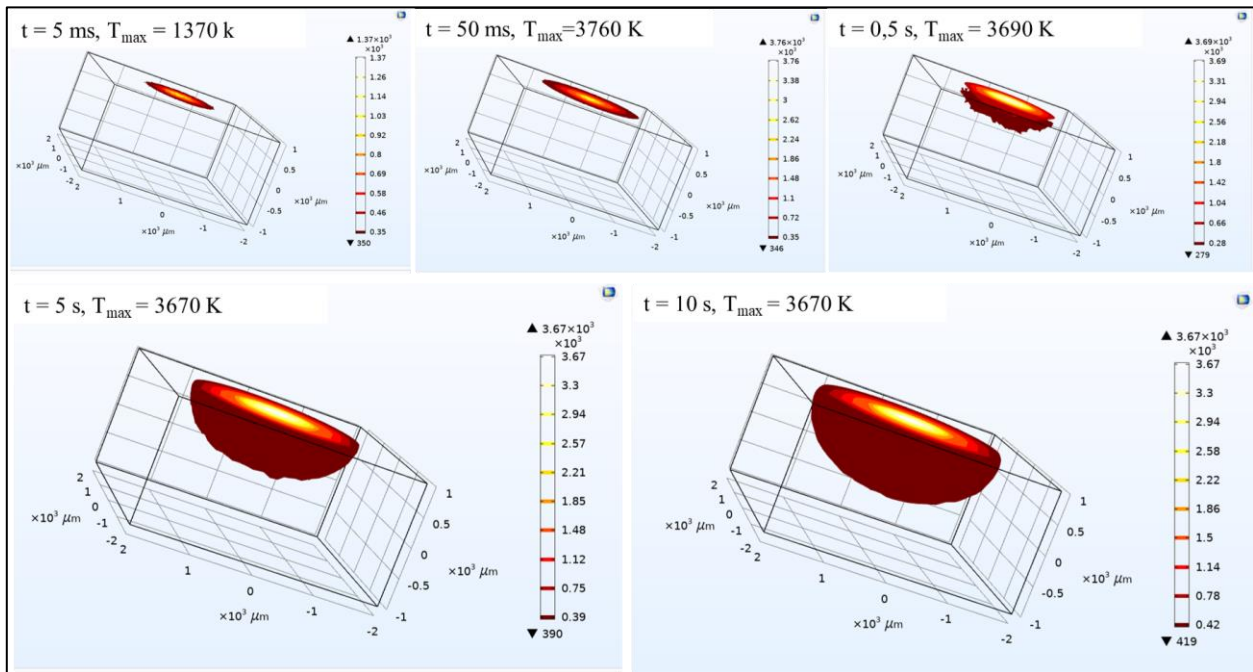


Fig. 1. Simulation of the evolution of the temperature in the static mode for 10 W and spot waist of 700  $\mu\text{m}$

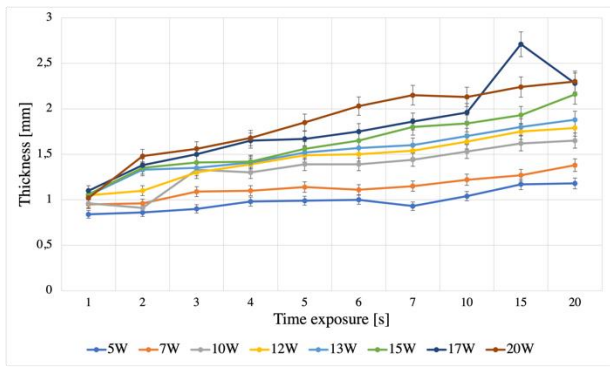


Fig. 2. Experimental results: Thicknesses of melted LMS-1 powder for various time and laser power

Regarding the dynamic mode, the multiphysics model was modified to observe the evolution of temperature when the laser spot is moving. The results displayed in Fig. 3 show the evolution of the melt pool from 10 to 100 ms with power of 25 W, laser speed of 50 mm/s, and spot waist of 700  $\mu\text{m}$ . From this simulation it can be seen that under these conditions, melting of the material happens during all printing process following by cooling coming slowly after. The cooling rate is important to monitor and control when multiple lines will be printed for 2D sample. This parameter has a strong impact on the residual stress and thus the structural integrity of the final printed samples.

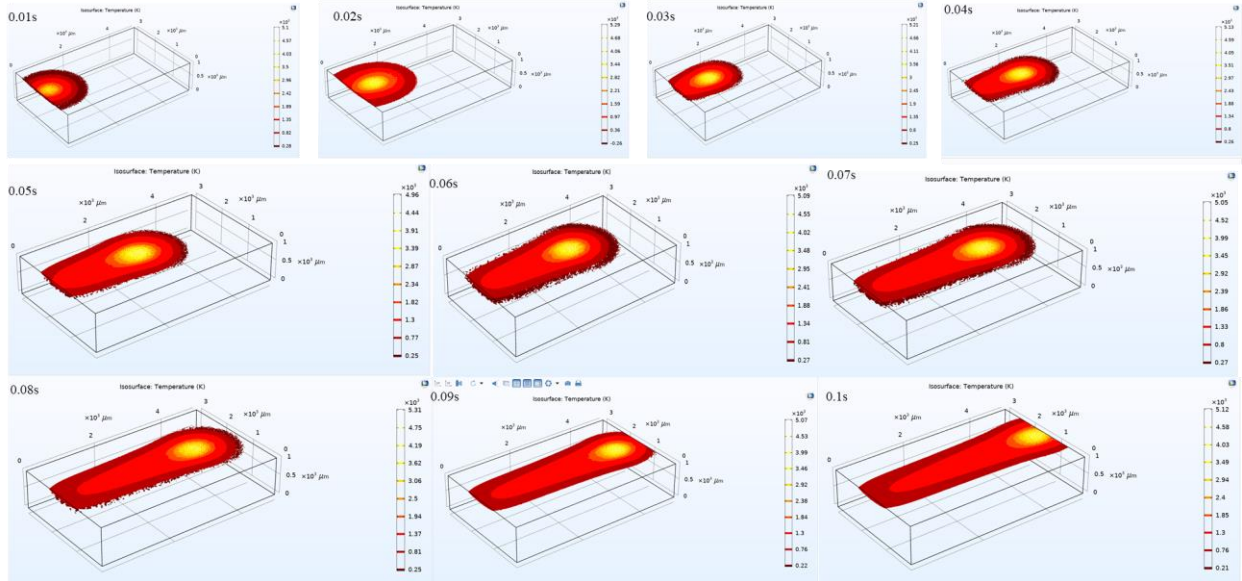


Fig. 3. Thermal analysis in dynamic mode done by COMSOL. 25 W power, laser spot waist of 700  $\mu\text{m}$ , 50 mm/s speed

Fig. 4 shows printed lines of JSC-2A simulant. It can be noticed that when the speed increases, the thickness of the samples is reduced. Likewise, for the same speed, if the power increases, the thickness increases as well.

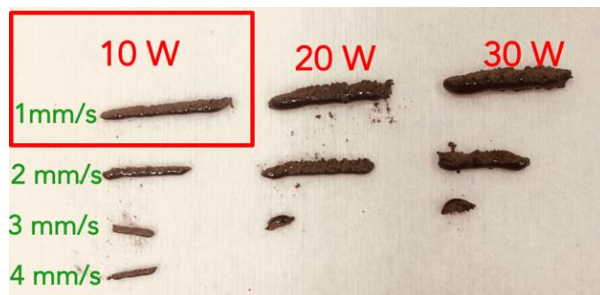


Fig. 4. JSC-2A printed lines under the different laser power and speed with selection of the best suitable combination

The next step in experimental part was to print a square using the best parameters what were applied for previously printed lines. A 10 W laser power and 1 mm/s speed were chosen (see Fig. 4) as a most suitable

combination for JSC-2A. The 3D printed square is shown in Fig. 5. The sample is a 10x10 mm square made of 43 lines with 0.2 mm hatches between lines.

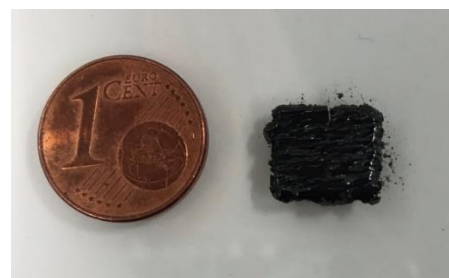


Fig. 5. JSC-2A printed squared

Fig. 6 displays the numerical and experimental results in dynamic mode. The power was varied from 40 to 95 W and speed between 10 and 24 mm/s were used numerically and experimentally. Similar results regarding the thicknesses of the printed samples and melt pool dimensions were found.

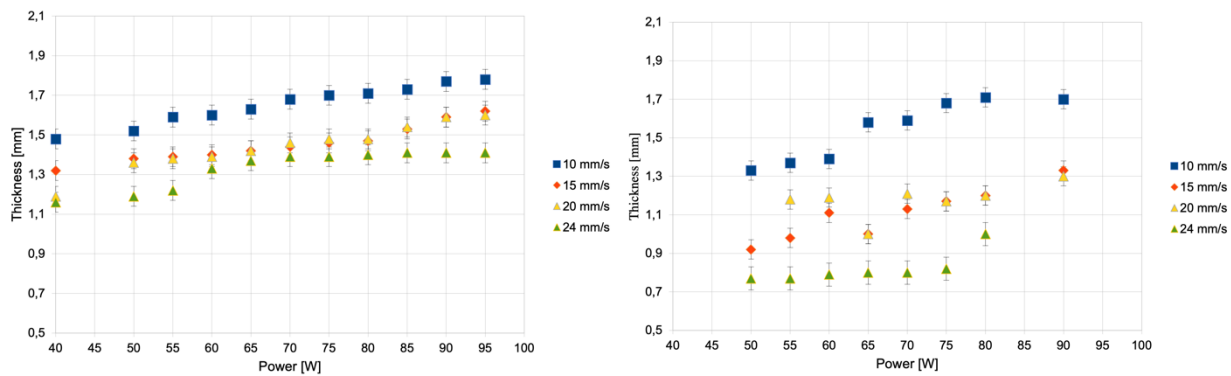


Fig. 6. Comparison between numerical (right) and experimental (left) results

#### 4. DISCUSSION

During the experimental tests it was noticed that laser power, speed of table motion (X direction), distance between printed lines (Y distance) are key parameters that can easily be tailored. The difficulties stand in the control of the energy deposited onto the powder during the processing. The melting and solidification process is governed by the adhesion between the melt pool and the raw material itself. In order to produce continuous lines and avoid the balling effect [16] (due to the surface tension and Marangoni effect), the laser processing parameters has to carefully be selected.

Another care has to be taken to select parameters giving lines with as little residual stress as possible to be able to 3D print surfaces made out of multiple lines. In this case, great care was taken in the optimization of the hatching space between the lines.

During the continuous printing process of a surface, lines one after the other in a raster pattern, the thermally induced mechanical stress and can build up line after line. The final printed samples can therefore present delamination and cracks.

The shape and grain distribution have not been investigated in the study and will surely have a big impact on the quality of the final product [17] Likewise the lack of adequate thermal control of the printed lines (second laser beam to preheat the material or slow down the cooling of the material [18]).

Involving a new laser and new material in any sintering experiment, the starting point is to understand the type of interactions under different conditions such as power and speed of table displacement where material is settled.

#### 5. CONCLUSION

There are several parameters which have to be taken into account before sintering procedures start such as the laser parameters, the composition of the raw materials and thus the overall heat transfer mechanism.

Regarding experimental laser tests, interaction of simulant with the laser beam was observed. experimental results are in a good term with COMSOL Multiphysics model. The present results indicate that this methodology of additive manufacturing could be successfully applied to build Lunar habitats.

Further study will include the testing of various powder compactness in a specifically design powder bed and spreader (hopper, blade and roller), test with a galvanic head instead of a stage to reach higher speed, test in a vacuum chamber, the use of other lunar soil simulants and optimization of the multiphysics model.

#### 6. REFERENCES

- [1] I.A. Crawford, Lunar resources: A review, *Prog. Phys. Geogr.* 39 (2015) 137–167. <https://doi.org/10.1177/0309133314567585>.
- [2] L.A. Taylor, C.M. Pieters, D. Britt, Evaluations of lunar regolith simulants, *Planet. Space Sci.* 126 (2016) 1–7. <https://doi.org/10.1016/j.pss.2016.04.005>.
- [3] M. Fateri, A. Grossmann, S. Fasoulas, A. Großmann, P. Schnauffer, P. Middendorf, Additive Manufacturing of Lunar Regolith for Extra-terrestrial Industry Plant, (2015). <https://doi.org/10.1016/j.expneurol.2007.12.026>.
- [4] L.P. Keller, D.S. McKay, The nature and origin of rims on lunar soil grains, *Geochim. Cosmochim. Acta.* 61 (1997) 2331–2341. [https://doi.org/10.1016/s0016-7037\(97\)00085-9](https://doi.org/10.1016/s0016-7037(97)00085-9).
- [5] E. Suescun-Florez, S. Roslyakov, M. Iskander, M. Baamer, Geotechnical Properties of BP-1 Lunar Regolith Simulant, *J. Aerosp. Eng.* 28 (2015) 04014124. [https://doi.org/10.1061/\(asce\)as.1943-5525.0000462](https://doi.org/10.1061/(asce)as.1943-5525.0000462).
- [6] W.D. Carrier, Particle Size Distribution of Lunar Soil, *J. Geotech. Geoenvironmental Eng.* 129 (2003) 956–959. [https://doi.org/10.1061/\(asce\)1090-0241\(2003\)129:10\(956\)](https://doi.org/10.1061/(asce)1090-0241(2003)129:10(956)).
- [7] Y. Li, X. Zeng, A. Wilkinson, Measurement of Small Cohesion of JSC-1A Lunar Simulant, *J. Aerosp. Eng.* 26 (2013) 882–886. [https://doi.org/10.1061/\(asce\)as.1943-5525.0000197](https://doi.org/10.1061/(asce)as.1943-5525.0000197).
- [8] M. Fateri, S. Pitikaris, M. Sperl, Investigation on Wetting and Melting Behavior of Lunar Regolith Simulant for Additive Manufacturing Application, *Microgravity Sci. Technol.* 31 (2019) 161–167. <https://doi.org/10.1007/s12217-019-9674-5>.
- [9] ISO 7884-2:1987 - Glass -- Viscosity and viscometric fixed points, 1987.
- [10] M.G.. J. Langseth, S.P.. J. Clark, J.L.. J. Chute, S.J.

- Keihm, A.E. Wechsler, Heat flow experiment, NASA. Manned Spacecr. Cent. Apollo 15 Prelim. Sci. Rept. (1972).
- [11] C.J. Cremers, Thermophysical properties of Apollo 14 fines, *J. Geophys. Res.* 80 (1975) 4466–4470. <https://doi.org/10.1029/JB080I032P04466>.
- [12] P. Richet, Y. Bottinga, Thermochemical properties of silicate glasses and liquids: A review, *Rev. Geophys.* 24 (1986) 1–25. <https://doi.org/10.1029/RG024I001P00001>.
- [13] J.F. Stebbins, I.S.E. Carmichael, L.K. Moret, Heat capacities and entropies of silicate liquids and glasses, *Contrib. to Mineral. Petrol.* 1984 862. 86 (1984) 131–148. <https://doi.org/10.1007/BF00381840>.
- [14] S.S. Schreiner, J.A. Dominguez, L. Sibille, J.A. Hoffman, Thermophysical property models for lunar regolith, *Adv. Sp. Res.* 57 (2016) 1209–1222. <https://doi.org/10.1016/J.ASR.2015.12.035>.
- [15] Y. Kang, K. Morita, Thermal conductivity of the CaO-Al<sub>2</sub>O<sub>3</sub>-SiO<sub>2</sub> system, *ISIJ Int.* 46 (2006) 420–426.
- [16] L. Moniz, Q. Chen, G. Guillemot, M. Bellet, C.A. Gandin, C. Colin, J.D. Bartout, M.H. Berger, Additive manufacturing of an oxide ceramic by laser beam melting—Comparison between finite element simulation and experimental results, *J. Mater. Process. Technol.* 270 (2019) 106–117. <https://doi.org/10.1016/J.JMATPROTEC.2019.02.004>.
- [17] S. Spath, H. Seitz, Influence of grain size and grain-size distribution on workability of granules with 3D printing, *Int. J. Adv. Manuf. Technol.* 70 (2014) 135–144. <https://doi.org/10.1007/S00170-013-5210-8>.
- [18] A. MJ, N. DS, P. HS, Investigation of SLM Process in Terms of Temperature Distribution and Melting Pool Size: Modeling and Experimental Approaches, *Mater. (Basel, Switzerland)*. 12 (2019). <https://doi.org/10.3390/MA12081272>.

**Authors: Danijela Ignjatović Stupar**, International Space University, 1 rue Dominique Cassini, 67400 Illkirch-Graffenstaden, France

E-mail: [danijela.stupar@isunet.edu](mailto:danijela.stupar@isunet.edu)

**Grégoire Robert Chabrol**, ECAM Strasbourg-Europe Espace Européen de l'Entreprise, 2 Rue de Madrid, 67300 Schiltigheim, France

E-mail: [Gregoire.Chabrol@ecam-strasbourg.eu](mailto:Gregoire.Chabrol@ecam-strasbourg.eu)

**Abdoul Razak Ibrahim Baraze, Sylvain Lecler, Alexandre Tessier**, INSA of Strasbourg -Unistra – CNRS, ICube, 300 bd Sébastien Brant – CS 10413, 67412 Illkirch Cedex, France

E-mail: [abdoulrazakbaraze@yahoo.com](mailto:abdoulrazakbaraze@yahoo.com);

[sylvain.lecler@insa-strasbourg.fr](mailto:sylvain.lecler@insa-strasbourg.fr);

[alexandre.tessier@insa-strasbourg.fr](mailto:alexandre.tessier@insa-strasbourg.fr)

**Thierry Cutard**, IMT Mines Albi-Carmaux, École Mines-Télécom, Campus Jarlard, 81013 Albi Ct Cedex 09, France

E-mail: [thierry.cutard@mines-albi.fr](mailto:thierry.cutard@mines-albi.fr)

**Jocelyne Brendle**, Institut de Science des Matériaux de Mulhouse, UMR CNRS-UHA 7361, 15 rue Jean Stracky, 68057Mulhouse Cedex, France

E-mail: [jocelyne.brendle@uha.fr](mailto:jocelyne.brendle@uha.fr)



Dekić, P., Milutinović, B., Tomić, M., Nikolić, S.

## INFLUENCE OF PRINTING PARAMETERS AT MECHANICAL PROPERTIES OF FDM PRINTINGS PARTS MADE FROM ABS

**Abstract:** In the modern world, the use of 3d printing is widespread both in scientific research and in engineering practice. The application is diverse and ranges from home use, biomedicine all the way to the space program. What is a problem in the application of this technology is the poor knowledge of the behavior of materials under different types of loads, and the influence of printing parameters on them. For the purposes of this research, samples were made and tested in accordance with ISO 527 and ISO 178 standards, whereby infill printing patterns and orientation of specimens were varied. Also, aging of the samples in the air was performed.

**Key words:** 3D printing, printing parameters, tensile properties, flexural strength

### 1. INTRODUCTION

Additive manufacturing (AM) or 3D printing is technologies that are increasingly supplanting classic technologies. These technologies are being used in various industries such as the automotive industry, biomedicine, construction, aerospace, food industries as well as in academic researches. The application of these technologies significantly accelerates the development and shortens the production time of new products. Additive technologies make it possible to make parts from just a few millimetres to entire residential buildings. The goal of additive technologies is to quickly and accurately create a three-dimensional object, based on CAD models, with the goal of significant cost reduction compared to traditional technologies. [1-6]

These technologies can be divided into several groups based on the principle of operation:

- Binder jetting
- Sheet lamination
- Material extrusion
- Direct energy deposition
- Material jetting
- Powder bed fusion
- Vat photo polymerization [6, 7]

The processes also differ according to the type of material from which the part is made:

- Polymers,
- Ceramics,
- Metal

Process of 3D printing consists of several steps. The first step is to create a 3D model and adjust the print parameters; this process is called pre-printing preparation. The next step is the production of the part, i.e. 3D printing. The last step is to remove the excess material and, if necessary, to correct the product and this process is called post processing. [8].

Fuse Deposition Modeling (FDM) is a typical representative of additive technologies and consists in the fact that the product is manufactured by building layer by layer of thermoplastic materials. The material is used in the form of a wire and is wound on a spool;

the wire can be of different diameters, as follows: 1.75 mm; 2.85mm and 3mm. The group of materials most commonly used includes for 3D printing:

- Acrylonitrile butadiene styrene - ABS
- Polylactic acid - PLA
- Polyethylene terephthalate glycol - PET-G
- Polyvinyl Alcohol - PVA

Typical FDM printer is shown in figure 1. The printing process consists in drawing a wire filament (fig. 1 position 1) through the hot extruder (fig. 1 position 2) set to melting temperature of the filament. In the extruder, the solid material turns into a liquid state and is applied layer by layer to the hot working bed (fig.1 position3), until the finished product is obtained.[8]

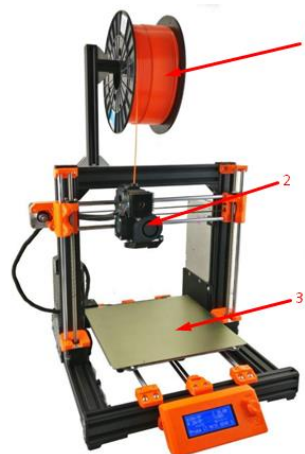


Fig. 1. Typical FDM printer [8]

Pre-printing preparation is one of the most important processes in FDM printing. During this process, a CAD model with the appropriate extension STL, OBJ, etc. needs to be processed by a piece of software called a "slicer," which converts the model into a series of thin layers and produces a G-code file. In this step it is necessary to set the following parameter:

- Working parameters
- Printing speed
- Layer thickness
- Infill pattern

- Infill density

Working parameters mainly depend on the type of material, so the manufacturer's recommendations for extruder and work bed temperatures are mainly used. Printing speed represents the speed of movement of the nozzle and the following speeds are distinguished: printing speed, infill speed and travel speed. Layer thickness denotes the height of layer which is stacked over other 3d printing is carried out by the addition of filament over layer. Infill pattern presents outer coated part of plastic which is inside the print. In 3D printing, different infill patterns can be used lines, concentric, zigzag, etc. Infill density is an amount of plastic whichever is incorporated inside the printing, usually ranging from 20 to 80 percent, rarely 100 percent is used. [8, 9]

All the above mentioned parameters affect the properties of the product. The influence of parameters can be divided into two basic categories:

- Impact on surface quality and dimensional stability
- Influence on mechanical properties.

This paper will present the influence of printing parameters on basic mechanical properties of products such as tensile and flexural properties.

## 2. EXPERIMENTAL

### 2.1 Material and device

For the purposes of this research, ABS thermoplastic with the following characteristics was used:

- Density 1.04g / cm<sup>3</sup>;
- Filament diameter 3 mm;
- Extruder temperature: 220-240 ° C;
- Bed temperature: 100-110 ° C.

The samples were made on a Pangu I3 printer with a nozzle diameter of 0.3 mm, with a print space size of 150x150x150mm, and printing temperature at 225° C

### 2.2. Dimensions and shapes of samples

For the purposes of this research, all samples were modeled in Solid Works and post processed in Repetier-Host software (Cura slicer).

For the purposes of testing of tensile properties, and in accordance with the ISO 527 standard, type 1B tubes were made, the CAD mode and realistic appearance of tube are shown in Figure 2.

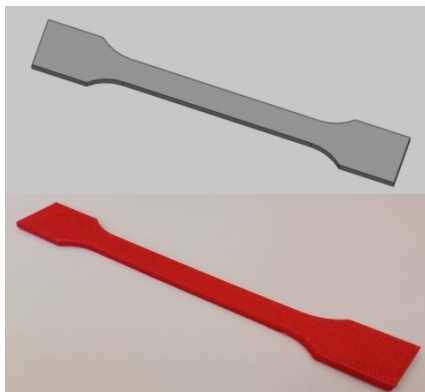


Fig. 2. Real model and CAD model of sample "1B"

Also for the purpose of testing of flexural properties, and in accordance with ISO 178 a test tube of the following dimensions was made: width 10 mm; length 80mm and height 4mm. The appearance of the CAD model and the real sample "2" are shown in Figure 3.

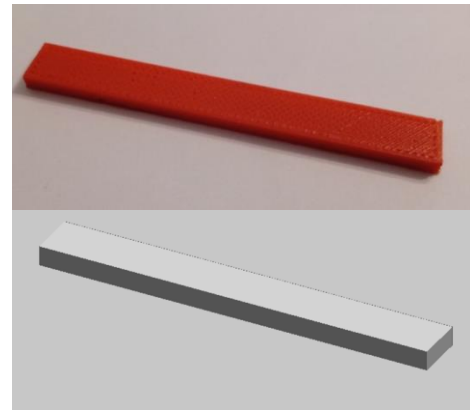


Fig. 3. Real model and CAD model of sample

### 2.3. Printing parameters and specimen orientation

A large number of studies have included the influence of the layer thickness and infill density parameters on the mechanical properties of the sample properties, so this is not considered by this study [2-6]. The sampling parameters were taken from the research of Đekić and all. [1] whereby only the infill parameter and specimen orientation were varied and their influence on tensile and flexural properties was analyzed.

Printing parameters are:

- Printing speed - 30mm / s
- Infill density - 30%
- Layer thickness - 0.2mm. [1]

The first part of the research referred to the influence of sample orientation during printing on the examined properties. Three cases are considered, which are shown in Figure 4.

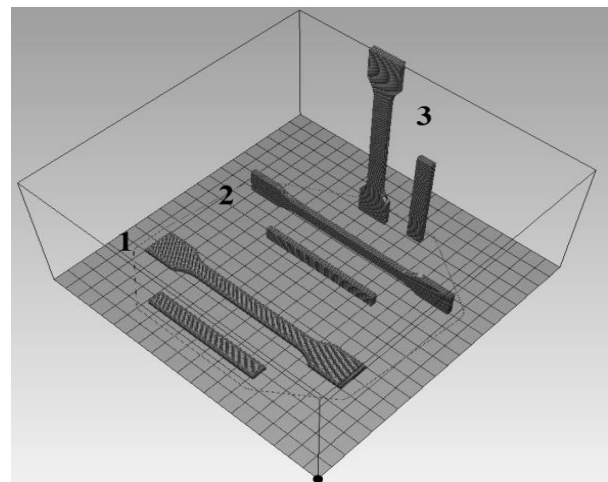


Fig. 4. Specimens orientation

After testing the tensile and flexural properties, it was determined that the best properties are obtained with the orientation under number 1.



When the optimal orientation of the sample was determined, which is case 1, a variation of the infill pattern was performed in the continuation of the research. The following cases of infill patterns which are considered are shown in Table 1.

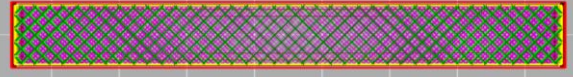
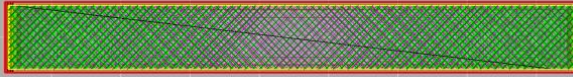
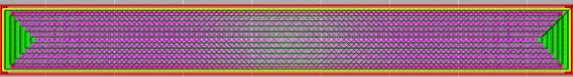

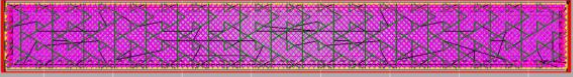
Infill pattern

Grid

Line

Concetric

Cristal

ZigZag

Table 1. Different types of infill

The test was performed on a Universal Testing Machine Amsler 40KN. Aging of the samples in air for 48 hours at a temperature of 200°C was also performed.

### 3. RESULT AND DISCUSSION

The test results of tensile strength and elongation at brake of different sample orientation during printing are shown in Figure 5 and 6.

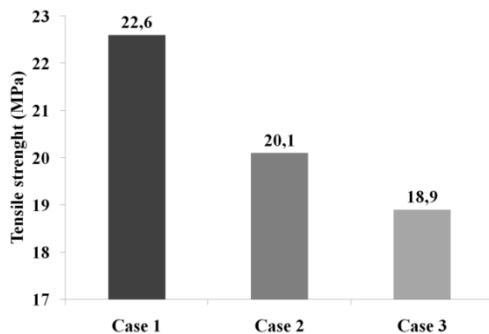


Fig. 5. Tensile strength

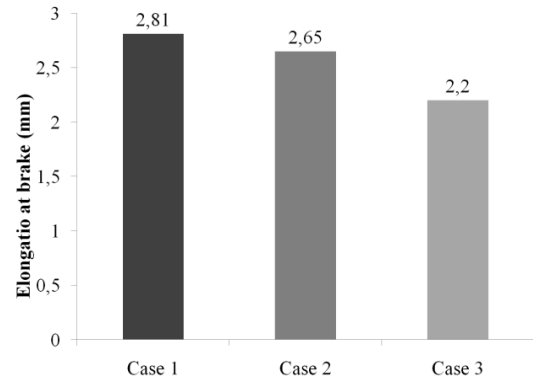
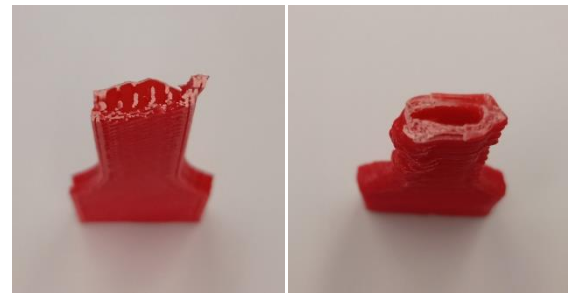


Fig. 6. Elongation at brake

Based on them, it can be concluded that the best properties are achieved in case 1 and the worst in case 3. This can be explained by the orientation of the layers and gaps when printing. In case 1 and 2, the applied load coincides with the orientation of the printed layers, which directly affects the properties of the material. In case 3, the load is perpendicular to the direction of the layers and delimitation of the layers occurs, i.e. the load is opposed by the adhesion of the layers, which is shown in figure 7.



Case 1. Case 3.

Fig. 7: Fracture surface vs. printing orientation

Figure 8. shows the influence of printing orientation on flexullar properties, from which the same regularity can be inferred as in the case of tensile properties.

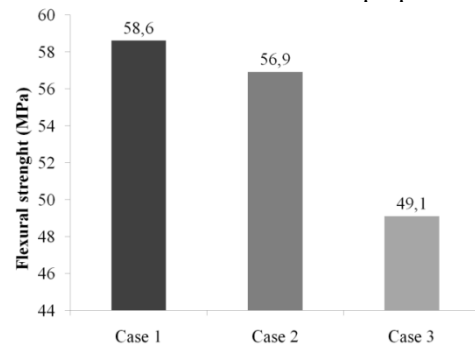


Fig. 7. Flexural strength

Test results of tensile strength and elongation at brake for different types of infill pattern are shown in figure 9 and 10.

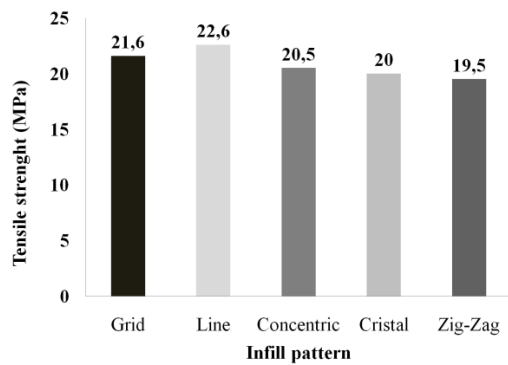


Fig. 9. Tensile strength vs. infill pattern

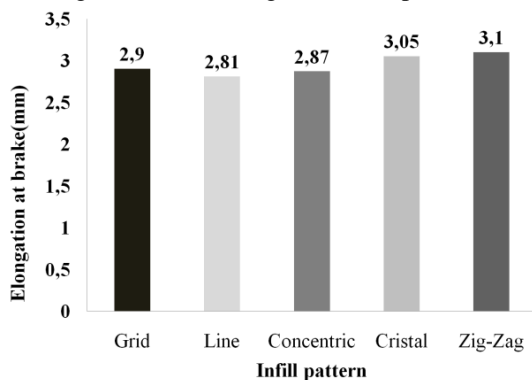


Fig. 10. Elongation at brake vs. infill pattern

This phenomenon can be explained by the load distribution shown in Figure 11. In the case of the Line infill pattern, the highest load is because it coincides with the print lines, but therefore the elongation is the lowest. While in the case of Zig-Zag infill pattern the resistance to tension depends on the strength of the adhesive layers and is usually the smallest, while the elongation is the largest.

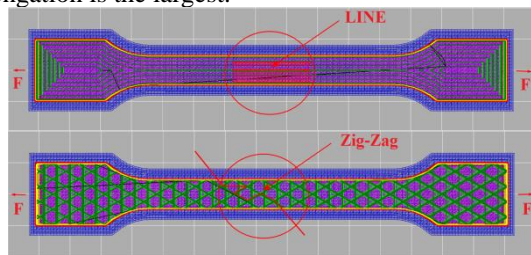


Fig. 11. Influence of infill pattern on properties

The results of the flexural strength test are shown in Figure 12. From these results it can also be concluded that the infill pattern affects this property as well as the tensile properties.

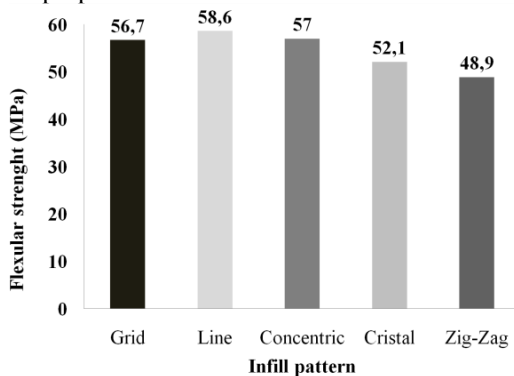


Fig. 12. Flexural strength vs. infill pattern

Aging did not have a significant effect on the examined properties.

#### 4. CONCLUSION

Although additive technologies are increasingly being applied and conventional technologies are slowly being suppressed, there are still a large number of problems related to the production of parts with 3D printing and their application.

Based on the performed tests, it can be concluded that the mechanical properties of the product significantly depend on the printing orientation and the infill pattern. When manufacturing the part, special care must be taken that the print lines coincide with the offensive load lines.

#### 5. REFERENCES

- [1] Djekić, P., Milutinović, B., Tomić, M., Nikolić, S.: *Influence of 3D printing parameters on the geometry and surface quality of manufactured parts on an FDM 3D printer*, X International Conference "Heavy Machinery-HM 2021", pp. B39-B44, Vrnjačka Banja, 23–25 June 2021
  - [2] Dixit, N., Jain K. P.: "3D printed carbon fiber reinforced thermoplastic composites: A review", *Materials Today: Proceedings* 43 pp. 678–681, (2021)
  - [3] Singh, T., Kumar, S., Sehgal, S.: "3D printing of engineering materials: A state of the art review," *Materials Today: Proceedings* 28, pp. 1927–1931, (2020)
  - [4] Prabhakar, M. M., Saravanan, K. A., Lenin, A., Jerinleno, I., Mayandi, K., Ramalingam S. P.: "A short review on 3D printing methods, process parameters and materials", *Materials Today: Proceedings* (2020)
  - [5] Safai, L., Cuellar, S. J., Smit, G., Zadpoor A. A.: "A review of the fatigue behavior of 3D printed polymers", *Additive Manufacturing* Vol: 28, pp. 87–97 (2019)
  - [6] Sandeep, B., Kannan, M. T. T., Chandradass, J., Ganesan, M., Rajan, J. A.: "Scope of 3D printing in manufacturing industries-A review", *A short review on 3D printing methods, process parameters and materials*", *Materials Today: Proceedings*, (2021)
  - [7] Khosravanian, R. M., Bertob, F., Ayatollahic, R. M., Reinicke, T.: "Fracture behavior of additively manufactured components: A review" *Theoretical and Applied Fracture Mechanics* Vol. 109, (2020)
  - [8] <https://www.prusa3d.com/>
  - [9] Morampudi, P., Ramana, N. S. V., Prabha A. K., Swetha, S., Brahmeswara Rao N. A.: "3D-printing analysis of surface finish", *Materials Today: Proceedings* 43, pp. 587–592 (2021)
- Authors: Senior Lecturer Petar Đekić, Senior Lecturer Biljana Milutinović**, The Academy of Applied Technical and Preschool Studies, Aleksandra Medvedeva 20, Niš.  
**Assoc. Prof. Mladen Tomić**, University of Novi Sad, Faculty of Technical Science.  
**Assoc. Prof. Saša Nikolić**, Faculty of Electronic Engineering, University of Niš.  
 E-mail: [petar.djekic@akademijanis.edu.rs](mailto:petar.djekic@akademijanis.edu.rs);  
[biljana.milutinovic@akademijanis.edu.rs](mailto:biljana.milutinovic@akademijanis.edu.rs);  
[mladen.tomic@uns.ac.rs](mailto:mladen.tomic@uns.ac.rs); [sasa.s.nikolic@elfak.ni.ac.rs](mailto:sasa.s.nikolic@elfak.ni.ac.rs)

Movrin, D., Pintać, D., Knežević, P., Milutinović, M., Kojić, S., Premčevski, V.

## COMPARISON OF MECHANICAL PROPERTIES OF REGULAR AND ANTIBACTERIAL 3D PRINTED PLA SPECIMENS

**Abstract:** The 3D printing technologies have a very wide industrial and medical use. Depending on the area of application, they must satisfy mechanical properties and if used for medical purpose, they should have good antimicrobial resistance. Looking at the most popular 3D printing technology, Fused Deposition Modeling (FDM), large numbers of 3D printing materials can be found on the market today, most being polymer materials like PLA, ABS, Nylon, PET, etc. The most popular and the most used material in the FDM technology is the Polylactic Acid (PLA), which belongs to the group of biodegradables, nontoxic and easy to print polymers. In this paper comparison of tensile strength and antimicrobial resistance of regular and antibacterial PLA is shown. Specimens were produced using FDM 3D printer Prusa research, and tested using methods which were in accordance with ISO standard.

**Key words:** 3D printing, PLA, Tensile strength, Antimicrobial test

### 1. INTRODUCTION

Today, Fused Deposition Modeling (FDM) presents one of the most widespread 3D printing (additive) technology and main reason for this is price, both, device and used material. Parallel with devices development, new materials with specific mechanical or other properties have been also developed. Last years, the most popular material for FDM 3D printing is Polylactic acid (PLA). It is a biodegradable thermoplastic aliphatic polyester derived from renewable resources, such as corn starch (in the United States), tapioca roots, chips or starch (mostly in Asia), or sugarcane (in the rest of the world). In some specifics form it can be biocompatible and used for implants production in medicine (surgery).

With the development of modern imaging modalities (Computed Tomography – CT or Magnetic Resonance Imaging MRI) which provided input data for CAD model generation, use of 3D printing technology in medicine became important.

Among numerous possible applications of 3D printing in medicine are:

- Possibility to improve diagnostic quality and help in pre-surgical planning. Simulating complicated surgical steps in advance using prototype model can help foresee complications during operation which may result in reduced procedure time.
- Use for implant and tissue design, both for bone reconstruction and replacement of the soft tissues, as 3D printing can be applied on a variety of materials.
- Opportunities for scientific research
- Use in medical training and education

One of the examples using 3D printing in medicine is presented in book [1], where is shown development of a methodology to design and fabricate a patient-specific ankle foot orthosis (AFO) redressing the

geometrically 3D scanned data cloud of patient's lower limb. AFO an assistive device used for support and correction of musculoskeletal structure. Similar research is described in [2] where presented a new approach to AFO manufacturing that utilizes digital and additive manufacturing technologies to customize the fit and form to an individual (Figure 1).



Fig. 1. FO being worn by the subject [2]

Expect for foot orthosis, 3D printing technology can be used for produces hand orthosis (Figure 2). In research [3,4] FDM technology is used for printing custom-made orthoses which provides significant advantages, including increased ventilation and lighter weights.



Fig. 2. Different modeling approaches for orthosis prototypes [3]

With expansion of field of 3D printing technologies

uses, as a relevant parameter has become mechanical properties of product material. The most used polymer materials in FDM technology are PLA, ABS, PETG etc. But, as it was mentioned, PLA is the most suitable material for medical purpose, and it can be found on the market in antibacterial variant. Antimicrobial properties of PLA have been achieved by adding silver or copper in nano dimensions. In some cases, those added elements can reduce main mechanical properties of final parts which is not preferably.

In presented research two PLA variants, regular and antibacterial, were tested and compared, from the standpoint of mechanical properties and antimicrobial properties. Antimicrobial testing was provided with three different microorganisms, two bacterial and yeast, using both type of PLA printed specimens. Tensile strength was also determined for both PLA type.

## 2. EXPERIMENTAL RESEARCH

Two types of PLA were used for all experiments; regular PLA (red color) from Devil Design (Poland) and antibacterial PLA (blue color) from Copper 3D (Chile). For each series of experiment different shapes of specimens were fabricated, rectangular thin plate (30x30x3mm) for antimicrobial testing, and special shaped specimens for tensile strength testing (Figure 4). All specimens were produced using parameters shown in Table 1.

### 2.1. Antimicrobial testing

Antimicrobial properties of the specimens were evaluated by the EPA method [5] used for testing the antimicrobial efficacy of copper alloy surfaces. Three microorganisms were applied: Escherichia coli ATCC 13706, representing Gram-negative bacteria, Staphylococcus aureus ATCC 11632, representing Gram-positive bacteria and Candida albicans ATCC 10231, representing yeasts. Luria-Bertani solid or liquid medium was used for bacteria, while Saburoad broth or agar was used for yeast growth. For experimental purposes, a 0.5 McFarland standard suspension of microorganisms was made and diluted in saline solution to the final concentration of  $5 \times 10^5$  /mL. 5.0% foetal bovine serum and 0.5% Triton-X were also added in order to evenly spread the suspension on the surface of the specimens. 20 $\mu$ L of suspension was applied to the specimen and the specimens were placed in a humid atmosphere, at 26 oC. After 2h, the specimens were immersed in 5 mL of saline solution and placed on a shaker for a certain amount of time. For the control, 20 $\mu$ L of microbial suspension was added to 5 mL of saline solution. The obtained suspensions were diluted 10 times and inoculated onto the surfaces. After the incubation, colonies were counted, the abundance of the microorganisms was transformed to a logarithmic scale and expressed as mean values  $\pm$  standard deviations, as shown in Figure 1. Significant difference was verified using ANOVA, after testing the normality of the results. In parallel, microorganisms were inoculated onto the surfaces and the specimens were placed on them. These surfaces were incubated, and after the

growth of the microorganisms, the specimens were removed in order to evaluate the growth. Results were obtained in two independent experiments and three repetitions

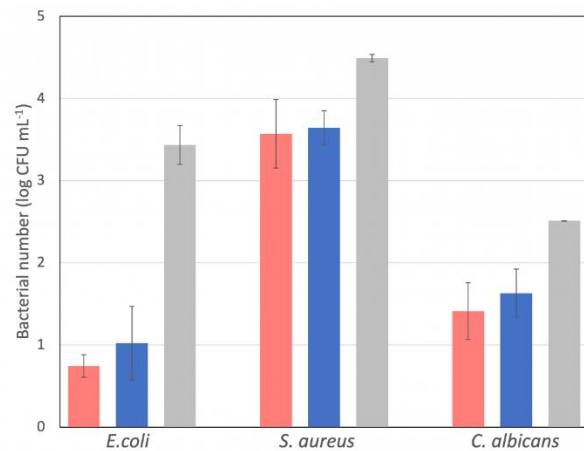


Fig. 3. Abundance of the microorganisms after 2h contact with the specimens

Figure 3 shows that the specimens had the best effect on *E. coli*, compared to the control ( $p < 0,001$ ), but a significant difference in antimicrobial properties was not evident between red and blue specimens ( $p = 0,174$ ). A difference between specimens was also not evident with *S. aureus* ( $p = 0,662$ ), but there was a significant decrease in bacterial number compared to the control ( $p < 0,001$ ). Similar results were obtained with *C. albicans*, where both blue ( $p = 0,009$ ) and red specimens ( $p = 0,016$ ) decreased the number of the microorganisms, but the difference was not statistically significant ( $p = 0,336$ ). As for the growth of the microorganisms, a similar effect can be seen on Fig. 4 – both specimens inhibit the growth of microorganisms during 24h incubation period.

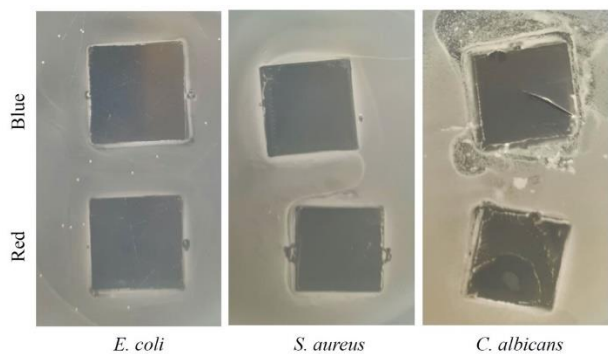


Fig.4 Growth inhibition of microorganisms exposed to specimens

Preliminary results from the conducted experiments indicate that there is no clear difference in the antimicrobial activity of the specimens, but both specimens decrease the abundance of tested microorganisms. It is very interesting to note a much better effect of the specimens towards Gram-negative bacteria, where it is possible that the material of the specimens damages the outer membrane comprised of lipopolysaccharides.

## 2.2. Mechanical testing

For production the testing specimens, Prusa i3 MK3 FDM printer (Prusa Research, Prague, Czech Republic), with a brass 0.4 mm nozzle diameters was used. All provided experiments for determination of tensile strength of both PLA, was conducted according to ISO 527-2 standard [6]. Shape and specific dimensions of the specimens are presented in figure 5, while series of printed specimens, before and after testing, are shown in figure 6 (antibacterial PLA).

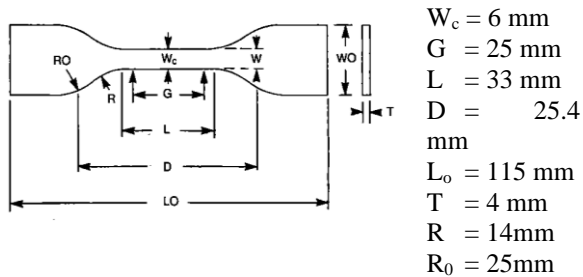


Fig. 5. Dimension and shape of specimen [6]

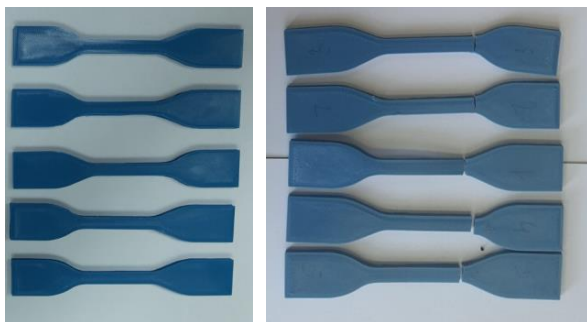


Fig. 6. Specimens before and after testing

Five specimens, for each type of PLA, were fabricated according to settings given in Table 1. Orientation of the specimen positioning on the printer's build plate, as well as schematic representation of raster angle (for better understanding), are given in Figure 7. As can be seen in Figure 7, dominant dimension of the specimens was oriented parallel to the printer's x-axis.

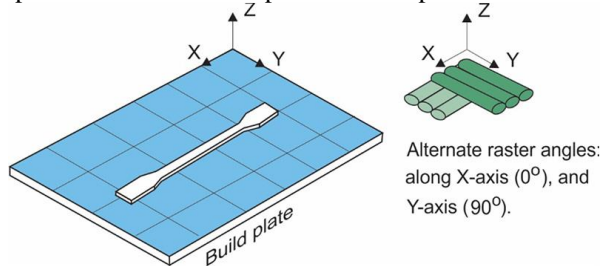


Fig 7. Specimen orientation and raster orientation used in the designed experiment [7]

Adopted process parameters, given in Table 1, were set up in way to eliminated influences of the other significant printing parameters such as raster shape, raster angle, etc. as well as to reduce number of experiments.

Processing parameter	Value
Number of shells	2
Number of top layers	2
Number of bottom layers	2
Raster angle	$0-90^\circ$
Infill	100%
Nozzle temperature	$215^\circ\text{C}$
Build plate temperature	$60^\circ\text{C}$

Table 1. Processing parameters

Universal tester, Ericsen, was used to test the specimens for tensile strength in compliance with the ISO 527-2: 2012 specification (ISO 527-2, 2012). Crosshead speed of 50mm/min was used, while the tests were conducted at  $22^\circ\text{C}$ . For force measuring load cell HBM 2kN was used, and for displacement inductive stroke sensor HBM  $\pm 10 \text{ mm}$ . Spider 8 amplifier and Catman Easy software made a connection between the sensors and computer to make results readable and gives possibility to export results to Excel.

Tensile force and the resulting stress are shown in Table 2. As can be seen from Table 2, there are small difference between the regular and antibacterial PLA. For regular PLA average tensile strength is 51.6 MPa while for antibacterial PLA average value is 51.7 MPa. Compared to declared value for COPPER 3, which is given from manufacturer (53MPa), there is difference about 2% which is not significant and can variate, depending on testing method. For Devil Design PLA is not available value of the tensile strength given by manufacturer, so it will be compared with values from the others authors' research. According to [8,9] values of tensile strength are between 50 and 54 MPa, which is corresponding values obtained in presented research.

No.	PLA		PLA antibacterial	
	F [N]	Rm [MPa]	F [N]	Rm [MPa]
#1	1192.92	49.7	1166.68	48.6
#2	1257.54	52.4	1269.77	52.9
#3	1234.50	51.4	1240.55	51.7
#4	1212.87	50.5	1248.27	52.0
#5	1299.12	54.1	1275.95	53.2
<b>Avg.</b>	<b>1239.39</b>	<b>51.6</b>	<b>1240.25</b>	<b>51.7</b>

Table 2. Tensile force and the resulting stress

### 3. FINAL REMARKS

In presented paper comparison of antimicrobial and mechanical properties of two different type of PLA filaments (antibacterial and regular) were presented. Two different tests were conducted and according to results, given in the paper were revealed following:

- There is no clear difference in the antimicrobial activity of regular and antibacterial PLA. Both PLA decrease the abundance of tested microorganisms.
- A much better effect of the both PLA towards Gram-negative bacteria, where it is possible that the material of the specimens damages the outer membrane comprised of lipopolysaccharides.
- There are not significant differences in values of tensile strength between the regular and antibacterial PLA. Difference between those two variants is less than 0.2%.
- Values of tensile strength for both PLA are very close declared values by manufacturer or results obtained by others authors.

Thru a future research, antimicrobial testing for more different bacteria should be done. Also, test on PLA with nano silver instead of nano copper should be provided, with following of mechanical properties of printed specimens.

### 4. REFERENCES

- [1] Mali H.S., Vasistha S. *Advances in Additive Manufacturing and Joining; Fabrication of Customized Ankle Foot Orthosis (AFO) by Reverse Engineering Using Fused Deposition Modelling*, Springer Nature Singapore Pte Ltd. 2018.
- [2] Walbran M., Turner K., McDaid A.J., *Customized 3D printed ankle-foot orthosis with adaptable carbon fibre composite spring joint*, Cogent Engineering, Vol. 3, No. 1, pp. 1-11, 2016
- [3] Li J., Tanaka H. *Feasibility study applying a parametric model as the design generator for 3D-printed orthosis for fracture immobilization*, 3D Printing in Medicine, Vol. 4, No. 1, 2018.
- [4] Portnova A.A., Mukherjee G., Peters K.M., Yamane A., Steele K.M. *Design of a 3D-printed, open-source wrist-driven orthosis for individuals with spinal cord injury*, PLoS ONE Vol. 13, No 2, 2018
- [5] United States Environmental Protection Agency. *Test Method for Efficacy of Copper Alloy Surfaces as a Sanitizer* (United States Environmental Protection Agency, Washington DC, 2008.
- [6] ISO 527-2, *Plastics – determination of tensile properties – part 2: test conditions for moulding and extrusion plastics*, 2nd ed., 2012.
- [7] Luzanin, O., Movrin, D., Stathopoulos, V., Pandis, P., Radusin, T. and Guduric, V., *Impact of processing parameters on tensile strength, in-process crystallinity and mesostructure in FDM-fabricated PLA specimens*, Rapid Prototyping Journal, Vol. 25 No. 8, pp. 1398-1410, 2019.
- [8] Dobrescu T., Pascu N.E., Jiga G., Simion I., Adir V., Enciu G., Tudose D. *Tensile Behavior of PLA and PLA Composite Materials Under Different Printing Parameters*, Materiale Plastice, Vol. 56 No. 4, pp. 783-800, 2019.
- [9] Vosynek P., Navrat T., Krejbychova A., Palousek D. *Influence of Process Parameters of Printing on Mechanical Properties of Plastic Parts Produced by FDM 3D Printing Technology*, 3<sup>rd</sup> International Conference on Design, Mechanical and Material Engineering (web conference), Chapter 2: Material Engineering, pp. 1-6, 2018.

**Authors: Assist. Prof. Dejan Movrin, Assoc. Prof Mladomir Milutinović**, University of Novi Sad, Faculty of Technical Sciences, Department of Production Engineering, Trg Dositeja Obradovića 6, 21000 Novi Sad, Serbia, Phone.: +381 21 485-23-24, Fax: +381 21 454-495.

E-mail: [movrin@uns.ac.rs](mailto:movrin@uns.ac.rs); [mladomil@uns.ac.rs](mailto:mladomil@uns.ac.rs)

**MSc Diandra Pintać**, University of Novi Sad Faculty of Sciences, Department of Chemistry, Biochemistry and Environmental Protection, Trg Dositeja Obradovića 3, 21000 Novi Sad, Serbia, Phone: + 381 21 485-2755

E-mail: [diandra.pintac@dh.uns.ac.rs](mailto:diandra.pintac@dh.uns.ac.rs)

**Assoc. Prof Petar Knežević**, University of Novi Sad Faculty of Sciences, Department of Biology and Ecology, Trg Dositeja Obradovića 3, 21000 Novi Sad, Serbia, Phone: + 381 21 485-2681

E-mail: [petar.knezevic@dbe.uns.ac.rs](mailto:petar.knezevic@dbe.uns.ac.rs)

**MSc Sanja Kojić**, University of Novi Sad, Faculty of Technical Sciences, Department of Power, Electronic and Telecommunication Engineering, Trg Dositeja Obradovića 6, 21000 Novi Sad, Serbia, Phone: +381 21 485-2557

E-mail: [sanjakojic@uns.ac.rs](mailto:sanjakojic@uns.ac.rs)

**MSc Velibor Premčevski**, University of Novi Sad, Technical Faculty “Mihajlo Pupin”, Đure Đakovića bb, 23101 Zrenjanin, Phone: +381 23 550-515

E-mail: [velibor.premcevski@tfzr.rs](mailto:velibor.premcevski@tfzr.rs)

**ACKNOWLEDGMENTS:** Results of investigation presented in this paper are part of the research realized in the framework of the project “Design of personalized insoles with a sensor system to help rehabilitation of patients“, financed by the Republic of Serbia, Autonomous Province of Vojvodina.

Ćirić Kostić, S., Bogojević, N., Croccolo, D., Olmi, G., Sindelić, V., Šoškić, Z.

## EFFECTS OF MACHINING ON THE FATIGUE STRENGTH OF STEEL COMPONENTS PRODUCED BY DMLS

**Abstract:** Direct metal laser sintering (DMLS) is the additive manufacturing (AM) technology that allows production of metal machine components with complex geometry. Due to the layer-wise production principle, its products usually require post-processing, predominantly machining, to achieve uniform or requested surface quality. Given the increasing application of DMLS technology in industry and insufficient published data about the effects of machining on the fatigue properties of steel, the focus of this research is put to investigation of the influence of thickness of allowance for machining to fatigue strength of DMLS products.

Previous studies revealed significant differences in the mechanical behaviour of samples made of different kinds of steels, both during production and testing. Unlike the samples made from maraging steel, the samples made from stainless steel often deformed during cooling due to the strong residual stresses, and revealed dependence of mechanical properties on orientation during production process.

To improve the understanding of the differences, fatigue testing according to ISO 1143 was performed on samples manufactured from two kinds of steel, maraging steel 1.2709 and stainless steel 15-5. Twelve sets of samples were tested with the aim to investigate the effects of machining allowance and build orientation according to an extensive DoE experimental plan.

**Key words:** Additive manufacturing, fatigue strength, machining allowance, build orientation

### 1. INTRODUCTION

The paper presents a part of research related to the Horizon 2020 project "Advanced design rules for optimal dynamic properties of additive manufacturing products - A\_MADAM", which represents a systematic study of fatigue behaviour of steel parts produced by Direct Metal Laser Sintering (DMLS) technology.

DMLS belongs to family of powder bed fusion (PBF) additive manufacturing (AM) technologies, where a product consist of subsequent layers, which are obtained by melting of powder particles. During the fast process of melting and cooling, the new layer is joined to the previous layer of the product. The melting is performed by focused laser beam, and the produced heat causes high temperature gradients in material during the manufacturing (also called "building") of the product. It is clear that the bonds within a layer and between the layers are not of the same strength, and the anisotropy of the produced material is reduced by heat treatment of the products.

The aim of the A\_MADAM project is to establish design rules for the best fatigue performances of DMLS parts. The interest for fatigue behaviour is driven by increasing production of lightweight, shape-integrated and optimized components in automotive and aerospace applications, which are known to subject the machine parts to dynamic loads. For these reasons, the previous research of the fatigue behaviour were focused to light metals and their alloys, in particular aluminium, magnesium and titanium. However, DMLS is also used in tooling applications, and the advanced tools are made from DMLS steels. Finally, DMLS is used also for production of advanced medical tools from stainless steel, and that were the reasons who motivated the research in the A\_MADAM project.

### 2. EXPERIMENT

#### 2.1. Material and specimen

Specimens were designed according to the experimental plan for testing campaign that comprised rotating bending following the ISO1143 [1] standard. The smallest dimension allowed by the standard, with diameter at gauge 6 mm, was chosen to reduce production costs. A drawing of the specimen with indication of all its dimensions and tolerances is shown in Fig. 1.

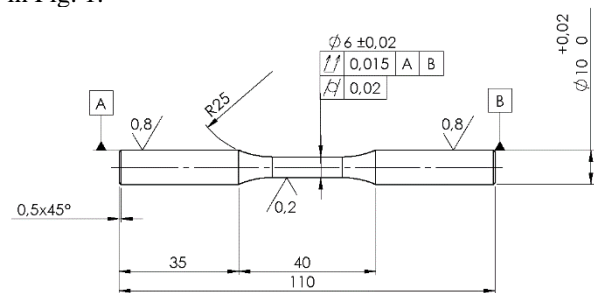


Fig. 1. Specimen with 6 mm diameter at gauge in agreement with ISO 1143 standard [1]

The experimental campaign involved two steels with chemical compositions given in Table 1: the maraging steel EOS MS1, equivalent to DIN 1.2709 [2], and the stainless steel EOS PH1 equivalent to DIN 1.4540 [2]. The experiments for each of the two materials were arranged using a 3-by-2 scheme, with three levels for the building orientation (horizontal (H), vertical (V) and slanted (S) (with an angle of 45 degrees to the base plate), and two levels for thickness of allowance (0.5 mm and 3mm for PH1 and 1mm and 3mm for MS1), with a total of 2x(3x2) specimen sets and 109

specimens. The complete experimental plan is summarized in Table 1. Each of the sets consisted of 7 to 13 specimens. The number of specimens in each of the sets is also reported in Table 1.

The specimens were manufactured by DMLS machine EOSINT M280 equipped with Ytterbium fibre laser with 200 W power and emitting 0.2032 mm thickness and 1064 nm wavelength infrared light beam. The process takes place in an inert environment and the scanning speed may range up to 7000 mm/s. The production chamber machine has a horizontal baseplate with dimensions 250×250 mm, and a production height of 325 mm.

Knowing that the materials and DMLS technology are relatively new, and wishing that the results of this research be used by majority of users of DMLS technology, the applied process parameters were selected according to the standard recommendations of manufacturer of the material. In particular, the layer thickness was set to 20 μm for the stainless steel (EOS “Surface” set of the parameters) and 40 μm for maraging steel (EOS “Performance” set of the parameters). A parallel scan strategy with alternating scan direction was adopted. Between the subsequent layers, the scanning direction was rotated by approximately 70°, in order to prevent or reduce in-plane property variations.

		Material				
		Thickness of allowance for machining				
		PH1		MS1		
Orientation of the longitudinal axis	Horizontal	1 mm	3 mm	0.5 mm	3 mm	
			PH <sub>H1</sub> 7 sp.	PH <sub>H3</sub> 9 sp.	MS <sub>H0.5</sub> 7 sp.	MS <sub>V3</sub> 10 sp.
	Vertical		PH <sub>V1</sub> 10 sp.	PH <sub>V3</sub> 10 sp.	MS <sub>V0.5</sub> 7 sp.	MS <sub>H3</sub> 13 sp.
		Slanted		PH <sub>S1</sub> 10 sp.	PH <sub>S3</sub> 9 sp.	MS <sub>S0.5</sub> 7 sp.

Table 1. Design of the experimental campaign (DoE)

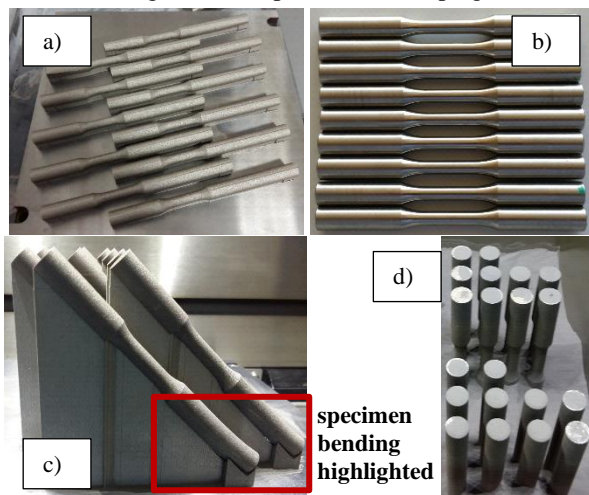


Fig. 2. Chosen stages of PH1 specimens' production: a) Set PH<sub>H1</sub> after DMLS process, b) Set PH<sub>H3</sub> after machining and finishing, c) Set PH<sub>S1</sub> before detachment, d) Sets PH<sub>V1</sub> and PH<sub>V3</sub> during residual powder removal

During the building process, the samples were connected to the base plate with the support structures. These structures have double role: to transfer the heat from the laser scanning area to base plate, and to keep the parts at fixed positions during the manufacturing process.

After the manufacturing by DMLS process, the samples were treated by micro-shot-peening by steel spheres with diameter of approximately 0.7 mm, under 5-bar flow pressure, for the purposes of cleaning of residual powder, closing the pores and improvement of the surface quality. After that, they were heat-treated according to the EOS materials data sheet recommendations [2]. MS1 specimens were exposed to temperature of 490°C for 6 hours, while the PH1 specimens were exposed to temperature of 482°C for 3 hours. After cooling process in fresh air, the specimens were removed from the building plate using wire electro discharge machine, and then, underwent machining and refining by grinding with the aim of achieving the roughness, dimensional specifications and improving of the fatigue performance. Figure 2 shows chosen stages of the manufacturing process.

The production of PH1 specimens required considerably more efforts and resources than production of MS1 specimens because of the large tensile residual stresses, caused by higher temperature gradients during production of PH1 and higher thermal expansion coefficients of PH1. The temperature gradients in DMLS production of PH1 are higher because the thicknesses of layers are twice smaller. As a result, some PH1 specimens bent and even detached from the supports, remaining permanently deformed (Fig.2c).

## 2.2. Test procedures

The aim of fatigue testing was to determine the S-N curves and the fatigue limits (FL) for each of the sets of specimens. The 4-point rotary bending tests with load ratio R=-1 and frequency of 60 Hz were performed. The initial stages of testing of each of the sets was aimed at determining fatigue behaviour in finite life domain by S-N curve. A life duration of 10<sup>7</sup> cycles was set as run-out. The results in the finite life domain were analysed according to the Standard ISO 12107 standard [4]. The staircase method was then used to determine the fatigue limit (FL). For this purpose, the series of failure and not-failure events was processed by the Dixon method [3].

Before the fatigue testing, according to the standard 1143, hardness, dimensions and roughness of the samples were measured. At the end of the experimental campaigns, fractographic and micrographic analyses were performed with two aims: 1) to identify of the crack nucleation point and of the zones of stable and unstable crack propagation, and 2) investigation of the possible presence of porosities, inclusions, spots of oxides and micro-cracks [5, 6].

## 3. SUMMARY OF RESULTS AND DISCUSSION

The obtained results have been statistically processed by the ANOVA method to assess the influence of the two observed factors and their interaction. The effects of the building orientation are presented in other research papers [5, 6] and in this paper we shortly discuss the influence of the thickness of allowance for machining.

Figures 3 and 4 show the graphs with fatigue curves in the finite life domain for all tested sets, presented by material type and levels of the DoE plan. The fatigue



limits are presented by material type in bar graphs in Figure 5.

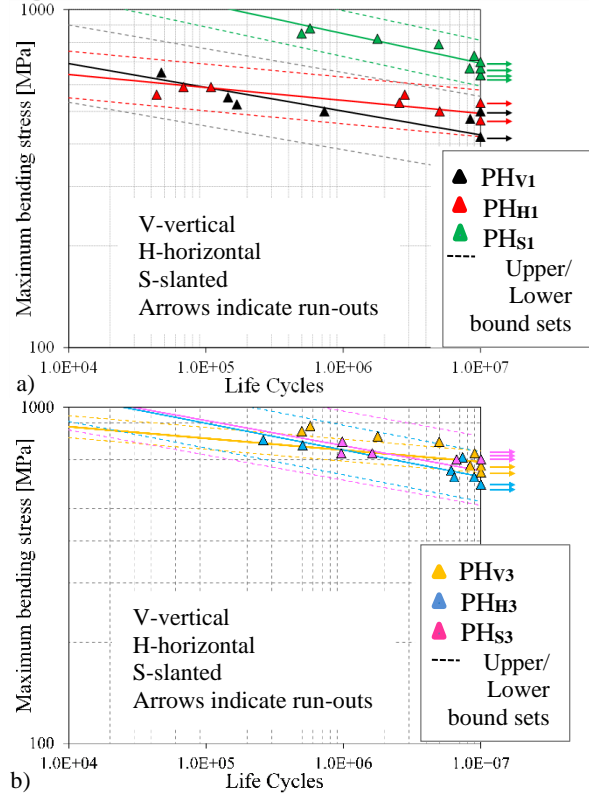


Fig. 3. S-N curves in the finite life domain for 3+3 sets of specimens manufactured from PH1 (two-factor design for one allowance level): a) allowance is 1 mm, and b) allowance is 3 mm

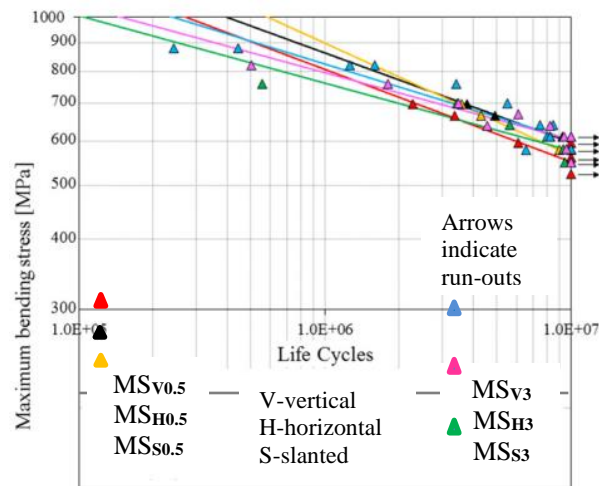


Fig. 4. S-N curves in the finite life domain for six specimens sets from MS1 (two-factor design for two allowance levels, 0.5 and 3 mm)

The results of the ANOVA analyses have shown that all the differences between the data describing different sets of maraging steel MS1 are negligible (3% significance level), meaning that the two factors do not have significant influences and that no interaction occurs. The ANOVA table for two factor design regarding maraging steel MS1 is given in top part of Table 2, and high levels of  $p$  ( $\gg 0,005$ ) indicate the insignificance of the studied factors. The result means that the heat treated maraging steel MS1 has an isotropic fatigue behaviour and that its fatigue response does not exhibit any significant variation for different thicknesses

of machining. The average value of the fatigue limit, involving all six sets, is 590 MPa, corresponding to 29% of the ultimate tensile stress (UTS) of the studied material following the heat treatment.

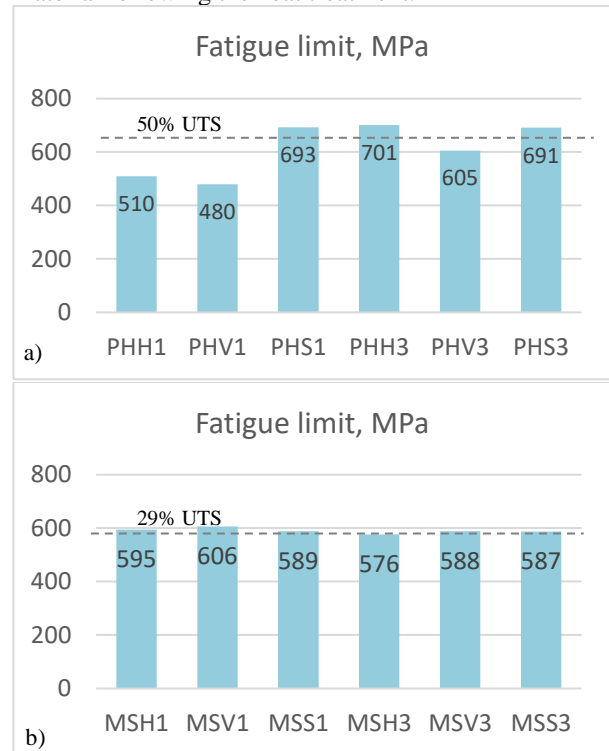


Fig. 5. Bar graph summarizing the fatigue limits for the six specimen types: a) stainless steel PH1, b) maraging steel MS1

	Factor	$p$
MS1	Orientation – 3 levels vertical-horizontal-slanted	0,65
	Thickness of allowance	0,04
	Interaction	0,28
PH1	Orientation – 3 levels vertical-horizontal-slanted	$4.0 \cdot 10^{-5}$
	Thickness of allowance	$3.1 \cdot 10^{-4}$
	Interaction	$3.4 \cdot 10^{-4}$
PH1	Orientation – 2 levels vertical-horizontal	0.45
	Thickness of allowance	$1.9 \cdot 10^{-5}$
	Interaction	0.22

Table 2. Two-factor ANOVA analysis

Conversely, the analyses of the results for samples sets made of stainless steel PH1 indicate that both of studied factors have influence on fatigue response. The results of two-factor ANOVA analysis with 3 orientation levels and 2 levels of allowance for the PH1 stainless steel is summarized in Table 1-middle, where low values

of p in the last column indicate that both of the factors and their interaction are highly significant. If ANOVA analysis is applied to the 2x2 scheme that excludes the slanted specimens (Table 2-down), then significance of the building orientation ceases (and so does the interaction of factors), while the thickness of allowance retains its high significance. This result confirms the influence of the thickness of the allowance for machining, and indicates the differences due to building orientation appear only when slanted specimens are taken into account. It should be noticed that increase of thickness of allowance for machining generally has the effect of increasing the fatigue limit (Fig.6 -right).

A probable reason for improvement of fatigue resistance of PH1 made by DMLS with increase of the thickness of allowance for machining could be removal of the surface layers with high residual stresses (Fig.2). The detrimental effects of residual stresses to fatigue behaviour are well known and documented [7].

Finally, it should be pointed out that the optimization of the considered factors leads to a fatigue strength that is compares favourably to that of wrought material, with ratio between the fatigue limit and the ultimate tensile strength being over 50%.

#### 4. CONCLUSIONS

The paper discusses the influence of the machining to fatigue strength of steels manufactured by DMLS. The study is based on fatigues testing of specimens of two different kinds of steels, stainless steel PH1 and maraging steel MS1 which were manufactured with different levels of thicknesses for allowance for machining: 1 and 3 mm for PH1 and 0.5 and 3 mm for MS1. Since the DMLS production is essentially an anisotropic process, the testing sets had also to consider variation of the building direction of the samples. Specimens belonging to individual sets were manufactured simultaneously, and all the specimens underwent micro-shot-peening and heat treatment recommended by manufacturer of the material.

The obtained results were analysed using ANOVA methodology, and the results have shown that machining has different influences to different types of steel. While the thickness of allowance increases fatigue strength of the stainless steel PH1 in finite life domain and FL, at least in the range of thicknesses 1-3 mm, the influence of thickness of allowance in the range 0.5-3 mm to fatigue behaviour of maraging steel MS1 could not be established.

Since the fatigue behaviour of steels is driven by surface quality, presence of the defects in microstructure and residual stresses, the obtained results suggest that the positive influence of thickness for machining is related to removal of the surface layers with internal stresses. Furthermore, the difference of influences of thickness of allowance for machining to different types of steels suggests that the factors that influence residual stresses, such as thermal expansion coefficients and thickness of the layers, should be carefully considered when fatigue behaviour of materials manufactured by DMLS is of interest.

#### 5. REFERENCES

- [1] International Organization for Standardization ISO 1143:2010, Standard - Metallic materials – Rotating bar bending fatigue testing, International Organization for Standardization (ISO), Geneva, Switzerland, 2010.
- [2] <https://www.eos.info/material-m> , last accessed 2021/07/10
- [3] Dixon, W. J., Massey, F. J.: *Introduction to statistical analysis*, Vol. 344, New York: McGraw-Hill, 1969.
- [4] International organization for standardization ISO 12107:2012. Metallic Materials – Fatigue Testing – Statistical Planning and Analysis of Data. Geneva, Switzerland: International Organization for Standardization (ISO); 2012.
- [5] Croccolo, D., De Agostinis, M., Fini, S., Olmi, G., Bogojevic, N., Ćirić-Kostić, S.: *Effects of build orientation and thickness of allowance on the fatigue behaviour of 15–5 PH stainless steel manufactured by DMLS*, Fatigue and Fracture of Engineering Materials and Structures, Vo. 41, pp. 900–916, 2018
- [6] Croccolo, D., De Agostinis, M., Fini, S., Olmi, Robusto, F., Ćirić-Kostić, S., Morača, S., Bogojević, N.: *Sensitivity of direct metal laser sintering Maraging steel fatigue strength to build orientation and allowance for machining*, Fatigue and Fracture of Engineering Materials and Structures, Vol.42, Iss.1, pp.374–386, 2019.
- [7] Loehe, D., Lang K.-H., Voehringer, O. *Residual stresses and fatigue behavior*. In: Totten GE, editor. Handbook of residual stress and deformation of steel. ASM international; 2002.

**Authors: Assoc. Prof. Snežana Ćirić Kostić, Assoc. Prof. Nebojša Bogojević, M.Sc. Vladimir Sindelić, Full Prof. Zlatan Šoškić**, University of Kragujevac, Faculty of Mechanical and Civil Engineering in Kraljevo, Dositejeva 19, 36000 Kraljevo, Serbia, Phone.: +381 36 383-380, Fax: +381 36 383-269.

E-mail: [cirickostic.s@mfkv.kg.ac.rs](mailto:cirickostic.s@mfkv.kg.ac.rs);

[bogojevic.n@mfkv.kg.ac.rs](mailto:bogojevic.n@mfkv.kg.ac.rs);

[sindjelic.v@mfkv.kg.ac.rs](mailto:sindjelic.v@mfkv.kg.ac.rs); [soskic.z@mfkv.kg.ac.rs](mailto:soskic.z@mfkv.kg.ac.rs)

**Full Prof. Dario Croccolo, Associate Prof. Giorgio Olmi**, University of Bologna, Department of Industrial Engineering (DIN)- Viale Risorgimento, 2 40136 Bologna, Italy, Phone.: +390 51 20-93413, Fax: +390 51 20-93413.

E-mail: [dario.croccolo@unibo.it](mailto:dario.croccolo@unibo.it); [giorgio.olmi@unibo.it](mailto:giorgio.olmi@unibo.it)

#### ACKNOWLEDGMENTS:

The research presented in this paper has received funding from the European Union's Horizon 2020 research and innovation programme under the Marie Skłodowska-Curie grant agreement No. 734455.

The authors also wish to acknowledge the support of Ministry of Education, Science and Technology Development of Republic of Serbia through Grant 451-03-9/2021-14/200108.

Sabotin, I., Jerman, M., Lebar, A., Valentinčič, J., Böttger, T., Kühnel, L., Zeidler, H.

## EFFECTS OF PLASMA ELECTROLYTIC POLISHING ON SLM PRINTED MICROFLUIDIC PLATFORM

**Abstract:** Additive manufacturing (AM) of metallic parts is gaining momentum in production industries. In view of producing a metal microproduct using AM the issue of high surface roughness is prominent. Plasma electrolytic Polishing (PeP) is a post processing technology that greatly reduces surface roughness of metallic parts. In this paper the effects of PeP of microfluidic platform, printed with selective laser melting (SLM) technology, is presented. The results show that surface roughness of the specimens was severely reduced. Also, some geometrical defects inherent to SLM technology were partly removed. It is shown, that for smaller geometrical microfeatures (sizes of less than 0.5 mm) the effectiveness of PeP is reduced. Through this investigation it can be concluded that PeP is a promising post-processing technology for SLM printed microparts since it significantly improves the overall part quality. However, further improvements of the process chain need to be implemented in order to render the microfluidic platform functional.

**Key words:** selective laser melting, plasma electrolytic polishing, microfluidics, additive manufacturing

### 1. INTRODUCTION

In the past two decades Additive Manufacturing (AM), popularly denoted as 3D printing, gained significant interest and has been spoken of as a disruptive technology. With AM technology predominantly polymer based materials as well as metallic materials can be manufactured. In AM a part is built stepwise in a layer by layer fashion. Since in the process of building the part the material is added, it opens up the possibility to complex part designs which cannot be manufactured by subtractive processes. AM also enables short lead-times at relatively low costs. Nowadays, AM has been successfully utilized in many areas such as aerospace, automotive, electronics, medical and biomedical industries where highly specialized and customizable parts are required [1,2].

Microfluidics is a research field that greatly embraced the AM technologies. The attraction stems from two aspects of AM technologies [1]. The first aspect relates to the ability to produce truly three-dimensional features. The second aspect relates to the ability to rapidly realize a 3D microfluidic device from constructed 3D model. This enables researchers to adopt the strategy of “fail fast and often”. Presently used AM technologies in microfluidics are inkjet 3D printing, fused deposition modelling, stereolithography and two photon polymerisation. Enlisted technologies are predominantly polymer based.

On the other hand the utilization of metallic materials in microproducts has gained momentum, largely due to its superior properties in view of microproduct performance [3]. Steel microfluidic platforms have several benefits over polymer based such as high robustness, being operational under elevated temperatures and pressures, compatibility with organic solvents and yielding high thermal conductivity coefficients [4].

Among the AM technologies that can print metallic

parts direct energy deposition (DED), selective laser sintering (SLS) and selective laser melting (SLM) are the most promising to be utilized in future microfluidic applications [5]. In the view of their implementation SLM has some advantages compared to the former two. SLM exhibits better resolution than DED and it does not need additional processing step, namely sintering, as it is the case with SLS.

SLM is a powder-bed fusion process. A layer of powder is first spread on the build substrate. In the next step laser beam scans the area related to the particular slice of the part geometry. The exerted heat melts the powder which after solidification joins with the adjacent regions and forms a solid metallic layer. In the next step a new layer of powder is applied to the part surface by a powder-recoating system and the lasers scans the region of the next part geometry slice. The process is repeated until the whole part is built.

An inherent disadvantage of SLM as well as for all metallic AM technologies is the achievable surface quality. Namely, partial melting and/or agglomeration of powder on the surrounding regions of the melt pool leads to high roughness in the range of 10  $\mu\text{m}$  to 30  $\mu\text{m}$  of Ra [6]. For many applications, and especially in microfluidics, these values are inadequate, thus surface finishing is required. A promising surface finish technology is plasma electrolytic polishing (PeP) [7].

PeP has gained attention in the metal finishing industry due to its capability to considerably enhance surface properties [8]. PeP is an innovative surface treatment, which renders smooth, high-gloss surfaces with improved corrosion resistance. The process is primarily determined by the dissolution of the anode (the workpiece) and plasma-chemical reactions. Commonly, the part to be polished is immersed in the electrolyte bath and DC current is applied between the anode/part and cathode. Advantageous aspects of PeP stem from being able to process complex 3D-shaped parts simultaneously over its entire surface and the use of environmentally

friendly aqueous electrolytes. The processing temperature at the part surface does not exceed the electrolyte boiling temperature which is below 120 °C.

In this paper a process chain for microfluidic platform consisting of SLM printing and PeP post processing is evaluated through dimensional characterization. Geometrical features of the planar microfluidic platform consist of microchannels and microgrooves, embedded on the microchannel floor, which are commonly applied in bottom groove micromixers.

## 2. MATERIALS AND METHODS

### 2.1. SLM 3D printer

For 3D printing of sample microfluidic platforms EOS M 290 SLM printer based on powder-bed fusion was used. It utilises Yb-fibre laser with maximum beam power of 400 W and a laser focus point of 100 µm. Materialise Magics Metal Package and EOSPRINT software was used for CAD/CAM settings.

### 2.2. SLM printing process parameters

Default process parameters suggested by the CAD/CAM software considering the material and layer depth were applied: laser beam power of 285 W, scanning speed of 960 mm/s, line ‘stripes’ scanning strategy, hatch spacing of 0.11 mm, powder layer depth of 0.04 mm, N<sub>2</sub> working atmosphere (cca. 0.15% O<sub>2</sub>) and the thickness of support layers of 5 mm. EOS Maraging Steel MS1 powder material was used (X3NiCoMoTi 18-9-5) with a predicted relative density of parts of 8.0 g/cm<sup>3</sup>.

Three specimens were printed with the same parameters the only difference being the orientation of the parts in *xy*-axis of the powder bed. Specimen 1 was oriented with microfeatures being aligned with the *x*-axis, microfeatures of specimen 2 were parallel to *y*-axis and specimen 3 was tilted for 45° with respect to the specimen 1.

### 2.3. PeP setup and process parameters

A Pilot plant vat/immersion based PeP machine with a maximum output current of 150 A was used (Fig. 1a). A stainless-steel vat (max. volume of 200 l) was used as a cathode and a spring clamp was holding the specimen immersed in the electrolyte (Fig. 1b).



Fig. 1. Pilot plant PeP machine. b) Holder for the specimen.

The previously obtained process parameters for used material to achieve high material removal rate, low surface roughness and high brightness were applied. The

used electrolyte was a water solution of ammonium sulphate (0.33 M). The temperature of the electrolyte was kept at 80°C and the specimen was anodically polarized, to sustain the current density of about 0.2 A/cm<sup>2</sup>, with the voltage of 350 V. The first specimen was treated for 10 min, the second for 15 min and the third for 20 min.

### 2.4. Microfluidic platform geometry

The design of microfeatures of the microfluidic platform is consistent with the feature shapes that are commonly applied in bottom grooved micromixers. The characteristic grooves at the bottom of the microchannel are either slanted at an angle of 45° with respect to the microchannel (so called slanted grooves - SG) or in a shape of a staggered herringbone (so called herringbone grooves – SH) (Fig. 2).

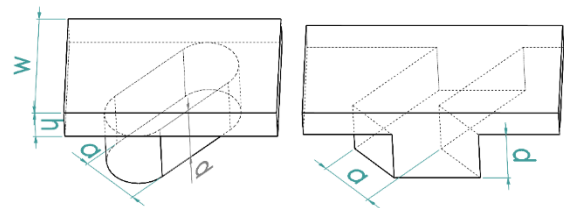


Fig. 2. The shape of a SG (left) and SH (right) grooves. Denotations of geometries are also presented.

The optimal aspect ratios of grooves (*d/a*) are a function of the microchannel aspect ratio (*h/w*) and were determined from research papers [9,10]. One should note, that the optimal aspect ratio of a SH groove is smaller compared to optimal SG groove.

Three sizes (L, M, S) of sample micromixer geometries were incorporated in the specimen design (Fig. 3). The dimensions of geometries are gathered in Table 1. Depths of features were set so, that they correspond to a multiplier of a single layer powder depth of 40 µm.

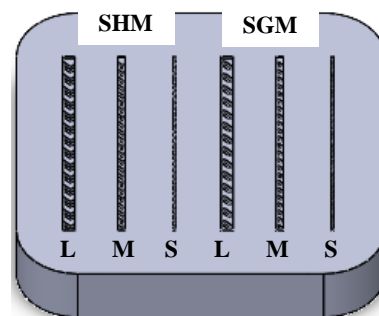


Fig. 3. 3D model of a microfluidic specimen (30x30x3 mm) with denotations: SHM – staggered herringbone micromixer design, SGM – slanted groove micromixer design.

Samples of groove micromixer geometries were modelled as parallel microchannels with descending sizes from large (L) to small (S).

### 2.5. Measurements

Characterisation measurements were conducted on a Keyence VHX-6000 digital microscope. The 3D surface was acquired using depth composition function. Profile roughness (*Ra*) was determined by MarSurf PS 10 profilometer.

Variant	Microfeature			
	w [ $\mu\text{m}$ ]	h [ $\mu\text{m}$ ]	a [ $\mu\text{m}$ ]	d [ $\mu\text{m}$ ]
SGM-L	1000	280	500	480
SGM-M	600	160	300	320
SGM-S	200	80	100	80
SHM-L	1000	280	500	400
SHM-M	600	160	300	240
SHM-S	200	80	100	80

Table 1. Nominal dimensions of micromixer designs

### 3. RESULTS AND DISCUSSION

#### 3.1. SLM printed specimens

The first observation of printed microfluidic platforms is, that different orientation of the parts on the machine  $xy$  table did not result in different print quality. This is due to the fact, that the laser trajectory at microfeature edges follows the edge contour, thus bulk hatch orientation influences only larger surfaces not crucial for microfeature geometries. Correspondingly, all the edges of microfeatures have a ridge of approximate height of  $\sim 10 \mu\text{m}$ .

As expected, larger (L) micromixer designs are printed with better geometrical quality (Fig. 4a,d). However, solidified microspheres with the diameter of used metal dust can be observed on the side walls of the microchannel and in the grooves (Fig. 5). Middle (M) sized designs are printed with bigger defects. In the grooves often a micropillar is present, which is a consequence of agglomerated resolidified dust particles (Fig. 6(left)). The explanation of mentioned artefacts lies in presence of dust particles near the edges of microfeatures which should not be melted by laser beam, however, they are melted due to excess heat. For the smallest designs (S) the microgrooves are below the printer's resolution (e.g. diameter of laser focus point is  $100 \mu\text{m}$ ) thus, they are printed into shapes that hardly correspond to a groove (Fig. 4c,f). Corresponding microchannels are printed more reliably with high relative width deviation.

The surface roughness was measured in the middle part of the specimens. The  $R_a$  value for all three specimens was measured to be  $18.5 \pm 0.4 \mu\text{m}$ , which is in a typical range for SLM printed parts. This roughness exceeds the values for typical microfluidic applications ( $R_a < 1 \mu\text{m}$ ) by a lot, thus specimens were subjected to PeP treatment to reduce it.

#### 3.2. Specimens after PeP treatment

At larger micromixer designs even after the shortest PeP treatment (specimen 1) significant improvement of the microfeatures quality is observed. Formed microspheres at the edges and on the bottom of the grooves were removed (Fig. 5). This is because higher electric field is present at pointy artefacts thus the PeP process removes them. Also, the waviness due to the laser scanning hatch pattern got severely reduced. Similar observations can be made with regards to medium sized microfeatures. Furthermore, the occasional micropillars within the grooves were also removed by the PeP as is evident from Fig. 6. However, a damaging effect of PeP can be observed on groove edges where excessive material removal occurred.

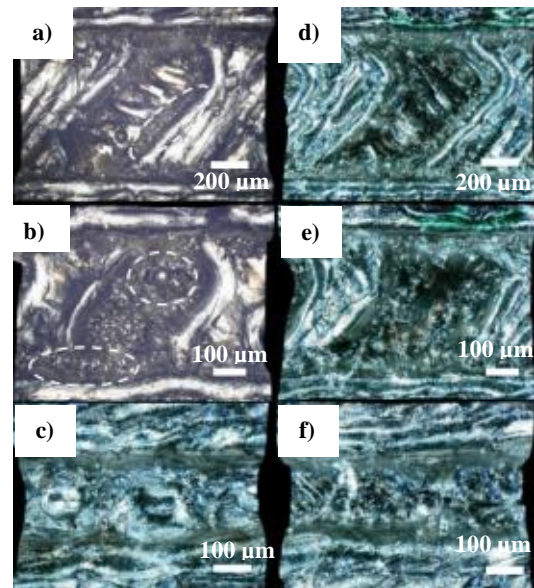


Fig. 4. Microscope images of single grooves (specimen 1). a) SG-L, dashed ellipse highlights solidified spheres, b) SG-M, in the groove a micropillar and solidified spheres at the channel edge are highlighted, c) SG-S, d) SH-L, e) SH-M and f) SH-S.

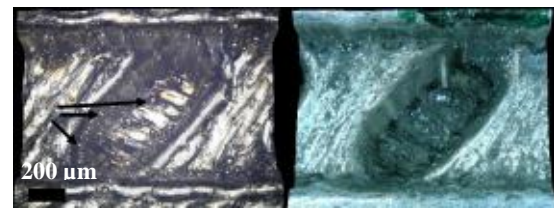


Fig. 5. Pre (left) and post (right) PeP treated specimen 1 detail (SG-L). The arrows point to solidified microspheres at the side and bottom of the groove.

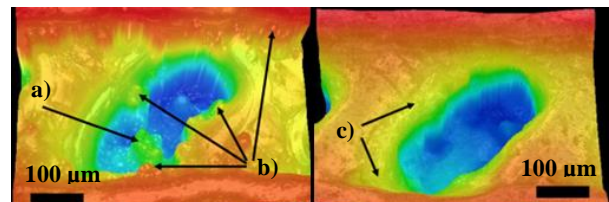


Fig. 6. A colored height microscopic image of a SG-M groove before (left) PeP treatment. Arrows a) point at a micropillar and b) at microspheres at the microfeature edges. SG-M groove after PeP treatment (right). Arrows c) point at excessive erosion at groove edge.

The influence of the PeP treatment duration can be extrapolated from Fig. 7. After shortest treatment time (10 min, Fig. 7b) the effects are consistent with above observations, namely, the microspheres and possible micropillars were eroded.

Longer PeP treatment (15 min, Fig. 7c) resulted in significant material removal also at the main channel side walls. 20 min PeP treatment (Fig. 7d) resulted in greater deterioration at the microchannel side walls. Furthermore, microcracks appeared at the groove edges and bottom.

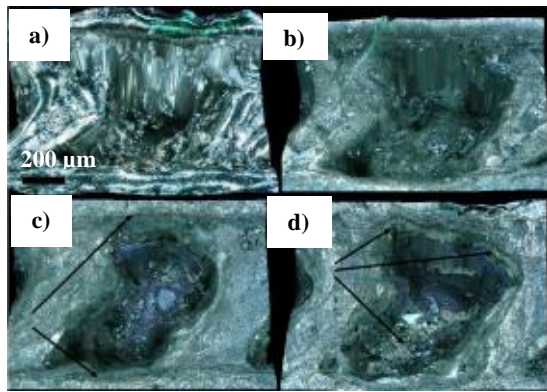


Fig. 7. SH-M grooves after PeP treatment. a) Untreated groove (specimen 1), b) PeP treated for 10 min (specimen 1), c) 15 min (specimen 2) where arrows point at microchannel wall material removal and d) 20 min (specimen 3), where arrows point to microcracks at the edge and the bottom of the groove.

The roughness on the flat surfaces of specimens was significantly reduced. Similar Ra values were measured on all three specimens regardless of the PeP treatment duration. For specimen 1 average roughness value was  $2.7 \pm 0.3 \mu\text{m}$ , for specimen 2  $2.8 \pm 0.3 \mu\text{m}$  and specimen 3  $2.5 \pm 0.3 \mu\text{m}$ . This means that the shortest PeP treatment was the best option since low frequency waviness of the pre-treated parts is harder to remove. However, the roughness still exceeds the values acceptable in microfluidics.

#### 4. CONCLUSIONS

In this paper, the influence of PeP treatment of SLM printed microfluidic platforms is presented. The results show that PeP treatment significantly improves microfeatures quality by removing resolidified microspheres at the feature edges and reduces overall roughness. Even the occasional occurrence of micropillar artefacts in the medium sized grooves were removed. Three durations of PeP were tested and the shortest treatment has proved to be the best. At longer PeP times, the edges of the microfeatures got eroded and there is a possibility of material surface microcracking.

This brief investigation shows, that PeP is a promising post-treatment technology which can improve the SLM printed microfluidic platforms quality.

#### 5. REFERENCES

- [1] Waheed, S., Cabot, J. M., Macdonald, N. P., Lewis, T., Guijt, R. M., Paull, B., and Breadmore, M. C., 2016, *3D Printed Microfluidic Devices: Enablers and Barriers*, Lab Chip, 16(11), pp. 1993–2013.
- [2] Guo, N., and Leu, M. C., 2013, *Additive Manufacturing: Technology, Applications and Research Needs*, Front. Mech. Eng., 8(3), pp. 215–243.
- [3] Alting, L., Kimura, F., Hansen, H. N., and Bissacco, G., 2003, *Micro Engineering*, CIRP Ann. - Manuf. Technol., 52(2), pp. 635–657.
- [4] Gjuraj, E., Kongoli, R., and Shore, G., 2012, *Combination of Flow Reactors with Microwave-Assisted Synthesis: Smart Engineering Concept for*

*Steering Synthetic Chemistry on the 'Fast Lane,'* Chem. Biochem. Eng. Q., 26(3), pp. 285–307.

- [5] Nagarajan, B., Hu, Z., Song, X., Zhai, W., and Wei, J., 2019, *Development of Micro Selective Laser Melting: The State of the Art and Future Perspectives*, Engineering, 5(4), pp. 702–720.
- [6] Zeidler, H., Böttger-Hiller, F., Krinke, S., Parenti, P., and Annoni, M., 2019, *Surface Finish of Additively Manufactured Parts Using Plasma Electrolytic Polishing*, 19th International Conference and Exhibition, EUSPEN 2019, pp. 228–229.
- [7] Zeidler, H., and Böttger-Hiller, F., 2018, *Surface Finish of Additively Manufactured Parts Using Plasma Electrolytic Polishing*, WCMNM 2018, J. Valentinčič, M.B.-G. Jun, K. Dohda, and S.S. Dimov, eds., Research Publishing, Singapore, Portorož, Slovenia.
- [8] Parfenov, E. V., Yerokhin, A., Nevyantseva, R. R., Gorbatkov, M. V., Liang, C. J., and Matthews, A., 2015, *Towards Smart Electrolytic Plasma Technologies: An Overview of Methodological Approaches to Process Modelling*, Surf. Coatings Technol., 269(1), pp. 2–22.
- [9] Sabotin, I., Tristo, G., Junkar, M., and Valentinčič, J., 2013, *Two-Step Design Protocol for Patterned Groove Micromixers*, Chem. Eng. Res. Des., 91(5).
- [10] Lynn, N. S., and Dandy, D. S., 2007, *Geometrical Optimization of Helical Flow in Grooved Micromixers*, Lab Chip, 7(5), pp. 580–587.

**Authors:** Tch. Asst. PhD. Izidor Sabotin, Res. Assoc. PhD. Marko Jerman, Asst. Prof. Andrej Lebar, Assoc. Prof. Joško Valentinčič, University of Ljubljana, Faculty of Mechanical Engineering, Chair of Manufacturing Technologies and Systems, Aškerčeva ulica 6, 1000 Ljubljana, Slovenia, Phone.: +386 1 477-17-74.

E-mail: [izidor.sabotin@fs.uni-lj.si](mailto:izidor.sabotin@fs.uni-lj.si);

[marko.jerman@fs.uni-lj.si](mailto:marko.jerman@fs.uni-lj.si), [andrej.lebar@fs.uni-lj.si](mailto:andrej.lebar@fs.uni-lj.si);

[jv@fs.uni-lj.si](mailto:jv@fs.uni-lj.si)

**Res. Assoc. Toni Böttger, Res. Assoc. PhD. Lisa Kühnel, Prof. Henning Zeidler**, Technical University Bergakademie Freiberg, IMKF, Chair of Additive Manufacturing, Agricolastrasse 1, 09599 Freiberg, Germany,

Beckmann-Institut für Technologieentwicklung, Annaberger Strasse 73, 09111 Chemnitz, Germany

E-mail: [Toni.Boettger@imkf.tu-freiberg.de](mailto:Toni.Boettger@imkf.tu-freiberg.de);

[Lisa.Kuehnel@imkf.tu-freiberg.de](mailto:Lisa.Kuehnel@imkf.tu-freiberg.de);

[Henning.Zeidler@imkf.tu-freiberg.de](mailto:Henning.Zeidler@imkf.tu-freiberg.de)

**ACKNOWLEDGMENTS:** This work was supported by the Slovenian Research Agency (ARRS) (Grant No. P2-0248 (B)) and EU EC H2020 funded Era Chair of Micro Process Engineering and Technology – COMPETE (Grant No. 811040). Authors wish to thank Boštjan Podlipec and SiEVA ltd. for providing resources for SLM printing.

# **MMA 2021**

---

**FLEXIBLE TECHNOLOGIES**

## **AUTHOR INDEX**





## Author Index

### A

Adamović Savka ..... 177  
Agarski Boris ..... 193  
Aleksić Anđelko ..... 49, 59  
Anania Florea Dorel ..... 107  
Antić Aco ..... 45, 59, 151  
Arandjelović Jovan ..... 127

### B

Baloš Sebastian ..... 167, 177, 181  
Banciu Felicia Veronica ..... 37, 123  
Barač Marina ..... 205  
Baralić Jelena ..... 53  
Baraze Abdoul Razak Ibrahim ..... 223  
Benić Juraj ..... 185  
Bisu Claudiu Florinel ..... 107  
Blagojević Vladislav ..... 135  
Bobić Zoran ..... 155  
Bogojević Nebojša ..... 237  
Borojević Stevo ..... 31  
Böttger Toni ..... 241  
Brendle Jocelyne ..... 223  
Budak Erhan ..... 1  
Budak Igor ..... 87, 193  
But Adrian ..... 107, 143

### C

Cajner Hrvoje ..... 131  
Canarache Marian Radu ..... 107, 143  
Carpanzano Emanuele ..... 3  
Cekić Erić Olivera ..... 167  
Chabrol Grégoire Robert ..... 223  
Cigić Lovro ..... 197  
Cipek Mihael ..... 185  
Colosimo Bianca Maria ..... 217  
Croccolo Dario ..... 237  
Cutard Thierry ..... 223

### Č

Čabrilo Aleksandar ..... 171

Čekada Miha ..... 159  
Čep Robert ..... 45  
Čepić Zoran ..... 193  
Čiča Đorđe ..... 31

### D

Demir Ali Gökhan ..... 217  
Demko Michal ..... 75  
Dimić Zoran ..... 63, 71  
Dramićanin Miroslav ..... 167, 177  
Drnovšek Aljaž ..... 103  
Dudić Branislav ..... 211  
Dujmović Miroslav ..... 205  
Dumanić Nađan ..... 205

### Đ

Đekić Petar ..... 91, 229  
Đukić Goran ..... 131

### F

Fajsi Angela ..... 139  
Feier Anamaria Ioana ..... 123

### G

Gal Lucian ..... 143  
Galantucci Luigi Maria ..... 5  
Gaška Adam ..... 13  
Gaška Piotr ..... 13  
Gečevska Valentina ..... 217  
Gostimirović Marin ..... 19, 23, 49, 59  
Greš Miroslav ..... 75  
Grešová Zuzana ..... 79  
Guerra Maria Grazia ..... 5

### H

Hadžistević Miodrag ..... 95, 99, 181  
Harmatys Wiktor ..... 13

## I

Ižol Peter ..... 75, 79

## J

Jakovljević Živana..... 119  
Janjatović Petar ..... 167, 177  
Janjić Mileta ..... 41  
Janković Predrag ..... 19, 95, 99  
Jerman Marko..... 241  
Jevtić Đorđe..... 189  
Jovković Srđan .....91

## K

Klobčar Damjan ..... 197  
Knežević Ivan..... 83  
Knežević Petar..... 233  
Kojić Sanja .....155, 233  
Kokotović Branko ..... 63  
Konjović Zoran ..... 163  
Kopač Janez ..... 201  
Korunović Nikola..... 127  
Kosec Borut..... 197  
Kostić Ćirić Snežana ..... 237  
Kostić Nikola.....91, 135  
Kovač Pavel..... 211  
Kovačević Lazar..... 103, 155, 159  
Kraišnik Milija ..... 163  
Kramar Davorin ..... 31  
Kühnel Lisa ..... 241  
Kukuruzović Dragan ..... 103, 159  
Kulundžić Nenad..... 23, 49, 177  
Kurbegović Ramiz..... 41  
Kuzmanović Bogdan ..... 147

## L

Lanc Zorana ..... 95, 181  
Lavecchia Fulvio ..... 5  
Lazarević Milovan..... 151  
Lebar Andrej ..... 241  
Lecler Sylvain ..... 223  
Lisjak Dragutin..... 185  
Lukić Dejan..... 45, 151

## M

Madić Miloš ..... 19, 23, 27, 99  
Majstorović Vidosav ..... 111  
Maňková Ildikó ..... 79  
Matin Ivan ..... 95  
Mićunović Ilić Milana..... 193, 197

Mijanović Krsto .....201  
Miletić Aleksandar ..... 103, 159  
Miljković Zoran .....189  
Milosavljević Marko.....139  
Milošević Mijodarag .....45, 151  
Milutinović Biljana .....91, 229  
Milutinović Mladomir.....135, 163, 233  
Mladenović Predrag .....99  
Morača Slobodan .....139  
Movrin Dejan ..... 135, 163, 233

## N

Nagode Aleš.....197  
Nedeljković Dušan.....119  
Nedić Bogdan .....53  
Nikolčić Milan.....91  
Nikolčić Saša .....229  
Nikolić Vukašin .....67  
Novaković Tamara.....193

## O

Olmi Giorgio.....237  
Opetuk Tihomir.....131  
Ostojić Gordana .....151

## P

Pamintas Eugen.....37, 123  
Panjan Peter .....159  
Pavković Danijel.....185  
Pavlović Milan .....91  
Pellegrini Alessandro .....5  
Petković Dušan .....19  
Petrović Bojan.....155  
Pintać Diandra.....233  
Plavac Filip .....185  
Premčevski Velibor.....233  
Previtali Barbara .....217  
Pušavecc Franci ..... 17

## R

Rackov Milan.....83  
Rajnović Dragan ..... 167, 177  
Randelović Sasa ..... 135, 163  
Ranisavljev Miloš .....95  
Ristić Miloš.....91  
Rodić Dragan ..... 19, 23, 49, 59

## S

Sabotin Izidor.....241

Santoši Željko.....	87
Savković Borislav .....	49, 59, 211
Sekulić Milenko .....	23, 49, 59
Sindelić Vladimir .....	237
Sladek Jerzy .....	13
Slavković Nikola.....	63
Sredanović Branislav.....	31
Stanivuk Tatjana.....	205
Stefanović Ljiljana .....	163
Stojadinović Slavenko.....	111
Stojanović Goran.....	155
Stojković Miloš .....	127
Stupar Ignjatović Danijela .....	223
Svorcan Jelena.....	189

## Š

Šejat Bojanić Mirjana.....	83
Šidānin Leposava .....	167
Škorić Branko.....	103, 147, 155, 159
Šokac Mario .....	87
Šoškić Zlatan .....	237
Štrbac Branko.....	95, 99, 181

## T

Tabaković Slobodan.....	67, 71
Tasić Nemanja.....	147
Terek Pal .....	103, 155, 159
Terek Vladimir .....	103, 155, 159
Tešić Saša .....	31
Tešić Zdravko.....	147
Tessier Alexandre.....	223
Tomić Mladen .....	229
Tomov Mite.....	115
Trifunović Milan .....	27
Trstenjak Maja .....	131, 185
Turudija Rajko .....	127

## U

Ungureanu Nikolae .....	45
-------------------------	----

## V

Valentinčić Joško .....	241
Varga Ján.....	75
Vasileska Ema.....	217
Velkoska Cvetanka.....	115
Vilotić Marko .....	163
Vitković Nikola .....	27
Vorkapić Nikola .....	63
Vrabel' Marek .....	75, 79
Vukelić Đorđe .....	87, 193

## Z

Zabunov Ivan .....	177
Zeidler Henning .....	241
Zeljковиć Milan.....	71, 181

## Ž

Živanović Saša .....	63, 71
Živković Aleksandar .....	83
Zlatanović Labus Danka .....	181



**IN MEMORIAM**



## IN MEMORIAM

### **Prof. Mikolaj Kuzinovski, Ph.D. (1956-2020)**



In Skopje at the age of 63, our esteemed and respected Prof. Mikolaj Kuzinovski Ph.D. left us. He was a full professor on the Faculty of Mechanical Engineering at the “Ss. Cyril and Methodius” University in Skopje, an exceptional collaborator and professor dedicated to his students. Professor Kuzinovski was born on 06.12.1956 in Legnica, Republic of Poland, and at the age of seven, together with his family he moved to Skopje, Republic of Macedonia, where he finished his primary, secondary and higher education. The academic career of the professor features many study visits to Poland, the country where he was born.

Professor Kuzinovski participated in the education process, teaching in the first, second and the third cycle of studies at the Faculty of Mechanical Engineering in Skopje. With respect to the Faculty and University bodies, he was appointed to several elective functions, including Vice Dean for Teaching, Senator in the University Senate, Head of the Laboratory for Metal Cutting Machines and Processing and Laboratory for Metrology of Geometric Characteristic and Quality Research, President of the Teaching and Studies Committee.

In the area of scientific and research he was considered as an exceptional researcher in the field of science, with 136 scientific papers published in conferences abroad and in the Republic of Macedonia, 38 scientific papers published in journals in the country and abroad, 4 scientific papers published in reputable journals with an impact factor, and 148 technical papers implemented for the purposes of the industry in the Republic of Macedonia. Of particular note is his contribution to 7 scientific and research projects and 4 development and research projects.

His legacy also includes his participation as a member of the Editorial Board of the following journals: Journal of the Balkan Tribological Association-Sofia, Tribology in Industry-Kragujevac, Journal of Production Engineering-Novis Sad, Mechanical Engineering-Scientific journal (MESJ)-Skopje and a member of the International Scientific Committee, as well as the following conferences: MMA-Flexible Technologies-Serbia, “Computer Aided Engineering”-Poland, Szkoły Obrobki Skrawaniem-Poland, Manufacturing and Management in the 21<sup>st</sup> Century-Macedonia.

Professor Kuzinovski was also a member of the Society of Production Engineering and the Society of Mechanics at the Faculty of Mechanical Engineering, as well as the Metrology Council within the Metrology Bureau. The 5 patents registered in the Republic of Macedonia duly represent his tireless and inexhaustible spirit for research and innovation. He authored the book *Machines and Processing Part II* – Faculty of Mechanical Engineering-Skopje, and coauthored the books: *Quality of Production and Products in the Industrial Companies in the Republic of Macedonia* and *Sterowalne i mechatroniczne narzedzia skrawajace*, WNT, Warszawa.

Professor Kuzonovski considered it a challenge and a responsibility to work in the field of international cooperation. In this regard, for many years he coordinated the cooperation between the Faculty of Mechanical Engineering in Skopje and the Institute of Machine Technology and Automatization at the Wroclaw University of Science and Technology in the Republic of Poland, as well as the cooperation between the Faculty of Mechanical Engineering Skopje and the Research and Development Center for Reductors and Motoreductors “REDOR” – Bielsko Biala, Poland.

The society at large in the Republic of Macedonia considered him as exceptionally knowledgeable about the field of accreditations in general, and higher education in particular, leaving an invaluable legacy as a President of the Accreditation Institute Council of the Republic of Macedonia and a deputy president of the Higher Education Accreditation and Evaluation Board of the Republic of Macedonia. He clearly expressed his visions and progressive ideas about improving the state of affairs in higher education and was dedicated to opening a dialogue for implementing improvements in all universities in the Republic of Macedonia.

In appreciation of his dedicated professional work Professor Kuzinovski received multiple awards, recognitions, and acknowledgements.

His departure left deep voids not only in the academic and student communities, but also in society at large in Macedonia, but his works will bear witness of the greatness of Professor Kuzonovski. It is the students and his coworkers who will continue his work. He will remain remembered by his cheerful spirit, modesty, love for his work, respect to interlocutors and his selfless strive for a better future in higher education.





# **MMA 2021**

---

**FLEXIBLE TECHNOLOGIES**

## **INFORMATION ABOUT SPONSORS AND DONATORS**



# MINISTRY OF EDUCATION, SCIENCE AND TECHNOLOGICAL DEVELOPMENT



Nemanjina 22-26  
11000 Beograd

[www.mpn.gov.rs](http://www.mpn.gov.rs)

## REPUBLIC OF SERBIA

# PROVINCIAL SECRETARIAT FOR HIGHER EDUCATION AND SCIENTIFIC RESEARCH



Bulevar Mihajla Pupina 16  
21108 Novi Sad

Tel: (021) 487 4641

Fax: (021) 456 044

E-mail: [secretary@apv-nauka.ns.ac.rs](mailto:secretary@apv-nauka.ns.ac.rs)

[www.vojvodina.gov.rs/en/autonomous-province-vojvodina](http://www.vojvodina.gov.rs/en/autonomous-province-vojvodina)

**REPUBLIC SERBIA**  
**AUTONOMOUS PROVINCE OF VOJVODINA**

# UNIVERSITY OF NOVI SAD



Dr Zorana Đinđića 1  
21001 Novi Sad  
Republic of Serbia  
Switchboard: +381 21 485 2000  
E-mail: [rektorat@uns.ac.rs](mailto:rektorat@uns.ac.rs)  
[www.uns.ac.rs](http://www.uns.ac.rs)

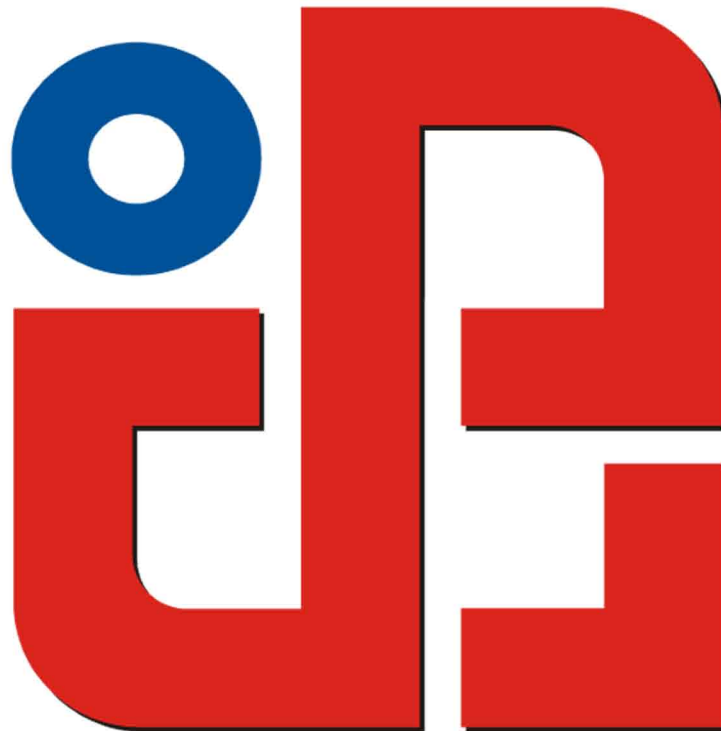
# FACULTY OF TECHNICAL SCIENCES



University of Novi Sad  
Faculty of Technical Sciences  
Trg Dositeja Obradovića 6  
21000 Novi Sad  
Republic of Serbia

Tel.: (+381) 21 450 810  
(+381) 21 6350 413  
Fax: (+381) 21 458 133  
E-mail: [ftndean@uns.ac.rs](mailto:ftndean@uns.ac.rs)  
[www.ftn.uns.ac.rs](http://www.ftn.uns.ac.rs)

# DEPARTMENT OF PRODUCTION ENGINEERING



University of Novi Sad  
Faculty of Technical Sciences  
Vladimira Perića-Valtera 2  
21000 Novi Sad  
Republic of Serbia

Secretariat of the Department:  
Tel: (021) 450-366, 485-23-20  
Fax: (021) 454-495  
E-mail: [dpm@uns.ac.rs](mailto:dpm@uns.ac.rs)  
[www.dpm.ftn.uns.ac.rs](http://www.dpm.ftn.uns.ac.rs)



Unimet provides its customers with CNC turned and machined parts, sheet metal parts, assembling and testing of parts and instruments. We employ more than 230 people. Our head office is situated in Kać, next to Novi Sad in north part of Serbia. We have two manufacturing locations, one in Kać and the other in Rudnik, 80 km south of Belgrade. In Kać we have five production facilities covering 6500 m<sup>2</sup> workspace and in Rudnik approximately 2000 m<sup>2</sup>.

Our highly productive CNC machines are capable of executing complex and precise demands. Our machines are of renowned Japanese, American and European brands. We currently have about 50 CNC machines at our disposal. Apart from the CNC machines, we have a large number of universal machines with accompanying equipment.

Materials that we machine are: Aluminium, Steel, Stainless steel, Brass and bronze, Titanium, Super alloys like Inconel and cobalt. Services that we offer: Turning from diameter 1 mm up to diameter 400mm, Milling, Sheet metal punching on CNC press and tool design for our mechanical presses, Grinding, Welding, Laser engraving.

Industries that we deliver our services to are process industries, automotive and aerospace.

Certificates that we hold are ISO9001, OHSAS18001, ISO14001 and AS9100.

We export all our goods and our main customers are Brovex Precision Engineering in Sweden, Trox in Germany, Knorr-Bremse Germany, Pratt and Whitney Canada and Telsonic Ultrasonic in Switzerland.

**Unimet d.o.o**

**Delfe Ivanic 51, 21241 Kac**

**Telephone: +381 21 6211 194**

**+381 21 6211 410**

**+381 21 6211 404**

**Fax: +381 21 6211 061**

**[www.unimet.rs](http://www.unimet.rs)**

**Email: [info@unimet.rs](mailto:info@unimet.rs)**





## Our Story

The company was founded in 1963 as a small craft-workshop thanks to the vision and entrepreneurship of Mr Slobodan Crnogorac. After a lot of hard work, deprivation and passion, we grew up into a serious, respectable, successful company known worldwide. We currently employ 360 people.

## For Reliability & Quality more than 50 years

We are TERMOVENT SC Company, a regional leader in production of industrial valves for process industry and thermo energetics. Legally, we are established as a limited liability company and classified as a medium-sized company.

Flexibility and reliability are characteristics that set us apart. We pay special consideration to cultural values. Traditional values, reliability, quality and sustainability – these are the basis of our work and existence.

We remained until today a company in private ownership and management structure, as for the past 50 years of presence.



## TODAY ...

Today, we are present with our products on almost all continents. TERMOVENT SC products are installed and functioning in many plants in more than 60 countries worldwide.

# 61

Countries Worldwide

### INDUSTRIAL VALVES

TERMOVENT SC  
Industrijska zona bb,  
21235 Temerin, Serbia  
+381 21 842 505  
office@termoventsc.rs

### STEEL FOUNDRY

Termovent SC Steel  
Foundry  
Industrijska zona bb,  
24300 Bačka Topola,  
Serbia  
+381 24 713 524  
office@livnica.com



Innovative ultrasonic welding tools  
**Sonotrodes**

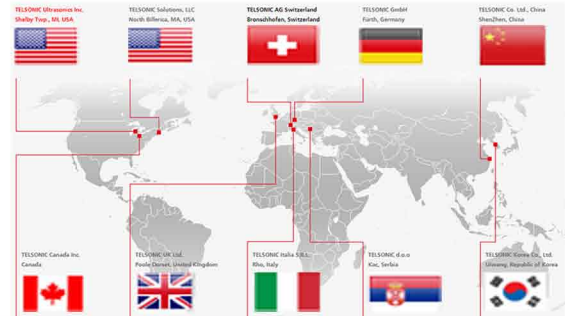


A long-standing and successful Swiss-Serbian Collaboration

In 2004, the TELSONIC Group opened a new subsidiary in Kac to produce ultrasonic welding sonotrodes and associated tooling. Last year an additional production building was commissioned to improve productivity, due to increased demands for tooling.

- Thousands of units used daily worldwide
- Innovative and patented designs
- Many years of expertise and experience
- State-of-the-art acoustic analysis for complex tooling

[www.telsonic.com](http://www.telsonic.com)



**THE POWERHOUSE OF ULTRASONICS**

**Booster**

**Sonotrodes for the packaging industry**



**Cutting Sonotrodes**

**Cut'n'Seal Sonotrodes**

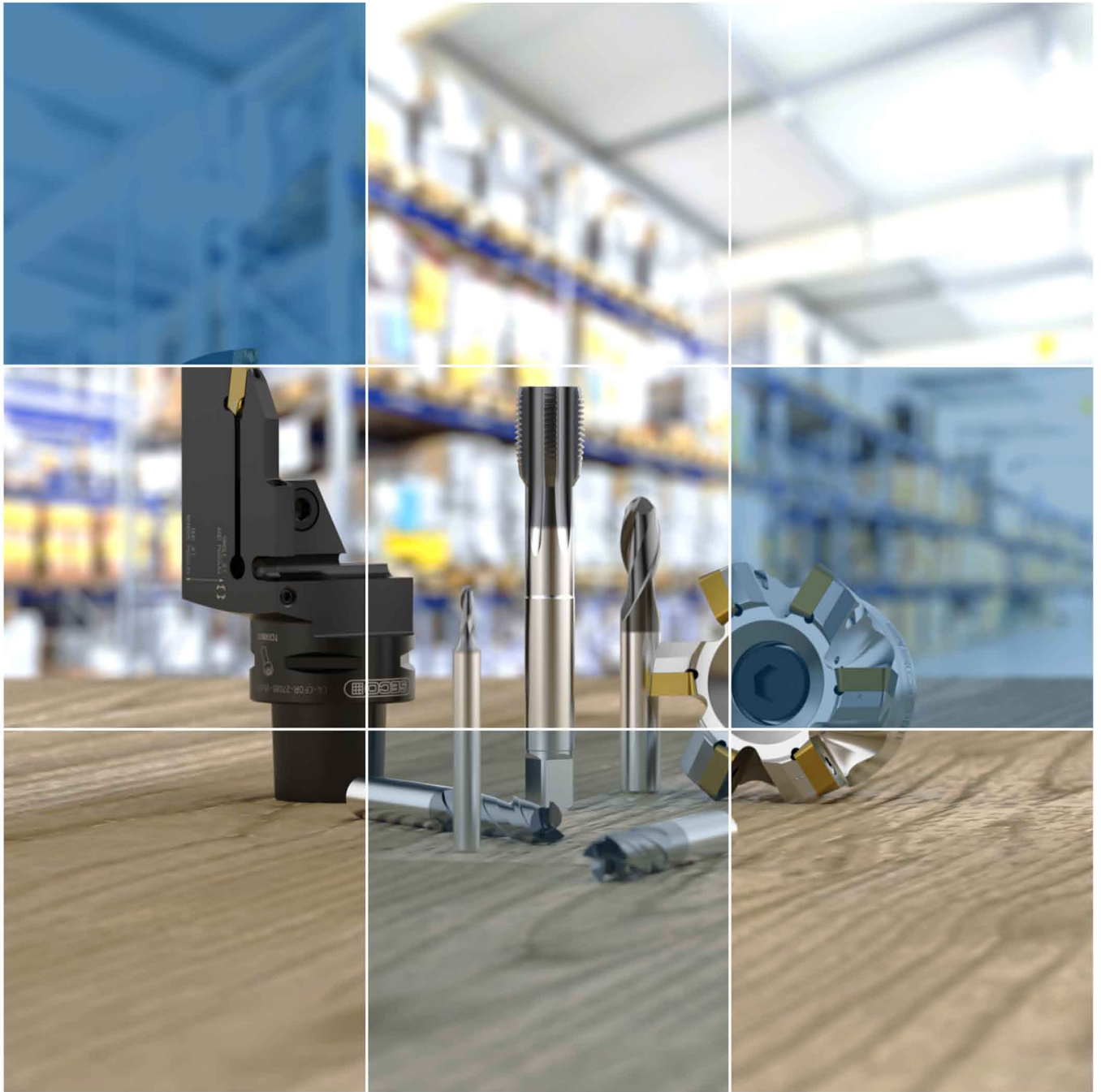


**Plastic Welding Sonotrodes**

**Metal Welding Sonotrodes**



TELSONIC d.o.o./ Atar 95, Kać, Serbia/ mob.: +381 21 2100 703/ mail: sales.rs@telsonic.com



**WE PROVIDE SUCCESS  
SOLUTION FOR YOUR BUSINESS**



SECO TOOLS SRB D.O.O.  
HAJDUK VELJKOVA 11  
21000 NOVI SAD  
[WWW.SECOTOOLS.COM](http://WWW.SECOTOOLS.COM)



# ATB SEVER

Technology in Motion



Our electric motors and generators are optimized in accordance with our client's technical and economical requests. Our clients will receive from us, within a very short notice, most advanced and high quality technical solutions of electric motors, generators, electric drives and complete technical solutions of small and middle sized hydroelectric power plants, along with economically most favourable conditions.

We are constantly moving your ideas. We are not just manufacturing motors and generators, we turn ambitious concepts of our clients into advanced, innovative and reliable products, which are unique and future oriented. Our reliability, creativity and flexibility will assist our clients in achieving their goals.

Keeping track with newest technological and technical solutions, our products are being constantly developed and therefore we are improving all our activities aimed to fulfil our client's requests. Our view of the future is oriented towards development of high power and big sized electric motors, hydrogenerators for small and middle sized hydroelectric power plants, as well as

## ATB SEVER DOO SUBOTICA

Magnetna polja 6

24 000 Subotica

Srbija

<http://www.sever.rs>

<http://www.atb-motors.com>

## Prodaja / Sales department:

Tel./Phone: +381 24 665 124

Fax: +381 24 665 125

## Servis / Service department:

Tel./Phone: +381 24 665 161

Fax: +381 24 665 125

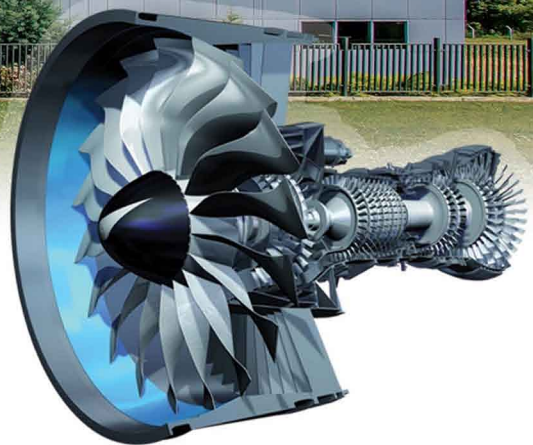




**BET SHEMESH  
ENGINES**

## **PRECISE CASTING PLANT ADA - SERBIA**

- \* **Precise Casting Plant - LPO DOO Ada was founded in 1978. The facility is in the industrial zone of Ada city.**
- \* **LPO is an expert in vacuum and air castings of superalloys and stainless steels, such as turbine blades, vanes and complex aerospace parts**



**LPO DOO ADA**  
**29. Novembra bb, Ada**  
**Tel.: +381 24 851 807**  
**Fax.: +381 24 851 475**  
**E-mail: preccast@lpo.rs**

 [www.lpo.rs](http://www.lpo.rs)





11 Hajduk Veljkova St.

21137 Novi Sad

Tel: +381 21 480 37 09

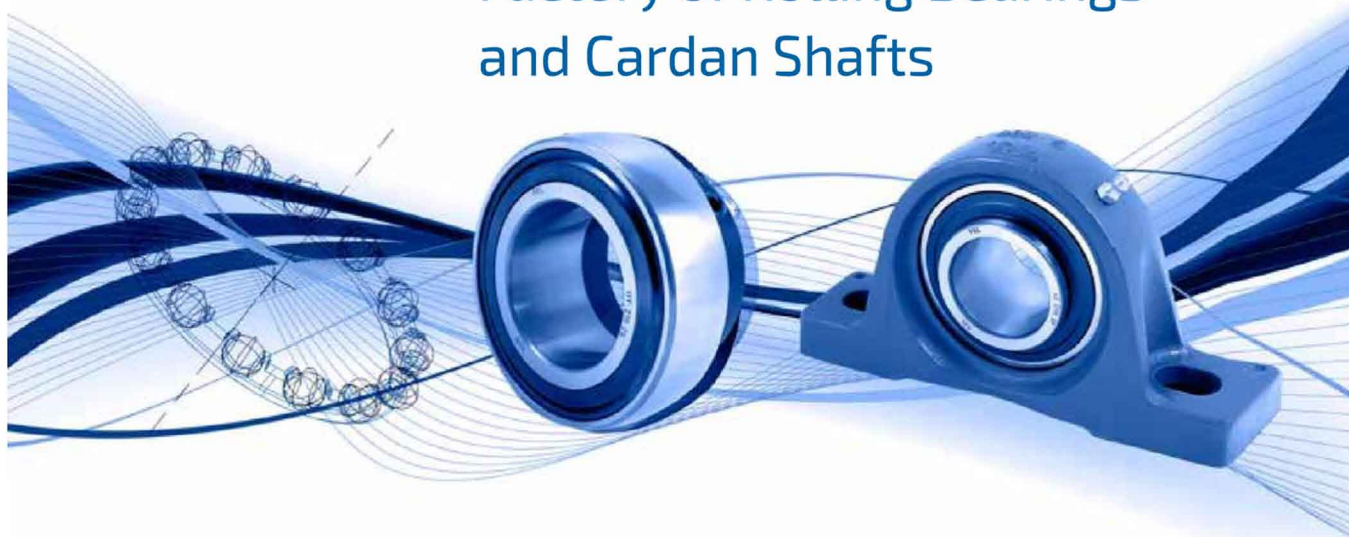
Fax: + 381 21 480 37 11

E-mail: [office@pkv.rs](mailto:office@pkv.rs)

[www.pkv.rs](http://www.pkv.rs)

# FKL®

Factory of Rolling Bearings  
and Cardan Shafts



Industrijska zona bb  
21235 Temerin  
SERBIA

Head of Sales +381 21 6841 222  
Foreign Markets +381 21 6841 190  
+381 21 6841 205  
+381 21 6841 201

[www.fkl-serbia.com](http://www.fkl-serbia.com)

[sales@fkl-serbia.com](mailto:sales@fkl-serbia.com)

[marketing@fkl-serbia.com](mailto:marketing@fkl-serbia.com)

**We are building,  
we are changing the future!**



**WE ARE INVESTING IN OUR FUTURE !**

If you want to be part of our team to become stronger,  
better, and more successful with you, join us.

Imperial Buildings d.o.o.  
Novi Sad, Đorđa Zličića 22  
Telefon/fax: 021 420 448  
office@imperialbuildings.rs





# STREIT

NOVA

Development  
Engineering  
Manufacturing



**STREIT NOVA**  
Evropska 11  
22300 STARA PAZOVA  
SERBIA  
+381 22 32 12 99  
Latitude = 44°59'27.75"N  
Longitude = 20°11'43.03"E

**P intraprofil** Company for the production of metal profiles



Intraprofil/ Đure strugara bb, Smederevo/ tel: 026- 642 940, 642 930/ fax: 026-642 942  
email: [profil@intraprofil.com](mailto:profil@intraprofil.com)/ [www.intraprofil.com](http://www.intraprofil.com)



## FLEXIBLE SOLUTIONS BY TEHNOEXPORT



## FLEXIBLE SOLUTIONS BY TEHNOEXPORT

**ADRESA:** Jovana Popovića 43, 22320 Indija

**TEL:** +381 (0) 22 553 453


**FAX:** +381 (0) 22 561 417

**E-MAIL:** [office@tehnoexport.co.rs](mailto:office@tehnoexport.co.rs)

**WEB:** [www.texo.rs](http://www.texo.rs), [www.tehnoexport.rs](http://www.tehnoexport.rs)



Private company Peštan is a leader in the Balkans in the production and distribution of products and solutions from the polymers. Company was founded in 1989 and has been producing water pipes made of polyethylene. Over time, we introduced new materials (polypropylene and PVC) and expanded product range. Today, in our offer you may find more than 8.000 products, divided into four categories:

 **PIPING SOLUTIONS**



 **BATHROOM SOLUTIONS**



 **AGRICULTURE SOLUTIONS**



 **HOUSEHOLD SOLUTIONS**



**PEŠTAN SERBIA - HEADQUARTERS**

Put 1300 kaplara 188, 34301 Bukovik, Arandelovac  
Phone: +38134700300  
Mail: office@pestan.net

Office Belgrade, Savska 33/II  
Phone: +381113610599  
Fax: +381113610599





**25**  
years and more we  
are synonymous  
with quality in the  
metal industry



About us

## DOO Vuves Commerce

DOO “Vuves Commerce” was founded in 1993., as a family company for production parts for machine industry, out of various materials, mainly metals.

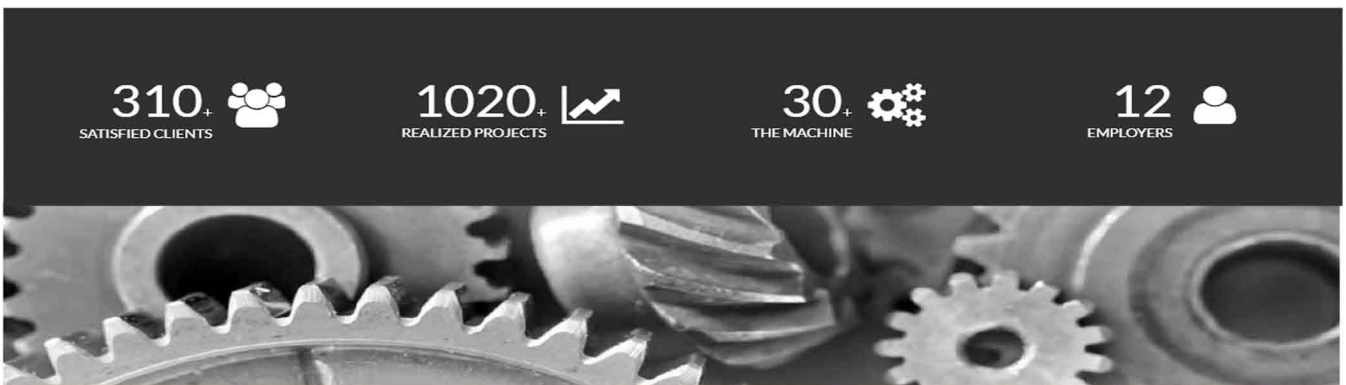
The company’s activity is based on service processing on CNC and universal metalworking machines, as well as on the production of spare parts for industrial vehicles (excavators, forklifts, tractors, combines, etc.) and for machines for the production of brick products.



Our guide is a motto:

## QUALITY - PRICE - DEADLINE

every day, we spread a network of satisfied partners, which is sufficient proof of the quality of our work and excellent motivation for future ventures



## YOUR LEADER IN MANUFACTURING

D.O.O. Vuves Commerce  
Svetosavksa 75, Kać  
Tel.: +381 21 621 3472  
Mob.: +381 69 111 6891 - Aleksandar

e-mail:  
Office: [office@vuves.co.rs](mailto:office@vuves.co.rs)  
Financial sector: [finansije@vuves.co.rs](mailto:finansije@vuves.co.rs)  
Engineering team: [inzenjering@vuves.co.rs](mailto:inzenjering@vuves.co.rs)



# DOO "GRUJIĆ I GRUJIĆ"

Bul. Vojvode Stepe 6, NOVI SAD, SRBIJA, Tel/fax: 021/518 381, 021/6403 091  
Mob. 063/865 78 79, e-mail:grujicgrujicns@gmail.com

## Shoulder endoprosthesis



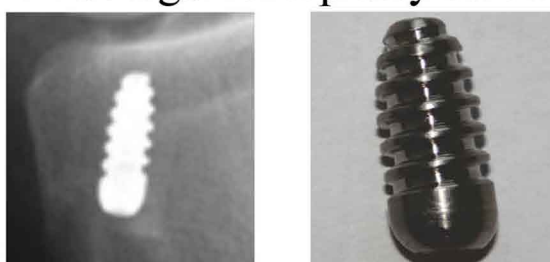
## Modular hip endoprosthesis



## Modular hip and knee endoprosthesis - "total femur"



## Knee ligamentoplasty screw



# KEYNOTE SPEAKERS

Prof. Dr. ERHAN BUDAK  
Sabanci University, Turkey



Dr. Budak is a professor at Sabanci University in Turkey. His areas of interest include machining processes and machine tools, intelligent manufacturing, process modelling and simulation, high precision/performance manufacturing, and machine dynamics. He is the founder of a spin-off company, Maxima Manufacturing R&D, which develops and implements machining solutions for various industries. He is the author/co-author of more than 200 articles and papers in conference proceedings with more than 10000 citations and an h-index of 50 (Google Scholar). He is a Fellow member of CIRP (currently Chair of Scientific Committee on Machines), Associate/Regional Editor, and Editorial Board Member of several journals.

Prof. Dr. EMANUELE CARPANZANO  
University of Applied Sciences and Arts of Southern Switzerland,  
Switzerland

Prof. Dr. Emanuele Carpanzano is Director of the Department of Innovative Technologies at the University of Applied Sciences and Arts of Southern Switzerland (SUPSI). He has led numerous research initiatives at international, European, national and regional levels, as well as industrial research and technology transfer projects. His research interests and activities focus on industrial control and automation systems and on the digitalization of industrial systems and value chains, including the development of related human aspects. He is Professor of Industrial Systems at SUPSI and author of more than 150 scientific papers and several industrial patents in his applied research areas. He is also Fellow member of the CIRP.



Prof. Dr. LUIGI MARIA GALANTUCCI  
Polytechnic University of Bari, Italy



Dr. Luigi Maria Galantucci is a professor at Polytechnic University of Bari in Italy. His areas of interest include 3D scanning and measurement of microcomponents, reverse engineering, rapid prototyping and additive manufacturing, laser machining, thermomechanical simulation of manufacturing processes, CAM, process planning, feature technology, analysis and simulation of manufacturing systems, biomechanics and anthropometry. Life Fellow of CIRP since 2006, now International Academy for Production Engineering. "Doctor Honoris Causa" awarded by the Academic Senate of the Polytechnic University of Tirana - PTU (Albania - October 16, 2009). CEO and President of Polishape 3D srl, a spin-off company of Polytechnic University of Bari.

Prof. Dr. ADAM GAŠKA  
Cracow University of Technology, Poland

Dr. Adam Gaška is a professor at the Cracow University of Technology (CUT) in Poland. His scientific interests include coordinate metrology, portable coordinate systems including AACMMs, LaserTrackers, triangulation and structured light scanners, topics related to measurements and system accuracy assessment, calibration of measurement systems and material standards, numerical methods in metrology, methods for identification and correction of geometric errors. He is author/co-author of more than 90 research papers and 3 patents. He presented his research at more than a dozen international conferences. He collaborates with many companies including Volkswagen, Fiat Auto Poland, ALSTOM Power, ArcelorMittal, Hexagon Metrology. He is a member of IMEKO (International Measurement Confederation).



Prof. Dr. FRANCI PUŠAVEC  
University of Ljubljana, Slovenia



Prof. Dr. Franci Pušavec is a researcher at the Faculty of Mechanical Engineering, University of Ljubljana (Slovenia), and heads the Department of Management of Manufacturing Technologies and the Laboratory of Machining. His research is mainly focused on sustainable development, upgrades, analysis, diagnosis and optimization of machining processes. He has published 62 original scientific articles with more than 1700 citations and an h-index of 20 (WoS, Scopus). He is also active in TRL on international patents and developing innovative solutions based on cryogenic cutting processes, polishing machine, high pressure jet assisted machining. The results of his work are visible in industry and prototyping. He is currently an Associate member of CIRP.

